Targeting *Acinetobacter baumannii* wound infections: From transcriptional profiling to drug repurposing and bioactive hydrogel development

A Thesis Submitted for the Degree of Doctor of Philosophy

By

Jie Han

Department of Biosciences, Brunel University London

2026

Abstract

Antimicrobial resistance (AMR) is an increasing public health emergency, driven largely by the overuse and misuse of antibiotics. Among multidrug-resistant pathogens, *Acinetobacter baumannii* is a major clinical concern due to its ability to survive in hospital environments. Recent studies have shown that artificial sweeteners, including acesulfame potassium (Ace-K), sodium saccharin (SACC), and sodium cyclamate (CYC), can inhibit bacterial growth, motility, and biofilm formation, and may enhance antibiotic activity *in vitro*. However, effective delivery of these compounds to wound infection sites remains a significant challenge.

This thesis investigates alternative non-antibiotic strategies for targeting *A. baumannii*, with a focus on artificial sweetener-loaded polyvinyl alcohol (PVA)-based hydrogels, behaviour changing in wound-mimic environment, 3D-printable hydrogel development, and screening of FDA-approved drugs that modulate virulence-associated pathways. PVA-Borax and freeze-thaw PVA hydrogels were formulated with Ace-K, SACC, and CYC and demonstrate strong antimicrobial activity. In addition, this thesis explores how *A. baumannii* behaves in a wound-mimic environment in Lubbock chronic wound biofilm (LCWB) medium. Under LCWB conditions, it induced reduced biofilm formation and iron-starvation responses. With iron supplementation, biofilm formation was restored. This highlights that iron is limited in the LCWB medium and is an important regulator of *A. baumannii* behaviour. Moreover, a 3D-printable PVA/hydroxypropyl methylcellulose (HPMC) hydrogel was then developed to improve mechanical properties and control antimicrobial release. The optimised PVA/HPMC/SACC formulation demonstrated improved printability, structural integrity, swelling behaviour, rapid SACC release and antimicrobial activity compared with non-printed formulations.

Finally, a high-throughput screen of an FDA-approved drug library identified compounds that regulate *pilA* expression and biofilm formation in *A. baumannii.* A cancer drug pomalidomide, was identified as a key hit that suppressed *pilA* expression, reduced twitching-associated behaviour, enhanced biofilm formation, and increased infection severity in *Galleria mellonella* and murine infection models.

Overall, these findings demonstrate that effective control of *A. baumannii* wound infections requires more than identifying antimicrobial compounds alone. It also requires wound-relevant testing models, rational biomaterial-based delivery systems, and careful evaluation of how non-antibiotic compounds influence bacterial physiology and virulence.

Acknowledgements

PhD is a journey filled with happiness, excitement, challenges and moments of uncertainty. Throughout this journey, I had the joy of discovery, the frustration of failed experiments, the pressure of deadlines, and the encouragement that comes from the support of others. These experiences have shaped me both as a researcher and as a person.

I would like to express my sincere gratitude to my supervisor, Professor Ronan McCarthy, for his continuous guidance, support and encouragement throughout my postgraduate years. Your scientific insight, feedback, patience and encouragement have been invaluable in shaping this project and helping me develop as a researcher.

I would like to thank all the members in the RMC lab (Dr Rubén de Dios, Dr Kavita Gadar, Dr Lyuboslava Harkova, Dr Sophie Howard, Dr Evagenia Maslova, Dr Chris Proctor, Dr Mohamed Soliman, Dominika Krawiel, Magdalena Howe and Ciaram Staber) who generously shared their knowledge, experience and advice with me, and I have had the great pleasure of working with all of you throughout my PhD. The PhD journey would have been much more difficult without the conversations, laughter and shared frustrations in the lab.

I am also deeply grateful to our collaborator, Dr Bin Zhang, in the Department of Mechanical Engineering at Brunel University of London, for her generous support, encouragement, and guidance throughout the development of the 3D-printable hydrogel work. I have truly enjoyed working with you, and I am thankful for your patience, kindness and willingness to help whenever I encountered difficulties.

Finally, a special thank you goes to my partner, my parents, my grandma, brother and cousin for their unconditional love, patience and support throughout my PhD and my life in general. Thank you for always believing in me and encouraging me during difficult moments. I would also like to thank my friends for standing beside me throughout this journey. I wouldn't be here without you.

Declaration of originality and collaborative work

I declare that the work presented in this thesis is my own. The contributions are appropriately referenced throughout the text and acknowledged below.

1. Chapter 2 is adapted from our paper in Advanced Healthcare Materials (Han *et al*., 2026).

- The cytocompatibility assay was conducted by Dominika Krawiel, a PhD student in our lab.
- The hydrogel-treated biofilm assessment was conducted by me and Dr Mohamed Soliman, a postdoctoral researcher in our lab.

2. The Cytocompatibility assay in Chapter 4 was conducted by Dr Mohamed Soliman.
3. The murine model experiment investigating pomalidomide exposure during *A. baumannii* infection was in Chapter 5, conducted by our collaborators in Dr Zurawski's group at Hartford HealthCare.

Contents

Abstract 2
Acknowledgements 4
Declaration of originality and collaborative work 6
Contents 7
List of Figures 13
List of Tables 17
Abbreviations 18
1. Introduction 20
1.1 The History of Antibiotics 20
1.2 Antimicrobial Resistance (AMR) 23
1.3 Mechanism of Antimicrobial Resistance 26
1.3.1 Limiting the Uptake of a Drug 28
1.3.2 Inactivation of the Antibiotic and Modifying Drug Targets 29
1.3.3 Efflux Pump of the Antibiotic 31
1.4 *Acinetobacter baumannii* 32
1.4.1 Prevalence and Types of Infection 35
1.4.2 The Virulence Factors of *A. baumannii* 37
1.4.3 *A. baumannii* Resistance Mechanism 49
1.5 Recent Progress to Tackle MDR *A. baumannii* Infection 51
1.6 Alternative Chemical Compounds and Agents to Tackle MDR Pathogens 52
1.7 Artificial Sweeteners and Their Antimicrobial Properties 55
1.8 Introduction of Hydrogel 60
1.8.1 Freeze-Thaw PVA Hydrogel 65
1.8.2 Poly (vinyl alcohol) Borax Hydrogel 67
1.8.3 3D Printable Hydrogel for Wound Dressing Application 69
1.9 Aims and Objectives 70
2. Develop a Novel Artificial Sweetener-Loaded PVA Hydrogel that Could Inhibit *A. baumannii*. 72

2.1 Introduction 72
2.2 Aim 1 76
2.3 Materials and Methods: 77
Bacterial strain 77
2.3.1 Formulation of Artificial Sweetener (AS) Loaded PVA-Borate Hydrogel 77
2.3.2 Preparation of Freezing- Thaw (FT) AS-loaded PVA Hydrogel 78
2.3.3 Hydrogel Zone of Inhibition Assays (ZOI) 79
2.3.4 Antimicrobial Time-Kill Assay and Drug Release Profile 80
2.3.5 Hydrogel-treated Biofilm Assays and Scanning Electron Microscopy (SEM) ... 81
2.3.6 *A. baumannii* AB5075 and *P. aeruginosa* PA14 Mixed Culture Assays 83
2.3.7 Haemolysis Assays Cytocompatibility Assessment 83
2.3.8 Degree of Swelling and Weight Loss 84
2.3.9 Hydrogel Morphology 85
2.3.10 Rheology 86
2.3.11 Attenuated Total Reflectance–Fourier Transform Infrared Spectroscopy (ATR-FTIR) and X-ray diffraction (XRD) 86
2.3.12 Phase 1 Clinical Study in Humans 86
2.3.13 Statistical Analysis 87
2.4 Results: 88
2.4.1 Formulation of Artificial Sweetener (AS) Loaded PVA-based Hydrogel. 88
2.4.2 Artificial sweetener-loaded hydrogels showed antimicrobial activity in the disk diffusion assay. 91
2.4.3 Artificial Sweetener-Loaded Freeze-Thaw PVA Hydrogels Antimicrobial Activity is Associated with the Concentration of PVA. 94
2.4.4 AS-Loaded Hydrogels Show Time-Dependent Inhibition of *A. baumannii* Viability *in vitro* 100
2.4.5 AS-loaded PVA Borax Hydrogels Exhibit Substantial Antibiofilm Activity Against *A. baumannii in vitro*. 105
2.4.6 AS-loaded PVA-Borax Hydrogels Outperform Commercial Antimicrobial Silver Alginate hydrogels in *A. baumannii* early biofilm *ex vivo* model. 108

2.4.7 AS-loaded hydrogels reduce the biofilm of polymicrobial culture. 110

2.4.8 AS Loaded-Hydrogels Have a Favourable Cytocompatibility Profile 112

2.4.9 Material Characterisation 113

2.4.10 Pilot Phase 1 Clinical Study in Humans 125

2.5 Discussion 129

2.6 Key Findings 135

3. Exploring How the Transcriptional Landscape of *A. baumannii* Changes and Hydrogel Performance in Lubbock Chronic Wound Biofilm Medium. 136

3.1 Introduction 136

3.2 Aim 2 139

3.3 Methods 140

Bacterial strain 140

3.3.1 Growth Curve Measurement Using LB, M9 Succinate, and Lubbock Chronic Wound Biofilm (LCWB) Model 140

3.3.2 Biofilm Assay 140

3.3.3 Transcriptome analysis of *Acinetobacter baumannii* grown in LB, M9 succinate, and the LCWB medium 141

3.3.4 Iron Supplement Assay in LCWB Medium 142

3.3.5 Time-Kill Assay of AS-Loaded Hydrogel in the LCWB Medium 142

3.3.6 Degree of Swelling and Weight Loss 142

3.3.7 Statistical Analysis 143

3.4 Results 144

3.4.1 Wound-Like LCWB Medium Supports Robust *A. baumannii* Proliferation 144

3.4.2 LB Broth Promotes *A. baumannii* Biofilm Formation More Than the LCWB medium or M9 Succinate Medium 145

3.4.3 LCWB Medium Induces Iron-Starvation Responses and Represses Environmental Persistence Pathways in *A. baumannii* 147

3.4.4 Wound-like Conditions Trigger a Global Shift Towards High Translational and T4P Activity When Compared to M9-succinate Medium in *A. baumannii* 150

3.4.5 Iron is a Key Factor in the *A. baumannii* Biofilms Formation in LCWB medium 154

3.4.6 Artificial Sweetener-Loaded-Hydrogel Demonstrates Antimicrobial Activity in a Host-Mimicking Wound Environment 156

3.4.7 Artificial Sweetener-Loaded-Hydrogel Showed Similar Swelling and Degradation behaviour in LCWB medium and PBS 157

3.5 Discussion 160

3.6 Key Findings 163

4. A 3D-Printable Poly(vinyl alcohol)/Hydroxypropyl Methylcellulose Hydrogel with Controllable Mechanical Properties and Drug Release 164

4.1 Introduction 164

4.2 Aim 3 167

4.3 Materials and methods 168

4.3.1 Material 168

4.3.2 Ink Formulation 168

4.3.3 Rheological measurement 169

4.3.4 Semi-solid extrusion (SSE) 3D Printing 170

4.3.5 Mechanical Strength Analysis 170

4.3.6 Attenuated Total Reflectance–Fourier Transform Infrared Spectroscopy (ATR-FTIR) 170

4.3.7 Degree of Swelling and Weight Loss 171

4.3.8 Hydrogel Surface Morphology 171

4.3.9 Drug Release and Antimicrobial Properties 172

4.3.10 *In vitro* Drug Release Test 172

4.3.11 Haemolysis Assays Cytocompatibility Assessment 173

4.3.12 Statistical Analysis 174

4.4 Results 175

4.4.1 Ink Printability Assessment 175

4.4.2 Material characterisation 181

4.4.3 Surface Morphology 186

4.4.4 Swell Ability and Degradation 186

4.4.5 Drug release profile and antimicrobial property 189

4.4.6 Biocompatibility of PVA+HPMC Hydrogel 193

4.5 Discussion 195

4.6 Key Findings 197

5.Identify bioactive compounds that regulate Type IV pilus expression in *A. baumannii* by screening the FDA-Approved drugs library 198

5.1 Introduction 198

5.2 Aims 4 201

5.3 Materials and Methods: 202

Bacterial strain 202

5.3.1 Validation of a GFP-based Gene Expression Assay for Ace-K 202

5.3.2 GFP-based Gene Expression assays on DiscoveryProbe™ FDA-Approved Drug Library. 203

5.3.3 Revalidate GFP-based Gene Expression Assays for Hit Drug Candidates. 203

5.3.4 Twitching Motility Assay 204

5.3.5 Minimum Inhibitory Concentration and Minimum Biofilm Inhibitory and Growth assays 204

5.3.6 RNA-Seq 205

5.3.7 Molecular Docking 206

5.3.8 In vivo Efficacy of Pomalidomide in *Galleria mellonella* 207

5.3.9 Murine Pulmonary Infection Model 207

5.3.10 Statistical Analysis 208

5.4 Results 209

5.4.1 Validation of a Green Fluorescent Protein (GFP) -based Gene Expression Assay for Ace-K 209

5.4.2 High-throughput GFP-based screening of an FDA-approved drug library identifies modulators of *pilA* expression. 211

5.4.3 Revalidation of *pilA* Expression of Hit Candidates and Determining their Growth and Biofilm Formation 216

5.4.4 Twitching assay of Primaquine Diphosphate, 2-Naphthol, Flavin adenine dinucleotide and Pomalidomide 221

5.4.5 Growth and Biofilm Effects of Selected Compounds Reveal that Pomalidomide Augments *A. baumannii* Biofilm Formation Without Affecting Growth 224

5.4.6 Pomalidomide Triggers Increases Expressed of the Biofilm-associated *CSU pili* 228

5.4.7 Pomalidomide Exhibits Strong Binding to Biofilm-associated csu pili Proteins by Using Molecular Docking 230

5.4.8 Pomalidomide Increases the Mortality of *A. baumannii* AB5075-infected *G. mellonella* 235

5.4.9 Pomalidomide Exposure Leads to Increase in Clinical Scores in a Murine Model of *A. baumannii* Infection 239

5.5 Discussion 244

5.6 Key Findings 247

6. Discussion 248

6.1 General Discussion 248

6.1.1 Development of Artificial Sweetener-Loaded Hydrogels as a Localised Antimicrobial Strategy 248

6.1.2 The Wound-like Environment Reshapes *A. baumannii* Physiology 250

6.1.3 3D-printable PVA/HPMC Hydrogels Provide a Tunable Drug Release and Improve Material Mechanical Properties. 252

6.1.4 Non-Antibiotic Drugs as Modulators of *A. baumannii* Virulence 254

6.2 Conclusion 256

7. Reference 258

Appendix 291

Chapter 2 Appendices 291

Chapter 3 Appendices 298

Chapter 5 Appendices 398

List of Figures

Figure 1.1. Antibiotic class diagram and its mechanism target. 22

Figure 1.2 Antimicrobial resistance mechanisms diagram. 28

Figure 1.3 The process of inactivation of tigecycline by Tetracycline destructases Tet(X4) ..29

Figure 1.4 Mutation of penicillin-binding proteins as a mechanism of β-lactam resistance in MRSA. 30

Figure 1.5 Timeline of resistance of *A. baumannii* to antibiotics. 35

Figure 1.6 *abaRMI* Quorum Sensing system in *A. baumannii* AB5075.....42

Figure 1.7 Biofilm formation includes five steps: reversible attachment, irreversible adhesion, small colony formation, maturation and cell separation. 45

Figure 1.8 Schematic representation of Type IV pilus-mediated natural transformation in *A. baumannii.* 48

Figure 1.9 Chemical structure of artificial sweeteners that have antimicrobial activity on *A. baumannii*. 59

Figure 1.10 Repeating units of poly(vinyl alcohol). 63

Figure 1.11 Schematic illustration of FT-PVA hydrogel formation. 66

Figure 1.12 Cross-linking of poly(vinyl alcohol) with borax. 67

Figure 2.1 Illustration of AS-Loaded PVA-Borax Hydrogel preparation 78

Figure 2.2 Illustration of *A. baumannii* AB5075 inoculation using the Kirby–Bauer disc diffusion method. 79

Figure 2.3 Schematic of the time-course assay to assess antimicrobial activity of control and AS-loaded hydrogels against *A. baumannii* AB5075 81

Figure 2.4 Image of 3% Ace-K loaded hydrogel 89

Figure 2.5 Antimicrobial activity of hydrogels loaded with (A) Ace-K, (B) SACC and (C) CYC against *A. baumannii*, assessed by disk diffusion assay. 94

Figure 2.6 Antimicrobial activity of FT-PVA hydrogels loaded with Ace-K, SACC and CYC against *A. baumannii*, assessed by disk diffusion assay. 95

Figure 2.7 Bar chart of the ZOI of FT-PVA Hydrogel against *A. baumannii*. 98

Figure 2.8 AS Loaded-PVA-Borax Hydrogel Effectiveness at 24 hours 101

Figure 2.9 This figure illustrates the log reduction in viable *A. baumannii* cell counts over a 24-hour period when exposed to 3% PVA FT-hydrogels loaded with varying concentrations of SACC, Ace-K, and CYC..... 104

Figure 2.11 Antibiofilm activity of AS-loaded hydrogels against *A. baumannii* in *ex vivo* porcine skin burn wound model..... 109

Figure 2.12 Antimicrobial activity of AS-loaded hydrogels against mixed infection biofilm *in vitro.*. 111

Figure 2.13 Blood compatibility and cell viability of AS-Loaded hydrogel. 113

Figure 2.14 Degree of swelling and weight loss of PVA-borax hydrogels:(A) Swelling degree (%) of PVA–borax hydrogels incorporated with different AS over a 48-hour period. 116

Figure 2.15 AS-Loaded Hydrogel Morphologies. 120

Figure 2.16 Rheological properties of control and 8% artificial sweetener-loaded PVA–borax hydrogels..... 122

Figure 2.17 FTIR Analysis of AS-Loaded Hydrogels. 124

Figure 2.18 Hydrogels were fixed with Tegaderm adhesive film (3M) to mimic clinical dressing conditions for 24 hours 128

Figure 3.1 Growth curve of *A. baumannii* strain AB5075 in Luria-Bertani (LB) broth, LCWB medium, and M9 succinate medium. 145

Figure 3.2 Biofilm formation of *A. baumannii* AB5075 in LCWB, M9 succinate medium, and LB broth. 146

Figure 3.3 Volcano plot of differentially expressed genes in *A. baumannii* AB5075 grown in LCWB medium compared to those grown in LB broth..... 150

Figure 3.4 Volcano plot of differentially expressed genes in *A. baumannii* AB5075 grown in LCWB medium compared to those grown in M9 succinate..... 154

Figure 3.5 Biofilm formation of *A. baumannii* under different iron supplement combinations in the LCWB medium. The biofilm was restored when Fe^{2+} and Fe^{3+}were presented..... 156

Figure 3.6 Time-kill assay of AS-loaded borate hydrogel against *A. baumannii* 157

Figure 3.7 Swelling and Weight loss 159

Figure 4.1 Printability assessment with manual dispensing of PVA and PVA+HPMC.....176

Figure 4.3 Printed filament fusion rate and width of 20%PVA+ 13/ 16.7%HPMC inks. 181

Figure 4.4 FTIR spectra of PVA-based hydrogels and components.. 184

Figure 4.5 Tensile stress–strain curves of FT-PVA (20%), FT-PVA+SACC, FT-PVA+13% HPMC, FT-PVA+16.7% HPMC and FT-PVA+16.7% HPMC+8% SACC (n=3).. 185

Figure 4.6 SEM micrographs of FT PVA-based hydrogels l 186

Figure 4.7 Swelling behaviour and degradation profile of PVA-based hydrogels 189

Figure 4.8 This figure illustrates the log reduction in viable *A. baumannii* cell counts over a 24-hour period when exposed to 20% PVA+16.7% HPMC hydrogel, 20% PVA+16.7% HPM hydrogel loaded with 8% SACC, and their 3D-printed counterparts 191

Figure 4.9 Release profiles of SACC from PVA-based hydrogels 192

Figure 4.10 Blood compatibility and cell viability of PVA+HPMC Hydrogel: (A) cell viability of PVA/HPMC-based hydrogel.....194

Figure 5.1 The graphs of Normalised fluorescence from the *PpilA::gfpmut3* transcriptional fusion show Ace-K could down-regulate the *pilA* (ABUW_0304) expression 210

Figure 5.2 Workflow of high-throughput screening of an FDA-approved drug library. 212

Figure 5.3. Identification of compounds that promote or inhibit *PilA* activity.. 213

Figure 5.4 *pilA* promoters and inhibitors identified in a single-repeat screen of the FDA drug library 216

Figure 5.5 Revalidation results of hit compounds at concentration of 0.05mM and 0.5mM. Data demonstrate the mean of three technical replicates and three biological replicates 218

Figure 5.6 Normalised fluorescence from *PpilA::gfpmut3* transcriptional fusion demonstrates that selected compounds have an effect on *pilA*. 220

Figure 5.7 Primaquine diphosphate, 2-naphthol and pomalidomide decrease the twitching motility in *A. baumannii*. 223

Figure 5.8 MIC and MBIC of (A, B) Primaquine Diphosphate, (C,D) 2-Naphthol (E, F) Pomalidomide. 225

Figure 5.9 Growth Curve of pomalidomide, 2-naphthol and primaquine diphosphate on the growth of *A. baumannii* AB5075.. 228

Figure 5.10 Volcano plot of differentially expressed genes in *Acinetobacter baumannii* AB5075 treated with 5 mM Pomalidomide compared to DMSO control, both grown in LB broth. ...230

Figure 5.11 Molecular docking of pomalidomide with the biofilm-associated CsuB protein of *A. baumannii*. 231

Figure 5.12 Molecular docking of pomalidomide with the biofilm-associated CsuC protein of *A. baumannii*.. 233

Figure 5.13 Molecular docking of pomalidomide with the 1,2-phenylacetyl-CoA epoxidase subunit A protein of *A. baumannii*.. 234

Figure 5.14 Survival of *Galleria mellonella* following DMSO and pomalidomide exposure 237

Figure 5.15 Survival study of *Galleria mellonella* following infection with *A. baumannii* AB5075 exposed to pomalidomide at different concentrations. 238

Figure 5.16 Pomalidomide increases clinical severity in a murine model of *A. baumannii* lung infection. 240

Figure 5.17 Pomalidomide increases clinical severity in a murine model of *A. baumannii* lung infection. 243

List of Tables

Table 1.1 Advantages and limitations of polymers commonly used in hydrogel wound dressings 63

Table 2.1 Formulation screening of AS-loaded PVA–borax hydrogels and their structural stability.....90

Table 2.2 Formulation screening of AS-loaded FT-PVA hydrogels and their structural stability 90

Table 2.3 Average CFU and Log Reduction of *A. baumannii* by AS-Loaded PVA Hydrogels at 24hrs.....104

Table 2.4 : Initial and Final Fry Weights of AS-loaded PVA–Borax Hydrogels for Weight Loss Evaluation 117

Table 4.1 PVA Base and PVA+HPMC ink Formulations. 168

Table 5.1 Molecular Weights and origin of compounds 204

Table 5.2 Medical use of compounds identified from the *PilA* promoter based on the screening. 213

Table 5.3 Medical use of compounds identified from the PilA inhibitor based on the screening. 214

Table 5.4 Medical uses of representative compounds affecting *PilA* activity 215

Abbreviations

3D	Three-dimensional
AACs	Aminoglycoside acetyltransferases
A. baumannii	*Acinetobacter baumannii*
Ace-K	Acesulfame potassium
AgNPs	Silver nanoparticles
AI	Artificial intelligence
AIF	Apoptosis-inducing factor
AIs	Autoinducers
AME	Aminoglycoside-modifying enzyme
AMR	Antimicrobial Resistance
AP	Aloe polysaccharide
ARGs	Antibiotic resistance genes
AS	Artificial sweeteners
borax	Sodium tetraborate
BSI	Bloodstream infection
CAMPs	Cationic antimicrobial peptides
CMC	Carboxymethylcellulose
COVID-19	Coronavirus disease 2019
CYC	Sodium cyclamate
DIW	Direct ink writing
DNA	Deoxyribonucleic acid
DS	Degree of swelling
E. faecalis	*Enterococcus faecalis*
E. coli	*Escherichia coli*
EPS	Extracellular polymeric substance
FT	Freezing-thawing
FTIR	Fourier Transform Infrared
GFP	Green fluorescent protein
G. mellonella	*Galleria mellonella*
HPMC	Hydroxypropyl methylcellulose
ICU	Intensive care units
Isox	Isoxazolidinone
K. pneumoniae	*Klebsiella pneumoniae*
LB	Luria-Bertani
LCWB	chronic wound biofilm (LCWB) model
LPS	LPS Lipopolysaccharide
MBIC	Minimum Biofilm Inhibitory Concentration

MDR	Multidrug-resistant
MIC	Minimal inhibitory concentration
MNPs	Metal-based nanoparticles
OmpA	Outer membrane protein A
OMPs	Outer membrane proteins
OTC	Over the counter
Oxa	Isomers oxazoline
P. aeruginosa	*Pseudomonas aeruginosa*
PCL	Polycaprolactone
PDR	Pan-drug-resistant
PLL/HA	poly(L-lysine)/hyaluronic acid
PVA	Polyvinyl alcohol
QQ	Quorum-quenching
QS	Quorum sensing
R&D	Research and development
SACC	Sodium saccharin
S. aureus	*Staphylococcus aureus*
SEM	Scanning Electron Microscopy
ssDNA	Single-stranded DNA
T4P	Type IV pilus
TBSA	Total body surface area
US	United States
VAP	Ventilator-associated pneumonia
VRP	Viscosity recovery percentage
WHO	World Health Organisation
XDR	Extensively drug-resistant
XRD	X-ray diffractometry
ZOI	Zone of Inhibition Assays

Chapter 1

1. Introduction

1.1 The History of Antibiotics

The discovery of antibiotics is one of the significant milestones in modern medicine. In 1910, the first antibiotic, salvarsan, was introduced, followed by the first commercial antibacterial agent, Sulphonamides, discovered by Gerhard Domagk in the early 1930s. A major breakthrough occurred in 1928 with Alexander Fleming's discovery of penicillin. This advancement initiated a "golden age" of antibiotic discovery. During the golden age period, naturally derived antimicrobial compounds such as streptomycin, tetracycline, and chloramphenicol were also discovered. These antibiotics reduced mortality dramatically from bacterial infections and saved millions of lives worldwide (Lobanovska and Pilla, 2017). Nowadays, antibiotics are widely used in different settings such as healthcare and agriculture. In clinical settings, antibiotics are essential for treating bacterial infections and preventing bacterial infections after surgery and in the intensive care unit. In agriculture, antibiotics have been widely used to promote livestock growth and prevent disease, contributing to food security and socio-economic development (Ding *et al.*, 2023). However, the extensive, often unregulated use of antibiotics in these settings has exerted strong selective pressure on bacterial populations, accelerating the emergence of antimicrobial resistance (AMR).

Antibiotics can target bacterial infections in different ways, such as inhibiting bacterial cell wall synthesis, bioprotein synthesis, deoxyribonucleic acid (DNA) replication, folic acid synthesis, and messenger ribonucleic acid (mRNA) translation (Walsh, 2005; Lettieri *et al.*, 2018). Inhibiting and damaging these cellular functions could lead to different outcomes for

bacteria, such as killing the cells or inhibiting bacterial growth (Figure 1.1). Based on their functional outcomes, antibiotics can be broadly divided into two groups: bacteriostatic and bactericidal. The bactericidal antibiotics have the ability to kill bacteria, such as penicillin. On the other hand, bacteriostatic antibiotics can inhibit bacterial growth, such as tetracycline, trimethoprim/sulfamethoxazole, and linezolid (Wright, 1999; Loree and Lappin, 2020; Verma *et al.*, 2022).

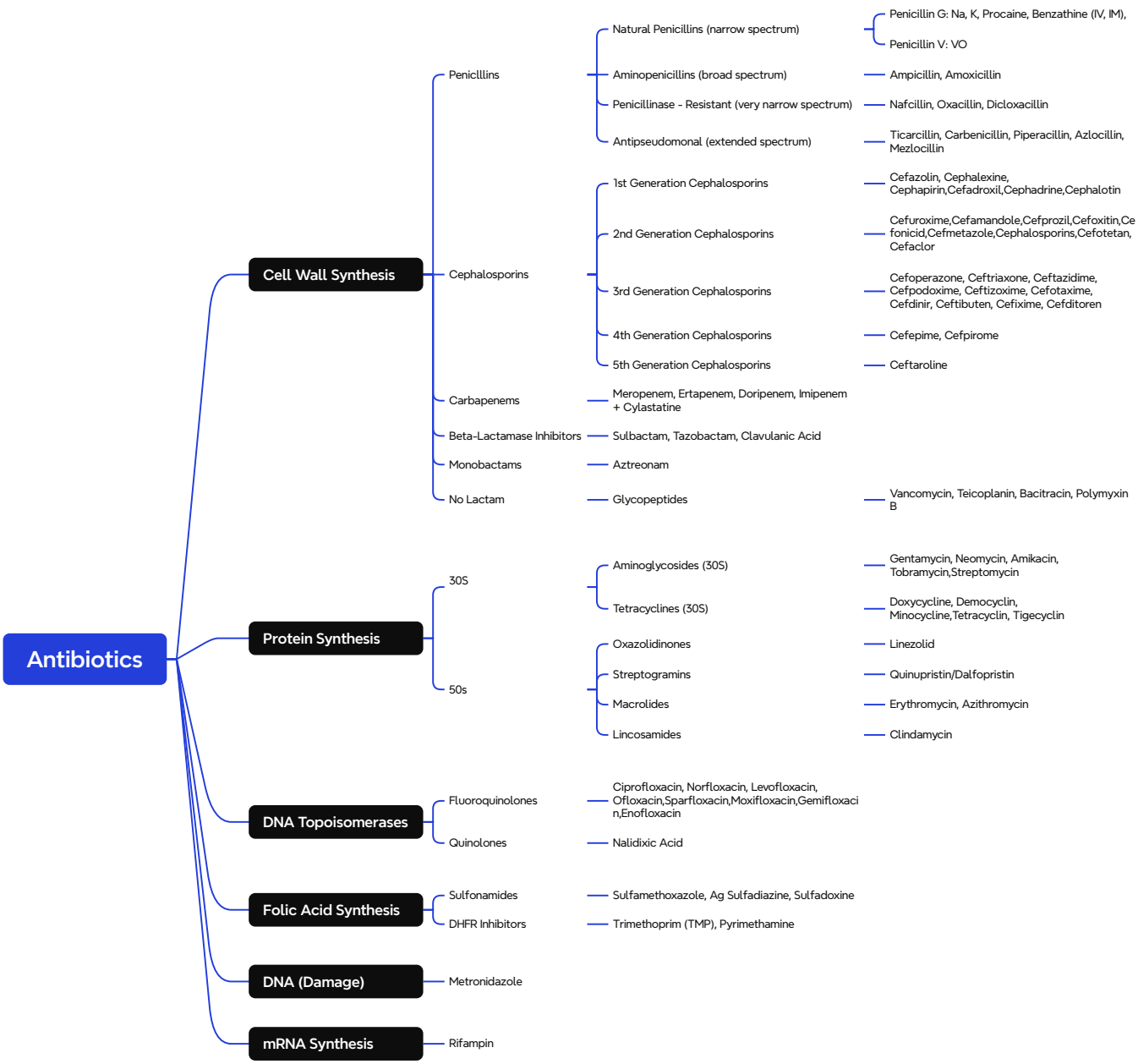

Figure 1.1. Antibiotic class diagram and its mechanism target. This image was created in Xmind.

Antibiotic research and development (R&D) progressed rapidly during the mid-twentieth century, and about half of the antibiotics commonly used nowadays were discovered or synthesised at that time. (Davies, 2006). Since the 1980s, progress in antibiotic R&D has slowed. In recent decades, fewer new antibiotics have been developed or marketed, while bacteria continue to develop resistance to antibiotics due to their overuse (Gargate, Laws and

Rahman, 2025). Limited funding for antimicrobial research hindered the development of antibiotics. However, even with substantial financial investment and scientific effort, only a few antibiotic candidates successfully pass clinical trials, and the average time required for development is approximately 10 to 15 years (Berdigaliyev and Aljofan, 2020). Moreover, many newly introduced antibiotics still belong to the same mechanistic classes as those developed between the late 1960s and early 1980s (C Lee Ventola, 2015). Because these agents share a similar mechanism of action, bacteria can develop cross-resistance more readily and rapidly, limiting the long-term effectiveness of newer drugs, including β-lactam antibiotics such as cephalosporins and penicillins (Belay *et al.*, 2024). Together, these factors illustrate that bacterial infection management has emerged as a major global health challenge and is explored in detail in the following section

1.2 Antimicrobial Resistance (AMR)

Antibiotics are one of the most important medicines in human history. During the Second World War, penicillin production increased significantly due to advances in production techniques. It saved millions of lives at the time and became an essential tool in our ability to treat infections. In 1942, scientists discovered that *Staphylococcus aureus* (*S. aureus*) had developed penicillin resistance, and by the late 1960s, 80% of *S. aureus* strains had become resistant (Lowy, 2003). In the 1960s, new synthetic antibiotics such as vancomycin and methicillin were developed, and it was believed that continued discovery of new antibiotics would address the AMR crisis (Mancuso *et al.*, 2021). Researchers soon realised that it is impossible to develop a large number of novel drugs to fight AMR within a short period of time.

AMR has become a critical global health challenge, threatening the effectiveness of existing antimicrobial therapies. It results in 23,000 deaths in the USA and 25,000 deaths in Europe annually (Auta *et al.*, 2019). In 2019, an estimated 4.95 million deaths were associated with bacterial AMR, and approximately 1.27 million were directly attributable to AMR globally (Murray *et al.*, 2022). Epidemiological analyses estimate that, without further action, there will be 10 million people killed annually by AMR after 2050, which would be greater than the deaths from cancer and diabetes combined (O'Neill, 2016). These data underscore the urgency of understanding both the scale of AMR and the factors driving its rapid escalation.

The slowdown in antibiotic development reflects both scientific and economic barriers. The discovery of new antimicrobial classes is technically challenging, while the clinical development pipeline is lengthy, costly, and associated with high failure rates. Between 2017 and 2024, only 13 new antibacterial drugs were approved, and only 2 of these antibiotics represented a new chemical class. This highlights the limited novelty of the recent pipeline (WHO, 2024b). This lack of innovation is further reflected in the development landscape: the number of antibiotic candidates in development against World Health Organisation (WHO) - priority pathogens decreased from 31 in 2017 to 27 in 2021 (WHO, 2021; WHO Antibacterial Pipeline Team, 2022). Another factor that slows antibiotic R&D is that the three phases of clinical trials are costly and time-consuming, with low success rates, making antibiotic development economically unattractive. The average time from preclinical to clinical development for potential antibiotic candidates is about 10-15 years. Only 1 out of 15 existing classes of novel antibiotics could survive from the preclinical to the clinical stage, and 1 out of 30 new classes of novel antibiotics could pass clinical trials (WHO Antibacterial Pipeline Team, 2022). As a result of these high costs and low success rates, 15 out of the 18 largest pharmaceutical companies have not invested in antibiotic research in the last 30 years (Dutescu and Hillier, 2021). Additionally, there are also financial constraints in adapting to research and

development. From 2010 to 2014, the U.S. National Institutes of Health invested $1.7 billion in AMR research, which was 15 times less than cancer research and 2 times less than diabetes research (O' Neil, 2014). These constraints highlight the urgent need for alternative strategies that complement or extend beyond traditional bactericidal approaches.

Apart from limitations in drug development, the overuse and inappropriate prescription of antibiotics is one of the most significant causes of AMR. According to the WHO's report, about 67% of antibiotics are available over the counter (OTC), and 50% of antibiotic prescriptions are inappropriate (WHO, 2014). For example, in some countries and regions, such as India, patients can purchase antibiotics without a prescription in pharmacies (Kotwani, Joshi and Lamkang, 2021). China is the biggest consumer of antibiotics. The antibiotic use per capita in China is about 10 times higher than in the United States (US). In a study, 79.1% of online pharmacies and 86.8% of community pharmacies sold antibiotics without a proper prescription (Gong *et al.*, 2020). Antibiotic overuse has also been reported in the US. In 2010, the average antibiotic consumption per person in the United States was 22 doses based on the number of antibiotics sold in pharmacies and hospitals (C. Lee Ventola, 2015). In Vaughn *et al.* study (2021), 21,825 patients with pneumonia or UTI in 46 US hospitals were studied, and about half of the patients (49.1%) used antibiotics more than they needed after discharge.

Antibiotic misuse occurs not only in human medicine but also extensively in the agricultural and livestock sectors. In the US, 80% of antibiotics are used in animal agriculture to promote animal growth and prevent infection (C. Lee Ventola, 2015). Drug-resistant bacteria could be transmitted to humans by contact with animals and undercooked or uncooked meat surfaces and could result in adverse health events (C. Lee Ventola, 2015; Martin, Thottathil and Newman, 2015).

Six major pathogens are linked with AMR. They are *Enterococcus faecium*, *S. aureus*, *Klebsiella pneumoniae*, *Acinetobacter baumannii*, *Pseudomonas aeruginosa (P. aeruginosa*) and other members of the *Enterobacterales* group, called the "ESKAPE" (Rice, 2008; Miller and Arias, 2024). These bacteria are highly virulent and commonly cause nosocomial infections, which could lead to high mortality and prolonged hospitalisation for patients. Among the pathogens contributing to the majority of AMR-associated morbidity and mortality, *Acinetobacter baumannii* (*A. baumannii*) has emerged as a critical threat, particularly in healthcare-associated infections. It has the ability to survive in hostile environments and adapt rapidly to antimicrobial and host-imposed stresses by evolving resistant factors (Lin and Lan, 2014).

In response to these scientific, economic and societal challenges, the G20 has decided to promote global cooperation on AMR research to develop the most effective strategies and stimulate R&D of antimicrobial molecules. The WHO also adopt the Global Action Plan on Antimicrobial Resistance which consist of improve awareness and understanding of AMR; to strengthen knowledge and the amount of data; to improve hygiene in medical setting and public awareness; to optimise the use of antimicrobial drug both in human and animal; to increase investment in R&D such as new drug, vaccines, diagnostic tools and other interventions (Terreni, Taccani and Pregnolato, 2021). This initiative reflects growing recognition that AMR poses a substantial and imminent threat to global health.

1.3 Mechanism of Antimicrobial Resistance

AMR is a major reason for the increasing morbidity and mortality in infection patients globally. The success of AMR pathogens is primarily attributable to four mechanisms of antimicrobial

resistance: limiting drug uptake, inactivating the antibiotic, effluxing the antibiotic, and altering the drug target. Gram-negative pathogens use all four mechanisms, whereas gram-positive pathogens use them less commonly, limiting drug uptake and efflux due to the lack of LPS (Lipopolysaccharide) in the outer membrane and drug efflux mechanisms (Reygaert, 2018).

These resistance mechanisms can arise through either intrinsic or acquired processes. Intrinsic resistance is an inherent structural or physiological feature of a bacterial species, such as low membrane permeability or the ability to pump the drug out via chromosomally encoded efflux pumps (Kostyanev and Can, 2017). In contrast, acquired resistance results from genetic changes, including mutation or horizontal gene transfer, that confer new resistance traits such as drug-inactivating enzymes or altered drug targets (Reygaert, 2018).

Bacteria have diverse strategies to become resistant to antibiotics, as mentioned above. These include the expression of antibiotic-inactivating enzymes, such as β-lactamases that degrade β-lactam antibiotics, the upregulation of efflux pumps that actively expel antimicrobial agents from the cell, and structural modifications that reduce antibiotic binding or entry. Additionally, bacteria can modify their drug targets or alter cell-surface structures, such as porins or Lipid A, to reduce the effectiveness of antibiotics (Figure 1.2) (McCarthy *et al.*, 2021).

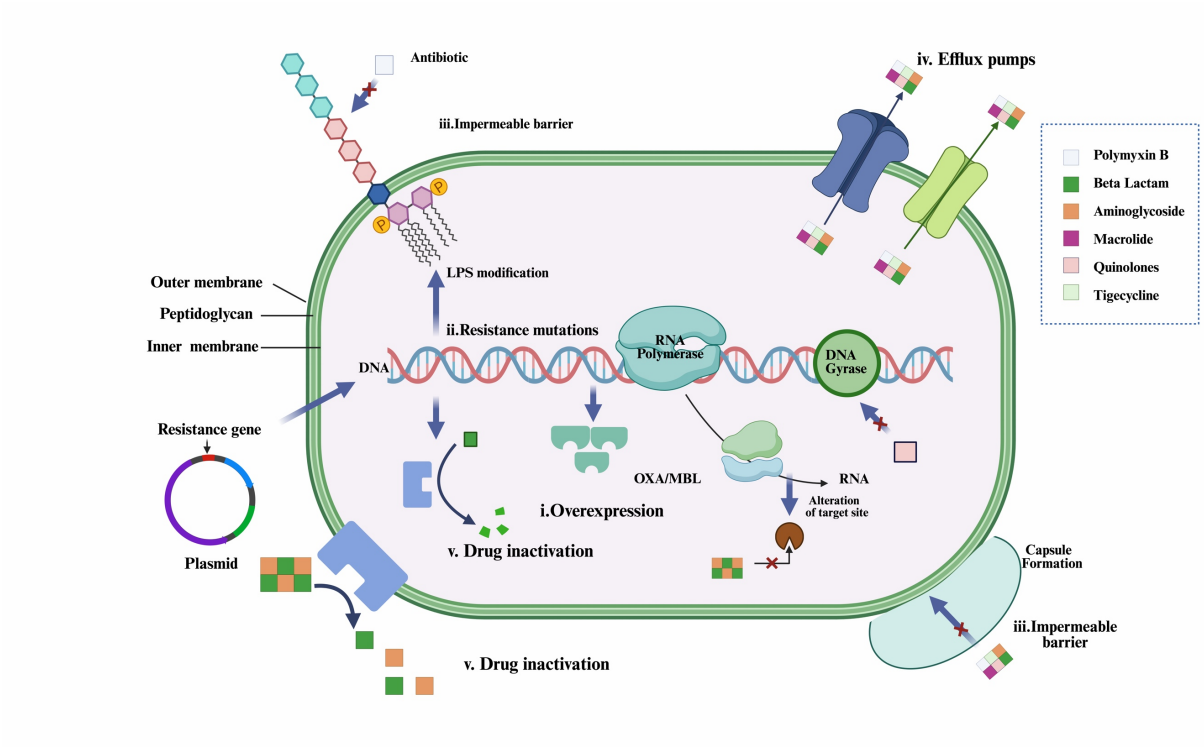

Figure 1.2 Antimicrobial resistance mechanisms diagram. Including (i) overexpression, (ii) resistance mutations, (iii)Impermeable barrier, (iv) efflux pumps, (v) Drug inactivation, Created with https://BioRender.com

1.3.1 Limiting the Uptake of a Drug

The ability of antibiotics to reach their intracellular targets is strongly influenced by bacterial cell envelope structure, and different bacterial species display markedly different capacities for drug uptake. For example, *Mycoplasma* and related species are intrinsically resistant to antibiotics that target the cell wall, such as β-lactams and glycopeptides, because they lack cell walls (Gautier-Bouchardon, 2018). In the last two decades, *S. aureus* has developed intermediate or complete resistance to vancomycin. This is due to their cell wall becoming thicker, making it more difficult for the drug to enter the cell (Cong, Yang and Rao, 2019). For bacteria with large outer membranes, drugs enter the cell through the porin channel. Bacteria can use porin channels to regulate drug entry, such as reducing the number of porin channels or mutating them to change their selectivity and improve the resistance (Reygaert, 2018).

Biofilm formation further restricts antibiotic uptake by creating a protective layer that protects bacterial cells from antimicrobial agents and host immune responses. The thick biofilm matrix is composed of polysaccharides and proteins. It creates a physical barrier that shields bacteria from harm (Flemming *et al.*, 2023; Almatroudi, 2025).

1.3.2 Inactivation of the Antibiotic and Modifying Drug Targets

Bacteria can achieve drug resistance by inactivating drugs or by modifying drug targets to which antibiotics bind. Antibiotic inactivation occurs primarily through two mechanisms: the degradation of the drug and the modification of the drug by transferring the functional group. For example, drugs such as tetracycline can be inactivated by the Tet(X) enzyme via monohydroxlation (Forsberg *et al.*, 2015). For example, tigecycline is a third-generation tetracycline and it is able to be inactivated by Tet(X) enzyme and produce inactive 11a-Hydroxytigecycline (Figure 1.3) (Beech *et al.*, 2025).

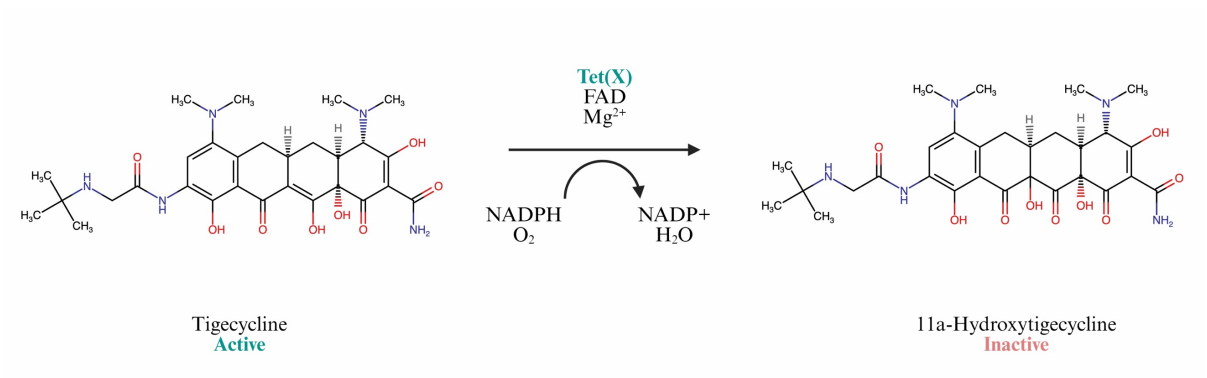

Figure 1.3 The process of inactivation of tigecycline by Tetracycline destructases Tet(X4)

A well-characterised mechanism of drug inactivation involves the hydrolysis of the β-lactam ring in β-lactam antibiotics by β-lactamases. This reaction disrupts the β-lactam structure that is essential for antimicrobial activity, thereby inactivating the drug (Bush and Bradford, 2016).

In addition, Gram-positive bacteria may modify the number, structure, or affinity of penicillin-binding proteins (PBPs). PBPs are transpeptidase enzymes that catalyse the cross-linking of peptidoglycan strands during the final step of bacterial cell wall biosynthesis (Lee *et al.*, 2001). Increasing the number of PBPs decreases drug binding, and altering their structure can also reduce binding, thereby diminishing the effectiveness of β-lactam antibiotics (Reygaert, 2018). For example, methicillin-resistant *Staphylococcus aureus* (MRSA) acquired the *mecA* gene, which encodes a PBP, called PBP2a. This PBP2a has a very low affinity for β-lactam antibiotics, allowing it to maintain new cell wall peptidoglycan synthesis in the presence of these drugs. This change makes MRSA insensitive to methicillin and all β-lactams that have been developed (Figure 1.4) (Foster, 2004). MRSA can also become resistant by picking up the *van* gene. This gene alters the structure of peptidoglycan precursors, making it much harder for drugs like vancomycin to bind to them (Reygaert, 2018).

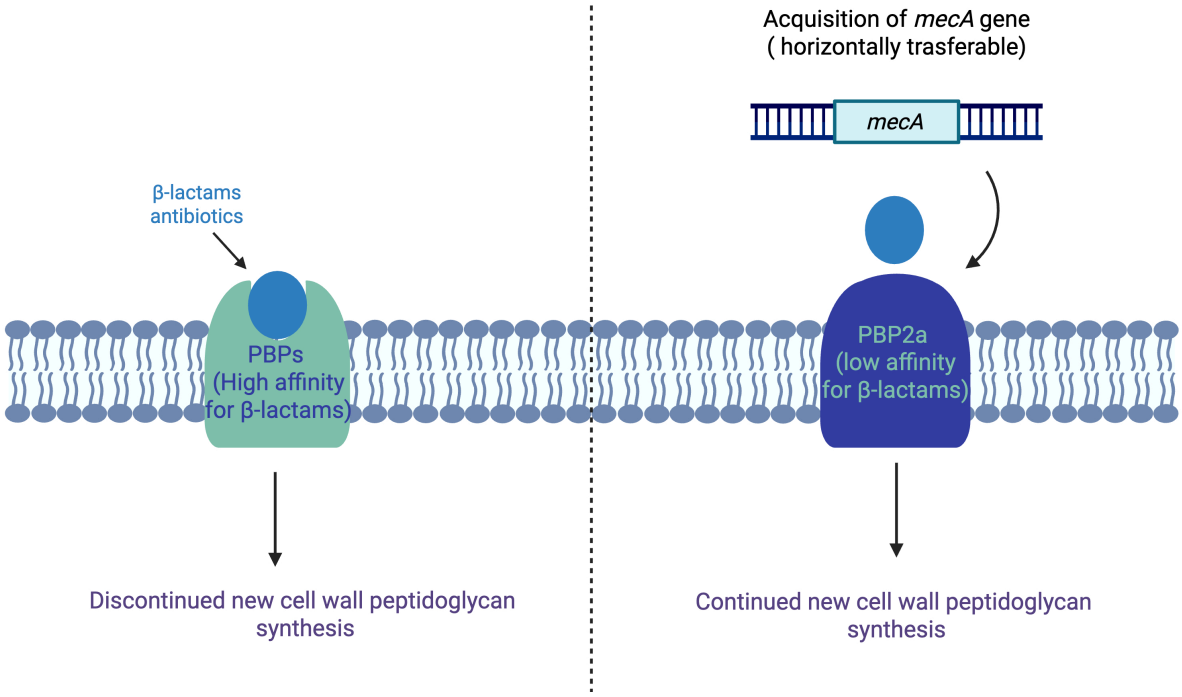

Figure 1.4 Mutation of penicillin-binding proteins as a mechanism of β-lactam resistance in MRSA. This figure was created by biorender https://BioRender.com.

Gram-negative pathogens, such as *A. baumannii,* that are resistant to carbapenems are also due to the drugs' inactivating ability. A highly transferable location gene encoding a Class D, OXA-type enzyme was discovered and shown to hydrolyse carbapenems, along with class B metallo-beta-lactamases (Brown and Amyes, 2006; Singh, Thangaraj and Chakrabarti, 2013). Inactivation of antibiotics also contributes to acquisition of genes.

1.3.3 Efflux Pump of the Antibiotic

Active efflux systems enable bacteria to pump out antimicrobial agents from the cell, thereby reducing intracellular drug concentrations below therapeutic levels. Efflux pump genes could be overexpressed and pump out toxic chemicals from bacterial cell. Most of the efflux pumps are multidrug transporters that have the ability to pump out different antibiotics (Kapoor, Saigal and Elongavan, 2017). These genes that are associated with multidrug efflux pump in multidrug resistant strains are often overexpressed (Nishino *et al.*, 2021).

There are six main efflux pump families: the ATP-binding cassette (ABC) family, the multidrug and toxic compound extrusion (MATE) family, the small multidrug resistance (SMR) family, the major facilitator superfamily (MFS), proteobacterial antimicrobial compound efflux (PACE) and the resistance-nodulation-cell division (RND) family (Nishino et al., 2021). The ABC transporter family is able to use the free energy that released from ATP hydrolysis to pump substrates across the lipid membrane into or out of the cell. The MATE family can expel cation drugs by H+ or Na+ exchange (Omote et al., 2006). The SMR family consist of small proteins (100-150 amino acid) with four transmembrane α-helical domains. They transfer the substrate by using proton gradient as energy recourse (Slipski *et al.*, 2019). The major MFS

family is one of the largest families of secondary active transporter. It has two mechanisms for transporting substrate: it use ion gradients during secondary active transport, and substrate gradients during uniport (Lekshmi *et al.*, 2024). The PACE family is primarily found in Gram-negative pathogens, and it can export biocides that are used as disinfectants and antiseptics by using the electrochemical gradient (proton-motive force) as an energy source (Hassan *et al.*, 2019). The RND efflux complexes consist of outer membrane protein, inner membrane protein and periplasmic adapter protein (PAP). The PAP is able to connect the outer membrane protein and the inner membrane protein together and form a duct that allowing compounds transport (Daury *et al.*, 2016)

1.4 *Acinetobacter baumannii*

A. baumannii is a Gram-negative, aerobic, non-motile, and opportunistic pathogen that has emerged as a major cause of healthcare-associated infections worldwide. In 1911, A Dutch scientist named Beijerinck discovered *A. baumannii* in a calcium acetate-rich soil environment. It was originally named *Micrococcus calco-aceticus* (Beijerinck, 1911). The name changed to *A. baumannii* because Bauman's 1969 study led to the formal recognition of the genus *Acinetobacte*r by an international committee in 1971 (Lessel, 1971). Before the 2000s, *A. baumannii* was considered a relatively manageable pathogen. Infection caused by *A. baumannii* could be treated more easily with frontline antibiotics. However, this situation changed during the Iraq and Afghanistan conflicts in the 2000s. There were increasing infections, and the isolated strain showed multidrug resistance (MDR) (McCarthy *et al.*, 2021). The outbreak of *A. baumannii* associated with the Iraq and Afghanistan conflict has several reasons. The first is due to Iraq's poor healthcare system. The trained staff were limited, which led to ineffective infection control and prevention (Abou Fayad *et al.*, 2023). Moreover, the diagnoses and drug

prescriptions were also inappropriate. The second reason is environmental pressure, such as exposure to heavy metals. When bacteria are exposed to excessive concentrations of Pb, Cd, Cu, As, Ag, and Zn, the cell wall can be damaged, which can lead to DNA damage and destabilised membrane integrity. It can also restrict essential ions from reaching their target sites by displacing unwanted heavy metals. There are six proposed mechanisms of heavy metal resistance: (1) Metal ions are released through extracellular barriers such as the capsule, cell wall and cell membrane. (2) Removal of intracellular metal ions through efflux systems or diffusion. (3) Intracellular sequestration of metal ions. (4) Extracellular sequestration of metal ions. (5) Enzymatic transformation or detoxification of toxic metal species. (6) Modification of cellular targets to reduce their susceptibility to metal ions (Bazzi *et al.*, 2020).

High exposure to heavy metals on the battlefield is a potential driver for AMR through co-selection (Abou Fayad *et al.*, 2023). There are three main co-selection mechanisms: co-resistance, cross-resistance, and co-regulation. When heavy metal resistance genes and antibiotic resistance genes (ARGs) are genetically linked on the same genetic element, co-resistance arises. Therefore, exposure to heavy metals can act as a co-selective factor for antibiotic resistance (AMR) even in the absence of antibiotics. Cross-resistance and co-regulation may also play a role, for example through shared efflux pumps or regulatory systems that confer resistance to both heavy metals and antibiotics (Baker-Austin *et al.*, 2006).

In the past two decades, *A. baumannii* has become an important cause of hospital-acquired infections, particularly in intensive care units (ICU). *A. baumannii* has become an MDR pathogen that is resistant to antibiotics, such as colistin, tigecycline, and carbapenems, via different resistance mechanisms, such as drug modifications, efflux pumps, and drug inactivation (Figure 1.5) (Oyejobi *et al.*, 2022; Whiteway *et al.*, 2022). Surveillance studies have reported rising isolation rates among Gram-negative pathogens. For example, a global

Tigecycline Evaluation and Surveillance Trial (TEST) was conducted, and the results showed that *A. baumannii* was the most MDR Gram-negative bacterium isolated globally from 2004 to 2014. The percentage increased from 23% in 2004 to 60% in 2014. In Europe, 2%-10% of infections in ICU were caused by *A. baumannii*, 2% in the United States and 20% globally (Hanberger *et al.*, 1999; Jones *et al.*, 2004; Oyejobi *et al.*, 2022).

Clinically isolated *A. baumannii* can form biofilms on abiotic surfaces more quickly than non-clinical strains. This faster biofilm development may facilitate quicker patient-to-patient transmission and potentially trigger outbreaks in healthcare environments. In the hospital, many surfaces are ideal for *A. baumannii* biofilm formation, including ventilators, polystyrene, polypropylene, polytetrafluoroethylene medical device tubes, and glass. This is the reason why *A. baumannii* infection has become a significant issue in hospitals and ICUs (Roy *et al.*, 2022). In 2016, *A. baumannii* was listed by the WHO as a critical priority pathogen for research and development of new antibiotics due to its resistance to carbapenems (Olivia, 2017). It remains in the list of 2024 WHO Bacterial Priority Pathogens List (WHO, 2024). It is because carbapenems are the last line of defence in treating *A. baumannii* infections.

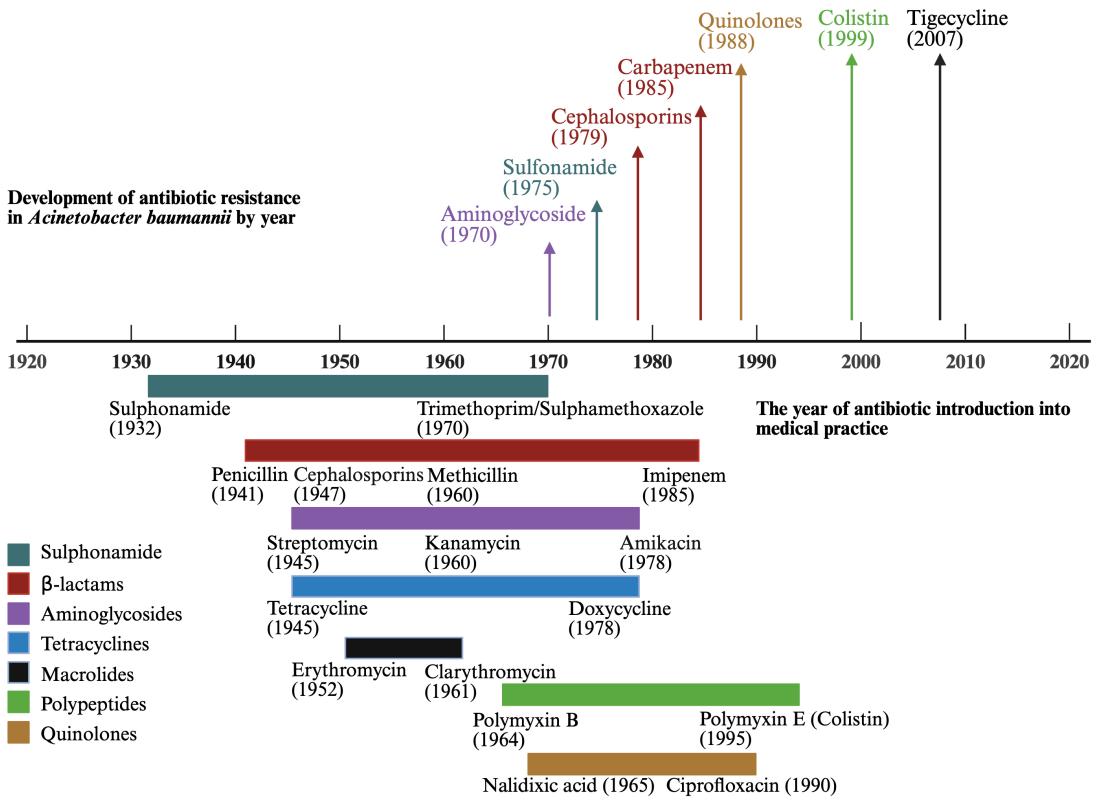

Figure 1.5 Timeline of resistance of *A. baumannii* to antibiotics. The top part demonstrates the year antimicrobial resistance was reported, and the lower part demonstrates the year antibiotics were introduced in the market. Created with https://BioRender.com

1.4.1 Prevalence and Types of Infection

A. baumannii is associated with a wide range of infections, including ventilator-associated pneumonia (VAP), urinary tract infection, meningitis, blood infection, endocarditis, burn infection, skin and other soft tissue infections (Gedefie, Demsis, *et al.*, 2021; Law and Tan, 2022). *A. baumannii* is highly associated with hospital-acquired infections. The patients in the ICU are susceptible to infection by this pathogen. Infections caused by *A. baumannii*, particularly pneumonia and bloodstream infections, are associated with high mortality rates. In the ICU setting, *A. baumannii* could spread through the ventilator and an open wound, prolonging hospitalisation and leading to death. For example, *A. baumannii* VAP infection, along with coronavirus disease 2019 (COVID-19), is associated with poor clinical outcomes.

In a single-centre cross-sectional investigation, 32 patients had co-infection with *A. baumannii* and COVID-19, and 115 had *A. baumannii* infection with other aetiologies. The survival rate was 18.8% in patients with *A. baumannii* co-infection and COVID-19 and 32.2% in patients with other aetiologies (Russo *et al.*, 2022). Another ICU report found 6.2% of ICU patients had *A. baumannii* respiratory infections. Within this 6.2% of patients, 93% of them developed ventilator-associated pneumonia. Moreover, 62% of these *A. baumannii* isolates were MDR, 35% were extensively Drug-Resistant (XDR), and 3% were pan-drug-resistant (PDR) (Hafiz *et al.*, 2023)

Bloodstream infection (BSI) caused by MDR Gram-negative bacteria are associated with high mortality and increased hospital cost (Zhen *et al.*, 2020; Yu *et al.*, 2021). *A. baumannii* was isolated from 8.2% of blood culture samples between January 2017 and December 2020 in Oman (Balkhair, Saadi and Adawi, 2023). Mortality associated with *A. baumannii* BSI is high, 61.2% of patients died within 14 days, and 70.6% died within 30 days (Russo *et al.*, 2019). Importantly, carbapenem is a first-line antibiotic used to treat *A. baumannii* and carbapenem resistance further increases risk (Maragakis and Perl, 2008). In the Chopra and their colleagues study (2013), 25% of BSI patients were associated with carbapenem-resistant *A. baumannii.* The mortality was 23% higher in patients involved in carbapenem-resistant *A. baumannii* when compared with non-carbapenem-resistant *A. baumannii* BSI patients.

As *A. baumannii* pneumonia and BSI, wound infections by *A. baumannii* have also become significant issues in healthcare settings (Irma D Fleming *et al.*, 2017). *A. baumannii* is more likely to infect patients with open wounds, as they lack skin and mucosal barriers. Furthermore, the medical device surface is suitable for the growth and biofilm formation of *A. baumannii*, which also helps them spread to patients with open wounds (Roy *et al.*, 2022). In Keen *et al.* a study (2010), 22% of burn injury infections were caused by *A. baumannii,* the most frequently

isolated strain. 53% of isolated *A. baumannii* strains tested MDR, a higher percentage than for other isolated strains, such as *P. aeruginosa* (15%) and *K. pneumoniae* (17%). This study evaluated burn severity and the percentage of infections caused by MDR isolates. This study also analysed burn size and the risk of infection with MDR isolates. The percentage of patients with a total body surface area (TBSA) of less than 30 who had MDR bacteria was 23%, compared with 33% for patients with a TBSA of 30–60% and 39% for patients with a TBSA greater than 60%. Another study showed that 73.6% of clinically isolated *A. baumannii* were resistant to quinolones, 71.3% to sulphonamides and 50-70% to cephalosporins and carbapenems (Chen *et al.*, 2017). Research on antibiotics and other antimicrobial agents is essential and urgent due to the robust transmission of *A. baumannii* and the emergence of resistance to existing antibiotics.

1.4.2 The Virulence Factors of *A. baumannii*

A virulence factor is a bacterial gene product or trait that enables bacteria to colonise the host, evade or suppress immune responses, acquire nutrients, and sense and adapt to their environment. These factors would help them establish and track infection progression (Mrsny, 2009; Castrejón-Jiménez *et al.*, 2022). Several virulence factors contribute to the pathogenesis of *A. baumannii.* They include outer membrane proteins (OMPs), the iron uptake systems, quorum sensing (QS), biofilm formation and motility (Harding, Hennon and Feldman, 2018; Law and Tan, 2022).

1.4.2.1 Outer Membrane Proteins

OMPs play a central role in the virulence and persistence of *A. baumannii*. It mediates interactions with host tissues, maintains cell envelope integrity, and contributes to responses to environmental and antimicrobial stress. Among these proteins, outer membrane protein A

(OmpA) is one of the most extensively characterised virulence-associated factors and has been implicated in both host cell damage and immune modulation (Scribano *et al.*, 2024). Moreover, OmpA is the most promising vaccine candidate for *A. baumannii* (Zanoos *et al.*, 2025). In *A. baumannii*, OmpA is the most abundant outer membrane porin, featuring an N-terminal eight-stranded β-barrel with four loops exposed outside, and a C-terminal domain in the periplasm that binds peptidoglycan, aiding cell-envelope stability (Iyer *et al.*, 2018). OmpA functions as a small-molecule channel and is involved in resistance to antibiotics and serum, biofilm formation, and host interaction (Gaddy, Tomaras and Actis, 2009; Iyer *et al.*, 2018; Scribano *et al.*, 2024).

Early studies showed that *A. baumannii* can trigger apoptosis in epithelial cells through OmpA. OmpA, a key component of outer membrane vesicles, promotes bacterial adhesion and gets into the epithelial cells and reaches the nucleus. Once inside, it activates host apoptotic pathways, involving the release of cytochrome c and apoptosis-inducing factor (AIF). AIF then facilitates chromosomal DNA breakdown. It will lead to cell death (Choi *et al.*, 2005). Meanwhile, structural changes to the outer membrane further help the bacteria evade host defences. The production of hepta-acylated lipid A increases resistance to cationic antimicrobial peptides (CAMPs) and enhances survival under dry conditions, supporting persistence on surfaces and in clinical settings (Boll *et al.*, 2015).

Recent studies demonstrate that OmpA-like proteins have roles beyond virulence at the gene level. It emphasises their functional diversity and unique contributions (Scribano *et al.*, 2024). In this study, AB5075 was used since it is a clinically significant strain. Scribano *et al.* (2024) created insertion mutants targeting multiple OmpA-like porins and compared them to the wild type. Their findings revealed that each OmpA-like porin plays a role in envelope integrity, stress resistance, and virulence-related features, and that disrupting specific porins can

influence antibiotic susceptibility. Overall, this research provides a gene-level functional map, demonstrating that OmpA-like porins are specialised components of the outer membrane that uniquely affect pathogenicity and drug response.

These results demonstrate that Omps are significant factors influencing the virulence and persistence of *A. baumannii*. OmpA and similar porins serve as both structural elements of the cell envelope and active regulators of host cell fate, immunological responses, and antibiotic susceptibility. Because it performs so many functions, the outer membrane is an important link between pathogenicity, environmental adaptation, and therapeutic failure.

1.4.2.2 Iron Acquisition System

The acquisition of iron is essential for the survival and proliferation of *A. baumannii* in host environments. It is important for DNA repair, replication, gene expression, and metabolic processes, such as enzymatic activation (Cook-Libin *et al.*, 2022). There are several ways *A. baumannii* acquires and utilises iron in the host environment. For example, *A. baumannii* can use haemolytic proteins to access iron within erythrocytes (Fiester *et al.*, 2016). Under iron-limited conditions, *A. baumannii* could obtain iron by lysis of erythrocytes by upregulating the phospholipase C genes (*plc1* and *plc2*) (Fiester *et al.*, 2016). After lysing the cell, *A. baumannii* imports iron by using heme uptake systems. The secreted hemophore HphA (heme scavenger) binds haemoglobin and free heme and delivers these iron sources to the outer membrane receptor HphR for cellular uptake (Bateman *et al.*, 2021).

Another way in which *A. baumannii* acquires and utilises iron in the host environment is through siderophore systems. *A. baumannii* produces siderophore, which is an iron chelator to obtain iron (Sheldon and Skaar, 2020). There are three classes of siderophores in *A. baumannii*:

acinetobactin, fimsbactins and baumannoferrins. The gene clusters for these siderophores are upregulated in iron-limited conditions (Sheldon and Skaar, 2020). Moreover, Sheldon and Skaar (2020) addressed that acinetobactin is essential for the *A. baumannii* growth when it acquires iron from the host. When there is less acinetobactin produced, *A. baumannii* survival rate will reduce in a mouse model.

Kim *et al.*, (2021) further refined this pathway-level understanding by dissecting the chemistry and uptake dynamics of acinetobactin isomers oxazoline (Oxa) and isoxazolidinone (Isox). Their findings indicate that the Oxa isomer mediates more efficient iron delivery due to preferential recognition by BauA (the cognate outer membrane receptor) and the formation of iron complexes with enhanced stability, reducing competitive diversion under restrictive conditions. In contrast, the Isox isomer contributes to iron capture by expanding the capacity for acquisition under severely limited iron availability. Together, these results support a model in which acinetobactin-mediated virulence depends not only on siderophore biosynthesis but also on isomer-specific transport and stability properties (Kim *et al.,* 2021).

1.4.2.3 Quorum Sensing

QS is a mechanism by which bacteria use signalling molecules called N-acyl-L-homoserine lactones (AHL) to communicate with one another to regulate physiological functions and pathogenesis (Cui *et al.*, 2025). *A. baumannii* QS genes consist of *abaR/abaI,* which were acquired from *Halothiobacillus neapolitanus* (Bhargava, Sharma and Capalash, 2010). The *abaI* encodes 183 amino acids and *abaR* gene encodes 238 amino acids. The AbaI proteins have a function in signal transduction, such as producing AHL molecules, while the AbaR protein is an autoinducer receptor (Figure 1.6B). (Sun *et al.*, 2021). The QS could facilitate biofilm formation and twitching motility (Clemmer, Bonomo and Rather, 2011; Bhargava *et*

al., 2015). Therefore, the QS system becomes a potential target for new drug development (Saipriya *et al.*, 2020)

López-Martín *et al.*, (2021) examined the influence of *abaM,* which is a third gene located between *abaR* and *abal*, by using an *abaM* mutant via a T26 insertion (Figure 1.6A). They found that surface-associated motility and biofilm formation were promoted *in vitro*, and the *abaM::T26* mutant showed reduced virulence compared with WTAB5075 and *abal::T26* Mutant in the *Galleria mellonella* model (Figure 1.6C). To connect phenotypes to molecular programs, they performed transcriptomic analysis to identify regulated genes, including modules associated with adhesion and biofilm formation, such as the *csu* pilus operon. The contribution is a regulatory explanation for why stronger quorum-sensing output does not necessarily translate into stronger pathogenicity, and it identifies *abaM* as a tunable node that reshapes group behaviours.

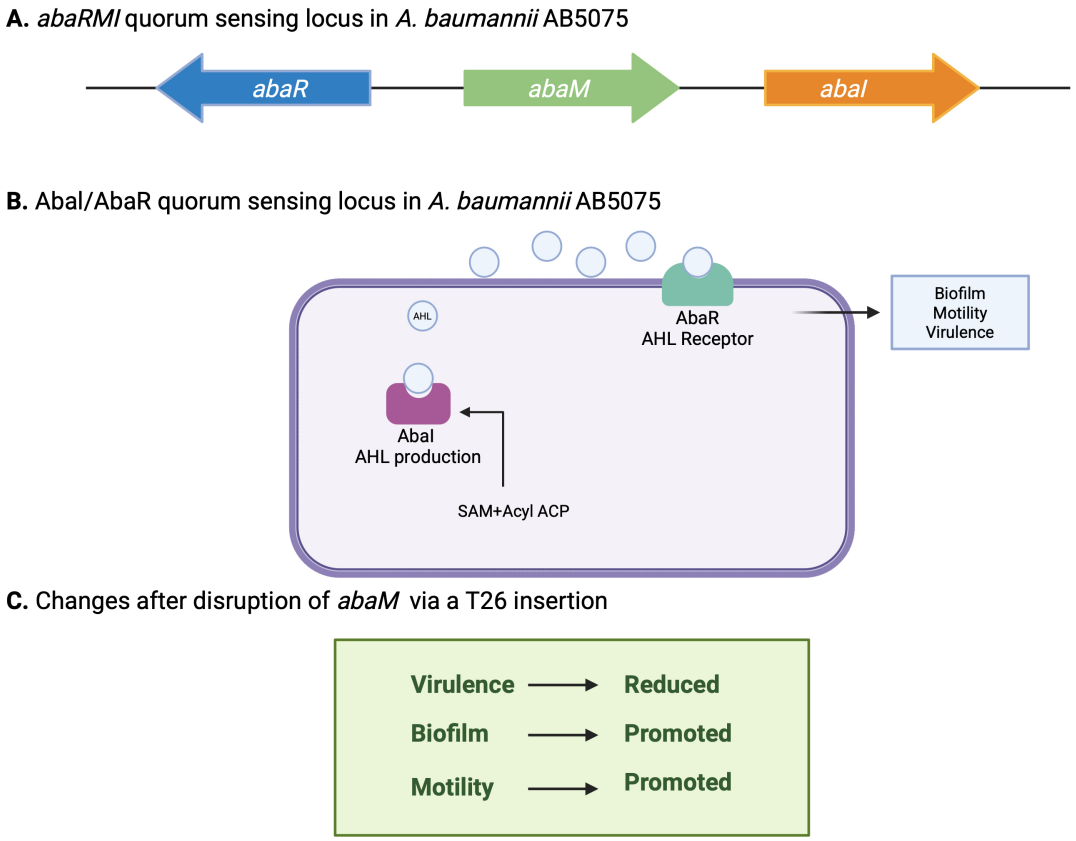

Figure 1.6 *abaRMI* Quorum Sensing system in *A. baumannii* AB5075. (A) abaRMI QS locus in *A. baumannii* AB5075 : three QS genes and their orientations. (B) the AbaI/AbaR quorum-sensing system(C) Phenotypic effects following disruption of *abaM* by T26 insertion. This figure was created by biorender https://BioRender.com.

1.4.2.4 Biofilm

Biofilm formation is a strategy that enables *A. baumannii* survival under hostile environmental conditions and contributes to chronic infection and treatment failure. *A. baumannii* has a higher biofilm formation rate compared with other species. Biofilms consist of bacterial communities, proteins, DNA and an EPS matrix (Shree *et al.*, 2023). Biofilm formation can support and protect bacteria in various ways. For example, biofilms help bacteria attach to surfaces such as the human body (biotic) and medical devices (Chiang *et al.*, 2018; Makvandi *et al.*, 2022). It could also be industrial equipment (abiotic). Biofilm formation on abiotic surfaces in hospital settings can lead to medical device-related infections and the spread of bacteria in the ICU, which plays a significant role in the development of nosocomial infections. Biofilm formation on biotic surfaces, such as epithelial cells, will result in host infection (Francesca, Claudia and Gianfranco, 2014). Additionally, biofilms provide protection against antimicrobials such as benzalkonium chloride, antibiotics, and ethanol against bacteria, thereby promoting cell-cell communication (quorum sensing) and enabling adaptation to changing environments and contribute to AMR (Flemming *et al.*, 2016).

There are five stages of biofilm formation, which are reversible attachment, irreversible adhesion, small colony formation, maturation, and eventual dispersal of planktonic cells (Figure 1.7) (Ding *et al.*, 2023). Planktonic cells can initially attach to a biotic or abiotic surface. In this stage, bacteria prefer hydrophobic, nonpolar surfaces, such as plastic, over hydrophilic

surfaces, such as stainless steel. Following stable adhesion, an irreversibly monolayer of bacteria will form. The EPS matrix will be produced at this stage, followed by colony formation. Moreover, once cells become irreversibly attached, they begin to organise into a more complex three-dimensional architecture, marking the transition from initial adhesion to biofilm maturation. Dispersal is triggered by nutrient and oxygen starvation. The saccharolytic enzymes will produce the dissolution of EPS, which allows the bacteria to release from biofilm and move onto a new surface and begin a new cycle (Gedefie, Demsis, *et al.*, 2021; G. Liu *et al.*, 2023).

Biofilm formation relies on several factors, including biofilm-associated protein (Bap), OmpA, QS, and efflux pumps. The biofilm-associated protein (Bap) has a high molecular weight of 8,620 amino acids. It is strongly associated with biofilm formation by increasing the adherence of cells, including epithelial cells, human neonatal keratinocytes, and bronchial epithelial cells (Loehfelm, Luke and Campagnari, 2008; De Gregorio *et al.*, 2015). On the other hand, Omps plays a pivotal role in biofilm formation. OmpA contributes to the development of robust biofilms on non-living surfaces (Gaddy, Tomaras and Actis, 2009). The Omp 33-36 kDa protein associates with growth rate, adherence, biofilm formation, and cytotoxicity on the biotic surface (Rumbo *et al.*, 2014).

In biofilm development, it contributes to the coordinated regulation of genes involved in surface attachment, extracellular matrix production, and community maturation. In the early stages of biofilm formation, QS could activate certain genes that subsequently secrete extracellular matrices, including EPS and proteins, and gradually establish a mature, complete biofilm structure. In the maturation stage, QS intercellular communication is also an important factor in control. Within the bacterial community, chemical signal molecules called

autoinducers are produced. The concentration of autoinducers (AIs) increases with the number of bacteria. When AIs increase to a certain threshold range, these AIs will enter bacterial cells and bind with the receptor, leading to multicellular responses in the bacterial population (Papenfort and Bassler, 2016; X. Liu *et al.*, 2023).

Efflux pumps are membrane-bound proteins that can transport antibiotics, detergents, dyes, poisons, and metabolic waste products. *A. baumannii* frequently use efflux pumps to mediate resistance through increased expression or altered substrate specificity of efflux systems. The upregulation of these pumps contributes not only to antibiotic resistance but also to enhanced survival under stress. (Singh, Thangaraj and Chakrabarti, 2013). Increasing evidence suggests that efflux pumps facilitate biofilm formation and maturation via various mechanisms, including the secretion of EPS and quorum-quenching (QQ) molecules that enhance matrix development, along with the indirect modulation of biofilm-associated genes and removal of antibiotics or metabolic intermediates (Rumbo-Feal *et al.*, 2013; Alav, Sutton and Rahman, 2018). AdeABC, AdeFGH, and AdeIJK are three RND efflux pumps associated with biofilm formation. Mutant *A. baumannii* strains lacking AdeABC, AdeFGH, or AdeIJK exhibit reduced biofilm formation compared with the wild-type strain (Yoon *et al.*, 2015).

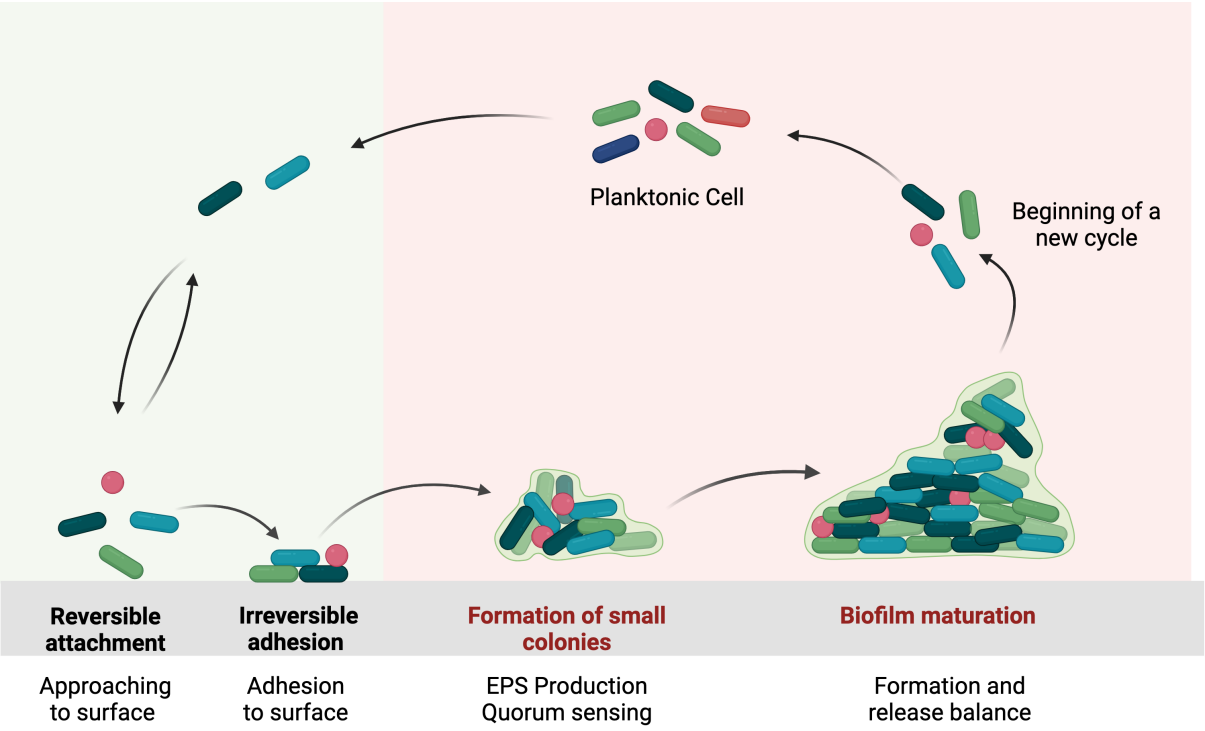

Figure 1.7 Biofilm formation includes five steps: reversible attachment, irreversible adhesion, small colony formation, maturation and cell separation. This figure was created by biorender https://BioRender.com.

Notably, *A. baumannii* demonstrates an exceptional propensity for biofilm formation relative to other *Acinetobacter* species. It prefers to form biofilms at the solid-liquid interface (80-91%), which is about three times higher than other Acinetobacter species (Martí *et al.*, 2011). In addition, *A. baumannii* can form a pellicle at the air-liquid interface, thereby enhancing its surface motility. Pellicle formation has been reported to occur at rates up to four times higher than in other *Acinetobacter* species (Roy *et al.*, 2022).

Biofilm formation complicates the treatment of *A. baumannii* infections. It increases the risk of patient transmission. *A. baumannii* is strongly associated with nosocomial infections in ICU

patients, often leading to outbreaks. Contaminated hospital and medical device surfaces, such as those involved in uterine skin rupture, bladder catheterisation, and contact with hospital staff, are significant factors in its transmission (Delamou *et al.*, 2019; Pompilio *et al.*, 2021). These medical devices would be used to gain access to the body and provide a better opportunity for *A. baumannii* to colonise body tissue. Moreover, biofilm formation is associated with antibiotic resistance. According to Qi and colleagues (2016), *A. baumannii* were isolated in China, and the report shows that *A. baumannii* with lower resistance tend to form more robust biofilms when antibiotics are introduced. High biofilm formation could protect cells and improve survival rates.

1.4.2.5 Type IV pilus

Many bacteria have hair-like structures on their surfaces, known as pili and fimbria. These structures are closely related to bacterial colonisation and infection. Type IV pilus (T4P), composed of oligomeric pilin proteins, forms cylindrical structures approximately 0.3 to 1 μm in length and 7 nm in diameter (Zhou and Li, 2015). These pili are widely distributed among Gram-negative bacteria, including *A. baumannii*, *Myxococcus xanthus, P. aeruginosa*, *Neisseria gonorrhoeae*., where they function as multifunctional virulence-associated structures (Craig, Forest and Maier, 2019; Ronish *et al.*, 2019)

Unlike flagella-driven motility, T4P mediate surface-associated movement known as twitching motility. This twitching motility relies on the repeated extension, surface attachment, and retraction of pili. It will generate a mechanical force that pulls the bacterial cell forward. Pilus extension and retraction are powered by distinct cytoplasmic ATPases, enabling rapid and reversible movement across semi-solid and abiotic surfaces (Mattick, 2002; Burrows, 2005).

In addition to motility, T4P facilitate DNA uptake (retraction-dependent functions) and biofilm formation and host–cell adherence (retraction-independent functions).

In *A. baumannii*, T4P are particularly important because the species lacks flagella and was historically considered non-motile (Baumann, Doudoroff and Stanier, 1968). However, later research found that *A. baumannii* could move relatively rapidly on semisolid and abiotic surfaces. Recent research revealed that *A. baumannii* could move through twitching mobility and surface-related motility (Clemmer, Bonomo and Rather, 2011; Harding *et al.*, 2013). Genome-wide analyses further confirmed the presence of conserved T4P gene clusters. Mutational studies established a direct link between T4P biogenesis and surface motility phenotypes (Harding *et al.*, 2013; Vijayakumar *et al.*, 2016).

Beyond motility, T4P plays a critical role in natural transformation, the ability to acquire horizontally acquired exogenous DNA. There are three steps in natural transformation: DNA uptake, DNA translocation, and ensuing homologous recombination (Ellison and Ellison, 2024). There are several key steps in DNA uptake: the ComEA can pull extracellular DNA into the periplasm by using PilQ to facilitate its passage through the outer membrane (Vesel and Blokesch, 2021). The DNA strand is then degraded; the remaining single-stranded DNA (ssDNA) is transported across the inner membrane via the ComA channel (ComEC in some species), with ComF acting as a transporter gene. Extracellular ssDNA will enter the cytoplasm at this stage. The extracellular ssDNA is stabilised by Ssb and DprA before being integrated into the host genome via RecA-mediated homologous recombination, or, alternatively, through illegitimate recombination or transposition (Figure 1.8) (Wilharm *et al.*, 2013; Hu, Zheng and Zhang, 2022). Moreover, *A. baumannii*'s natural competence has been shown to be surface-dependent, suggesting that T4P-mediated motility and DNA uptake are spatially and

functionally coupled (Harding et al., 2013). This dual role enhances both genetic adaptability and the rapid acquisition of antimicrobial resistance determinants in clinical environments.

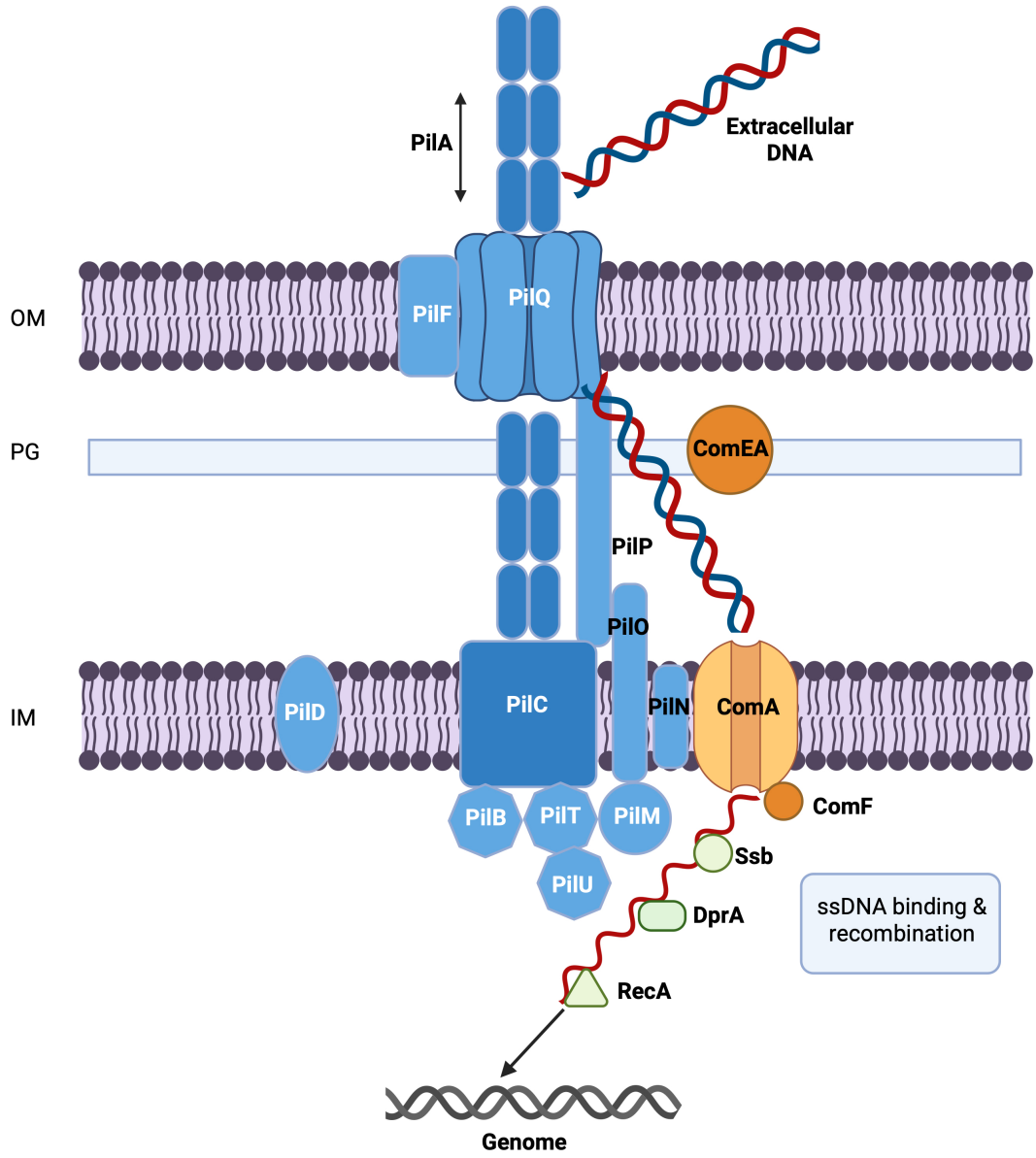

Figure 1.8 Schematic representation of Type IV pilus-mediated natural transformation in *A. baumannii.* This figure was created by biorender https://BioRender.com.

T4P are also closely linked to biofilm development by promoting initial attachment and facilitating microcolony expansion. T4P contribute to the early stages of biofilm formation. Their role in surface exploration and aggregation enhances the development of biofilms and

reinforces persistence on medical devices and host tissues (Harding et al., 2013; Vesel and Blokesch, 2021). However, there is a trade-off between motility and biofilm formation, in which stronger biofilm formation correlates with weaker motility (Ronish *et al.*, 2019).

Based on the characteristics of their primary pilin protein and the arrangement of their pilus genes, T4P can be broken down into type IVa (T4aP) and type IVb (T4bP) subgroups. Moreover, T4P could withstand substantial stresses above 100 pN, demonstrating its excellent biomechanical properties. Type IV pili are beneficial to many bacterial species because of their twitching motility.

1.4.3 *A. baumannii* Resistance Mechanism

The rapid development of antibiotic resistance in *A. baumannii* has made it one of the most problematic pathogens in modern healthcare settings. AMR in *A. baumannii* is driven by several mechanisms. Firstly, *A. baumannii* can inactivate β-lactam antibiotics through the production of β-lactamase enzymes, which hydrolyse the β-lactam ring. These antibiotics include penicillins, cephalosporins, and carbapenems (Smani *et al.*, 2014). Outer membrane proteins also play an important role in *A. baumannii* resistance when they work with β-lactamases. The OmpA is the main non-specific porin in *A. baumannii,* which can remove antibiotics from the cell (Smani *et al.*, 2014).

In addition, OXA-type inactivating enzymes are Ambler class D β-lactamases that can break down β-lactams. When the number OXA-type inactivating enzymes are increasing, it could lead to high levels of resistance when combined with other mechanisms, such as porin deletion. Moreover, *A. baumannii* naturally comes with small and fewer porins, which can protect the drug from getting to the target site. Secondly, aminoglycoside-modifying enzyme (AME) and

16 s rRNA methylase production result in *A. baumannii*'s resistance to aminoglycosides. Aminoglycoside resistance is due to gene exchange between pathogens through transposons, integrons, and plasmids through transformation and transduction. In the transformations and transductions, three classes of AMEs are involved: aminoglycoside acetyltransferases (AACs), aminoglycoside nucleotidyltransferases (ANTs), and aminoglycoside phosphotransferases (APHs), encoded by *aac*, *ant*, and *aph*, respectively. AMEs contribute to AMR by modifying aminoglycoside groups, changing covalent bonds, preventing aminoglycosides antibiotics through acetylation, nucleotidylation, or phosphorylation and prevent it from reaching the target ribosome and inhibiting bacterial protein production and contributing to AMR. These genes can be carried on mobile genetic elements such as integrons, transposons and plasmids. This could facilitate the spread of aminoglycoside resistance among bacterial populations (Ramirez and Tolmasky, 2010). 16S rRNA methylation can also confer aminoglycoside resistance. There were 10 16S rRNA methylase genes reported, and they are *armA, rmtA, rmtB, rmtC, rmtD, rmtE, rmtF, rmtG, rmtH and npmA* (Gholami *et al.*, 2017). *A. baumannii* has many *armA* genes, which can further promote the aminoglycoside resistance.

Moreover, biofilm formation is an important contributor to antimicrobial resistance. *A. baumannii* is one of the bacteria that frequently forms biofilms, and biofilm can create a physical and physiological barrier that prevents antimicrobial agents from reaching the target site. There are several ways to do that: changing permeability, inactivation of drugs via antimicrobial-inactivating enzymes immobilised on the biofilm surface, nutrient and oxygen limitations, biofilm phenotype uniqueness, and immune evasion (Shi *et al.*, 2024).

Finally, these resistance mechanisms, such as enzymatic drug inactivation, genetic adaptability, and biofilm-associated tolerance, work together and enable *A. baumannii* to survive against diverse antimicrobial challenges. This multifactor resistance profile explains the limited

efficacy of conventional bactericidal strategies and suggests that alternative approaches, including anti-virulence interventions, vaccines, and drug repurposing strategies, should be designed to disrupt persistence rather than rely on antibiotics alone.

1.5 Recent Progress to Tackle MDR *A. baumannii* Infection.

Bacterial resistance to antibiotics is becoming increasingly significant. Therefore, the development of new antibiotics and antibacterial agents is a matter of great urgency. *A. baumannii* was listed by the WHO as a top-priority bacterium requiring new treatment. Therefore, the G20 countries have begun collaborating closely to develop antibacterial agents.

From 2017 to 2021, 12 novel antibiotics have been developed and approved, 10 of them are derivatives of an existing class of compounds. The novel antibiotics are cefiderocol, ceftazidime/avibactam, eravacycline, delafloxacin, meropenem-vaborbactam combination, plazomicin, pretomanid and omadacycline (Terreni, Taccani and Pregnolato, 2021). Among these antibiotics, eravacycline showed an inhibitory effect on *A. baumannii* MDR and was resistant to carbapenem strains *in vitro* MIC90 experiment and showed 4 -fold more active than tigecycline (Abdallah *et al.*, 2015). However, antibiotics still treat carbapenem-resistant *A. baumannii* are limited, despite the progress made in pharmaceutical research against tuberculosis and *Clostridium difficile* (Terreni, Taccani and Pregnolato, 2021).

In 2023, research on antibiotics targeting *A. baumannii* made significant progress with the use of artificial intelligence (AI). Scientists discovered a new antibiotic, named abaucin, through an innovative experiment. In this study, the growth of *A. baumannii* was monitored against 7,500 different compounds. AI was then used to model the structure of these compounds and predict their potential impact on *A. baumannii*. The AI also explored the relationship between chemical structure and growth inhibition.

Building on the initial model, the researchers screened an additional 6,680 previously unknown compounds to identify top candidates that differed structurally from existing antibiotics. This process led to the discovery of abaucin, a narrow-spectrum antibiotic effective against *A. baumannii* by disrupting lipoprotein trafficking through a mechanism involving LolE (G. Liu et al., 2023). The efficacy of abaucin was further confirmed in a mouse model, where it successfully treated *A. baumannii*-infected wounds. This experiment marks a breakthrough in antibiotic discovery, demonstrating how AI can provide a new and faster approach to developing targeted treatments for bacterial infections.

1.6 Alternative Chemical Compounds and Agents to Tackle MDR Pathogens

AMR is a global issue requiring novel approaches to resolution. While developing novel antibiotics, several alternative compounds and agents are being explored for their potential to combat AMR, including antimicrobial proteins, bacteriophages (phages), probiotics, and plant-based substances (Łojewska and Sakowicz, 2021).

Bacteriophages are viruses that can infect bacteria and kill them. It was discovered by Frederick William Twort and Felix d'Hérelle separately in 1915 and 1917. In 1922, phages were first used therapeutically in the United States and have regained attention due to the rise of antibiotic resistance (Aswani and Shukla, 2021). Phages kill bacteria by injecting their genetic material into the host, using the bacterial cell to replicate and produce new phages. Eventually, this leads to the lysis of the bacterial cell and the release of new phages (Mitropoulou *et al.*, 2022). Clinical studies have reported the successful use of intravenous phage therapy, such as in a patient with *staphylococcal* infection who was also taking cefazolin and oral minocycline, without disruption to the gut microbiota (Mu *et al.*, 2021). Phage therapy offers several

advantages, including host specificity, low toxicity, and a reduced likelihood of antibiotic cross-resistance. Additionally, new phages can be isolated from natural environments or waste facilities and tailored to target specific bacteria. However, phages have limitations: bacteria can develop resistance to phages over time, and phages typically target a narrow range of bacteria. To address this, phage therapy often involves a combination of phages or phages with antibiotics (Chang *et al.*, 2022). In Gordillo Altamirano *et al.*, (2022), using phase with ceftazidime to treat *A. baumannii* increased effectiveness compared to either treatment alone. In another study, the treatment of a 68-year-old man with necrotizing pancreatitis complicated by a MDR *A. baumannii* infection failed after multiple antibiotics and drainage procedures. A phage cocktail was administered via intravenous and percutaneous routes, leading to clinical recovery (Schooley *et al.*, 2017).

Another promising approach to overcoming AMR is the use of plant-based substances. Plants produce a wide array of bioactive compounds as they lack an immune system like animals and must defend themselves against pathogens. These functional compounds include polyphenols, phenols, micronutrients, phytochemicals, and essential oils. In Tajkarimi and collaborators' study (2010), 30,000 compounds with phenol groups were extracted from more than 1340 plants, many of which are used in the food industry. Most antimicrobial essential oils were extracted from herbs and spices such as clove, cinnamon, garlic, ginger, and oregano. The oregano essential oils showed the ability to inhibit *E. coil* protein synthesis and potentially limit flagellin synthesis (Burt *et al.*, 2007). In another study, a natural flavanol flavonoid, kaempferol was identified as a potentiator of the antimicrobial activity of colistin. Complete inhibition of bacterial growth was observed when 1.22 μg/mL colistin was combined with 0.375 mM kaempferol (Gadar *et al.*, 2023).

The probiotic could alleviate diarrhoea symptoms caused by pathogen infections (Paula Rosa, 2017). Probiotics also offer a strategy against AMR by positively affecting pathogen-induced diarrhoea and competing with pathogens for colonisation. They can trigger the immune system to fight off infections and have shown potential against foodborne pathogens (Łojewska and Sakowicz, 2021). In a *Galleria mellonella* (*G. mellonella*) burn wound infection model, larvae infected with *P. aeruginosa* PA14 were treated with *Limosilactobacillus reuteri* CCUG44144. Treatment resulted in a survival rate exceeding 60% at 72 hours post-infection, whereas survival in untreated *P. aeruginosa* PA14–infected larvae remained below 10% (Maslova, Osman and McCarthy, 2023). In Rodriguez *et al.*, study (2023), shown *Lacticaseibacillus rhamnosus* CRL 2244 has a killing effect when co-cultured with *A.baumannii* AB5075.

In recent years, there has been an increasing interest in metal nanoparticle applications in the medical field. The metal nanoparticle could serve as an antimicrobial agent against WHO-listed priority pathogens, such as *A. baumannii.* Metal-based nanoparticles (MNPs) can slow bacterial resistance. This is because MNP does not bind with bacterial receptors. They inhibit both Gram-positive and Gram-negative bacteria by binding to negatively charged bacterial cell walls and disrupting them.

Many MNPs, such as gold, zinc oxide, copper, and silver, are being investigated as potential strategies to combat AMR (Sánchez-López *et al.*, 2020). Among these MNPs, silver was studied intensively. Silver ions released from silver nanoparticles could interact with sulphur and phosphorus in DNA, disrupting DNA replication and cell reproduction, or causing bacterial death (Durán, Nakazato and Seabra, 2016). In addition to releasing ions, silver nanoparticles (AgNPs) could pass through the cell wall due to their size and alter the cell membrane's

structure. They could also lead to cell lysis and organelle rupture because of cytoplasmic membrane denaturation. Moreover, AgNPs could disrupt the signal transduction of bacteria, cause bacterial cell death and inhibit cell growth (Yin *et al.*, 2020).

In Malcher and colleagues study (2008) poly(L-lysine)/hyaluronic acid (PLL/HA) multilayer films and liposomes loaded with silver ions were created. $AgNO_3$ was added to liposomes and deposited on PLL/HA multilayer films. The minimal inhibitory concentration (MIC) of AgNO3 was confirmed, and the antibacterial activity of the $AgNO_3$ coating (120 ng/cm^2) was tested against *E. coli*. After 120 minutes of exposure to the $AgNO_3$ coating, a 4-log reduction in viable *E. coli* cells was observed. However, recent study reveal that *A. baummanii* development resistant agains AgNPs by biofilm formation, upregulations of outer membrane proteins, and membrane and capsule synthesis genes. The membrane integrity was also enhance in the resistant strain (McNeilly *et al.*, 2025).

Therefore, to effectively combat AMR, research must continue across multiple approaches and on a large scale. Bacteria constantly evolve and mutate, allowing them to develop resistance to new antibacterial agents and antibiotics.

1.7 Artificial Sweeteners and Their Antimicrobial Properties

Artificial sweeteners (AS) are widely used in modern society to reduce sugar and calorie intake. More than 250,000 tonnes of artificial sweeteners are consumed each year globally (Luo, Wu, *et al.*, 2019). They are present in various aspects of daily life, including beverages, food, and certain medications. Despite FDA and European Union approval, the potential long-term health effects of ASs remain controversial. Recent research has linked artificial sweeteners to health concerns such as cardiovascular disease, cancer, and gestational diabetes (Goran, Plows and

Ventura, 2019; Debras *et al.*, 2022; Fornasini, Robles-Rodríguez and Baldeon, 2023). Long-term safety of AS that have not been tested by using randomised clinical trials. The study Witkowski and colleagues study (2023) shows that erythritol intake could lead to an increased risk of cardiovascular events. Their mechanistic studies demonstrate that platelet reactivity and thrombosis risk increase with increasing erythritol levels. In addition to human health impacts, the effects of AS on microorganisms, particularly gut microbiota, are also concerning. The gut microbiota plays a crucial role in metabolism, energy balance, and immune system function (Jandhyala *et al.*, 2015). Studies have shown that AS like saccharin and sucralose can disrupt the gut microbiota, potentially leading to dysbiosis and adverse effects on gut health (Ruiz-Ojeda *et al.*, 2019).

AS consumption has increased significantly. AS can be tracked via wastewater analysis because they are not metabolised by the body and are therefore excreted unchanged (Zhang *et al.*, 2016). This means they could enter the wastewater system directly through urine. A long-term study of artificial sweetener consumption through wastewater was conducted in Australia (Li *et al.*, 2021). In the result, it revealed that daily per capita intake of individual sweeteners ranged from 2.4 ± 0.8 mg/day/person for saccharin to 7.8 ± 2.0 mg/day/person for acesulfame between 2012 and 2018. It also demonstrates a trend change over six years of study. Consumption of sucralose and sodium saccharin (SACC) increased substantially. However, sodium cyclamate (CYC) consumption decreased, consistent with market survey data. Specifically, sucralose and saccharin saw average annual increases of 10% and 6.0%, respectively, while CYC experienced an average annual decline of 11% from 2012 to 2018 (Li *et al.*, 2021). The increasing use of AS results in concentrations of up to 2.5 mg/L in wastewater treatment plants (Loos *et al.*, 2013).

The effects of these compounds on bacteria, particularly those relevant to the human gut, remain understudied (Ruiz-Ojeda *et al.*, 2019). However, the growing concern about the environmental and public health impacts of increasing AS levels in wastewater has led to recent research investigating their potential influence on bacterial evolution and contribution to antibiotic resistance. In Yu and Guo study (2022), they performed MIC against *K. pneumoniae, Escherichia coli (E. coli)* and *Bacillus subtili,* the concentration of AS (SACC, sucralose, aspartame and Ace-K) was over 1500 mg/L, which is much higher than the daily dosage of AS (300 mg/L). However, the LIVE/DEAD assay revealed a significant increase in cell damage and death at 300 mg/L. Their ROS results show AS significantly increasing intracellular ROS levels compared to the control. At a 300 mg/L concentration, the ROS was increased most significantly. The acesulfame potassium (Ace-K) group resulted in up to a 1.9-fold increase in ROS in *E. coli* and *Bacillus subtilis*, and aspartame caused a 2.1-fold increase in *K. pneumoniae*. Antibiotic treatments also elevated ROS production, whereas sucrose and glucose had no effect on ROS levels. Notably, glucose decreased ROS production in *E. coli*. In this study, AS also increase cell-envelope permeability and efflux-pump activity.

On the other hand, AS showed potential as an antimicrobial candidate. In de Dios *et al.* research (2023), aspartame was shown to increase the growth of *A. baumannii*, while others like CYC, SACC, Ace-K exhibit inhibitory effects on bacterial growth both *A. baumannii* AB5075 and *P. aeruginosa* PA14 (Figure 1.9). In addition, Ace-K could not serve as a carbon source for the growth of *A. baumannii* AB5075 and *P. aeruginosa* PA14. In this study, Ace-K exhibited significant broad-spectrum antimicrobial activity, effectively inhibiting the growth of *A. baumannii* AB5075 at 0.89% The 50% inhibition (IC_{50}) against *A. baumannii* AB5075 at 2.20%. The near-maximal inhibition at 4.43% and above for *A. baumannii*.

Ace-K completely inhibited biofilm formation in *A. baumannii* AB5075 at 2.66% and in *P. aeruginosa* PA14 at 1.77%. It also eradicates biofilm formation by 48.8% in AB5075 and 69.7% in PA14 at a concentration of 8.85%. It showed the most potent antimicrobial effect and prevented biofilm establishment, demonstrating potential against both *A. baumannii* AB5075 and *P. aeruginosa* PA14. Additionally, Ace-K was observed to limit twitching motility in *A. baumannii* due to its downregulation of T4P assembly genes. RNA-seq analysis showed that several *pil* genes (*pilA*, *fimT*, *pilVWXY*, p*ilGHIJL, pilZ, pilTU, pilBCD and pilR* in Ace-K) regulating twitching motility were down-regulated, and this transcriptional response was further confirmed by the twitching motility assays. This inhibition of motility is important because it can reduce the bacteria's ability to adhere and form biofilms. Moreover, transcriptomic analysis also revealed that several peptidoglycan amide and glycoside hydrolases were differentially expressed (including ABUW_0928, ABUW_3204, and ABUW_4116). This indicates that the disruption of the balance between peptidoglycan synthesis and degradation ultimately compromises cell envelope structural integrity, leading to the formation of bulges in the cell envelope that ultimately trigger lysis (de Dios *et al.,* 2023). Taken together, these findings suggest the antimicrobial activity of Ace-K because it disrupts type IV pili-associated motility and cell-envelope homeostasis, thereby impairing biofilm formation and compromising bacterial cell integrity.

The combination of Ace-K with antibiotics showed greater inhibition of *A. baumannii* than antibiotics alone when tested against polymyxin B, gentamicin, and carbapenems. These findings are particularly relevant because *A. baumannii* is a significant cause of hospital-acquired wound infections. An *ex vivo* porcine skin model was used to test Ace-K in a practical scenario to further assess its efficacy. The skin infected with *A. baumannii* was treated with gauze soaked in 8.85% Ace-K. This treatment resulted in a 1.86 log reduction in viable bacterial

cells compared to a control water treatment, highlighting Ace-K's potential as an effective antimicrobial agent.

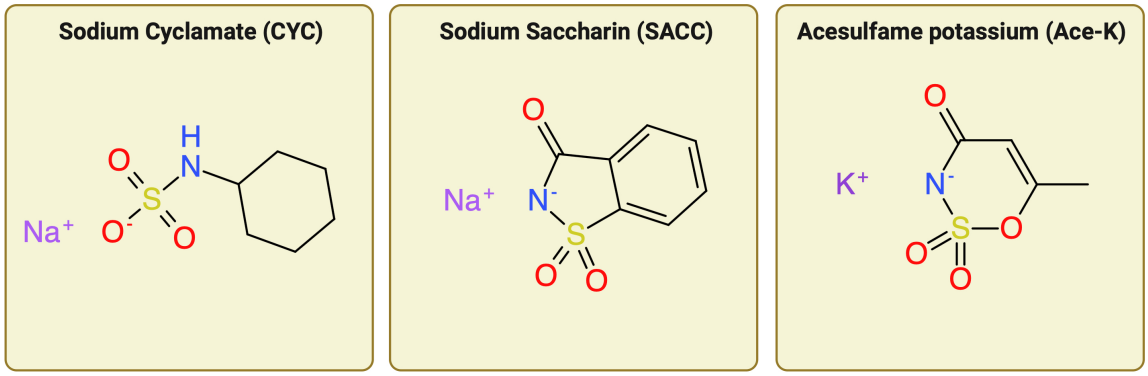

Figure 1.9 Chemical structure of artificial sweeteners that have antimicrobial activity on *A. baumannii*. Created in https://BioRender.com

In their later study, SACC exhibited antimicrobial activity through a dual mechanism that affected both cell-envelope stability and DNA-replication dynamics (de Dios *et al.*, 2025). Saccharin showed increasing inhibitory activity against *A. baumannii* AB5075 with an IC_{50} of approximately 1.2%. Near-maximal inhibition was observed at concentrations of approximately 5% and above for *A. baumannii* AB5075. SACC induces *E. coli* cell filamentation, bulging, and ultimately lysis. Transcriptomic and microscopy analyses demonstrate that SACC impacts the expression of membrane-associated genes and induces DNA repair pathways, indicating replication stress and damage that extends beyond origin-initiated synthesis. Global transcriptomic analysis revealed that SACC could downregulate *A. baumannii* genes involved in pili and fimbriae biogenesis (ABUW_0648, ABUW_1632, ABUW_1633, ABUW_2052, ABUW_2053 and ABUW_2310), which are closely associated with bacterial adhesion and biofilm formation. Moreover, several *pil* genes (*pilN,pilO, pilA*) regulating twitching motility were down-regulated, and this was further confirmed by the twitching motility assays. This was validated by biofilm formation and twitching assays. The

treatment with SACC could enhanced antibiotic efficacy against MDR *A. baumannii* AB5075 by increasing membrane permeability, which enhances antibiotic uptake and re-sensitises *A. baumannii* AB5075 to carbapenems. Finally, a saccharin-loaded polyvinyl alcohol hydrogel demonstrated antimicrobial efficacy against *A. baumannii* biofilms both *in vitro* and in an *ex vivo* porcine burn wound model (de Dios *et al.*, 2025).

In summary, AS such as Ace-K, CYC, and SACC have emerged as promising candidates with notable antimicrobial properties, offering biofilm inhibition, antibiotic sensitisation, and broad-spectrum activity. When AS solutions are applied directly to a wound, they may disperse rapidly, be diluted by wound exudate, or dry quickly at the surface, which can shorten the contact time between the active compounds and the infected tissue. Therefore, repeated application may be required to maintain therapeutic activity. In addition, once dried, ASs may crystallise or form powdery residues on the wound surface, which could be difficult to remove, reduce patient comfort and re-damage the wound site. These drawbacks can be improved by a better delivery system. In this context, loading AS into moist hydrogel can be a promising approach for wound management.

1.8 Introduction of Hydrogel

Hydrogels are three-dimensional (3D) structured hydrophilic macromolecular networks with cross-linked polymer (Kamoun, E. R. S. Kenawy and Chen, 2017; Waresindo *et al.*, 2023). These materials are excellent candidates for medical applications due to their hydrophilicity, soft-tissue-like water content, and biocompatibility (Kamoun, E. R. S. Kenawy and Chen, 2017; Mei *et al.*, 2024). The first modern hydrogel for biological use was made of crosslinked 2-hydroxyethyl methacrylate (HEMA) and ethylene dimethacrylate, was introduced by Wichterle and Lim in 1954 (Wheeler *et al.*, 1996). Initially used for eye enucleation and contact lenses (Wichterle and Lím, 1960). Since then, numerous studies have explored hydrogels for

various applications. In the late 1970s, chitin-based materials were reported and used as wound covers (Kamoun, E. R. S. Kenawy and Chen, 2017; Mei *et al.*, 2024). Today, hydrogels are extensively studied in fields such as cosmetics, tissue engineering, and healthcare (Correa *et al.*, 2021).

The widespread use of hydrogels in the biomedical field is largely due to their biocompatibility. This biocompatibility is primarily attributed to factors such as high-water content, chemical composition, degradation behaviour, and mechanical properties. The high-water content of hydrogels mimics the body's aqueous environment, enhancing biocompatibility and reducing potential adverse effects on tissue. Hydrogels can also improve cell adhesion, survival, and proliferation by swelling and absorbing fluids (Hoffman, 2012). Hydrogels are an excellent wound-dressing material that maintains moisture balance and provides adhesion-free coverage of the open wound, reducing pain and enabling loading with bioactive compounds for better treatment results. A moist wound environment provides several benefits for wound healing, including enhanced keratinocyte migration and re-epithelialisation, increased collagen synthesis and autolytic debridement, as well as reduced tissue necrosis, inflammation and scar formation (Nuutila and Eriksson, 2021). Some hydrogels can respond to different pH values, and changes in the charge on the polymer chains lead to swelling and drug release (Rizwan *et al.*, 2017). In contrast, traditional gauze dressings are widely known for their use in wound application. They are easily accessible, cost-effective, and easy to manufacture. However, using this gauze can cause rapid dehydration and promote bacterial growth, leading to contamination. Furthermore, it is difficult to remove after treatment and can lead to bleeding (Kamoun, E. R. S. Kenawy and Chen, 2017; Mei *et al.*, 2024).

Hydrogels could act as vehicles to deliver drugs effectively. In El-Aassar *et al.* study (2015), a hydrogel membrane was made by cross-linking kappa carrageenan and hyaluronic acid with epichlorohydrine. The cumulative release of L-carnosine was 28% to 93% when the hyaluronic acid concentration was increased (El-Aassar *et al.*, 2015). In another study, gentamicin sulphate was used as a model drug. A citric acid crosslinked carboxymethylcellulose (CMC)-polyvinyl alcohol (PVA) hydrogel was developed. This CMC-PVA-based hydrogel film was shown to reduce drug release as the PVA content increased. However, the hydrogel film with the highest PVA concentration showed a greater tendency to control the release (Ghorpade *et al.,* 2019)

Hydrogels can be produced using both natural polymers and synthetic polymers. Both polymers have their strengths and weaknesses (Table 1.1). The natural polymers include alginate, collagen, chitosan, agarose, gelatin, hyaluronic acid and cellulose. Natural polymers provide exceptional characteristics, including biocompatibility and biodegradability. Nevertheless, natural polymers exhibit comparatively low mechanical strength and pose maintenance challenges. Additionally, natural polymers may be limited by resource availability, immunogenicity, and the risk of pathogen transmission (Garbayo *et al.*, 2017). Moreover, the use of natural polymers such as gelatin may be restricted in some countries due to their animal origin (Feuilloley *et al*., 2024). Conversely, synthesising hydrogels allows for convenient adjustment of their physical and chemical properties, making it more feasible to achieve the appropriate mechanical properties (Bashir *et al.*, 2020). However, synthetic polymers such as Polyethene glycol (PEG), Polyvinylpyrrolidone (PVP), and PVA exhibit weaker biological activity than natural polymers (Zhu, 2010; Asy-Syifa *et al.*, 2022). PVA is a well-studied, water-soluble material and one of the most widely used synthetic polymers for the preparation of hydrogels (Figure 1.10) (Teodorescu *et al.*, 2016). It has biocompatibility, high water content, and non-toxicity, which make PVA a friendly polymer for body tissues (Wang *et al.*, 2021).

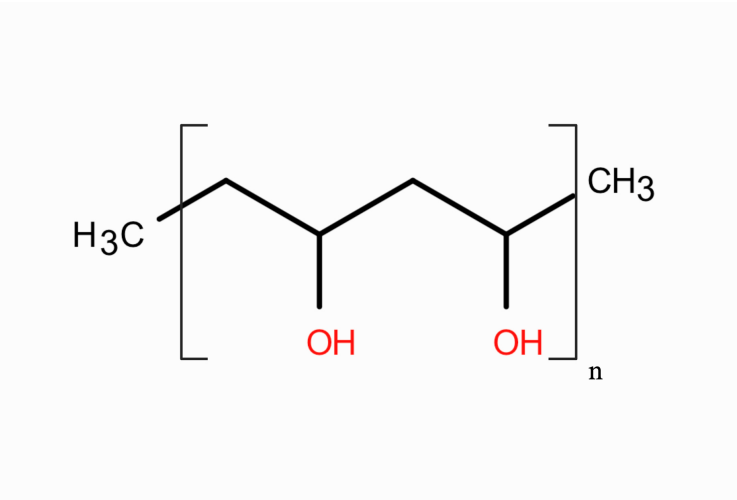

Figure 1.10 Repeating units of poly(vinyl alcohol). Created in https://BioRender.com.

Additionally, PVA has strong mechanical and degradable properties, which make it commonly used in wound dressings, cartilage, and orthopaedic applications (He *et al.*, 2018). Hydrogels are generally formed by physical or chemical interactions between polymers, a process called crosslinking. The hydrogel would obtain water-absorbing properties due to the mesh structure after crosslinking (Kamoun, E. R. S. Kenawy and Chen, 2017). The PVA can form a hydrogel by physical and chemical cross-linking, which makes PVA more interesting, as it can be tuned to adjust its physical properties (Fan *et al.*, 2016; Shamloo *et al.*, 2021).

Table 1.1 Advantages and limitations of polymers commonly used in hydrogel wound dressings

Polymer	Type	Main Advantage	Limitation	Reference
Alginate- A natural polysaccharide derived mainly from brown algae.	Natural	Support tissue repair, moisture retention, biocompatibility and promotes cell proliferation and angiogenesis.	Weak mechanical strength and limited cell adhesion.	(Teng *et al.*, 2021; Wen *et al.*, 2022).
Agarose- A natural polysaccharide derived from red algae.	Natural	Biocompatible and non-toxic, low-cost polysaccharide and moisture retention.	Exhibits brittleness and contractility and limited cell adhesion.	(Jiang *et al.*, 2023; S. Li *et al.*, 2025)
Chitosan- A natural polymer derived from	Natural	Antimicrobial, biodegradable and accelerates wound healing.	Poor solubility at neutral pH, weaker mechanics and low blood compatibility.	(Dhiman and Agnihotri, 2020; Guarnieri *et*

deacetylation of chitin.				*al.*, 2022; Lin *et al.*, 2026)
Collagen- A structural protein that is a major component of the extracellular matrix.	Natural	Stops the bleeding, promote tissue regeneration, biocompatible, and biodegradable	Easy to degrade, weak mechanical properties	(Gaspar-Pintiliescu, Stanciuc and Craciunescu, 2019; Zhang *et al.*, 2023; Jin *et al.*, 2026)
Gelatin- A polypeptide generated by hydrolysis and denaturation of collagen.	Natural	Biocompatibale, biodegradable and low immunogenicity.	Poor thermal/mechanical stability unless modified, usage restriction due to animal origin in some countries.	(Xing *et al.*, 2014; Feuilloley *et al.*, 2024; Maeso *et al.*, 2026)
Hyaluronic acid- A naturally occurring glycosaminoglycan.	Natural	Excellent biocompatibility, high water retention, supports cell migration and wound healing	Weak mechanical strength, poor structural stability, rapid clearance, limiting its use in load-bearing tissues or long-term applications.	(Segneanu *et al.*, 2025; Wang, Zhou and Xie, 2025)
PVA- A colorless, odorless, and water-soluble synthetic polymer containing hydroxyl groups	Synthetic	Good mechanical strength, biocompatible, and easy processing.	Limited cell adhesion and lack of antibacterial activity.	(Chen *et al.*, 2022; Pavita *et al.*, 2025; Tian *et al.*, 2026)
PEG- A synthetic polyether polymer composed of repeating ethylene glycol units	Synthetic	Nontoxicity, water soluble, flexibility, and nonimmunogenic.	Brittleness and low hydrophilicity.	(Li *et al.*, 2017; Ge *et al.*, 2020; Deng, Gould and Ali, 2022)
PVP- A synthetic water-soluble polymer derived from N-vinylpyrrolidone.	Synthetic	Nontoxicity, adequate adhesion, high water retention, and biocompatible.	Low swelling capacity and weak mechanical property	(Kariduragana var, Kittur and Kamble, 2014; Roy and Saha, 2012; Huang *et al.*, 2017; Gounden and Singh, 2024)

1.8.1 Freeze-Thaw PVA Hydrogel

The physical crosslinked PVA hydrogel was first developed in 1975, when it was found that the PVA solution changed to a gel form after repetitive freezing-thawing (FT) due to phase separation and crystallisation (Peppas, 1975). When water molecules crystallise at low temperatures, they force the PVA chains to come closer together and increase hydrogen-bond interactions, which act as physical crosslinking points after thawing (Figure 1.11) (Adelnia *et al.*, 2022). An ideal wound dressing should maintain a moist environment, absorb exudate, protect the wound surface, and minimise secondary damage during dressing changes. The FT-PVA hydrogels have high-water content and soft-tissue-like characteristics. It can provide a hydrated wound environment while also providing non-adherent coverage (S. *et al.*, 2020). The U.S. Food and Drug Administration (FDA) has approved its PVA for biomedical applications, such as tissue engineering and drug delivery, due to its biocompatibility. Studies indicate that PVA hydrogels are applicable in numerous wound dressing scenarios (Loughlin *et al.*, 2008; Murphy *et al.*, 2012; Q. Zhang *et al.*, 2022). Furthermore, PVA hydrogel has a porous and swollen network structure, which could enable it to act as a carrier for bioactive compounds (Machado-Torres *et al.*, 2025). This allows the local delivery of therapeutic agents, including drugs, DNA, growth factors, nanoparticles, and proteins, to the wound site (Jin, 2022). For the treatment of infected wounds, agents such as antibiotics, honey, and AgNPs can be used to accelerate wound healing (Shamloo *et al.*, 2021; Thet *et al.*, 2024).

The physical and mechanical properties of the FT-PVA hydrogel can be influenced by formulation parameters such as molecular weight, solution concentration, hydrolysis, the number of FT cycles and freeze-thaw temperature (Adelnia *et al.*, 2022; Waresindo *et al.*, 2023). Increasing the molecular weight of PVA generally enhances chain entanglement and increases the number of cross-linking points, thereby improving gel strength and mechanical integrity

(Ma *et al.*, 2019; Waresindo *et al.*, 2023). Increasing the PVA concentration in the solution can lead to higher viscosity and a denser network, resulting in a stiffer gel (Waresindo *et al.*, 2021; Asy-Syifa *et al.*, 2022). The number of FT cycles also plays an important role. More FT cycles could increase crystallinity and crosslink density, thereby strengthening the hydrogel. Moreover, the lower the freezing temperature, the more cross-linking points are formed. It can lead to a smaller pore size. The smaller pore size directly influences the swelling ability of PVA hydrogel (Figueroa-Pizano *et al.*, 2018). The degree of hydrolysis can affect the properties of the hydrogel because a higher degree of hydrolysis means more hydroxyl groups. It can lead to more hydrogen bonding between PVA chains. As a result, it strengthens the gel structure and network integrity (Adelnia *et al.*, 2022).

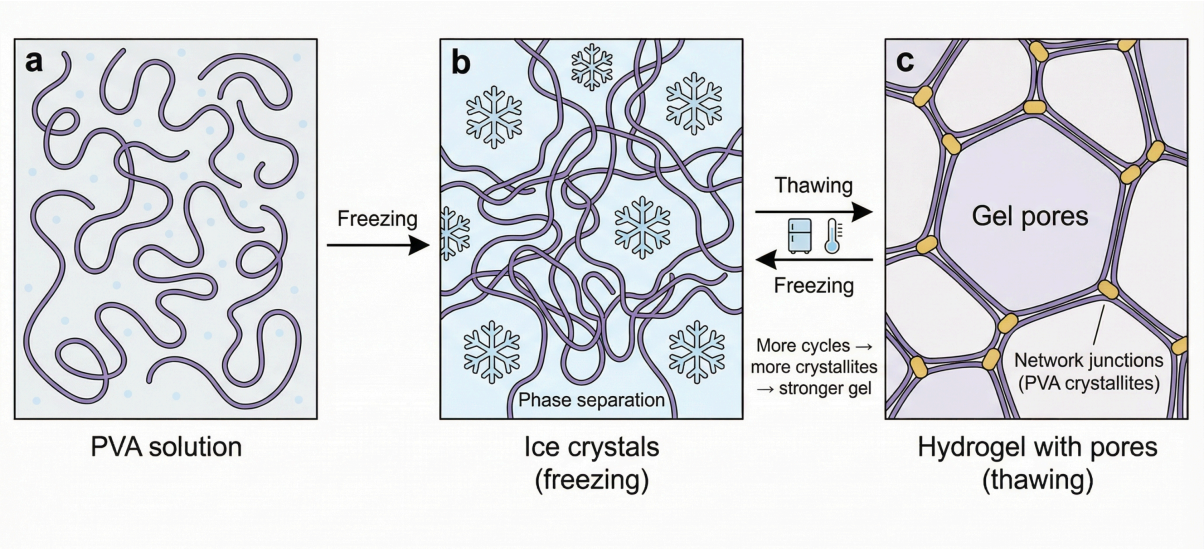

Figure 1.11 Schematic illustration of FT-PVA hydrogel formation: (A) PVA dissolved in solution forms free chains. (B) Freezing leads to water crystallising into ice and to phase separation, which traps the PVA chain between ice crystals and forms hydrogel bonds. (C) A gel network forms, and ice crystals become pores in the hydrogel. With more cycles of FT, the gel becomes stronger. This figure was created by biorender https://BioRender.com.

1.8.2 Poly (vinyl alcohol) Borax Hydrogel

The PVA-Borax hydrogel is notable for its ability to load drugs for topical delivery. One major advantage of PVA-Borax hydrogel is its enhanced mechanical properties achieved by cross-linking PVA with borax. This modification not only improves the structural integrity of the hydrogel but also imparts unique rheological properties, such as dilatancy, in which viscosity increases with the rate of shear strain. This feature is particularly beneficial in wound dressing applications as it allows the hydrogel to conform to the wound site effortlessly, minimising pain and potential re-injury. Additionally, the formation of diol-borate ester bonds between borax and PVA enhances the hydrogel's water-retention capacity (Figure 1.12) (Zandraa *et al.*, 2021). These properties provide a moist environment for the wound, promote healing, and even deliver the drugs it needs.

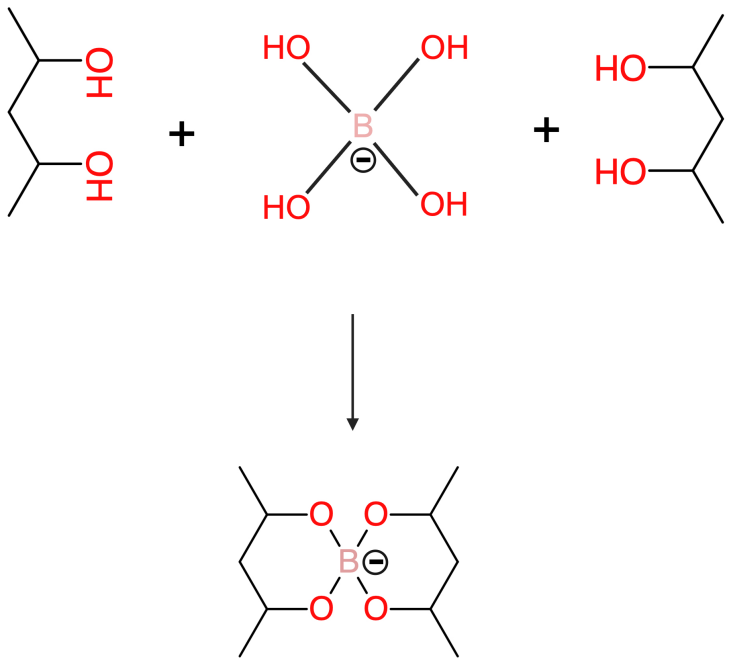

Figure 1.12 Cross-linking of poly(vinyl alcohol) with borax. This figure was created by biorender https://BioRender.com.

In Zhang and collaborator's study (2022), aloe polysaccharide (AP) and honey were added to the PB hydrogel for better wound healing and antibacterial properties. In this study, various properties were tested. This hydrogel demonstrated inhibitory effects on *S. aureus, E. coli, and Candida albicans.* Different honey concentrations significantly affect antimicrobial activity. In this experiment, bacterial inhibition increased proportionally as the honey concentration rose from 5% to 10%. However, the antibacterial activity was less pronounced when the concentration increased from 10% to 20%. In addition, hydrogel loaded with more than 7.5% honey showed a better inhibitory effect on *S. aureus.* This experiment also examined the cytocompatibility and blood compatibility of AP solution and PVA-AP-H10 hydrogels. The test lasted five days, and the number of dead cells was measured on days 1,3 and 5. The results show that a relatively small number of cells were dyed in the PVA-AP-H10 hydrogel, indicating the biocompatibility of this PVA borax-based hydrogel. Also, in this study, both the rheological and mechanical properties of the hydrogel were examined, highlighting the importance of its physical properties. According to the results, adding AP and honey improves the rheological and mechanical properties. Finally, tests on wound healing have demonstrated that PVA-AP-H10 hydrogel-healed wounds have smoother skin and less scarring in mice.

In wound care, antimicrobial substances, including honey and other antiseptic solutions, are frequently used due to their broad-spectrum efficacy. However, these liquid agents are facing constraints. For example, it could dry out or be readily wiped or washed away. Therefore, their therapeutic concentrations at the wound site are inconsistent. Additionally, these agents are not ideal because they cannot effectively seal the wound or maintain the moist environment required for optimal healing. The long-term protection against infections caused by pathogens is limited.

PVA-Borax hydrogels loaded with antimicrobial agents have shown promising results in recent studies (Yalei Liu *et al.*, 2022). These hydrogels provide a stable environment that maintains therapeutic concentrations for extended periods. For example, incorporating carboxymethyl chitosan and AgNPs into PVA-Borax hydrogels resulted in exceptional antimicrobial efficacy against *S. aureus* and *E. coli* while minimising cytotoxicity. Cell viability reached 98% after 96 hours in culture (Yalei Liu *et al.*, 2022). This highlights the potential of PVA-Borax hydrogels as effective carriers for antimicrobial agents.

1.8.3 3D Printable Hydrogel for Wound Dressing Application

Conventional hydrogels have demonstrated considerable value in wound-dressing applications and can be tailored by varying formulation parameters. However, dressing performance can also be influenced by structural features such as shape, porosity and thickness. Recently, three-dimensional (3D) direct ink writing (DIW) printing has emerged as a promising fabrication strategy for hydrogel-based wound dressings. It can mimic natural extracellular matrix components, and a porous structure provides space for cell adhesion, integration and differentiation. It is also able to tune its release that will contribute to wound healing (Pop and Almquist, 2017; Alizadehgiashi *et al.*, 2021). In Harmanci *et al.* study (2022), PVA and Polycaprolactone (PCL) were 3D printed via DIW as bi-layer and tri-layer sandwich scaffolds to load metformin. The results show that this 3D-printed PVA/PCL scaffold increases the bioavailability and half-life of metformin. In Alizadehgiashi *et al.* study (2021), a hydrogel prepared by cellulose nanocrystals and chitosan loaded with AgNPs and vascular endothelial growth factor showed a controlled release profile with antimicrobial property and a rapid and customisable fabrication potential for wound dressing.

Overall, this thesis will develop conventional and 3D printed hydrogel systems that optimise the antimicrobial efficacy of ASs and prolong agent retention at the wound site, thereby overcoming the limitations of conventional liquid antimicrobials and improving wound-healing quality. It will explore how the transcriptional landscape of *A. baumannii* changes in the synthetic wound medium (LCWB) and how the hydrogel performs in this medium and identify bioactive compounds regulating T4P expression in *A. baumannii* by screening the FDA-approved drugs library.

1.9 Aims and Objectives

Aim one:

Aim one is to develop PVA-based hydrogels loaded with artificial sweeteners (AS) and investigate their potential as antimicrobial wound-dressing against *A. baumannii.* This will provide a novel approach to delivering artificial sweeteners at the wound site while investigating their antimicrobial activity. At the same time, the growth of *A. baumannii* in the Lubbock Chronic Wound Biofilm (LCWB) model, the biofilm formation and global gene expression profile, will be investigated to assess the suitability of LCWB for hydrogel testing. Moreover, the hydrogel system will subsequently be optimised using 3D printing to enhance AS release and antimicrobial activity. This will be achieved by the following objectives:

1. Develop and characterise PVA-based hydrogels loaded with artificial sweeteners using PVA-borate and freeze-thaw PVA (FT-PVA) hydrogel systems.
2. Investigate the global gene expression profile of *A. baumannii* in LCWB medium and evaluate the suitability of LCWB for assessing the antimicrobial activity of PVA-based hydrogels.

3. Develop 3D-printed PVA-based hydrogels to investigate whether controlled hydrogel architecture can enhance artificial sweetener release and improve antimicrobial activity against *A. baumannii*.

Aim two:

Aim two is to identify FDA-approved drugs that demonstrate potential to modulate *pilA* expression and virulence-associated phenotypes in *A. baumannii*. This will identify potential compounds that may change bacterial motility and biofilm formation without directly targeting bacterial viability. The identified hit compounds will be further validated *in vitro,* and the molecular mechanisms underlying their effects will be investigated at the transcriptomic level, followed by *in vivo* validation. This will be achieved by the following objectives:

1. Screen the FDA-approved drug library for compounds that modulate *pilA* expression and biofilm formation in *A. baumannii*.
2. Investigate the mechanisms of action of hit candidates against *A. baumannii* AB5075 by using RNA-Seq analysis.
3. Validate the virulence activity of hit candidate *in vivo.*

Chapter 2

2. Develop a Novel Artificial Sweetener-Loaded PVA Hydrogel that Could Inhibit *A. baumannii*.

2.1 Introduction

AMR has become a public health crisis globally. In 2019, antimicrobial-resistant pathogens were associated with nearly 5 million deaths (Murray *et al.*, 2022). The misuse of antibiotics has accelerated the widespread of dissemination of resistance among pathogens and created an urgent need for novel alternative antimicrobial strategies. Amongst the most recalcitrant pathogens is carbapenem-resistant *A. baumannii* which has been classified at the top of the World Health Organisations's list of critical priority pathogens in urgent need of novel therapeutic interventions (WHO, 2024).

A. baumannii is an opportunistic nosocomial pathogen that is frequently associated with wound infections, ventilator-associated pneumonia, bloodstream infections and urinary-tract infections (Dijkshoorn, Nemec and Seifert, 2007; Ayoub Moubareck and Hammoudi Halat, 2020; Aswathanarayan *et al.*, 2022). In 2021, *A. baumannii* accounted for 15.2% of all deaths attributable to AMR. The proportion of *A. baumannii*-attributable deaths in patients aged five years and younger increased from 10.1% in 1990 to 13% in 2021 (Naghavi *et al.*, 2024). Resistance among these strains is a major problem, with up to 99% of *A. baumannii* clinical isolates in some Mediterranean EU countries being multidrug-resistant. These rates are nearly 4 times higher than those observed for other Gram-negative pathogens such as *P. aeruginosa* (Foglia *et al.*, 2025).

While its capacity to evolve or acquire resistance to antibiotics is one pillar supporting the pathogenic success of *A. baumannii*, its ability to form robust biofilms is another. Biofilms are groups of cells encased in an exopolysaccharide matrix which protects them from the rigours of disinfection, antibiotics or the host immune system. As a result of this capacity to form robust biofilms, *A. baumannii* is frequently associated with chronic wound infections where there are limited, if any, effective treatment options (Maslova *et al.*, 2021).

Recent studies have demonstrated that AS have the ability to kill multidrug-resistant bacteria through bulge-mediated cell lysis and can attenuate *A. baumannii* virulence behaviour by limiting motility and biofilm formation. Global transcriptomic analysis revealed that these sweeteners, at sub-lethal concentrations, could trigger the downregulation of genes associated with mediating biofilm formation and motility. Moreover, combining sweeteners with antibiotics such as carbapenems has been shown to resensitise *A. baumannii* and enhance antibiotic efficacy *in vitro*, overcoming native resistance mechanisms (de Dios *et al.*, 2023a). However, despite the remarkable *in vitro* antimicrobial activity of these sweeteners, a major challenge is how to effectively deliver them to the site of infection, particularly in wound environments where traditional methods may not provide sufficient localised concentration or may desiccate, reducing their effectiveness.

Hydrogels provide a promising solution to this challenge. Hydrogels are three-dimensional (3D) structured hydrophilic macromolecular networks with cross-linked polymers (Waresindo *et al.*, 2021). They are widely used as medical applications for their ability to maintain a moist wound environment while also serving as vehicles for the controlled release of antimicrobial compounds (Salomé Veiga and Schneider, 2013). The hydrophilic nature and biocompatibility

of hydrogels make them ideal candidates for wound dressing, as they not only maintain moisture balance but also create a pathogen-free environment conducive to healing. Hydrogels can be made from synthetic or natural polymers, or both. Natural polymers such as collagen, gelatin, chitosan and hyaluronic acid provide exceptional characteristics, including biocompatibility and biodegradability. Nevertheless, they can exhibit comparatively low mechanical strength and can be degraded by enzymes, which creates challenges in terms of maintenance (Hu *et al.*, 2024). As a result, synthetic hydrogels are increasingly used in biomedical applications due to their excellent mechanical properties and low cost (Gounden and Singh, 2024).

PVA-based hydrogels have been widely studied for topical application due to their ability to retain moisture, conform to wound surfaces and release bioactive compounds in a controlled manner and enhanced mechanical properties (Abdelkader *et al.*, 2018; Q. Zhang *et al.*, 2022). PVA-based hydrogels can form stable networks by using several crosslinking methods. The two main fabrication techniques of PVA-based hydrogel are chemical crosslinking and physical crosslinking (Liang *et al.*, 2024). The crosslinking method plays an important role in defining hydrogel performance. Freeze–thaw-crosslinked PVA hydrogels rely on the formation of crystalline domains that act as stable physical crosslinking points, resulting in mechanically robust and durable networks widely used in wound dressings and tissue engineering (Adelnia *et al.*, 2022). In contrast, borax-crosslinked PVA hydrogels form dynamic diol–borate ester bonds, producing viscoelastic, self-healing networks with enhanced conformability and responsiveness (Wang *et al.*, 2022). These distinct crosslinking mechanisms enable PVA hydrogels to be tailored for specific clinical applications. For example, PVA-borax hydrogel's diol-borate ester bonds in the hydrogel matrix improve its structural integrity, making it more robust for clinical applications. On the other side, the FT-PVA hydrogel was widely used as

wound dressing, a drug delivery system and tissue engineering due to its mechanical and biocompatible properties (Waresindo *et al.*, 2021).

Through this study we developed a series of highly potent artificial sweetener-loaded PVA based-hydrogels that were optimised based on their swelling behaviour, mechanical properties, gel porosity and antimicrobial efficacy against *A. baumannii* biofilm using *in vitro* models and *ex vivo* burn wound porcine skin models. To further demonstrate the translational potential of these hydrogels, we carried out a pilot Phase I human clinical study to investigate the short-term safety and irritancy of the optimised formulations in healthy volunteers, demonstrating no adverse effects. This research provides a novel blueprint for effectively treating biofilm-associated wound infections and addressing the critical issue of AMR in clinical settings.

2.2 Aim 1

The overall aim of this chapter is to develop and evaluate artificial sweetener-loaded PVA-based hydrogels as potential antimicrobial wound-dressing. This includes optimising the hydrogel formulation and evaluating its antimicrobial efficacy *in vitro* and *ex vivo*. It will also characterise its material properties and biocompatibility. Follow by investigating its potential application in a Phase 1 clinical study.

1. Identify the most stable hydrogel formulation with the highest concentration of artificial sweetener.
2. Test artificial sweetener-loaded PVA-Borax and FT-PVA hydrogels *in vitro.*
3. Examine artificial sweetener-loaded PVA-Borax hydrogels and FT-PVA *ex vivo.*
4. To assess the cytocompatibility and haemocompatibility of the developed hydrogel system for PVA-Borax hydrogel as wound-dressing application.
5. Material characterisation of artificial sweetener-loaded PVA-borax hydrogel
6. Investigation of artificial sweetener-loaded PVA-borax hydrogel Phase 1 clinical study in humans.

2.3 Materials and Methods:

Bacterial strain

A. baumannii strain AB5075 (virulent colony variant) was used in this study (de Dios *et al.*, 2025). The overnight stocks were grown for 18 hours at 37 °C and 180 rpm in Luria- Bertani (LB) Broth (ThermoFisher). The stocks were frozen in 20% Glycerol and kept at -80 °C.

2.3.1 Formulation of Artificial Sweetener (AS) Loaded PVA-Borate Hydrogel

Artificial Sweetener either sodium saccharin (SACC), sodium Cyclamte (CYC) (99+%, Thermo scientific) or acesulfame potassium (Ace-K) (99%, Sigma-Aldrich), together with sodium tetraborate (borax) (99%, Alfa Aesar), and Polyvinyl alcohol (PVA) (Mw=115,000,100% hydrolysed, Sigma-Aldrich) were accurately weighed and added into a beaker (Figure 2.1). Different formulations were tested. The PVA was prepared at concentrations of 3%, 4%, 5%, 6% and 8% (W/W) and borax was at concentrations of 0.3%, 0.6%, 1%, 2%, 3%, 4%, and 5%. Deionised water was added to the beaker and mixed with a glass stirring rod. The initial mass of the whole system (beaker and contents) was recorded. The mixture was then heated in a water bath at 80°C for 3 hours, covered with an aluminium foil to minimise evaporation. The mixture was stirred every 1 hour to promote homogeneity and gel formation. Any evaporated water was replenished to maintain the original volume. Once the hydrogel was obtained, it was transferred into custom-made 3D-printed moulds to achieve uniform shape and size. The mould diameter is 10 mm, and the height is 6.5 mm. The mould was 3D-printed in a Mars 2 Pro 2K resin 3D printer (Elegoo). Freshly printed moulds were UV-cured in a Wash & Cure 2.0 chamber (Anycubic).

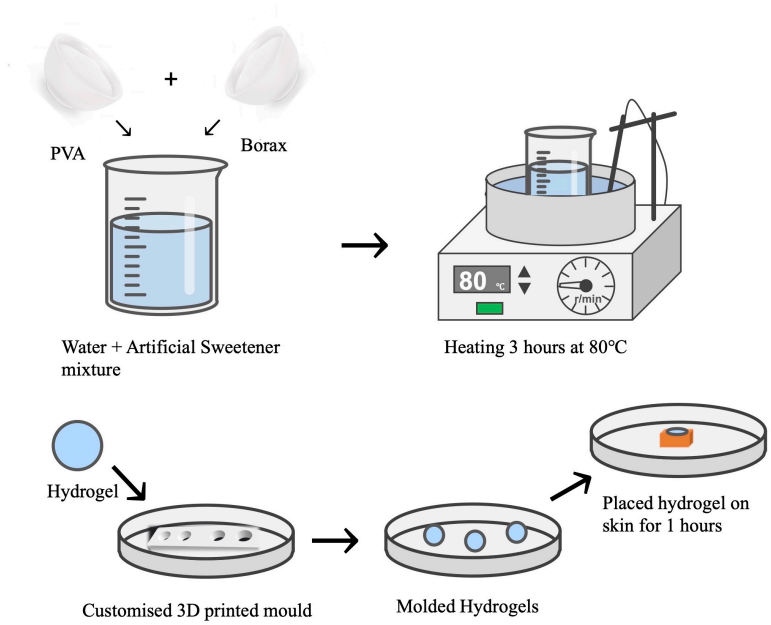

Figure 2.1 Illustration of AS-Loaded PVA-Borax Hydrogel preparation. Steps include: (1) transferring PVA, AS and borax into a beaker with water (2) The beaker was heated for 3 hours at 80°C (3) Hydrogel was transferred into petri dish with 3-D printed mould (4) Removed hydrogels from mould. (5) Hydrogel was placed on the infected skin.

2.3.2 Preparation of Freezing- Thaw (FT) AS-loaded PVA Hydrogel

The PVA (Mw=115,000,100% hydrolysed, Sigma-Aldrich) (10% 5% or 3%, w/w) were weighed and added into a sterile conical flask with sterile water. The solution was heated by a magnetic water bath at 80°C for 3 hours in order to reach a homogeneous state. After 3 hours, SACC, Ace-K or CYC were added in different PVA solution flasks, then stirred for another 1 hour at 80 °C. Once the solution is obtained, it is transferred into the prepared mound and placed in a freezer at -20°C for 20 hours. After 20 hours, the PVA gels were transferred to the

bench and thawed at room temperature for four hours. Subsequently, it was transferred to the freezer, and this process was repeated for a total of three cycles.

2.3.3 Hydrogel Zone of Inhibition Assays (ZOI)

The OD_{600} was adjusted to 0.5 McFarland standard from *A. baumannii* AB5075 overnight culture using Luria- Bertani (LB) Broth (ThermoFisher) (CLSI, 2015). The Kirby-Bauer disc diffusion method was used. The whole plate was swabbed five times in a linear pattern with *A. baumannii* AB5075 from 0° to 180°, followed by a sixth swab along the circumference to ensure even distribution at the edges (Figure 2.2). Moulded hydrogel (0.6 g) was plated on top of agar and then incubated for 18 or 24 hours at 37°C. Three biological replicates of the zone of inhibition were measured by following: (d2-d1) to avoid uneven distribution of the PVA-borax hydrogel.

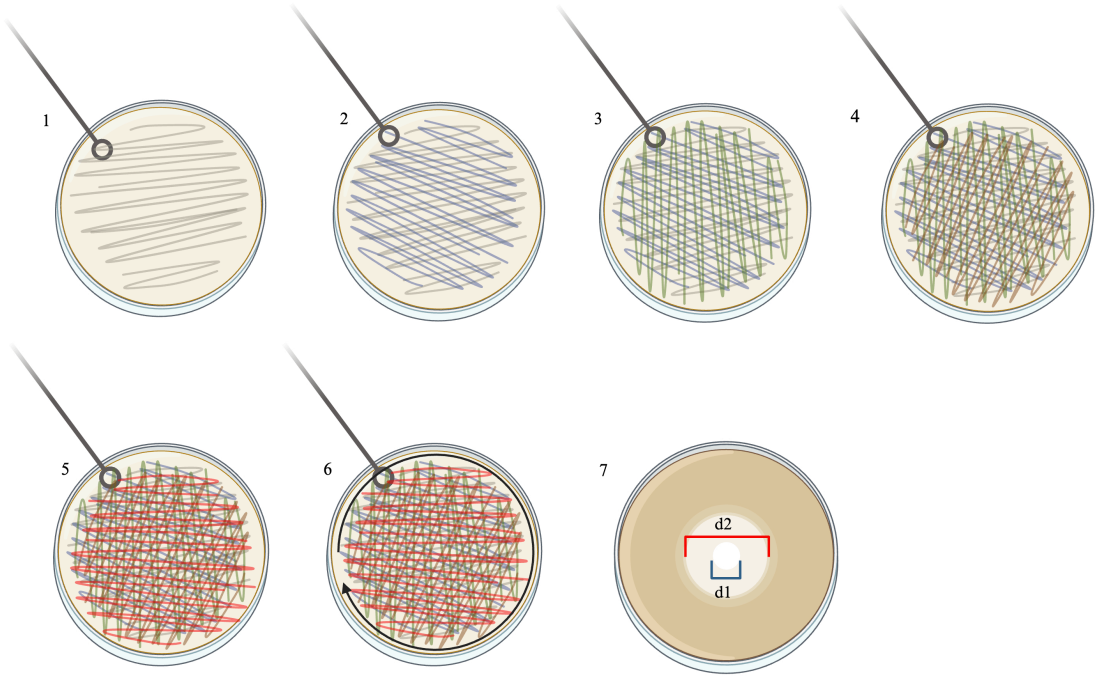

Figure 2.2 Illustration of *A. baumannii* AB5075 inoculation using the Kirby–Bauer disc diffusion method. The agar plate was swabbed five times (every 45°) in a linear pattern from

0° to 180°, followed by a sixth swab along the circumference to ensure even distribution at the edges. Created in BioRender.

The agar plate was swabbed five times (every 45°) in a linear pattern from 0° to 180°, followed by a sixth swab along the circumference to ensure even distribution at the edges. Created by biorender.com.

2.3.4 Antimicrobial Time-Kill Assay and Drug Release Profile

Control hydrogels and AS-loaded hydrogels were prepared, weighed (0.6 g), and placed each gel into a well of sterile 24-well plates and incubated for 15 minutes at 37°C to ensure that the hydrogel fully covered the bottom of each well. A 1 mL suspension of *A. baumannii* AB5075, adjusted to an OD_{600} of 0.5 from an overnight culture, was then added on top of each hydrogel, and the plates were incubated at 37°C. This setup was repeated for each time point (0, 2, 4, 6, 8, and 24 hours), and at each time point, the bacterial suspension from each well was collected, serially diluted, and plated to enumerate viable cells (Figure 2.3).

The *in vitro* drug-release behaviour of the drug-loaded hydrogel was evaluated using a modified pharmaceutical dissolution test. The hydrogels were placed in 25 mL solution at pH 7.4 and pH 5.5 at 100 rpm at 37 °C in a KS 3000 control incubator shaker (IKA, Staufen, Germany). At predetermined time intervals, 2 mL samples were withdrawn and replaced with an equal volume of fresh release medium. The absorbance of the collected samples was measured using UV–Vis spectrophotometry (VWR) at λ = 270 nm, the wavelength of maximum absorption for SACC. Drug content was calculated based on the established calibration curve. All experiments were conducted in triplicate.

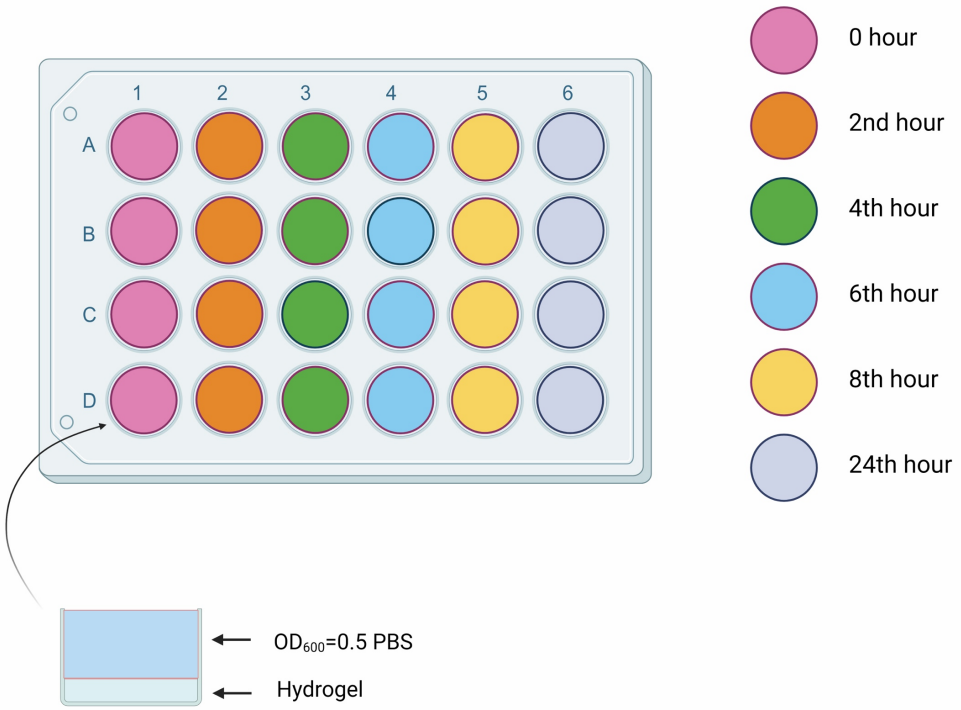

Figure 2.3 Schematic of the time-course assay to assess antimicrobial activity of control and AS-loaded hydrogels against *A. baumannii* AB5075. Hydrogels (0.6 g) were placed in 24-well plates. A 1 mL bacterial suspension ($OD_{600} = 0.5$) was added to each well. Samples were collected at 0, 2, 4, 6, 8, and 24 hours for viable cell enumeration. Coloured wells represent different time points. This figure was created by biorender https://BioRender.com.

2.3.5 Biofilm Assays and Scanning Electron Microscopy (SEM)

The OD_{600} of an *A. baumannii* AB5075 overnight culture was adjusted to 0.05 using sterile phosphate buffer (PBS). 1 mL of molten LB agar was applied to each well and allowed to solidify in a 12 well plate. A 5 µL inoculum of *A. baumannii* AB5075 was applied to the agar surface and allowed to dry. For an early-established biofilm, the inoculated agar was incubated for 3.5 hours at 37°C and then treated with either the control hydrogel or the AS-loaded hydrogel for 1 hour. For muture biofilm, the inoculated agar was then incubated for 24 hours

at 37°C and treat with hydrogels. At time points 0, 2, 4, 6, 8, and 24 hours the treatments were removed, and the biofilm was dispersed with 1 mL sterile PBS and washed for thrice. The collected PBS was serially diluted to 10^{-7} and plated to enumerate viable cells.

For the *ex vivo* assay, fresh porcine belly skin was purchased from Fine Food Specialist (London, UK). To mimic an acute burn wound, an array containing 20 steel pins was heated to 140°C for one hour and placed on the 20 cm^2 pre-cut skin for 60 seconds. The skin was cut into 1.5 cm^2 pieces after the array was removed. Each side of the skin was sterilised under UV light for 30 minutes. The OD_{600} of an *A. baumannii* AB5075 overnight suspension was then adjusted to 0.05 using PBS. A 5 µL inoculum of AB5075 was applied to burnt skin and allowed to dry. The burnt skin was incubated for 3 hours to form an early-stage biofilm representing acute infection. The moulded hydrogel was applied on the top of the infected area. Also, Tegaderm Alginate Silver Dressing from MEDISAVE UK LTD (Dorset, UK) was cut into 1.5 cm^2 pieces and placed on the infected skin. Then, burnt skins were transferred back to the incubator for an extra 1 hour. After incubation, the hydrogel or dressing was removed, and the skin was washed with 1 mL of sterile PBS three times. The collected PBS was serially diluted as before and plated to enumerate viable cells.

SEM was used to examine the biofilm formation of *A. baumannii* when it was exposed to AS-Loaded PVA hydrogels. AS-load hydrogel was added to an OD_{600}=0.1 inoculum with a sterile glass slide and incubated for 24 h. They were immobilised using 2.5% glutaraldehyde, 2% paraformaldehyde, and 0.15% alcian blue in 0.1 M PBS for 2 h, then treated with 1% osmium tetroxide in distilled water, dehydrated, critical-point dried, gold-coated, and observed by SEM (JEOL IT200, JEOL, USA).

2.3.6 *A. baumannii* AB5075 and *P. aeruginosa* PA14 Mixed Culture Assays

In a 12-well plate, 1 mL of molten LB agar was applied to each well and allowed to solidify. The OD_{600} was adjusted to 0.05 for each overnight suspension culture of *A. baumannii* AB5075 and *P. aeruginosa* PA14 using sterile PBS. A 500 µL of *A. baumannii* inoculum and a 500 µL of *P. aeruginosa* inoculum were transferred into a tube and the tube was mixed for 3 times. A 5 µL of *A. baumannii* and *P. aeruginosa* mixture inoculum was applied to the surface of the agar. Once it dried, the agar was incubated for 3.5 hours at 37°C to form a biofilm. The moulded hydrogel was applied to the biofilm. Then, agar was transferred back to the incubator for an additional 1 hour. The hydrogel was removed, and the agar surface was washed with 1 mL of sterile PBS to resuspend the biofilm. The washing process was repeated 3 times, the PBS was collected, and viable cells were enumerated. To enumerate viable cells of *P. aeruginosa* PA14, the *Pseudomonas* isolation agar (Sigma-Aldrich) was used. To enumerate viable cells of *A. baumannii* AB5075*,* 20 mg/mL of gentamicin was added to LB agar. The LB agar was melted and transferred to a 40°C water bath for half an hour. The solution was prepared at a concentration of 20 mg/mL and filtered sterile with a pore size of 0.2 µm. The final concentration of the agar was 20 µg/mL.

2.3.7 Haemolysis Assays and Cytocompatibility Assessment

To evaluate haemolysis, the erythrocytes were collected from horse blood defibrinated (TCS Bioscience, UK) by centrifuging whole blood at 3000 rpm for 10 min, then washing 3 times with PBS to obtain clean erythrocytes. Hydrogel extracts were prepared by incubating hydrogels in PBS at 37 °C for 24 h. For the haemolysis test, the erythrocyte suspension and the mixture were incubated at room temperature for 1 hour, with deionised water as the positive control and PBS as the negative control. The mixture was centrifuged again, and the supernatant was collected and transferred to a 96-well plate. Haemoglobin release was

quantified by measuring absorbance at 541 nm using a CLARIOstar Plus plate reader (BMG Labtech). The haemolysis rate was calculated by following the equation:

$$\text{Haemolysis rate (\%)} = (OD_{exp} - OD_{neg}) / (OD_{pos} - OD_{neg}) \times 100\%$$

where OD_{exp}, OD_{neg}, and OD_{pos} represent the OD values for the experimental, negative, and positive groups (Xin *et al.*, 2025).

Hydrogel cytocompatibility was assessed using an MTT assay on dermal fibroblasts (2DD cell line isolated by Bridger *et al.*, (1993). In 24-well plates, Cells (5×10^4/well) in DMEM supplemented with 10% FBS, 2 mM L-glutamine, and 1% penicillin/streptomycin were incubated at 37°C with 5% CO2 for 24 h. Non-adherent cells were removed by washing twice with PBS, and fresh medium or hydrogel extract medium (500 µL) was added to fibroblast-seeded wells and incubated for 24 h. After treatment, the cells were washed twice with PBS. The assay involved three groups: a blank group (untreated cells), a control group (cells treated with PVA hydrogel extract), and an AS-loaded hydrogel group (cells treated with AS-loaded hydrogel extracts). Cells were then incubated with 500 µL of MTT solution (0.5 mg/mL) for 3 h, after which 250 µL of the MTT solution was removed, and the formazan crystals were dissolved in 750 µL DMSO. Absorbance was measured at 570 nm using a CLARIOstar Plus plate reader (BMG Labtech). Cell viability was expressed as the percentage of absorbance in treated wells relative to untreated wells.

2.3.8 Degree of Swelling and Weight Loss

The degree of swelling was determined by the maximum amount of liquid that hydrogels could absorb (Zhang *et al.*, 2025). In In this experiment, the pH of the PBS solution was set at 7.4 to mimic wound sites. AS loaded PVA Hydrogel was dried at -55 °C overnight to ensure that the final weight remains unchanged, and placed in pH-adjusted PBS for 48 hours at 37 °C. The

weight of hydrogels was measured at 0, 3, 6, 9, 24 and 48 hours. The degree of swelling (DS) was calculated by

$$SD = \frac{m_i - m_0}{m_0}$$

The m_i is the weight at a specific hour, and m_0 is the weight of the dry hydrogel.

The weight loss observed in the hydrogel can be an indicator of its degradation (Zhang *et al.*, 2025). To determine this, the hydrogel was initially dried at -55°C. The dried hydrogels were measured then immersed in a PBS solution with a pH of 7.4 and incubated at 37°C for 48 hours. After incubation, the hydrogels were dried again using a freeze dryer at -55°C. The dry weight of the hydrogel was then measured, and the weight loss was calculated. W_i is the initial dry weight, and W_d is the weight of the re-dried hydrogel after 48 hours of soaking.

$$WL = \frac{W_i - W_d}{W_i}$$

2.3.9 Hydrogel Morphology

SEM was used to characterise the morphological properties of the PVA hydrogels. Samples were freeze dried, mounted onto carbon disc then gold coated and analysed using SEM (Microscope Jeol IT200, JEOL, USA). SEM images at magnifications of 250x were employed to examine the pore size and cross-linking density of the hydrogels after freeze-drying. The pore size of the hydrogels was measured using ImageJ software. The measurements were obtained from SEM images taken at 250x magnification. For each hydrogel, three images were analysed, each covering an area of 512.5µm x 383.9µm.

2.3.10 Rheology

Rheological properties of the hydrogels were measured using a TA Instruments Discovery Core Rheometer (TA Instruments, USA) with a 40 mm parallel plate geometry. A solvent trap was applied to reduce water evaporation during testing. The amplitude sweep was conducted to assess the linear viscoelasticity of the hydrogel, and the frequency sweep was performed to determine the gel stiffness. The strain range of the amplitude sweep was 0.01-100% at 1 Hz. The frequency sweep was measured between 0.1-100 rad/s at 0.1% strain. All measurements were performed at 37°C to mimic physiological conditions. All tests were conducted in triplicate.

2.3.11 Attenuated Total Reflectance–Fourier Transform Infrared Spectroscopy (ATR-FTIR) and X-ray diffraction (XRD)

Fourier Transform Infrared (FTIR) spectroscopy was measured by using Spectrum One (PerkinElmer, USA) used to investigate the chemical interaction between the functional groups in the cross-linked structure of the hydrogels. FTIR spectra were used to study the structural changes in PVA hydrogel loaded with different AS. Samples were compared for the identification of any shifts or variations in the characteristic peaks, which could reflect changes in the bonding pattern and interaction between PVA and the sweetener molecules. Measurements were taken in a wavelength region of 600–4000 cm^{-1} with 10 scans. The crystalline profiles of AS-Loaded hydrogels were studied using an X-ray diffractometer (D8 Advance, Bruker). The X-ray source used Cu-Ka radiation at 40 kV and 40 mA; 2θ was from 5 to 100.

2.3.12 Phase 1 Clinical Study in Humans

To explore the short-term dermal compatibility of AS-Loaded PVA-borax hydrogel in healthy human volunteers, with a focus on assessing any immediate skin reactions or adverse effects.

A Phase 1 clinical study in humans was conducted. This experiment protocol was accepted by the University Research Ethics Committee (UREC) at Brunel University London, UK. The Ethical approval number is 47765-MHR-Nov/2024-53276-3**.** In the study, 12 healthy adult volunteers aged 18-65 from Brunel University of London were recruited. All participants had no irritated or abraded skin at the measurement sites and had not suffered from any skin conditions, including eczema and dermatitis. The participant's skin condition was assessed by a self-questionnaire and the researcher. Four skin sites were chosen: lower left forearm (LL), upper left arm (UL), lower right forearm (LR), and upper right arm (UR). Each site had an area of skin 1.5 x 3 cm tested. On each site, 3 replicates of hydrogel were applied and monitored. A film dressing (TEGADERM Film Dressings, 3M) was applied on top of hydrogels. All participants were observed at 1, 3, 6, 9, and 24 h.

2.3.13 Statistical Analysis

Data are expressed as mean ± standard deviation (SD). Statistical analyses were performed using GraphPad Prism and Origin Pro. Two-way ANOVA with Tukey correction and one-way ANOVA with Dunnett's correction were used. Statistical significance was established at p-values of < 0.05 (*), 0.01 (**), 0.001 (***) or 0.0001 (****).

2.4 Results:

2.4.1 Formulation of Artificial Sweetener (AS) Loaded PVA-based Hydrogel.

The artificial sweeteners Ace-K, SACC and CYC have displayed promising therapeutic potential when administered in solution in *in vitro* assays (de Dios *et al.*, 2023, 2025). Proper wound care is essential for promoting healing, preventing infection, and minimising patient discomfort. Inadequate management can lead to prolonged treatment due to bacterial colonisation and infection, underscoring the need for effective wound dressings that combine protection with antimicrobial functionality (Q. Zhang *et al.*, 2022). A major roadblock to the translation of novel antimicrobials is effective delivery solutions that can be applied *in vivo*.

PVA-based hydrogels can be prepared using different crosslinking approaches, including chemical and physical crosslinking. Common approaches for physical and chemical cross-linking of PVA include freeze–thaw cycling and borax cross-linking (Zhong *et al.*, 2024). To determine a suitable crosslinking approach for incorporating artificial sweeteners while maintaining hydrogel integrity and antimicrobial activity, both approaches were investigated. First, different PVA-borax formulations were screened to optimise the structural stability of the AS-loaded hydrogels. Initial tests showed that the addition of 3% (w/w) AS resulted in phase separation among AS, water, and the gel matrix, causing turbidity and instability in several formulations (Figure 2.4). To solve this, a series of hydrogels were prepared by combining 3%, 4%, 5%, 6% and 8% (w/w) PVA with 0.3%, 0.6%, 1%, 2%, 3%, 4% and 5% (w/w) sodium tetraborate (borax), each with 4%, 6% and 8% (w/w) of AS. When 4% (w/w) artificial sweetener was added, hydrogels made with 3%, 4%, and 5% (w/w) PVA and 2%–5% (w/w) borax remained structurally stable. However, when the AS concentration was increased to 6% (w/w), only 3% PVA combined with 2%–5% borax produced stable hydrogels. The 4%

PVA also formed hydrogels under these conditions. However, the hydrogel began to change from transparent to milky in appearance, and phase separation occurred during the transition, which was within 30 minutes. At 8% (w/w) AS concentration, only the 3% PVA with 3%–5% borax resulted in structurally stable gels, while all other tested formulations failed to form hydrogels or exhibited phase separation. Based on these results, the formulation of 3% PVA and 3% borax was selected for all subsequent experiments, as it consistently supported gel formation across all AS concentrations tested (4%, 6%, and 8%) while maintaining adequate mechanical and visual stability (Table 2.1).

A B

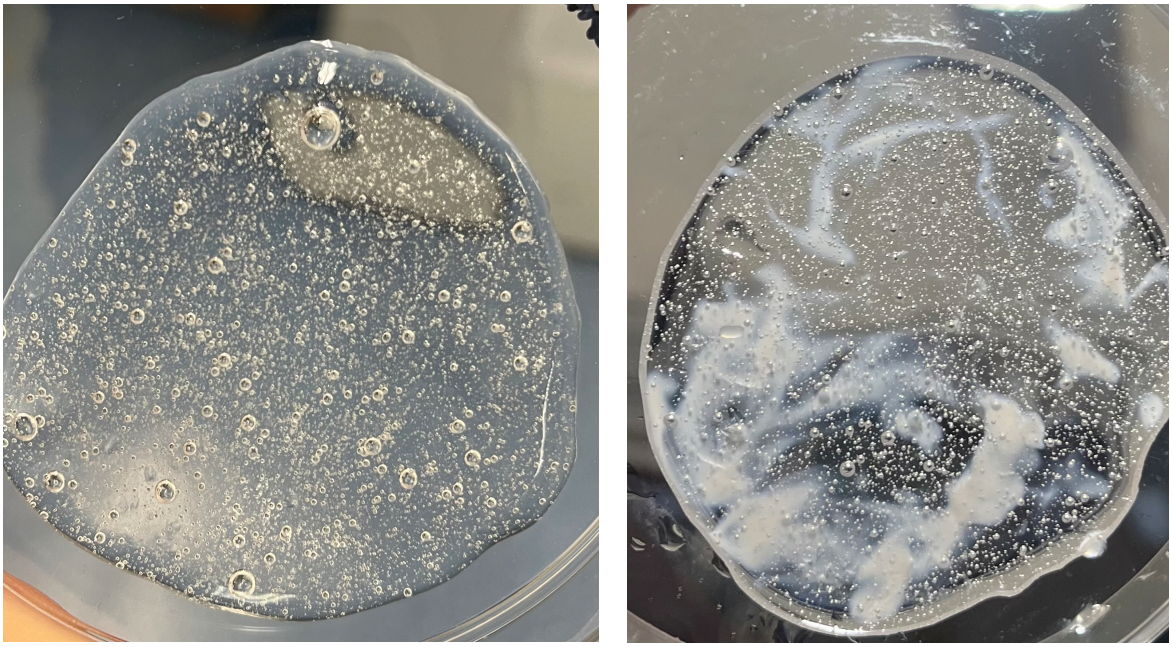

Figure 2.4 Image of 3% Ace-K loaded hydrogel (A) Digital photos of the 3% Ace-K loaded hydrogels (after 1 minute). (B) Digital images of the 3% Ace-K loaded hydrogels (after 30 minutes).

Table 2.1 Formulation screening of AS-loaded PVA–borax hydrogels and their structural stability

PVA(% w/w)	AS (%w/w)	Borax (%w/w)	Gel formation
3, 4, 5, 6 ,8	4	0.3, 0.6%, 1%	Phase separation, low elastic, brittle gel
3, 4, 5	4	2%–5%	Stable gel
6 ,8	4	2%–5%	Phase separation, low elastic, brittle gel
3	6	2%–5%	Stable gel
4, 5	6	2%–5%	Phase separation, low elastic, brittle gel
3	8	3%–5%	Stable gel
3	8	2%	Phase separation, low elastic, brittle gel

AS-loaded FT-PVA hydrogels were developed and evaluated concurrently. The rationale behind evaluating the freeze thaw method as a crosslinking approach is the chemical cross linking can alter the mechanical properties by adding AS and resulting in phase separation and increased brittleness and crumbling when forced to significant pressure. As a result, AS-loaded FT-PVA hydrogel solved previous problems such as stability. The hydrogel will stay in shape in long period of time both in room temperature and 37°C. Moreover, adding different sweeteners also has a substantial impact on the physical properties of the hydrogel. For example, by adding SACC can lead to softer and more transparent gel. The higher the concentration of SACC, the softer the gel was (Table 2.2).

Table 2.2 Formulation screening of AS-loaded FT-PVA hydrogels and their structural stability

PVA(% w/w)	AS (%w/w)	Gel formation

10	10%,8%, 6%	Stable gel
5	10%,8%, 6%	Stable gel, the SACC gels are softer and more transparent at higher concentration.
3	10%,8%, 6%	Stable gel, the SACC gels are softer and more transparent at higher concentration.

2.4.2 Artificial sweetener-loaded hydrogels showed antimicrobial activity in the disk diffusion assay.

After developing the PVA-borax AS hydrogel formulae, the hydrogels were tested for their antimicrobial properties using the disk diffusion method. Ace-K, SACC and CYC-loaded hydrogels showed significant dose-dependent antimicrobial properties when compared to the control hydrogel when assessed against a multidrug-resistant clinical isolate of *A. baumannii*. As shown in Figure 5, the higher the concentration of AS, the more antimicrobial activity it is. For 1%-2% Ace-K-loaded hydrogels, the average zone of inhibition (ZOI) was larger (4.83 mm and 5.33 mm) compared to control hydrogels (3.5 mm). The control gel also had a ZOI, which is in agreement with the known antiseptic effect of borate (Sun *et al.,* 2024). The CYC-loaded hydrogels showed concentration-dependent antimicrobial effects similar to other developed AS hydrogels. CYC hydrogels start to show significant antimicrobial activity compared with the control gels beginning at concentrations of 4%. Notably, the antimicrobial efficacy significantly increased at 4%, 6%, and 8% CYC concentrations, with average ZOI values of 5.83 mm, 7.17 mm, and 8.83 mm (Figure 2.5A). For Ace-K hydrogels, there was a substantial increase in ZOI when the concentration of Ace-K increased from 4% to 6% and 8%, showing an average ZOI of 5.5, 6.17 and 8 mm. (Figure 2.5B) The ZOI for the 1% SACC hydrogel was 4.16 mm, for the 2% SACC hydrogel it was 5 mm, and for the 4% SACC hydrogel it was 5.17 mm. The 6% SACC-loaded hydrogel exhibited an average ZOI of 5.67

mm, while the 8% SACC -loaded hydrogel showed an average ZOI of 7 mm (Figure 2.5C). All three AS-loaded hydrogels at 6% and 8% concentration showed the highest antimicrobial activity and therefore, they were selected for further study.

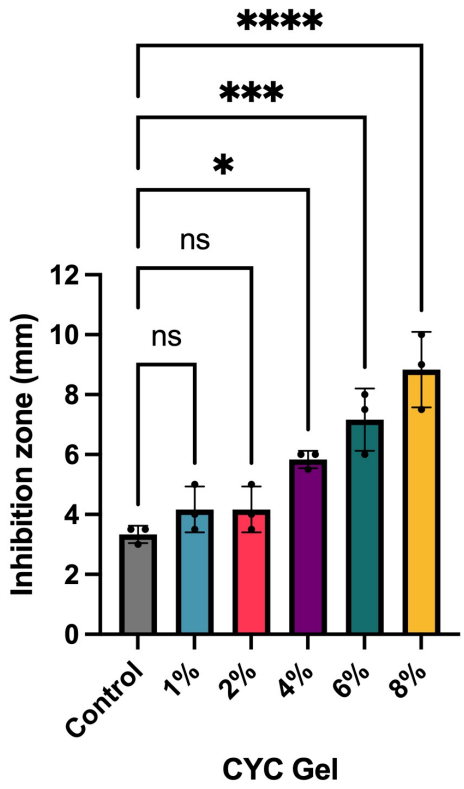
****
***
*
ns
ns
Inhibition zone (mm)
0
2
4
6
8
10
12
Control
1%
2%
4%
6%
8%
CYC Gel

A

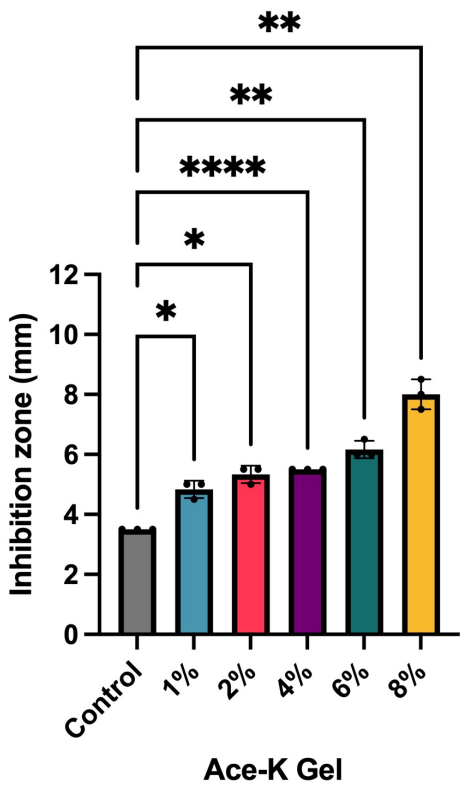
**
**
****
*
*
Inhibition zone (mm)
0
2
4
6
8
10
12
Control
1%
2%
4%
6%
8%
Ace-K Gel

B

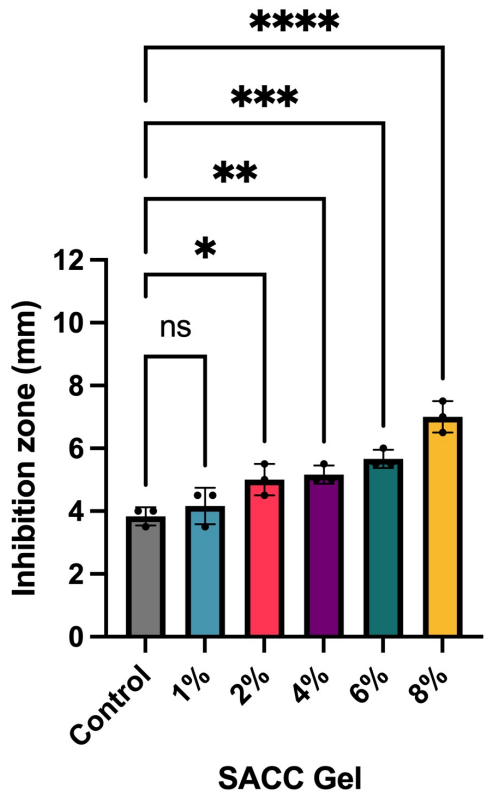
****
***
**
*
ns
Inhibition zone (mm)
0
2
4
6
8
10
12
Control
1%
2%
4%
6%
8%
SACC Gel

C

Figure 2.5 Antimicrobial activity of hydrogels loaded with (A) Ace-K, (B) SACC and (C) CYC against *A. baumannii*, assessed by disk diffusion assay. Antimicrobial activity increases proportionally with AS concentration. Among all AS-loaded hydrogels, CYC hydrogel showed the Largest ZOI at 8%. The ZOI increased significantly with higher concentrations of Ace-K (≥4%), SACC (≥6%), and CYC (≥4%), compared to control hydrogels. Data represent the mean ± SD from three biological replicates. Statistical significance was determined by ordinary one-way ANOVA (ns>0.05, *p-value < 0.05,**p-value < 0.01, *** p-value < 0.001, **** p-value < 0.0001)

2.4.3 Artificial Sweetener-Loaded Freeze-Thaw PVA Hydrogels Antimicrobial Activity is Associated with the Concentration of PVA.

To investigate the impact of different crosslinking methods on the antibacterial efficacy of PVA hydrogels, we also prepared FT-AS-loaded hydrogels. To understand the efficacy of FT-AS-loaded hydrogel's antibacterial properties. AS-loaded FT-PVA hydrogels were prepared and tested at 8% w/w PVA and varying AS concentrations. 8% FT-PVA AS-loaded hydrogels were tested on both agar and the burnt porcine skin model. As a result, all the AS-loaded hydrogels showed better antibacterial properties than the control FT-PVA hydrogel. In the *in vitro* model, the 8% SACC FT-PVA hydrogel shows the best antibacterial properties among the three hydrogels. The 8% SACC FT-PVA hydrogel demonstrated a 2.32 log reduction in viable *A. baumannii* cells compared to the control FT-PVA hydrogel. The 8% Ace-K FT-PVA hydrogel exhibited a 1.77 log reduction, and the 8% CYC FT-PVA hydrogel exhibited a 1.57 log reduction (Figure 2.6).

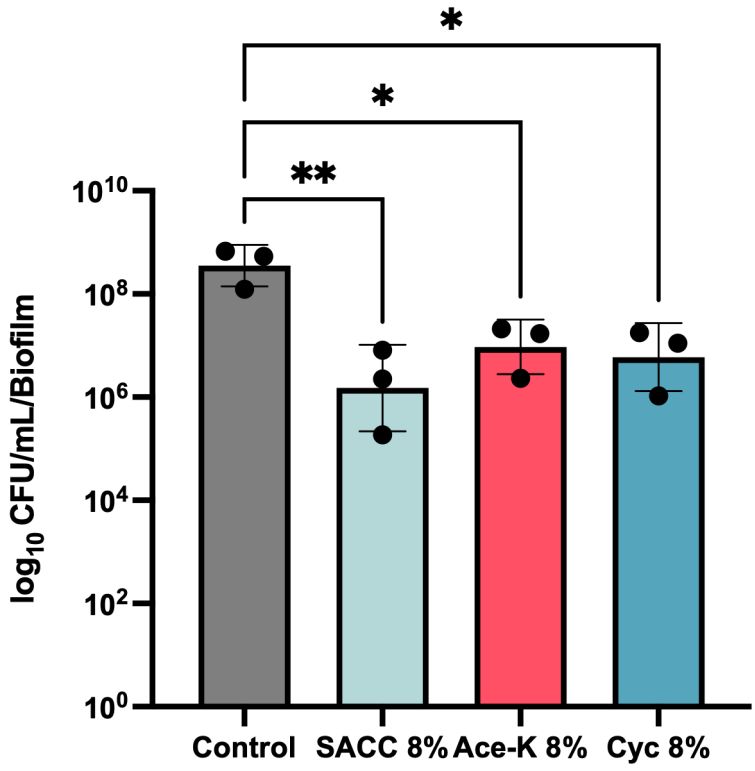

Figure 2.6 Antimicrobial activity of FT-PVA hydrogels loaded with Ace-K, SACC and CYC against *A. baumannii*, assessed by disk diffusion assay**.** Data demonstrate the mean of three biological and 3 technical replicates. Error bars represent standard deviation (SD). Statistical analysis was performed through ordinary one-way ANOVA between the control and treated samples for 8 % Ace-K, SACC and CYC FT-loaded hydrogels. (*p-value < 0.05,** p-value < 0.01)

To determine whether the concentration of PVA and AS affects antimicrobial efficacy, varying concentrations of PVA were tested. Antimicrobial efficacy was assessed using the ZOI method. The hydrogel contains 3 different AS with different concentrations (0%, 2%, 4%, 6%, 8%), which were papered with varying PVA concentrations (3%, 5%, and 10%), and were assessed using the ZOI method (Figure 2.7).

The ZOI increased with the concentration of AS increased. Moreover, the ZOI values of 10% PVA hydrogels were generally lower than those observed for the 3, 5% PVA hydrogels (Table 2.3). The control group showed no inhibition since the PVA itself does not have an antibacterial property. For 10% FT-PVA SACC hydrogels, 2% SACC hydrogel exhibited no ZOI. At 4% SACC, a small ZOI of average 0.544 mm was observed. As the concentration increased, the ZOI increased as well. The ZOIs for 6% and 8% SACC were measured at an average of 1.22 mm and 3.22 mm, respectively. The average ZOI was 4.5mm at 10% SACC (Figure 2.7A). For CYC gels, the average ZOI was 3.05 mm at 10% CYC. The rest of the hydrogel showed no inhibition (Figure 2.7D). For 10% PVA Ace-K hydrogel, the average ZOI of 4% was 0.62mm and increased to 1.67mm at 6%. At 8% and 10%, the average ZOI were 2mm and 3.05mm (Figure 2.7G).

In Figure 2.7B, the ZOI of 5% PVA/SACC hydrogel were shown. In the result, the control (0% sodium saccharin) showed no inhibition. The ZOI for 2% SACC was minimal, ranging from 0 to 0.33 mm. As the SACC concentration increased, the ZOI grew significantly, with a maximum ZOI of 7 mm and an average of 5.83mm at 10% SACC. Intermediate concentrations also showed considerable antimicrobial activity, with average ZOIs of 1.22 mm for 4% SACC and 3.44 mm for 6% saccharin. The 8% SACC hydrogel exhibited ZOIs ranging from 3 to 5 mm with an average of 4 mm. For the 5%PVA CYC hydrogel, there was no inhibition for the control and 2% CYC loaded hydrogel. The inhibition started to be shown at 4% with a 0.44mm zone. At 6%, the zone increased slightly to 0.67mm. At 8% and 10%, the zone increased significantly to 2.44mm and 3.16mm (Figure 2.7E). For the 5% PVA Ace-K hydrogel, the inhibitory effect started to appear at 4% with an average of 2.44mm. The ZOI increased with increasing concentration. They were 2.89mm, 3.22mm and 3.89mm at 6%, 8% and 10% (Figure 2.7H).

The 3% PVA hydrogel showed the highest ZOI values among the different PVA concentrations, which is consistent with other studies reporting that lower PVA concentrations are associated with improved drug release (Rahman Khan and Rumon, 2025). A lower polymer concentration is associated with reduced crystallinity, increased porosity, reduced cross-linking density and greater water absorption. (Waresindo *et al.*, 2023; Liang *et al.*, 2024). The lower cross-linking density can lead to accelerated drug transport and release (Anwar *et al.*, 2026). The control hydrogel displayed no antimicrobial activity. The ZOI for 2% SACC was absent in all trials. For the 4% SACC in hydrogel, the ZOI ranged from 1.66-2.16 mm. The 6% SACC hydrogel showed substantial inhibition, with ZOIs ranging from 4.16 to 5.33 mm. The highest antimicrobial activity was observed in the 10% SACC hydrogel, with ZOIs ranging from 6.66 to 7.66 mm (Figure 2.7C). CYC hydrogel continues to show lower inhibition when compared with other AS hydrogels. At 6% the average ZOI was 0.56mm. At 8% and 10%, the average ZOI were 1.39 and 3.22mm (Figure 2.7F). In Figure 2.7I, the ZOI of 3% FT-PVA hydrogel loaded with Ace-K is shown. For the 4% Ace-K hydrogel, the average ZOI was 0.62mm. The 6% Ace-K hydrogel showed slightly increased inhibition, with an average 1.17mm ZOI. The highest antimicrobial activity was observed in the 10% Ace-K hydrogel, with 3.56mm ZOI. The 8% Ace-K hydrogel showed a slightly lower ZOI when compared with 10% Ace-K hydrogel, with 2 mm ZOI. In this assay, the 5% and 3% FT-PVA hydrogel shown better antibacterial properties.

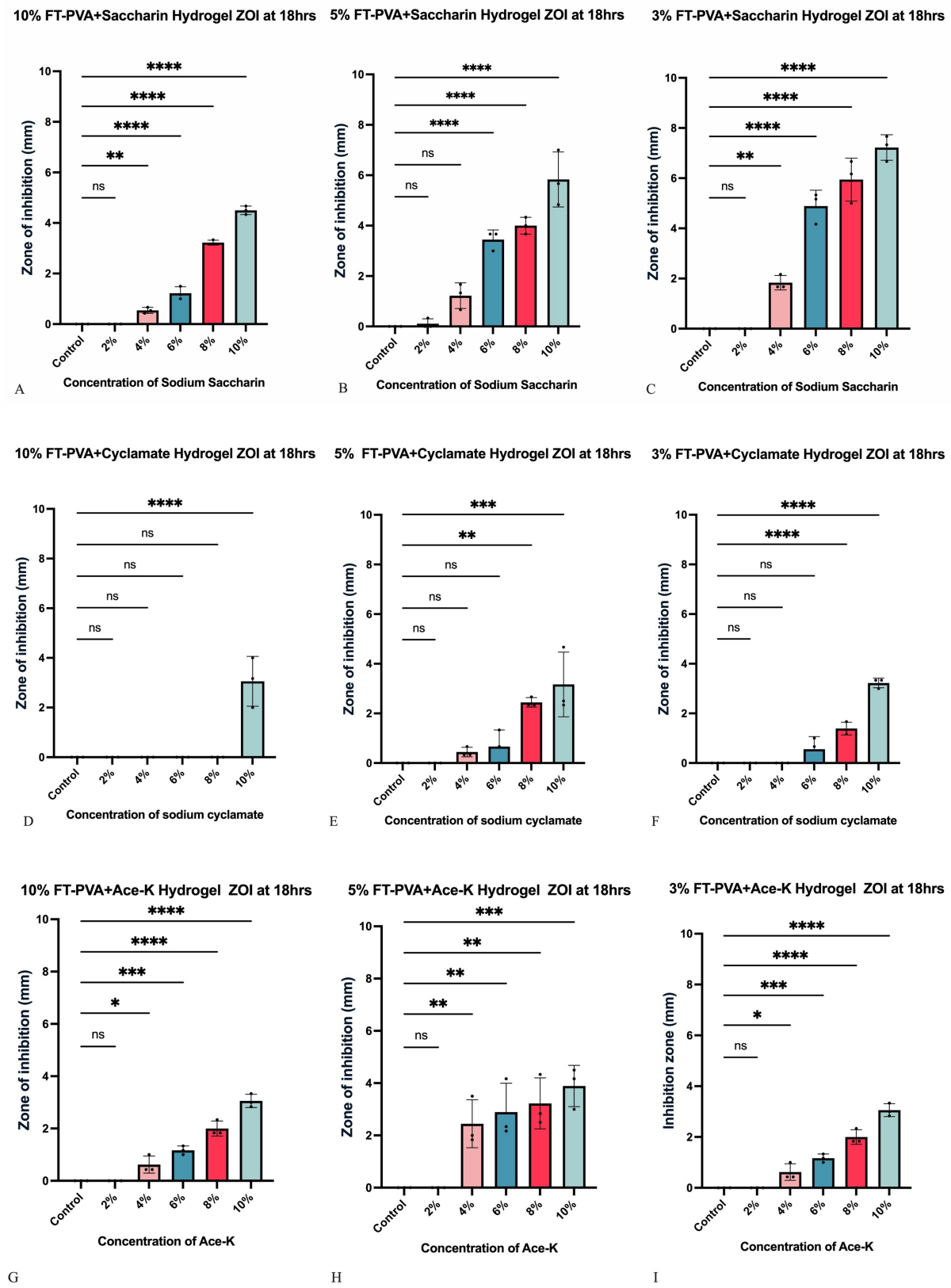

Figure 2.7 Bar chart of the ZOI of FT-PVA Hydrogel against *A. baumannii*. The chart illustrates the relationship between sweetener concentration (0% to 10%) and polyvinyl alcohol

(PVA) percentages (3%, 5%, and 10%) on the measured values of hydrogels loaded with Saccharin, Cyclamate, and Ace-K after 18 hours. Overall, increasing sweetener concentration results in higher measured values across all sweeteners and PVA percentages. Notably, SACC-loaded FT-PVA hydrogels exhibit the highest measured values under the same conditions, indicating the best inhibition among the sweeteners tested. Lower PVA percentages (3% PVA) show higher ZOI in SACC AND Ace-K gel at 10% concentration, suggesting enhanced release of the sweeteners in hydrogels with lower PVA content. Data demonstrate the mean of three biological and 3 technical replicates. Error bars represent standard deviation (SD). Statistical analysis was performed through ordinary one-way ANOVA between the control and AS loaded samples for (ns >0.05, * p-value < 0.05, ** p-value < 0.01, ***p-value <0.001, **** p value < 0.0001).

Table 2.3 Comparison of ZOI values of SACC-, CYC-, and Ace-K-loaded hydrogels prepared with different PVA concentrations.

	Mean values of ZOI		
	10%PVA (mm)	5% PVA (mm)	3% PVA (mm)
8% SACC	3.22	4	5.94
8% CYC	0	2.44	1.38
8% Ace-K	2	3.22	2
10% SACC	4.5	5.83	7.22
10% CYC	3.05	3.16	3.22
10% Ace-K	3.05	3.89	3.05

2.4.4 AS-Loaded Hydrogels Show Time-Dependent Inhibition of *A. baumannii* Viability *in vitro*

For hydrogel wound dressing applications, the treatment interval typically ranges from 1 to 3 days. A slow release of the AS profile can prolong its activity at the wound site and help prevent bacterial contamination during the treatment period and also be more effective against established biofilms (Gámez-Herrera *et al.*, 2020; Britto *et al.*, 2025). In earlier results, all PVA-based AS-loaded hydrogels exhibited dose-dependent antimicrobial activity against *A. baumannii*. Moreover, this effect was more pronounced when higher amounts of AS were loaded, as more AS was released from the gel matrix (Figure 2.8) The key metric here is antimicrobial activity, so to determine whether slow-release kinetics at concentrations sufficient to mediate antimicrobial activity could be achieved from the AS-loaded hydrogels, the hydrogels were submersed in PBS containing a known concentration of bacterial cells. PBS was used to limit the bacterial proliferation while maintaining cell viability. This approach would ensure any changes in bacterial counts were primarily attributable to AS activity.

The samples were collected every 2 hours from 0 hour to 8th hour. Figure 2.8A&B shows the AS release from the PVA borax hydrogel matrix in a time-dependent manner because *A. baumannii* cell viability reduced over time. Most significantly, after 24 hours, all AS-loaded PVA borax hydrogels showed a significant reduction, whereas the bacterial cell count in the control gel was reduced by only around 1.03 log CFU/mL compared with the untreated group. Among all AS-loaded hydrogels, both Ace-K and CYC demonstrated the most potent antimicrobial activity. After 24 hours, hydrogels loaded with 6% AS showed an average bacterial reduction of ~5.30 log in CFU count compared to the growth control. The 6% CYC-loaded hydrogel exhibited the highest reduction of ~6.29 log CFU/mL, followed by the 6% Ace-K-loaded hydrogel with a ~5.49 log CFU/mL of reduction and the 6% SACC-loaded hydrogel with a ~4.10 log of reduction in CFU count (Figure 2.8A&C). Increasing the AS

concentration further enhanced inhibition as an indication of higher AS release over time. Hydrogels loaded with 8% AS achieved an average bacterial reduction of ~6.13 log in CFU count compared to the growth control. The 8% CYC-loaded hydrogel again demonstrated the highest reduction of ~6.42 log in CFU/mL after 24 h, while the 8% Ace-K-loaded hydrogel achieved a slightly greater reduction of ~6.40 log. The 8% SACC-loaded hydrogel reduced bacterial growth by ~5.56 log. In contrast, the control hydrogel showed a non-significant reduction in CFU count (Figure 2.8B&D). These results highlight the dose-dependent antimicrobial activity of AS-loaded hydrogels, with consistent release over time. The CYC hydrogel provides the strongest inhibition, followed by the Ace-K and SACC hydrogels.

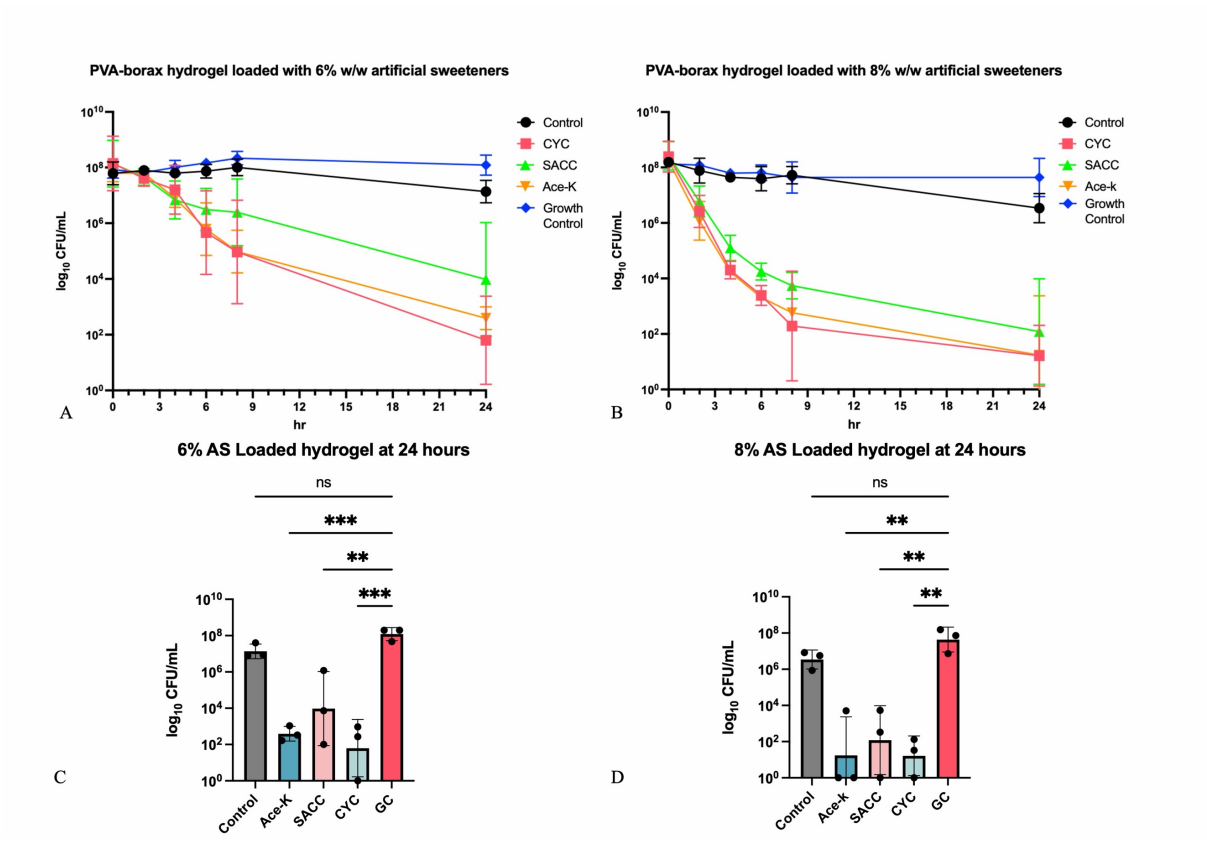

Figure 2.8 AS Loaded-PVA-Borax Hydrogel Effectiveness at 24 hours: (A, B) Antimicrobial profile of AS-loaded hydrogels at different AS concentrations (C, D) Antimicrobial Activity of 6% and 8% AS-Loaded Hydrogels Against *A. baumannii* at 24 Hours. Data demonstrate the

mean of three biological replicates. Error bars represent standard deviation (SD). Statistical analysis was performed by one-way ANOVA between the control and treated samples. (**p-value < 0.01, *** p-value < 0.001)

The releasing profile of FT-PVA hydrogels was also investigated. Most AS-loaded hydrogel showed inhibitory effect was more pronounced when lower of PVA concentration were used, as more AS was released from the gel matrix (Figure 2.9). 3% PVA FT-hydrogel were studied because they outperformed the 10% and 5% FT-PVA concentration in the ZOI assay. The inhibition of *A. baumannii* cells by 3% FT-PVA hydrogels loaded with sweeteners and CYC shows notable variation across different concentrations. In the initial phase, all gels exhibit a similar level of antimicrobial activity. However, by hour 24 the efficacy of AS-loaded FT-PVA hydrogel becomes significantly more pronounced compared to the control gel (Figure 2.9A, B). For the SACC FT-PVA hydrogel, the effectiveness increased relative to the increasing concentration of SACC. The log reductions were 3.69, 3.92, and 5.20. Similarly, Ace-K hydrogel at 6% and 8% concentrations shows less inhibition than SACC hydrogel. The log reductions were 1.27 at 6%, 1.78 at 8%. At 10% concentration, an enhanced antimicrobial effect was observed, with 4.46 log reduction in viable cell count. The 6%, 8%, and 10% CYC gels achieve log reductions of 1.87, 2.04, and 3.62. This confirms the robust antimicrobial potential of the 10% AS-loaded 3% FT-PVA hydrogel against *A. baumannii* (99.9% inhibition). The control gel has an insignificant log reduction, reinforcing the active roles of sweeteners.

The FT-PVA hydrogels exhibited some bactericidal activity. But their efficacy was significantly lower than that of borax-crosslinked PVA hydrogels. In particular, the 10% AS-loaded FT-3%PVA hydrogels exhibit the best performance among all hydrogels. However, there was about only a 3-log (99.9%) reduction in viable cells at the 24-hour time point for all the 10%AS FT- 3% PVA hydrogels (Table 2.4). In contrast, borax-based hydrogels achieved

significantly higher reduction at 24 hours (Figure 2.9C). Due to this significant difference in antimicrobial performance, FT-PVA hydrogels were not pursued further in this study.

A

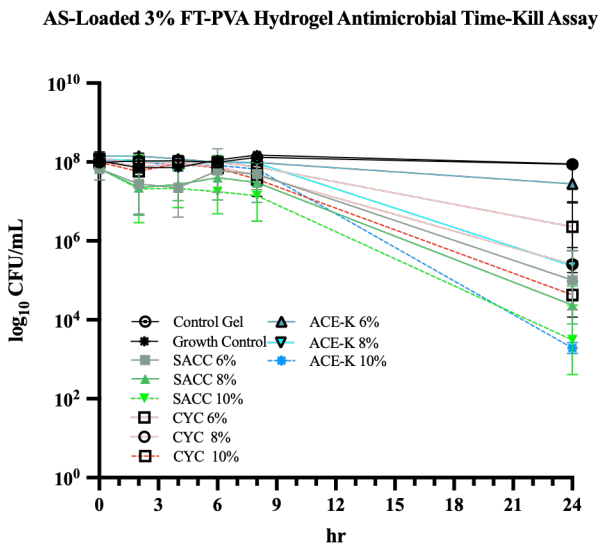

B

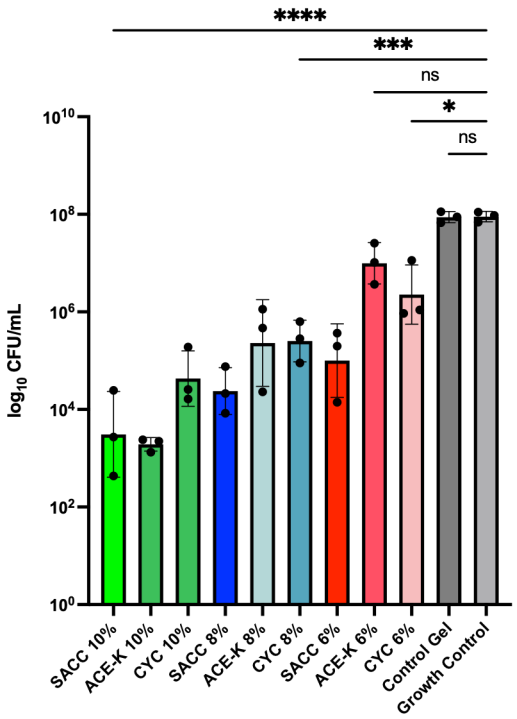

C

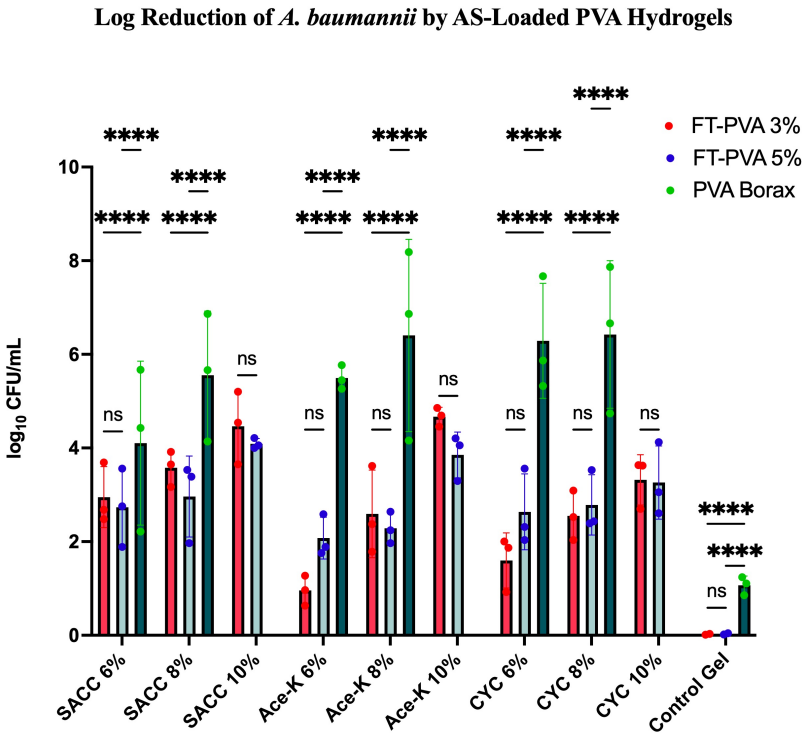

Figure 2.9 This figure illustrates the log reduction in viable *A. baumannii* cell counts over a 24-hour period when exposed to 3% PVA FT-hydrogels loaded with varying concentrations of SACC, Ace-K, and CYC (A) Time-kill assay results for 3% PVA hydrogels with sweeteners, showing *A. baumannii* CFU counts over 24 hours (B) Focused results at 24 hours, displaying CFU log reductions of *A. baumannii* for various sweetener concentrations in 3% PVA hydrogels. (C) Log Reduction of A. baumannii Following Treatment with AS-Loaded PVA Hydrogels Compared with the Untreated Control. Data demonstrate the mean of three 3 technical replicates and biological replicates. Error bars represent standard deviation (SD). Statistical analysis was performed using ordinary one-way ANOVA to compare the growth control with AS-loaded hydrogel samples (A&B). Two-way ANOVA was used to compare the effects of hydrogel formulation (FT-PVA 3%, FT-PVA 5%, and PVA-Borax) and AS concentration on *A. baumannii* growth (C). (ns >0.05, * p-value < 0.05, ** p-value < 0.01, ***p-value <0.001, **** p value < 0.0001)

Table 2.4 Average CFU and Log Reduction of *A. baumannii* by AS-Loaded PVA Hydrogels at 24hrs

Concentration	CFU Log Reduction (3% FT-PVA)	CFU Log Reduction (FT-5% PVA)	CFU Log Reduction (PVA-Borax Hydrogel)
SACC 6%	2.95±0.64	2.73±0.84	4.10±1.75
SACC 8%	3.58±0.38	2.96±0.86	5.56±1.37
SACC 10%	4.46±0.78	4.09±0.11	-
ACE-K 6%	0.96±0.32	2.08±0.45	5.49±0.26
ACE-K 8%	2.59±0.94	2.28±0.34	6.40±2.05
ACE-K 10%	4.66±0.20	3.85±0.49	-
CYC 6%	1.60±0.58	2.64±0.81	6.29±1.23
CYC 8%	2.55±0.53	2.78±0.64	6.42±1.58
CYC 10%	3.32±0.54	3.26±0.78	-
Control Gel	0.01±0.19	-0.05±0.14	1.03±0.27

2.4.5 AS-loaded PVA Borax Hydrogels Exhibit Substantial Antibiofilm Activity Against *A. baumannii in vitro*.

Many antimicrobials show limited efficacy against biofilms with bacteria in a biofilm requiring between 10-1,000 times higher concentration to be eradicated than their planktonic counterparts (Kalia, Patel and Lee, 2023). These sweeteners have demonstrated antibiofilm potential previously via the dysregulation of key genes linked to biofilm formation (de Dios *et al.*, 2023, 2025). To evaluate if this antibiofilm potential was maintained with the AS were formulated part of a hydrogel, we used the colony biofilm agar model, and we initially checked early-stage biofilm (3.5 hours) (de Dios *et al.*, 2023). The control hydrogel (borate-based, without sweeteners) after 1 h treatment demonstrated a reduction (~ 1.98 log CFU; $p < 0.01$) in viable cells of *A. baumannii* when compared with the untreated group, as expected (Figure 2.10A). Notably, loading hydrogels with artificial sweeteners led to significantly enhanced biofilm eradication. The 8% Ace-K hydrogel achieved ~4.00 log reduction in CFUs, which corresponds to more than a 99.99% reduction in viable biofilm cells. SACC and CYC hydrogels demonstrated even higher efficacy, with reductions of 5.44 and 5.67 log CFU, respectively, indicating near complete biofilm eradication after just 1 h of treatment. These results highlight the potent and rapid antibiofilm activity of AS-loaded hydrogels against early-stage biofilms.

In the 24-hour established biofilm model (Figures 2.10B – D), AS-loaded hydrogels showed a significant time-dependent biofilm reduction over 24 h compared to the control gel. The control gel only showed ~1.77 log reduction in CFU/biofilm without further reduction observed up to 24 h when compared with the untreated group, showing the limited effect of the control gel. In contrast, Ace-K hydrogel produced a ~1.74 log reduction at 2 h, with continued decline in biofilm burden over time, reaching ~2.51 log at 8 h and ~4.48 log at 24 h when compared with the untreated group. Similarly, SACC hydrogel caused a ~1.84 log reduction at 2 h, improving

to ~2.82 log and ~4.79 log by 8 h and 24 h. The CYC hydrogel also showed ~1.07 and 2 log reduction in CFU within 2 and 4 h, culminating in 3.94 log reduction after 24 h of treatment. These results confirm a sustained and potent antibiofilm effect likely due to the controlled release of AS from the hydrogel matrix. To visualise these antibiofilm and antibacterial effects, we performed SEM on established biofilms treated for 24 hours with the AS-loaded hydrogels. The SEM image of the AS-loaded hydrogel reveals excellent antibacterial and anti-biofilm properties (Figure 2.10E). In the untreated group, bacterial cells were densely distributed, indicating surface colonisation and biofilm development. The control hydrogel showed a reduction in bacterial cell counts, but numerous attached cells remained visible. Compared to the control and untreated groups, the AS-loaded hydrogel exhibited significantly reduced *A. baumannii*. Moreover, CYC reduces the least amount of *A. baumannii*. This finding aligns with Figures 2.10B, C, and D and further confirms the antibiofilm potential of these AS-loaded hydrogels.

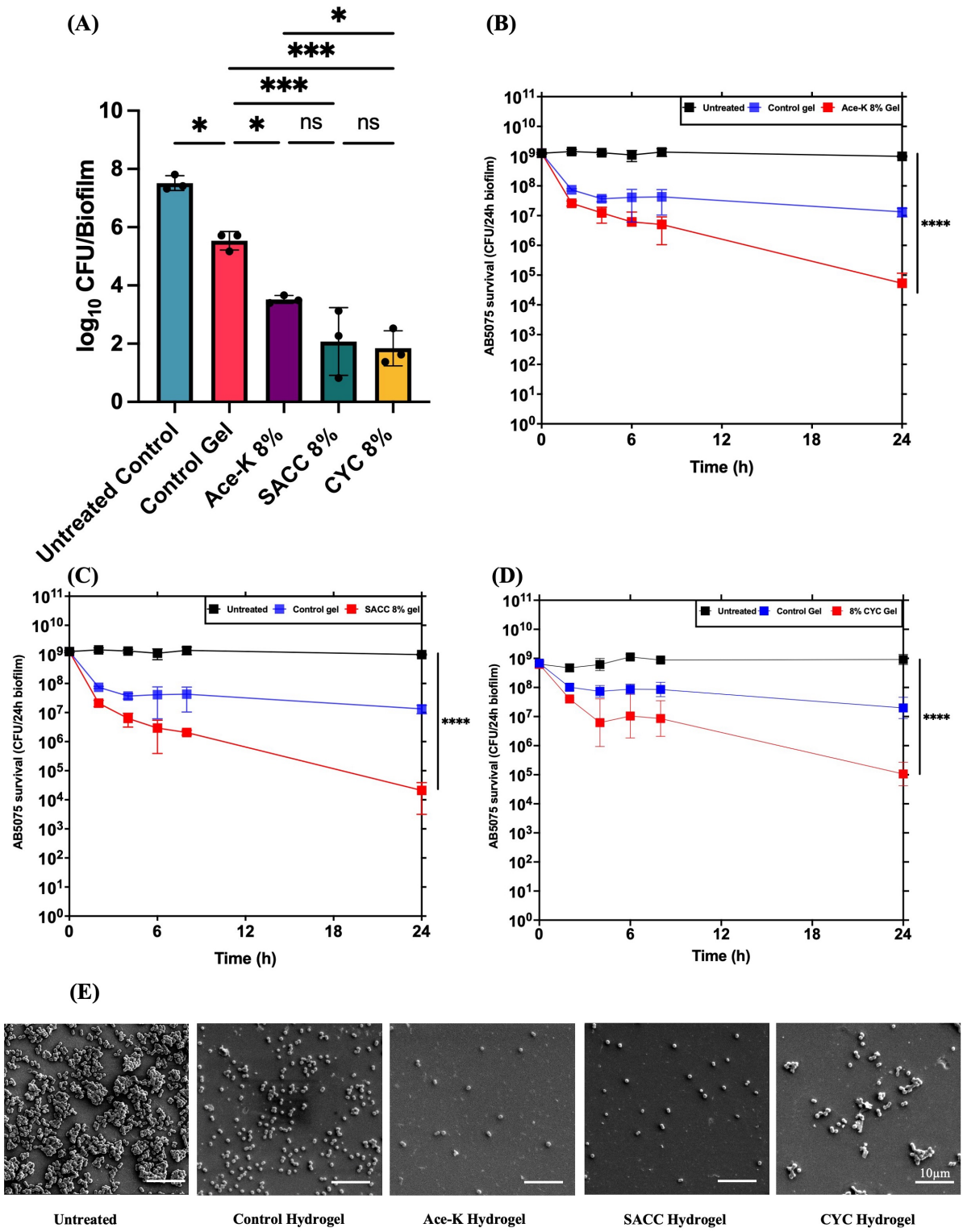

Figure 2.10 Antibiofilm activity of AS-loaded hydrogels against *A. baumannii in vitro*. (A) Viable cell counts ($\log_{10}$ CFU/biofilm) of 3.5h *A. baumannii* biofilms following 1 h treatment with either control hydrogel or 8% AS-loaded hydrogels. Sweetener hydrogels significantly

reduced the biofilm compared to control hydrogel (n=3 ± SD). One-way ANOVA with multiple comparisons was performed to assess statistical significance. (B-D) Time-kill kinetics of mature *A. baumannii* biofilms treated with AS-loaded hydrogels (B) 8% Ace-K, (C) 8% SACC and (D) 8% CYC. CFUs were quantified at 2, 4, 6, 8, and 24 h post-treatment. SACC and Ace-K hydrogels exhibited a sustained and significant reduction in viable biofilm cells over 24 h compared to control hydrogel. (E) Representative SEM image of *A. baumannii* with 24-hour treatment AS-Loaded PVA hydrogel, Control hydrogel and Untreated Control. (n=3 ± SD) One-way ANOVA with multiple comparisons was performed to assess statistical significance. (**p-value < 0.01, **** p-value < 0.0001)

2.4.6 AS-loaded PVA-Borax Hydrogels Outperform Commercial Antimicrobial Silver Alginate hydrogels in *A. baumannii* early biofilm *ex vivo* model.

To further validate the antibiofilm potential of AS-loaded hydrogels in a more clinically relevant setting, a porcine *ex vivo* burn wound infection model was employed to compare their efficacy against a commercially available silver dressing (De Dios *et al.,* 2023). After 1 hour of treatment, the control gel resulted in a slight, yet non-significant, reduction in the *A. baumannii* biofilm burden, indicating limited activity under short exposure times (Figure 2.11). In contrast, all AS-loaded hydrogels demonstrated significantly enhanced antibiofilm activity when compared with the control gel. The Ace-K hydrogel achieved a significant reduction in CFU/biofilm by ~1.48 log, while SACC- and CYC-loaded hydrogels followed a similar pattern of the *in vitro* assay and demonstrated the highest antibiofilm activity, reducing the bacterial cell numbers by ~2.64 and ~2.76 log in biofilm when compared with control gel and ~2.37, ~3.53, and ~3.65 log when compared with the untreated group. These findings indicate a strong and rapid disruption of early biofilms by our developed AS hydrogels, with SACC and CYC showing the most potent effects, with more than 99 % biofilm reduction within 1 h.

Surprisingly, the commercial silver dressing, a widely used standard for topical antimicrobial treatment, showed no significant effect on the *A. baumannii* biofilm under short-term exposure, highlighting the limited efficacy of current frontline treatments against bacterial biofilms. Taken together, these results demonstrate that the AS-loaded hydrogels not only exhibit rapid and potent antibiofilm properties but also significantly outperform the commercial silver dressing under short-contact conditions.

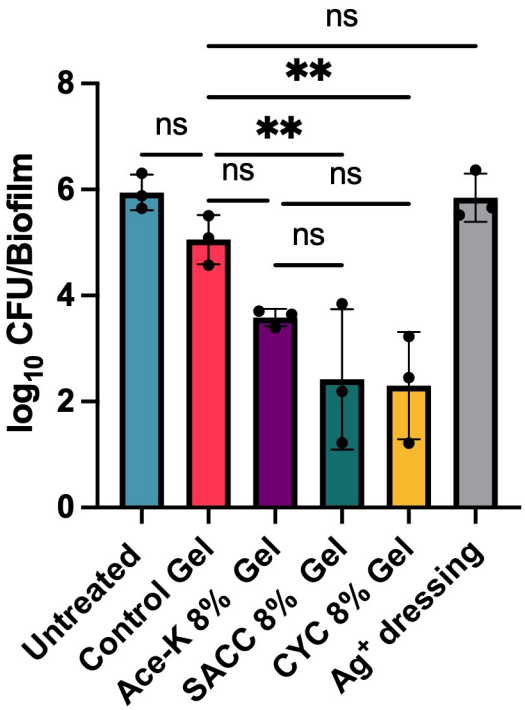

Figure 2.11 Antibiofilm activity of AS-loaded hydrogels against *A. baumannii* in *ex vivo* porcine skin burn wound model. Viable cell counts ($\log_{10}$ CFU/biofilm) of 3.5 h *A. baumannii* biofilms following 1 h treatment with either control hydrogel, 8% AS-loaded hydrogels or silver dressing. Sweetener hydrogels significantly reduced the biofilm compared to control hydrogel and silver dressing (n=3 ± SD). One-way ANOVA with multiple comparisons was performed to assess statistical significance (ns >0.05, ** p-value < 0.01)

2.4.7 AS-loaded hydrogels reduce the biofilm of dual-microbial culture.

In a clinical setting, biofilms are rarely found as monospecies, instead they typically comprise of multiple different microorganisms in a polymicrobial biofilm (Maslova *et al.*, 2021). These polymicrobial biofilms offer even greater protection against the host immune system and antimicrobials which are more difficult to treat (Bertesteanu *et al.*, 2014; Thattaruparambil Raveendran *et al.*, 2019). Apart from *A. baumannii*, *P. aeruginosa* is a major contributor to chronic wound infection, with prevalence rates ranging from 20% to 75% in such infections, making it a key target for treatment (De Oliveira *et al.*, 2017; Phan *et al.*, 2023). To assess the efficacy of AS-loaded hydrogels against a polymicrobial biofilm, we utilised an *in vitro* mixed-culture biofilm model combining *A. baumannii* and *P. aeruginosa*, followed by plating on selective media after treatment which would only allow the growth of either *A. baumannii* or *P. aeruginosa*.

As shown in Figure 2.12, all 8% (% w/w) AS-loaded hydrogels demonstrated significant polymicrobial biofilm inhibition. The CYC-loaded hydrogel had the most potent impact on bacterial survival, reducing *A. baumannii* viable cells by ~4.46 log. SACC and Ace-K-loaded hydrogel demonstrated ~3.56 and ~3.75 log reductions in *A. baumannii* viable cells. All AS-loaded hydrogels demonstrated more than a 3-log reduction compared with the untreated group, while the control hydrogel showed a 1.63-log reduction (Figure 2.12A). This means that all AS-loaded hydrogels achieved 99.9% inhibition.

For *P. aeruginosa* (Figure 2.12B), the CYC-loaded hydrogel achieved the highest efficacy, with a reduction of ~4.38 log compared with the untreated group, followed by SACC (~3.93 log) and Ace-K-loaded hydrogel (~2.19 log), while the control hydrogel showed a 0.97 log.

Given the prevalence of *P. aeruginosa* in chronic wounds and its role in biofilm formation, the broad-spectrum antimicrobial properties of AS-loaded hydrogel present a promising therapeutic approach for managing such complex infections.

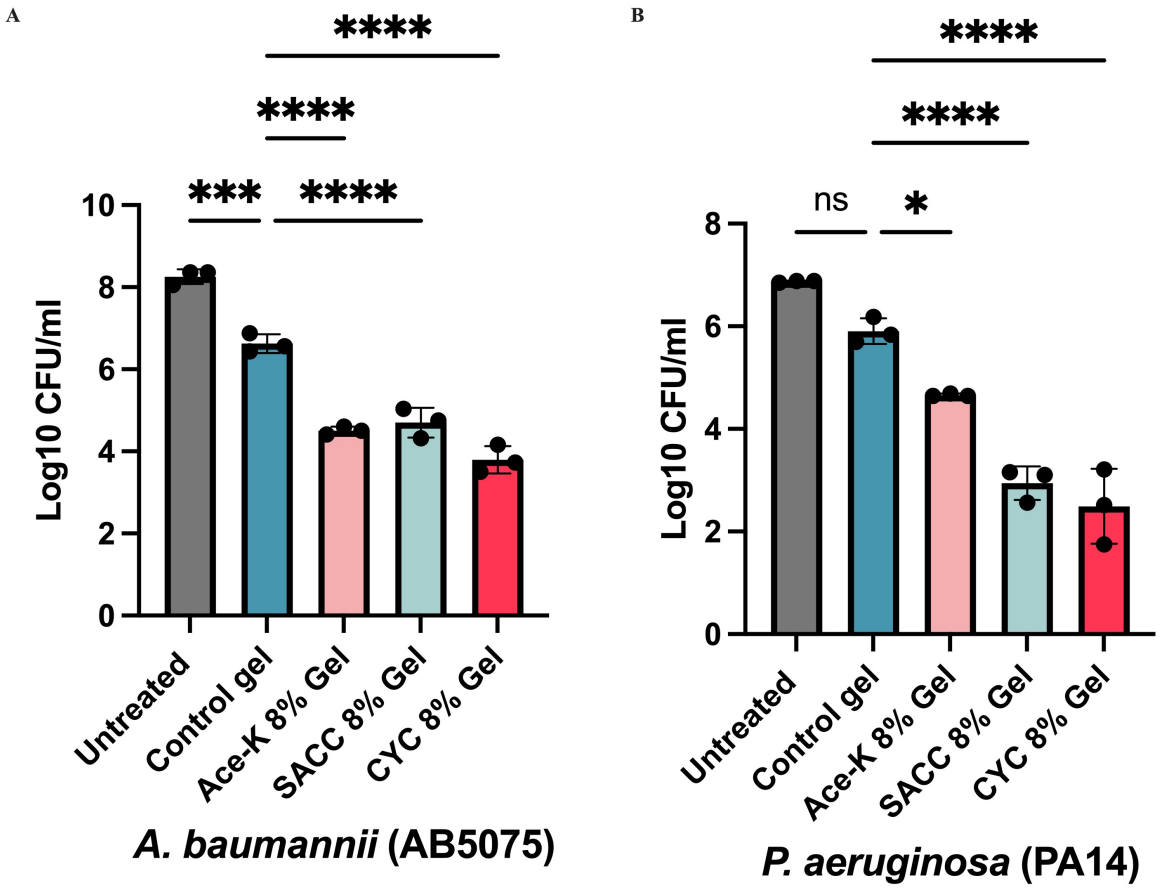

Figure 2.12 Antimicrobial activity of AS-loaded hydrogels against mixed infection biofilm *in vitro*. (A) Viable cell counts (Log_{10}CFU/mL) of *A. baumannii* AB5075 after treatment with AS-loaded hydrogel. (B) Viable cell counts (Log_{10}CFU/mL) of *P. aeruginosa* PA14 after treatment with AS-loaded hydrogel. All AS-loaded hydrogels reduce bacterial viability compared to untreated and control hydrogel groups. The CYC-loaded hydrogels demonstrating the highest ability to against both species. Data demonstrate the mean of three biological replicates. Error bars represent standard deviation (SD). Statistical analysis was performed by one-way ANOVA between the control and treated samples. (ns>0.05, *p-value < 0.05, *** p-value < 0.001, **** p-value < 0.0001).

2.4.8 AS Loaded-Hydrogels Have a Favourable Cytocompatibility Profile

Haemocompatibility is a material's capacity to contact blood without triggering harmful or adverse reactions, which is an important factor for biomaterials. The material has poor blood compatibility, which could lead to unwanted physiological responses such as immune responses, thrombosis, and haemolysis (Zhang *et al.*, 2024). In this study, the blood compatibility of AS-Loaded PVA hydrogels was studied (Figure 2.13A). All the hydrogels have an average haemolysis rate below 1.5%, which is significantly lower than the ASTM (Advancing Standards Transforming Markets) F756-17 standard of 5%. Furthermore, the haemolysis rates of all hydrogels are considered non-haemolytic according to the ASTM standard (0-2%= non-haemolytic, 2-5% = slightly haemolytic and 5% above= haemolytic). Cell viability is widely used to assess the cytotoxicity and biocompatibility of materials for wound-dressing applications. To assess the potential cytotoxicity of our AS-loaded PVA hydrogels, we exposed them to human dermal fibroblasts. Each of the formulations exhibited excellent cell viability compared with the blank control, with no significant differences (Figure 2.13B). Moreover, all groups treated with hydrogel showed less than 30% reduction and can be considered non-cytotoxic (Gruber and Nickel, 2023).

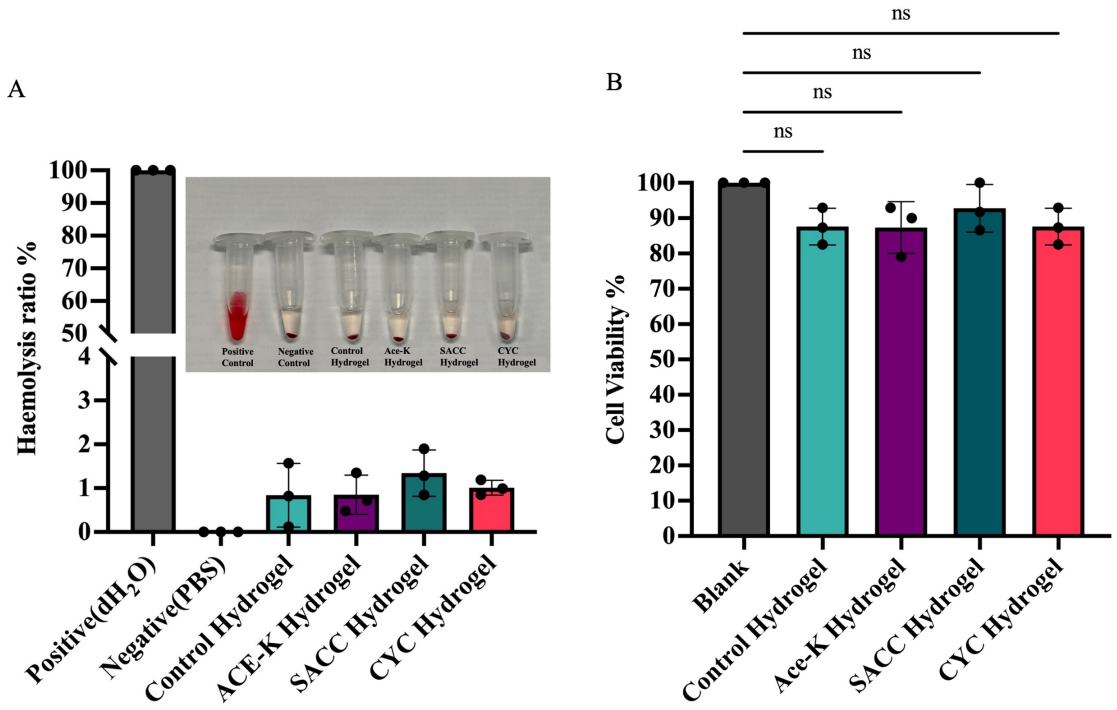

Figure 2.13 Blood compatibility and cell viability of AS-Loaded hydrogel. (A) *In vitro* haemolysis assay of AS-Loaded hydrogels. (B) cell viability percentage. Data are presented as the mean of three biological replicates. Error bars represent standard deviation (SD). Statistical analysis was performed using one-way ANOVA to compare the control and treated samples. (ns>0.05).

2.4.9 Material Characterisation

Given that we had now demonstrated potent antimicrobial activity of these AS-loaded hydrogels, we next sought to investigate their material properties to gain further insights into their therapeutic potential. To assess the water-absorption and retention capacity of the hydrogels, the degree of swelling (DS) was measured. Swelling behaviour is a critical factor for blood and wound exudate, the release of loaded agents, and the transfer of nutrients and metabolites (Feng and Wang, 2023).

The DS of AS-loaded PVA-Borax hydrogel was tested over a 48-hour period (Figure 2.14A). The control gel had the highest swelling rate compared to the AS-loaded hydrogels during the study. Maximum overall swelling was observed at the 3rd hour (Figure 2.14B). The control hydrogel reached an average DS of 498.25 ± 18.57%, significantly higher than all other groups. In contrast, the 6% and 8% Ace-K hydrogels showed lower swelling degrees of 217.51 ± 10.11% and 187.44 ± 85.71%, respectively. Similarly, the 6% and 8% SACC hydrogels exhibited swelling degrees of 212.54 ± 18.25% and 167.93 ± 7.05%, while the 6% and 8% CYC hydrogels showed 219.73 ± 12.71% and 189.67 ± 54.54%, respectively. At 6 h, the control group maintained the highest DS (511.8% ± 58.68), while AS hydrogels exhibited lower swelling values compared with those observed at 3 h. The 6% and 8% Ace-K hydrogels had swelling degrees of 182.9 ± 14.82% and 155.4 ± 73.76%, the 6% and 8% SACC hydrogels showed 200.9% ± 23.96 and 136.2 ± 20.14%, and the 6% and 8% CYC hydrogels achieved 187.35 ± 10.99% and 173.57 ± 57.52%, respectively. By 48 hours, the control group maintained significantly higher DS (297.3 ± 177.29%) than all other groups. The DS of Ace-K groups decreased to 147.4 ± 4.94 % (6%) and 97.1 ± 38.35% (8%), the SACC groups were 158.6 ± 23.80% (6%) and 110.3 ± 18.03% (8%), and the CYC groups were 154.74 ± 8.27 % (6%) and 125.64 ± 36.71% (8%), where a similar trend of less swelling being observed as the AS concentration increases. Overall, these results demonstrate that incorporation of artificial sweeteners significantly modulates the swelling behaviour of PVA–borax hydrogels in a concentration-dependent manner. This high swelling ability is because of PVA's hydrophilic surface (Asy-Syifa *et al.*, 2022).

Weight loss is an important parameter for wound dressings. It reflects the hydrogel's stability and degradation profile under physiological conditions (Mndlovu *et al.*, 2024). The weight loss

(%) of AS-loaded PVA-borax hydrogel was measured (Figure 2.14C). The control hydrogel exhibited the highest average weight loss at 63.66 ± 22.61% and was significantly lower than other hydrogels. Hydrogels loaded with 8% sweeteners generally showed higher weight loss than the control hydrogel and the 6% AS-loaded hydrogel. The average weight loss of 8% Ace-K hydrogel was 76.57 ± 0.99%, 77.21 ± 1.19% for 8% SACC hydrogel, and 74.12 ±2.01% for 8% CYC hydrogel. Hydrogels containing 6% Ace-K, 6% SACC, and 6% CYC showed slightly lower weight loss than 8% hydrogels. The values were 70.49 ± 1.25%, 70.38± 1.89%, and 68.19 ± 3.64%. As Table 2.5 demonstrates, their final average weights were similar to those of the control gel. Overall, the percentage weight loss of the AS-loaded hydrogel is significantly higher than that of the control hydrogel. This observation can be due to the artificial sweetener being highly water-soluble and completely dissolved in PBS solution.

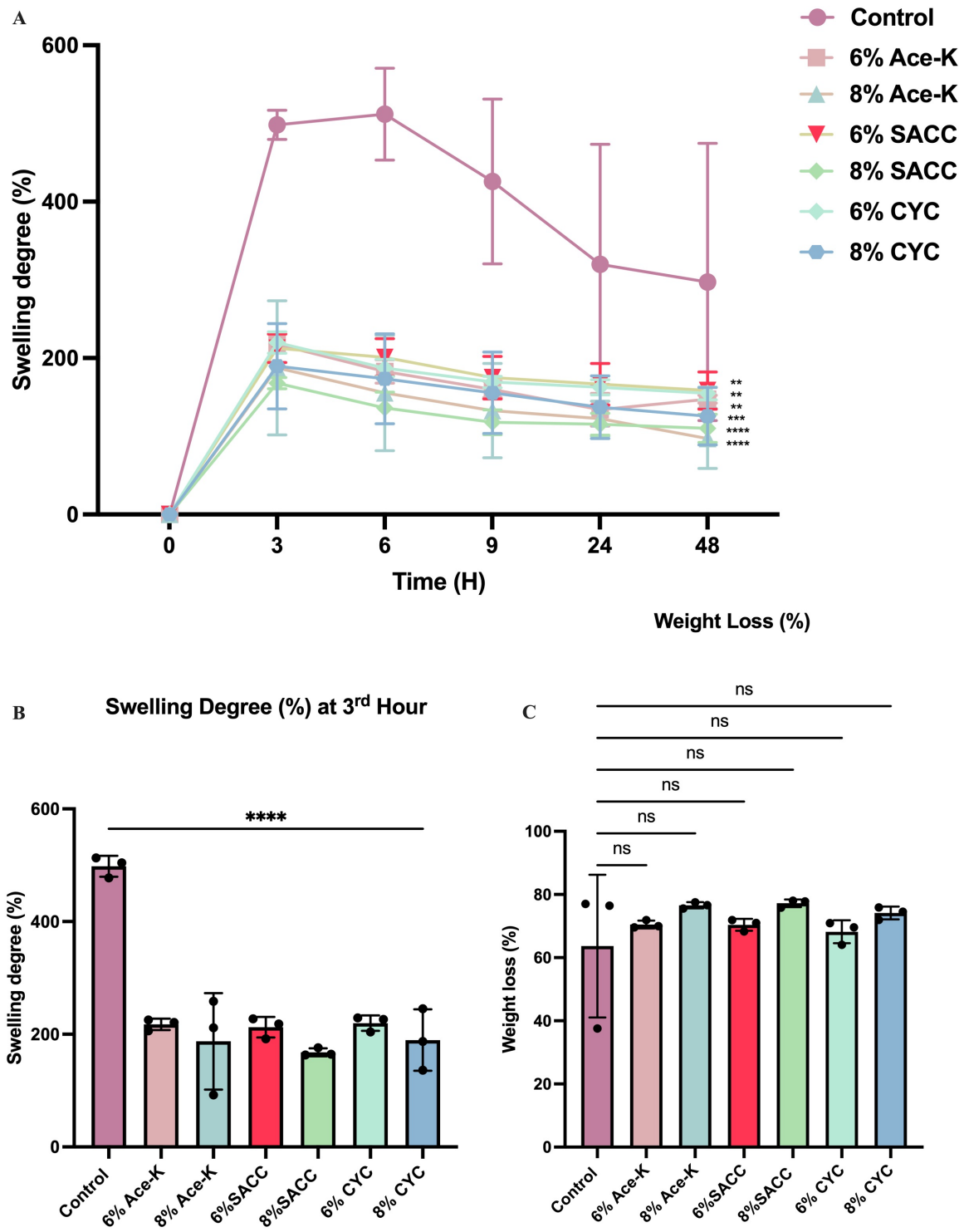

Figure 2.14 Degree of swelling and weight loss of PVA-borax hydrogels:(A) Swelling degree (%) of PVA–borax hydrogels incorporated with different AS over a 48-hour period. Hydrogels were measured at 3, 6, 9, 24, and 48 hours. The control hydrogel exhibits the highest DS% when compared to other hydrogels. (B) Comparison of the highest average swelling degree at

3 hours among the control and AS-loaded groups. The control hydrogel shows the highest DS%. The lower the AS concentration, the higher the DS%. (C) Weight loss (%) was measured at 48 h after re-drying, the hydrogels containing 6% or 8% (w/w) of Ace-K, SACC, or CYC, along with a control hydrogel. The control hydrogels shown highest weight loss. The weight loss shows concentration dependent when compared with AS-loaded hydrogels. Data are presented as mean ± standard deviation (n = 3). Error bars represent standard deviation (SD). Statistical analysis for A used two-way ANOVA with Tukey correction between the AS-loaded hydrogel and the control hydrogels. Statistical analysis for B and C were performed by one-way ANOVA with Dunnett's correction between the control and AS-loaded hydrogel (ns>0.05, *p-value < 0.05,**p-value < 0.01, *** p-value < 0.001, **** p-value < 0.0001).

Table 2.5 : Initial and Final Fry Weights of AS-loaded PVA–Borax Hydrogels for Weight Loss Evaluation

	Control	6% Ace-K	8% Ace-K	6% SACC	8% SACC	6% CYC	8% CYC
Initial dry weight (g)	0.133±0.015	0.262±0.004	0.324±0.017	0.262±0.007	0.319±0.046	0.259±0.007	0.332+0.031
After dry weight (g)	0.046±0.023	0.077±0.037	0.076±0.062	0.077±0.049	0.072±0.098	0.083±0.117	0.086±0.020

The pore structure, size, and porosity can influence swelling rate, fluid retention, and

mechanical properties (Xing *et al.*, 2018). The different pore sizes of the hydrogel would be more suitable for some applications than others. For example, for neovascularisation applications, 5 μm is ideal, and 5-15 μm is more suitable for fibroblast growth. In skin regeneration of adult mammals, 20-125 μm is the optimal (Waresindo *et al.*, 2021). The hydrogel morphology is shown in Figure 2.15. The control hydrogel showed a smaller average pore size, which is 12.00 ± 9.83 μm. The average pore size of Ace-K hydrogel is 20.75 ± 14.31 μm. The CYC hydrogel shows a slightly larger average pore size (14.38 ± 8.27 μm) when compared to the control hydrogel. The SACC hydrogel showed the largest pore size at ~ 27.42 ± 20.03 μm.

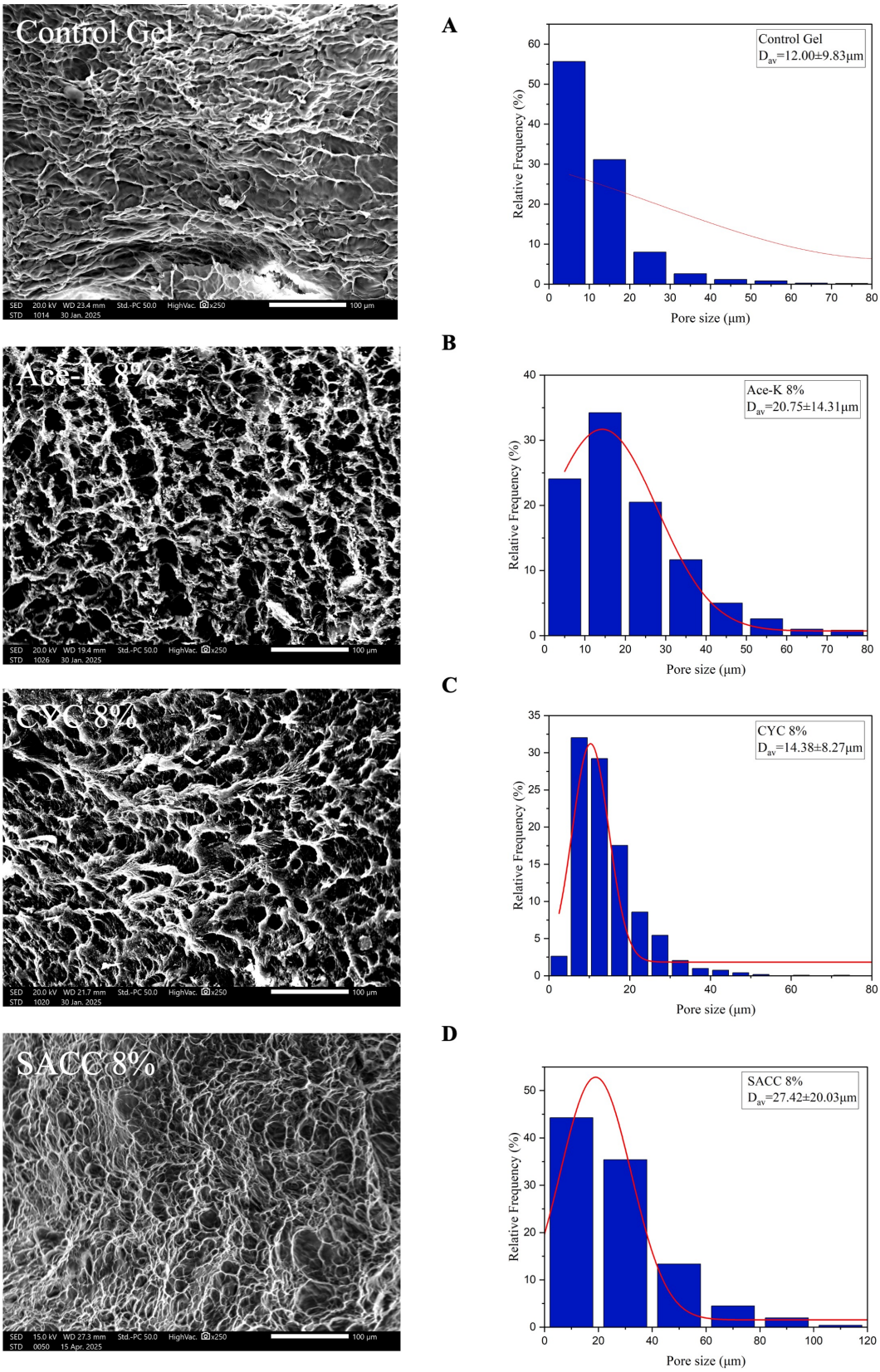
Control Gel
A
Control Gel
D_{av}=12.00±9.83µm
Relative Frequency (%)
Pore size (µm)
Ace-K 8%
B
Ace-K 8%
D_{av}=20.75±14.31µm
Relative Frequency (%)
Pore size (µm)
CYC 8%
C
CYC 8%
D_{av}=14.38±8.27µm
Relative Frequency (%)
Pore size (µm)
SACC 8%
D
SACC 8%
D_{av}=27.42±20.03µm
Relative Frequency (%)
Pore size (µm)

Figure 2.15 AS-Loaded Hydrogel Morphologies: Visualisation of different pore morphologies of PVA Borax hydrogels with different artificial sweeteners (Control gel, Ace-K 8%, CYC 8%, and SACC 8%) using SEM Nonlinear curve fitting in OriginPro software, using the Gaussian peak function, was used to determine pore size distributions of PVA borax hydrogels (n=3).

It is important to understand the rheological behaviour of hydrogels, as it provides an insight into their mechanical stability. To assess differences in mechanical and rheological properties, rheological analysis was performed on the most effective AS-loaded PVA–borax hydrogel formulations, specifically those containing 8% artificial sweeteners (SACC, CYC, and Ace-K), as well as a control hydrogel. In Figure 2.16A, the SACC-loaded hydrogel has the highest storage modulus and loss modulus in the frequency scanning range of 0-15.92 Hz, followed by the CYC and Ace-K-loaded hydrogel. All AS-loaded hydrogels exhibited a higher storage modulus compared to the control gel, while their loss modulus remained lower than the storage modulus across the frequency scanning range of 0–15.92 Hz. All the gels showed higher storage modules (G’) than the loss modulus (G’’), which indicates a stronger gel intensity (Nesrinne and Djamel, 2017). In addition, the higher (G’) was observed in the SACC-loaded hydrogel indicates a stronger and more rigid network structure compared to other formulations.

Figure 2.16B shows the variation of storage modulus (G') and loss modulus (G") of artificial sweetener-loaded hydrogels under increasing strain% (0–100%), which can be studied for quantified viscoelastic behaviour of the gels. At lower strains, AS-loaded hydrogels showed higher G' than G", which indicates that the material behaved more solid-like. With increasing strains, AS-loaded hydrogels reached a “crossover point” where the G" started to have higher values than G', and the gel became more liquid-like and could flow. This shows the gels are non-Newtonian shear-thinning fluids. The SACC-loaded PVA borax demonstrated the highest

storage modulus across the entire strain range. The Ace-K-loaded hydrogel showed a moderately high storage modulus, slightly lower than SACC but higher than CYC and control hydrogels. The CYC-loaded hydrogel exhibited a storage modulus similar to or slightly higher than the control hydrogel. This enhanced rigidity can improve the hydrogel's stability on the wound surface, which complies with the pilot study.

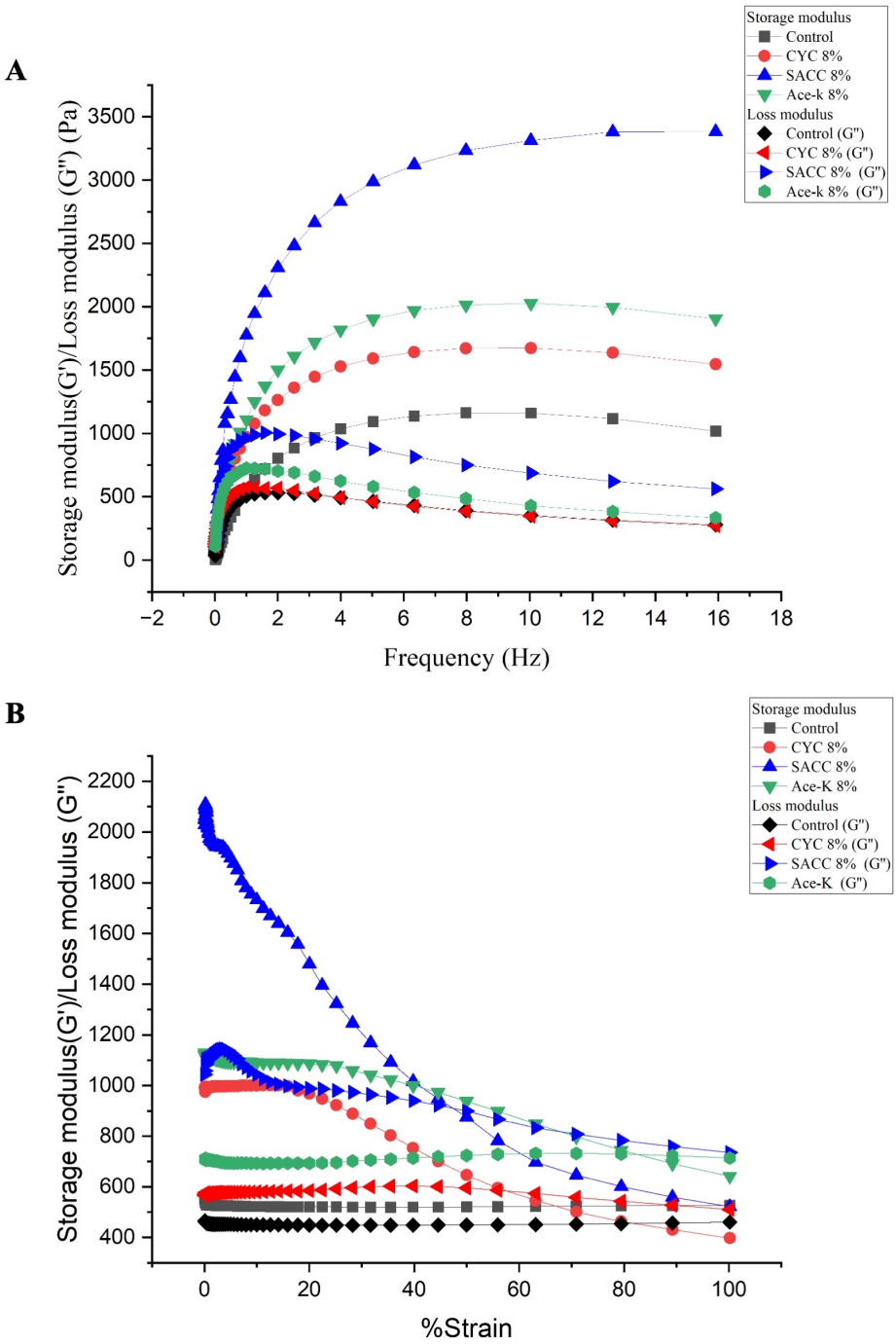

Figure 2.16 Rheological properties of control and 8% artificial sweetener-loaded PVA–borax hydrogels. (A) Frequency sweep analysis showing storage modulus (G′) and loss modulus (G″) as a function of frequency (0–15.92 Hz). The SACC-loaded hydrogel exhibited the highest storage modulus, indicating increased stiffness, while all hydrogels showed G′ values greater than G″ across the frequency range, demonstrating elastic solid-like behaviour. (B) Strain sweep analysis showing storage modulus (G′) and loss modulus (G″) as a function of strain (0–100%). All hydrogels exhibited decreasing G′ and G″ with increasing strain, indicating shear-thinning behaviour. Data represent mean values from three biological replicates.

Fourier Transform Infrared Spectroscopy **(**FTIR) analysis was performed to identify the functional groups and molecular interactions in the PVA–borax hydrogels. It is also used to confirm if there is any chemical interaction between AS and PVA–borax hydrogels. In the FTIR spectrum of PVA, the characteristic peak at approximately 3250 cm^{-1} is assigned to the O-H stretching vibration of hydroxyl groups. The characteristic peaks at 2940 cm^{-1} and 2905 cm^{-1} are attributed to CH_2 asymmetric stretching vibrations. The peak at 1415 cm^{-1} corresponds to the C-H bending vibration of -CH_2- groups, while the peak at 1320 cm^{-1} represents the CH and OH bending groups. The absorption peak at 1145 cm^{-1} indicates the C-O stretching vibration of the -CH_2OH hydroxyl groups in PVA molecules, which was previously described (Figure 2.17) (Omkaram, Sreekanth Chakradhar and Lakshmana Rao, 2007; Jipa *et al.*, 2012; Zidan *et al.*, 2019). In Figure 2.17, the PVA hydrogel shows a broad peak at 3250 cm^{-1}, which indicates stretching vibration of the O-H group. Peaks at 2940 cm^{-1} and 2905 cm^{-1} were assigned to C–H stretching, and bands at 1415 cm^{-1} and 1320 cm^{-1} corresponded to -CH_2 bending and CH+OH bending groups. A reduced peak at 3250 cm^{-1} means the number of hydroxyl species has reduced. This reduction indicated the formation of a boric ester bond (Wang *et al.*, 2022). In Ace-K-loaded PVA hydrogels (Figure 2.17A), characteristic peaks of

Ace-K were observed at 1650 cm^{-1} (C=O stretching), 1590 cm^{-1} (N–H bending), and 1075 cm^{-1} (S=O stretching), confirming that there is no chemical interaction of Ace-K with the hydrogel matrix (Armenta, Garrigues and de la Guardia, 2004). The B–O stretching vibration at 997 cm^{-1} remained visible in the Ace-K-loaded PVA hydrogels, indicating the presence of borate crosslinking. In Figure 2.17B, CYC-loaded hydrogels showed a sharp N–H stretching peak at 3275 cm^{-1} and a broad O–H stretching band (3200–3500 cm^{-1}). Other peaks were found to be at 3275 cm^{-1}, 2935 cm^{-1} and 2856 cm^{-1} (C–H stretching), 1432 cm^{-1} (C–H bending); 1170 cm^{-1} and 1035 cm^{-1} (S=O stretching); and 683 cm^{-1} (C–S bending), which substantiate the addition of CYC in the hydrogel system (Tosa *et al.*, 2012). In Figure 2.17C, SACC-loaded hydrogels showed clear peaks at 3567 cm^{-1} and 3487 cm^{-1} corresponding to O–H stretching and hydrogen bonding, which match the SACC powder spectra. Aromatic stretching C=C (1630 cm^{-1} and 1583 cm^{-1}), the sulfonyl group peak (1255 cm^{-1} and 957), and C–S-related peaks at 748 cm^{-1} and 674 cm^{-1} were identified both in SACC powder and SACC-loaded hydrogel (Srivastava *et al.*, 2012). The FTIR spectra confirm the successful incorporation of AS into the PVA-borax hydrogel network, and there was no chemical interaction between the PVA-borax hydrogel and AS.

The X-ray diffractometry (XRD) patterns of AS-Loaded hydrogels are presented in Figure 10D. The PVA powder exhibited a sharp diffraction peak at $2\theta = 20.03°$, indicating its semi-crystalline nature. This crystallinity arises from strong intermolecular hydrogen bonding between PVA chains, as previously reported (Ricciardi *et al.*, 2004). In contrast, the PVA-borax hydrogel exhibited two broad peaks (Figure 2.17D), suggesting a significant reduction in crystallinity. This change is attributed to borax crosslinking, which sterically interferes with the regular arrangement and hydrogen bonding of PVA chains within the network structure (Wang *et al.*, 2022). The AS samples exhibited characteristic crystalline peaks, confirming

their crystalline structure (Figure 2.17D). After incorporation into the PVA hydrogel matrix, the broad diffraction peak of the PVA hydrogel disappeared and was replaced by the characteristic peaks of AS. However, the intensity of these AS peaks decreased compared to pure AS, indicating reduced crystallinity. This reduction suggests that AS was molecularly dispersed or partially embedded within the amorphous regions of the hydrogel network, thereby distorting its ordered crystalline structure.

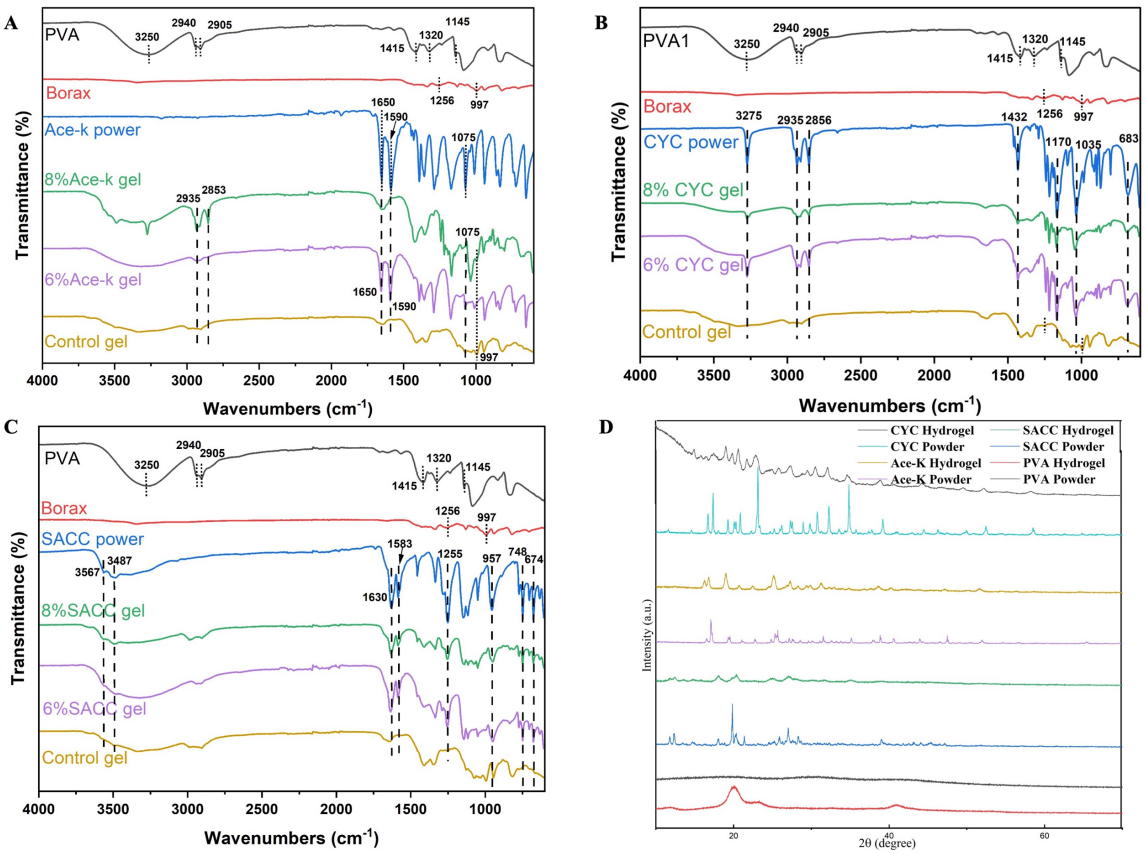

Figure 2.17 FTIR Analysis of AS-Loaded Hydrogels (A) FTIR spectra of PVA, sodium tetraborate, Ace-K, 8% Ace-K hydrogel, 6% Ace-K hydrogel and control hydrogel (B) sodium tetraborate, CYC, 8% CYC hydrogel, 6% CYC hydrogel and control hydrogel. (C) FT-IR spectra of PVA, sodium tetraborate, SACC, 8% SACC hydrogel, 6% SACC hydrogel and

control hydrogel. (D) XRD spectra of PVA powder, PVA hydrogel, CYC powder, CYC Hydrogel, SACC powder, SACC hydrogel, Ace-K powder, Ace-K hydrogel.

2.4.10 Pilot Phase 1 Clinical Study in Humans

To evaluate whether the AS hydrogel causes any effects on healthy human skin, such as irritation, discomfort, or other adverse events, a pilot Phase I clinical study was conducted. In this study, 12 healthy volunteers were recruited. The 4 different hydrogels (control, Ace-K, SACC and CYC) were placed on their healthy and undamaged skin. To keep the hydrogel in place, an adhesive film (TEGADERM Film Dressing, 3M) was used (Figure 2.18A). This study also aimed to assess potential issues related to the adhesion and removal of the hydrogel from the skin, as well as its degradation over time. In the Participant Feedback on Hydrogel Application Study – Section 1: Comfort and Sensation, the majority of participants (75%) rated the hydrogel as highly comfortable (score of 5). The remaining 25% rated it as 4 initially, suggesting it was well-tolerated (Figure 2.18B). One participant reported an increasing comfort sensation of the hydrogel over time (Figure 2.18C). After 24 hours, 50% of participants rated the sensation as 5, and 25% rated it as 4 (Figure 2.18D). The majority of participants did not experience discomfort, but one participant reported itchiness due to the adhesive tape securing the hydrogel (Figure 2.18E).

In the adhesion and removal section, the feedback shows that 58.33% of participants rated hydrogel's stability as excellent, with 33.33% rating it as 4 and 8.33% giving it 3 for structural integrity (Figure 2.18F). All participants reported that phase separation occurred in both the CYC and Ace-K hydrogels during the test. Most of the participants experience 8% CYC hydrogel phase separation within the first three hours. However, there were two participants (both male) whose CYC hydrogels phase separated at the 6th-hour observation time point. This could due to males typically have higher skin temperatures than female (Marins *et al.*, 2014;

Chudecka and Lubkowska, 2015). Ace-K-loaded hydrogel phase separated between 9- and 24-hour time points. Hydrogel loaded with SACC and control hydrogel maintained their structural integrity over 24 hours (Figure 2.18G). The removal processing of hydrogel was relatively easy. There were 66.67% of participants who found the process very easy (score of 5), and 33.33% found it slightly difficult (score of 4) (Figure 2.18H). One participant reported discomfort due to the strong adhesive of transparent film (Figure 2.18I).

In the skin reaction section, four participants experienced redness or swelling post-hydrogel removal. These reactions were localised to the area where the transparent film was applied, rather than the hydrogel application site (Figure 2.18J). This is due to repeated application and removal of the adhesive film which irritated the skin the skin. Moreover, one participant reported an itching/burning sensation that was also confined to the area covered with the adhesive film (Figure 2.18K). None of the participants observed any skin changes such as dryness or flakiness after hydrogel application (Figure 2.18L). These findings suggest that while a minority of participants experienced mild and transient redness and itching due to the commercially available transparent film that was on top of the hydrogels, the majority reported no adverse effects. The reactions were limited to the site of the transparent film and not on the AS-loaded hydrogel sites, indicating that the AS-loaded hydrogels are well tolerated on healthy skin during the applications.

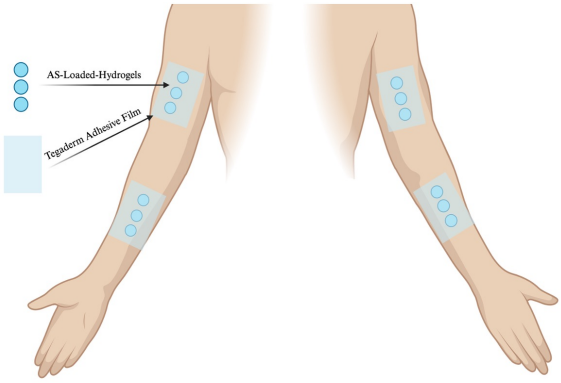

A

How comfortable was the hydrogel on your skin immediately after application? (Score 1-5)

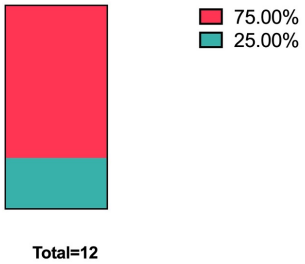

B

Did the sensation of the hydrogel change over time?

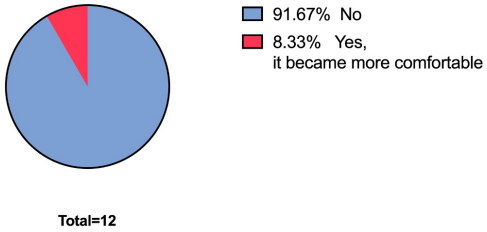

C

How would you rate the sensation of the hydrogel on your skin after 24 hours?

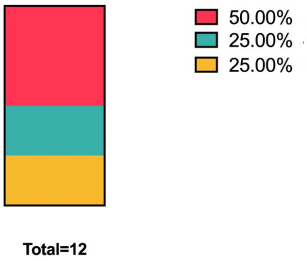

D

Did you experience any discomfort while the hydrogel was on your skin?

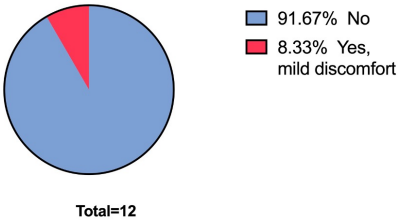

E

How well did the hydrogel maintain in shape to your skin?

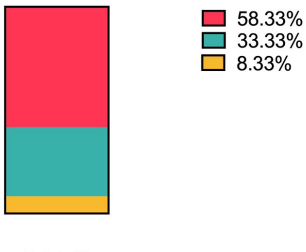

F

Did the hydrogel stay in place throughout the observation period?

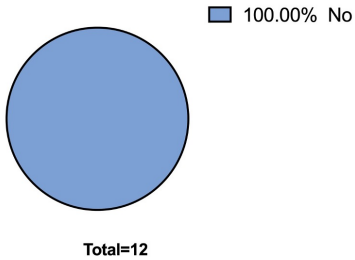

G

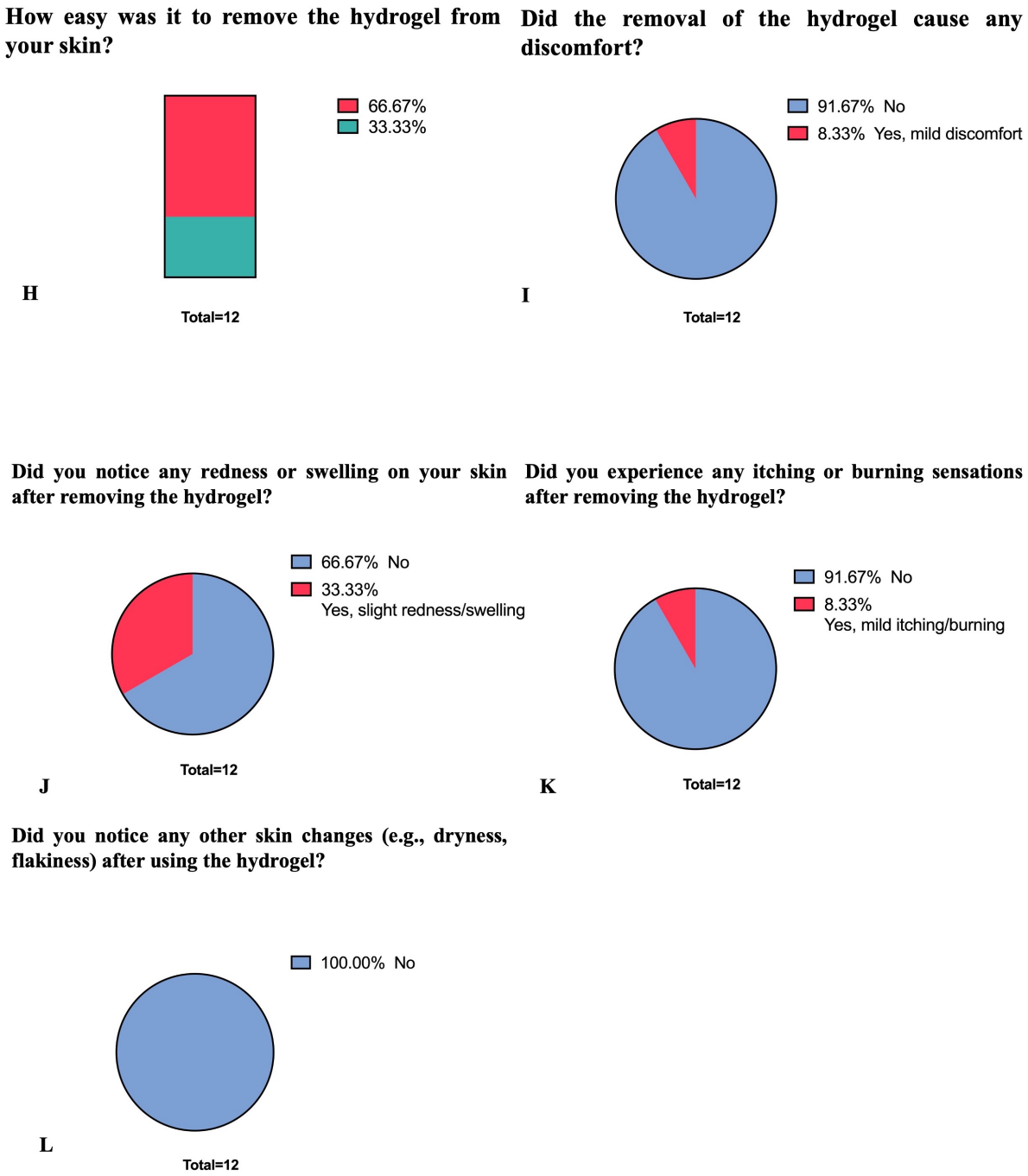

Figure 2.18 Hydrogels were fixed with Tegaderm adhesive film (3M) to mimic clinical dressing conditions for 24 hours (A) Participant Feedback on Hydrogel Application Study – Section 1: Comfort and sensation (B-E), Section 2: Adhesion and Removal (F-I), Section 3: Skin Reaction (J-L), Score interpretation: Higher scores indicate more favourable outcomes,

including greater satisfaction, ease of removal, and hydrogel stability. Scoring criteria varied between questions. Created in BioRender. Han, J. (2025) https://BioRender.com/6sdwcby

2.5 Discussion

Artificial sweeteners are ubiquitous in our lives. The market scale of artificial sweeteners is increasing every year (Luo, Zhang, *et al.*, 2019). In our previous studies, AS such as Ace-K, SACC and CYC showed the ability to inhibit the growth of common wound infection AMR pathogens, including the *A. baumannii* AB5075 and *P. aeruginosa* PA14 (de Dios *et al.*, 2023a, 2025). We also demonstrated a range of antivirulence properties including the inhibition of biofilm formation, natural transformation and motility. In this prior work, we extensively explored the underlying mechanism of action using bacterial cytological profiling and transcriptomics, uncovering that these AS triggered the downregulation of key genes associated with these phenotypes and the cell death was mediated via bulge mediated cell lysis. This study focused on trying to further demonstrate the translational potential of these sweeteners by developing novel formulations for their topical application. An initial screening using the ZOI assay was conducted to assess the antimicrobial potential of hydrogels loaded with different AS concentrations. Interestingly, the AS-loaded hydrogels showed a concentration-dependent effect consistent with our previous findings which used AS solutions directly (de Dios *et al.*, 2023, 2025). This demonstrated the efficacy of this hydrogel as a vehicle for the AS and that they maintained their activity. As 8% AS-loaded hydrogels showed the highest ZOI, they were selected for testing against biofilm.

Biofilm is a leading factor that contributes to prolonged wound healing (Metcalf and Bowler, 2013). It leads to a burden of $386.8 billion in health systems globally (Cámara *et al.*, 2022). The anti-biofilm activity of our AS-loaded hydrogels was tested against early-stage biofilm

(3.5 h) and mature biofilm (24 h). For early-stage biofilm, *in vitro* and *ex vivo* porcine skin model were evaluated. There was a ≥ 99.99% reduction in viable biofilm cells observed after 1-hour treatment in the *in vitro* model for all the. This was also confirmed in the *ex vivo* porcine skin model, where all AS-loaded hydrogels demonstrated ~99% reduction in viable cells in early-established biofilm, while the control gel showed no significant efficacy against the biofilm. Moreover, all AS-PVA hydrogels outperformed the commercial silver dressing, which failed to show any efficacy against the early biofilm, highlighting the inefficacy of current frontline therapeutic interventions when treating biofilm-associated infections. This confirms the potential use of our dressing in early-stage wound infections. In the established biofilm model, ~99% reduction in viable biofilm cells was also observed within 2 h and increased over time, achieving ≥99.99% biofilm removal in 24 h. SEM analysis confirmed these findings. Interestingly, it was noted the few remaining cells in the sweetener-treated groups displayed an altered cell morphology, with cells being larger and rounder than their untreated counterparts; this aligns with our previous reporting of the altered *A. baumannii* cell morphology induced by sweetener exposure (de Dios *et al.*, 2023, 2025). We hypothesised that the hydrogel would allow a controlled release of the AS for continuous eradication of biofilms in chronic wounds. This was further validated by time-kill assays, where hydrogels loaded with 6% and 8% AS significantly reduced *A. baumannii* viability over 24 hours. To explore potential real-world applications, we extended our investigation to an *in vitro* polymicrobial biofilm model. The *A. baumannii* AB5075 and *P. aeruginosa* PA14 were selected due to their common association with chronic wound infections (Hou *et al.,* 2024; Ruamsap *et al.,* 2023). This polymicrobial efficacy further highlights the delivery ability and broad-spectrum potential of this AS hydrogel to be used in wound infections. Moreover, the AS-Loaded PVA hydrogel demonstrates excellent hemocompatibility, with a haemolytic rate below 2% and excellent cell viability within a non-cytotoxic range (less than 30% reduction) (Gruber and Nickel, 2023).

These results demonstrate that AS-Loaded PVA borate hydrogels have excellent biocompatibility and antimicrobial efficacy. Future work will explore the impact of these hydrogels on wound healing and the effects of longer exposure periods on the host.

In this study, the antimicrobial activity of FT-PVA hydrogel against *A. baumannii* was confirmed by the disk diffusion assay. The FT- PVA hydrogels exhibited concentration-dependent antimicrobial properties, with higher AS concentrations correlating with a larger zone of inhibition (ZOI). Interestingly, we found that in FT- PVA hydrogels system higher concentrations of PVA led to a reduction in antimicrobial efficacy. Higher PVA concentration will lead to higher cross-linking density of the hydrogel (Waresindo *et al.*, 2021). A denser cross-linking matrix may reduce the diffusion of AS which limiting its ability to spread to surrounding areas and inhibit bacterial growth effectively (Wu, Joseph and Aluru, 2009). This observation emphasizes the importance of balancing PVA concentration in the formulation, as higher concentrations may compromise the antimicrobial activity by trapping the AS within the hydrogel network. In conclusion, the FT- PVA hydrogels have potential to be developed as antimicrobial wound dressings capable of inhibiting the growth of pathogens like *A. baumannii*. However, their effectiveness needs to be improved when compared with PVA-borax hydrogel. This is the reason why FT- PVA hydrogels were not being studied further in this chapter.

In addition to their antimicrobial efficacy, the physical properties of AS-loaded hydrogels were evaluated to understand how material characteristics influence hydrogel performance. The degree of swelling of PVA-hydrogel was monitored over 48 hours. The control gel reached its maximum swelling at 3 h and that was maintained till 6 h before starting to degrade. In contrast, sweetener-containing hydrogels showed less swelling compared to control gel and started to degrade earlier at 3 h. These findings suggest that AS incorporation reduces the swelling

capacity of the hydrogel. However, all the hydrogels reached more than 150% swelling at the 3-hour time point, and a high swelling rate could enable the hydrogels to exhibit high wound exudate absorption capacity and high drug release, which is ideal for deployment in wound applications (Feng and Wang, 2023). Over time, all groups showed a gradual reduction in swelling indicating the biodegradability of the hydrogels. The average pore size was around 12.00 μm for the control gel, 20.75 ± 14.31 μm for Ace-K gel, 14.38 ± 8.27 μm for CYC gel and 27.42 ± 20.03 μm for CYC gel. However, the swelling rate trend does not align with the porosity that was observed by SEM. These different observations could be due to the fact of the high-water solubility of the AS. The AS hydrogel has a higher initial weight compared to the control hydrogel, and ASs are highly water soluble. Therefore, AS might rapidly dissolve after liquid immersion, which results in a lower swelling rate.

In this study, the incorporation of artificial sweeteners changed the viscoelastic behaviour of the PVA–borax hydrogels. When the storage modulus (G′) is lower than the loss modulus (G″), the material behaves as a viscous fluid. When storage modulus (G′) is higher than the loss modulus (G″), the material behaves as a gel. In the results, it showed that at lower frequencies, the hydrogels tended to exhibit viscous behaviour, whereas at higher frequencies, the storage modulus (G′) exceeded the loss modulus (G″), indicating elastic solid-like behaviour under these conditions. Incorporation of artificial sweeteners increased the storage modulus compared to the control hydrogel. Specifically, the storage modulus of the SACC-loaded PVA–borax hydrogel was approximately three times higher than that of the control gel, while CYC- and Ace-K-loaded hydrogels exhibited increases of approximately 1.5-fold and 1.8-fold.

Given that the AS-loaded hydrogels had displayed potent antimicrobial and antibiofilm activity we wanted to further explore their therapeutic potential. A pilot Phase I clinical study was

conducted to evaluate the subjective experience and skin compatibility of AS-loaded hydrogels in healthy human participants. The goal was to assess both subjective comfort and skin compatibility under conditions simulating topical application. The majority of participants reported that AS hydrogels were comfortable to wear. However, a few cases of mild itchiness and redness were reported after removing the adhesive film. Importantly, these reactions were localised to the adhesive area rather than the hydrogel contact zone, which indicated the hydrogel did not induce irritation. However, repeated application and removal of the adhesive film might cause skin damage in sensitive individuals. To minimise such reactions in future experiment designs, we would reduce the number of application intervals to reduce the skin damage.

In terms of formulation stability during wear, hydrogel stability varied among the formulations. SACC hydrogel maintained its integrity during the 24 h application period. In contrast, the CYC hydrogel phase separated within 3 hours of application, whereas the Ace-K hydrogel phase separated between 9 and 24 hours. These differences highlight the impact of sweetener type on the mechanical properties of the hydrogel under physiological conditions. The findings reinforce the need for hydrogel formulations to balance not only antimicrobial efficacy but also practical usability and wearability in real-world applications. Future work will look to conduct a full Phase 1 clinical trial which will evaluate the effects of dose escalation, pharmacokinetics, with predefined clinical endpoints.

In conclusion, this study demonstrates that AS-loaded PVA–borax hydrogels have both antimicrobial and antibiofilm efficacy and favourable material properties for topical application in acute and chronic wounds when compared to the control hydrogel. The hydrogels effectively inhibited *A. baumannii* both in planktonic and biofilm conditions. The antimicrobial activity was observed in both mono- and polymicrobial models. The swelling and porosity of

the hydrogels were influenced by sweetener type and concentration, with solubility playing a key role in observed variability. SEM analysis and adjusted swelling degree calculations further clarified these effects. Importantly, human testing indicated good comfort and biocompatibility, although improvements in adhesive application and hydrogel stability, particularly for Ace-K and CYC formulations are essential. Overall, these findings highlight the promise of AS-loaded hydrogels as an innovative platform for wound care and localised infection management.

2.6 Key Findings

1. Development of PVA-Borax and FT-PVA Formulation with the addition of AS.
2. Demonstration of antimicrobial activity of artificial sweetener-loaded hydrogels against *A. baumannii* and AS-Loaded borax hydrogels outperforms commercial antimicrobial silver alginate hydrogels and AS-Loaded FT-PVA hydrogel.
3. Demonstration of strong antibiofilm activity against *A. baumannii in vitro* and *ex vivo* and mixed-species biofilms.
4. AS-Loaded PVA-Borax hydrogel shows excellent biocompatibility and translational potential.
5. Material characterisation demonstrated that the incorporation of an artificial sweetener influenced the physicochemical properties of PVA-borax hydrogels.

Chapter 3

3. Exploring How the Transcriptional Landscape of *A. baumannii* Changes and Hydrogel Performance in Lubbock Chronic Wound Biofilm Medium.

3.1 Introduction

Wounds can be defined as an opening or breaking of skin integrity, damaged muscle or organ. It could be due to physical, chemical or thermal injuries (Kamoun, Kenawy and Chen, 2017). Under normal physiological conditions, wound healing can be classified into four stages: haemostasis, inflammation, proliferation and tissue remodelling (Singh, Young and McNaught, 2017). Patients who progress through these stages successfully could restore their skin barrier and prevent further complications. However, there are an abundance of factors that can disrupt this healing process and lead to impaired recovery and increase infection risk (Guo and DiPietro, 2010).

Wound infection leads to a significant burden to healthcare systems worldwide, such as prolonged hospitalisation and increased healthcare costs. It is estimated that around 8.2 million medicare beneficiaries in the US suffer from wounds with or without infection, resulting in $28.1 billion to 96.8 billion in medical treatment costs (Sen, 2019). Wounds can be classified as acute or chronic. Acute wounds have a lower bacterial burden and can be healed on time through the healing stages, leading to minimal scarring. However, chronic wounds on the other side is hard to treat. Chronic wounds are wounds that fail to heal after 4 to 12 weeks. There are many factors that can lead to chronic wounds such as the patient's medical condition, gender, age, condition of blood circulation, immune system and infection (Guo and DiPietro, 2010).

Pathogenic infection is one of the factors that leads to an unhealed or slow-to-heal wound. These infections not only delay healing but can also progress to severe complications such as sepsis and limb amputation (Zhao *et al.*, 2016). Therefore, understanding the challenges caused by chronic wound infections is critical for developing targeted therapeutic approaches. One of the key factors contributing to the chronicity of these wounds is the formation of microbial biofilms, which can be found in 90% of chronic wound infections (Attinger and Wolcott, 2012).

To understand the bacterial behaviour within the environment. A range of *in vitro* wound-like models has been developed to mimic the biochemical and physiological conditions at infection sites, such as the human plasma biofilm model and the Lubbock chronic wound biofilm (LCWB) model. The LCWB model has been widely used because it mimics the human wound environment, such as damaged tissue, red blood cells, and serum. It provides a rapid way for screening of clinical isolates and polymicrobial populations for antimicrobial susceptibility and biofilm formation (Dowd *et al.*, 2009; Diban *et al.*, 2023). It consists of 50% plasma, 5% freeze-thawed horse red blood cells, and 45% Bolton broth. This model was developed by Sun et al. (2008) to screen for polymicrobial biofilm formation by *P. aeruginosa, Enterococcus faecalis (E. faecalis), and S. aureus. P. aeruginosa, Candida albicans,* and β-hemolytic *streptococci* are the primary pathogens that delay wound healing and cause infection (Diban *et al.*, 2023). Ever since then, the LCWB Model has been widely used in different settings. In DeLeon *et al.* study (2014), the *P. aeruginosa and S. aureus* showed significantly higher antibiotic tolerance when compared with single cultured strains. In another study, LCWB Model supplemented with 1% of gelatine was used to mimic the wound bed for wound dressing application (Kucera *et al.*, 2014). Moreover, the LCWB Model was used to test graphene oxide's antibiofilm property. The colony-forming Units (CFU) was reduced by 59.31% and 70.24% (Di Giulio *et al.*, 2020).

While *P. aeruginosa, E. faecalis, and S. aureus* remain the most commonly recognised pathogens in wound infections, they have been studied intensively at phenotypic and transcriptomic levels (Bessa *et al.*, 2015; Gonzalez *et al.*, 2018; D'Arpa *et al.*, 2021; Thaarup and Bjarnsholt, 2021). However, *A. baumannii* has increasingly emerged as an important wound-associated pathogen, particularly in trauma, burn, and healthcare-associated wound settings. These infections are common problems in both the injured military setting and the nonmilitary setting (Guerrero *et al.*, 2010; Irma D. Fleming *et al.*, 2017). Understanding how *A. baumannii* adapts to wound conditions at the transcriptional level remains limited even though individual blood components and their impact on *A. baumannii* gene expression have been studied (Quinn *et al.*, 2018; Martinez *et al.*, 2021; Pimentel *et al.*, 2021; Ghavanloughajar *et al.*, 2025). Therefore, in this study, we used the LCWB model as a physiologically relevant medium to examine growth, biofilm formation and transcriptional adaptations in *A. baumannii* under wound-like conditions.

3.2 Aim 2

The overall aim of this chapter is to establish the LCWB model as a suitable and physiologically relevant model for investigating *A. baumannii* as a chronic wound pathogen and for testing PVA-based hydrogels. This will be achieved by comparing bacterial growth, biofilm and global gene expression in LCWB medium and compare with standard laboratory media and evaluating the relevance of the observed biofilm-associated and virulence-related responses to chronic wound infection.

1. To apply the LCWB model to investigate *Acinetobacter baumannii* as a wound pathogen.
2. To compare the growth dynamics of *A. baumannii* in LCWB medium with standard laboratory media M9 succinate medium and Luria-Bertani broth using growth curve analysis.
3. To analyse global gene expression profiles of *A. baumannii* grown in LCWB medium versus M9 and LB media by performing RNA-seq. To determine whether the LCWB medium induces biofilm-related genes and virulence factors that are relevant to chronic wound infections.
4. To validate the suitability of the adapted LCWB model for future studies on *A. baumannii* and for testing PVA-based hydrogels.

3.3 Methods

Bacterial strain

A. baumannii strain AB5075 was used in this study. The overnight stocks were grown for 18 hours at 37 °C and 180 rpm in Luria-Bertani (LB) Broth (Thermo Fisher). The stocks were frozen in 20% Glycerol and kept at -80 °C.

3.3.1 Growth Curve Measurement Using LB, M9 Succinate, and Lubbock Chronic Wound Biofilm (LCWB) Model

A Growth Curve assay was performed using 3 different media: LB broth. The LCWB medium was made using 45% Bolton broth, 50% Bovine plasma, 5% freeze–thaw laked horse red blood cells (RBC), and M9 succinate medium. The *A. baumannii* was normalised to $1x10^6$ CFU/mL for each medium. For each condition, 20 mL of the inoculated medium was dispensed into a conical flask. The flasks were incubated at 37 °C with shaking (180 rpm). At predetermined time points (0, 1, 2, 4, 6, 8 and 24 hours), 100 µL aliquots were removed, serially diluted in phosphate-buffered saline, and plated on LB agar for viable count determination. Plates were incubated at 37 °C for 18 hours before colony enumeration. All conditions were tested in 3 technical triplicate and 3 biological triplicates.

3.3.2 Biofilm Assay

The OD_{600} of different media was adjusted to 0.1 from *A. baumannii* AB5075 overnight in LB, LCWB medium and M9 succinate. Every 200 µL of inoculum was transferred into a 96-well plate, then incubated for 24 hours at 37°C and 180 rpm. After 24 hours, the liquid cultures were removed from the plate and washed 3 times with deionised water. 200 µL of a 0.1% solution of crystal violet in water was added to a 96-well microtiter plate and left for 10 min. Then, the crystal violet was removed from each well and washed with deionised water 5 times. The plate

was turned upside down and left to dry for about 1 hour. The 200 µL of 99% ethanol was added to each well. The plate was incubated at room temperature for 10 to 15 min. The absorbance was read in the SPECTROstar Nano plate reader (BMG Labtech) at 570 nm using 200 µL of 99% ethanol as the blank.

3.3.3 Transcriptome analysis of *Acinetobacter baumannii* grown in LB, M9 succinate, and the LCWB medium

To understand *A. baumannii* transcriptomic differences in LB, M9 succinate and the LCWB medium**.** The AB5075 overnight culture was diluted to an OD_{600} of 0.05 in 20 mL of the media accordingly. Cells were grown to an OD_{600} of 0.6-0.7, which is mid-exponential phase. The cells were collected into Eppendorf tubes, spun down, and washed in RNAlater for storage while maintaining the integrity of RNA at -80°C. To isolate RNA, the RNAeasy Kit with on-column DNAase digestion (Qiagen) was used. The RNA integrity was confirmed by gel visualisation. Samples were processed for RNA sequencing on an Illumina MiSeq with 12 million reads per sample, and further analysed at SeqCenter (Pittsburgh, Pennsylvania, USA). Quality control and adapter trimming were performed with bcl-conver (Version 4.2.4). Read mapping was performed with HISAT2 (Version 2.2.0). Read quantification was performed using Subread's feature Counts (Version 2.0.1) functionality. The reference *A. baumannii* AB5075-UW gene annotation was used (GenBank accession number NZ_CP008706.1 (Gallagher *et al.*, 2015). 1375 genes were identified as being significantly differentially expressed, greater than $|logFC| > 1$ and $P < 0.05$ between LB versus M9 Succinate media, 684 genes were identified between LCWB medium versus LB and 1515 were identified between LCWB medium versus M9 Succinate media. VolcaNoseR was used for create a volcano plot (Goedhart and Luijsterburg, 2020). Genes were defined as differentially expressed if Log2(fold change) ≥ 1 or ≤ -1 and p value < 0.05.

3.3.4 Iron Supplement Assay in LCWB Medium

The media was supplemented with 100 μM $FeCl_3$, $FeCl_2$, or both. The media was adjusted to an OD_{600} of 0.1 from an overnight culture of *A. baumannii* AB5075. The plate was incubated at 37°C and 180 rpm for 24 hours. Biofilm was treated and measured as described previously in the biofilm assay.

3.3.5 Time-Kill Assay of AS-Loaded Hydrogel in the LCWB Medium

AS-loaded hydrogels were prepared, weighed (0.6 g), and placed into wells of sterile 24-well plates. A 1 mL suspension of *A. baumannii* AB5075, adjusted to CFU=$1x10^6$ from an overnight culture, was then added to each hydrogel, and the plates were incubated at 37°C for 24 hours. At each time point (0, 2, 4, 6, 8, and 24 hours), the bacterial suspension from each well was collected, serially diluted, and plated to enumerate viable cells.

3.3.6 Degree of Swelling and Weight Loss

The DS was determined by the maximum amount of liquid that hydrogels could absorb (Zhang *et al.*, 2025). In this experiment, the LCWB medium was used to mimic wound-site exudate. AS-Loaded PVA borax hydrogels were freeze-dried overnight until their final weight remained unchanged. The dried hydrogels were then immersed in wound-like medium for 48 hours at 37°C, and their weight was measured at 0, 3, 6, 9, 24 and 48 hours. The DS was calculated by using the formula below. The m_i is the weight at a specific hour, and m_0 is the weight of the dry hydrogel at 0 hours.

$$SD = \frac{m_i - m_0}{m_0} \times 100$$

The weight loss observed in the hydrogel can be an indicator of its degradation (Zhang *et al.*, 2025). To determine this, the swollen hydrogel was freeze-dried again at the end of the swelling test. The hydrogel's dry weight was measured, and the weight loss (WL) was calculated. The W_i is the initial dry weight, and W_d is the weight of the re-dried hydrogel after 48 hours of soaking.

$$WL = \frac{W_i - W_d}{W_d} \times 100$$

3.3.7 Statistical Analysis

Data are expressed as mean ± standard deviation (SD). Statistical analyses were performed using GraphPad Prism. Two-way ANOVA with Tukey correction and one-way ANOVA with Dunnett's correction. Statistical significance was established at p-values of >0.05 (ns), < 0.05 (*), 0.01 (**), 0.001 (***) or 0.0001 (****).

3.4 Results

3.4.1 Wound-Like LCWB Medium Supports Robust *A. baumannii* Proliferation

To evaluate how *A. baumannii* AB5075 responds to different nutritional environments, its growth was examined in LB broth, M9 succinate medium, and LCWB medium. The LB broth is a nutrient-rich environment. Using this to compare with the LCWB medium, we can directly understand if *A. baumannii* proliferates similarly in the LCWB medium. In contrast, M9 succinate medium is a nutrient-limited environment in which succinate is added as the primary carbon source. It works as a baseline control in this condition. Comparing growth across these three media helped understand whether the wound-like LCWB medium alters bacterial growth behaviour when compared with standard laboratory conditions. In this result, *A. baumannii* exhibited robust growth in all three conditions during the 24-hour incubation period. However, minor variations were observed in growth rates and final cell counts.

During the initial exponential phase (4 h), cultures grown in LB and LCWB showed higher CFU counts than those grown in M9 succinate medium, indicating more rapid early proliferation under nutrient-rich and wound-like conditions. This trend remained consistent throughout the experiment, with both LB and LCWB generally supporting greater bacterial growth than M9 succinate. By 6 to 8 hours, bacterial count in LCWB medium attained a level that similar to or marginally exceeding those in LB, whereas M9 succinate demonstrate a lower in growth. After 24 hours, cultures in LCWB exhibited the highest CFU counts, indicating that the wound-like formulation supports effective proliferation of *A. baumannii* (Figure 3.1).

The findings demonstrate that the LCWB medium provides a nutrient-rich environment that

promotes the growth of *A. baumannii,* comparable to conventional nutrient-rich lab media and more effective than minimal medium. This demonstrates its suitability for biofilm and transcriptomic analysis under conditions similar to those of chronic wound infections.

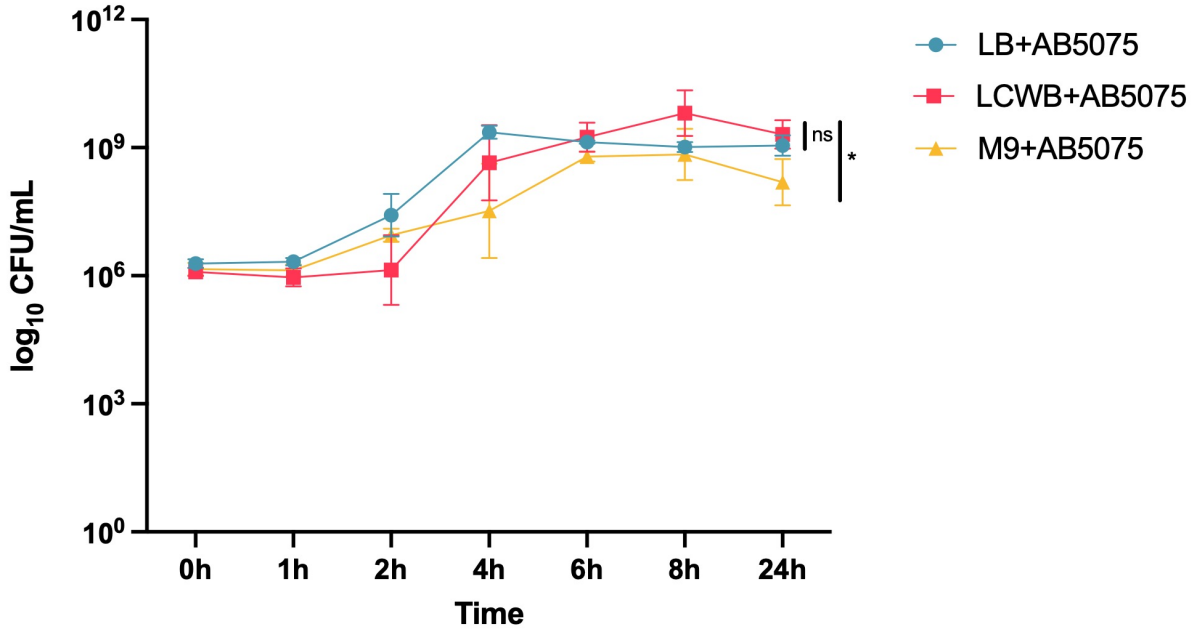

Figure 3.1 Growth curve of *A. baumannii* strain AB5075 in Luria-Bertani (LB) broth, LCWB medium, and M9 succinate medium. Bacterial cultures were normalised to an initial inoculum of 1×10^6 CFU/mL and incubated at 37 °C. CFU cell counts were measured at specified time points (0, 1, 2, 4, 6, 8, and 24 hours). Data represent mean values ± standard deviation from three technical and biological replicates. (ns>0.05, *p-value < 0.05).

3.4.2 LB Broth Promotes *A. baumannii* Biofilm Formation More Than the LCWB medium or M9 Succinate Medium

To determine whether the wound-like LCWB medium influences biofilm formation differently from standard laboratory media, biofilm formation by *A. baumannii* was assessed in LCWB medium, LB, and M9 succinate medium. Biofilm formation of *A. baumannii* AB5075 was measured after 24-hour incubation. In Figure 3.2, LB broth shows the highest level of biofilm

formation, with an average OD_{570} value of approximately 0.49. However, biofilm in LCWB was significantly lower, with an OD_{570} value of around 0.23. The M9 succinate medium exhibited the lowest biofilm formation with an OD_{570} value around 0.15.

The results show that *A. baumannii* can form biofilms in all the media tested. LB broth significantly increased biofilm biomass compared to both wound-like and minimal media. These results suggest that the nutrient-rich LB broth promotes biofilm formation by *A. baumannii*. In contrast, LCWB medium appears to support planktonic growth more strongly than biofilm formation.

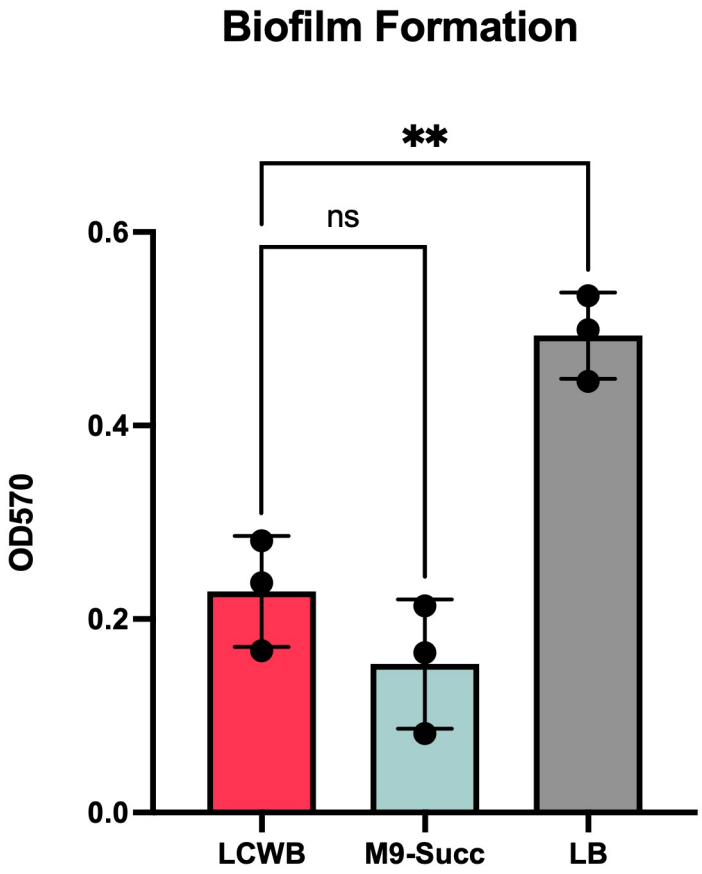

Figure 3.2 Biofilm formation of *A. baumannii* AB5075 in LCWB, M9 succinate medium, and LB broth. Biofilm biomass was quantified using crystal violet staining after incubation, and absorbance was measured at 570 nm. Data represent the mean ± standard deviation from three technical and biological replicates. (ns>0.05, **p-value < 0.01).

3.4.3 LCWB Medium Induces Iron-Starvation Responses and Represses Environmental Persistence Pathways in *A. baumannii*

In previous assays, differences in growth and biofilm formation were observed. However, they cannot explain the molecular mechanisms underlying these changes. To investigate how *A. baumannii* adapts to a host-mimicking wound environment transcriptional level, we conducted RNA-sequencing (RNA-seq) to profile global transcriptional changes in LCWB medium compared with two commonly used laboratory conditions, LB and M9-succinate. The LB represents a nutrient-rich, non-host environment, and M9-succinate serves as a defined minimal medium.

The LCWB medium and LB comparison allowed us to identify genes specifically induced by host-associated stresses. We found that 684 genes were expressed differentially. Among all genes, 308 are upregulated and 376 are downregulated (Figure 3.3). We further analysed our dRNA-seq data by performing Gene Set Enrichment Analysis with FUNAGE-Pro to understand the functionality of the gene that was regulated differently (de Jong, Kuipers and Kok, 2022). In Gene Set Enrichment Analysis, the current *A. baumannii* AB5075-UW annotated genome was used (Gallagher *et al.*, 2015; Gadar *et al.*, 2023). In Gene Ontology comparison, iron ion homeostasis, siderophore transport, siderophore uptake transmembrane transporter activity, and isochorismatase activity were upregulated. Iron plays an important role in the growth and virulence of bacteria such as *A. baumannii* because it is a cofactor of DNA synthesis, cellular respiration and oxidative stress management. There are six gene clusters for active iron uptake in *A. baumannii:* the *feo* cluster, which transports Fe^{2+} through the cytoplasmic membrane; the haem uptake, which produces transport systems for haem and haem-binding protein (*hem*T and *hem*O gene clusters); and synthesis and transport of baumannoferrin(s) (*bfn* gene cluster), acinetobactin (*bas/bau* gene cluster) and fimsbactin(s) (*fbs* gene cluster) siderophores (Artuso *et al.*, 2023).

In this study, genes related to iron ion homeostasis (ABUW_0159, ABUW_1646, ABUW_1655, ABUW_1800, ABUW_2165, ABUW_2182, *pfe*A, ABUW_2987, ABUW_3403, *feo*B) were upregulated. In these genes, ABUW_2182 and ABUW_3403 encode a TonB-dependent receptor, and *pfe*A encodes the TonB-dependent outer membrane siderophore. The TonB complex helps iron carriers such as siderophores and haemophores to enter the periplasm by converting the proton gradient into energy that is needed to open the gated channel on the outer membrane receptor (Artuso *et al.*, 2023).

Moreover, the whole acinetobactin iron-acquisition cluster (*bar*A-B, *bas*A-J, *bau*A-F) was upregulated, and the acinetobactin siderophore is the most important iron-uptaking molecule in *A. baumannii*. The *feo*A&B in the *feo* gene cluster was upregulated as well, and the *feo* system works as a conserved ferrous iron acquisition system (Antunes *et al.*, 2011). Along with *fum*C, which encodes class II fumarate hydratase, it is produced in iron-limited conditions (Nwugo *et al.*, 2011). These observations indicate the LCWB medium provides limited iron resources for *A. baumannii,* indicating that it recapitulates the real wound conditions and stresses *A. baumannii* experiences in the human host as most iron is bound and unavailable (Law and Tan, 2022).

Furthermore, genes that regulated the siderophore transport (ABUW_0159, *bau*A, ABUW_1800, ABUW_3403), siderophore uptake transmembrane transporter activity (ABUW_0143, ABUW_0159, *bau*A, ABUW_1646, ABUW_1655, ABUW_1800, ABUW_2165, ABUW_2182, ABUW_2828, ABUW_2916, ABUW_3403) and isochorismatase activity (*bas*F, ABUW_2075) were also upregulated. According to Sheldon and Skaar (2020), under iron-restricted conditions, siderophore-associated loci are upregulated,

whereas excess iron inhibits siderophore production by the *A. baumannii*. This would further indicate that *A. baumannii* in the LCWB medium is in an iron-limited environment.

We next examined pathways that were significantly downregulated in the LCWB medium compared with LB. Gene set enrichment analysis revealed a coordinated repression of several metabolic modules typically associated with environmental carbon utilisation. Notably, both genes encoding the ferritin-like ferroxidases (*bfr*1 and *bfr* 2; 2/2) were downregulated, suggesting cells try to promote iron storage under wound-like conditions (Gadar *et al.*, 2023). In addition, all four components of the phenylacetyl-CoA 1,2-epoxidase complex (*paa*A-C, *paa*E; 4/4) and the majority of genes involved in the broader phenylacetate degradation pathway (12/16; including *paa*A–*paa*E, *paa*G, *paa*I2, *paa*K, *paa*Z, *cai*D, *dca*H, and ABUW_1006) were significantly repressed. Likewise, both genes associated with 3-hydroxybutyryl-CoA dehydrogenase activity (*dca*H, *paa*C; 2/2) showed decreased expression. The PAA catabolic pathway encoded by the *paa* operon is an important route in the catabolism of several aromatic compounds that converge and are directed to the Krebs cycle. Together, these findings indicate that in LCWB medium (rich in peptides, amino acids, lipids, and host proteins), it can use these carbon sources, so PAA catabolism is switched off. These *paa* genes were downregulated, which could also due to the iron availability. According to Robin *et al.* (2022), disruption of iron homeostasis in *A. baumannii macAB-tolC* mutants resulted in up to 15-fold downregulation of five proteins in the PAA pathway (PaaA, PaaG, PaaZ, PaaJ, and PaaH). These findings suggest that the expression of PAA-associated genes may be modulated by iron status. Moreover, the downregulated *paa* could leads to virulence reduction since the global virulence regulator *gac*A was also downregulated (Cerqueira *et al.*, 2014). Furthermore, *csu*A/B, *csu*A, *csu*B, *csu*C, *and csu*D were downregulated, together with *mai*A, in the LCWB

medium, which could be the reason why there was less biofilm formed (Rumbo-Feal *et al.*, 2013).

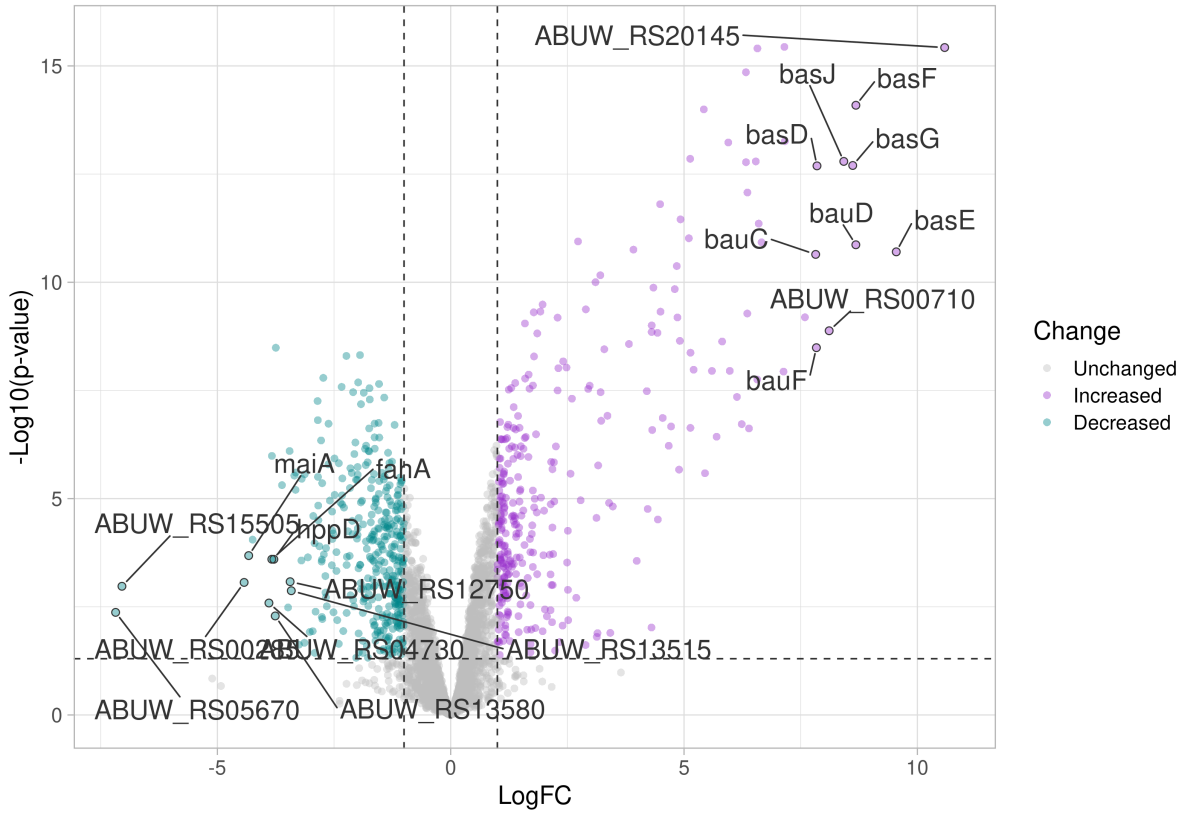

Figure 3.3 Volcano plot of differentially expressed genes in *A. baumannii* AB5075 grown in LCWB medium compared to those grown in LB broth (n=3). The x-axis represents $\log_2$ fold change (LogFC), while the y-axis shows $-\log_{10}$(p-value). Purple dots indicate significantly upregulated genes, teal dots indicate significantly downregulated genes, and grey dots represent genes with no significant change in expression.

3.4.4 Wound-like Conditions Trigger a Global Shift Towards High Translational and T4P Activity When Compared to M9-succinate Medium in *A. baumannii*

To understand how *A. baumannii* genes regulate differently from a nutrient-limited state to a host-associated, nutrient-rich environment, we carried out differential RNA-sequencing

(dRNA-seq) comparing bacteria grown in LCWB medium with those in M9 minimal medium. We found that 1515 genes were expressed differentially. Among all the genes, 745 are being upregulated, and 770 genes are being downregulated (Figure 3.4). We further analysed our dRNA-seq data by performing Gene Set Enrichment Analysis with FUNAGE-Pro to understand the functionality of the gene that regulated differently (de Jong, Kuipers and Kok, 2022). A striking feature of the LCWB medium transcriptome was the upregulated genes that related to the ribosomes, such as translation machinery, ribosomes, ribosome biogenesis, ribonucleoprotein complex, structural constituent of ribosome, large and small ribosomal subunits, ribosomal large subunit assembly, large ribosomal subunit rRNA binding, and ribosomal small subunit biogenesis. Numerous genes related to ribosomal translation (*rpl*A-F, I-J, L-Y, *rpm*A-J, *rsp*A, B, D-U, ABUW_0258, *ett*A-C, *pth*) were upregulated. The genes related to ribosome (*rpl*C-F, I, K, L, M, P-Y, *rpm*A-C, E, G-J, *rsp*F, H-K, M-U), ribosome biogenesis (ABUW_0380, *cgt*A, ABUW_3111, *der* and *nus*A), Ribonucleoprotein complex (*rpl*C-F, *rpl*I, *rpl*K-M, *rpl*P-U, *rpl*W-Y, *rpm*A-J, *rps*F, *rps*H-U), Structural constituent of ribosome (*rpl*A-F, *rpl*I-Y, *rpm*A-J, *rps*A-U), large ribosomal subunit (*rpl*A, B, J, N, O, V and *rpm*D, F), small ribosomal subunit (*rps*B, D, E, G, L, S), large ribosomal subunit assembly (typA, *rpl*T and ABUW_0381), large ribosomal subunit rRNA binding (*rpl*J, K) and ribosomal small subunit biogenesis (*rsg*A, *rim*M, P and *era*) were also upregulated in LCWB medium conditions when compared with M9. Alone with phenylalanyl-tRNA aminoacylation and phenylalanine-tRNA ligase activity (*phe*T, S). These changes indicate a shift from a low-growth, resource-limited state in M9–succinate to a highly active translational regime in the LCWB medium (Calabrese, Ciandrini and Cosentino Lagomarsino, 2024).

Additionally, in the LCWB medium, the genes related to T4P biogenesis, machinery and regulation were upregulated. T4P is the key structure in *A. baumannii* that regulates the bacterial twitching motility. It also regulated transformation and natural competence of *A.*

baumannii due to DNA uptake machinery, DNA binding and recombination. In this study, *pil*A, *pil*B, *pil*G, *pil*T, *pil*V-Z, and *fim*V were upregulated. Moreover, several genes annotated as *com* (*com*MNOPQ, with locus tags ABUW_0290– 0294) were also upregulated (de Dios *et al.*, 2023a). These genes should be part of *pil* clusters based on the current AB5075 annotation (Gallagher *et al.*, 2015). These upregulations of *pil* genes could potentially promote natural transformation and twitching motility (Ellison *et al.*, 2021; Vesel Nina and Blokesch Melanie, 2021). Furthermore, the *dprA* is one of the genes directly involved in DNA uptake and stabilisation, and it was also upregulated (de Dios *et al.*, 2023). This competence-associated state could enhance *A. baumannii* to adopt a competence-like state that favours DNA acquisition. Such a shift could increase the potential for exogenous DNA uptake, with possible implications for adaptation and resistance development.

We next examined pathways that were significantly downregulated in the LCWB medium compared with M9. 3-hydroxybutyryl-CoA epimerase activity, 3-isopropylmalate dehydratase activity, 3-oxoadipate enol-lactonase activity, 3-phenylpropionate catabolic process, propionate metabolic process, methylcitrate cycle, poly-hydroxybutyrate (PHB) biosynthetic process. These pathways are associated with growth under stress conditions, such as limited nutrient conditions. For example, poly-hydroxybutyrate (PHB) is one of the common polyhydroxyalkanoates (PHA), which can be produced by 40 to 60 species of microorganism (D. Li *et al.*, 2025) Bacteria will use it under the carbon limited condition, and 3-hydroxybutyryl-CoA is one of the intermediate products in PHB production (Prados and Maicas, 2016; Jia *et al.*, 2025). The methylcitrate cycle is an analogous pathway to the tricarboxylic acid cycle, and it involves the catabolism of propionyl-CoA, which can prevent the accumulation of toxic propionyl-CoA and provide energy (Korn, Brock and Schuster, 2025). They downregulated in the LCWB medium indicates that *A. baumannii* does not depend on

these scavenging and storage strategies compared with M9-succinate. It could use the nutrients directly from the LCWB medium.

In addition to the metabolic pathway, there are gene groups associated with biofilm formation, interbacterial competition and secretion system that were also downregulated in the LCWB medium. For example, *csu*AB, *csu*B, ABUW_1634 (Csu type fimbrial protein), ABUW_1634 (Csu type fimbrial protein) were downregulated in the LCWB medium, and these genes are associated with Csu pili, and they can help with initiation attachment and biofilm formation on abiotic surfaces (Ahmad *et al.*, 2023). Fimbrial usher porin activity *(*ABUW_1163, ABUW_2054, ABUW_2312) is associated with the largest β-barrel outer membrane proteins (OMPs), and it moves bacteria on the surface (Palomino, Marín and Fernández, 2011). Toxin sequestering activity (ABUW_1158, ABUW_2618) is associated with the antitoxin system and type VI secretion system Vgr family protein.

Type VI secretion system: *tss*B, *tss*C, *tss*F, ABUW_2817 (type VI secretion system Vgr family protein), ABUW_2578 (Hcp family type VI secretion system effector), ABUW_2618 (type VI secretion system Vgr family protein) were also downregulated in the LCWB medium. The Type VI secretion system can inject toxins into both eukaryotic cells and prokaryotic cells and work as a weapon in interbacterial competition. It can also reduce *A. baumannii* biofilm formation (Dong *et al.*, 2022). This could be why genes associated with Csu pili were downregulated, while biofilm formation remained higher than in M9-succinate. In the LCWB medium, *A. baumannii* shifts its focus from competitive interactions to growth and host colonisation.

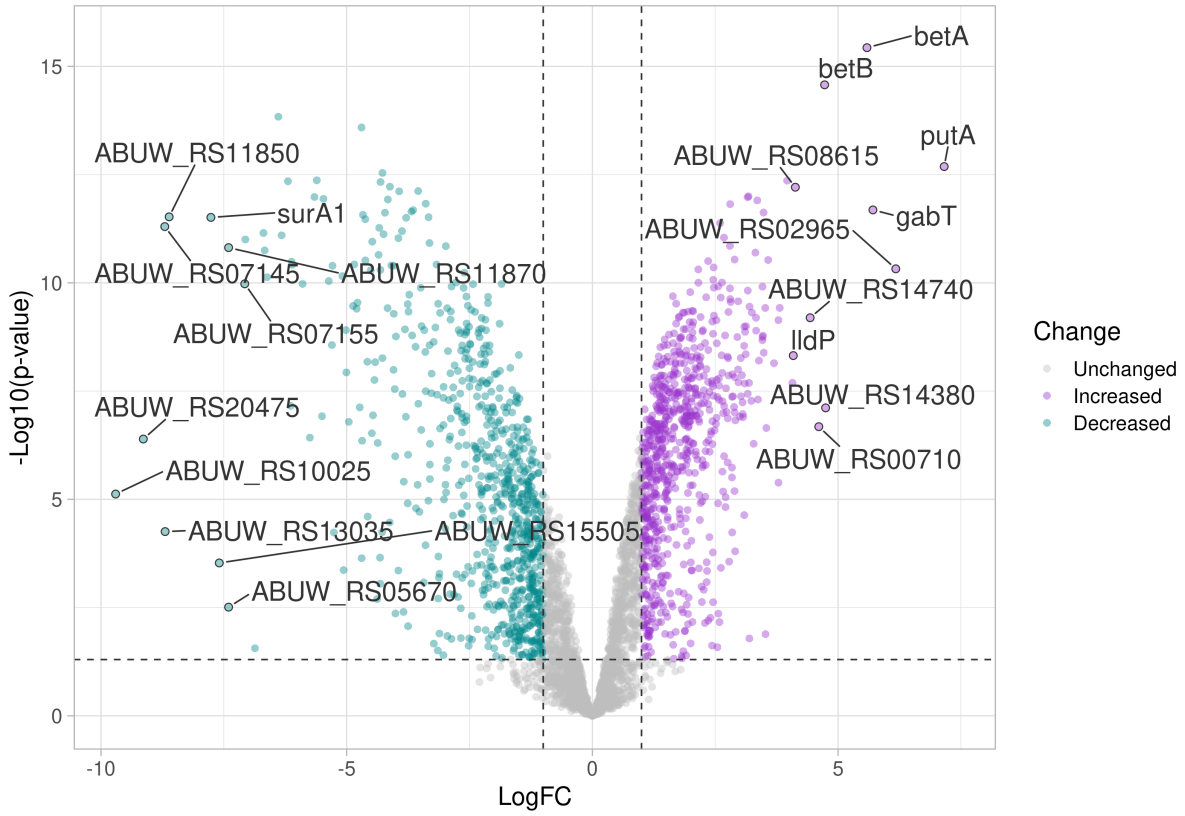

Figure 3.4 Volcano plot of differentially expressed genes in *A. baumannii* AB5075 grown in LCWB medium compared to those grown in M9 succinate. (n=3). The x-axis represents $\log_2$ fold change (LogFC), while the y-axis shows $-\log_{10}$(p-value). Purple dots indicate significantly upregulated genes, teal dots indicate significantly downregulated genes, and grey dots represent genes with no significant change in expression.

3.4.5 Iron is a Key Factor in the *A. baumannii* Biofilms Formation in LCWB medium

In our previous RNA-Seq experiments, we observed that genes associated with iron uptake were up-regulated in LCWB medium. Furthermore, biofilm formation in the LCWB medium was relatively reduced compared to that in the LB medium. Iron is essential for *A. baumannii* nutrition and virulence, and iron availability can influence different *A. baumannii* strains form

biofilms differently, as they respond to iron differently (Zimbler *et al.*, 2009; Gentile *et al.*, 2014). According to Gentile *et al.*, (2014), iron limitation influenced biofilm formation in *A. baumannii* in a strain-dependent manner: 42% *A. baumannii* isolates produced significantly enhanced biofilm in iron-deficient media, 24% showed reduced biofilm formation, and 34% showed no effect. In our study, biofilm formation was reduced in the LCWB medium compared with LB. Based on these findings, we hypothesise that iron availability may contribute to the regulation of biofilm formation in *A. baumannii* AB5075 under LCWB conditions. Therefore, the media was supplemented with 100 µM $FeCl_3$, $FeCl_2$ or $FeCl_3$ and $FeCl_2$. The addition of 100 µM $FeCl_3$ promotes biofilm formation from OD_{570}= 0.26 to 0.35. Supplementation with $FeCl_3$ and $FeCl_2$ together restores biofilm formation levels to OD_{570}= 0.44, which is similar to that in LB medium (OD_{570}= 0.50) (Figure 3.5). It could due to the Fe (III) acquisition appears to be more predominant than Fe (II) uptake in this strain (Runci *et al.*, 2019).

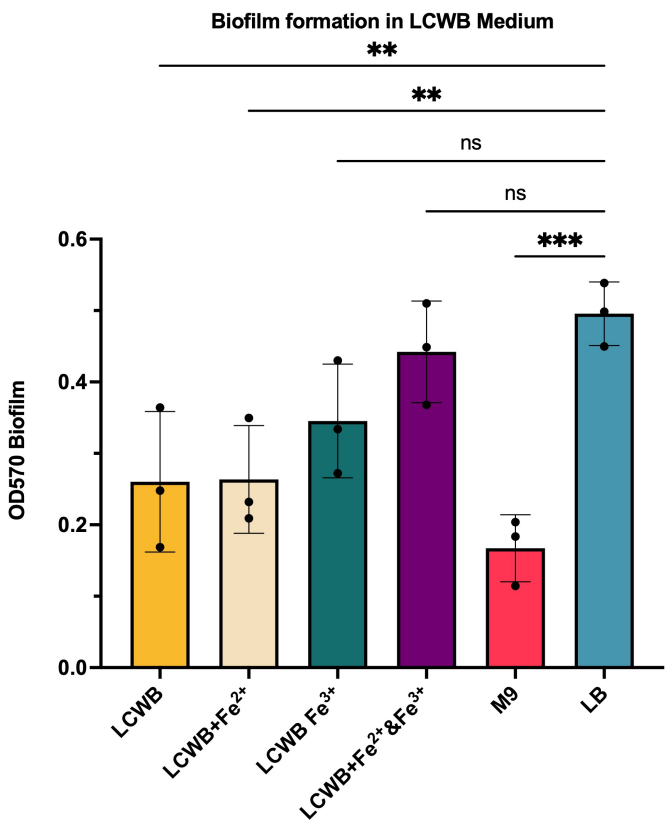

Figure 3.5 Biofilm formation of *A. baumannii* under different iron supplement combinations in the LCWB medium. The biofilm was restored when Fe^{2+} and Fe^{3+}were presented. Data are presented as mean ± SD and n=3. Statistical significance was determined using one-way ANOVA to compare the LB, M9 and LCWB media and their iron-supplemented samples. (ns>0.05, *p-value < 0.05,**p-value < 0.01, *** p-value < 0.001).

3.4.6 Artificial Sweetener-Loaded-Hydrogel Demonstrates Antimicrobial Activity in a Host-Mimicking Wound Environment

From previous results, the LCWB medium provides limited iron resources for *A. baumannii*, which is a host-mimicking wound condition (Law and Tan, 2022). This media provides a practical platform for evaluating the hydrogels developed in the previous chapter, as it provides more detailed information on their performance at the intended site of application. In this nutrient-rich broth, the control hydrogel maintained the bacterial population at a stable level, as borate has an antimicrobial effect. However, as the hydrogels gradually released their AS from the system, the effect became more apparent, although the initial antibacterial effect was not particularly significant (Figure 3.6A). At the 24-hour time point, all the Ace-K-Loaded PVA borate hydrogel reduces cell viability by about 2.95 log, the CYC-Loaded PVA borate hydrogel reduces 2.38 log, and the SACC-Loaded PVA borate hydrogel showed the highest inhibition, which is about 4.23 log (Figure 3.6B). In our previous finding in chapter 2, the 8% CYC-loaded hydrogel demonstrated the reduction of ~6.42 log in CFU/mL after 24 h, while the 8% Ace-K-loaded hydrogel achieved a reduction of ~6.40 log. The 8% SACC-loaded hydrogel reduced bacterial growth by ~5.56 log. The greater apparent inhibition observed in this assay may be partly attributable to the use of PBS, which does not provide nutrients to support bacterial growth.

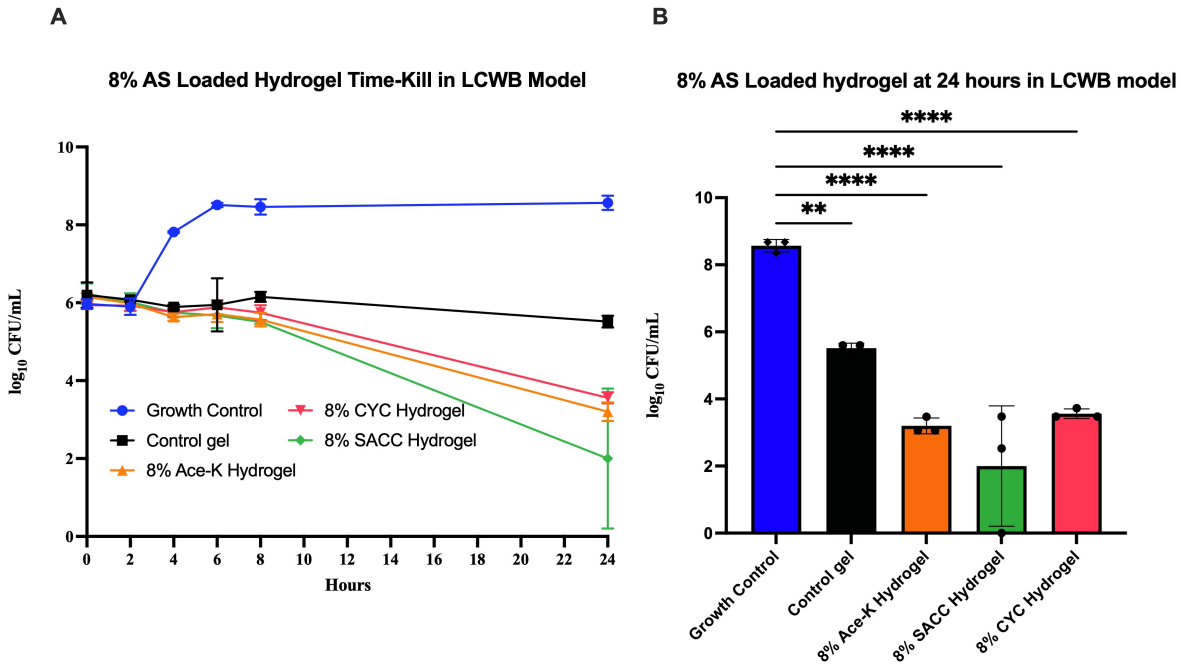

Figure 3.6 Time-kill assay of AS-loaded borate hydrogel against *A. baumannii* (A) Time-kill of AS-loaded hydrogel against *A. baumannii* in LCWB medium (B) Bactericidal activity of 8% AS-Loaded Hydrogels Against *A. baumannii* at 24 Hours (n=3 ± SD). Statistical analysis was performed using one-way ANOVA to compare the control and treated samples. (**p-value < 0.01, **** p-value < 0.0001)

3.4.7 Artificial Sweetener-Loaded-Hydrogel Showed Similar Swelling and Degradation behaviour in LCWB medium and PBS

Swelling behaviour is a critical factor for hydrogel wound dressings, as it absorbs blood and wound exudate, and is important for the release of loaded agents, nutrient delivery, and metabolite transfer (Feng and Wang, 2023; Xin *et al.*, 2025). In Figure 3.7A, the control hydrogel absorbs LCWB medium quickly, and the DS reaches 478.97% at 3h. The DS further increased to a maximum of 535.22% at 6h. Thereafter, the DS gradually declined to 386% but remained higher than that of the loaded hydrogels after 48 h.

Moreover, all 8% AS-loaded hydrogels showed lower DS than the control hydrogel in PBS (Figure 3.7A). The DS of AS-Loaded hydrogels remained within a relatively narrow range of approximately 160–220% over 48 h. Among these formulations, the 8% CYC hydrogel generally displayed the highest DS of 207%, whereas the 8% SACC hydrogel showed the lowest overall DS, around 162.15%. The 8% Ace-K hydrogel exhibited an intermediate profile, with DS around 184.26%. Furthermore, all loaded hydrogels reached their initial swelling equilibrium within the first 3 h and remained comparatively stable thereafter, with no pronounced secondary swelling phase observed. The minor reduction in DS observed in the CYC and Ace-K hydrogels may be due to AS diffusion from the hydrogel system into the medium. However, at the 6th hour, the AS was released completely, and a slight increase in DS was observed. It could be due to the system still absorbing water, nutrients and proteins from the medium. The weight loss percentage of the control hydrogel was about 45.02% after 48 hours. The sweetener hydrogel shows a higher weight loss percentage, with 68.64% for SACC-Loaded hydrogel, 64.51% for CYC-Loaded hydrogel, and 66.46% for-Ace-K Loaded hydrogel (Figure 3.7B). This higher weight-loss percentage could be due to the artificial sweetener diffusing from the hydrogel system into the LCWB Medium. Overall, AS-Loading hydrogels in LCWB Medium showed a similar DS profile and degradation to that in PBS.

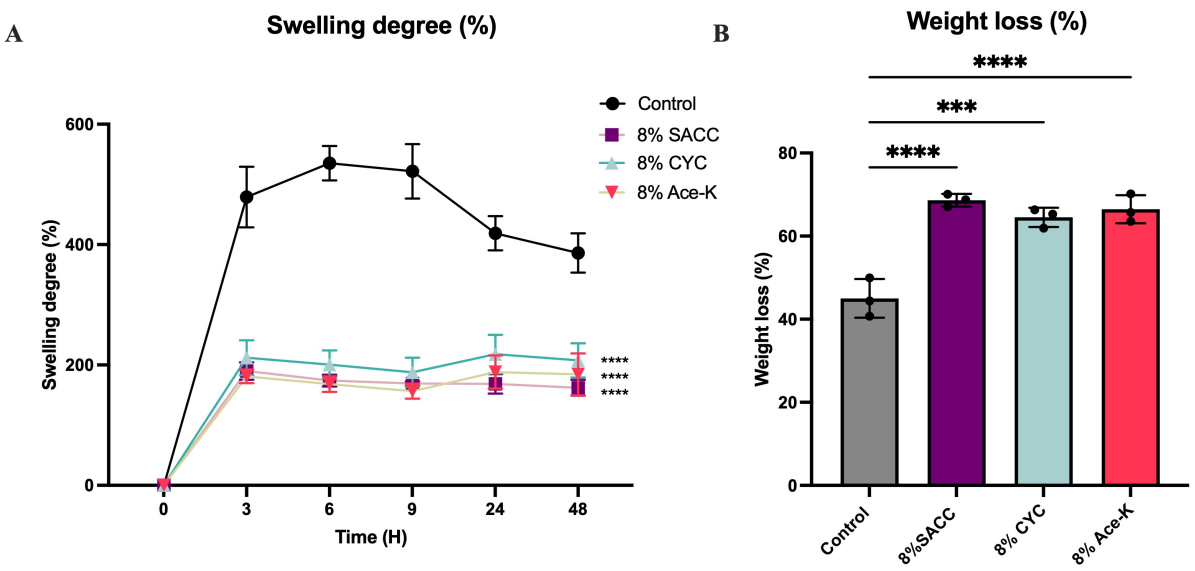

Figure 3.7 Swelling and Weight loss: (A) Swelling degree (%) of PVA–borax hydrogels incorporated with different AS over a 48-hour period in LCWB medium. Hydrogels were measured at 3, 6, 9, 24, and 48 hours. The control hydrogel exhibits the highest SD% among the hydrogels. (B) Weight loss (%) was measured at 48 h after re-dry, with hydrogels containing 8% (w/w) Ace-K, SACC, CYC and a control hydrogel. Data are presented as mean ± standard deviation (n = 3). Error bars represent standard deviation (SD). Statistical analysis for A was using two-way ANOVA with Tukey correction between the AS-loaded hydrogel and the control hydrogels. Statistical analysis for B were performed by one-way ANOVA with Dunnett's correction between the control and AS-loaded hydrogel. (*** p-value < 0.001, **** p-value < 0.0001)

3.5 Discussion

This study showed that the LCWB medium induces a coordinated transcriptional and phenotypic reprogramming in *A. baumannii*, reflecting adaptation to a host-mimicking wound environment. The growth of *A. baumannii* in LB and LCWB media was relatively similar. However, the biofilm formation was reduced in LCWB media. Therefore, we performed RNA-Seq in LB, M9 succinate, and LCWB media to determine why these changes occur across different media.

Compared with LB, *A. baumannii* in LCWB medium reveals iron acquisition systems, including siderophore biosynthesis (Bas/Bau clusters), TonB-dependent receptors, and ferrous iron transport systems, which were strongly upregulated. This means the LCWB medium is a nutrient-rich, but iron-limited environment, which is similar to the macromolecular nutritional environment experienced by *A. baumannii* in wounds (Law and Tan, 2022). Moreover, due to the iron-limited environment, *paa* genes were downregulated and it was reported in other studies (Nwugo *et al.*, 2011b; Robin *et al.*, 2022). The downregulation of *paa* could reduce virulence, as the global virulence regulator *gac*A was also downregulated (Cerqueira *et al.*, 2014). Furthermore, *csu*A/B, *csu*A, *csu*B, *csu*C, *and csu*D were downregulated, together with *mai*A, in the LCWB medium, which may explain the reduced biofilm formation (Rumbo-Feal *et al.*, 2013). Quinn *et al.*, (2018) reported that biofilm formation decreased with additional human serum albumin. The genes associated with biofilm formation were downregulated, including *fimA*, *ompA*, *csuA,* and *csuC.* In another study, the biofilm formation by *A. baumannii* AB5075 was also reduced with additional human serum albumin and pooled normal human serum in LB when compared with LB alone (Pimentel *et al.*, 2021). The genes *csuA/B, csuB, and csuE were* expressed at lower levels in these media than in LB. Together, these studies and

our research suggest that host-derived macromolecules can shift *A. baumannii* away from a classic abiotic biofilm toward host-adaptation strategies.

Compared with M9 minimal medium, LCWB supported enhanced bacterial growth and was associated with global upregulation of ribosomal proteins and ribosome-associated synthetases, consistent with the higher nutritional availability of the medium. This indicates a change towards a highly active translational and biosynthetic state. These results suggest that *A. baumannii* transitions from a nutrient-limited, low-growth condition to a metabolically active regime when exposed to wound-like conditions. Moreover, genes associated with pil were also upregulated. These upregulations of *pil* genes could potentially promote natural transformation and twitching motility (Ellison *et al.*, 2021; Vesel Nina and Blokesch Melanie, 2021). Furthermore, the *dprA* is one of the genes directly involved in DNA uptake and stabilisation, and it was also upregulated (de Dios *et al.*, 2023).

Apart from upregulated genes and pathways, there were some metabolic pathways that were downregulated. For example, poly-hydroxybutyrate (PHB) usually active when bacteria under the carbon limited condition (Prados and Maicas, 2016). The methylcitrate cycle is involves the catabolism of propionyl-CoA, which prevents the accumulation of toxic propionyl-CoA and provides energy (Korn, Brock and Schuster, 2025). They downregulated in the LCWB medium indicates that *A. baumannii* does not depend on these scavenging and storage strategies compared with M9-succinate. It could use the nutrients directly from the LCWB medium. In addition to the metabolic pathway, the gene associated with biofilm formation, interbacterial competition and the secretion system were also downregulated in the LCWB medium such as *csu*AB, *csu*B, ABUW_1634 (Csu type fimbrial protein), ABUW_1634 (Csu type fimbrial protein) (Ahmad *et al.*, 2023) and genes in the Type VI secretion system. Upregulation of

Type VI secretion system + isolates showed a lower biofilm formation activity (Dong *et al.*, 2022). In this case, genes associated with Type VI secretion system + were downregulated. This could be why genes associated with Csu pili were downregulated, while biofilm formation remained higher than in M9-succinate. These results also indicated that in the LCWB medium, *A. baumannii* shifts its focus from competitive interactions to growth and host colonisation.

Interestingly, biofilm formation in LCWB was lower than in LB despite robust bacterial growth. And the iron uptake-related gene was upregulated in LCWB, so we supplemented with Fe^{3+}, Fe^{2+}/or combined Fe^{2+}/Fe^{3+} restored biofilm to levels comparable to LB. In the Fe^{2+}/Fe^{3+} group, the biofilm was restored to a level similar to that in LB, highlighting iron as a critical regulator linking metabolism and biofilm behaviour. In the meantime, we assess AS-Loaded hydrogel behaviour in this wound-like LCWB medium against *A. baumannii.* As a result, both AS-loaded PVA borate hydrogels showed activity against *A. baumannii* in this wound-mimic condition. Therefore, the LCWB not only can be used as a model for studying wound-associated issues at the molecular level, but also as a practical platform for evaluating antimicrobial hydrogel.

3.6 Key Findings

1. Validation of the LCWB medium as a wound-like model for *A. baumannii.*
2. Identification of iron limitation as a major transcriptional signal in the LCWB medium when compared with the LB medium.
3. Compared with M9, LCWB provides a more nutrient-rich environment and more closely mimics host-associated conditions, as supported by transcriptional analysis.
4. Demonstration that iron availability regulates biofilm formation in LCWB medium.
5. Validation of the LCWB model for testing antimicrobial hydrogels and swelling and degradation behaviour.

Chapter 4

4. A 3D-Printable Poly(vinyl alcohol)/Hydroxypropyl Methylcellulose Hydrogel with Controllable Mechanical Properties and Drug Release

4.1 Introduction

The skin is the largest organ in the human body and provides several physiological functions, including acting as a physical barrier, maintaining haemostasis, and regulating body temperature. It also provides immunological, neurosensory and metabolic roles (Todorova and Mandinova, 2020). The functions of the skin can be disrupted by damage to the epithelial and connective tissues caused by various injuries and systemic diseases, thereby disrupting the body's haemostasis (Xu *et al.*, 2024). Combined with damaged skin and disturbed haemostasis, the risk of infection and the potential resulting in chronic, non-healing wounds could increase (Q. Zhang *et al.*, 2022; Zegadło *et al.*, 2023). Therefore, effective wound management is essential to minimise bacterial infection and promote proper healing.

Wound dressings are widely used in wound management as temporary barriers that protect the wound bed. An ideal wound dressing should absorb wound exudate, maintain a moist environment, prevent infection, allow gas and nutrient exchange, and exhibit excellent biocompatibility (Graça *et al.*, 2020). Hydrogels are considered excellent candidates for wound dressings due to their hydrophilic nature, soft-tissue-like water content, tuneable mechanical strength, and biocompatibility (Kamoun, Kenawy and Chen, 2017; Xu *et al.*, 2024). PVA is a widely used synthetic polymer in biomedical applications due to its excellent biocompatibility, tissue adhesion properties, and gel-forming capabilities, which have been extensively studied for wound dressing applications as a vehicle of drug delivery (Harmanci *et al.*, 2022; Q. Zhang *et al.*, 2022). Conventionally, drug release from PVA hydrogels can be tailored by varying the

freeze–thaw cycles, molecular weight, and polymer concentration (Quispe-Siccha *et al.*, 2024). However, in the previous chapter study, the AS-loaded PVA borax hydrogels have excellent antimicrobial properties, but their mechanical properties were changed by adding AS, resulting in phase separation. The gel can become brittle and crumble under significant pressure. To address these limitations, FT-PVA hydrogels were explored as a more stable alternative. Although the FT-PVA system improved gel integrity, it did not meet sufficient antibacterial activity, even with a better release approach when the PVA concentration was reduced and the number of FT cycles. Additionally, using a low number of FT cycles and low PVA concentration compromises the hydrogel's mechanical properties, which are critical for wound-dressing applications. Therefore, an alternative strategy is required to improve drug release from FT-PVA hydrogels while maintaining robust mechanical properties.

In recent years, direct ink writing (DIW) based three-dimensional (3D) printing has emerged as a promising fabrication strategy for drug-delivery platforms, enabling the production of complex geometries with controllable internal architectures and tuneable drug loading and release behaviours (Harmanci *et al.*, 2022). This creates the way to producing dressings with tailored geometry, porosity, and surface area for a potential better antimicrobial property. 3D printing could also offer potentially bespoke wound dressings designed for different wound sizes, depths, or exudate conditions. However, the low viscosity of PVA solutions limits their printability, and 3D printing of PVA typically requires low-temperature plates (−5 to −40 °C) to maintain structural fidelity (Kim *et al.*, 2018). This approach introduces several limitations. Under uncontrolled room-temperature conditions, plate temperatures may fluctuate over time, resulting in unstable sample fabrication. Additionally, long printing durations can further alter plate temperature. During multilayer printing, PVA near the cold plate may solidify, while layers farther away remain unfrozen, constraining both design flexibility and printing

versatility. To overcome these challenges, cellulose derivatives have been increasingly explored as rheology modifiers and structural enhancers in bioprinting inks (Sharma *et al.*, 2025). Incorporating cellulose derivatives can improve the biocompatibility, mechanical strength, and thermal properties of PVA hydrogels, providing a versatile platform for tailoring ink rheology and printability (Sargur Ranganath *et al.*, 2022).

Among cellulose derivatives, hydroxypropyl methylcellulose (HPMC) is a biocompatible hydrophilic polymer widely used as a binder and controlled-release agent in the pharmaceutical industry. HPMC can form hydrogels upon swelling in water and rapidly absorb water due to the presence of hydrophilic residues, such as hydroxypropyl and methyl groups, within its network (Li *et al.*, 2019). This high water-absorption capacity is a key characteristic for hydrogel-based wound dressing applications (Vo *et al.*, 2022).

In this study, a 3D printable PVA-based ink incorporating HPMC was developed to fabricate drug-loaded hydrogels using a freeze-thaw method. The incorporation of HPMC was intended to improve ink rheology, printability, and structural stability while maintaining favourable drug-release characteristics. The SACC was added into PVA+HPMC hydrogels system, because SACC shown excellent antimicrobial property in ZOI and established biofilm model previously. Therefore, we use SACC as a sample molecule. The printing performance and gel properties were systematically evaluated by comparing rheological behaviour, printability, mechanical properties, and drug-release profiles. This work provides insight into the design of cellulose-modified PVA inks and proposes a versatile strategy for fabricating 3D-printed drug-delivery systems with controllable release characteristics for wound-dressing applications.

4.2 Aim 3

The overall aim of this chapter is to develop a 3D-printable PVA hydrogel incorporating sodium saccharin as a model antimicrobial agent. Follow by evaluating its potential for wound-dressing applications. This study will assess the rheological and printability properties of the hydrogel, as well as its release behaviour, antimicrobial performance, cytocompatibility and haemocompatibility.

1. To formulate a printable PVA based ink.
2. To evaluate the rheological and printability properties.
3. To incorporate sodium saccharin as a model antimicrobial agent.
4. To determine whether 3D printing enhances release behaviour and antimicrobial performance.
5. To assess the cytocompatibility and haemocompatibility of the developed hydrogel system for potential wound-dressing application.

4.3 Materials and methods

4.3.1 Material

Poly (vinyl alcohol) (PVA) (61,000 Mw) was purchased from Sigma-Aldrich (USA). The Hydroxypropyl Methylcellulose (HPMC) (METOLOSE® SR 90SH-4000, Mw 270000 g mol−1, Tokyo, Japan) was donated by Shin-Etsu Chemical Co. Ltd (Tokyo, Japan). The sodium saccharin (99%) was purchased from Sigma-Aldrich (USA). The dermal fibroblast cell line was donated by Professor Bridger's group (Bridger *et al.*, 1993). The horse blood defibrinated was purchased from TCS Bioscience (UK).

4.3.2 Ink Formulation

A PVA solution was prepared by dissolving PVA in water under continuous heating in a water bath at 90 °C for 1 hour to ensure uniform dissolution with difference formulation (Table 4.1). Once the PVA was completely dissolved, HPMC was added to the solution and mixed thoroughly until a homogeneous mixture was obtained. To determine which concentration of PVA performs better in printing, we first tested different concentrations of PVA (10 to 30%) by using the manual dispensing assessment based on Zhang *et al.* study (2021). For each sample, a 20-gauge nozzle tip was used, and the pressure was applied on the plunger until the sample was extruded. After confirming the PVA concentration, different HPMC concentrations (The same manual dispensing method was used for PVA+HPMC ink, and pictures were taken. For saccharin-loaded ink, 8% w/w sodium saccharin (SACC) (Thermo Scientific) was added to a PVA/water mixture. Once PVA was dissolved after heated for 1 hour, HPMC was added accordingly.

Table 4.1 PVA Base and PVA+HPMC ink Formulations.

Name of Sample	PVA(w/w)	HPMC(w/w)	SACC(w/w)
10% PVA	10%	-	-

20 % PVA	20%	-	-
30 % PVA	30%	-	-
20%PVA+ 9.1%HPMC	20%	9.1%	-
20%PVA+ 13%HPMC	20%	13%	-
20%PVA+ 16.7%HPMC	20%	16.7%	-
20%PVA+ 16.7%HPMC+8%SACC	20%	16.7%	8%

4.3.3 Rheological measurement

Rheological properties of the hydrogels were measured using a TA Instruments Discovery Core Rheometer (TA Instruments, USA) with a 40 mm parallel plate geometry with 1mm distance. A solvent trap was applied to reduce water evaporation during testing. The creep recovery test was conducted to assess the printability of the ink, and the flow sweep was performed to determine the viscoelastic properties (Smith *et al.*, 2018; Zhang *et al.*, 2021). The time sweep was conducted in three steps. Approximately 1.5 mL of ink was applied on the geometry with a low shear rate of 1 s^{-1} for 100s and a high shear rate of 200 s^{-1} for 10s, then followed by a recovery step at 1 s^{-1} for 100s. The flow sweep was measured between 0.1s^{-1} and 100s^{-1}. The viscosity recovery percentage (VRP) was calculated by the equation (Zhang *et al.*, 2021):

$$\mathrm{VRP} = \frac{\eta\mathrm{Recovery}}{\eta\mathrm{Initial}}$$

Where η Recovery is the viscosity at time 210s and η Initial at time 100s. All measurements were performed at 25°C. All tests were conducted in triplicate.

4.3.4 Semi-solid extrusion (SSE) 3D Printing

An SSE 3D printer (BioX, Cellink Life Sciences, Gothenburg, Sweden) was used to fabricate the drug-free and drug-loaded 3D samples. The G-code of the design was generated in accordance with the predesigned CAD model. All printing was performed at 25°C. To extrude the ink, 22 gauge nozzle and 3mL syringe were used. The internal diameter (ID) of the Gauge nozzle was 610 µm. The filament fusion was calculated by equation: d2 is the width of the filament, d1 is the measured width of two fused adjacent filaments after printing.

$$FF\% = \frac{d1 - d2}{d2} * 100$$

After printing, the hydrogels were subjected to freeze–thaw treatment. This involved freezing the printed hydrogels at –20 °C for 20 hours, followed by thawing at room temperature for 4 hours. This cycle was repeated three times.

4.3.5 Mechanical Strength Analysis

The PVA-HPMC hydrogel was prepared in 30 x 30 x 1.5 mm moulds. After three cycles of FT, tensile analysis was conducted using a TA.XT Plus Texture Analyser (Stable Microsystems, UK). Samples were held by the tensile grips accessory and loaded into the tensile grips with an approximate height of 25 mm. Extension of the sample was conducted at 1 mm/s until the yield of the sample.

4.3.6 Attenuated Total Reflectance–Fourier Transform Infrared Spectroscopy (ATR-FTIR)

FTIR spectroscopy was measured by using Spectrum One (PerkinElmer, USA) used to investigate the chemical interaction between the functional groups in the cross-linked structure of the hydrogels. FTIR spectra were used to study the structural changes in PVA hydrogel loaded with different AS. Samples were compared for the identification of any shifts or

variations in the characteristic peaks, which could reflect changes in the bonding pattern and interaction between PVA and the sweetener molecules. Measurements were taken in a wavelength region of 600–4000 cm^{-1} with 10 scans.

4.3.7 Degree of Swelling and Weight Loss

The degree of swelling was determined by the maximum amount of liquid that hydrogels could absorb. In this experiment, the pH of the PBS solution was set at 7.4 to mimic wound sites to exudate. The hydrogels were freeze-dried overnight until their final weight remained unchanged. The dried hydrogels were then immersed in pH-adjusted PBS for 48 hours at 37°C, and their weight was measured at 0, 2, 4, 6, 8, 24 and 48 hours. The DS was calculated by using the formula below. The m_i is the weight at a specific hour, and m_0 is the weight of the dry hydrogel at 0 hours.

$$SD = \frac{m_i - m_0}{m_0} \times 100$$

The weight loss observed in the hydrogel can be an indicator of its degradation. To determine this, the freeze-dried hydrogel was soaked in PBS for 48 hours, then freeze-dried again. The hydrogel's dry weight was measured, and the weight loss (WL) was calculated. The W_i is the initial dry weight, and W_d is the weight of the re-dried hydrogel after 48 hours of soaking.

$$WL = \frac{W_i - W_d}{W_i} \times 100$$

4.3.8 Hydrogel Surface Morphology

The morphology of hydrogels was observed by using SEM (Jeol IT200, JEOL, USA). SEM images at 500x magnification were captured to examine the pore size of the hydrogel. The pore size of the hydrogels was measured using ImageJ software (Bethesda, Maryland, USA) and

then plotted by Origin 2025 (Northampton, Massachusetts, USA). For each hydrogel, three images were analysed.

4.3.9 Drug Release and Antimicrobial Properties

Control PVA hydrogels, and 8% (w/w) SACC-loaded hydrogels, and 3D-printed hydrogels were prepared, weighed (～0.6 g), and each gel was placed into a well of sterile 24-well plates. 1 mL of suspension of *A. baumannii* AB5075 with 1×10^6 CFU/mL was added to the hydrogel, and the plates were incubated at 37°C. This setup was repeated for each time point (0, 2, 4, 6, 8, and 24 hours), and at each time point, the bacterial suspension from each well was collected, serially diluted, and plated to enumerate viable cells.

4.3.10 *In vitro* Drug Release Test

The *in vitro* drug-release behaviour of the drug-loaded constructs was evaluated using a modified pharmaceutical dissolution test. The 3D constructs were placed in 25 mL of pH 7.4 PBS and agitated at 100 rpm at 37 °C in a KS 3000 control incubator shaker (IKA, Staufen, Germany). Three types of 3D structures were tested: (1) DIW 3D-printed PVA/HPMC/SAAC scaffolds, and two solid structures of the same total weight (with identical SACC content), namely (2) PVA/SACC and (3) PVA/HPMC/SACC produced by solvent casting. Sink conditions were maintained throughout the release study. At predetermined time intervals, 2 mL samples were withdrawn and replaced with an equal volume of fresh release medium. The absorbance of the collected samples was measured using UV–Vis spectrophotometry (VWR) at $\lambda = 270$ nm, the maximum absorption for SACC. Drug content was calculated based on the established calibration curve. All experiments were conducted in triplicate.

4.3.11 Haemolysis Assays Cytocompatibility Assessment

To evaluate haemolysis, the erythrocytes were collected from horse blood defibrinated (TCS Bioscience, UK) by centrifuging whole blood at 3000 rpm for 10 min, then washing 3 times with PBS to obtain clean erythrocytes. Hydrogel extracts were prepared by incubating 0.2 g of hydrogel in 0.8 mL PBS at 37 °C for 24 h. For the haemolysis test, 190 µL of hydrogel extract was mixed with 10 µL of washed erythrocyte suspension, and the mixture was incubated at room temperature for 1 hour, with deionised water as the positive control and PBS as the negative control. The mixture was centrifuged again, and the supernatant was collected and transferred to a 96-well plate. Haemoglobin release was quantified by measuring absorbance at 541 nm using a microplate reader. The haemolysis rate was calculated by following the equation (Xin *et al.*, 2025):

$$\text{Haemolysis rate (\%)} = (OD_{exp} - OD_{neg}) / (OD_{pos} - OD_{neg}) \times 100\%$$

where OD_{exp}, OD_{neg}, OD_{pos} represent the OD values for the experimental, negative, and positive groups.

Hydrogel cytocompatibility was assessed using an MTT assay on dermal fibroblasts (2DD cell line isolated by Bridger *et al.*(1993). In 24-well plates, Cells (5 × 10^4/well) in DMEM supplemented with 10% FBS, 2 mM L-glutamine, and 1% penicillin/streptomycin were incubated at 37°C with 5% CO_2 for 24 h. Non-adherent cells were removed by washing twice with PBS, and fresh medium (500 µL) was added. The assay involved three groups: a blank group (untreated cells), a control group (cells treated with PVA hydrogel or PVA/HPMC hydrogel), and a saccharin-loaded hydrogel group (cells treated with saccharin-loaded hydrogels).

Hydrogel samples were placed in polyester membrane inserts (6.5 mm, 0.4 µm pore size), and UV-sterilised for 30 min before use. Inserts were transferred to fibroblast-seeded wells and

incubated for 24 h. Following treatment, inserts were removed, and cells were washed twice with PBS. Cells were then incubated with 500 µL of MTT solution (0.5 mg/mL) for 3 h, after which 250 µL of the MTT solution was removed, and the formazan crystals were dissolved in 750 µL DMSO. Absorbance was measured at 570 nm using a microplate reader. Cell viability was expressed as the percentage of absorbance in treated wells relative to untreated wells.

4.3.12 Statistical Analysis

Data are expressed as mean ± standard deviation (SD). Statistical analyses were performed using GraphPad Prism and Origin Pro. One-way ANOVA with Dunnett's correction and t-test were used. Statistical significance was established at p-values of 0.05 (ns), < 0.05 (*), 0.01 (**), 0.001 (***) or 0.0001 (****).

4.4 Results

4.4.1 Ink Printability Assessment

4.4.1.1 Manual dispensing

An important requirement for developing a DIW printable ink is its ability to form a consistent, cylindrical filament, as the ink must be extrudable through the nozzle while retaining its printed shape. The PVA concentration directly affects the viscosity of the PVA solution. To determine an appropriate PVA concentration as the base of the ink, different PVA concentrations (10%,20% and 30% w/w) were first screened using a manual dispensing method to simulate the DIW printing process and identify an appropriate base formulation. In Figure 4.1A, 10% w/w PVA was too liquid, and it dropped as droplets. For a 30% w/w PVA solution, the ink formed a filament shape, but its viscosity was high. The filament at this concentration was relatively thick, and when it extruded, it stuck to itself due to high viscosity. This high viscosity was not beneficial to subsequent printing, particularly when HPMC is added. It could cause the ink to be unable to be extruded from a syringe, forcing the needle out if higher pressure is applied. The 20% w/w PVA demonstrates a filament shape that meets the requirements for DIW printing. In Figures 4.1B, 1g, 1.5g, and 2g, HPMC (9.1%, 13.0%, and 16.7% w/w) was added, and all inks formed filament-shaped structures. However, when extruded, the 9.1% HPMC+PVA ink could not be extruded consistently, whereas 13.0% and 16.7% could hold their shape and will be studied further.

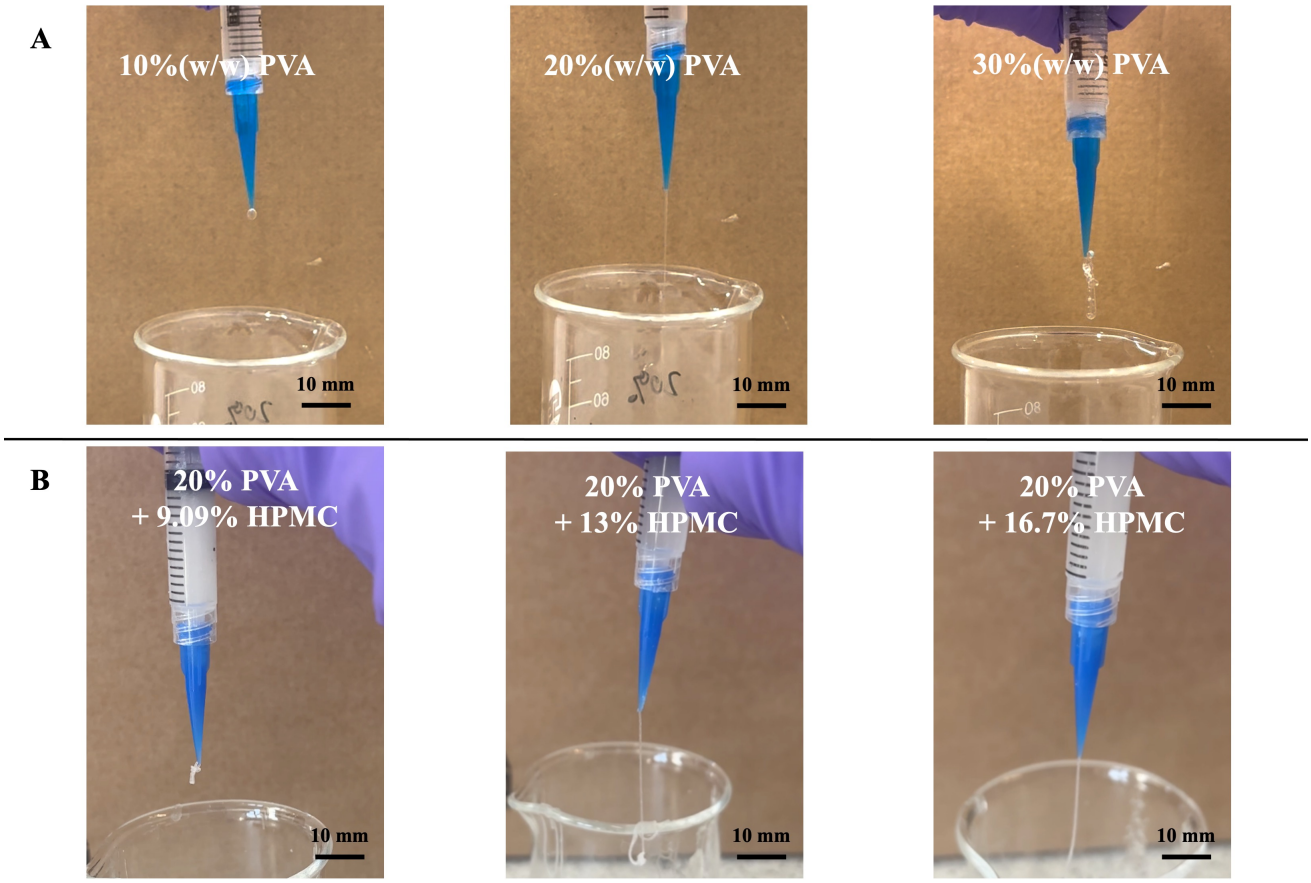

Figure 4.1 Printability assessment with manual dispensing of PVA and PVA+HPMC (A) Different concentrations of PVA inks (B) 20% PVA with different weights of HPMC.

4.4.1.2 Ink Rheology of PVA+HPMC Inks

There are 3 requirements a bioink should meet for optimal DIW printing: a cohesive filament should form after printing, it should exhibit shear-thinning properties, and it should have thixotropic properties (above 80% VRP) (Zhang *et al.*, 2022). Therefore, the shear-thinning behaviour of inks was evaluated by flow sweep (Figure 4.2A). All formulations exhibited similar shear-thinning behaviours, with viscosity decreased when shear rate increased from 0.01 s^{-1} to 100 s^{-1} (Schwab *et al.*, 2020). This feature is important for ensuring smooth ink flow from a nozzle during direct-write 3D printing (Smith *et al.*, 2018). To understand the printability of the inks, a three-step recovery test was performed. In this test, it can be

determined whether the inks exhibit thixotropy. Thixotropy enables bioinks to flow smoothly under shear during extrusion while rapidly recovering their viscosity and structural integrity after deposition (Figure 4.2B). The inks were subjected to a low shear rate of 1 s^{-1} for 100s and a high shear rate of 200 s^{-1} for 10s, then followed by a recovery step at 1 s^{-1} for 100s to simulate the printing process. After a higher shear rate was applied to the 20% PVA, PVA+13 % HPMC, and PVA+16.7 % HPMC inks, the viscosity of all the bioinks recovered rapidly. The 20% PVA ink VRP was 98.94%, the PVA+13 % HPMC ink VRP was 91.41%, and PVA+16.7 % HPMC VRP was106.09% after 100 seconds when high shear (100 s^{-1}) was applied, indicating the thixotropic property (Rathan *et al.*, 2019). However, the viscosity of PVA did not change much under high shear rates, from 4.29 to 3.51 Pa.s, further proving that it is not suitable for DIW printing. For the PVA+13 % HPMC and PVA+16.7 % HPMC inks, viscosity dropped 22.99- and 6.84-fold when the shear rate changed from 1 to 100 s^{-1}, which again showed a shear-thinning property. The PVA+13 % HPMC and PVA+16.7 % HPMC inks exhibit shear-thinning properties; each was considered suitable for DIW printing and was therefore printed for further evaluation.

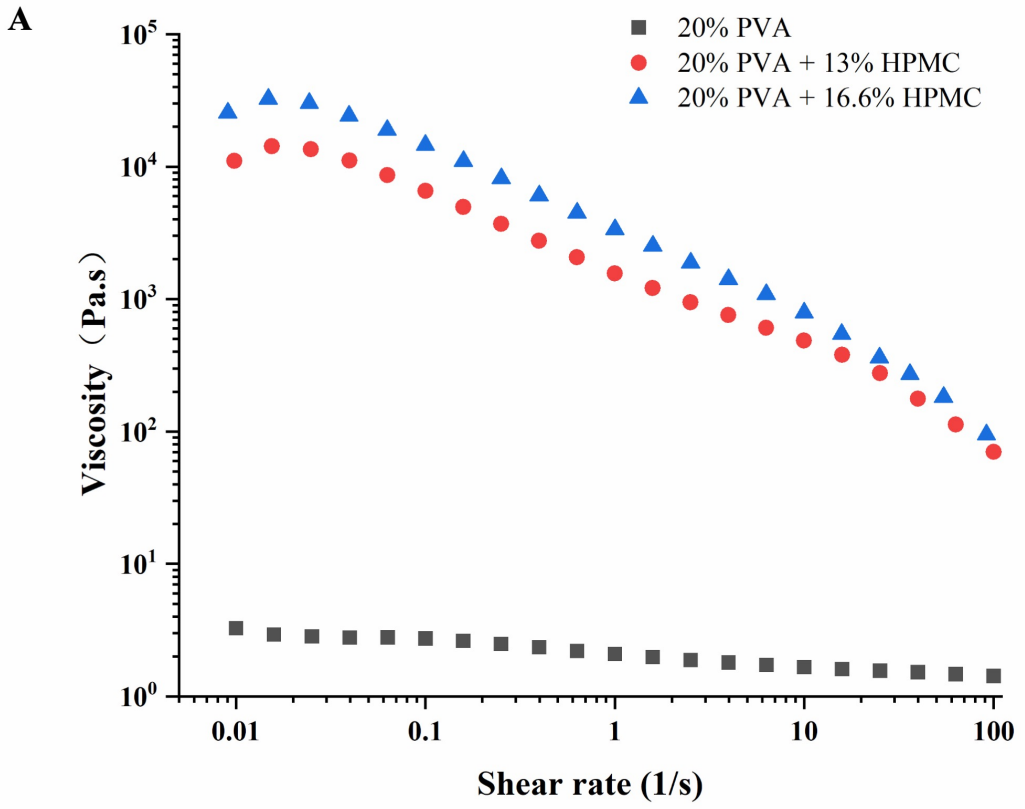
A
20% PVA
20% PVA + 13% HPMC
20% PVA + 16.6% HPMC
Viscosity（Pa.s）
Shear rate (1/s)
0.01
0.1
1
10
100

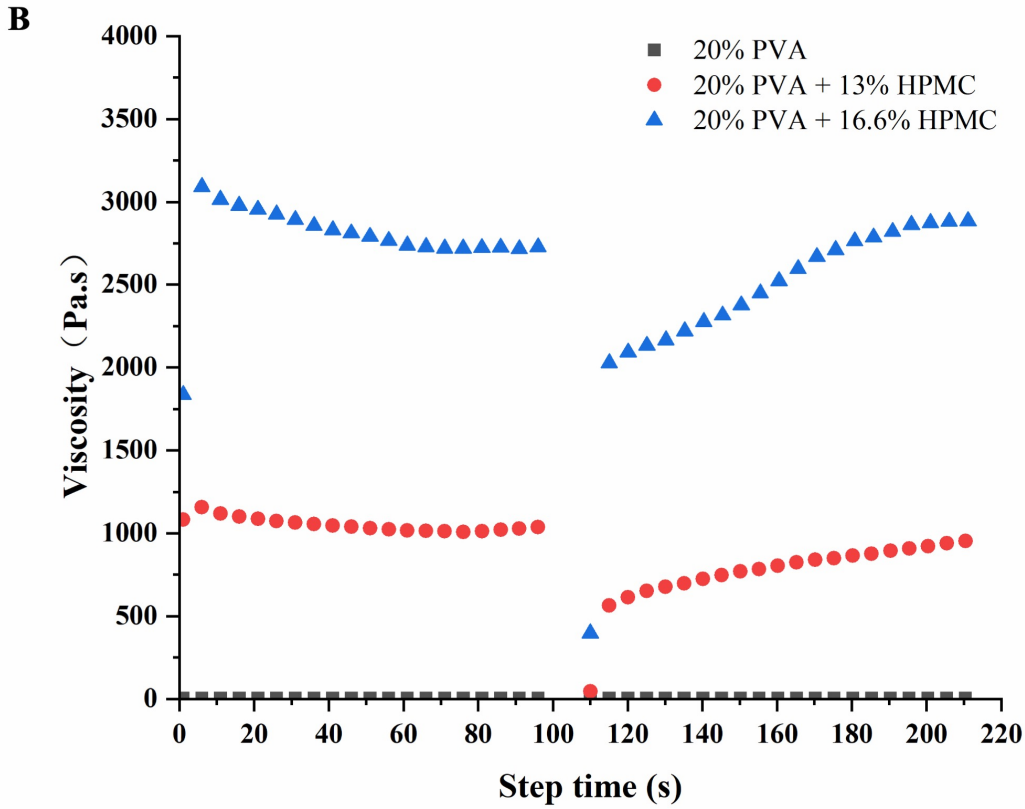
B
20% PVA
20% PVA + 13% HPMC
20% PVA + 16.6% HPMC
Viscosity（Pa.s）
Step time (s)

Figure 4.2 Rheological properties of PVA and PVA+HPMC inks. (A) The shear rate-viscosity flow curves. (B) creep recovery test of 20% PVA, PVA+13% HPMC, PVA+16.7% HPMC inks. Data demonstrate the mean of three 3 replicates and biological replicates. Error bars represent standard deviation (SD)

4.4.1.3 3D Printability of PVA+HPMC Inks

Figure 4.3A shows that the formulation containing 20% PVA and 9.1% HPMC had poor formability, with adjacent filaments fusing easily, resulting in low shape fidelity and difficulty in producing multilayer structures. The addition of HPMC improved printability and structural integrity, particularly at 16.7% HPMC. In Figure 4.3B, the filament fusion rate was calculated. The filament fusion rate decreases when HPMC concentration increases. This suggests that the printed filaments were less likely to merge, thereby maintaining the designed structure. Moreover, the filament width decreases with increasing HPMC concentration (Figure 4.3C). This indicates less spreading after extrusion and better shape fidelity with a higher HPMC concentration, whereas a lower concentration could lead to inadequate printing of multi-layer structures. These findings suggest that adding HPMC improves filament definition and enables more reliable layer-by-layer deposition.

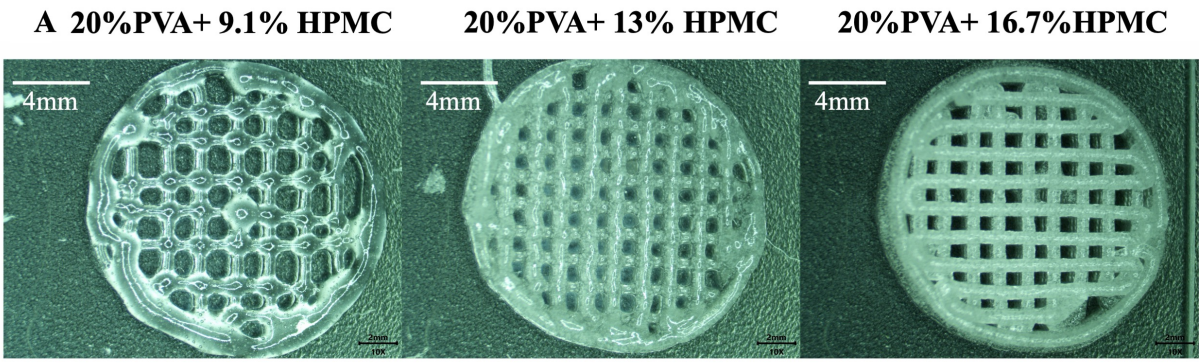
A 20%PVA+ 9.1% HPMC
20%PVA+ 13% HPMC
20%PVA+ 16.7%HPMC
4mm
4mm
4mm

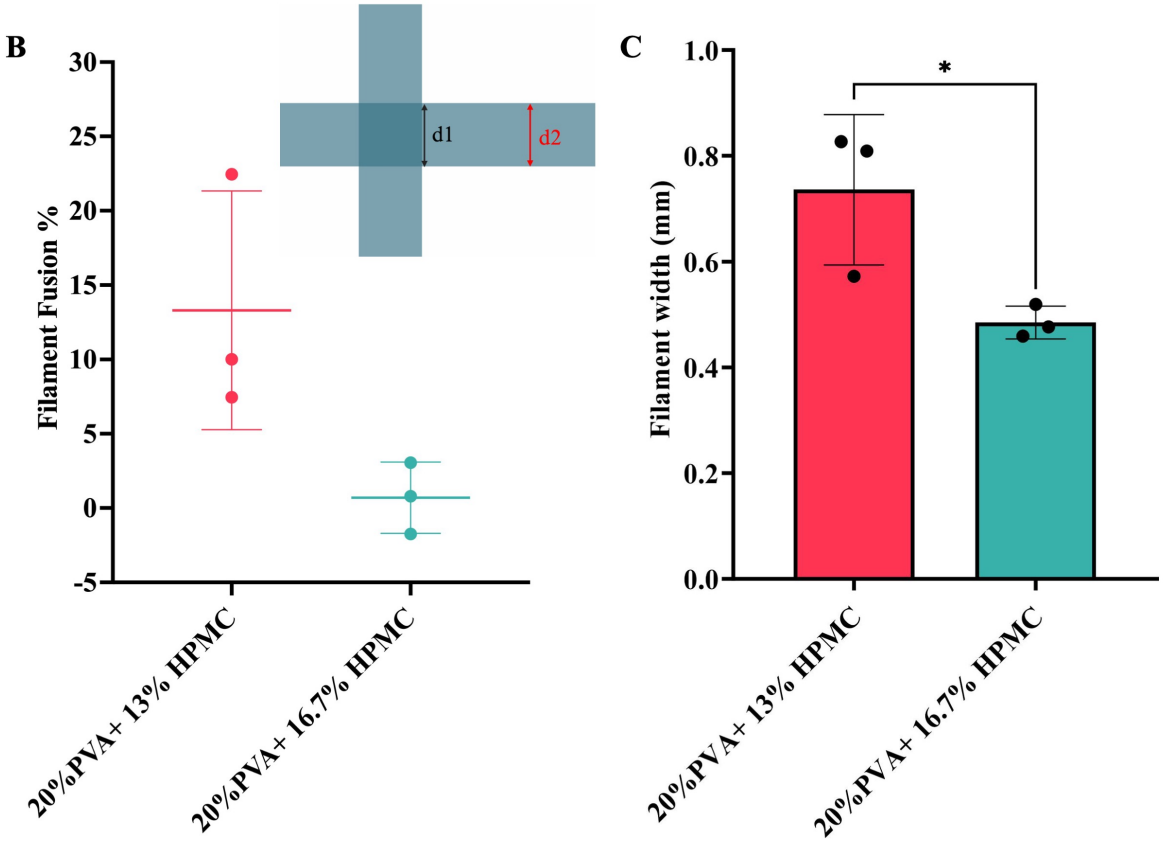
B
Filament Fusion %
30
25
20
15
10
5
0
-5
d1
d2
20%PVA+ 13% HPMC
20%PVA+ 16.7% HPMC
C
Filament width (mm)
1.0
0.8
0.6
0.4
0.2
0.0
*
20%PVA+ 13% HPMC
20%PVA+ 16.7% HPMC

Figure 4.3 Printed filament fusion rate and width of 20%PVA+ 13/ 16.7%HPMC inks (A) image of printed scaffold (B) the filament fusion rate, d1 is the width at cross-merge points, and d2 is the width of non-cross-merge points (C) width of PVA+HPMC inks. Data demonstrate the mean of three 3 replicates and biological replicates. Error bars represent standard deviation (SD). Statistical analysis was performed through t-test between 20%PVA+13%HPMC and 20%PVA+16.7%HPMC group.

4.4.2 Material characterisation

FTIR analysis was performed to identify the functional groups and molecular interactions in the PVA–HPMC hydrogels. It is also used to confirm if there is any chemical interaction between AS and PVA–HPMC hydrogels. In the FTIR spectrum of PVA, the characteristic peak at approximately 3250 cm^{-1} is assigned to the O-H stretching vibration of hydroxyl groups. The characteristic peaks at 2944 cm^{-1} and 2905 cm^{-1} are attributed to CH_2 asymmetric stretching vibrations. The peak at 1416 cm^{-1} corresponds to the C-H bending vibration of -CH_2- groups. The absorption peak at 1086 cm^{-1} indicates the C-O stretching vibration of the -CH_2OH hydroxyl groups in PVA molecules, which was previously described (Figure 4.4) (Zidan *et al.*, 2019). In Figure 4.4A, the FT-20% PVA hydrogel shows a broad peak at 3250 cm^{-1}, which indicates stretching vibration of the O-H group. The wider peak at 3250 cm^{-1} is caused by PVA polymer chain crystallisation that forms a hydrogen bond during the FT process (Sirousazar and Khodamoradi, 2020). Peaks at 2944 cm^{-1} and 2904 cm^{-1} were assigned to C–H stretching, and bands at 1415 cm^{-1} and 1320 cm^{-1} corresponded to -CH_2 bending and CH+OH bending groups. The peaks at 1715 and 1651 corresponded to carbonyl -C=O- and C=C groups (Wang *et al.*, 2022). The HPMC shows a peak at 3420 cm^{-1}, assigned to the hydroxyl (-OH) group. Other bands at 2893 cm^{-1} and 1050 cm^{-1} were observed, which corresponded to C-H and C-O.

These peaks were similar to those reported in the previous study (Furqan, Iqbal and Tulain, 2017). The PVA+HPMC hydrogel shows a peak similar to that of the PVA hydrogel. However, the peaks at 2944 cm^{-1} and 2904 cm^{-1} become less sharp and move to 2930 and 2950 cm^{-1}. This could be due to the HPMC peak at 2893 cm^{-1} reducing sharpness. The peaks at 1051 and 945 indicate that HPMC is successfully incorporated into the PVA hydrogel system.

In Figure 4.4B, the absorption peak at 3567 cm^{-1} in the infrared spectrum of sodium saccharin (SACC) is related to the O-H stretching vibration in water molecules, representing the stretching motion of hydroxyl bonds in water. The peak at 3487 cm^{-1} arises due to hydrogen bonding between SACC molecules and water molecules or other functional groups (such as amide or amino groups). The absorption peak at 1630 cm^{-1} generally corresponds to the C=C stretching vibration in aromatic rings or the bending vibration of heteroaromatic rings linked to C=N in saccharin sodium. The peak at 1580 cm^{-1} is also associated with the C=C stretching vibration of aromatic rings in saccharin sodium molecules.

SACC-loaded PVA+HPMC hydrogels showed broad peaks at 3271 cm^{-1} corresponding to O–H stretching and hydrogen bonding, which match the PVA hydrogel spectra. Aromatic stretching C=C (1630 cm^{-1} and 1580 cm^{-1}), the sulfonyl group peak (1255 cm^{-1} and 957) was identified both in SACC powder and SACC-loaded hydrogel (Srivastava *et al.*, 2012). The FTIR spectra confirm the successful incorporation of SACC into the PVA+HPMC hydrogel network, and there was no chemical interaction between the PVA-HPMC hydrogel and AS.

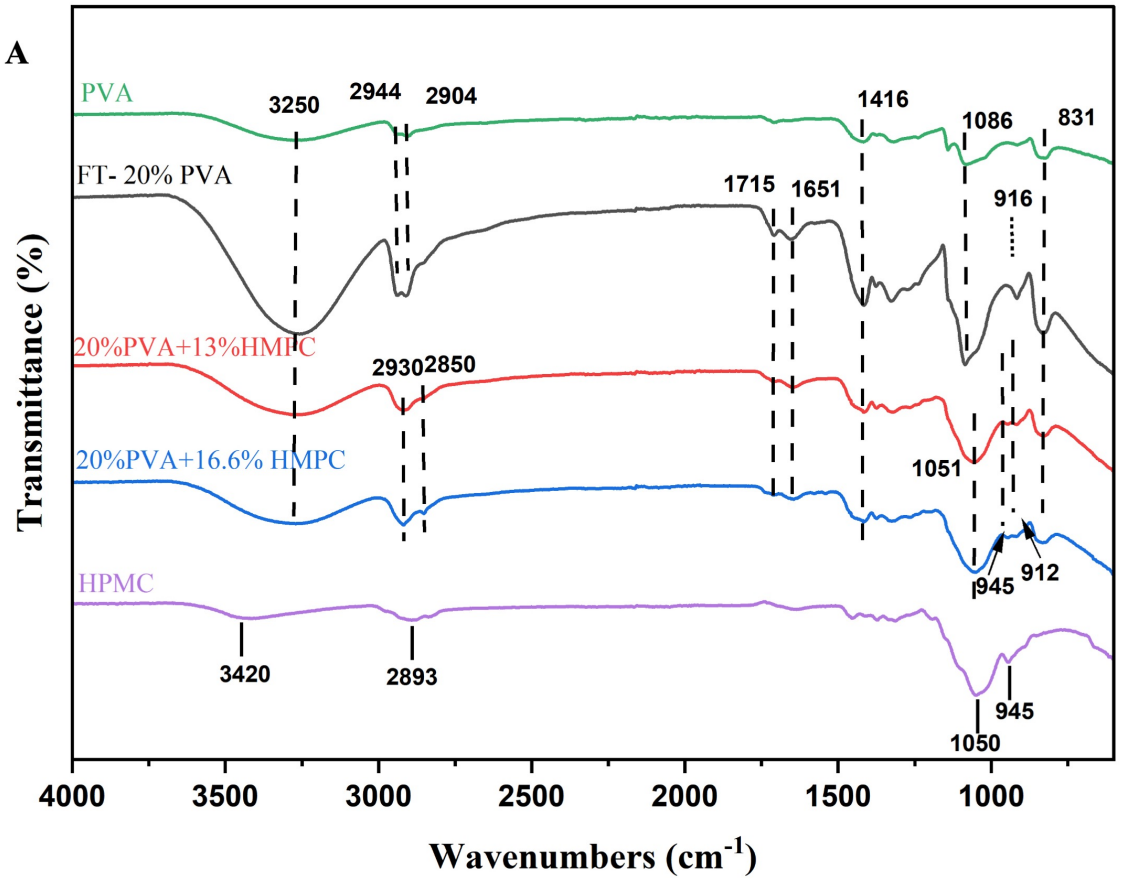
A
PVA
FT- 20% PVA
20%PVA+13%HMPC
20%PVA+16.6% HMPC
HPMC
3250
2944
2904
1416
1086
831
1715
1651
916
2930
2850
1051
945
912
3420
2893
945
1050
Transmittance (%)
4000
3500
3000
2500
2000
1500
1000
Wavenumbers (cm-1)

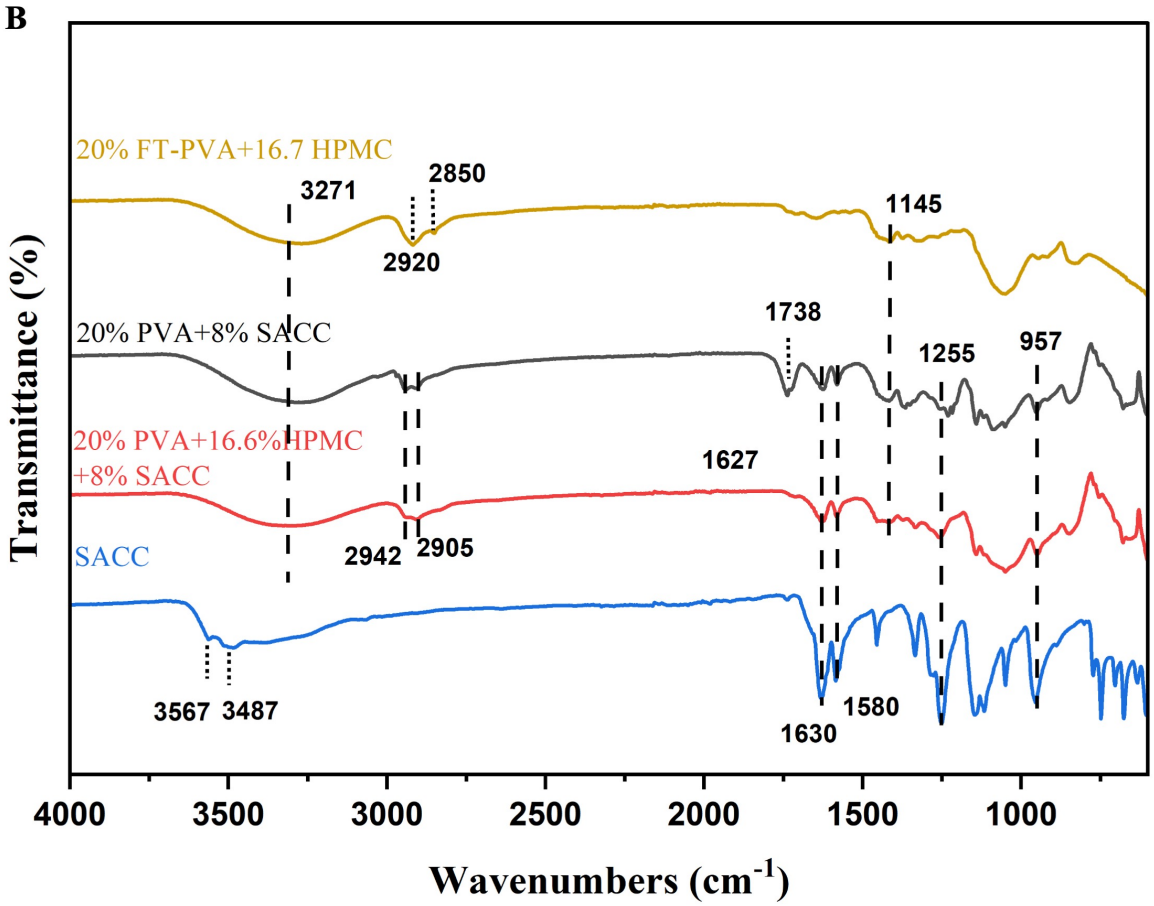
B
20% FT-PVA+16.7 HPMC
20% PVA+8% SACC
20% PVA+16.6%HPMC
+8% SACC
SACC
3271
2850
2920
1145
1738
1255
957
1627
2942
2905
3567
3487
1630
1580
Transmittance (%)
4000
3500
3000
2500
2000
1500
1000
Wavenumbers (cm-1)

Figure 4.4 FTIR spectra of PVA-based hydrogels and components. (A) Spectra of PVA, FT-PVA hydrogel, PVA/HPMC hydrogels, and HPMC. (B) Spectra of PVA-based formulations with/without SACC and SACC alone.

To understand the effects of adding HPMC and SACC on the mechanical properties of the hydrogel, tensile strain was measured (Figure 4.5). Adding 8% SACC, the largest tensile is around 50%, which is lower than FT-PVA itself (about 80%). However, the tensile strain was significantly improved by adding HPMC. After incorporating 13% w/w HPMC, tensile strain reached approximately 100%. When a higher HPMC content (16.7%) was added, tensile strain increased to around 120%. Moreover, SACC alone reduces mechanical properties, whereas its incorporation into the PVA+HPMC system yields the highest stress values, exceeding 2000 kPa at ~100% strain. In general, the mechanical strength of hydrogel is within 1-100 kPa, which is significantly lower than that of traditional gauze or cotton wool, which has a storage modulus of around 1MPa to 1GPa (Chen *et al.*, 2023). Hydrogels with lower mechanical strength are more compatible with applications such as soft robots and intravenous delivery (Yu *et al.*, 2019). However, hydrogels with improved mechanical properties are important for wound-dressing applications. These PVA+HPMC formulations are outperforming the PVA hydrogel. By adding 13%(w/w) of HPMC, the mechanical strength increased 3.00-fold compared with FT-PVA itself. When the HPMC content increased to 16.7%, mechanical strength increased 4.23-fold. Additionally, the mechanical strength of FT-PVA decreased upon the addition of SACC. Without SACC, the PVA stress was approximately 292.10; with SACC, it decreased to 31.11. This corresponds to an 8.82-fold reduction. However, adding SACC into the PVA+HPMC system shows an opposite effect. With SACC incorporated, mechanical strength increased 1.79-fold compared with PVA+16%HPMC and 66.90-fold compared with

PVA+SACC. These results demonstrate that the addition of HPMC and SACC significantly enhances the mechanical strength of the hydrogel.

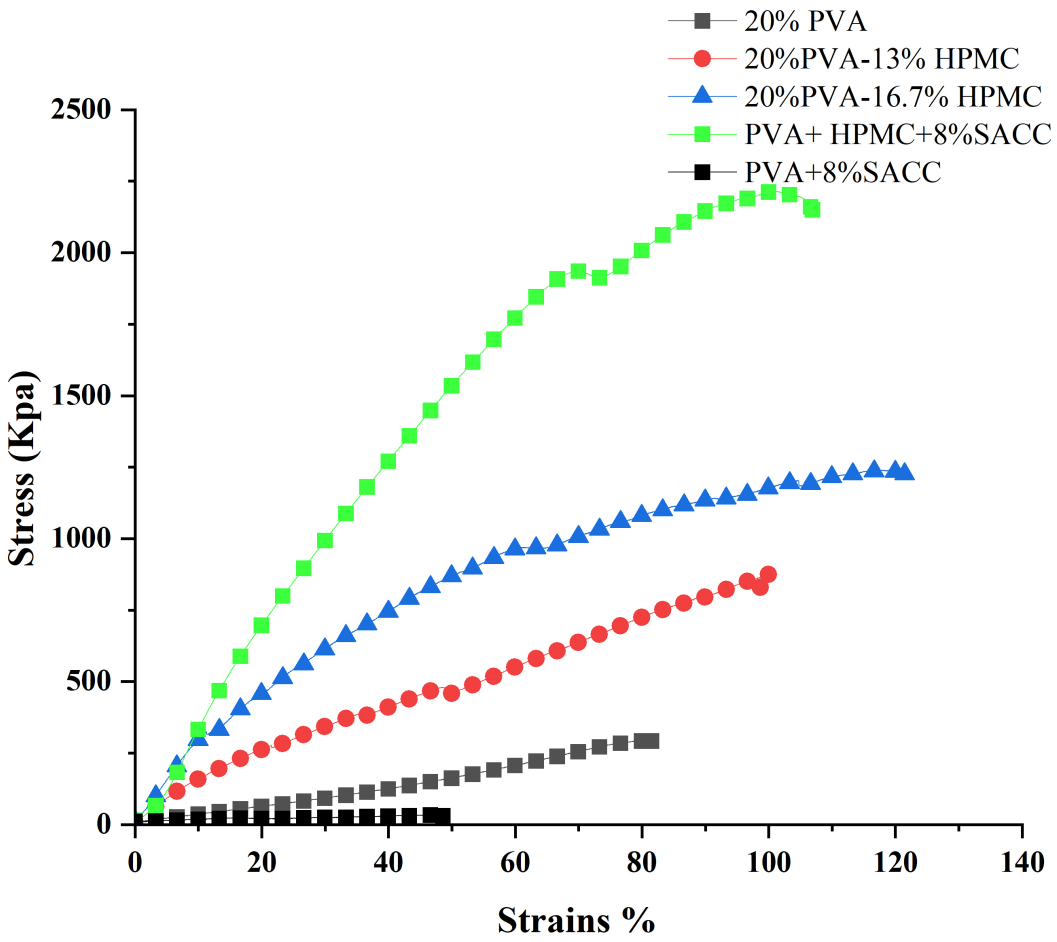

Figure 4.5 Tensile stress–strain curves of FT-PVA (20%), FT-PVA+SACC, FT-PVA+13% HPMC, FT-PVA+16.7% HPMC and FT-PVA+16.7% HPMC+8% SACC (n=3). The incorporation of HPMC markedly enhances the mechanical strength of the PVA matrix, with higher HPMC content resulting in higher stress at a given strain. While the addition of SACC alone provides limited mechanical reinforcement. But it combines with HPMC, resulting in better mechanical properties.

4.4.3 Surface Morphology

SEM images revealed distinct microstructural differences between 20% FT-PVA and 20% FT-PVA + 16.7% HPMC hydrogels (Figure 4.6). The 20% FT-PVA hydrogel exhibited a relatively heterogeneous porous structure, with irregular pores that were distributed throughout the matrix (Figure 4.6A). On the other hand, the incorporation of 16.7% HPMC resulted in a more homogeneous porous architecture (Figure 4.6B). The pores appeared more uniformly distributed and were relatively rounded. In Figure 4.6C, the addition of HPMC changed the microstructure from an irregular morphology to a more uniform porous network, which may contribute to the enhanced swelling behaviour observed in the HPMC-containing hydrogels. The addition of SACC had minimal impact on this HPMC-induced architecture.

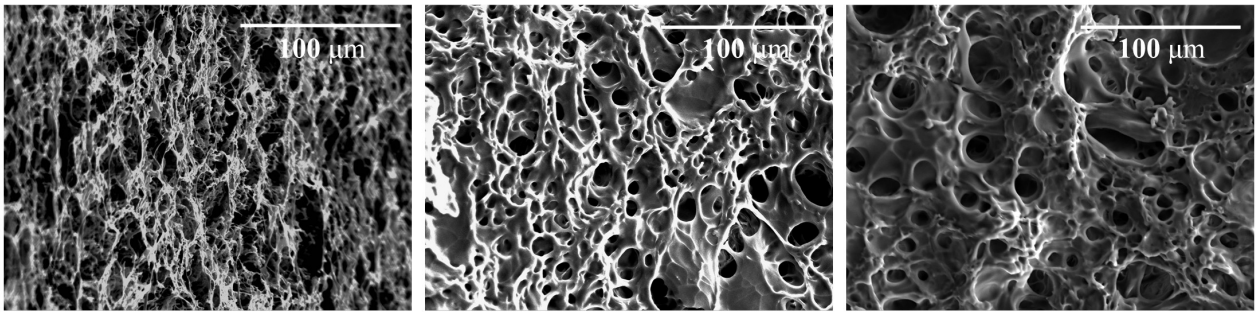

A. 20% PVA **B. 20% PVA+ 16.7%HPMC** **C.20%PVA+16.7%HPMC +8% SACC**

Figure 4.6 SEM micrographs of FT PVA-based hydrogels (A) PVA hydrogel (B) 20%PVA + 16.7% HPMC hydrogel (C) 20%PVA + 16.7% HPMC+8% SACC hydrogel

4.4.4 Swell Ability and Degradation

Swelling behaviour is a critical factor for hydrogel wound dressings, as it helps them absorb blood and wound exudate. It is also important for the release of loaded agents and nutrients, as well as for metabolite transfer (Feng and Wang, 2023; Xin *et al.*, 2025). The DS of

PVA+HPMC hydrogel was tested over a 48-hour period (Figure 7A). The DS of PVA+HPMC hydrogels are outperformance the FT-PVA hydrogels. The DS of FT-PVA is 211.33%. By the addition of HPMC, the DS reaches to 624.752%. However, additional SACC reduced DS. It could be because SACC is highly water-soluble and it releases into PBS over time, resulting in a low final weight of the gel.

Weight loss reflects the hydrogel's stability and degradation profile under physiological conditions. It is an important parameter for wound dressings (Mndlovu *et al.*, 2024). As a result, the FT-PVA+SACC hydrogel showed the highest weight loss (59.30%), while the FT-PVA hydrogel showed the lowest (8.61%) (Figure 4.7B). The FT-PVA+ HPMC showed a higher weight loss than the FT-PVA hydrogel (17.82%). However, the FT-PVA+ HPMC+ SACC hydrogel showed less weight loss when compared with the FT-PVA+SACC hydrogel.

The DS and weight loss were tested in LWCB medium (Figure 4C,D). The DS of hydrogel reached its peak at 48 h, slightly later than in PBS (Figure 4D). This indicated that the hydrogel absorbed the LWCB medium more slowly than PBS. The DS of PVA+HPMC hydrogels are outperformance the FT-PVA hydrogels. The DS of FT-PVA is 238.50%. By the addition of HPMC, the DS reaches to 539.79%. However, additional SACC reduced the DS to 481.34%. It could be because SACC is highly water-soluble and it releases into media over time, resulting in a low final weight of the gel. The weight loss FT-PVA+SACC hydrogel showed the highest weight loss (31.45%), while the FT-PVA hydrogel showed the lowest (3.07%) (Figure 4.7D). The FT-PVA+HPMC showed a higher weight loss than the FT-PVA hydrogel (8.70%). However, the FT-PVA+ HPMC+ SACC hydrogel showed less weight loss when compared with the FT-PVA+SACC hydrogel which is 17.27%. The lower weight loss observed could due to the slower DS previously recorded in LCWB medium. In addition, the hydrogel may

absorb proteins and red blood cells present in LCWB, which could further influence the measured weight change.

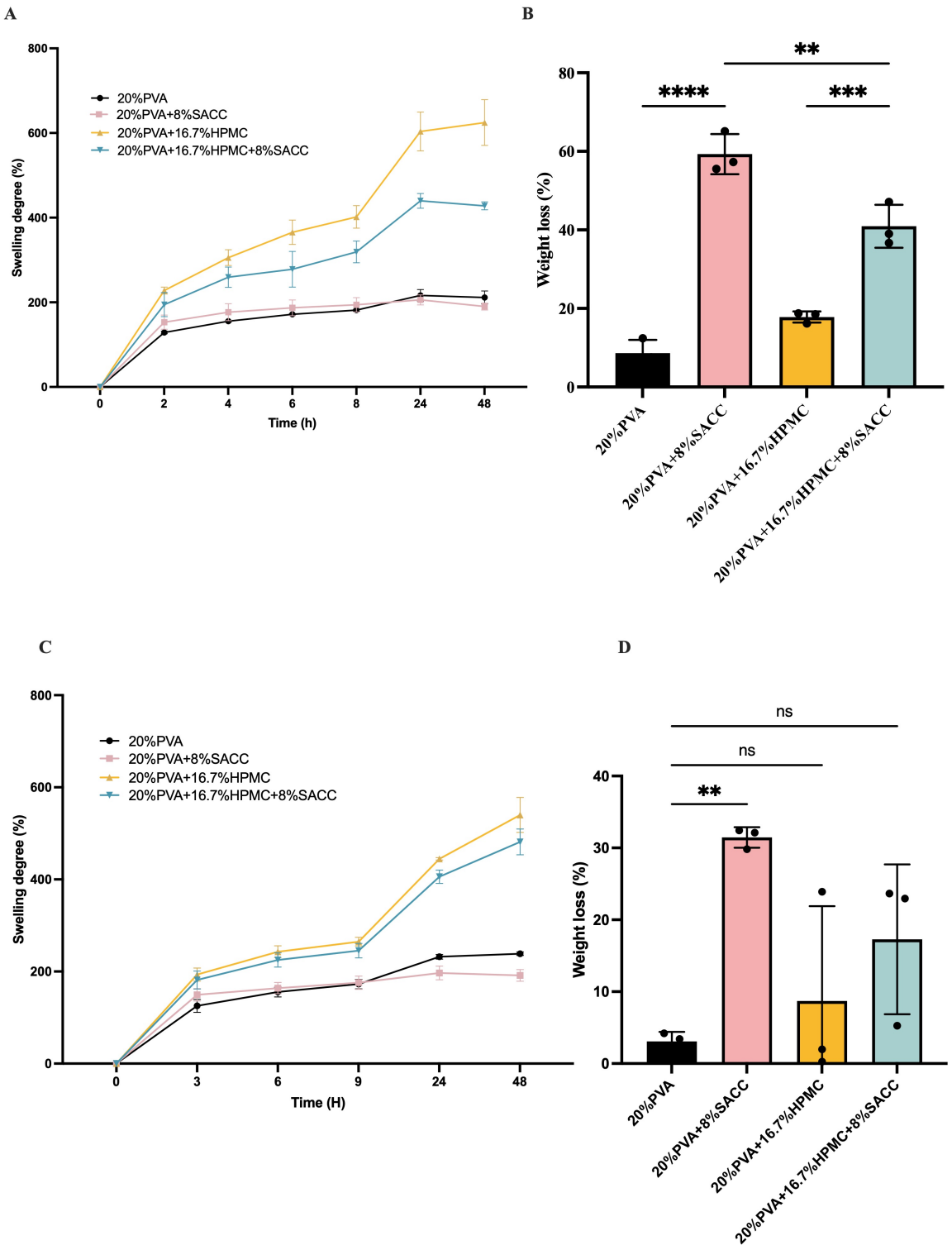

Figure 4.7 Swelling behaviour and degradation profile of PVA-based hydrogels. (A) Time-dependent swelling degree (%) of PVA, 20% PVA + 8% SACC, 20%PVA + 16.7%HPMC, and 20%PVA + 16.7%HPMC + 8% SACC hydrogels over 48 h. The incorporation of HPMC significantly increased water uptake capacity, with PVA + HPMC exhibiting the highest swelling degree at 24–48 h. (B) Weight loss (%) of hydrogels after 48 h incubation under the same conditions. The addition of SACC markedly increased degradation, whereas HPMC-containing formulations exhibited improved structural stability. (C) Time-dependent swelling degree (%) of PVA, 20% PVA + 8% SACC, 20%PVA + 16.7%HPMC, and 20%PVA + 16.7%HPMC + 8% SACC hydrogels over 48 h in LCWB medium (D) Weight loss (%) of hydrogels after 48 h incubation in LCWB medium. Data demonstrate the mean of three 3 replicates and biological replicates. Error bars represent standard deviation (SD). Statistical analysis was performed through ordinary one-way ANOVA between all samples (ns>0.05,**p-value < 0.01, *** p-value < 0.001, **** p-value < 0.0001).

4.4.5 Drug release profile and antimicrobial property

In the previous chapter, the FT-PVA+ 8% SACC hydrogel demonstrated limited antimicrobial activity, achieving only approximately a 3-log reduction in CFU after 24 hours. For this study, we utilised 3D printing to increase the contact surface area and enhance release efficiency. All the samples were prepared with the same weight and diameter to ensure a consistent comparison. As shown in Figure 4.8, additional HPMC did not affect the antimicrobial activity and it has been reported previously (Mohamed *et al.,* 2025). The 20%PVA+16.7% HPMC +8%SACC hydrogel exhibited a reduction of ~2.93 log CFU/mL when compared with growth control, corresponding to a reduction of less than 99.9%. This result is similar to the reduction of *A. baumannii* observed in our previous study using an 8% SACC-loaded FT-PVA hydrogel.

However, the inhibition of the 3D-printed counterparts was significantly greater than that of the untreated control, reaching ~3. 91 logs.

Meanwhile, the PVA+HPMC hydrogel and its 3D printed counterpart were tested in LCWB medium. In Figure 4.8C, the number of *A. baumannii* in the control 20%PVA+16.7% HPMC hydrogel group was increased significantly, which is similar to the growth control group. Moreover, the inhibitory effect improved significantly after the addition of SACC. For the 20%PVA + 16.7% HPMC + SACC hydrogel, cell viability decreases by approximately 4.97 log. However, the 3D-printed 20%PVA+16.7% HPMC +SACC hydrogel shows a 7.14 log reduction in cell viability at 24 hours when compared with growth control group, which is a much stronger inhibitory effect than the other group (Figure 4.8D).

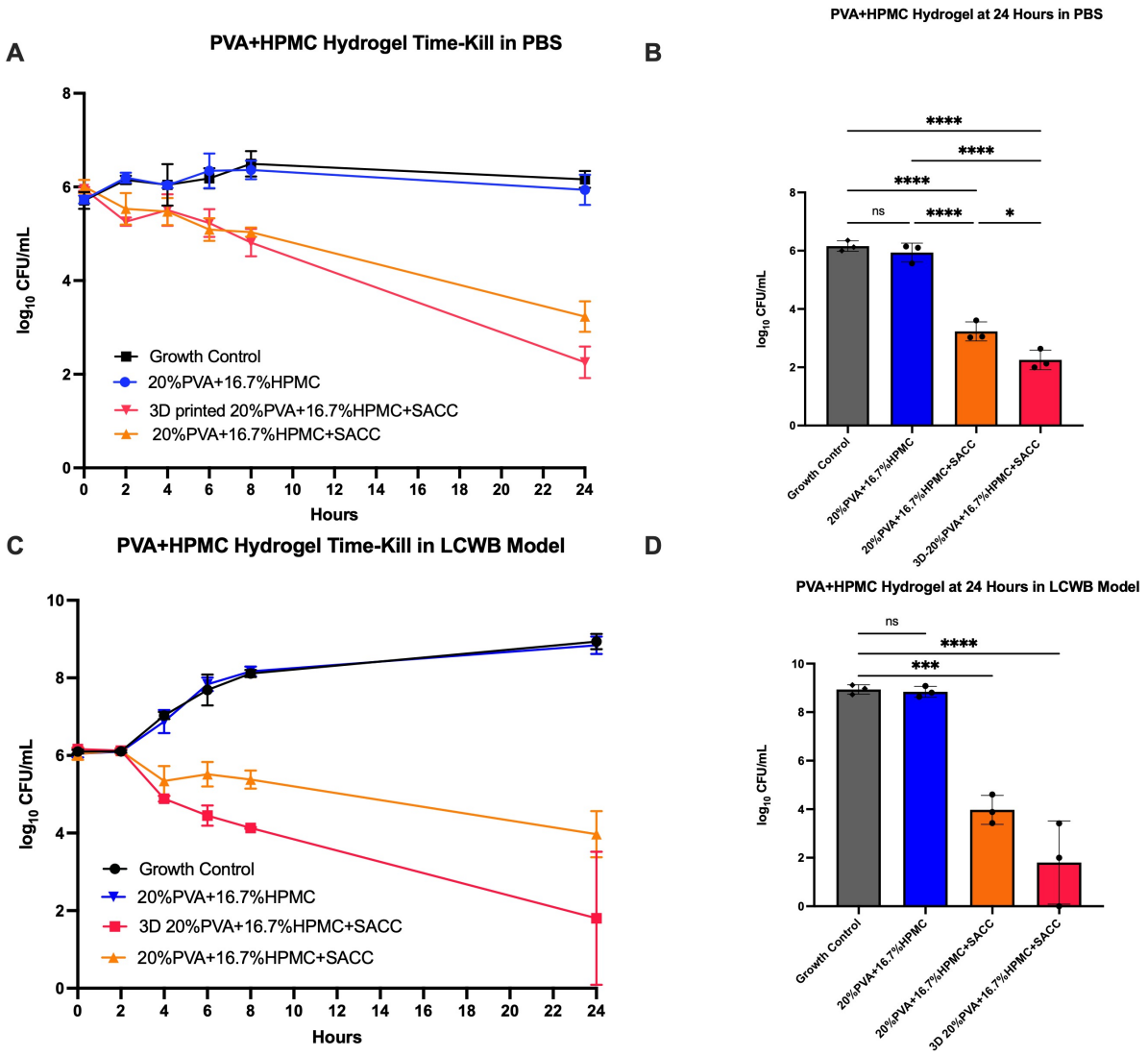

Figure 4.8 This figure illustrates the log reduction in viable *A. baumannii* cell counts over a 24-hour period when exposed to 20% PVA+16.7% HPMC hydrogel, 20% PVA+16.7% HPM hydrogel loaded with 8% SACC, and their 3D-printed counterparts. (A) Time- kill assay results for PVA+HPMC, 20%PVA +16.7%HPMC hydrogel loaded with 8% SACC, and 3D printed counterparts hydrogels showing *A. baumannii* CFU counts over 24 hours. (B) Focused results at 24 hours, displaying CFU log reductions of *A. baumannii*. (C) Bactericidal Activity of PVA+HPMC, 20%PVA +16.7%HPMC hydrogel loaded with 8% SACC, and 3D printed counterparts' hydrogels against *A. baumannii* at 24 Hours in LCWB media (D) Focused results at 24 hours. Data demonstrate the mean of three 3 technical replicates and biological replicates.

Error bars represent standard deviation (SD). Statistical analysis was performed through ordinary one-way ANOVA between the 3D printed FT-PVA+HPMC+SACC hydrogel and other samples (ns>0.05, *** p-value < 0.001, **** p-value < 0.0001)

Additionally, we used UV spectroscopy to monitor SACC release (Figure 4.9). Results showed that the release rate of the 3D-printed PVA+HPMC+SACC hydrogel was significantly faster than that of the non-3D-printed PVA+HPMC+SACC hydrogel. The 3D-printed hydrogel released nearly all of its contents within approximately 30 minutes, whereas the non-3D-printed hydrogel took 240 minutes to complete release. Moreover, the addition of HPMC in the non-3D-printed hydrogel further slowed the release process.

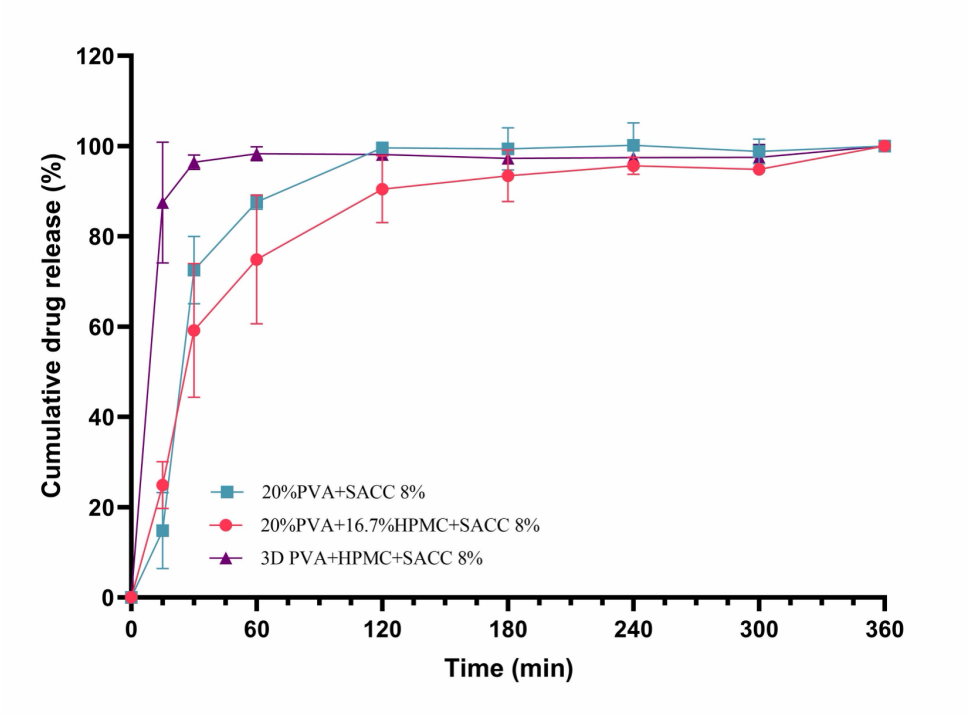

Figure 4.9 Release profiles of SACC from PVA-based hydrogels. Cumulative release (%) of SACC over 360 min from PVA + HPMC + 8% SACC, PVA + 8% SACC, and 3D PVA + HPMC + 8% SACC formulations. The 3D-printed hydrogel showed a faster early-stage release, while HPMC-containing formulations demonstrated a more controlled release behaviour at later time points. Data are presented as mean ± SD (n = 3).

4.4.6 Biocompatibility of PVA+HPMC Hydrogel

Cell viability assessment is a fundamental step in toxicological and biomaterial studies to evaluate the cellular response to newly developed materials. Cytocompatibility is particularly critical for materials intended for biomedical applications, such as wound dressings and tissue engineering scaffolds, where prolonged contact with living cells is expected. Dermal fibroblasts were chosen due to their central role in wound healing through the synthesis and remodelling of the extracellular matrix (ECM), which provides structural support for tissue regeneration and angiogenesis (Tracy, Minasian and Caterson, 2016; Nilforoushzadeh *et al.*, 2017).

In this study, the cytocompatibility of the developed 3D-printed hydrogels was examined using the MTT colourimetric assay after 24 h of exposure to 2DD dermal fibroblasts. The MTT assay is widely used to determine cell metabolic activity as an indirect measure of cell viability, based on the mitochondrial reduction of tetrazolium salts into insoluble formazan crystals by viable cells. Control hydrogels, including PVA hydrogel and PVA+HPMC hydrogels, exhibited high cytocompatibility, maintaining nearly 100% cell viability consistent with previous reports (Figure 4.10A) (Schmedlen, Masters and West, 2002; Díez *et al.*, 2022; Oh, Hwang and Na, 2022). Similarly, saccharin-loaded hydrogels exhibited high biocompatibility, with cell viability around 91.4%. The maintained fibroblast viability indicates that saccharin incorporation did not adversely affect the cytocompatibility of the formulations. This further supports the potential use of saccharin-loaded hydrogels as wound dressing.

A material's haemocompatibility is an important factor for biomaterials. Excellent haemocompatibility would allow a biomaterial to contact blood without triggering harmful or adverse reactions. The material has poor blood compatibility, which could lead to unwanted

physiological responses, including immune responses, thrombosis, and haemolysis (Zhang *et al.*, 2024). In this study, deionised water as the positive control, and PBS as the negative control. The samples were measured at 540nM after 1 hour. As shown in Figure 4.10B, the PVA+HPMC and PVA+HPMC+8% SACC hydrogels exhibited excellent haemolysis, with haemolysis rates of 0.32% and 1.85%, respectively. This haemolysis rate is significantly lower than the ASTM (Advancing Standards Transforming Markets) F756-17 standard of 5%, suggesting both PVA+HPMC hydrogel and SACC-loaded hydrogel have reliable blood compatibility.

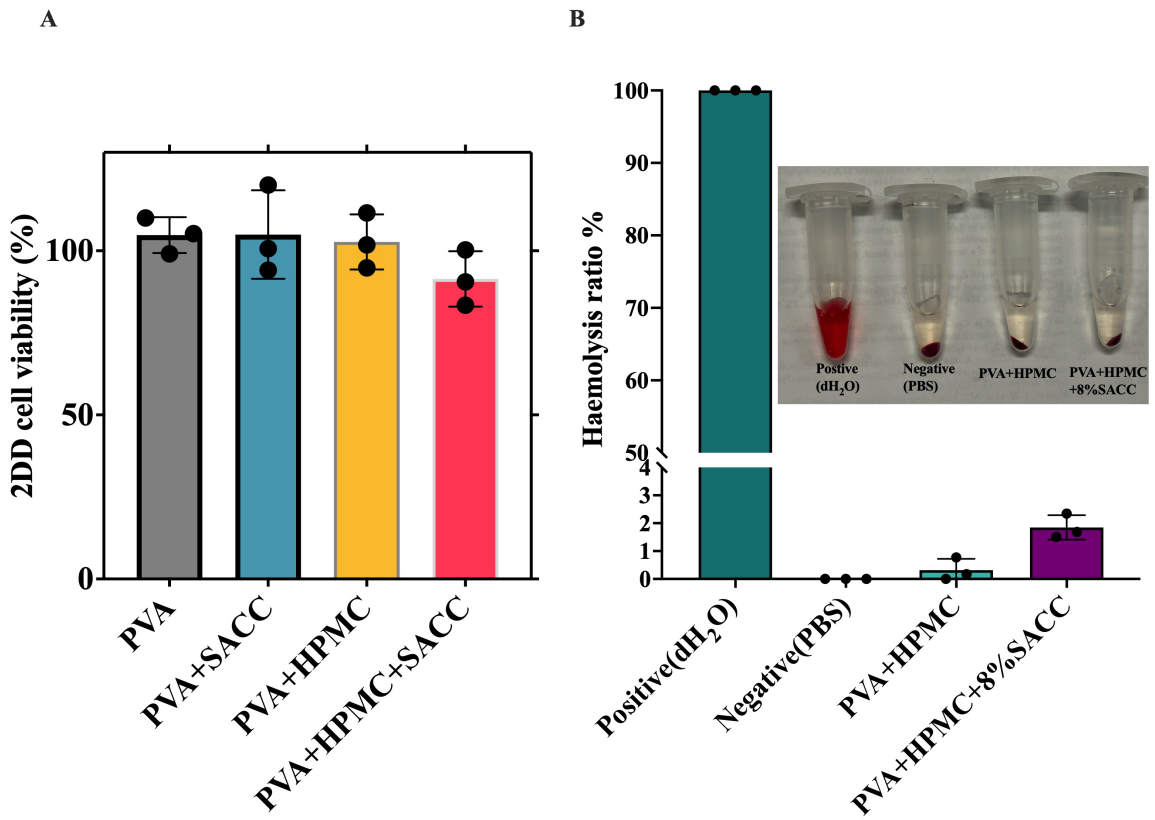

Figure 4.10 Blood compatibility and cell viability of PVA+HPMC Hydrogel: (A) cell viability of PVA/HPMC-based hydrogel. No significant cytocompatibility differences between the control and hydrogel treatment groups. (B) *In vitro* haemolysis assay of PVA+HPMC hydrogel

shows excellent blood compatibility. The positive control (dH2O) induced complete haemolysis, and PBS served as the negative control. Results are expressed as the percentage mean ± standard deviations (n=3) (ns>0.05).

4.5 Discussion

In our previous experiments, sodium saccharin demonstrated excellent antibacterial properties. However, freeze-thaw PVA did not yield satisfactory release efficiency. Therefore, in this study, we incorporate HPMC into FT-PVA hydrogel systems, which provides a viable strategy to enhance printability, mechanical strength, swelling capacity, and drug-release performance while maintaining biocompatibility.

To understand the printability of the ink, manual dispensing and rheological assessment were performed. The results showed that 20% PVA (MW 61,000) is most suitable for further development of 3D printing ink. Furthermore, additional HPMC improves the printability and structural integrity after printing of PVA bases inks, allowing the hydrogel to hold its shape before cross-linking. All formulations exhibited shear-thinning and behaviours, which is essential for direct ink writing. The recovery test reveals thixotropic behaviour. This behaviour enables the ink to rapidly restore viscosity following high shear.

In FTIR analysis, there is no chemical interaction between PVA, HPMC and sodium saccharin, indicating that the system is physically crosslinked rather than chemically modified. Moreover, the improved mechanical performance was observed in tensile testing, while SACC alone weakened the FT-PVA matrix. Its incorporation into the PVA–HPMC system resulted in increased stress values. This suggests that adding HPMC could counteract SACC's effects by reinforcing intermolecular interactions and improving structural integrity.

Surface morphology was studied by using SEM. In the SEM images, adding HPMC transformed the microstructure from irregular, heterogeneous pores to a more uniform, interconnected porous network. These structural changes are related to the degree of swelling. HPMC's hydrophilic substituents enhance water uptake, while the porosity facilitates fluid diffusion (Annabi *et al.,* 2010; Vlad *et al.,* 2025). Hydrogel has a swelling degree of 150% or more, indicating a high-swelling hydrogel (Feng and Wang, 2023). This high swelling behaviour is beneficial for skin wound healing because it can absorb wound exudate, transfer nutrients and metabolites, and allow better drug delivery.

In Chapter 2, FT-PVA hydrogel did not provide desirable release, so we developed a 3D-printable ink to work as a carrier for SACC. In our results, the 3D-printed hydrogel shows better inhibition of *A. baumannii* in the Time-kill assay. Therefore, we assume the 3D printed PVA+HPMC+SACC hydrogel can release SACC more effectively. The release kinetics is performed to understand the release of SACC in real time. As a result, SACC was released effectively and reached about 100% releasing at first 30 minutes. The non-3D printed hydrogels reached their complete release at the 2nd hour. This difference could be advantageous for early-stage antimicrobial intervention. The enhanced bacterial reduction observed with 3D-printed scaffolds supports this interpretation, demonstrating that architectural control can significantly influence therapeutic performance.

Finally, cytocompatibility and hemocompatibility assays confirmed that all formulations maintained high cell viability and low haemolysis rates. These results indicate the suitability for wound-dressing applications. Overall, these findings highlight the synergistic effect of compositional modification and structural design in tuning the functional properties of PVA-based hydrogels. Additional HPMC allows the printability of PVA hydrogel.

4.6 Key Findings

5. Formulation of a printable PVA-based ink through HPMC incorporation.
5. Material characterisation demonstrates that the additional HPMC improved the hydrogel's structural integrity.
5. The 3D-printed 20% PVA + 16.7% HPMC hydrogel demonstrates better release behaviour and antimicrobial performance than its non-3D-printed counterpart.
5. The 20% PVA + 16.7% HPMC hydrogel demonstrates excellent biocompatibility and haemocompatibility.

Chapter 5

5. Identify bioactive compounds that regulate Type IV pilus expression in *A. baumannii* by screening the FDA-Approved drugs library

5.1 Introduction

More than 95% of drugs currently available on the global pharmaceutical market are non-antibiotic compounds (Chen *et al.*, 2025). Despite their widely use in clinical settings, the potential impact on AMR remains poorly understood. While antibiotics are traditionally regarded as the primary drivers of resistance development, growing evidence indicates that non-antibiotic drugs can also exert pressure on bacterial populations and potentially influence microbial physiology and evolutionary trajectories.

Recent studies have demonstrated that non-antibiotic drugs can directly affect bacterial growth and gene transfer. For instance, a study by Maier *et al.*, (2018) revealed that more than 200 drugs that available on market can inhibit the growth of gut bacteria. This finding suggests that these compounds possess unintended antimicrobial activity. Importantly, such effects could not be restricted to commensal species. Another research conducted by Wang *et al.*, (2020), reported that anti-inflammatory drugs (NSAIDs) such as ibuprofen, naproxen, diclofenac, as well as gemfibrozil and propranolol, can significantly increase the frequency of transformation in *Acinetobacter baylyi.* In another study, Lu *et al.* (2022) found that antidepressants play a role in antibiotic resistance by accelerating the horizontal transfer of antibiotic resistance genes (ARGs). When *A. baylyi* ADP1 is exposed to clinical concentrations of antidepressants, ARG transformation increases 2.3-fold. Antidepressants also enhance cell membrane permeability

and porosity, aiding the passage of endogenous DNA through the outer membrane (Lu *et al.*, 2022a).

These findings suggest that non-antibiotic drugs may contribute to the development of AMR not only by inhibiting bacterial growth but also by reshaping bacterial membrane properties and gene exchange mechanisms. However, while the influence of non-antibiotic drugs on resistance acquisition has begun to attract attention, their potential effects on bacterial virulence regulation remain largely unexplored (Wang *et al.*, 2020).

T4P are surface appendages that are critical virulence factors in many bacteria, including *A. baumannii*. In *A. baumannii*, T4P are involved in several key processes, such as twitching motility, natural competence, biofilm formation, and host-cell adhesion (Ronish *et al.*, 2019b). Although *A. baumannii* lacks flagella and is theoretically incapable of surface motility, it can spread rapidly on surfaces through twitching motility powered by T4P (Tomaras *et al.*, 2003).

Given the importance of T4P in both virulence and horizontal gene transfer, modulation of T4P expression could provide a potential link between exposure to non-antibiotic drugs and enhanced bacterial pathogenicity. Nevertheless, whether FDA-approved non-antibiotic drugs can alter T4P regulation in *A. baumannii* remains unexplored.

In this chapter, we examine how FDA-approved drugs affect the expression of *pilA*, the major structural gene encoding Type IV pili in *A. baumannii*. By screening a library of FDA-approved drugs, we aim to identify compounds that modulate *pilA* expression, potentially affecting the bacterium's motility, biofilm formation, and overall pathogenicity. We further assess how these compounds influence bacterial growth, twitching motility, biofilm formation, and virulence *in*

vivo. This research has significant implications for understanding the broader impact of pharmaceuticals on microbial ecology and public health. By identifying non-antibiotic drugs that influence T4P expression and, consequently, *A. baumannii* virulence, we can better assess the potential risks associated with their widespread use. Ultimately, this work could inform strategies to mitigate the unintended consequences of non-antibiotic drug use in clinical and environmental settings, helping to combat the global challenge of antimicrobial resistance.

5.2 Aims 4

The overall aim of this chapter is to identify FDA-approved drugs that can modulate *pilA* expression and virulence-associated phenotypes in *A. baumannii.* Potential compounds affecting *pilA* expression, bacterial motility and biofilm formation will be identified through drug screening. The identified hit compounds will then be validated *in vitro*, and the molecular mechanisms underlying their effects will be investigated at the transcriptomic level, followed by *in vivo* validation. This will be achieved through the following objectives:

1. Screening the FDA-Approved drugs library on *pilA* expression in *A. baumannii.*
2. Screening the FDA-approved drugs library on biofilm formation of *A. baumannii.*
3. Identify the hit compounds.
4. Validate the pomalidomide compound *in vitro.*
5. Understand the effect of pomalidomide on *A. baumannii* AB5075 at the transcriptomic level.
6. Validate pomalidomide *in vivo.*

5.3 Materials and Methods:

Bacterial strain

de Dios *et al.*, (2023), developed a miniTn7-based *PpilA::gfpmut3* transcriptional fusion to monitor expression from the *PpilA* promoter. The *PpilA* region was amplified via PCR using the oligonucleotides PpilA fw EcoRI and PpilA rv BamHI. After digestion, the amplified fragment was ligated into the pUC18T-miniTn7T-zeo-gfpmut3, resulting in the construct pUC18T-miniTn7T-zeo-PpilA::gfpmut3. *A. baumannii* strain *AB5075/miniTn7T-zeo-PpilA::gfpmut3* was used for testing the *PpilA* expression in this study. The overnight stocks were grown for 18 hours at 37 °C and 180 rpm in LB Broth (ThermoFisher). The stocks were frozen in 20% Glycerol and kept at -80 °C.

5.3.1 Validation of a GFP-based Gene Expression Assay for Ace-K

To test the *PpilA* expression, the miniTn7T-based insertion bearing a *PpilA::gfpmut3* transcriptional fusion (*AB5075/miniTn7T-zeo-PpilA::gfpmut3*) was used as the sample. The OD_{600} was adjusted to 0.1 from *an A. baumannii AB5075/miniTn7T-zeo-PpilA::gfpmut3* overnight culture using LB Broth (ThermoFisher) and water in a 1:9 ratio. In each well, the final concentration of Ace-K was 1% (w/w) Ace-K. For the control, the same amount of water was used with the inoculum. The cultures were incubated in a CLARIOstar Plus plate reader (BMG Labtech) at 37°C, 200 rpm. The OD_{600} and GFP fluorescence (excitation: 485 nm; emission: 535 nm) of the samples were measured over time.

5.3.2 GFP-based Gene Expression assays on DiscoveryProbe™ FDA-Approved Drug Library.

DiscoveryProbe™ FDA-approved drug library (APExBIO) is a collection of 2320 FDA-approved drugs supplied as pre-dissolved DMSO solutions. All 2,320 FDA-approved drugs were packed into 96-well microplates, totalling 27 plates. Each well contained 20 µL of the drug solution at a 10 mM concentration. To test the *PpilA* expression, the miniTn7T-based insertion bearing a *PpilA::gfpmut3* transcriptional fusion (*AB5075/miniTn7T-zeo-PpilA::gfpmut3*) was used. The OD_{600} was adjusted to 0.1 from *A. baumannii AB5075/miniTn7T-zeo-PpilA::gfpmut3* overnight culture using Luria-Bertani (LB) Broth (ThermoFisher) and water mixture in a ratio of 1:10 for accurate fluorescent measurement. In each well, 1µL of the drug solution was added to a 96-well plate along with 199µL of the inoculum to make the drug concentration 0.05 mM. The 1% (w/w) Ace-K was used as the positive control. The DMSO was used as a negative control. The 1:10 LB and water mix solution was used as a sterile control (200mL). The cultures were incubated in a CLARIOstar Plus plate reader (BMG Labtech) at 37°C, 200 rpm. The OD_{600} and GFP fluorescence (excitation: 485 nm; emission: 535 nm) of the samples were read hourly for 18 hours.

5.3.3 Revalidate GFP-based Gene Expression Assays for Hit Drug Candidates.

To revalidate GFP-based gene expression assays for hit drug candidates. Drugs were purchased from MedChemExpress or Fisher Scientific (Table 5.1). The OD_{600} was adjusted to 0.1 from an *A. baumannii AB5075/miniTn7T-zeo-PpilA::gfpmut3* overnight culture using Luria-Bertani (LB) Broth (ThermoFisher) and water in a 1:10 ratio. In each well, 1 µL of the drug solution was added to a 96-well plate along with 199 µL of the inoculum. The 1:10 LB and water mix solution was used as a sterile control. The cultures were incubated in a CLARIOstar Plus plate

reader (BMG Labtech) at 37°C, 200 rpm. The OD_{600} and GFP fluorescence (excitation: 485 nm; emission: 535 nm) of the samples were measured every hour for 18 hours. Three biological replicates were performed.

Table 5.1 Molecular Weights and origin of compounds

Compound	Order from	
2-Naphthol	Thermo Scientific	144.17g/mol
Primaquine Diphosphate	MedChemExpress	455.34g/mol
Flavin adenine dinucleotide disodium	Thermo Scientific	829.52g/mol
Pomalidomide	Thermo Scientific	273.34g/mol

5.3.4 Twitching Motility Assay

Twitching assays were carried out in twitching media, which consisted of tryptone (10 g/L), yeast extract (5 g/L), sodium chloride (2.5 g/L), and agar (10 g/L). After autoclaving, pomalidomide or DMSO was added to the twitching media at 45°c. Then, 10 ml of the agar mixture was poured into 90 mm Petri dishes and left next to a Bunsen burner for 10 minutes to cool. A pipette tip was used to pick up a colony from a freshly grown AB5075 plate and stab it into the bottom of the plate to inoculate it. Before measuring motility, the plates were incubated at 37°C in high humidity condition for 48 hours. Three biological replicates were performed for each experimental condition.

5.3.5 Minimum Inhibitory Concentration and Minimum Biofilm Inhibitory and Growth assays

MIC and Minimum Biofilm Inhibitory Concentration (MBIC) assays were carried out in cation-adjusted Muller-Hinton broth (CAMHB). The bacterial overnight culture was adjusted to an OD_{600} of 0.1. To test MIC, the concentration of primaquine diphosphate in the first well was 0.125 mM from a 100 mM Stock. In the second well, the concentration was 0.25 mM;

thereafter, the concentrations were 0.5 mM, 1 mM, 1.5 mM, 2 mM, 2.5 mM, 3 mM, 3.5 mM, 4 mM, 4.5 mM, and 5 mM. The concentration of 2-Naphthol was the same as that of primaquine diphosphate, but the final concentration was 4.5 mM. The testing concentration of pomalidomide was 0.5 mM, 1 mM, 1.5 mM, 2 mM, 2.5 mM, 3 mM, 3.5 mM, 4 mM, 4.5 mM, and 5 mM. For the control group, the same amount of DMSO was added to each well. The plates were incubated at 37°C and 180 rpm for 18 hours. After incubation, the plates were measured at OD_{600} using a microplate reader, the SPECTROstar Nano (BMG LabTech).

To assess biofilm formation, the CAMHB and planktonic cells were removed from the plate and washed 3 times with deionised water. The 200 mL of 0.1% crystal violet solution was added to a 96-well microtiter plate and left for 10 min. Then, the crystal violet was removed from each well and the wells were washed with deionised water 5 times. The plate was turned upside down and air-dried. The 200 mL of 99% ethanol was added to each well. The plate was incubated at room temperature for 15 min. The absorbance was read in the SPECTROstar Nano plate reader (BMG Labtech) at 570 nm using 200 mL of 99% ethanol as the blank.

To assess growth kinetics, an overnight bacterial culture was adjusted to an OD_{600} of 0.1 in CAMHB. Different concentrations of compound and DMSO control were selected based on MIC result: pomalidomide at 0.5, 2.5 and 5 mM, 2-naphthol at 0.125, 1 and 2.5 mM and Primiquine diphosphate at 0.5, 1.5 and 2.5 mM. Plates were incubated in a CLARIOstar Plus plate reader (BMG Labtech) at 37°C, and OD_{600} was measured hourly for 18 h using a microplate reader with shaking at 200 rpm between readings.

5.3.6 RNA-Seq

To understand the *A. baumannii* transcriptome differences under 5mM pomalidomide conditions. The AB5075 overnight culture was diluted to OD_{600}=0.05 in 20mL of the LB broth that was adjusted to 5mM pomalidomide accordingly. Cells were grown to an OD_{600} of 0.6-0.7, which is mid-exponential phase. The cells were collected into Eppendorf tubes, spun down, and washed with RNAlater for storage to maintain RNA integrity. To isolate RNA, the RNAeasy Kit with on-column DNAase digestion (Qiagen) was used. The RNA integrity was confirmed by gel visualisation. Samples were processed for RNA sequencing on an Illumina MiSeq with 12 million reads per sample, and further analysed at SeqCenter (Pittsburgh, Pennsylvania, USA). Quality control and adapter trimming were performed with bcl-conver (Version 4.2.4). Read mapping was performed with HISAT2 (Version 2.2.0). Read quantification was performed using Subread's featureCounts (Version 2.0.1) functionality. The reference *A. baumannii* AB5075-UW gene annotation was used (GenBank accession number NZ_CP008706.1; (Gallagher *et al.*, 2015)). 94 genes were identified as being significantly differentially expressed, with a greater than $|logFC| > 1$ and $P < 0.05$ between 5mM Pomalidomide and DMSO control LB broth. VolcaNoseR was used to create a volcano plot (Goedhart and Luijsterburg, 2020). Genes were defined as differentially expressed if Log2(fold change) ≥ 1 or ≤ -1 and p value < 0.05.

5.3.7 Molecular Docking

The 3D structure of the small-molecule ligand was retrieved from DrugBank (http://go.drugbank.com). High-resolution crystal structures of the target proteins were obtained from UniProt (www.uniprot.org).Use PyMOL to perform dehydration on the proteins and save the results as PDB files. The binding sites' centre and size were detected by using CB-Dock2 (https://cadd.labshare.cn/cb-dock2) and molecular docking was performed using AutoDock Vina 2 software to explore protein-ligand interactions (Yang Liu *et al.*, 2022). To

visualise interactions between test pomalidomide and the target protein, the Discovery Studio 2019 was used to generate 2D and 3D plots.

5.3.8 In vivo Efficacy of Pomalidomide in *Galleria mellonella*

The *A. baumanni* AB5075 was adjusted to OD_{600}=1.0, then 10 times diluted 3 times in PBS to make the concentration at 2.56 x10^5 CFU/mL. To avoid contamination, the ethanol was taken into a Hamilton 25 µL syringe needle (Sigma-Aldrich) and allowed to sit for 15 minutes. The ethanol was removed and washed 6 times with ethanol, and 6 times with PBS, then 5µL of pomalidomide solution was injected. After 15 minutes, 10 µL of bacterial inoculum was injected into the *G. mellonella* (Live Food Ltd).

5.3.9 Murine Pulmonary Infection Model

Mice will be rendered transiently neutropenic by injecting cyclophosphamide IP at 150 mg/kg four days and 100 mg/kg one day prior to inoculation. Two transfers of ACB 395 (original ID BEI MRSN 959/AB5075) will be performed onto Trypticase Soy Agar plates containing 5% sheep blood (Becton, Dickinson & Co.; Sparks, MD) and incubated at 37°C for approximately 24 hours. After 18-24 hours of incubation of the second transfer, a bacterial inoculum of approximately 1×10^7 CFU/mL will be confirmed by serial dilution and culture of an aliquot from each inoculum suspension for quality control.

The mice will be lightly anaesthetised using vaporised isofluorane (2-3% v/v in an oxygen carrier) until the respiratory rate is decreased upon visual inspection. Pneumonia will be induced via intranasal inoculation with 0.05 ml of the bacterial suspension. All mice will be

housed in an oxygen-enriched chamber until they have fully recovered from anaesthesia. Mice will be randomised into control and different pomalidomide dose groups before any dosing interventions. The control group (n = 5 mice per group) will receive drug vehicle (5% DMSO in PBS) in the same volume (0.1 mL) and schedule as the most frequent pomalidomide regimen. Pomalidomide groups (n = 5 mice per group) will receive 0.1 mL IP doses of pomalidomide (5 – 30 mg/kg).

5.3.10 Statistical Analysis

Data are expressed as mean ± standard deviation (SD). Statistical analyses were performed using GraphPad Prism. Two-way ANOVA with Tukey correction, one-way ANOVA with Dunnett's correction and t-test were used. Statistical significance was established at p-values of < 0.05 (*), 0.01 (**), 0.001 (***) or 0.0001 (****).

5.4 Results

5.4.1 Validation of a Green Fluorescent Protein (GFP) -based Gene Expression Assay for Ace-K

To establish a reliable platform for high-throughput screening of *pilA* expression, a GFP-based transcriptional reporter assay was first validated using acesulfame potassium (Ace-K) as a positive control. A diluted growth medium (1:10 LB/water) was employed to minimise background fluorescence and enable accurate simultaneous measurement of optical density (OD_{600}) and GFP signal by using the CLARIOstar Plus plate reader.

The *A. baumannii AB5075/miniTn7T-zeo-PpilA::gfpmut3* strain can grow in diluted medium, allowing stable monitoring of fluorescence over time. OD_{600} and GFP fluorescence were measured hourly for 18 hours. Ace-K treatment resulted in an clear reduction in *pilA* promoter activity compared to the water control (Figure 5.1), confirming its suitability as a positive control for *pilA* repression.

As shown in Figure 5.1, the GFP fluorescence of the growth control increased over time. At the 16-hour time point, the GFP fluorescence between the growth control and Ace-K 1% showed significantly different results. Based on these observations, the 16-hour time point was selected as the standard endpoint for subsequent screening assays. These results demonstrate that the 1:10 LB/water medium supports bacterial growth and sensitive detection of *pilA* GFP expression. The assay provides a robust and scalable method for screening FDA-approved drugs for their effects on *pilA* regulation in *A. baumannii*.

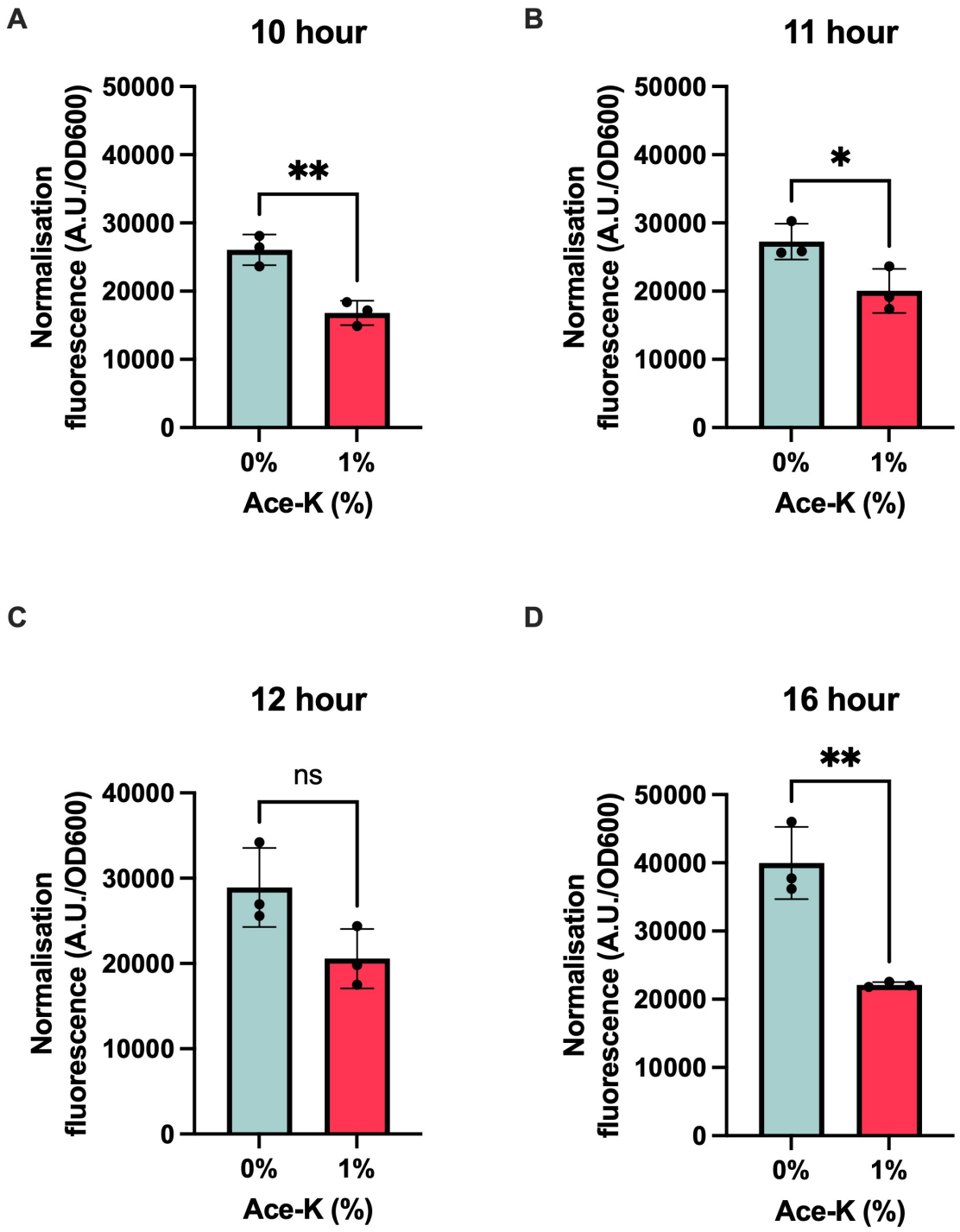

Figure 5.1 The graphs of Normalised fluorescence from the *PpilA::gfpmut3* transcriptional fusion show Ace-K could down-regulate the *pilA* (ABUW_0304) expression. (A) Normalised fluorescence at the 10th hour (B) Normalised fluorescence at the 11th hour (C) Normalised fluorescence at the 12th hour (D) Normalised fluorescence at the 16th hour. Data demonstrate

the mean of three biological replicates. Error bars represent standard deviation (SD). Statistical analysis was performed by an unpaired t-test between Ace-K and the control sample (ns>0.05, * p-value < 0.05, ** p-value < 0.01)

5.4.2 High-throughput GFP-based screening of an FDA-approved drug library identifies modulators of *pilA* expression.

Following validation of the GFP-based *PpilA* reporter assay, a high-throughput screen was conducted using the DiscoveryProbe™ FDA-approved drug library to identify compounds that modulate *pilA* expression in *A. baumannii*. The library comprises 2,320 FDA-approved compounds supplied as pre-dissolved solutions across 27 individual 96-well plates. These 27 plates were analysed independently for three parameters: bacterial growth (OD_{600}), *pilA*- GFP fluorescence, and biofilm formation. Normalised GFP fluorescence values were obtained by using the value from the 16th hour minus the 0 hour and dividing by the OD_{600} value for each well. To minimise inter-plate variability and enable comparison across the entire library, fluorescence values were further normalised relative to the DMSO growth control within each plate. The GFP fluorescence value of the compounds was divided by the normalised GFP fluorescence value of the DMSO control. Doing this would allow for the generation of a ratio-based normalised values that enabled robust cross-plate comparison.

Using this approach, the top five and bottom five compounds from each plate were picked, 270 drugs in total, which could regulate the *pilA* expression obtained (Figure 5.2). These 270 compounds were ranked across all plates, and the 10 strongest up-regulators (promotors) and 10 strongest down-regulators (inhibitors) of *pilA* expression were identified and checked for

their medical use (Figure 5.3). In Tables 5.2 and 5.3, the medical uses of these compounds were identified.

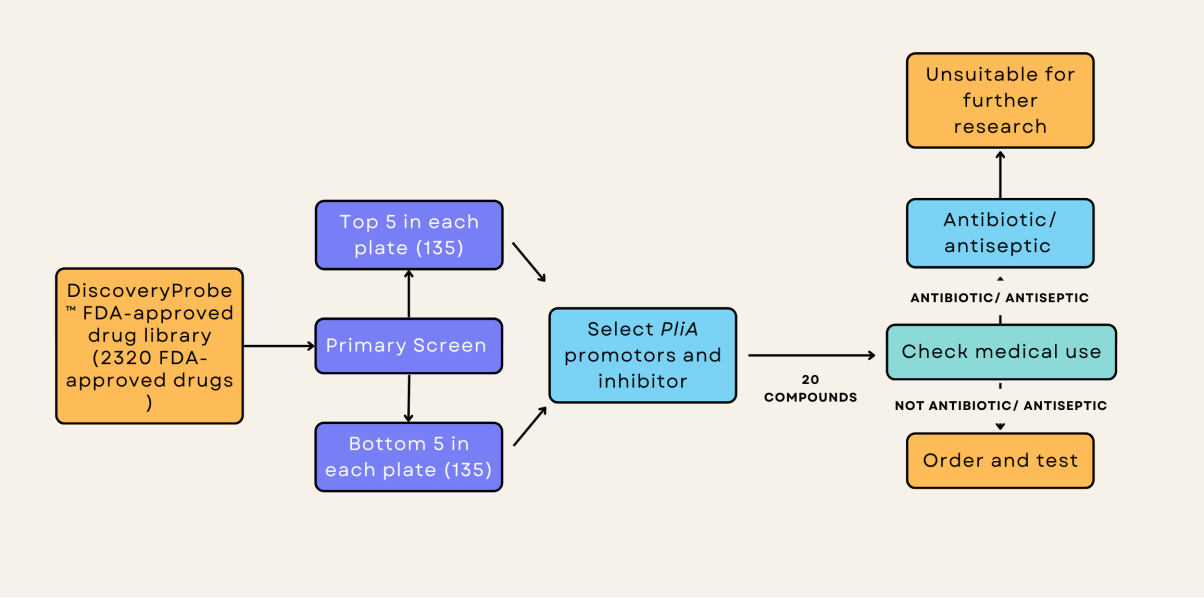

Figure 5.2 Workflow of high-throughput screening of an FDA-approved drug library. A GFP-based primary screen was performed using the DiscoveryProbe™ FDA-approved drug library (2,320 compounds). The top and bottom five compounds from each 135-compound plate were selected based on normalised reporter activity. Compounds were subsequently classified as putative PilA promoter activators or inhibitors. Antibiotic and antiseptic compounds were excluded from further analysis, while non-antibiotic candidates were selected for follow-up validation.

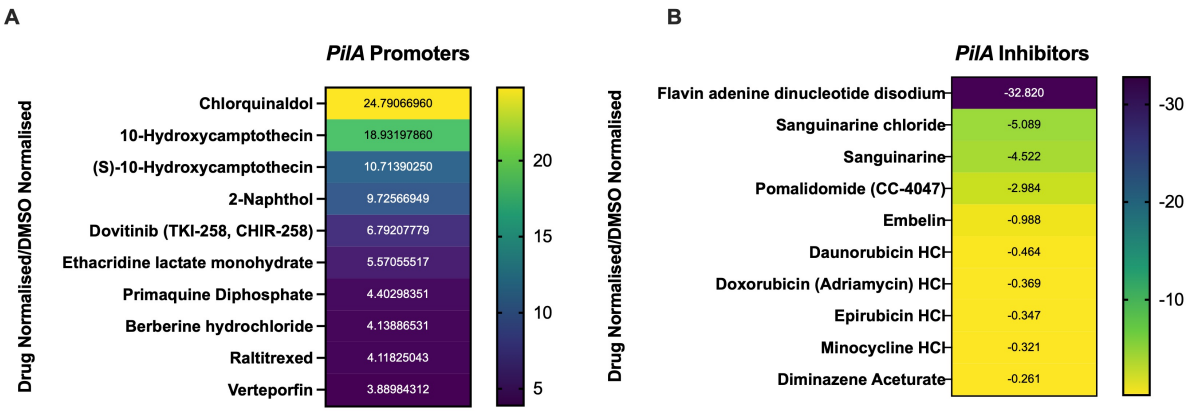

Figure 5.3. Identification of compounds that promote or inhibit *PilA* activity. Heatmaps show the effects of selected compounds on *PilA* promoter–driven reporter activity. Compounds are grouped into *PilA* promoters (A) and *PilA* inhibitors (B) based on their relative effects on *pilA* activity. The ratio was calculated by dividing the normalised GFP value of each compound by that of the normalised DMSO control. Compounds at the top of each heatmap showed the strongest promoting or inhibitory activity.

Table 5.2 Medical use of compounds identified from the *PilA* promoter based on the screening.

Compound Name (*PilA* promoters)	**Primary Functional Classification**
Chlorquinaldol	Antimicrobial agent; quinoline derivative; metal chelator(Bortolin *et al.*, 2017).
10-Hydroxycamptothecin	Anticancer agent; topoisomerase I inhibitor (Zhang *et al.*, 1998).
(S)-10-Hydroxycamptothecin	Anticancer agent; stereospecific topoisomerase I inhibitor (Song *et al.*, 2019).
2-Naphthol	Azo dyes, used as derivatising reagent for metal ion determination(Cu^{2+},Co^{2+}, Ni^{2+}), Used in non-steroidal anti-inflammatory drug (naproxen), antifungals(tolnaftate) and antibiotic (nafcillin) drugs synthesis (Aurelio-Soria *et al.*, 2026).
Dovitinib (TKI-258, CHIR-258)	Multikinase inhibitor; receptor tyrosine kinase inhibitor (Porta *et al.*, 2015).
Ethacridine lactate monohydrate	Dye with antiseptic properties (Mei *et al.*, 2014).
Primaquine Diphosphate	Antimalarial agent; redox-active antimicrobial ('Primaquine Diphosphate: Comprehensive Profile', 2005).

Berberine hydrochloride	Anti-inflammatory, antioxidant, and anticancer effects (Song *et al.*, 2025).
Raltitrexed	Thymidylate synthase inhibitor (Van Cutsem *et al.*, 2002).
Verteporfin	Photosensitizer; photodynamic therapy agent; ophthalmology for treating age-related macular degeneration (AMD) disease (Greco *et al.*, 2021).

Table 5.3 Medical use of compounds identified from the PilA inhibitor based on the screening.

Compound Name (*PilA* inhibitors)	**Primary Functional Classification**
Diminazene Aceturate	Antiparasitic agent (Da Silva Oliveira and De Freitas, 2015).
Minocycline HCl	Tetracycline-class antibiotic (Garrido-Mesa, Zarzuelo and Gálvez, 2013).
Daunorubicin HCl	Anthracycline antibiotic; also used for severe leukemia, lymphoma, breast and ovarian cancer, and other solid tumors (Vardanyan and Hruby, 2006).
Embelin	Natural benzoquinone; anti-cancer & antimicrobial properties (Prabhu *et al.*, 2018; Banerjee *et al.*, 2025).
Pomalidomide (CC-4047)	Immunomodulatory drug (IMiD) for multiple myeloma (Chanan-Khan *et al.*, 2013).
Sanguinarine	Plant-derived alkaloid; nuclear factor- κB modulator; antimicrobial; apoptosis inducer (Mackraj, Govender and Gathiram, 2008).
Sanguinarine chloride	Alkaloid salt form; antimicrobial property (Zhang *et al.*, 2018).
Flavin adenine dinucleotide (FAD) disodium	Cofactor for flavoproteins (Molano-Arevalo *et al.*, 2014), and use for vitamin B2 deficiency eye condition .
Epirubicin HCl	Anticancer agent; interference with the DNA synthesis (Cersosimo and Hong, 1986).
Doxorubicin (Adriamycin) HCl	Anthracycline anticancer agent (Carvalho *et al.*, 2009).

Four compounds were selected for detailed follow-up analysis based on pharmacological relevance, availability, and cost-effectiveness: 2-Naphthol, Primaquine Diphosphate, Pomalidomide, and Flavin adenine dinucleotide disodium (Table 5.4). Primaquine diphosphate has been used as an antimalarial agent in patients since the 1950s. 2-Naphthol is a colourless solid with several uses, including dyes, pigments, fats, oils, insecticides, pharmaceuticals, perfumes, antiseptics, the synthesis of fungicides, and antibiotics (Aurelio-Soria *et al.*, 2026). Both demonstrated increased *PilA* expression. Pomalidomide and FAD on the other hand,

reduced *PilA* expression. Pomalidomide is a second-generation immunomodulatory drug approved by the FDA in 2013 for the treatment of myeloma (Lacy and McCurdy, 2013). FAD can be found in the active sites of a and b monoamine oxidases, which are responsible for dopamine metabolism (Medrades *et al.*, 2022). FAD is used to treat vitamin B2 deficiency-related eye diseases.

Table 5.4 Medical uses of representative compounds affecting *PilA* activity

	Name	Medical use
PilA promotor	2-Naphthol	Dyes, pigments and perfume
	Primaquine Diphosphate	Antimalarial
PilA inhibitor	Pomalidomide	Antimyeloma agents
	Flavin adenine dinucleotide disodium	Vitamin B2 deficiency eye diseases

In the screen, 2-naphthol was promoting *pilA* expression by 9.73 times compared to DMSO control, and Primaquine Diphosphate showed promoting *pilA* expression by 4.40 times (Figure 5.4A, B). Pomalidomide inhibited *pilA* expression by 3.98 times, and FAD inhibited *pilA* expression by 33.82 times (Figure 5.4C, D). Therefore, further investigation is needed.

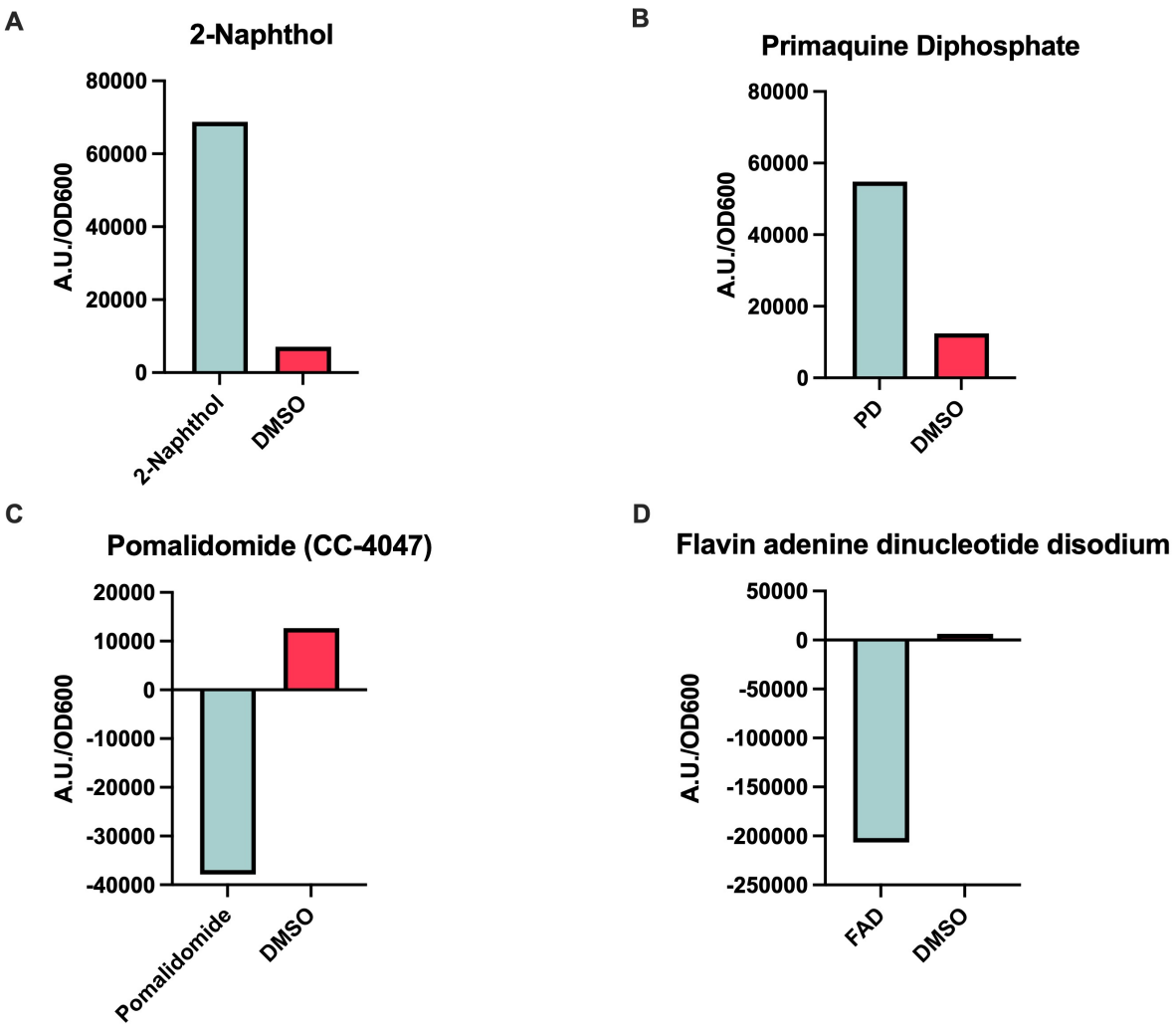

Figure 5.4 *pilA* promoters and inhibitors identified in a single-repeat screen of the FDA drug library (A)2-Naphthol increased *pilA* expression by a factor of 9.73 compared to the control group treated with DMSO. (B) Primaquine Diphosphate increased *pilA* expression by a factor of 4.40. (C) Pomalidomide inhibited *pilA* expression by 3.98-fold. (D) FAD was inhibiting *pilA* expression by 33.82- fold

5.4.3 Revalidation of *pilA* Expression of Hit Candidates and Determining their Growth and Biofilm Formation

To validate the initial screening results, these four compounds were tested at 0.05 mM, the same concentration used in the primary screen, and at 0.5 mM, which is tenfold higher than the

screening concentration. For 2-Naphthol promoted *pilA* expression by 8.74-fold at 0.05 mM and by 43.93-fold at 0.5 mM (Figure 5.5A). Similarly, Primaquine diphosphate promoted *pilA* expression by 28.62-fold at 0.05 mM and by 83.97-fold at 0.5 mM (Figure 5.5B). For the *pilA* inhibitor, the 0.05 mM pomalidomide reduced *pilA* expression by 3.44-fold (Figure 5.5C), which is consistent with previous experimental results. When the concentration was increased tenfold, 0.5 mM pomalidomide reduced *pilA* expression by 29.20-fold. For the FAD, inhibited *pilA* expression by 10.37-fold at 0.05 mM and by 15.40-fold at 0.5 mM (Figure 5.5D). Therefore, the promoting and inhibitory effects of the selected compounds are proportional to their concentrations.

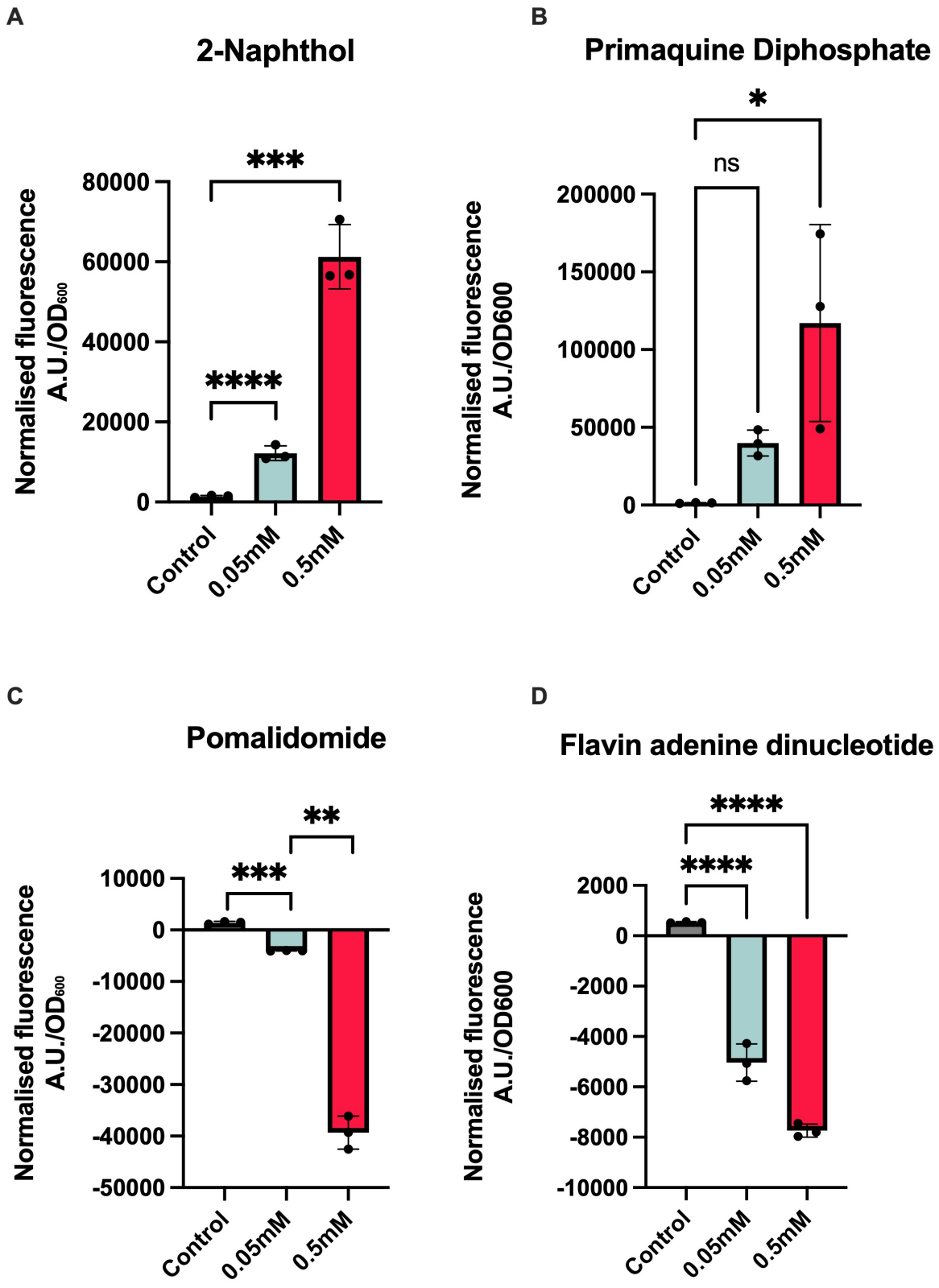

Figure 5.5 Revalidation results of hit compounds at concentration of 0.05mM and 0.5mM. Data demonstrate the mean of three technical replicates and three biological replicates. Error

bars represent standard deviation (SD). Statistical analysis was performed through ordinary one-way ANOVA between DMSO control (Untreated) and compounds treated groups.(ns>0.05, **p-value < 0.05, ** p-value < 0.01, **** p-value < 0.0001)

The levels of *pilA* expression were found to be proportional to concentration, with levels measured at 0.05 mM to 0.5 mM. To further characterise the regulatory effects of the selected hit compounds on *pilA* expression, a concentration-response analysis was performed. Six concentrations ranging from 0.025 mM to 1 mM were tested for 2-naphthol, primaquine diphosphate, pomalidomide, and FAD.

In the experiment with 2-naphthol, *pilA* expression increased with increasing 2-naphthol concentration. This provides evidence supporting the previous hypothesis that concentration is related to the rise in *pilA* expression. For primaquine diphosphate, *pilA* expression was similar to that of 2-naphthol. Expression increased with higher concentrations (Figure 5.6A, B). However, it was highest at 0.5 mM and decreased at 1mM. *pilA* expression is inhibited by FAD in a concentration-dependent manner as the FAD concentration increases from 0.025 mM to 0.5 mM (Figure 5.6D). Inhibition becomes more pronounced at higher concentrations, peaking at 0.25 mM and 0.5 mM, where expression levels reach highly negative values. As in previous tests, pomalidomide inhibits *pilA* expression. The inhibition increased with increasing concentration (Figure 5.6C).

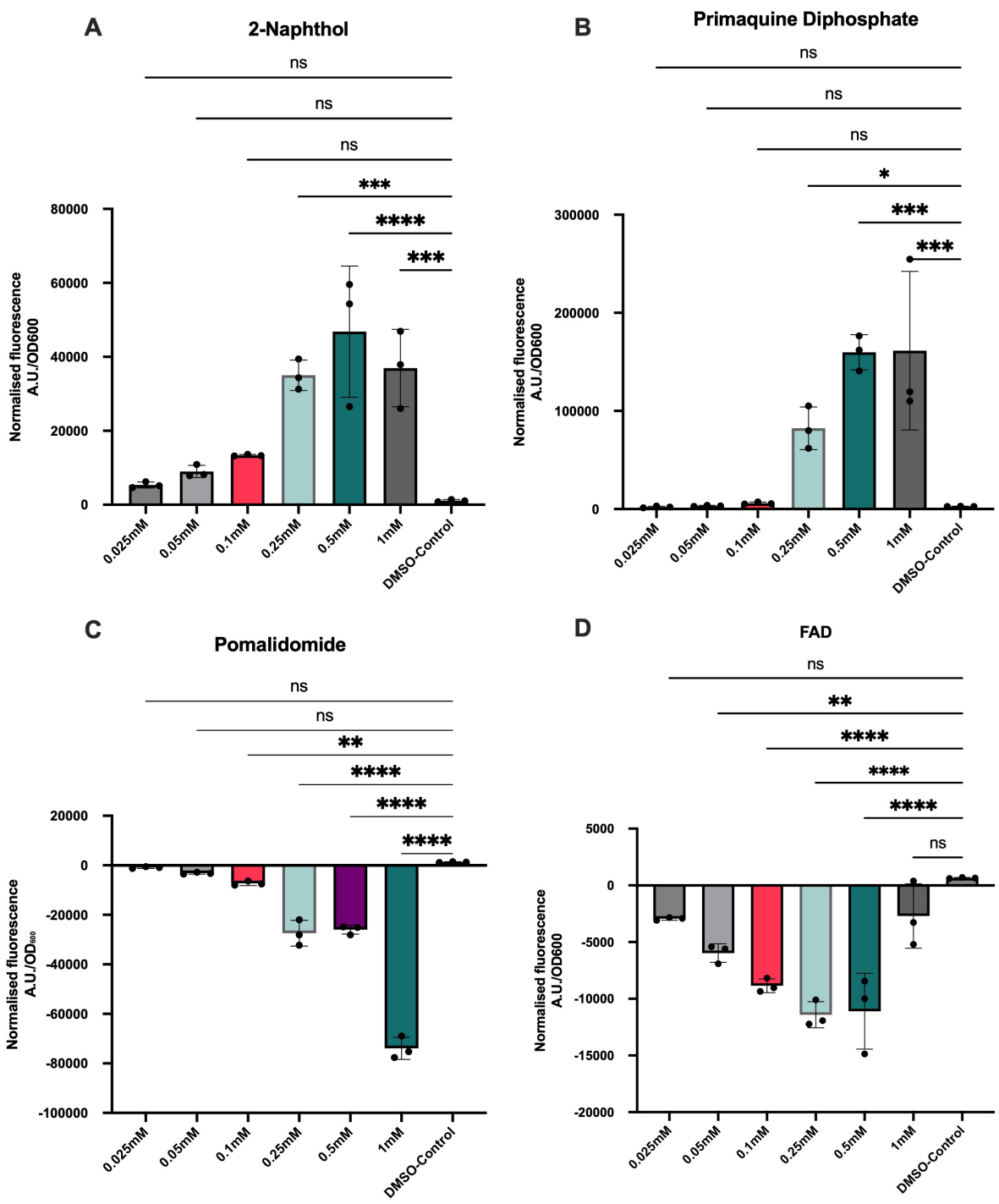

Figure 5.6 Normalised fluorescence from *PpilA::gfpmut3* transcriptional fusion demonstrates that selected compounds have an effect on *pilA*. Error bars represent standard deviation (SD). Statistical analysis was performed through ordinary one-way ANOVA between the DMSO control (Untreated) and the compound-treated groups. (ns>0.05, *p-value < 0.05, ** p-value < 0.01,*** p-value < 0.001, **** p-value < 0.0001).

5.4.4 Twitching assay of Primaquine Diphosphate, 2-Naphthol, Flavin adenine dinucleotide and Pomalidomide

To determine whether compound-induced modulation of *pilA* expression translated into functional changes in Type IV pilus activity, twitching motility assays were performed. Three conditions were tested for each compound: DMSO control, 0.05 mM, and 0.5 mM. Twitching zones were measured after 48 hours of incubation under high-humidity conditions.

Primaquine diphosphate markedly reduced twitching motility in a concentration-dependent manner (Figure 5.7A). At 0.05 mM, the mean twitching zone diameter was 25.5 mm, decreasing to 9.94 mm at 0.5 mM. This pronounced reduction suggests strong impairment of Type IV pilus–mediated surface motility.

In contrast, 2-naphthol decreased twitching motility at both lower and higher concentrations, with an average twitching zone of 27.5 mm at 0.05 mM. At 0.5 mM, twitching motility was further reduced to 8.89 mm. These responses indicate that the effect of 2-naphthol on twitching motility is concentration dependent (Figure 5.7B).

For the pomalidomide-treated group, the average twitching zone was 29.0 mm at 0.05 mM and 29.45 mm at 0.5 mM. And the average twitching zone of the control group was 34.33 mm. Both concentrations demonstrated similar twitching zones and showed effective inhibition of twitching compared to the DMSO-Control. These results suggest that pomalidomide reduces the twitching zone in a dose-independent manner (Figure 5.7C).

There was no significant difference in twitching motility observed between the FAD-treated and DMSO control groups. The twitching zone for the DMSO control was 23 mm, 21.55 mm at 0.05 mM, and 22 mm at 0.5 mM (Figure 5.7D).

Notably, the observed twitching phenotypes did not always correlate directly with *pilA* expression levels, particularly at higher concentrations of primaquine diphosphate and 2-naphthol. This observation suggested that additional factors, such as growth inhibition or broader physiological stress, may contribute to reduced motility under these conditions, prompting further investigation using growth and biofilm assays. Moreover, FAD did not significantly affect twitching motility and was therefore not pursued in further study.

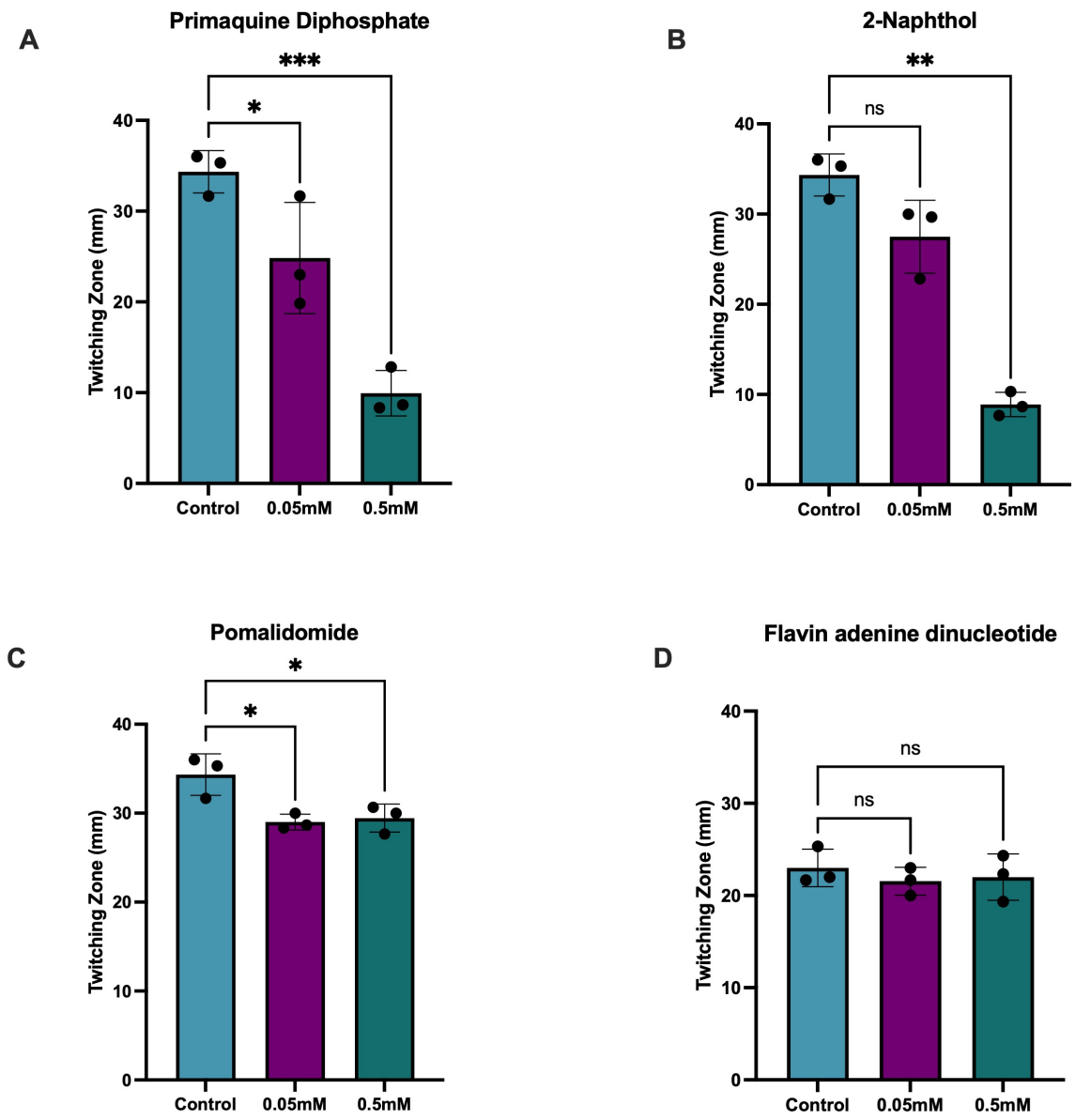

Figure 5.7 Primaquine diphosphate, 2-naphthol and pomalidomide decrease the twitching motility in *A. baumannii* (A) Twitching zone of primaquine diphosphate (B) Twitching zone of 2-naphthol (C) Twitching zone of pomalidomide. (D) Twitching zone of Flavin adenine dinucleotide. Data demonstrate the mean of three biological replicates. Error bars represent standard deviation (SD). Statistical analysis was performed through ordinary one-way ANOVA between the DMSO control (Untreated) and the compound-treated groups. (ns>0.05, **p-value < 0.05, ** p-value < 0.01, *** p-value < 0.001).

5.4.5 Growth and Biofilm Effects of Selected Compounds Reveal that Pomalidomide Augments *A. baumannii* Biofilm Formation Without Affecting Growth

To determine whether modulation of *pilA* expression occurred independently of bacteriostatic or bactericidal effects, growth and biofilm assays were performed with 2-naphthol, primaquine diphosphate, and pomalidomide. A range of concentrations from 0.125 mM to 5 mM was tested in cation-adjusted Mueller–Hinton broth.

In the growth and biofilm assays, Primaquine diphosphate exhibited a clear inhibitory effect on bacterial growth, with complete inhibition observed at 2.5 mM. Biofilm formation was more sensitive, with complete inhibition occurring at 1.5 mM, indicating that biofilm inhibition occurred at sub- MIC levels (Figure 5.8A, B).

Similarly, 2-naphthol inhibited *A. baumannii* growth in a concentration-dependent manner, with complete growth inhibition observed at 3.5 mM. Biofilm formation was fully inhibited at 1 mM, again demonstrating that antibiofilm activity preceded growth inhibition. (Figure 5.8C, D).

The pomalidomide did not inhibit bacterial growth across the entire tested concentration range. Instead, bacterial growth increased slightly at concentrations greater than 2 mM. For the biofilm formation, pomalidomide promoted biofilm formation at higher concentrations, indicating a distinct biological effect compared to the other compounds tested. (Figure 5.8E, F).

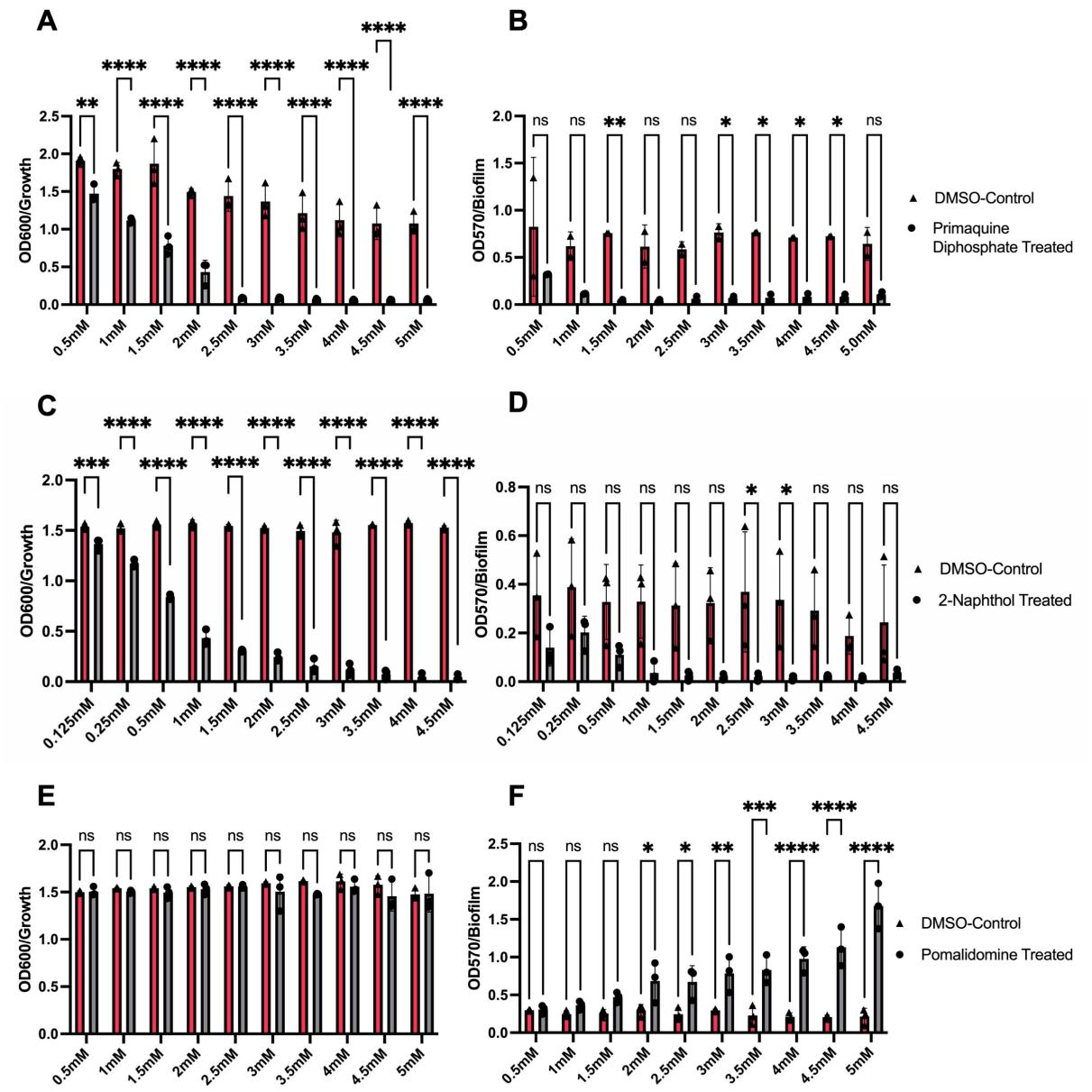

Figure 5.8 MIC and MBIC of (A, B) Primaquine Diphosphate, (C,D) 2-Naphthol (E, F) Pomalidomide. Data demonstrate the mean of three technical and biological replicates. Error bars represent standard deviation (SD). Statistical analysis was performed using a two-way ANOVA between the DMSO control (Untreated) and the compound-treated groups. (ns>0.05, *p-value < 0.05,**p-value < 0.01, *** p-value < 0.001, **** p-value < 0.0001).

To further understand and validate the growth profiles of 2-naphthol, pomalidomide, and primaquine diphosphate, growth curves were performed. In the result, pomalidomide growth curves show a similar trend to the MIC assay (Figure 5.9A). There is no significant difference in growth between the DMSO control and the pomalidomide-treated group. For 2-naphthol and primaquine diphosphate, the growth curve and growth assay results were consistent with the MIC result (Figure 5.9B, C). At 0.125 mM, the growth curve showed no difference between the DMSO control group and the treated group. However, growth began to decrease once the concentration reached 1 mM. Growth was inhibited entirely at a concentration of 2.5 mM. The 0.5 mM of primaquine diphosphate showed no difference between the DMSO control group and the treated group. However, at 1.5 mM, a semi-inhibitory state is observed, and at 2.5 mM, complete inhibition occurs. This result demonstrates that 2-naphthol and primaquine diphosphate have an inhibitory effect on *A. baumannii,* and this could be the reason why the twitching motility was reduced in the previous assay. The pomalidomide modulates *pilA* expression without promoting the growth of *A. baumannii* or antimicrobial activity. Therefore, pomalidomide was selected for further investigation.

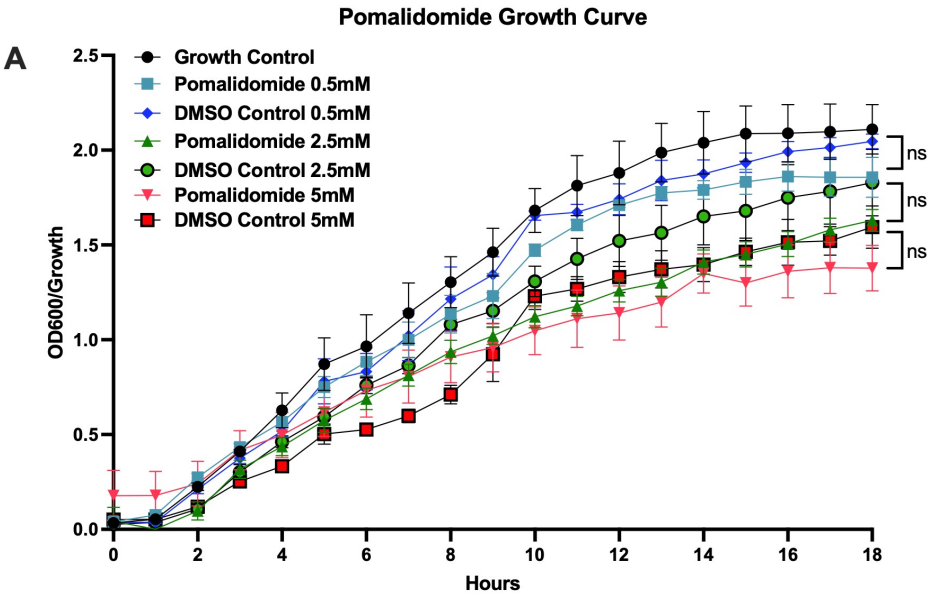
Pomalidomide Growth Curve
A
Growth Control
Pomalidomide 0.5mM
DMSO Control 0.5mM
Pomalidomide 2.5mM
DMSO Control 2.5mM
Pomalidomide 5mM
DMSO Control 5mM
ns
ns
ns
OD600/Growth
Hours

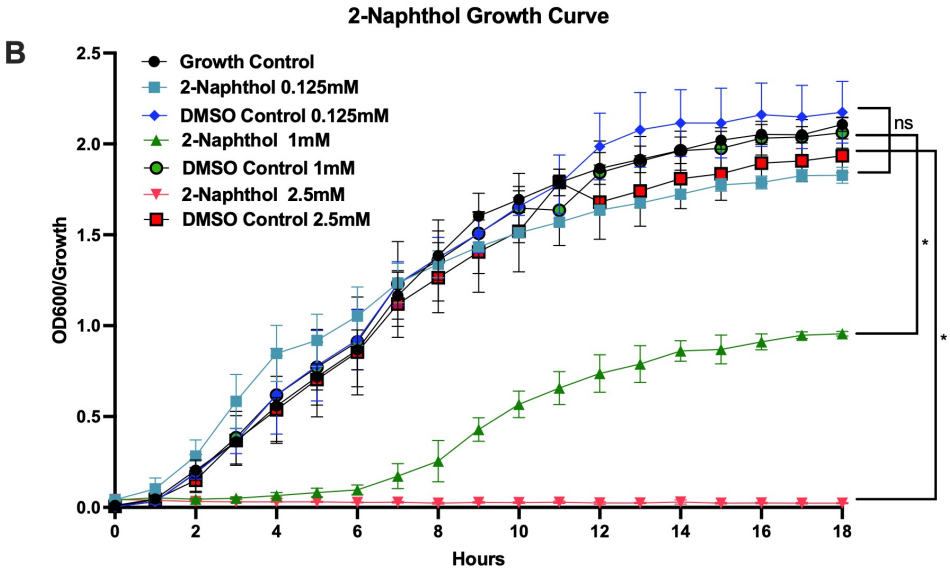
2-Naphthol Growth Curve
B
Growth Control
2-Naphthol 0.125mM
DMSO Control 0.125mM
2-Naphthol 1mM
DMSO Control 1mM
2-Naphthol 2.5mM
DMSO Control 2.5mM
ns
*
*
OD600/Growth
Hours

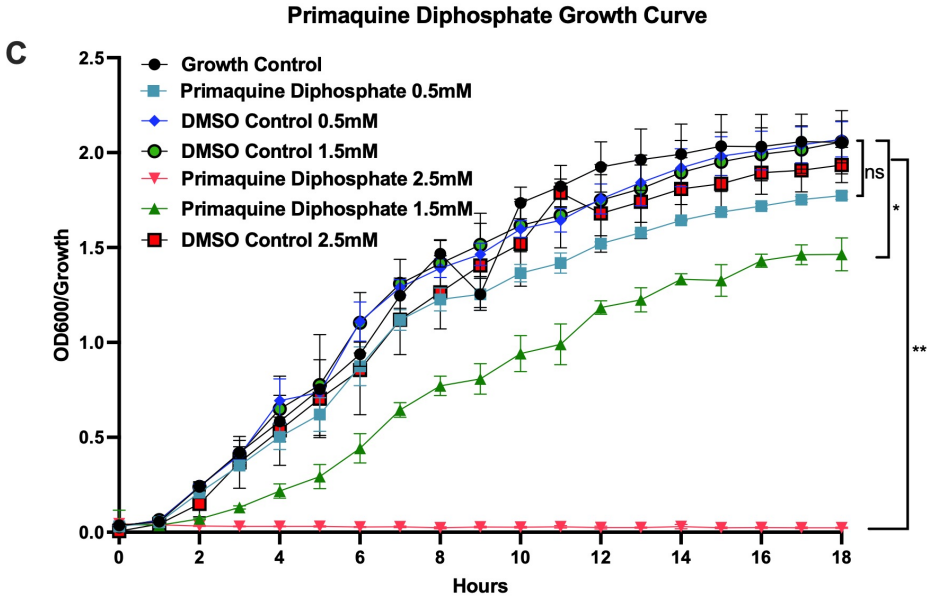
Primaquine Diphosphate Growth Curve
C
Growth Control
Primaquine Diphosphate 0.5mM
DMSO Control 0.5mM
DMSO Control 1.5mM
Primaquine Diphosphate 2.5mM
Primaquine Diphosphate 1.5mM
DMSO Control 2.5mM
ns
*
**
OD600/Growth
Hours

Figure 5.9 Growth Curve of pomalidomide, 2-naphthol and primaquine diphosphate on the growth of *A. baumannii* AB5075. Growth curves were monitored by OD_{600} measurements over 18 h in the presence of increasing concentrations of each compound. (A) pomalidomide at 0.5, 2.5 and 5 mM. (B) 2-naphthol at 0.125, 1 and 2.5 mM. (C) Primiquine diphosphate at 0.5, 1.5 and 2.5 mM. Data demonstrate the mean of three technical and biological replicates. Error bars represent standard deviation (SD). Statistical analysis was performed through ordinary two-way ANOVA between DMSO control (Untreated) and compounds treated groups. (ns>0.05, *p-value < 0.05,**p-value < 0.01, *** p-value < 0.001, **** p-value < 0.0001).

5.4.6 Pomalidomide Triggers Increases Expressed of the Biofilm-associated *CSU pili*

Pomalidomide is an immunomodulatory agent for multiple myeloma. However, infection-related adverse events have been reported (Dimopoulos *et al.*, 2016; Richardson *et al.*, 2019; Balmaceda *et al.*, 2021). In the STRATUS phase 3b study of pomalidomide plus low-dose dexamethasone, infection is the most frequent nonhaematological grade 3/4 adverse event, occurring in 28.1% patients, including grade 3/4 pneumonia in 10.9% (Dimopoulos *et al.*, 2016). In another phase 3 trial, infection was also the most frequent nonhaematological grade 3/4 adverse event, affecting 31% of patients who received pomalidomide, bortezomib, and dexamethasone. However, this number decreased to 18% in patients receiving bortezomib and dexamethasone. The patients with pomalidomide treatment are also associated with a higher risk of neutropenia than patients who received bortezomib and dexamethasone (Richardson *et al.*, 2019). In a systematic review and meta-analysis of randomised myeloma trials showed that the monthly risk for grade III or higher infection of patients who taking pembrolizumab/pomalidomide/dexamethasone is 3.9%, and 3.5 for patients taking bortezomib/pomalidomide/dexamethasone at 3.5%. Moreover, in the relapsed/refractory MM setting, pembrolizumab/pomalidomide/dexamethasone had the highest monthly incidence of grade 3 or higher pneumonia (3.2%), whereas Daratumumab/bortezomib/dexamethasone was

associated with a lower rate of approximately 0.8% (Balmaceda *et al.*, 2021). These data indicate that patients receiving pomalidomide-based therapy have a higher risk of severe infection. In the study by Miguel *et al.* (2013), it was reported that 66% of patients who did not develop neutropenia still experienced infections. Based on our previous findings together with these clinical studies, we hypothesise that pomalidomide may directly influence the pathogenicity of pathogens such as *A. baumannii*.

To investigate the global transcriptional response of *A. baumannii* to pomalidomide exposure, RNA sequencing was performed on strain AB5075 grown in LB broth supplemented with 5 mM pomalidomide and compared with a DMSO-treated control. In total, 94 genes were differentially expressed ($|\log_2 \text{fold change}| \geq 1$, $p < 0.05$; Figure 5.10). Notably, several genes associated with biofilm formation were upregulated, including *csuC* and *csuB*. These findings suggest that exposure to pomalidomide may enhance biofilm formation and potentially promote *A. baumannii* infection.

On the other hand, *paaA*, *paaB*, *paaC*, *paaD*, and *paaZ*, were all upregulated. In Bhuiyan et al. (2016) study, *paaA* was investigated and zebrafish were used as the animal model. When infected with wild-type *A. baumannii*, the survival rate at 96 hours was only 25%. However, when *paaA* was knocked out, the survival rate at 96 hours increased to 75%, highlighting the importance of *paaA* in virulence. This may explain the lower survival rate observed in the pomalidomide-treated larvae in our animal model.

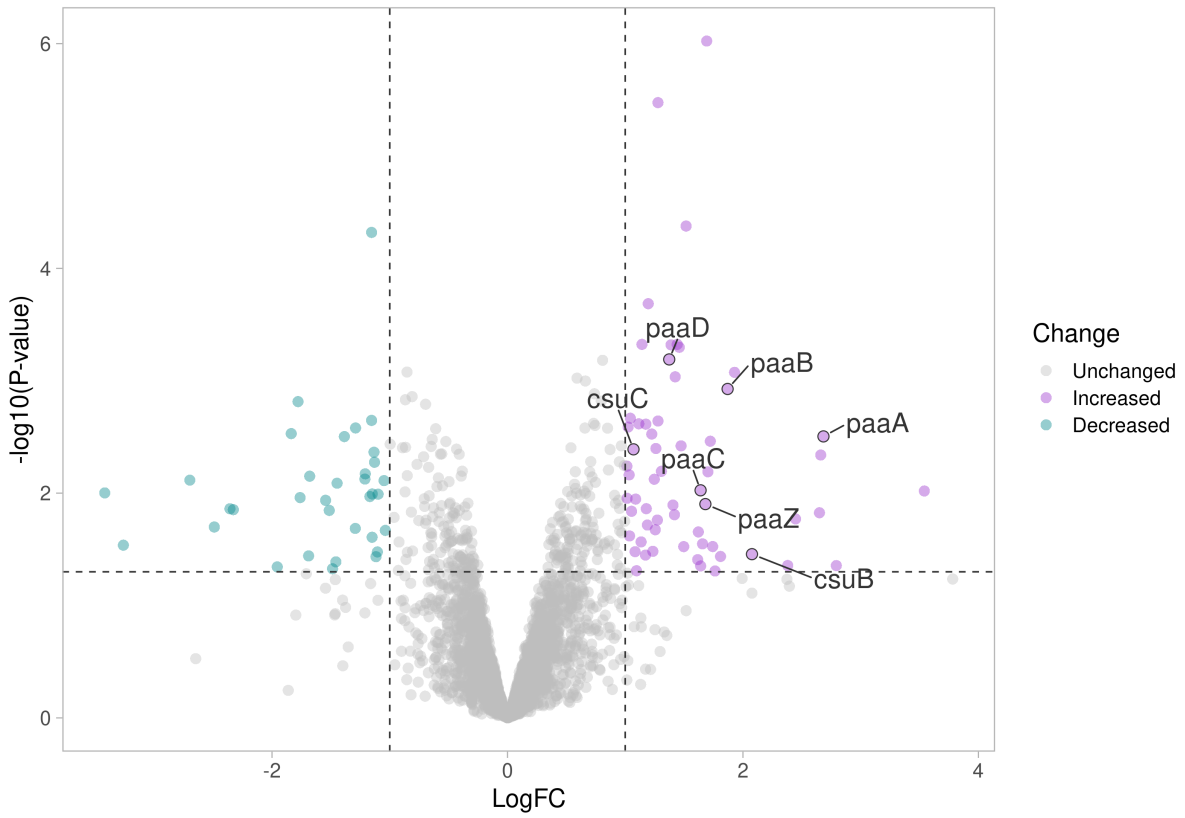

Figure 5.10 Volcano plot of differentially expressed genes in *Acinetobacter baumannii* AB5075 treated with 5 mM Pomalidomide compared to DMSO control, both grown in LB broth. The x-axis represents $\log_2$ fold change (LogFC), while the y-axis shows $-\log_{10}$(p-value). Purple dots indicate significantly upregulated genes, teal dots indicate significantly downregulated genes, and grey dots represent genes with no significant change in expression.

5.4.7 Pomalidomide Exhibits Strong Binding to Biofilm-associated csu pili Proteins by Using Molecular Docking

Molecular docking analysis predicted that pomalidomide interacts with the biofilm-associated Csu pili proteins CsuB and CsuC. In the CsuB protein, the pomalidomide formed a hydrogen bond with TYR162, and the bond distance is 2.1 Å. The ILE161 residue on the CsuB forms hydrophobic interactions with the ligand. Additionally, the LYS52, GLY51, GLY160, SER54,

SER57, LEU150, LEU108, and LYS163 residues on the CsuB form van der Waals interactions with the pomalidomide. There was carbon–hydrogen bonding interactions between pomalidomide and HIS157 and ALA55 (Figure 5.11). The lowest binding energy (BE) is -7.7 kcal/mol, which means it is in a favourable binding mode (Figure 5.11D).

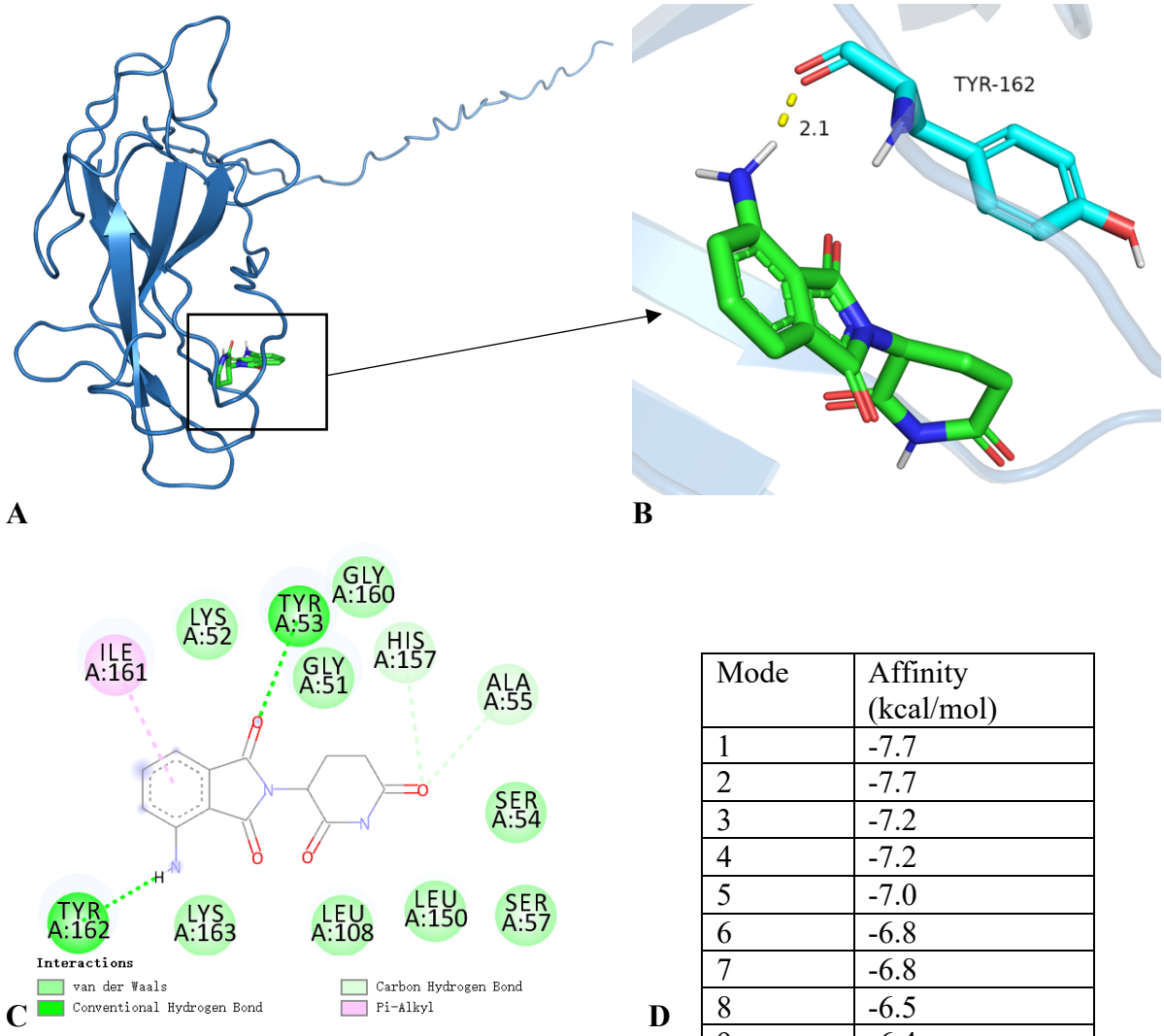

Mode	Affinity (kcal/mol)
1	-7.7
2	-7.7
3	-7.2
4	-7.2
5	-7.0
6	-6.8
7	-6.8
8	-6.5
9	-6.4

Figure 5.11 Molecular docking of pomalidomide with the biofilm-associated CsuB protein of *A. baumannii*. (A) Overall binding pose of pomalidomide within the predicted binding pocket of CsuB (B) Enlarged view of the binding site, highlighting key ligand–protein interactions (C) Two-dimensional interaction diagram illustrating the interaction network between pomalidomide and surrounding CsuB residues.

The molecular interaction between pomalidomide and CsuC was tested. In the result, residues SER159, ASN169, and LYS201 in the CsuC protein have hydrogen bond interactions with the pomalidomide. Additionally, GLN166, ALA175, ALA170, ALA173, ASN172, LYS176, GLY160, LEU161, ILE259, and GLY258 on the CsuC form van der Waals interactions with the pomalidomide (Figure 5.12). The lowest predicted binding energy for the pomalidomide–CsuC complex was –6.5 kcal/mol (Figure 5.12D), indicating a favourable, though comparatively weaker, binding activity than that observed for CsuB.

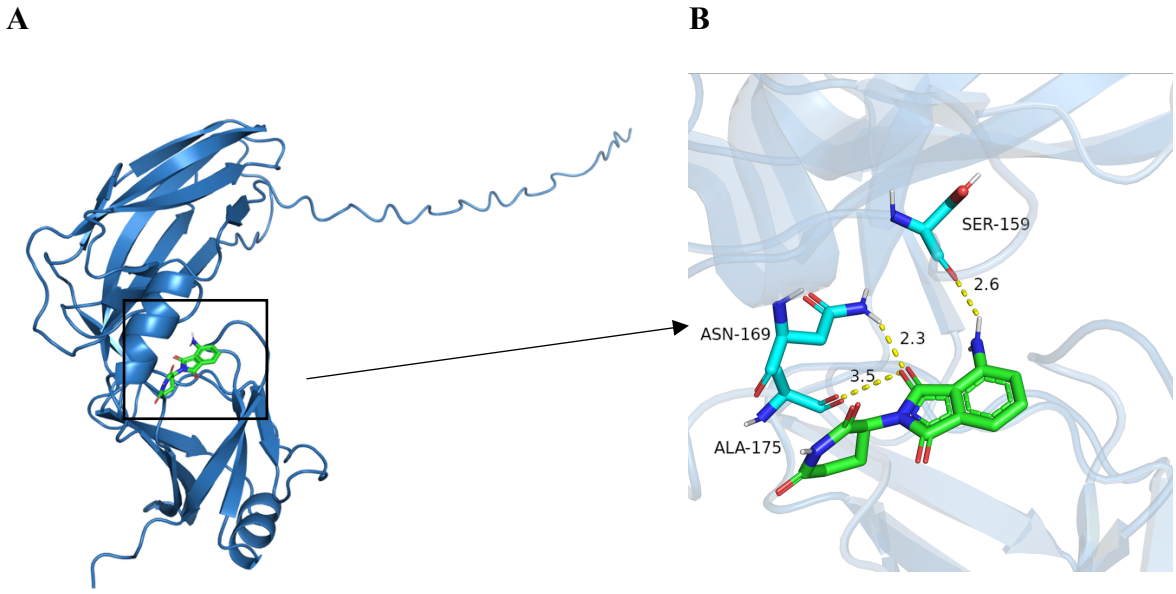

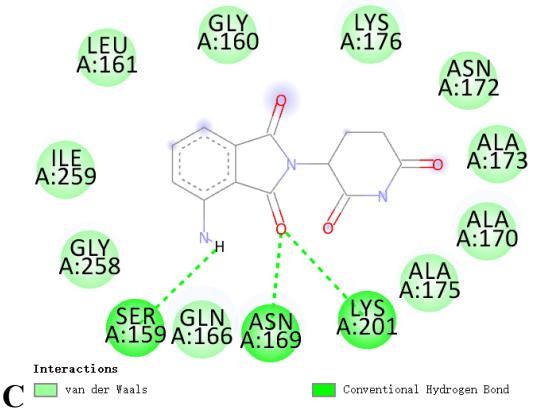

C

D

Mode	Affinity (kcal/mol)
1	-6.5
2	-6.5
3	-6.4
4	-6.4
5	-6.3
6	-6.2
7	-6.2
8	-6.2
9	-6.2

Figure 5.12 Molecular docking of pomalidomide with the biofilm-associated CsuC protein of *A. baumannii*. (A) Overall binding pose of pomalidomide within the predicted binding pocket of CsuC (B) Enlarged view of the binding site, highlighting key ligand–protein interactions (C) Two-dimensional interaction diagram illustrating the interaction network between pomalidomide and surrounding CsuC residues.

In addition to Csu pili proteins, 1,2-phenylacetyl-CoA epoxidase subunit A protein, where the *paaA* gene is encoded by was also tested (Figure 5.13). In the result, the residues MET194, SER42, TYR145, and GLN35 on the 1,2-phenylacetyl-CoA epoxidase subunit A form hydrogen bond interactions with pomalidomide. The residues PRO198, GLY197, ILE269, PHE265, PHE196, MET195, SER107, HIS39, LEU137, ASN133, and GLN38 on the 1,2-phenylacetyl-CoA epoxidase subunit A form van der Waals interactions with pomalidomide. The pomalidomide and 1,2-phenylacetyl-CoA epoxidase subunit A protein demonstrates a favourable binding activity, with the lowest predicted binding energy of –8.0 kcal/mol (Figure 5.13D).

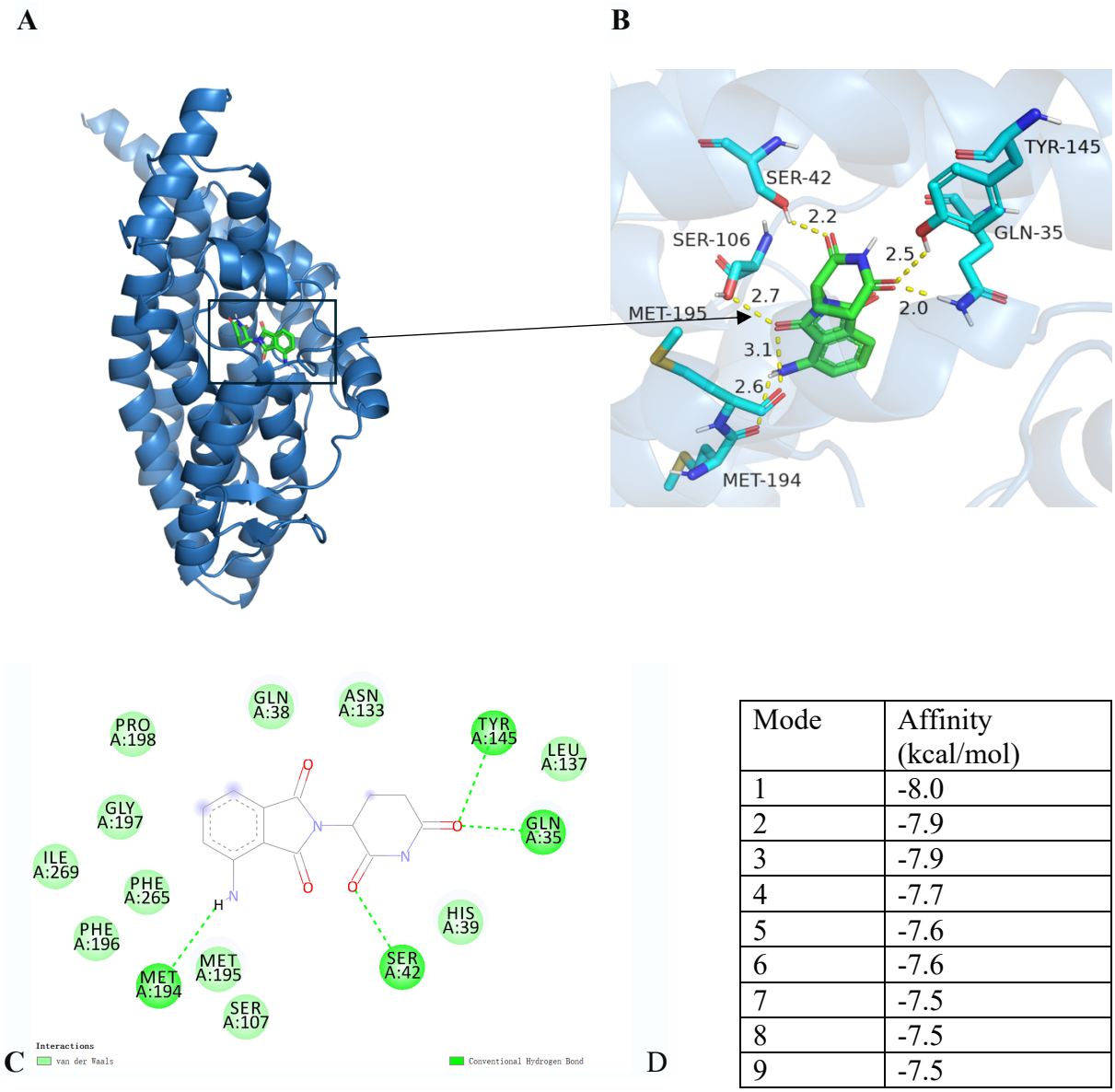

Mode	Affinity (kcal/mol)
1	-8.0
2	-7.9
3	-7.9
4	-7.7
5	-7.6
6	-7.6
7	-7.5
8	-7.5
9	-7.5

Figure 5.13 Molecular docking of pomalidomide with the 1,2-phenylacetyl-CoA epoxidase subunit A protein of *A. baumannii*. (A) Overall binding pose of pomalidomide within the predicted binding pocket of 1,2-phenylacetyl-CoA epoxidase subunit A (B) Enlarged view of the binding site, highlighting key ligand and protein interactions (C) Two-dimensional interaction diagram illustrating the interaction network between pomalidomide and the surrounding 1,2-phenylacetyl-CoA epoxidase subunit A residues.

5.4.8 Pomalidomide Increases the Mortality of *A. baumannii* AB5075-infected *G. mellonella*

According to reports, the clinical treatment of pomalidomide (POMA) increases the chance of bacterial infections in patients. Approximately 75% of patients experience infections in the Gram-negative respiratory tract and urinary tract (Munshi, Longo and Anderson, 2022). Immunodeficiency is the underlying cause of the increased rate of bacterial infections, as indicated by earlier findings. For instance, B-cell dysfunction, reduced CD4+ cell counts, and natural killer cell dysfunction (Dimopoulos *et al.*, 2014). We next assessed whether pomalidomide-induced transcriptional and phenotypic changes influenced bacterial virulence *in vivo* using the *Galleria mellonella* model. *G. mellonella* has innate immune system that shares key functional similarity to mammalian innate immunity such as phagocytic haemocytes and antimicrobial peptide response. It has been widely used to assess for drug toxicity and pathogen virulence, and the results from this insect show similarity and correlation with result obtained in mice (Pereira *et al.*, 2018; Maslova *et al.*, 2020). Prior to infection experiments, the toxicity of the solvent DMSO and pomalidomide alone was evaluated to establish appropriate injection volumes and concentrations.

The analysis of survival rates over 48 hours for different DMSO volumes in *G. mellonella* shows a clear dose-dependent toxicity (Figure 5.14A). At the highest concentration (10 µL), survival rates decreased rapidly, reaching 12.9% at 22nd hours and 0% at 40 hours, which indicates severe toxicity. Moderate concentrations (5 µL) show a more gradual decline, with survival decreasing to 58.57% by 47hours and 48.89% by 48 hours. With a 4µL DMSO injection, the survival rate at the 40th hour was 53.33%, and it decreased to 48.49% at the 48th time point. In contrast, at lower volumes (3 µL, and 2 µL) it exhibits less toxicity, with 3 µL and 2 µL maintaining high survival rates above 86.67% and 96. 67% at 48 hours. These results suggest that while higher DMSO volumes are highly toxic, lower volumes are much safer,

highlighting the importance of dose considerations in biological applications involving DMSO. Based on these results, a 5 µL injection volume was selected for later experiments to minimise solvent-associated mortality while keeping the compound concentration within its solubility limit. Given a solubility of 183 mM and a 5 µL injection volume, the maximum achievable concentration in *G. mellonella* was 4 mM. Therefore, pomalidomide was used at 4 mM in all further experiments.

With DMSO toxicity established, the focus shifted to assessing the toxicity of pomalidomide in *G. mellonella*. Analysis of survival rates in larvae treated with a 5 µL injection of pomalidomide at different concentrations revealed toxicity (Figure 5.14B). There was no significant difference between the different concentrations tested. At the physiological concentration (0.06 mg/kg), the survival rate was 50%, whereas the DMSO control showed a survival rate of 58.4%. At higher concentrations (1.5 mM and 4 mM), similar moderate toxicity was observed, with survival rates of 56.7% and 50%, respectively. These results indicate that pomalidomide exhibits minimal toxicity and that the majority of the observed toxicity is attributable to DMSO.

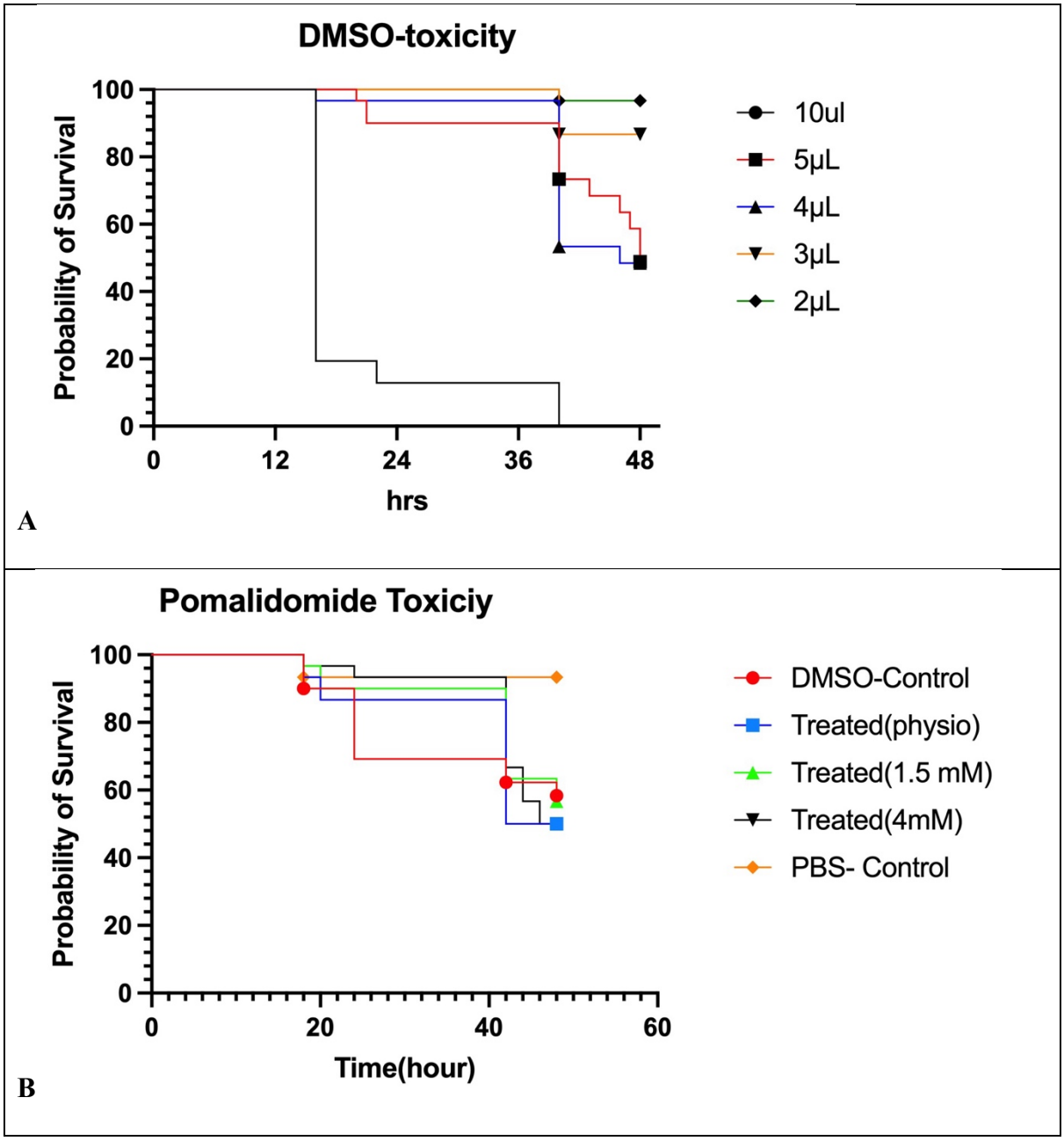

Figure 5.14 Survival of *Galleria mellonella* following DMSO and pomalidomide exposure (A) Survival curves of *G. mellonella* injected with increasing concentrations of DMSO. (B) Survival curves of *G. mellonella* following injection with varying concentrations of pomalidomide (POMA). For both assays, experiments were performed in biological triplicate, with 30 larvae per treatment group (N = 30).

From the previous results, we observed that pomalidomide affects biofilm formation, potentially altering virulence in *A. baumannii,* and that DMSO and pomalidomide are toxic.

We next assessed whether pomalidomide-induced transcriptional and phenotypic changes influenced bacterial virulence *in vivo*. Survival assays were performed using the *G. mellonella* infection model with *A. baumannii* AB5075 exposed to pomalidomide at different concentrations. As shown in Figure 5.15, pomalidomide treatment resulted in a dose-dependent reduction in larval survival compared with the untreated and DMSO control groups. In the 4 mM pomalidomide-treated group, all larvae died within 48 hours. At 1.5 mM, fewer than 10% of total larvae survived (2 survived). At the physiological concentration, approximately 40% of larvae survived (10 survived), which was significantly lower than the survival rate observed in the AB5075 + DMSO control group. This effect was significant at both 1.5 mM (p value = 5.34×10^{-6}) and 4 mM (p value = 5.38×10^{-8}), with the stronger effect observed at the higher concentration. These results indicate that pomalidomide exposure enhances *A. baumannii* virulence in the *G. mellonella* model, consistent with the upregulation of biofilm and adhesion-associated genes observed at the transcriptomic level.

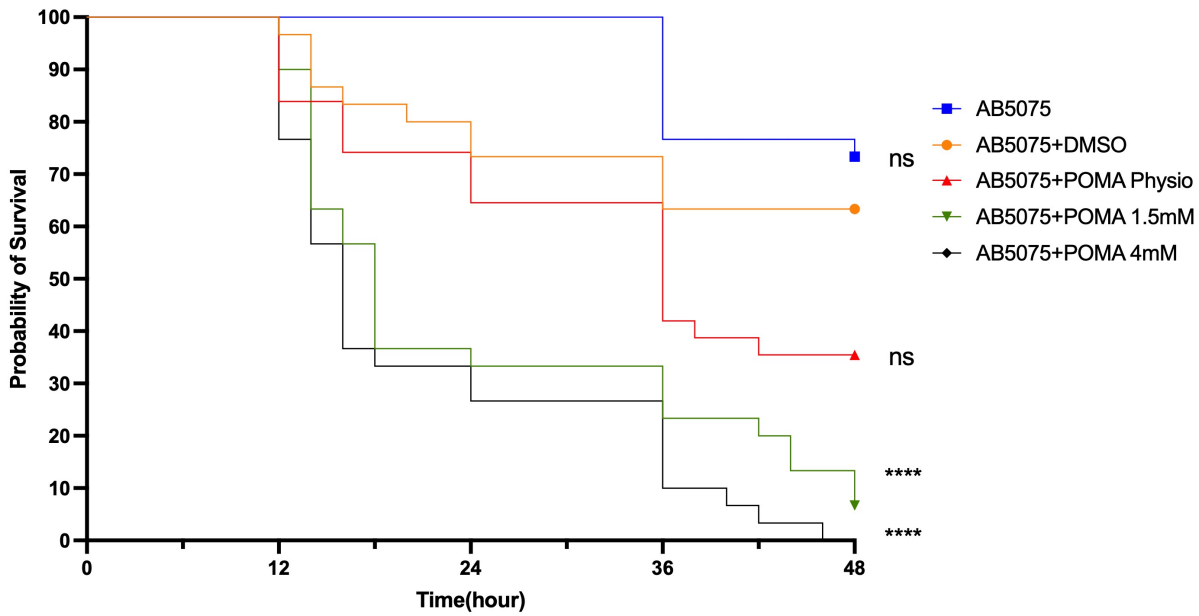

Figure 5.15 Survival study of *Galleria mellonella* following infection with *A. baumannii* AB5075 exposed to pomalidomide at different concentrations. Larvae were infected with *A.*

baumannii alone or with pomalidomide (1.5 mM, 4 mM, or physiological concentration), or with a DMSO control. Larval survival was monitored over a 48-hour period, plotted as survival curves and analysed using Long-rank (Mantel-Cox) test. (n=30). (ns>0.05, **** p-value < 0.0001)

5.4.9 Pomalidomide Exposure Leads to Increase in Clinical Scores in a Murine Model of *A. baumannii* Infection

Based on the findings from the *G. mellonella* model, we next validated whether pomalidomide increases *A. baumannii* pathogenicity in a mammalian host. In this section, a murine infection model was established using immunocompetent BALB/c mice. Initially, pomalidomide was injected with various concentrations (5, 10, 20, 30mg/kg). As a result, pomalidomide +AB5075 groups showed an increased clinical score when compared with the vehicle control group from day 0 to day 3 (Clinical scores were recorded based on each animal's general appearance, behaviour, hydration status, respiratory effort, weight, and external body temperature). Particularly in the AB5075+ 10 mg/kg, AB5075+ 20 mg/kg, and AB5075+ 30 mg/kg Pomalidomide groups. On Day 1, the clinical score for AB5075+ 10 mg/kg was 7, AB5075+ 20 mg/kg was 8, and AB5075+ 30 mg/kg was 7.6. The control group's clinical score was 6.2. By day three, the clinical scores for AB5075 + 10mg/kg were 10.25, and both the AB5075 + 20 mg/kg pomalidomide and AB5075+ 30 mg/kg pomalidomide groups had risen to 9.8, while the control group's score was 9.5 (Figure 5.16A). In the second run, clinical scores on day 1 were higher in both the AB5075 + 20 mg/kg pomalidomide and AB5075 + 30 mg/kg pomalidomide groups than in the control group (Figure 5.16B). The scores were 9.8 and 9.2, respectively, compared with 8.8 in the control group. By day 3, the control group showed the high clinical score (12.75), whereas the AB5075 + 20 mg/kg and AB5075 + 30 mg/kg pomalidomide groups had scores of 11.75 and 12.33, respectively.

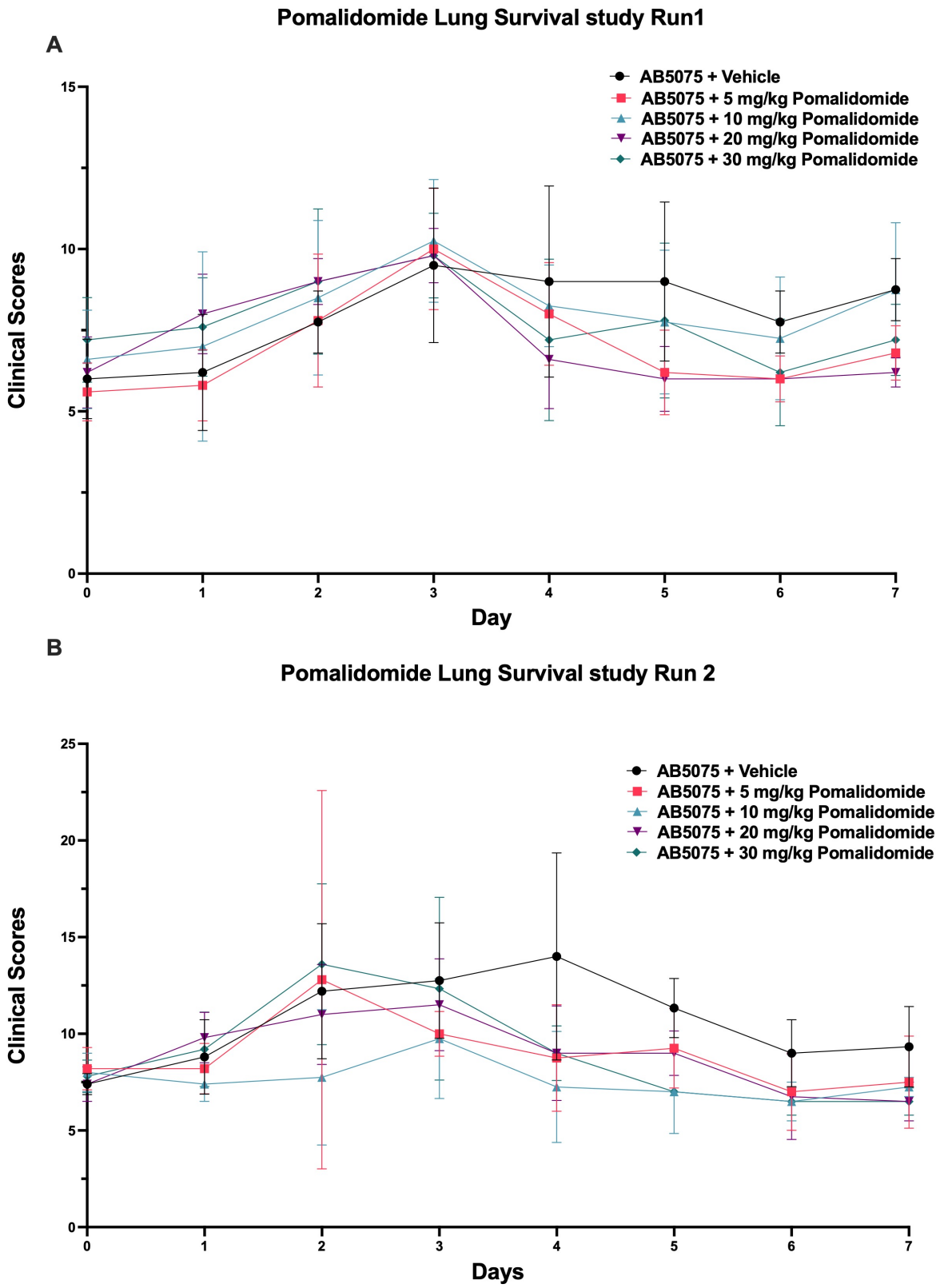

Figure 5.16 Pomalidomide increases clinical severity in a murine model of *A. baumannii* lung infection. (A) clinical scores of experiment 1 (B) clinical scores of experiment 2. BALB/c mice

were infected with *A. baumannii* strain AB5075 with increasing doses of pomalidomide (5, 10, 20, or 30 mg/kg). Clinical scores were assessed daily over a 7-day period. Data represent mean ± SD for each group (n = 5 per group).

To further validate the phenotype, the AB5075 + 30 mg/kg pomalidomide group was tested again an *in vivo* experiment and directly compared with the vehicle-treated control group (Figure 5.17A). Similar to previous studies, 5 mice were used. A similar result was observed with the initial findings. In this result, the AB5075+ 30 mg/kg Pomalidomide groups show higher clinical scores than the control group at day 1, day 2, day 4 and day 7 in run 3.

To better characterise the changes in clinical scores observed across the three-run mouse study, daily clinical scores were plotted for the AB5075 + 30 mg/kg pomalidomide group (Figure 5.17B). The clinical scores were significantly elevated on day 1 in the pomalidomide-treated group. The pomalidomide-treated group reached a clinical score of 8.87, compared with 7.13 in the control group. This also represented an increase from 6.07 on day 0 in the pomalidomide-treated group. These results indicated an early exacerbation of infection severity following pomalidomide exposure.

Pomalidomide Lung Survival study Run 3

A

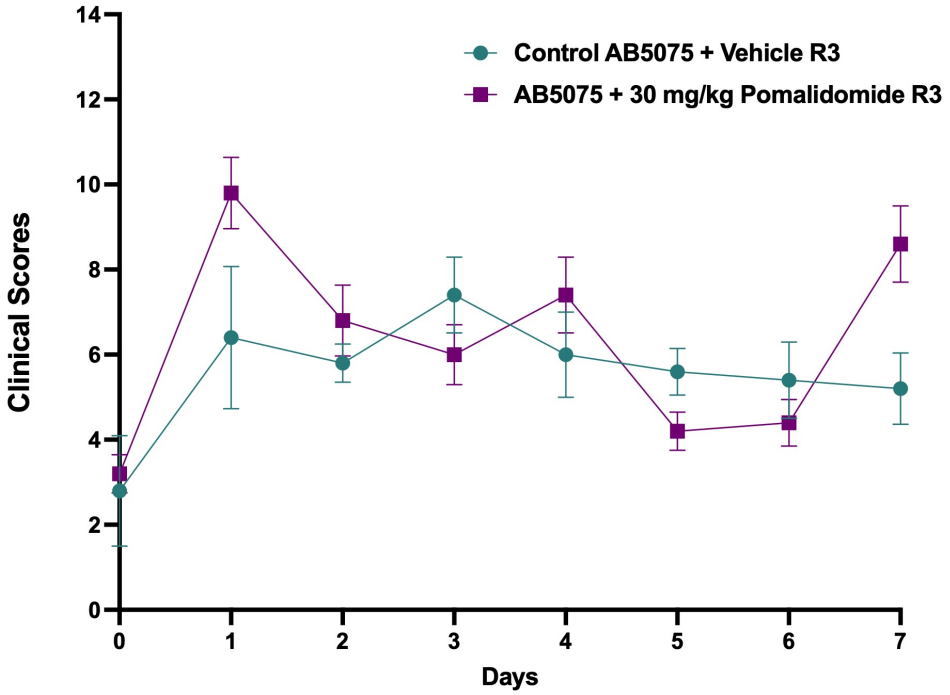

B

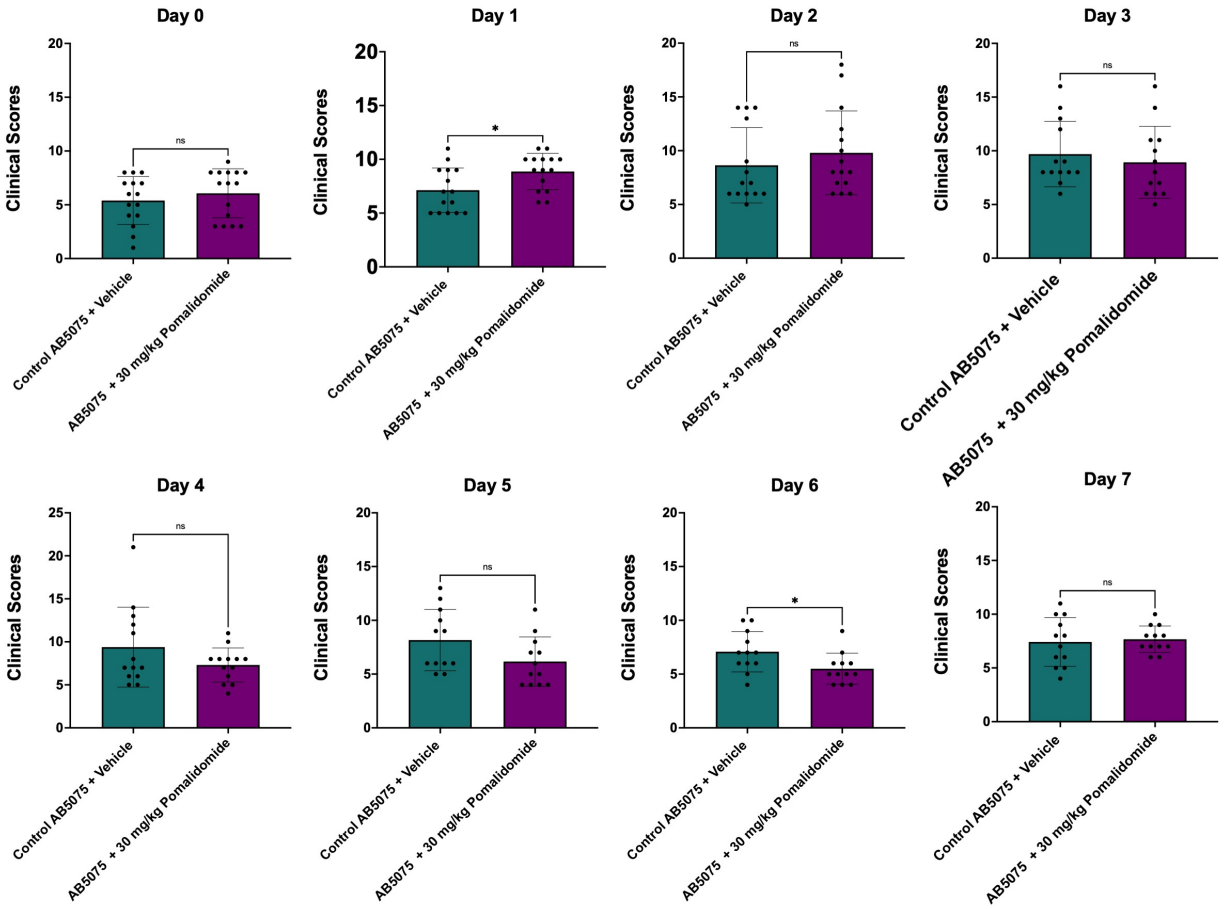

Figure 5.17 Pomalidomide increases clinical severity in a murine model of *A. baumannii* lung infection. (A) Overall clinical scores for 7 days in exprinment 3 (B) Clinical score at day 0 to day 7 on 30mg/kg group. Clinical scores were assessed daily for 7 days. Data represent mean ± SD for each group ((A)n = 5 per group and (B) n = 5 per group). Error bars represent standard deviation (SD). Statistical analysis was performed through a t-test between the DMSO control (Untreated) and the compound-treated groups. (**p-value < 0.01, *** p-value < 0.001)

5.5 Discussion

In this study, the effects of FDA-approved non-antibiotic drugs on Type IV pilus (T4P) regulation and biofilm formation in *A. baumannii*, with a particular focus on *pilA* expression, were systematically investigated. By integrating high-throughput screening, growth and biofilm assays, twitching assay, transcriptomic profiling, and an *in vivo* infection model, this work demonstrates that non-antibiotic compounds can exert biologically meaningful effects on bacterial behaviour beyond classical growth inhibition. Together, these findings expand current understanding of how pharmaceutical exposure may unintentionally reshape bacterial pathogenicity.

The high-throughput screening demonstrated the feasibility of the 1:9 LB/Water growth medium for measuring GFP fluorescence and OD_{600} simultaneously. Using this medium, both GFP fluorescence and OD_{600} could be measured simultaneously for FDA-approved compounds with the CLARIOstar Plus plate reader. It provides one of the most comprehensive assessments to date of the effects of non-antibiotic drugs on T4P regulation in *A. baumannii.* Among the screened drugs, 40 candidates were selected based on their effects on biofilm formation and GFP fluorescence associated with *pilA* expression. From these candidates, 4 compounds were picked for further investigation. Notably, the pomalidomide and Flavin adenine dinucleotide disodium showed significant inhibition of *pilA* expression, while two other drugs, namely 2-Naphthol and primaquine diphosphate, showed up-regulated *pilA* expression. Moreover, the effects of the selected drugs on biofilm formation and *pilA* expression were tested under the same conditions, confirming the consistency of the previous experiments.

One of most interesting findings is this study was pomalidomide's effect on *pilA* expression. Pomalidomide suppressed *pilA* expression, but it promoted biofilm formation by dose-

dependent manner without increasing antimicrobial activity. This trade-off behaviour between biofilm formation and twitching motility has been report by Ronish *et al.* (2019)

In the RNA-Seq analysis data, pomalidomide demonstrate resulted in differential expression of 94 genes, including upregulation of the *csu* chaperone– Type 1 chaperon usher pili (*csuB* and *csuC*), which are known as major player in mediating the irreversible attachment of cells to a surface in *A. baumannii* (Upmanyu, Haq and Singh, 2022). This induction of *csu* pili provides a molecular explanation for enhanced biofilm formation which suggesting a shift from T4P-dependent motility toward biofilm formation at 5mM. Additionally, pomalidomide also upregulated the paa operon, including *paaA*, which has been directly implicated in virulence (Bhuiyan *et al.*, 2016). Previous studies have demonstrated that deletion of *paaA* significantly reduced *A. baumannii* pathogenicity in zebrafish infection models. The upregulation of *csu* and *paa* genes suggests that pomalidomide promotes *A. baumannii* pathogenicity. To explore potential molecular mechanisms underlying these phenotypes, molecular docking analysis was performed using proteins upregulated by pomalidomide exposure. The CsuB, CsuC and PaaA proteins were selected as docking targets. Pomalidomide exhibited favourable binding affinities with all three proteins, suggesting potential direct interaction. To confirm this interaction further study is needed for solid validation.

These transcriptomic findings were confirmed through an *in vivo G. mellonella* infection model. Pomalidomide with DMSO exhibited only modest toxicity, but when administered with *A. baumannii, it* resulted in a pronounced, concentration-dependent increase in larval mortality. Moreover, mice infected with *A. baumannii* and treated with pomalidomide exhibited increased clinical scores at early time points. It confirms that pomalidomide exacerbates infection severity *in vivo.* This observation is important because, as previous reports indicate, the

increased adverse events of Gram-negative bacterial infections in patients receiving pomalidomide treatment are attributable to host immunosuppression (Dimopoulos *et al.*, 2014). These findings suggest that changes within the bacteria themselves also contribute to this increased susceptibility.

5.6 Key Findings

1. Establishment of a high-throughput screening platform to identify regulators of *pilA* expression in *A. baumannii*:
2. The pomalidomide is the most relevant hit compound for further study.
3. The pomalidomide alters virulence-associated phenotypes in vitro.
4. Identification of transcriptomic changes of *A. baumannii* associated with pomalidomide. Prediction of direct interaction between pomalidomide and biofilm-associated targets:
5. Pomalidomide enhances virulence *in vivo.*

Chapter 6

6. Discussion

6.1 General Discussion

AMR remains one of the most urgent challenges to global health. The development of new antibiotics has not kept pace with the emergence and spread of multidrug-resistant pathogens, which threatens millions of lives. Among these multidrug-resistant pathogens, *A. baumannii is* particularly problematic and can cause persistent healthcare-associated infections due to its ability to thrive on both biotic and abiotic surfaces, readily acquire resistance determinants, and form biofilms (Roy *et al.*, 2022). In this thesis, the challenge of *A. baumannii* wound infections is addressed as a problem that cannot be addressed through antibiotic discovery alone but requires alternative approaches that combine the development of AS-loaded PVA-based hydrogels as localised antimicrobial delivery systems, the utilization of the wound-like LCWB model to advance our understanding of the *A. baumannii* transcriptional response to the host, the design of a 3D-printable PVA/HPMC hydrogel platform with controllable drug release, and the ability of FDA-approved drugs to modulate Type IV pilus-associated virulence behaviours.

6.1.1 Development of Artificial Sweetener-Loaded Hydrogels as a Localised Antimicrobial Strategy

In our previous study, artificial sweeteners such as CYC, SACC and Ace-K showed antimicrobial and anti-virulence ability against multidrug-resistant bacteria, including *A. baumannii* (de Dios *et al.*, 2023, 2025). These findings suggest that artificial sweeteners could work as non-traditional antimicrobial agents. However, the real challenge in translational medicine lies in delivering them effectively to the wound site. There are many factors can

reduce the effectiveness. For example, wound exudate can dilute the AS, reducing its concentration. Moreover, the solution can dry out quickly, reducing contact time at the infection site. In our research, we demonstrate that PVA-based hydrogels serve as a carrier vehicle for AS and evaluate whether their antimicrobial activity can be translated into a topical delivery format. In chapter 2, the addition of AS at the initial stage alters the physical properties of the PVA-borax hydrogel, leading to phase separation, increased brittleness, and crumbling under significant pressure. We optimised this issue by testing different formulations and crosslinking methods. We found that 3% PVA + 3% borax is the most stable combination and provides the most promising antimicrobial properties, with a high AS percentage.

The antibiofilm activity of the AS-loaded hydrogels is particularly important because biofilm formation is a major factor that makes *A. baumannii* wound infections difficult to treat (Gedefie, Demsiss, *et al.*, 2021). Our research demonstrates that the AS-loaded PVA-borax hydrogels exhibit strong antibiofilm activity against both early-stage and mature *A. baumannii* biofilms. This effect was further supported by the ex vivo porcine burn wound model, in which AS-loaded hydrogels significantly reduced early biofilm formation and outperformed a commercial silver dressing. Moreover, the hydrogel shows excellent cytocompatibility and haemocompatibility, making it a promising candidate for wound-dressing applications. To further evaluate dermal compatibility, a pilot Phase I study was conducted using healthy adult volunteers. This study was designed to examine whether the PVA-borax hydrogel caused immediate irritation or adverse skin reactions. The AS-loaded PVA-borax hydrogel safety and tolerability are supported by the absence of major adverse effects.

Overall, this part of the thesis demonstrates that AS can be successfully incorporated into PVA-borax hydrogel systems and delivered as localised antimicrobial agents against *A. baumannii* biofilm. This research helps improve the application of AS in topical application, as antimicrobial activity alone is insufficient for its use in wound care. The active compound

needs to be incorporated into a stable, biocompatible system that maintains contact with the wound surface over time and releases the compound effectively.

Next steps:

Future work will first focus on the optimisation of AS-loaded hydrogel. The AS can potentiate the effectiveness of antibiotics against *A. baumannii* AB5075, including polymyxin B, gentamicin, doripenem, imipenem, and meropenem (de Dios *et al.*, 2023, 2025). Their use in combination treatment would be worth investigating. Different concentrations of antibiotics could be combined with ASs to assess their antibacterial activity. In addition to *A. baumannii*, other wound pathogens, such as *P. aeruginosa* and *S. aureus*, could also be tested against AS and AS-loaded hydrogels.

In this study, the pilot Phase I study involved 12 participants. In the future, the number of participants can be increased, the adhesive dressing replaced, or the observation interval reduced to prevent irritation from repeated adhesive dressing removal. If no contact-related adverse effects are observed in a larger cohort, the AS-loaded hydrogel could be further evaluated to phase I clinical testing for infected wounds.

6.1.2 The Wound-like Environment Reshapes *A. baumannii* Physiology

Although the AS-loaded hydrogels showed promising antimicrobial and antibiofilm activity, wound infection cannot be fully represented by standard laboratory media. The wound environment contains host-derived components, fluctuating nutrients, red blood cells, plasma proteins, and limited freely available iron, all of which may influence bacterial growth, biofilm formation, and the antimicrobial response. Therefore, it was important to examine how *A. baumannii* behaves under wound-like conditions before further evaluating hydrogel

performance. The LCWB model was widely used as a host-mimicking medium to study pathogens such as *E. faecalis, P. aeruginosa, S. aureus*, its biofilm formation, effect of biofilm treatment, antimicrobial susceptibility or antimicrobial dressing (Sun *et al.*, 2008; Dowd *et al.*, 2009; Kucera *et al.*, 2014; Staneviciute *et al.*, 2019; Diban *et al.*, 2023). In this study, the LCWB model was used as a host-mimicking medium to investigate A. baumannii physiology and to determine whether it could be used for antimicrobial susceptibility testing of *A. baumannii*. We performed growth and biofilm assay initially, and the LCWB medium supported robust bacterial growth which is similar to nutrient-rich LB. RNA-seq allows us to better understand how the relatively low iron content in the LCWB medium, compared to LB, affects biofilm formation. Following the addition of iron, biofilm formation was restored. We then tested the AS-loaded PVA-borax hydrogel, which showed an inhibitory effect and swelling behaviour, further confirming that the LCWB medium can be used to assess antimicrobial susceptibility.

Together, these findings show that *A. baumannii* adapts actively to wound-like conditions rather than simply growing in a nutrient-rich environment. This has important implications for antimicrobial testing. Because treatments developed in standard media may not fully predict bacterial behaviour or therapeutic performance in wound-relevant conditions.

Next steps:

The LCWB medium used in this thesis provided important insight into how wound-like conditions reshape *A. baumannii* physiology. However, this study compared the LCWB medium with LB and M9 succinate medium. In the future, we would like to explore transcriptomic differences in *A. baumannii* grown in LCWB medium, rabbit blood, and human whole blood. If similar transcriptional patterns are observed in LCWB and the blood-based environment, these pathways may play an important role in *A. baumannii* adaptation during

infection. Conversely, differences between these conditions would help identify environment-specific responses and clarify how different host components influence bacterial behaviour. This would allow a deeper understanding of how *A. baumannii* reacts to the host-derived environment. Moreover, hydrogels can be tested in polymicrobial LCWB systems as they mimic the real wound condition that is infected with different pathogens.

6.1.3 3D-printable PVA/HPMC Hydrogels Provide a Tunable Drug Release and Improve Material Mechanical Properties.

Building on the earlier AS-loaded PVA hydrogel work, the PVA+HPMC system was developed to explore whether drug release could be more precisely controlled through 3D-printed architecture. AS-loaded PVA-borax hydrogels exhibit strong antimicrobial activity, but the addition of AS compromises their mechanical properties. The FT-PVA hydrogel system also presents a trade-off between release and mechanical properties when PVA concentration is reduced or during freeze-thaw cycles. DIW 3D printing PVA-based hydrogel was introduced to overcome these issues. 3D printing allows the fabrication of controllable geometry, pore distribution and surface area. With predesign geometry and pore distribution, the contact surface between the hydrogel and the surrounding medium can be increased, which potentially accelerates drug diffusion and improves antimicrobial performance.

The HPMC play an important role in this 3D printable PVA based system. The PVA itself has low viscisity which make it difficult to print under standard conditions. The addition of HPMC improved the rheological behaviour of the ink, enabling it to form continuous filaments and maintain shape after extrusion. The 20% PVA was identified as an appropriate base and the addition of HPMC further improved filament formation and structural fidelity. Moreover, adding HPMC increases the mechanical properties.

The antimicrobial performance of the hydrogel was tested. The non-printed 20%PVA+ 16.7% HPMC+ 8%SACC hydrogel showed antimicrobial activity against *A. baumannii*. However, the 3D-printed counterpart showed a greater reduction in bacterial viability. This improvement was associated with a faster SACC release profile. The 3D-printed 20%PVA+16.7% HPMC+8%SACC hydrogel released nearly all of its SACC within approximately 30 minutes. The non-printed PVA+HPMC+SACC hydrogel required a much longer period to complete release. This suggests that the printed structure increased release efficiency, most likely by increasing the exposed surface area and shortening the diffusion distance between the loaded compound and the external medium. Moreover, This PVA+HPMC hydrogel also showed excellent cytocompatibility and haemocompatibility. This rapid and customisable strategy may be useful in hospitals in conflict zones, where *A. baumannii* infections are prevalent (Granata *et al.*, 2024). It offers the potential to tailor treatment to individual wound characteristics, particularly in deeper wounds. Moreover, the rapid release of the loaded agent can enhance the early suppression of bacterial growth.

Overall, this mechanically robust and 3D-printable hydrogel system demonstrated controllable release behaviour by varying its porosity. These findings suggest that future antimicrobial wound dressings should be developed not only by selecting active compounds, but also by engineering the material platform, such as structural design.

Next steps:

The 3D-printable PVA+HPMC hydrogel also provides several opportunities for future development. The drug release and antimicrobial performance can be change by printed hydrogel architecture. In future work, it should systematically investigate how pore size, filament spacing, scaffold thickness and infill density affect swelling, degradation, release kinetics and bacterial killing. This would allow the wound dressings with tailored release

profiles. For example, with proper design, rapid release can be used on the wound site for sterilisation or acute infection and slower release for chronic infection. The hydrogel could also be expanded to multi-agent delivery, such as artificial sweeteners with conventional antibiotics or wound-healing agents.

6.1.4 Non-Antibiotic Drugs as Modulators of *A. baumannii* Virulence

The earlier parts of this thesis focused on antimicrobial delivery and wound-relevant infection modelling. The final experimental chapter expanded the discussion towards the broader effects of non-antibiotic compounds on *A. baumannii* virulence. This is important because many drugs used in clinical settings are not designed as antimicrobials, but they can influence bacterial physiology, such as bacterial growth, membrane permeability, gene transfer and resistance-related behaviours (Maier *et al.*, 2018b; Wang *et al.*, 2020; Lu *et al.*, 2022b). However, their effects on virulence-associated pathways remain less well understood. In this research, the screening of FDA-approved compounds for their ability to alter *pilA* expression in *A. baumannii* was investigated. The *pilA* encodes the major pilin subunit of T4P, changes in its expression may influence twitching motility, surface attachment, biofilm formation and natural transformation (Salinas *et al.*, 2025).

In this screening, pomalidomide was the most important hit compound identified in this chapter because its inhibition of *pilA* expression was reflected in decreased twitching motility and increased biofilm formation, without altering growth. Additionally, transcriptomic analysis also supported this interpretation. Pomalidomide exposure in *A. baumannii* resulted in differential expression of 94 genes, including the upregulation of *csuB* and *csuC*. These are associated with surface attachment and biofilm formation. This explains the increased biofilm formation observed after pomalidomide treatment. In addition, pomalidomide upregulated

genes within the *paa* operon, including *paaA*, which has previously been linked to *A. baumannii* virulence (Bhuiyan *et al.*, 2016). Molecular docking analysis also suggested possible interactions between pomalidomide and CsuB, CsuC and PaaA proteins.

The virulence associated with biofilm formation and the *paa* operon was supported by the *in vivo* findings. In the *G. mellonella* model, *A. baumannii* infection with pomalidomide increased larval mortality in a concentration-dependent manner. Similarly, in the murine infection model, pomalidomide-treated infected mice showed higher clinical scores at early time points. These findings illustrated that infection-related adverse events in patients receiving pomalidomide are often understood mainly through the lens of host immunosuppression. The findings of this thesis suggest an additional possibility: pomalidomide may act directly on *A. baumannii* to enhance infection-associated phenotypes. This indicates that bacterial responses to the drug may contribute to infection severity and that this effect can be exacerbated by host-mediated factors. These findings suggest that the administration of pomalidomide should be carefully re-evaluated in patients with *A. baumannii* infection to avoid the potential exacerbation of bacterial pathogenicity.

Next steps:

In the future, further investigation of pomalidomide could involve using mutant strains, such as *csuB and csuC*, in biofilm assays to determine whether the observed phenotypes are consistent with the transcriptomic data. Moreover, increased biofilm formation after pomalidomide treatment, and the RNA-seq data also showed upregulation of biofilm-associated genes. A biotinylated pomalidomide probe could be a useful next step to investigate whether pomalidomide directly interacts with the identified bacterial proteins in RNA-Seq data on biofilm formation.

6.2 Conclusion

This thesis investigated alternative strategies to targeting *A. baumannii* infections by using artificial sweetener in hydrogel development, transcriptional profiling in wound-like LCWB medium, and the effect on *A. baumannii* with a non-antibiotic compound. This research delivers a multidimensional approach to targeting *A. baumannii* with non-antibiotic strategies. The development of AS-loaded PVA-based hydrogels demonstrated that non-traditional antimicrobial compounds can be incorporated into localised wound-dressing platforms while retaining antibacterial and antibiofilm activity. This hydrogel has excellent cytocompatibility, haemocompatibility, and tolerability in healthy participants, further supporting its potential for future topical application. The LCWB model showed wound-associated transcriptional changes. For example, iron acquisition, nutrient adaptation, translation and surface-associated behaviours. These data highlight the importance of testing antimicrobial agents in physiologically relevant models rather than relying only on standard laboratory media. Building on the hydrogel work, the PVA+HPMC 3D-printable hydrogel demonstrated that polymer composition and printed architecture can be used to improve drug-release behaviour, antimicrobial performance, and mechanical properties. This shows that material design is central to effective localised therapy. Non-antibiotic drugs can modulate *A. baumannii* virulence-associated phenotypes was demonstrated by screening FDA-approved drug library. The pomalidomide reduced *pilA* expression and twitching motility but enhanced biofilm formation and infection severity, suggesting that non-antibiotic compounds may redirect bacterial behaviour in clinically relevant ways.

Overall, the findings demonstrate that effective control of *A. baumannii* wound infection requires more than the identification of antibacterial compounds alone. It also requires consideration of how active agents are delivered, how bacteria respond to wound-like environments, and how non-antibiotic chemical exposures may influence virulence-associated behaviours.

7. Reference

Abdallah, M. *et al.* (2015) 'Activity of eravacycline against Enterobacteriaceae and *Acinetobacter baumannii*, including multidrug-resistant isolates, from New York City', *Antimicrobial Agents and Chemotherapy*, 59(3). Available at: https://doi.org/10.1128/AAC.04809-14.

Abdelkader, D.H. *et al.* (2018) 'Enhanced cutaneous wound healing in rats following topical delivery of insulin-loaded nanoparticles embedded in poly(vinyl alcohol)-borate hydrogels', *Drug Delivery and Translational Research*, 8(5), pp. 1053–1065. Available at: https://doi.org/10.1007/s13346-018-0554-0.

Abou Fayad, A. *et al.* (2023) 'Antimicrobial resistance and the Iraq wars: Armed conflict as an underinvestigated pathway with growing significance', *BMJ Global Health*, 7. Available at: https://doi.org/10.1136/bmjgh-2022-010863.

Adelnia, H. *et al.* (2022) 'Freeze/thawed polyvinyl alcohol hydrogels: Present, past and future', *European Polymer Journal*, 164, p. 110974. Available at: https://doi.org/10.1016/j.eurpolymj.2021.110974.

Ahmad, I. *et al.* (2023) 'Csu pili dependent biofilm formation and virulence of *Acinetobacter baumannii*', *NPJ biofilms and microbiomes*, 9(1), p. 101. Available at: https://doi.org/10.1038/s41522-023-00465-6.

Alav, I., Sutton, J.M. and Rahman, K.M. (2018) 'Role of bacterial efflux pumps in biofilm formation', *Journal of Antimicrobial Chemotherapy*, 73(8), pp. 2003–2020. Available at: https://doi.org/10.1093/jac/dky042.

Alizadehgiashi, M. *et al.* (2021) 'Multifunctional 3D-Printed Wound Dressings', *ACS Nano*, 15(7), pp. 12375–12387. Available at: https://doi.org/10.1021/acsnano.1c04499.

Almatroudi, A. (2025) 'Biofilm Resilience: Molecular Mechanisms Driving Antibiotic Resistance in Clinical Contexts', *Biology*, 14(2), p. 165. Available at: https://doi.org/10.3390/biology14020165.

Annabi, N. *et al.* (2010) 'Controlling the Porosity and Microarchitecture of Hydrogels for Tissue Engineering', *Tissue Engineering Part B: Reviews*, 16(4), pp. 371–383. Available at: https://doi.org/10.1089/ten.teb.2009.0639.

Antunes, L.C.S. *et al.* (2011) 'Genome-assisted identification of putative iron-utilization genes in *Acinetobacter baumannii* and their distribution among a genotypically diverse collection of clinical isolates', *Research in Microbiology*, 162(3), pp. 279–284. Available at: https://doi.org/10.1016/j.resmic.2010.10.010.

Anwar, M.Z. *et al.* (2026) 'Hybrid hydrogels for biomedical applications: Addressing challenges in drug delivery through advanced crosslinking and nanocarrier integration', *Journal of Controlled Release*, 392, p. 114719. Available at: https://doi.org/10.1016/j.jconrel.2026.114719.

Armenta, S., Garrigues, S. and de la Guardia, M. (2004) 'FTIR Determination of Aspartame and Acesulfame-K in Tabletop Sweeteners', *Journal of Agricultural and Food Chemistry*, 52(26), pp. 7798–7803. Available at: https://doi.org/10.1021/jf0492181.

Artuso, I. *et al.* (2023) 'Genomics of *Acinetobacter baumannii* iron uptake', *Microbial Genomics*, 9(8). Available at: https://doi.org/10.1099/mgen.0.001080.

Aswani, V.H. and Shukla, S.K. (2021) 'An Early History of Phage Therapy in the United States: Is it Time to Reconsider?', *Clinical Medicine & Research*, 19(2), pp. 82–89. Available at: https://doi.org/10.3121/cmr.2021.1605.

Aswathanarayan, J.B. *et al.* (2022) 'Biofilm-Associated Infections in Chronic Wounds and Their Management', in G. Donelli (ed.) *Advances in Microbiology, Infectious Diseases and Public Health*. Cham: Springer International Publishing (Advances in Experimental Medicine and Biology), pp. 55–75. Available at: https://doi.org/10.1007/5584_2022_738.

Asy-Syifa, N. *et al.* (2022) 'The Study of the Swelling Degree of the PVA Hydrogel with varying concentrations of PVA'. *Journal of Physics: Conference Series*. Available at: https://doi.org/10.1088/1742-6596/2243/1/012053.

Attinger, C. and Wolcott, R. (2012) 'Clinically Addressing Biofilm in Chronic Wounds', *Advances in Wound Care*, 1(3), pp. 127–132. Available at: https://doi.org/10.1089/wound.2011.0333.

Aurelio-Soria, D. *et al.* (2026) 'Analytical methods for the determination of α-naphthol and β-naphthol in biological and environmental samples: a review', *Microchemical Journal*, 220, p. 116456. Available at: https://doi.org/10.1016/j.microc.2025.116456.

Auta, A. *et al.* (2019) 'Global access to antibiotics without prescription in community pharmacies: A systematic review and meta-analysis', *Journal of Infection*, 78(1), pp. 8–18. Available at: https://doi.org/10.1016/j.jinf.2018.07.001.

Ayoub Moubareck, C. and Hammoudi Halat, D. (2020) 'Insights into *Acinetobacter baumannii*: A Review of Microbiological, Virulence, and Resistance Traits in a Threatening Nosocomial Pathogen', *Antibiotics*, 9(3). Available at: https://doi.org/10.3390/antibiotics9030119.

Baker-Austin, C. *et al.* (2006) 'Co-selection of antibiotic and metal resistance', *Trends in Microbiology*, 14(4), pp. 176–182. Available at: https://doi.org/10.1016/j.tim.2006.02.006.

Balkhair, A., Saadi, K.A. and Adawi, B.A. (2023) 'Epidemiology and mortality outcome of carbapenem- and colistin-resistant *Klebsiella pneumoniae*, *Escherichia coli*, *Acinetobacter baumannii*, and *Pseudomonas aeruginosa* bloodstream infections', *IJID Regions*, 7. Available at: https://doi.org/10.1016/j.ijregi.2023.01.002.

Balmaceda, N. *et al.* (2021) 'Infection risks in multiple myeloma: a systematic review and meta-analysis of randomized trials from 2015 to 2019', *BMC Cancer*, 21(1), p. 730. Available at: https://doi.org/10.1186/s12885-021-08451-x.

Banerjee, D. *et al.* (2025) 'Exploration of Phytochemicals as Anti-biofilm Agents against Pathogenic Bacteria: Their Potential and Challenges', *Infectious Disorders - Drug Targets*, 25(6), p. e18715265324950. Available at: https://doi.org/10.2174/0118715265324950241204182204.

Bashir, S. *et al.* (2020) 'Fundamental Concepts of Hydrogels: Synthesis, Properties, and Their Applications', *Polymers*, 12(11), p. 2702. Available at: https://doi.org/10.3390/polym12112702.

Bateman, T.J. *et al.* (2021) 'A Slam-dependent hemophore contributes to heme acquisition in the bacterial pathogen *Acinetobacter baumannii*', *Nature Communications*, 12(1), p. 6270. Available at: https://doi.org/10.1038/s41467-021-26545-9.

Baumann, P., Doudoroff, M. and Stanier, R.Y. (1968) 'A Study of the Moraxella Group II. Oxidative-negative Species (Genus Acinetobacter)', *Journal of Bacteriology*, 95(5), pp. 1520–1541. Available at: https://doi.org/10.1128/jb.95.5.1520-1541.1968.

Bazzi, W. *et al.* (2020) 'Heavy Metal Toxicity in Armed Conflicts Potentiates AMR in A. baumannii by Selecting for Antibiotic and Heavy Metal Co-resistance Mechanisms', *Frontiers in Microbiology*, 11, p. 68. Available at: https://doi.org/10.3389/fmicb.2020.00068.

Beech, M.J. *et al.* (2025) 'Binding assays enable discovery of Tet(X) inhibitors that combat tetracycline destructase resistance', *Chemical Science*, 16(22), pp. 9691–9704. Available at: https://doi.org/10.1039/D5SC00964B.

Beijerinck, M.W. (1911) 'Über pigmentbildung bei essigbakterien', *Bakteriol Parasitenk*, 29.

Belay, W.Y. *et al.* (2024) 'Mechanism of antibacterial resistance, strategies and next-generation antimicrobials to contain antimicrobial resistance: a review', *Frontiers in Pharmacology*, 15, p. 1444781. Available at: https://doi.org/10.3389/fphar.2024.1444781.

Berdigaliyev, N. and Aljofan, M. (2020) 'An Overview of Drug Discovery and Development', *Future Medicinal Chemistry*, 12(10), pp. 939–947. Available at: https://doi.org/10.4155/fmc-2019-0307.

Bertesteanu, S. *et al.* (2014) 'Polymicrobial wound infections: Pathophysiology and current therapeutic approaches', *International Journal of Pharmaceutics*, 463(2), pp. 119–126. Available at: https://doi.org/10.1016/J.IJPHARM.2013.12.012.

Bessa, L.J. *et al.* (2015) 'Bacterial isolates from infected wounds and their antibiotic susceptibility pattern: some remarks about wound infection', *International Wound Journal*, 12(1), pp. 47–52. Available at: https://doi.org/10.1111/iwj.12049.

Bhargava, N. *et al.* (2015) 'Attenuation of Quorum Sensing-Mediated Virulence of *Acinetobacter Baumannii* by *Glycyrrhiza Glabra* Flavonoids', *Future Microbiology*, 10(12), pp. 1953–1968. Available at: https://doi.org/10.2217/fmb.15.107.

Bhargava, N., Sharma, P. and Capalash, N. (2010) 'Quorum sensing in *Acinetobacter* : an emerging pathogen', *Critical Reviews in Microbiology*, 36(4), pp. 349–360. Available at: https://doi.org/10.3109/1040841X.2010.512269.

Bhuiyan, M.S. *et al.* (2016) '*Acinetobacter baumannii* phenylacetic acid metabolism influences infection outcome through a direct effect on neutrophil chemotaxis', *Proceedings of the National Academy of Sciences*, 113(34), pp. 9599–9604. Available at: https://doi.org/10.1073/pnas.1523116113.

Boll, J.M. *et al.* (2015) 'Reinforcing lipid a acylation on the cell surface of acinetobacter baumannii promotes cationic antimicrobial peptide resistance and desiccation survival', *mBio*, 6(3). Available at: https://doi.org/10.1128/mBio.00478-15.

Bortolin, M. *et al.* (2017) 'In vitro Antimicrobial Activity of Chlorquinaldol against Microorganisms Responsible for Skin and Soft Tissue Infections: Comparative Evaluation with Gentamicin and Fusidic Acid', *Frontiers in Microbiology*, 8, p. 1039. Available at: https://doi.org/10.3389/fmicb.2017.01039.

Bridger, J.M. *et al.* (1993) 'Internal lamin structures within G1 nuclei of human dermal fibroblasts', *Journal of Cell Science*, 104(2), pp. 297–306. Available at: https://doi.org/10.1242/jcs.104.2.297.

Britto, E.J. *et al.* (2025) 'Wound Dressings', *StatPearls*. Treasure Island (FL): StatPearls Publishing. Available at: http://www.ncbi.nlm.nih.gov/books/NBK470199/ (Accessed: 7 October 2025).

Brown, S. and Amyes, S. (2006) 'OXA β-lactamases in Acinetobacter: The story so far', *Journal of Antimicrobial Chemotherapy*, 57(1). Available at: https://doi.org/10.1093/jac/dki425.

Burrows, L.L. (2005) 'Weapons of mass retraction', *Molecular Microbiology*, 57(4). Available at: https://doi.org/10.1111/j.1365-2958.2005.04703.x.

Burt, S.A. *et al.* (2007) 'Carvacrol induces heat shock protein 60 and inhibits synthesis of flagellin in *Escherichia coli* O157:H7', *Applied and Environmental Microbiology*, 73(14). Available at: https://doi.org/10.1128/AEM.00340-07.

Bush, K. and Bradford, P.A. (2016) 'β-Lactams and β-Lactamase Inhibitors: An Overview', *Cold Spring Harbor Perspectives in Medicine*, 6(8), p. a025247. Available at: https://doi.org/10.1101/cshperspect.a025247.

Calabrese, L., Ciandrini, L. and Cosentino Lagomarsino, M. (2024) 'How total mRNA influences cell growth', *Proceedings of the National Academy of Sciences*, 121(21), p. e2400679121. Available at: https://doi.org/10.1073/pnas.2400679121.

Cámara, M. *et al.* (2022) 'Economic significance of biofilms: a multidisciplinary and cross-sectoral challenge', *npj Biofilms and Microbiomes*, 8(1), p. 42. Available at: https://doi.org/10.1038/s41522-022-00306-y.

Carvalho, C. *et al.* (2009) 'Doxorubicin: The Good, the Bad and the Ugly Effect', *Current Medicinal Chemistry*, 16(25), pp. 3267–3285. Available at: https://doi.org/10.2174/092986709788803312.

Castrejón-Jiménez, N.S. *et al.* (2022) 'Candida glabrata is a successful pathogen: An artist manipulating the immune response', *Microbiological Research*, 260, pp. 127038–127038. Available at: https://doi.org/10.1016/J.MICRES.2022.127038.

Cerqueira, G.M. *et al.* (2014) 'A Global Virulence Regulator in *Acinetobacter baumannii* and Its Control of the Phenylacetic Acid Catabolic Pathway', *The Journal of Infectious Diseases*, 210(1), pp. 46–55. Available at: https://doi.org/10.1093/infdis/jiu024.

Cersosimo, R.J. and Hong, W.K. (1986) 'Epirubicin: a review of the pharmacology, clinical activity, and adverse effects of an adriamycin analogue.', *Journal of Clinical Oncology*, 4(3), pp. 425–439. Available at: https://doi.org/10.1200/JCO.1986.4.3.425.

Chanan-Khan, A.A. *et al.* (2013) 'Pomalidomide: the new immunomodulatory agent for the treatment of multiple myeloma', *Blood Cancer Journal*, 3(9), pp. e143–e143. Available at: https://doi.org/10.1038/bcj.2013.38.

Chang, R.Y.K. *et al.* (2022) 'Novel antimicrobial agents for combating antibiotic-resistant bacteria', *Advanced Drug Delivery Reviews*, 187, pp. 114378–114378. Available at: https://doi.org/10.1016/J.ADDR.2022.114378.

Chen, H. *et al.* (2025) 'The effect of commonly used non-antibiotic medications on antimicrobial resistance development in *Escherichia coli*', *Npj Antimicrobials and Resistance*, 3(1), p. 73. Available at: https://doi.org/10.1038/s44259-025-00144-w.

Chen, L.K. *et al.* (2017) 'Clinical Antibiotic-resistant *Acinetobacter baumannii* Strains with Higher Susceptibility to Environmental Phages than Antibiotic-sensitive Strains', *Scientific Reports*, 7(1). Available at: https://doi.org/10.1038/s41598-017-06688-w.

Chen, S.-Q. *et al.* (2023) 'Mechanical properties and wound healing potential of bacterial cellulose-xyloglucan-dextran hydrogels', *Carbohydrate Polymers*, 321, p. 121268. Available at: https://doi.org/10.1016/j.carbpol.2023.121268.

Chen, Ying *et al.* (2022) 'Synthesis and properties of Poly(vinyl alcohol) hydrogels with high strength and toughness', *Polymer Testing*, 108, p. 107516. Available at: https://doi.org/10.1016/j.polymertesting.2022.107516.

Chiang, S.R. *et al.* (2018) 'Desiccation and ethanol resistances of multidrug resistant *Acinetobacter baumannii* embedded in biofilm: The favorable antiseptic efficacy of combination chlorhexidine gluconate and ethanol', *Journal of Microbiology, Immunology and Infection*, 51(6). Available at: https://doi.org/10.1016/j.jmii.2017.02.003.

Choi, C.H. *et al.* (2005) 'Outer membrane protein 38 of *Acinetobacter baumannii* localizes to the mitochondria and induces apoptosis of epithelial cells', *Cellular Microbiology*, 7(8). Available at: https://doi.org/10.1111/j.1462-5822.2005.00538.x.

Chopra, T. *et al.* (2013) 'Epidemiology of bloodstream infections caused by *Acinetobacter baumannii* and impact of drug resistance to both carbapenems and ampicillin-sulbactam on clinical outcomes', *Antimicrobial Agents and Chemotherapy*, 57(12). Available at: https://doi.org/10.1128/AAC.01520-13.

Chudecka, M. and Lubkowska, A. (2015) 'Thermal maps of young women and men', *Infrared Physics & Technology*, 69, pp. 81–87. Available at: https://doi.org/10.1016/j.infrared.2015.01.012.

Clemmer, K.M., Bonomo, R.A. and Rather, P.N. (2011) 'Genetic analysis of surface motility in *Acinetobacter baumannii*', *Microbiology*, 157(9), pp. 2534–2544. Available at: https://doi.org/10.1099/mic.0.049791-0.

Cong, Y., Yang, S. and Rao, X. (2019) 'Vancomycin resistant *Staphylococcus aureus* infections: A review of case updating and clinical features', *Journal of Advanced Research*, 21, pp. 169–176. Available at: https://doi.org/10.1016/j.jare.2019.10.005.

Cook-Libin, S. *et al.* (2022) 'Iron Acquisition Mechanisms and Their Role in the Virulence of *Acinetobacter baumannii*', *Infection and Immunity*, 90(10), p. e0022322. Available at: https://doi.org/10.1128/iai.00223-22.

Correa, S. *et al.* (2021) 'Translational Applications of Hydrogels', *Chemical Reviews*, 121(18). Available at: https://doi.org/10.1021/acs.chemrev.0c01177.

Craig, L., Forest, K.T. and Maier, B. (2019) 'Type IV pili: dynamics, biophysics and functional consequences', *Nature Reviews Microbiology*, 17(7), pp. 429–440. Available at: https://doi.org/10.1038/s41579-019-0195-4.

Cui, B. *et al.* (2025) 'Signaling in *Acinetobacter baumannii*: Quorum sensing and nucleotide second messengers', *Computational and Structural Biotechnology Journal*, 27, pp. 2168–2175. Available at: https://doi.org/10.1016/j.csbj.2025.05.032.

Da Silva Oliveira, G.L. and De Freitas, R.M. (2015) 'Diminazene aceturate—An antiparasitic drug of antiquity: Advances in pharmacology & therapeutics', *Pharmacological Research*, 102, pp. 138–157. Available at: https://doi.org/10.1016/j.phrs.2015.10.005.

D'Arpa, P. *et al.* (2021) '*Pseudomonas aeruginosa* transcriptome adaptations from colonization to biofilm infection of skin wounds', *Scientific Reports*, 11(1), p. 20632. Available at: https://doi.org/10.1038/s41598-021-00073-4.

Daury, L. *et al.* (2016) 'Tripartite assembly of RND multidrug efflux pumps', *Nature Communications*, 7, p. 10731. Available at: https://doi.org/10.1038/ncomms10731.

Davies, J. (2006) 'Where have all the antibiotics gone?' *Canadian Journal of Infectious Diseases and Medical Microbiology*. Available at: https://doi.org/10.1155/2006/707296.

Davis, K.A. *et al.* (2005) 'Multidrug-Resistant *Acinetobacter* Extremity Infections in Soldiers', *Emerging Infectious Diseases*, 11(8), pp. 1218–1224. Available at: https://doi.org/10.3201/1108.050103.

De Gregorio, E. *et al.* (2015) 'Biofilm-associated proteins: news from Acinetobacter', *BMC Genomics*, 16(1), p. 933. Available at: https://doi.org/10.1186/s12864-015-2136-6.

Debras, C. *et al.* (2022) 'Artificial sweeteners and cancer risk: Results from the NutriNet-Santé population-based cohort study', *PLoS Medicine*, 19(3). Available at: https://doi.org/10.1371/journal.pmed.1003950.

de Jong, A., Kuipers, O.P. and Kok, J. (2022) 'FUNAGE-Pro: comprehensive web server for gene set enrichment analysis of prokaryotes', *Nucleic Acids Research*, 50(W1), pp. W330–W336. Available at: https://doi.org/10.1093/nar/gkac441.

Delamou, A. *et al.* (2019) 'Trends of and factors associated with cesarean section related surgical site infections in Guinea', *Journal of Public Health in Africa*, 10(1). Available at: https://doi.org/10.4081/jphia.2019.818.

DeLeon, S. *et al.* (2014) 'Synergistic Interactions of *Pseudomonas aeruginosa* and *Staphylococcus aureus* in an *In Vitro* Wound Model', *Infection and Immunity*. Edited by B.A. McCormick, 82(11), pp. 4718–4728. Available at: https://doi.org/10.1128/IAI.02198-14.

De Oliveira, F.P. *et al.* (2017) 'Prevalence, antimicrobial susceptibility, and clonal diversity of pseudomonas aeruginosa in chronic wounds', *Journal of Wound, Ostomy and Continence Nursing*, 44(6). Available at: https://doi.org/10.1097/WON.0000000000000373.

Deng, X., Gould, M. and Ali, M.A. (2022) 'A review of current advancements for wound healing: Biomaterial applications and medical devices', *Journal of Biomedical Materials Research Part B: Applied Biomaterials*, 110(11), pp. 2542–2573. Available at: https://doi.org/10.1002/jbm.b.35086.

Dhiman, N.K. and Agnihotri, S. (2020) 'Hierarchically aligned nano silver/chitosan–PVA hydrogel for point-of-use water disinfection: contact-active mechanism revealed', *Environmental Science: Nano*, 7(8), pp. 2337–2350. Available at: https://doi.org/10.1039/D0EN00405G.

Di Giulio, M. *et al.* (2020) 'Graphene Oxide affects *Staphylococcus aureus* and *Pseudomonas aeruginosa* dual species biofilm in Lubbock Chronic Wound Biofilm model', *Scientific Reports*, 10(1), p. 18525. Available at: https://doi.org/10.1038/s41598-020-75086-6.

Diban, F. *et al.* (2023) 'Biofilms in Chronic Wound Infections: Innovative Antimicrobial Approaches Using the In Vitro Lubbock Chronic Wound Biofilm Model', *International Journal of Molecular Sciences*, 24(2), p. 1004. Available at: https://doi.org/10.3390/ijms24021004.

Díez, B. *et al.* (2022) 'Chemically cross-linked poly(vinyl alcohol) electrospun fibrous mats as wound dressing materials', *Journal of Chemical Technology & Biotechnology*, 97(3), pp. 620–632. Available at: https://doi.org/10.1002/jctb.7006.

Dijkshoorn, L., Nemec, A. and Seifert, H. (2007) 'An increasing threat in hospitals: multidrug-resistant *Acinetobacter baumannii*', *Nature Reviews Microbiology*, 5(12), pp. 939–951. Available at: https://doi.org/10.1038/nrmicro1789.

Dimopoulos, M.A. *et al.* (2014) 'Expert panel consensus statement on the optimal use of pomalidomide in relapsed and refractory multiple myeloma', *Leukemia*, 28(8). Available at: https://doi.org/10.1038/leu.2014.60.

Dimopoulos, M.A. *et al.* (2016) 'Safety and efficacy of pomalidomide plus low-dose dexamethasone in STRATUS (MM-010): a phase 3b study in refractory multiple myeloma', *Blood*, 128(4), pp. 497–503. Available at: https://doi.org/10.1182/blood-2016-02-700872.

Ding, D. *et al.* (2023) 'The spread of antibiotic resistance to humans and potential protection strategies', *Ecotoxicology and Environmental Safety*, 254, pp. 114734–114734. Available at: https://doi.org/10.1016/J.ECOENV.2023.114734.

de Dios, R. *et al.* (2023) 'Artificial sweeteners inhibit multidrug-resistant pathogen growth and potentiate antibiotic activity', *EMBO Molecular Medicine*, 15(1), pp. e16397–e16397. Available at: https://doi.org/10.15252/emmm.202216397.

de Dios, R. *et al.* (2025) 'Saccharin disrupts bacterial cell envelope stability and interferes with DNA replication dynamics', *EMBO Molecular Medicine*, 17(5), pp. 993–1017. Available at: https://doi.org/10.1038/s44321-025-00219-1.

Dong, J.-F. *et al.* (2022) 'The type VI secretion system in *Acinetobacter baumannii* clinical isolates and its roles in antimicrobial resistance acquisition', *Microbial Pathogenesis*, 169, p. 105668. Available at: https://doi.org/10.1016/j.micpath.2022.105668.

Dowd, S.E. *et al.* (2009) 'Effects of biofilm treatments on the multi-species Lubbock chronic wound biofilm model', *Journal of Wound Care*, 18(12), pp. 508–512. Available at: https://doi.org/10.12968/jowc.2009.18.12.45608.

Durán, N., Nakazato, G. and Seabra, A.B. (2016) 'Antimicrobial activity of biogenic silver nanoparticles, and silver chloride nanoparticles: an overview and comments', *Applied Microbiology and Biotechnology*, 100(15). Available at: https://doi.org/10.1007/s00253-016-7657-7.

Dutescu, I.A. and Hillier, S.A. (2021) 'Encouraging the Development of New Antibiotics: Are Financial Incentives the Right Way Forward? A Systematic Review and Case Study', *Infection and Drug Resistance*, Volume 14, pp. 415–434. Available at: https://doi.org/10.2147/IDR.S287792.

El-Aassar, M.R. *et al.* (2015) 'Controlled drug release from cross-linked κ-carrageenan/hyaluronic acid membranes', *International Journal of Biological Macromolecules*, 77. Available at: https://doi.org/10.1016/j.ijbiomac.2015.03.055.

Ellison, C.K. *et al.* (2021) '*Acinetobacter baylyi* regulates type IV pilus synthesis by employing two extension motors and a motor protein inhibitor', *Nature Communications*, 12(1), p. 3744. Available at: https://doi.org/10.1038/s41467-021-24124-6.

Ellison, T.J. and Ellison, C.K. (2024) 'DNA binding is rate-limiting for natural transformation', *bioRxiv: The Preprint Server for Biology*, p. 2024.06.06.597730. Available at: https://doi.org/10.1101/2024.06.06.597730.

Fan, L. *et al.* (2016) 'Preparation and characterization of chitosan/gelatin/PVA hydrogel for wound dressings', *Carbohydrate Polymers*, 146, pp. 427–434. Available at: https://doi.org/10.1016/j.carbpol.2016.03.002.

Feng, W. and Wang, Z. (2023) 'Tailoring the Swelling-Shrinkable Behavior of Hydrogels for Biomedical Applications', *Advanced Science*, 10(28), p. 2303326. Available at: https://doi.org/10.1002/advs.202303326.

Feng, W. and Wang, Z. (2023b) 'Tailoring the Swelling-Shrinkable Behavior of Hydrogels for Biomedical Applications', *Advanced Science*, 10(28), p. 2303326. Available at: https://doi.org/10.1002/advs.202303326.

Feuilloley, C. *et al.* (2024) 'Genipin-Crosslinked Gelatin Hydrogel for the Detection and Treatment of Active Metalloprotease Releasing *Pseudomonas aeruginosa*.' Available at: https://doi.org/10.26434/chemrxiv-2024-vm2dc.

Fiester, S.E. *et al.* (2016) 'Iron-Regulated Phospholipase C Activity Contributes to the Cytolytic Activity and Virulence of *Acinetobacter baumannii*', *PloS One*, 11(11), p. e0167068. Available at: https://doi.org/10.1371/journal.pone.0167068.

Figueroa-Pizano, M.D. *et al.* (2018) 'Effect of freeze-thawing conditions for preparation of chitosan-poly (vinyl alcohol) hydrogels and drug release studies', *Carbohydrate Polymers*, 195, pp. 476–485. Available at: https://doi.org/10.1016/j.carbpol.2018.05.004.

Fleming, Irma D *et al.* (2017) 'Modeling *Acinetobacter baumannii* wound infections: The critical role of iron.', *The journal of trauma and acute care surgery*, 82(3), pp. 557–565. Available at: https://doi.org/10.1097/TA.0000000000001338.

Fleming, Irma D. *et al.* (2017) 'Modeling *Acinetobacter baumannii* wound infections: The critical role of iron', *The Journal of Trauma and Acute Care Surgery*, 82(3), pp. 557–565. Available at: https://doi.org/10.1097/TA.0000000000001338.

Flemming, H.C. *et al.* (2016) 'Biofilms: An emergent form of bacterial life', *Nature Reviews Microbiology*, 14(9). Available at: https://doi.org/10.1038/nrmicro.2016.94.

Flemming, H.-C. *et al.* (2023) 'The biofilm matrix: multitasking in a shared space', *Nature Reviews Microbiology*, 21(2), pp. 70–86. Available at: https://doi.org/10.1038/s41579-022-00791-0.

Foglia, F. *et al.* (2025) 'Prevalence of *Acinetobacter baumannii* Multidrug Resistance in University Hospital Environment', *Antibiotics*, 14(5), p. 490. Available at: https://doi.org/10.3390/antibiotics14050490.

Fornasini, M., Robles-Rodríguez, J. and Baldeon, M.E. (2023) 'The traffic light labeling could induce consumers to increase intake of artificial sweeteners and potentially enhance their cardiovascular risk: the case of Ecuador', *Public Health* [Preprint]. Available at: https://doi.org/10.1016/j.puhe.2023.01.006.

Forsberg, K.J. *et al.* (2015) 'The Tetracycline Destructases: A Novel Family of Tetracycline-Inactivating Enzymes', *Chemistry and Biology*, 22(7). Available at: https://doi.org/10.1016/j.chembiol.2015.05.017.

Foster, T.J. (2004) 'The Staphylococcus aureus "superbug"', *Journal of Clinical Investigation*, 114(12), pp. 1693–1696. Available at: https://doi.org/10.1172/JCI200423825.

Francesca, L., Claudia, V. and Gianfranco, D. (2014) 'Biofilm formation in acinetobacter baumannii', *New Microbiologica*, 37(2), pp. 119–127.

Furqan, M., Iqbal, F. and Tulain, U.R. (2017) 'Microwave radiation induced synthesis of hydroxypropyl methylcellulose-graft-(polyvinylalcohal-co-acrylic acid) polymeric network and its in vitro evaluation', *Acta Poloniae Pharmaceutica - Drug Research*, 74, pp. 527–541.

Gadar, K. *et al.* (2023) 'Disrupting iron homeostasis can potentiate colistin activity and overcome colistin resistance mechanisms in Gram-Negative Bacteria', *Communications Biology*, 6(1), p. 937. Available at: https://doi.org/10.1038/s42003-023-05302-2.

Gaddy, J.A., Tomaras, A.P. and Actis, L.A. (2009) 'The *Acinetobacter baumannii* 19606 OmpA Protein Plays a Role in Biofilm Formation on Abiotic Surfaces and in the Interaction of This Pathogen with Eukaryotic Cells', *Infection and Immunity*, 77(8), pp. 3150–3160. Available at: https://doi.org/10.1128/IAI.00096-09.

Gallagher, L.A. *et al.* (2015) 'Resources for Genetic and Genomic Analysis of Emerging Pathogen *Acinetobacter baumannii*', *Journal of Bacteriology*. Edited by T.J. Silhavy, 197(12), pp. 2027–2035. Available at: https://doi.org/10.1128/JB.00131-15.

Gámez-Herrera, E. *et al.* (2020) 'Drug-eluting wound dressings having sustained release of antimicrobial compounds', *European Journal of Pharmaceutics and Biopharmaceutics*, 152, pp. 327–339. Available at: https://doi.org/10.1016/j.ejpb.2020.05.025.

Garbayo, E. *et al.* (2017) 'Bioresorbable polymers for next-generation cardiac scaffolds', *Bioresorbable Polymers for Biomedical Applications: From Fundamentals to Translational Medicine*, pp. 445–467. Available at: https://doi.org/10.1016/B978-0-08-100262-9.00019-7.

Gargate, N., Laws, M. and Rahman, K.M. (2025) 'Current economic and regulatory challenges in developing antibiotics for Gram-negative bacteria', *npj Antimicrobials and Resistance*, 3(1), p. 50. Available at: https://doi.org/10.1038/s44259-025-00123-1.

Garrido-Mesa, N., Zarzuelo, A. and Gálvez, J. (2013) 'Minocycline: far beyond an antibiotic', *British Journal of Pharmacology*, 169(2), pp. 337–352. Available at: https://doi.org/10.1111/bph.12139.

Gaspar-Pintiliescu, A., Stanciuc, A.-M. and Craciunescu, O. (2019) 'Natural composite dressings based on collagen, gelatin and plant bioactive compounds for wound healing: A review', *International Journal of Biological Macromolecules*, 138, pp. 854–865. Available at: https://doi.org/10.1016/j.ijbiomac.2019.07.155.

Gautier-Bouchardon, A.V. (2018) 'Antimicrobial Resistance in *Mycoplasma spp*', *Microbiology Spectrum*, 6(4). Available at: https://doi.org/10.1128/microbiolspec.ARBA-0030-2018.

Ge, P. *et al.* (2020) 'Full Poly(ethylene glycol) Hydrogels with High Ductility and Self-Recoverability', *ACS Applied Materials & Interfaces*, 12(33), pp. 37549–37560. Available at: https://doi.org/10.1021/acsami.0c08716.

Gedefie, A., Demsis, W., *et al.* (2021) '*Acinetobacter baumannii* biofilm formation and its role in disease pathogenesis: A review', *Infection and Drug Resistance*, 14. Available at: https://doi.org/10.2147/IDR.S332051.

Gedefie, A., Demsiss, W., *et al.* (2021) '*Acinetobacter baumannii* Biofilm Formation and Its Role in Disease Pathogenesis: A Review', *Infection and Drug Resistance*, Volume 14, pp. 3711–3719. Available at: https://doi.org/10.2147/IDR.S332051.

Gentile, V. *et al.* (2014) 'Iron and *Acinetobacter baumannii* Biofilm Formation', *Pathogens*, 3(3), pp. 704–719. Available at: https://doi.org/10.3390/pathogens3030704.

Ghavanloughajar, H. *et al.* (2025) 'Transcriptomic and functional profiling of *Acinetobacter baumannii* reveals adaptation to burn patient blood and time-dependent responses to human serum', *Frontiers in Microbiology*, 16, p. 1635690. Available at: https://doi.org/10.3389/fmicb.2025.1635690.

Gholami, M. *et al.* (2017) 'Frequency of 16S rRNA Methylase and Aminoglycoside-Modifying Enzyme Genes among Clinical Isolates of *Acinetobacter baumannii* in Iran', *Iranian Journal of Pathology*, 12(4), pp. 329–338.

Ghorpade, V.S. *et al.* (2019) 'Citric acid crosslinked carboxymethylcellulose-polyvinyl alcohol hydrogel films for extended release of water soluble basic drugs', *Journal of Drug Delivery Science and Technology*, 52, pp. 421–430. Available at: https://doi.org/10.1016/j.jddst.2019.05.013.

Giammanco, A. *et al.* (2017) 'Global Assessment of the Activity of Tigecycline against Multidrug-Resistant Gram-Negative Pathogens between 2004 and 2014 as Part of the Tigecycline Evaluation and Surveillance Trial', *mSphere*, 2(1). Available at: https://doi.org/10.1128/msphere.00310-16.

Goedhart, J. and Luijsterburg, M.S. (2020) 'VolcaNoseR is a web app for creating, exploring, labeling and sharing volcano plots', *Scientific Reports*, 10(1), p. 20560. Available at: https://doi.org/10.1038/s41598-020-76603-3.

Gong, Y. *et al.* (2020) 'Over-the-counter antibiotic sales in community and online pharmacies, China', *Bulletin of the World Health Organization*, 98(7), pp. 449–457. Available at: https://doi.org/10.2471/BLT.19.242370.

Gonzalez, M.R. *et al.* (2018) 'Transcriptome Analysis of *Pseudomonas aeruginosa* Cultured in Human Burn Wound Exudates', *Frontiers in Cellular and Infection Microbiology*, 8, p. 39. Available at: https://doi.org/10.3389/fcimb.2018.00039.

Goran, M.I., Plows, J.F. and Ventura, E.E. (2019) 'Effects of consuming sugars and alternative sweeteners during pregnancy on maternal and child health: Evidence for a secondhand sugar effect'. *Proceedings of the Nutrition Society*. Available at: https://doi.org/10.1017/S002966511800263X.

Gordillo Altamirano, F.L. *et al.* (2022) 'Phage-antibiotic combination is a superior treatment against *Acinetobacter baumannii* in a preclinical study', *eBioMedicine*, 80, p. 104045. Available at: https://doi.org/10.1016/j.ebiom.2022.104045.

Gounden, V. and Singh, M. (2024) 'Hydrogels and Wound Healing: Current and Future Prospects', *Gels*, 10(1). Available at: https://doi.org/10.3390/gels10010043.

Graça, M.F.P. *et al.* (2020) 'Hyaluronic acid—Based wound dressings: A review', *Carbohydrate Polymers*, 241, p. 116364. Available at: https://doi.org/10.1016/j.carbpol.2020.116364.

Granata, G. *et al.* (2024) 'The impact of armed conflict on the development and global spread of antibiotic resistance: a systematic review', *Clinical Microbiology and Infection*, 30(7), pp. 858–865. Available at: https://doi.org/10.1016/j.cmi.2024.03.029.

Greco, A. *et al.* (2021) 'Nanotechnology, a booster for the multitarget drug verteporfin', *Journal of Drug Delivery Science and Technology*, 64, p. 102562. Available at: https://doi.org/10.1016/j.jddst.2021.102562.

Gruber, S. and Nickel, A. (2023) 'Toxic or not toxic? The specifications of the standard ISO 10993-5 are not explicit enough to yield comparable results in the cytotoxicity assessment of an identical medical device', *Frontiers in Medical Technology*, 5, p. 1195529. Available at: https://doi.org/10.3389/fmedt.2023.1195529.

Guarnieri, A. *et al.* (2022) 'Antimicrobial properties of chitosan from different developmental stages of the bioconverter insect Hermetia illucens', *Scientific Reports*, 12(1), p. 8084. Available at: https://doi.org/10.1038/s41598-022-12150-3.

Guerrero, D.M. *et al.* (2010) '*Acinetobacter baumannii* -Associated Skin and Soft Tissue Infections: Recognizing a Broadening Spectrum of Disease', *Surgical Infections*, 11(1), pp. 49–57. Available at: https://doi.org/10.1089/sur.2009.022.

Guo, S. and DiPietro, L.A. (2010) 'Factors Affecting Wound Healing', *Journal of Dental Research*, 89(3), pp. 219–229. Available at: https://doi.org/10.1177/0022034509359125.

Hafiz, T.A. *et al.* (2023) 'A two-year retrospective study of multidrug-resistant *Acinetobacter baumannii* respiratory infections in critically Ill patients: Clinical and microbiological findings', *Journal of Infection and Public Health*, 16(3). Available at: https://doi.org/10.1016/j.jiph.2023.01.004.

Han, J. *et al.* (2026) 'Hydrogels Augmented With Artificial Sweeteners can Inhibit Multidrug-Resistant *Acinetobacter baumannii* Growth and Biofilm Formation While Demonstrating Safety in Pre-Clinical Pilot Human Trials', *Advanced Healthcare Materials*, p. e05777. Available at: https://doi.org/10.1002/adhm.202505777.

Hanberger, H. *et al.* (1999) 'Antibiotic susceptibility among aerobic gram-negative bacilli in intensive care units in 5 European countries', *JAMA*, 281(1). Available at: https://doi.org/10.1001/jama.281.1.67.

Harding, C.M. *et al.* (2013) '*Acinetobacter baumannii* strain M2 produces type IV pili which play a role in natural transformation and twitching motility but not surface-associated motility.', *mBio*, 4(4). Available at: https://doi.org/10.1128/mBio.00360-13.

Harding, C.M., Hennon, S.W. and Feldman, M.F. (2018) 'Uncovering the mechanisms of *Acinetobacter baumannii* virulence', *Nature Reviews Microbiology*, 16(2). Available at: https://doi.org/10.1038/nrmicro.2017.148.

Harmanci, S. *et al.* (2022) 'Production of 3D Printed Bi-Layer and Tri-Layer Sandwich Scaffolds with Polycaprolactone and Poly (vinyl alcohol)-Metformin towards Diabetic Wound Healing', *Polymers*, 14(23), p. 5306. Available at: https://doi.org/10.3390/polym14235306.

Hassan, K.A. *et al.* (2019) 'Short-chain diamines are the physiological substrates of PACE family efflux pumps', *Proceedings of the National Academy of Sciences*, 116(36), pp. 18015–18020. Available at: https://doi.org/10.1073/pnas.1901591116.

He, F. *et al.* (2018) 'Facile and large-scale synthesis of curcumin/PVA hydrogel: effectively kill bacteria and accelerate cutaneous wound healing in the rat', *Journal of Biomaterials Science, Polymer Edition*, 29(4), pp. 325–343. Available at: https://doi.org/10.1080/09205063.2017.1417002.

Hoffman, A.S. (2012) 'Hydrogels for biomedical applications', *Advanced Drug Delivery Reviews*, 64(SUPPL.), pp. 18–23. Available at: https://doi.org/10.1016/J.ADDR.2012.09.010.

Hou, J. *et al.* (2024) 'A Standardized Mouse Model for Wound Infection with Pseudomonas aeruginosa', *International Journal of Molecular Sciences*, 25(21). Available at: https://doi.org/10.3390/ijms252111773.

Hu, T. *et al.* (2024) 'Advances of naturally derived biomedical polymers in tissue engineering', *Frontiers in Chemistry*, Volume 12-2024. Available at: https://www.frontiersin.org/journals/chemistry/articles/10.3389/fchem.2024.1469183.

Hu, Y., Zheng, J. and Zhang, J. (2022) 'Natural Transformation in *Acinetobacter baumannii* W068: A Genetic Analysis Reveals the Involvements of the CRP, XcpV, XcpW, TsaP, and TonB2', *Frontiers in Microbiology*, 12, p. 738034. Available at: https://doi.org/10.3389/fmicb.2021.738034.

Huang, M. *et al.* (2017) 'High performances of dual network PVA hydrogel modified by PVP using borax as the structure-forming accelerator', *Designed Monomers and Polymers*, 20(1), pp. 505–513. Available at: https://doi.org/10.1080/15685551.2017.1382433.

Iyer, R. *et al.* (2018) '*Acinetobacter baumannii* OmpA Is a Selective Antibiotic Permeant Porin', *ACS Infectious Diseases*, 4(3), pp. 373–381. Available at: https://doi.org/10.1021/acsinfecdis.7b00168.

Jarosławiecka, A. and Piotrowska-Seget, Z. (2014) 'Lead resistance in micro-organisms', *Microbiology*, 160(1), pp. 12–25. Available at: https://doi.org/10.1099/mic.0.070284-0.

Jandhyala, S.M. *et al.* (2015) 'Role of the normal gut microbiota', *World Journal of Gastroenterology*, 21(29). Available at: https://doi.org/10.3748/wjg.v21.i29.8787.

Jia, L. *et al.* (2025) 'A Review of Polyhydroxybutyrate Biosynthesis by Different Microorganisms', *ChemBioChem*, 26(23), p. e202500562. Available at: https://doi.org/10.1002/cbic.202500562.

Jiang, F. *et al.* (2023) 'Extraction, Modification and Biomedical Application of Agarose Hydrogels: A Review', *Marine Drugs*, 21(5), p. 299. Available at: https://doi.org/10.3390/md21050299.

Jin, H. *et al.* (2026) 'Recent progress of collagen-based hydrogels for wound healing: a review', *Collagen and Leather*, 8(1), p. 1. Available at: https://doi.org/10.1186/s42825-025-00225-6.

Jin, S.G. (2022) 'Production and Application of Biomaterials Based on Polyvinyl alcohol (PVA) as Wound Dressing', *Chemistry – An Asian Journal*, 17(21), p. e202200595. Available at: https://doi.org/10.1002/asia.202200595.

Jipa, I. *et al.* (2012) 'Potassium sorbate release from poly(vinyl alcohol)-bacterial cellulose films', 66(2), pp. 138–143. Available at: https://doi.org/10.2478/s11696-011-0068-4.

Jones, M.E. *et al.* (2004) 'Emerging resistance among bacterial pathogens in the intensive care unit - A European and North American surveillance study (2000-2002)', *Annals of Clinical Microbiology and Antimicrobials*, 3. Available at: https://doi.org/10.1186/1476-0711-3-14.

Kariduraganavar, M.Y., Kittur, A.A. and Kamble, R.R. (2014) 'Polymer Synthesis and Processing', *Natural and Synthetic Biomedical Polymers*. Elsevier, pp. 1–31. Available at: https://doi.org/10.1016/B978-0-12-396983-5.00001-6.

Kalia, V.C., Patel, S.K.S. and Lee, J.-K. (2023) 'Bacterial biofilm inhibitors: An overview', *Ecotoxicology and Environmental Safety*, 264, p. 115389. Available at: https://doi.org/10.1016/j.ecoenv.2023.115389.

Kamoun, E.A., Kenawy, E.R.S. and Chen, X. (2017) 'A review on polymeric hydrogel membranes for wound dressing applications: PVA-based hydrogel dressings', *Journal of Advanced Research*, 8(3). Available at: https://doi.org/10.1016/j.jare.2017.01.005.

Kamoun, E.A., Kenawy, E.-R.S. and Chen, X. (2017) 'A review on polymeric hydrogel membranes for wound dressing applications: PVA-based hydrogel dressings', *Journal of Advanced Research*, 8(3), pp. 217–233. Available at: https://doi.org/10.1016/j.jare.2017.01.005.

Kapoor, G., Saigal, S. and Elongavan, A. (2017) 'Action and resistance mechanisms of antibiotics: A guide for clinicians', *Journal of Anaesthesiology, Clinical Pharmacology*, 33(3), pp. 300–305. Available at: https://doi.org/10.4103/joacp.JOACP_349_15.

Keen, E.F. *et al.* (2010) 'Prevalence of multidrug-resistant organisms recovered at a military burn center', *Burns*, 36(6). Available at: https://doi.org/10.1016/j.burns.2009.10.013.

Kim, H. *et al.* (2018) 'Gelatin/PVA scaffolds fabricated using a 3D-printing process employed with a low-temperature plate for hard tissue regeneration: Fabrication and characterizations', *International Journal of Biological Macromolecules*, 120, pp. 119–127. Available at: https://doi.org/10.1016/j.ijbiomac.2018.07.159.

Kim, M. *et al.* (2021) 'Distinctive Roles of Two Acinetobactin Isomers in Challenging Host Nutritional Immunity', *mBio*. Edited by P.E. Klebba and G.D. Wright, 12(5), pp. e02248-21. Available at: https://doi.org/10.1128/mBio.02248-21.

Korn, L., Brock, M. and Schuster, S. (2025) 'Metabolic pathway analysis of the methylcitrate cycle in bacteria and fungi identifies methylcitrate synthase as an antiinfective drug target', *microLife*, 6, p. uqaf009. Available at: https://doi.org/10.1093/femsml/uqaf009.

Kostyanev, T. and Can, F. (2017) 'The Global Crisis of Antimicrobial Resistance', *Antimicrobial Stewardship*. Elsevier, pp. 3–12. Available at: https://doi.org/10.1016/B978-0-12-810477-4.00001-5.

Kotwani, A., Joshi, J. and Lamkang, A.S. (2021) 'Over-the-counter sale of antibiotics in india: A qualitative study of providers' perspectives across two states', *Antibiotics*, 10(9). Available at: https://doi.org/10.3390/antibiotics10091123.

Kucera, J. *et al.* (2014) 'Multispecies biofilm in an artificial wound bed—A novel model for in vitro assessment of solid antimicrobial dressings', *Journal of Microbiological Methods*, 103, pp. 18–24. Available at: https://doi.org/10.1016/j.mimet.2014.05.008.

Lacy, M.Q. and McCurdy, A.R. (2013) 'Pomalidomide', *Blood*, 122(14), pp. 2305–2309. Available at: https://doi.org/10.1182/BLOOD-2013-05-484782.

Law, S.K.K. and Tan, H.S. (2022) 'The role of quorum sensing, biofilm formation, and iron acquisition as key virulence mechanisms in *Acinetobacter baumannii* and the corresponding anti-virulence strategies', *Microbiological Research*, 260, pp. 127032–127032. Available at: https://doi.org/10.1016/J.MICRES.2022.127032.

Lee, W. *et al.* (2001) 'A 1.2-A snapshot of the final step of bacterial cell wall biosynthesis', *Proceedings of the National Academy of Sciences of the United States of America*, 98(4), pp. 1427–1431. Available at: https://doi.org/10.1073/pnas.98.4.1427.

Lekshmi, M. *et al.* (2024) 'Major facilitator superfamily efflux pumps in human pathogens: Role in multidrug resistance and beyond', *Current Research in Microbial Sciences*, 7, p. 100248. Available at: https://doi.org/10.1016/j.crmicr.2024.100248.

Lessel, E.F. (1971) 'International Committee on Nomenclature of Bacteria Subcommittee on the Taxonomy of Moraxella and Allied Bacteria: Minutes of the Meeting, 11 August 1970. Room Constitution C, Maria-Isabel Hotel, Mexico City, Mexico', *International Journal of Systematic Bacteriology*, 21(2). Available at: https://doi.org/10.1099/00207713-21-2-213.

Lettieri, T. *et al.* (2018) *State of the art on the contribution of water to antimicrobial resistance*. Publications Office. Available at: https://doi.org/10.2760/771124.

Li, D. *et al.* (2021) 'Trends in artificial sweetener consumption: A 7-year wastewater-based epidemiology study in Queensland, Australia', *Science of the Total Environment*, 754. Available at: https://doi.org/10.1016/j.scitotenv.2020.142438.

Li, D. *et al.* (2025) 'Review of Biopolymer Polyhydroxybutyrate (PHB) and Blends: Modification of Thermal and Mechanical Properties via Additive Manufacturing Processing', *Polymers*, 17(22), p. 3083. Available at: https://doi.org/10.3390/polym17223083.

Li, J. *et al.* (2019) 'An optical fiber relative humidity sensor based on hollow-core fiber and hydroxypropyl methylcellulose hydrogel film', *Optik*, 195, p. 163172. Available at: https://doi.org/10.1016/j.ijleo.2019.163172.

Li, L. *et al.* (2017) 'Synthesis and wound healing of alternating block polyurethanes based on poly(lactic acid) (PLA) and poly(ethylene glycol) (PEG): Pula- *Alt* -PEG for Wound Healing and Skin Regeneration', *Journal of Biomedical Materials Research Part B: Applied Biomaterials*, 105(5), pp. 1200–1209. Available at: https://doi.org/10.1002/jbm.b.33670.

Li, S. *et al.* (2025) 'Bioactive agarose-based hydrogels with granulated microstructures for accelerating diabetic wound healing', *International Journal of Biological Macromolecules*, 330, p. 148061. Available at: https://doi.org/10.1016/j.ijbiomac.2025.148061.

Liang, X. *et al.* (2024) 'Polyvinyl Alcohol (PVA)-Based Hydrogels: Recent Progress in Fabrication, Properties, and Multifunctional Applications', *Polymers*, 16(19), p. 2755. Available at: https://doi.org/10.3390/polym16192755.

Lin, C. *et al.* (2026) 'Formulating Smart All-in-One Chitosan Hydrogel for High Performance Wound Dressing', *Advanced Healthcare Materials*, 15(4), p. e02971. Available at: https://doi.org/10.1002/adhm.202502971.

Lin, M.-F. and Lan, C.-Y. (2014) 'Antimicrobial resistance in *Acinetobacter baumannii*: From bench to bedside', *World Journal of Clinical Cases*, 2(12), pp. 787–814. Available at: https://doi.org/10.12998/wjcc.v2.i12.787.

Liu, G. *et al.* (2023) 'Deep learning-guided discovery of an antibiotic targeting *Acinetobacter baumannii*', *Nature Chemical Biology* [Preprint]. Available at: https://doi.org/10.1038/s41589-023-01349-8.

Liu, X. *et al.* (2023) 'Biofilm Formation and Control of Foodborne Pathogenic Bacteria', *Molecules*, 28(6), pp. 2432–2432. Available at: https://doi.org/10.3390/molecules28062432.

Liu, Yang *et al.* (2022) 'CB-Dock2: improved protein–ligand blind docking by integrating cavity detection, docking and homologous template fitting', *Nucleic Acids Research*, 50(W1), pp. W159–W164. Available at: https://doi.org/10.1093/nar/gkac394.

Liu, Yalei *et al.* (2022) 'Polyvinyl alcohol/carboxymethyl chitosan hydrogel loaded with silver nanoparticles exhibited antibacterial and self-healing properties', *International Journal of*

Biological Macromolecules, 220, pp. 211–222. Available at: https://doi.org/10.1016/J.IJBIOMAC.2022.08.061.

Lobanovska, M. and Pilla, G. (2017) 'Penicillin's Discovery and Antibiotic Resistance: Lessons for the Future?', *The Yale Journal of Biology and Medicine*, 90(1), pp. 135–145.

Loehfelm, T.W., Luke, N.R. and Campagnari, A.A. (2008) 'Identification and characterization of an *Acinetobacter baumannii* biofilm-associated protein', *Journal of Bacteriology*, 190(3). Available at: https://doi.org/10.1128/JB.01416-07.

Łojewska, E. and Sakowicz, T. (2021) 'An Alternative to Antibiotics: Selected Methods to Combat Zoonotic Foodborne Bacterial Infections', *Current Microbiology*, 78(12). Available at: https://doi.org/10.1007/s00284-021-02665-9.

Loos, R. *et al.* (2013) 'EU-wide monitoring survey on emerging polar organic contaminants in wastewater treatment plant effluents', *Water Research*, 47(17). Available at: https://doi.org/10.1016/j.watres.2013.08.024.

López-Martín, M. *et al.* (2021) 'AbaM Regulates Quorum Sensing, Biofilm Formation, and Virulence in *Acinetobacter baumannii*', *Journal of Bacteriology*. Edited by Y.V. Brun, 203(8). Available at: https://doi.org/10.1128/JB.00635-20.

Loree, J. and Lappin, S.L. (2020) *Bacteriostatic Antibiotics*. (StatPearls).

Loughlin, R.G. *et al.* (2008) 'Modulation of gel formation and drug-release characteristics of lidocaine-loaded poly(vinyl alcohol)-tetraborate hydrogel systems using scavenger polyol sugars', *European Journal of Pharmaceutics and Biopharmaceutics*, 69(3). Available at: https://doi.org/10.1016/j.ejpb.2008.01.033.

Lowy, F.D. (2003) 'Antimicrobial resistance: the example of *Staphylococcus aureus*', *The Journal of Clinical Investigation*, 111(9), pp. 1265–1273. Available at: https://doi.org/10.1172/JCI18535.

Lu, J. *et al.* (2022a) 'Antidepressants promote the spread of extracellular antibiotic resistance genes via transformation', *ISME Communications*, 2(1), pp. 63–63. Available at: https://doi.org/10.1038/s43705-022-00147-y.

Lu, J. *et al.* (2022b) 'Antidepressants promote the spread of extracellular antibiotic resistance genes via transformation', *ISME Communications*, 2(1), pp. 63–63. Available at: https://doi.org/10.1038/s43705-022-00147-y.

Luo, J., Zhang, Q., *et al.* (2019) 'Ecotoxicity and environmental fates of newly recognized contaminants-artificial sweeteners: A review', *Science of The Total Environment*, 653, pp. 1149–1160. Available at: https://doi.org/10.1016/j.scitotenv.2018.10.445.

Luo, J., Wu, L., *et al.* (2019) 'Review on the determination and distribution patterns of a widespread contaminant artificial sweetener in the environment', *Environmental Science and Pollution Research*, 26(19). Available at: https://doi.org/10.1007/s11356-019-05261-4.

Ma, W. *et al.* (2019) 'Swelling Resistance and Mechanical Performance of Physical Crosslink-Based Poly(Vinyl Alcohol) Hydrogel Film with Various Molecular Weight', *Journal of Polymer Science Part B: Polymer Physics*, 57(24), pp. 1673–1683. Available at: https://doi.org/10.1002/polb.24902.

Machado-Torres, K. *et al.* (2025) 'Self-healing PVA/PVP micelle–hydrogel composite system for potential phenytoin repositioning in wound healing', *Journal of Biological Engineering*, 20(1), p. 6. Available at: https://doi.org/10.1186/s13036-025-00587-9.

Mackraj, I., Govender, T. and Gathiram, P. (2008) 'Sanguinarine', *Cardiovascular Drug Reviews*, 26(1), pp. 75–83. Available at: https://doi.org/10.1111/j.1527-3466.2007.00037.x.

Maeso, L. *et al.* (2026) 'Recent advances in the use of gelatin as a biomaterial for tissue engineering', *International Journal of Pharmaceutics*, 696, p. 126828. Available at: https://doi.org/10.1016/j.ijpharm.2026.126828.

Maier, L. *et al.* (2018a) 'Extensive impact of non-antibiotic drugs on human gut bacteria', *Nature*, 555(7698), pp. 623–628. Available at: https://doi.org/10.1038/nature25979.

Maier, L. *et al.* (2018b) 'Extensive impact of non-antibiotic drugs on human gut bacteria', *Nature*, 555(7698), pp. 623–628. Available at: https://doi.org/10.1038/nature25979.

Makvandi, P. *et al.* (2022) 'Bioinspired microneedle patches: Biomimetic designs, fabrication, and biomedical applications', *Matter*, 5(2), pp. 390–429. Available at: https://doi.org/10.1016/J.MATT.2021.11.021.

Malcher, M. *et al.* (2008) 'Embedded silver ions-containing liposomes in polyelectrolyte multilayers: Cargos films for antibacterial agents', *Langmuir*, 24(18). Available at: https://doi.org/10.1021/la8014755.

Mali, K.K. *et al.* (2018) 'Citric acid crosslinked carboxymethyl cellulose-based composite hydrogel films for drug delivery', *Indian Journal of Pharmaceutical Sciences*, 80(4). Available at: https://doi.org/10.4172/pharmaceutical-sciences.1000405.

Mancuso, G. *et al.* (2021) 'Bacterial antibiotic resistance: the most critical pathogens', *Pathogens*, 10(10). Available at: https://doi.org/10.3390/pathogens10101310.

Maragakis, L.L. and Perl, T.M. (2008) '*Acinetobacter baumannii*: Epidemiology, antimicrobial resistance, and treatment options', *Clinical Infectious Diseases*, 46(8). Available at: https://doi.org/10.1086/529198.

Marins, J.C.B. *et al.* (2014) 'Thermal body patterns for healthy Brazilian adults (male and female)', *Journal of Thermal Biology*, 42, pp. 1–8. Available at: https://doi.org/10.1016/j.jtherbio.2014.02.020.

Martí, S. *et al.* (2011) 'Biofilm formation at the solid-liquid and air-liquid interfaces by *Acinetobacter* species', *BMC Research Notes*, 4. Available at: https://doi.org/10.1186/1756-0500-4-5.

Martin, M.J., Thottathil, S.E. and Newman, T.B. (2015) 'Antibiotics overuse in animal agriculture: A call to action for health care providers', *American Journal of Public Health*, 105(12). Available at: https://doi.org/10.2105/AJPH.2015.302870.

Martinez, J. *et al.* (2021) 'Cerebrospinal fluid (CSF) augments metabolism and virulence expression factors in *Acinetobacter baumannii*', *Scientific Reports*, 11(1), p. 4737. Available at: https://doi.org/10.1038/s41598-021-81714-6.

Maslova, E. *et al.* (2020) 'An Invertebrate Burn Wound Model That Recapitulates the Hallmarks of Burn Trauma and Infection Seen in Mammalian Models', *Frontiers in Microbiology*, 11, p. 998. Available at: https://doi.org/10.3389/fmicb.2020.00998.

Maslova, E. *et al.* (2021) 'Burns and biofilms: priority pathogens and in vivo models', *npj Biofilms and Microbiomes*, 7(1), p. 73. Available at: https://doi.org/10.1038/s41522-021-00243-2.

Maslova, E., Osman, S. and McCarthy, R.R. (2023) 'Using the Galleria mellonella burn wound and infection model to identify and characterize potential wound probiotics', *Microbiology*, 169(6). Available at: https://doi.org/10.1099/mic.0.001350.

Mattick, J.S. (2002) 'Type IV Pili and Twitching Motility', *Annual Review of Microbiology*, 56(1), pp. 289–314. Available at: https://doi.org/10.1146/annurev.micro.56.012302.160938.

McCarthy, R.R. *et al.* (2021) 'Antibiotic Resistance Mechanisms and Their Transmission in *Acinetobacter baumannii*', pp. 135–153. Available at: https://doi.org/10.1007/978-3-030-67452-6_7.

McNeilly, O. *et al.* (2025) 'Molecular insights into silver nanoparticle resistance in *Acinetobacter baumannii* and unique adaptations to ionic silver', *npj Antimicrobials and Resistance*, 3(1), p. 92. Available at: https://doi.org/10.1038/s44259-025-00161-9.

Medrades, J. de P. *et al.* (2022) 'Flavin adenine dinucleotide functionalized gold nanoparticles for the electrochemical detection of dopamine', *Sensors and Actuators Reports*, 4, pp. 100085–100085. Available at: https://doi.org/10.1016/J.SNR.2022.100085.

Mei, Q. *et al.* (2014) 'Effectiveness of mifepristone in combination with ethacridine lactate for second trimester pregnancy termination', *European Journal of Obstetrics & Gynecology and Reproductive Biology*, 178, pp. 12–15. Available at: https://doi.org/10.1016/j.ejogrb.2014.04.041.

Mei, Y. *et al.* (2024) 'Versatile hydrogel-based drug delivery platform for multimodal cancer therapy from bench to bedside', *Applied Materials Today*, 39, pp. 102341–102341. Available at: https://doi.org/10.1016/J.APMT.2024.102341.

Metcalf, D.G. and Bowler, P.G. (2013) 'Biofilm delays wound healing: A review of the evidence', *Burns & Trauma*, 1(1), pp. 2321-3868.113329. Available at: https://doi.org/10.4103/2321-3868.113329.

Miguel, J.S. *et al.* (2013) 'Pomalidomide plus low-dose dexamethasone versus high-dose dexamethasone alone for patients with relapsed and refractory multiple myeloma (MM-003):

a randomised, open-label, phase 3 trial', *The Lancet Oncology*, 14(11), pp. 1055–1066. Available at: https://doi.org/10.1016/S1470-2045(13)70380-2.

Miller, W.R. and Arias, C.A. (2024) 'ESKAPE pathogens: antimicrobial resistance, epidemiology, clinical impact and therapeutics', *Nature Reviews Microbiology*, 22(10), pp. 598–616. Available at: https://doi.org/10.1038/s41579-024-01054-w.

Mitropoulou, G. *et al.* (2022) 'Phage therapy for respiratory infections', *Revue Medicale Suisse*, 18(804). Available at: https://doi.org/10.53738/REVMED.2022.18.804.2150.

Mndlovu, H. *et al.* (2024) 'A review of biomaterial degradation assessment approaches employed in the biomedical field', *npj Materials Degradation*, 8(1), p. 66. Available at: https://doi.org/10.1038/s41529-024-00487-1.

Mohamed, S.A.A. *et al.* (2025) 'Potential application of new antimicrobials biological macromolecule of CNT/ZnO-NPs based on hydroxypropyl methylcellulose/shellac as packaging films', *International Journal of Biological Macromolecules*, 306, p. 141421. Available at: https://doi.org/10.1016/j.ijbiomac.2025.141421.

Molano-Arevalo, J.C. *et al.* (2014) 'Flavin Adenine Dinucleotide Structural Motifs: From Solution to Gas Phase', *Analytical Chemistry*, 86(20), pp. 10223–10230. Available at: https://doi.org/10.1021/ac5023666.

Mrsny, R.J. (2009) 'Lessons from nature: "Pathogen-Mimetic" systems for mucosal Nano-medicines', *Advanced Drug Delivery Reviews*, 61(2), pp. 172–192. Available at: https://doi.org/10.1016/J.ADDR.2008.09.009.

Mu, A. *et al.* (2021) 'Assessment of the microbiome during bacteriophage therapy in combination with systemic antibiotics to treat a case of staphylococcal device infection', *Microbiome*, 9(1). Available at: https://doi.org/10.1186/s40168-021-01026-9.

Murphy, D.J. *et al.* (2012) 'Physical characterisation and component release of poly(vinyl alcohol)-tetrahydroxyborate hydrogels and their applicability as potential topical drug delivery systems', *International Journal of Pharmaceutics*, 423(2). Available at: https://doi.org/10.1016/j.ijpharm.2011.11.018.

Murray, C.J. *et al.* (2022) 'Global burden of bacterial antimicrobial resistance in 2019: a systematic analysis', *The Lancet*, 399(10325), pp. 629–655. Available at: https://doi.org/10.1016/S0140-6736(21)02724-0.

Munshi, N.C., Longo, D.L. and Anderson, K.C. (2022) 'Plasma Cell Disorders', in J. Loscalzo et al. (eds) *Harrison's Principles of Internal Medicine, 21e*. New York, NY: McGraw-Hill Education. Available at: accessmedicine.mhmedical.com/content.aspx?aid=1198034860.

Naghavi, M. *et al.* (2024) 'Global burden of bacterial antimicrobial resistance 1990–2021: a systematic analysis with forecasts to 2050', *The Lancet*, 404(10459), pp. 1199–1226. Available at: https://doi.org/10.1016/S0140-6736(24)01867-1.

Nesrinne, S. and Djamel, A. (2017) 'Synthesis, characterization and rheological behavior of pH sensitive poly(acrylamide-co-acrylic acid) hydrogels', *Arabian Journal of Chemistry*, 10(4), pp. 539–547. Available at: https://doi.org/10.1016/j.arabjc.2013.11.027.

Nilforoushzadeh, M.A. *et al.* (2017) 'Dermal Fibroblast Cells: Biology and Function in Skin Regeneration', *Journal of Skin and Stem Cell*, In Press(In Press). Available at: https://doi.org/10.5812/jssc.69080.

Nishino, K. *et al.* (2021) 'Function and Inhibitory Mechanisms of Multidrug Efflux Pumps', *Frontiers in Microbiology*, 12, p. 737288. Available at: https://doi.org/10.3389/fmicb.2021.737288.

Nuutila, K. and Eriksson, E. (2021) 'Moist Wound Healing with Commonly Available Dressings', *Advances in Wound Care*, 10(12), pp. 685–698. Available at: https://doi.org/10.1089/wound.2020.1232.

Nwugo, C.C. *et al.* (2011a) 'Deciphering the iron response in *Acinetobacter baumannii*: A proteomics approach', *Journal of Proteomics*, 74(1), pp. 44–58. Available at: https://doi.org/10.1016/j.jprot.2010.07.010.

Nwugo, C.C. *et al.* (2011b) 'Deciphering the iron response in *Acinetobacter baumannii*: A proteomics approach', *Journal of Proteomics*, 74(1), pp. 44–58. Available at: https://doi.org/10.1016/j.jprot.2010.07.010.

O' Neil, J. (2014) *Review on Antibiotic resisitance. Antimicrobial Resistance : Tackling a crisis for the health and wealth of nations*.

Oh, N.G., Hwang, S.Y. and Na, Y.H. (2022) 'Fabrication of a PVA-Based Hydrogel Microneedle Patch', *ACS Omega*, 7(29), pp. 25179–25185. Available at: https://doi.org/10.1021/acsomega.2c01993.

Olivia, D. (2017) 'WHO publishes list of bacteria for which new antibiotics are urgently needed', *World Health Organization* [Preprint]. Available at: https://www.who.int/news/item/27-02-2017-who-publishes-list-of-bacteria-for-which-new-antibiotics-are-urgently-needed.

Omkaram, I., Sreekanth Chakradhar, R.P. and Lakshmana Rao, J. (2007) 'EPR, optical, infrared and Raman studies of VO2+ ions in polyvinylalcohol films', *Physica B: Condensed Matter*, 388(1), pp. 318–325. Available at: https://doi.org/10.1016/j.physb.2006.06.134.

Omote, H. *et al.* (2006) 'The MATE proteins as fundamental transporters of metabolic and xenobiotic organic cations', *Trends in Pharmacological Sciences*, 27(11), pp. 587–593. Available at: https://doi.org/10.1016/j.tips.2006.09.001.

O'Neill, J. (2016) *Tackling drug-resistant infections globally: final report and recommendations*. Available at: https://apo.org.au/node/63983.

Oyejobi, G.K. *et al.* (2022) '*Acinetobacter baumannii*: More ways to die', *Microbiological Research*, 261, pp. 127069–127069. Available at: https://doi.org/10.1016/J.MICRES.2022.127069.

Palomino, C., Marín, E. and Fernández, L.Á. (2011) 'The fimbrial usher FimD follows the SurA-BamB pathway for its assembly in the outer membrane of *Escherichia coli*', *Journal of Bacteriology*, 193(19), pp. 5222–5230. Available at: https://doi.org/10.1128/JB.05585-11.

Papenfort, K. and Bassler, B.L. (2016) 'Quorum sensing signal-response systems in Gram-negative bacteria', *Nature Reviews Microbiology*, 14(9). Available at: https://doi.org/10.1038/nrmicro.2016.89.

Paula Rosa, A.C. de (2017) 'Diarrheagenic Escherichia Coli and Probiotic Activity against Foodborne Pathogens: A Brief Review', *Gastroenterology & Hepatology: Open Access*, 7(5). Available at: https://doi.org/10.15406/ghoa.2017.07.00248.

Pavita, T.G. *et al.* (2025) 'Advances in Polyvinyl Alcohol Based Hydrogels for Sensing Technologies', *Polymers for Advanced Technologies*, 36(10), p. e70372. Available at: https://doi.org/10.1002/pat.70372.

Peppas, N.A. (1975) 'Turbidimetric studies of aqueous poly(vinyl alcohol) solutions', *Die Makromolekulare Chemie*, 176(11), pp. 3433–3440. Available at: https://doi.org/10.1002/macp.1975.021761125.

Pereira, T.C. *et al.* (2018) 'Recent Advances in the Use of Galleria mellonella Model to Study Immune Responses against Human Pathogens', *Journal of Fungi*, 4(4), p. 128. Available at: https://doi.org/10.3390/jof4040128.

Phan, S. *et al.* (2023) 'Relative Abundance and Detection of Pseudomonas aeruginosa from Chronic Wound Infections Globally', *Microorganisms*, 11(5). Available at: https://doi.org/10.3390/microorganisms11051210.

Pimentel, C. *et al.* (2021) 'Interaction of *Acinetobacter baumannii* with Human Serum Albumin: Does the Host Determine the Outcome?', *Antibiotics*, 10(7), p. 833. Available at: https://doi.org/10.3390/antibiotics10070833.

Pompilio, A. *et al.* (2021) 'Gram-negative bacteria holding together in a biofilm: The acinetobacter baumannii way', *Microorganisms*, 9(7). Available at: https://doi.org/10.3390/microorganisms9071353.

Pop, M.A. and Almquist, B.D. (2017) 'Biomaterials: A potential pathway to healing chronic wounds?', *Experimental Dermatology*, 26(9), pp. 760–763. Available at: https://doi.org/10.1111/exd.13290.

Porta, C. *et al.* (2015) 'Dovitinib (CHIR258, TKI258): Structure, Development and Preclinical and Clinical Activity', *Future Oncology*, 11(1), pp. 39–50. Available at: https://doi.org/10.2217/fon.14.208.

Prabhu, K.S. *et al.* (2018) 'Embelin: A Benzoquinone Possesses Therapeutic Potential for the Treatment of Human Cancer', *Future Medicinal Chemistry*, 10(8), pp. 961–976. Available at: https://doi.org/10.4155/fmc-2017-0198.

Prados, E. and Maicas, S. (2016) 'Bacterial Production of Hydroxyalkanoates (PHA)', *Universal Journal of Microbiology Research*, 4(1), pp. 23–30. Available at: https://doi.org/10.13189/ujmr.2016.040104.

'Primaquine Diphosphate: Comprehensive Profile' (2005) *Profiles of Drug Substances, Excipients and Related Methodology*. Elsevier, pp. 153–208. Available at: https://doi.org/10.1016/S0099-5428(05)32007-7.

Qi, L. *et al.* (2016) 'Relationship between antibiotic resistance, biofilm formation, and biofilm-specific resistance in *Acinetobacter baumannii*', *Frontiers in Microbiology*, 7(APR). Available at: https://doi.org/10.3389/fmicb.2016.00483.

Quinn, B. *et al.* (2018) 'Human serum albumin alters specific genes that can play a role in survival and persistence in *Acinetobacter baumannii*', *Scientific Reports*, 8(1), p. 14741. Available at: https://doi.org/10.1038/s41598-018-33072-z.

Quispe-Siccha, R.M. *et al.* (2024) 'Development of Polyvinyl Alcohol Hydrogels for Controlled Glucose Release in Biomedical Applications', *Gels (Basel, Switzerland)*, 10(10), p. 668. Available at: https://doi.org/10.3390/gels10100668.

Rahman Khan, M.M. and Rumon, Md.M.H. (2025) 'Synthesis of PVA-Based Hydrogels for Biomedical Applications: Recent Trends and Advances', *Gels*, 11(2), p. 88. Available at: https://doi.org/10.3390/gels11020088.

Ramirez, M.S. and Tolmasky, M.E. (2010) 'Aminoglycoside modifying enzymes', *Drug Resistance Updates: Reviews and Commentaries in Antimicrobial and Anticancer Chemotherapy*, 13(6), pp. 151–171. Available at: https://doi.org/10.1016/j.drup.2010.08.003.

Rathan, S. *et al.* (2019) 'Fiber Reinforced Cartilage ECM Functionalized Bioinks for Functional Cartilage Tissue Engineering', *Advanced Healthcare Materials*, 8(7), p. 1801501. Available at: https://doi.org/10.1002/adhm.201801501.

Ramirez, M.S. and Tolmasky, M.E. (2010) 'Aminoglycoside modifying enzymes', *Drug Resistance Updates: Reviews and Commentaries in Antimicrobial and Anticancer Chemotherapy*, 13(6), pp. 151–171. Available at: https://doi.org/10.1016/j.drup.2010.08.003.

Reygaert, W.C. (2018) 'An overview of the antimicrobial resistance mechanisms of bacteria.', *AIMS microbiology*, 4(3), pp. 482–501. Available at: https://doi.org/10.3934/microbiol.2018.3.482.

Ricciardi, R. *et al.* (2004) 'X-ray Diffraction Analysis of Poly(vinyl alcohol) Hydrogels, Obtained by Freezing and Thawing Techniques', *Macromolecules*, 37(5), pp. 1921–1927. Available at: https://doi.org/10.1021/ma035663q.

Rice, L.B. (2008) 'Federal Funding for the Study of Antimicrobial Resistance in Nosocomial Pathogens: No ESKAPE', *The Journal of Infectious Diseases*, 197(8), pp. 1079–1081. Available at: https://doi.org/10.1086/533452.

Richardson, P.G. *et al.* (2019) 'Pomalidomide, bortezomib, and dexamethasone for patients with relapsed or refractory multiple myeloma previously treated with lenalidomide

(OPTIMISMM): a randomised, open-label, phase 3 trial', *The Lancet Oncology*, 20(6), pp. 781–794. Available at: https://doi.org/10.1016/S1470-2045(19)30152-4.

Rizwan, M. *et al.* (2017) 'pH Sensitive Hydrogels in Drug Delivery: Brief History, Properties, Swelling, and Release Mechanism, Material Selection and Applications', *Polymers*, 9(4), p. 137. Available at: https://doi.org/10.3390/polym9040137.

Robin, B. *et al.* (2022) 'MacAB-TolC Contributes to the Development of *Acinetobacter baumannii* Biofilm at the Solid–Liquid Interface', *Frontiers in Microbiology*, 12, p. 785161. Available at: https://doi.org/10.3389/fmicb.2021.785161.

Rodriguez, C. *et al.* (2023) 'Antimicrobial activity of the Lacticaseibacillus rhamnosus CRL 2244 and its impact on the phenotypic and transcriptional responses in carbapenem resistant *Acinetobacter baumannii*', *Scientific Reports*, 13(1), p. 14323. Available at: https://doi.org/10.1038/s41598-023-41334-8.

Ronish, L.A. *et al.* (2019) 'The structure of *pilA* from *Acinetobacter baumannii* AB5075 suggests a mechanism for functional specialization in Acinetobacter type IV pili', *Journal of Biological Chemistry*, 294(1). Available at: https://doi.org/10.1074/jbc.RA118.005814.

Ronish, L.A. *et al.* (2019) 'The structure of *pilA* from *Acinetobacter baumannii* AB5075 suggests a mechanism for functional specialization in Acinetobacter type IV pili', *Journal of Biological Chemistry*, 294(1), pp. 218–230. Available at: https://doi.org/10.1074/jbc.RA118.005814.

Roy, N. and Saha, N. (2012) 'PVP-based hydrogels: Synthesis, properties and applications', *Hydrogels: Synthesis, Characterization and Applications*, pp. 227–252.

Roy, S. *et al.* (2022) 'Convergence of Biofilm Formation and Antibiotic Resistance in *Acinetobacter baumannii* Infection', *Frontiers in Medicine*, 9. Available at: https://doi.org/10.3389/fmed.2022.793615.

Ruamsap, N. *et al.* (2023) 'Chronic Wound Infection Model of Acinetobacter baumannii in Outbred Mice', *Military Medicine*, 188(7–8), pp. e1708–e1716. Available at: https://doi.org/10.1093/milmed/usac020.

Ruiz-Ojeda, F.J. *et al.* (2019) 'Effects of Sweeteners on the Gut Microbiota: A Review of Experimental Studies and Clinical Trials'. *Advances in Nutrition*. Available at: https://doi.org/10.1093/advances/nmy037.

Rumbo, C. *et al.* (2014) 'The *Acinetobacter baumannii* Omp33-36 Porin Is a Virulence Factor That Induces Apoptosis and Modulates Autophagy in Human Cells', *Infection and Immunity*. Edited by C.R. Roy, 82(11), pp. 4666–4680. Available at: https://doi.org/10.1128/IAI.02034-14.

Rumbo-Feal, S. *et al.* (2013) 'Whole Transcriptome Analysis of *Acinetobacter baumannii* Assessed by RNA-Sequencing Reveals Different mRNA Expression Profiles in Biofilm Compared to Planktonic Cells', *PLoS ONE*. Edited by G.F. Kaufmann, 8(8), p. e72968. Available at: https://doi.org/10.1371/journal.pone.0072968.

Runci, F. *et al.* (2019) 'Contribution of Active Iron Uptake to *Acinetobacter baumannii* Pathogenicity', *Infection and Immunity*. Edited by A.J. Bäumler, 87(4), pp. e00755-18. Available at: https://doi.org/10.1128/IAI.00755-18.

Russo, A. *et al.* (2019) 'Bloodstream infections caused by carbapenem-resistant *Acinetobacter baumannii*: Clinical features, therapy and outcome from a multicenter study', *Journal of Infection*, 79(2). Available at: https://doi.org/10.1016/j.jinf.2019.05.017.

Russo, A. *et al.* (2022) 'Multidrug-resistant *Acinetobacter baumannii* infections in COVID-19 patients hospitalized in intensive care unit', *Infection*, 50(1). Available at: https://doi.org/10.1007/s15010-021-01643-4.

S., S. *et al.* (2020) 'A nonadherent chitosan-polyvinyl alcohol absorbent wound dressing prepared via controlled freeze-dry technology', *International Journal of Biological Macromolecules*, 150, pp. 129–140. Available at: https://doi.org/10.1016/j.ijbiomac.2020.01.292.

Saipriya, K. *et al.* (2020) 'Quorum-sensing system in *Acinetobacter baumannii* : a potential target for new drug development', *Journal of Applied Microbiology*, 128(1), pp. 15–27. Available at: https://doi.org/10.1111/jam.14330.

Salinas, J.H. *et al.* (2025) 'Phenotypic Characterization of pilA, pilB, and pilD Mutants of *Acinetobacter baumannii* 5075: Impacts on Growth, Biofilm Formation, and Tazobactam Response', *Antibiotics*, 14(8), p. 816. Available at: https://doi.org/10.3390/antibiotics14080816.

Salomé Veiga, A. and Schneider, J.P. (2013) 'Antimicrobial hydrogels for the treatment of infection', *Peptide Science*, 100(6), pp. 637–644. Available at: https://doi.org/10.1002/bip.22412.

Sánchez-López, E. *et al.* (2020) 'Metal-based nanoparticles as antimicrobial agents: An overview', *Nanomaterials*, 10(2). Available at: https://doi.org/10.3390/nano10020292.

Sargur Ranganath, A. *et al.* (2022) 'Evaluating 3D-printability of polyvinyl alcohol (PVA) and microfibrillated cellulose (MFC) composite inks', *Materials Today: Proceedings*, 70, pp. 6–11. Available at: https://doi.org/10.1016/j.matpr.2022.08.483.

Schafer, J.J. and Mangino, J.E. (2008) 'Multidrug-Resistant *Acinetobacter baumannii* Osteomyelitis from Iraq', *Emerging Infectious Diseases*, 14(3), pp. 512b–5514. Available at: https://doi.org/10.3201/eid1403.070128.

Schmedlen, R.H., Masters, K.S. and West, J.L. (2002) 'Photocrosslinkable polyvinyl alcohol hydrogels that can be modified with cell adhesion peptides for use in tissue engineering', *Biomaterials*, 23(22), pp. 4325–4332. Available at: https://doi.org/10.1016/S0142-9612(02)00177-1.

Schooley, R.T. *et al.* (2017) 'Development and Use of Personalized Bacteriophage-Based Therapeutic Cocktails To Treat a Patient with a Disseminated Resistant *Acinetobacter baumannii* Infection', *Antimicrobial Agents and Chemotherapy*, 61(10), pp. e00954-17. Available at: https://doi.org/10.1128/AAC.00954-17.

Schwab, A. *et al.* (2020) 'Printability and Shape Fidelity of Bioinks in 3D Bioprinting', *Chemical Reviews*, 120(19), pp. 11028–11055. Available at: https://doi.org/10.1021/acs.chemrev.0c00084.

Scribano, D. *et al.* (2024) '*Acinetobacter baumannii* OmpA-like porins: functional characterization of bacterial physiology, antibiotic-resistance, and virulence', *Communications Biology*, 7(1), p. 948. Available at: https://doi.org/10.1038/s42003-024-06645-0.

Segneanu, A.-E. *et al.* (2025) 'Advancements in Hydrogels: A Comprehensive Review of Natural and Synthetic Innovations for Biomedical Applications', *Polymers*, 17(15), p. 2026. Available at: https://doi.org/10.3390/polym17152026.

Sen, C.K. (2019) 'Human Wounds and Its Burden: An Updated Compendium of Estimates', *Advances in Wound Care*, 8(2), pp. 39–48. Available at: https://doi.org/10.1089/wound.2019.0946.

Shamloo, A. *et al.* (2021) 'Fabrication and evaluation of chitosan/gelatin/PVA hydrogel incorporating honey for wound healing applications: An in vitro, in vivo study', *International Journal of Pharmaceutics*, 592, p. 120068. Available at: https://doi.org/10.1016/j.ijpharm.2020.120068.

Sharma, C. *et al.* (2025) 'Cellulose-based 3D printing bio-inks for biomedical applications: A review', *International Journal of Biological Macromolecules*, 305, p. 141174. Available at: https://doi.org/10.1016/j.ijbiomac.2025.141174.

Sheldon, J.R. and Skaar, E.P. (2020) '*Acinetobacter baumannii* can use multiple siderophores for iron acquisition, but only acinetobactin is required for virulence', *PLOS Pathogens*. Edited by D.S. Weiss, 16(10), p. e1008995. Available at: https://doi.org/10.1371/journal.ppat.1008995.

Shi, J. *et al.* (2024) '*Acinetobacter baumannii*: an evolving and cunning opponent', *Frontiers in Microbiology*, 15, p. 1332108. Available at: https://doi.org/10.3389/fmicb.2024.1332108.

Shree, P. *et al.* (2023) 'Biofilms: Understanding the structure and contribution towards bacterial resistance in antibiotics', *Medicine in Microecology*, 16, p. 100084. Available at: https://doi.org/10.1016/j.medmic.2023.100084.

Singh, H., Thangaraj, P. and Chakrabarti, A. (2013) '*Acinetobacter baumannii*: A brief account of mechanisms of multidrug resistance and current and future therapeutic management', *Journal of Clinical and Diagnostic Research*, 7(11). Available at: https://doi.org/10.7860/JCDR/2013/6337.3626.

Singh, S., Young, A. and McNaught, C.-E. (2017) 'The physiology of wound healing', *Wound Management*, 35(9), pp. 473–477. Available at: https://doi.org/10.1016/j.mpsur.2017.06.004.

Sirousazar, M. and Khodamoradi, P. (2020) 'Freeze-thawed humic acid/polyvinyl alcohol supramolecular hydrogels', *Materials Today Communications*, 22, p. 100719. Available at: https://doi.org/10.1016/j.mtcomm.2019.100719.

Slipski, C.J. *et al.* (2019) 'Plasmid transmitted small multidrug resistant (SMR) efflux pumps differ in gene regulation and enhance tolerance to quaternary ammonium compounds (QAC) when grown as biofilms'. Microbiology. Available at: https://doi.org/10.1101/768630.

Smani, Y. *et al.* (2014) 'Role of OmpA in the Multidrug Resistance Phenotype of *Acinetobacter baumannii*', *Antimicrobial Agents and Chemotherapy*, 58(3), pp. 1806–1808. Available at: https://doi.org/10.1128/AAC.02101-13.

Smith, P.T. *et al.* (2018) 'Chemical modification and printability of shear-thinning hydrogel inks for direct-write 3D printing', *Polymer*, 152, pp. 42–50. Available at: https://doi.org/10.1016/j.polymer.2018.01.070.

Song, C. *et al.* (2025) 'Berberine hydrochloride attenuates avian pathogenic *Escherichia coli*-induced macrophage inflammation via NAD^+/NADH-SIRT1-NF-κB regulatory axis', *Animals and Zoonoses*, 1(3), pp. 234–242. Available at: https://doi.org/10.1016/j.azn.2025.06.001.

Song, M. *et al.* (2019) '(S)-10-Hydroxycamptothecin Inhibits Esophageal Squamous Cell Carcinoma Growth In Vitro and In Vivo Via Decreasing Topoisomerase I Enzyme Activity', *Cancers*, 11(12), p. 1964. Available at: https://doi.org/10.3390/cancers11121964.

Srivastava, S. *et al.* (2012) 'Forensic examination of the spurious health drinks: Glucose', *Egyptian Journal of Forensic Sciences*, 2(4), pp. 131–138. Available at: https://doi.org/10.1016/j.ejfs.2012.06.001.

Staneviciute, E. *et al.* (2019) 'New in vitro model evaluating antiseptics' efficacy in biofilm-associated *Staphylococcus aureus* prosthetic vascular graft infection', *Journal of Medical Microbiology*, 68(3), pp. 432–439. Available at: https://doi.org/10.1099/jmm.0.000939.

Sun, N. *et al.* (2024) 'Composite Hydrogels with Rapid Self-Healing, Stretchable, Moldable and Antibacterial Properties Based on PVA/ε-Poly-l-lysine/Hyaluronic Acid', *Molecules*, 29(19), p. 4666. Available at: https://doi.org/10.3390/molecules29194666.

Sun, X. *et al.* (2021) 'The abaI/abaR Quorum Sensing System Effects on Pathogenicity in *Acinetobacter baumannii*', *Frontiers in Microbiology*, 12, p. 679241. Available at: https://doi.org/10.3389/fmicb.2021.679241.

Sun, Y. *et al.* (2008) 'In vitro multispecies Lubbock chronic wound biofilm model', *Wound Repair and Regeneration*, 16(6), pp. 805–813. Available at: https://doi.org/10.1111/j.1524-475X.2008.00434.x.

Szivák, I., Behra, R. and Sigg, L. (2009) 'METAL-INDUCED REACTIVE OXYGEN SPECIES PRODUCTION IN *CHLAMYDOMONAS REINHARDTII* (CHLOROPHYCEAE)[1]', *Journal of Phycology*, 45(2), pp. 427–435. Available at: https://doi.org/10.1111/j.1529-8817.2009.00663.x.

Tajkarimi, M.M., Ibrahim, S.A. and Cliver, D.O. (2010) 'Antimicrobial herb and spice compounds in food', *Food Control*, 21(9), pp. 1199–1218. Available at: https://doi.org/10.1016/J.FOODCONT.2010.02.003.

Teng, K. *et al.* (2021) 'Recent Development of Alginate-Based Materials and Their Versatile Functions in Biomedicine, Flexible Electronics, and Environmental Uses', *ACS Biomaterials Science & Engineering*, 7(4), pp. 1302–1337. Available at: https://doi.org/10.1021/acsbiomaterials.1c00116.

Teodorescu, M. *et al.* (2016) 'Viscoelastic and structural properties of poly(vinyl alcohol)/poly(vinylpyrrolidone) hydrogels', *RSC Advances*, 6(46), pp. 39718–39727. Available at: https://doi.org/10.1039/C6RA04319D.

Terreni, M., Taccani, M. and Pregnolato, M. (2021) 'New Antibiotics for Multidrug-Resistant Bacterial Strains: Latest Research Developments and Future Perspectives.', *Molecules (Basel, Switzerland)*, 26(9). Available at: https://doi.org/10.3390/molecules26092671.

Thaarup, I.C. and Bjarnsholt, T. (2021) 'Current *In Vitro* Biofilm-Infected Chronic Wound Models for Developing New Treatment Possibilities', *Advances in Wound Care*, 10(2), pp. 91–102. Available at: https://doi.org/10.1089/wound.2020.1176.

Thattaruparambil Raveendran, N. *et al.* (2019) 'Ciprofloxacin-and Fluconazole-Containing Fibrin-Nanoparticle-Incorporated Chitosan Bandages for the Treatment of Polymicrobial Wound Infections', *ACS Applied Bio Materials*, 2(1), pp. 243–254. Available at: https://doi.org/10.1021/acsabm.8b00585.

Thet, N.T. *et al.* (2024) 'On-demand release of silver from composite hydrogel by cold atmospheric plasma jet for wound infection control', *Applied Physics Letters*, 124(21), p. 211902. Available at: https://doi.org/10.1063/5.0206812.

Thomson, J.M. and Bonomo, R.A. (2005) 'The threat of antibiotic resistance in Gram-negative pathogenic bacteria: β-lactams in peril!', *Current Opinion in Microbiology*, 8(5). Available at: https://doi.org/10.1016/j.mib.2005.08.014.

Tian, Y. *et al.* (2026) 'Polyvinyl alcohol Hydrogels: Structure, Preparation, Modification Strategies and Biomedical Applications', *European Polymer Journal*, 244, p. 114517. Available at: https://doi.org/10.1016/j.eurpolymj.2026.114517.

Todorova, K. and Mandinova, A. (2020) 'Novel approaches for managing aged skin and nonmelanoma skin cancer', *Advanced Drug Delivery Reviews*, 153, pp. 18–27. Available at: https://doi.org/10.1016/j.addr.2020.06.004.

Tomaras, A.P. *et al.* (2003) 'Attachment to and biofilm formation on abiotic surfaces by *Acinetobacter baumannii*: involvement of a novel chaperone-usher pili assembly system.', *Microbiology (Reading, England)*, 149(Pt 12), pp. 3473–3484. Available at: https://doi.org/10.1099/mic.0.26541-0.

Tosa, N. *et al.* (2012) 'Simultaneous determination of some artificial sweeteners in ternary formulations by FT-IR and EI-MS'. *PROCESSES IN ISOTOPES AND MOLECULES (PIM 2011)*, Cluj Napoca, Romania, pp. 98–101. Available at: https://doi.org/10.1063/1.3681976.

Tracy, L.E., Minasian, R.A. and Caterson, E.J. (2016) 'Extracellular Matrix and Dermal Fibroblast Function in the Healing Wound', *Advances in Wound Care*, 5(3), pp. 119–136. Available at: https://doi.org/10.1089/wound.2014.0561.

Upmanyu, K., Haq, Q.Mohd.R. and Singh, R. (2022) 'Factors mediating *Acinetobacter baumannii* biofilm formation: Opportunities for developing therapeutics', *Current Research in Microbial Sciences*, 3, p. 100131. Available at: https://doi.org/10.1016/j.crmicr.2022.100131.

Van Cutsem, E. *et al.* (2002) 'Raltitrexed: current clinical status and future directions', *Annals of Oncology*, 13(4), pp. 513–522. Available at: https://doi.org/10.1093/annonc/mdf054.

Vardanyan, R.S. and Hruby, V.J. (2006) 'Antineoplastics', *Synthesis of Essential Drugs*. Elsevier, pp. 389–418. Available at: https://doi.org/10.1016/B978-044452166-8/50030-3.

Vaughn, V.M. *et al.* (2021) 'Antibiotic Overuse After Hospital Discharge: A Multi-hospital Cohort Study', *Clinical Infectious Diseases*, 73(11), pp. e4499–e4506. Available at: https://doi.org/10.1093/cid/ciaa1372.

Ventola, C. Lee (2015) 'The antibiotic resistance crisis: part 1: causes and threats', *P & T: A Peer-Reviewed Journal for Formulary Management*, 40(4), pp. 277–283.

Ventola, C Lee (2015) 'The Antibiotics Resistance Crisis Part: Part 1: Causes and Threats', *Pharmacy and therapeutics.*, 40(4).

Verma, T. *et al.* (2022) 'Current challenges and advancements towards discovery and resistance of antibiotics', *Journal of Molecular Structure*, 1248, pp. 131380–131380. Available at: https://doi.org/10.1016/j.molstruc.2021.131380.

Vesel Nina and Blokesch Melanie (2021) 'Pilus Production in *Acinetobacter baumannii* Is Growth Phase Dependent and Essential for Natural Transformation', *Journal of Bacteriology*, 203(8), p. 10.1128/jb.00034-21. Available at: https://doi.org/10.1128/jb.00034-21.

Vijayakumar, S. *et al.* (2016) 'Biofilm Formation and Motility Depend on the Nature of the *Acinetobacter baumannii* Clinical Isolates.', *Frontiers in public health*, 4, pp. 105–105. Available at: https://doi.org/10.3389/fpubh.2016.00105.

Vlad, R.-A. *et al.* (2025) 'Hydroxypropyl Methylcellulose—A Key Excipient in Pharmaceutical Drug Delivery Systems', *Pharmaceutics*, 17(6), p. 784. Available at: https://doi.org/10.3390/pharmaceutics17060784.

Vo, T.S. *et al.* (2022) 'Enhancement of water absorption capacity and compressibility of hydrogel sponges prepared from gelatin/chitosan matrix with different polyols', *Progress in Natural Science: Materials International*, 32(1), pp. 54–62. Available at: https://doi.org/10.1016/j.pnsc.2021.10.001.

Walsh, C. (2005) 'Antibiotics: Actions, Origins, Resistance', *Natural Product Reports*, 22(2), pp. 304–305. Available at: https://doi.org/10.1039/B417591N.

Wang, C. *et al.* (2022) 'Facile fabrication and characterization of high-performance Borax-PVA hydrogel', *Journal of Sol-Gel Science and Technology*, 101(1), pp. 103–113. Available at: https://doi.org/10.1007/s10971-021-05584-0.

Wang, L., Zhou, F. and Xie, W. (2025) 'Advances in hyaluronic acid-based biomaterials: applications in cancer therapy, wound healing, and disease management', *Journal of Materials Science. Materials in Medicine*, 36(1), p. 91. Available at: https://doi.org/10.1007/s10856-025-06946-8.

Wang, M. *et al.* (2021) 'Poly(vinyl alcohol) Hydrogels: The Old and New Functional Materials', *International Journal of Polymer Science*. Edited by C. Vasile, 2021, pp. 1–16. Available at: https://doi.org/10.1155/2021/2225426.

Wang, Y. *et al.* (2020) 'Non-antibiotic pharmaceuticals enhance the transmission of exogenous antibiotic resistance genes through bacterial transformation', *The ISME Journal*, 14(8), pp. 2179–2196. Available at: https://doi.org/10.1038/s41396-020-0679-2.

Waresindo, W.X. *et al.* (2021) 'A freeze-thaw PVA hydrogel loaded with guava leaf extract: physical and antibacterial properties', *RSC Advances*, 11(48). Available at: https://doi.org/10.1039/d1ra04092h.

Waresindo, W.X. *et al.* (2023) 'Freeze-thaw hydrogel fabrication method: basic principles, synthesis parameters, properties, and biomedical applications', *Materials Research Express*, 10(2). Available at: https://doi.org/10.1088/2053-1591/acb98e.

Wen, Y. *et al.* (2022) 'Comparative Study of Physicochemical Properties of Alginate Composite Hydrogels Prepared by the Physical Blending and Electrostatic Assembly Methods', *Gels*, 8(12), p. 799. Available at: https://doi.org/10.3390/gels8120799.

Wheeler, J.C. *et al.* (1996) 'Evolution of hydrogel polymers as contact lenses, surface coatings, dressings, and drug delivery systems', *Journal of Long-Term Effects of Medical Implants*, 6(3–4), pp. 207–217.

Whiteway, C. *et al.* (2022) '*Acinetobacter baumannii*', *Trends in Microbiology*, 30(2), pp. 199–200. Available at: https://doi.org/10.1016/J.TIM.2021.11.008.

Williams, C.L. *et al.* (2016) 'Copper Resistance of the Emerging Pathogen Acinetobacter baumannii', *Applied and Environmental Microbiology*. Edited by E.G. Dudley, 82(20), pp. 6174–6188. Available at: https://doi.org/10.1128/AEM.01813-16.

WHO (2014) 'Antimicrobial resistance. Global report on surveillance', *World Health Organization*, 61(3). Available at: https://doi.org/10.1007/s13312-014-0374-3.

WHO (2021) *2021 Antibacterial Agents in Clinical and Preclinical Development: an overview and analysis*. (World Health Organization 2021).

WHO (2024a) *WHO Bacterial Priority Pathogens List 2024: Bacterial Pathogens of Public Health Importance, to Guide Research, Development, and Strategies to Prevent and Control Antimicrobial Resistance*. 1st ed. Geneva: World Health Organization.

WHO (2024b) 'WHO releases report on state of development of antibacterials'. Available at: https://www.who.int/news/item/14-06-2024-who-releases-report-on-state-of-development-of-antibacterials.

WHO Antibacterial Pipeline Team (2022) 'Lack of innovation set to undermine antibiotic performance and health gains'. Available at: https://www.who.int/news/item/22-06-2022-22-06-2022-lack-of-innovation-set-to-undermine-antibiotic-performance-and-health-gains.

WICHTERLE, O. and LÍM, D. (1960) 'Hydrophilic Gels for Biological Use', *Nature*, 185(4706), pp. 117–118. Available at: https://doi.org/10.1038/185117a0.

Wilharm, G. *et al.* (2013) 'DNA Uptake by the Nosocomial Pathogen *Acinetobacter baumannii* Occurs during Movement along Wet Surfaces', *Journal of Bacteriology*, 195(18), pp. 4146–4153. Available at: https://doi.org/10.1128/JB.00754-13.

Witkowski, M. *et al.* (2023) 'The artificial sweetener erythritol and cardiovascular event risk', *Nature Medicine*, 29(3), pp. 710–718. Available at: https://doi.org/10.1038/s41591-023-02223-9.

Wright, A.J. (1999) 'The penicillins'. *Mayo Clinic Proceedings*. Available at: https://doi.org/10.4065/74.3.290.

Wu, Y., Joseph, S. and Aluru, N.R. (2009) 'Effect of Cross-Linking on the Diffusion of Water, Ions, and Small Molecules in Hydrogels', *The Journal of Physical Chemistry B*, 113(11), pp. 3512–3520. Available at: https://doi.org/10.1021/jp808145x.

Xin, H. *et al.* (2025) 'Macro/Microgel-Encapsulated, Biofilm-Armored Living Probiotic Platform for Regenerating Bacteria-Infected Diabetic Wounds', *Advanced Healthcare Materials*, 14(7), p. 2403476. Available at: https://doi.org/10.1002/adhm.202403476.

Xing, L. *et al.* (2018) 'Yeast fermentation inspired Ca-alginate hydrogel membrane: lower transparency, hierarchical pore structure and higher hydrophobicity', *RSC Advances*, 8(5), pp. 2622–2631. Available at: https://doi.org/10.1039/C7RA10904K.

Xing, Q. *et al.* (2014) 'Increasing mechanical strength of gelatin hydrogels by divalent metal ion removal', *Scientific Reports*, 4, p. 4706. Available at: https://doi.org/10.1038/srep04706.

Xu, J. *et al.* (2024) 'Chitosan-Based Hydrogels as Antibacterial/Antioxidant/Anti-Inflammation Multifunctional Dressings for Chronic Wound Healing', *Advanced Healthcare Materials*, 13(30), p. 2401490. Available at: https://doi.org/10.1002/adhm.202401490.

Yin, I.X. *et al.* (2020) 'The antibacterial mechanism of silver nanoparticles and its application in dentistry', *International Journal of Nanomedicine*, 15. Available at: https://doi.org/10.2147/IJN.S246764.

Yoon, E.-J. *et al.* (2015) 'Contribution of Resistance-Nodulation-Cell Division Efflux Systems to Antibiotic Resistance and Biofilm Formation in *Acinetobacter baumannii*', *mBio*. Edited by G.D. Wright, 6(2), pp. e00309-15. Available at: https://doi.org/10.1128/mBio.00309-15.

Yu, K. *et al.* (2021) 'Bloodstream infections caused by ST2 *Acinetobacter baumannii*: risk factors, antibiotic regimens, and virulence over 6 years period in China', *Antimicrobial Resistance and Infection Control*, 10(1). Available at: https://doi.org/10.1186/s13756-020-00876-6.

Yu, Y. *et al.* (2019) 'Multifunctional "Hydrogel Skins" on Diverse Polymers with Arbitrary Shapes', *Advanced Materials*, 31(7), p. 1807101. Available at: https://doi.org/10.1002/adma.201807101.

Yu, Z. and Guo, J. (2022) 'Non-caloric artificial sweeteners exhibit antimicrobial activity against bacteria and promote bacterial evolution of antibiotic tolerance', *Journal of Hazardous Materials*, 433. Available at: https://doi.org/10.1016/j.jhazmat.2022.128840.

Zandraa, O. *et al.* (2021) 'Development of dual crosslinked mumio-based hydrogel dressing for wound healing application: Physico-chemistry and antimicrobial activity', *International Journal of Pharmaceutics*, 607, pp. 120952–120952. Available at: https://doi.org/10.1016/J.IJPHARM.2021.120952.

Zanoos, K.A. *et al.* (2025) 'OmpA virulence factor, a promising conserved vaccine candidate against *Acinetobacter baumannii*, could trigger autoreactive immune responses in susceptible population', *BMC Immunology*, 26(1), p. 85. Available at: https://doi.org/10.1186/s12865-025-00766-9.

Graça, K. *et al.* (2023) 'Bacterial Motility and Its Role in Skin and Wound Infections', *International Journal of Molecular Sciences*, 24(2), p. 1707. Available at: https://doi.org/10.3390/ijms24021707.

Zhang, B. *et al.* (2021) 'Direct ink writing of polycaprolactone / polyethylene oxide based 3D constructs', *Progress in Natural Science: Materials International*, 31(2), pp. 180–191. Available at: https://doi.org/10.1016/j.pnsc.2020.10.001.

Zhang, B. *et al.* (2022) 'Direct ink writing of vancomycin-loaded polycaprolactone/ polyethylene oxide/ hydroxyapatite 3D scaffolds', *Journal of the American Ceramic Society*, 105(3), pp. 1821–1840. Available at: https://doi.org/10.1111/jace.18048.

Zhang, J. *et al.* (2025) 'Carboxymethyl Chitosan-Based Antioxidant Hydrogel Accelerates Diabetic Wound Healing', *Advanced Healthcare Materials*, 14(4), p. 2403198. Available at: https://doi.org/10.1002/adhm.202403198.

Zhang, L. *et al.* (2024) 'Research progress on blood compatibility of hemoperfusion adsorbent materials', *Frontiers in Bioengineering and Biotechnology*, 12, p. 1456694. Available at: https://doi.org/10.3389/fbioe.2024.1456694.

Zhang, Q. *et al.* (2022) 'Preparation of aloe polysaccharide/honey/PVA composite hydrogel: Antibacterial activity and promoting wound healing', *International Journal of Biological Macromolecules*, 211, pp. 249–258. Available at: https://doi.org/10.1016/J.IJBIOMAC.2022.05.072.

Zhang, R. *et al.* (1998) 'Preclinical pharmacology of the natural product anticancer agent 10-hydroxycamptothecin, an inhibitor of topoisomerase I', *Cancer Chemotherapy and Pharmacology*, 41(4), pp. 257–267. Available at: https://doi.org/10.1007/s002800050738.

Zhang, T. *et al.* (2016) 'Occurrence of artificial sweeteners in human liver and paired blood and urine samples from adults in Tianjin, China and their implications for human exposure',

Environmental Science: Processes and Impacts, 18(9). Available at: https://doi.org/10.1039/c6em00130k.

Zhang, Y. *et al.* (2018) 'Natural compound sanguinarine chloride targets the type III secretion system of *Salmonella enterica* Serovar Typhimurium', *Biochemistry and Biophysics Reports*, 14, pp. 149–154. Available at: https://doi.org/10.1016/j.bbrep.2018.04.011.

Zhang, Y. *et al.* (2023) 'Application of Collagen-Based Hydrogel in Skin Wound Healing', *Gels*, 9(3), p. 185. Available at: https://doi.org/10.3390/gels9030185.

Zhao, R. *et al.* (2016) 'Inflammation in Chronic Wounds', *International Journal of Molecular Sciences*, 17(12). Available at: https://doi.org/10.3390/ijms17122085.

Zhen, X. *et al.* (2020) 'Clinical and economic burden of carbapenem-resistant infection or colonization caused by klebsiella pneumoniae, pseudomonas aeruginosa, acinetobacter baumannii: A multicenter study in China', *Antibiotics*, 9(8). Available at: https://doi.org/10.3390/antibiotics9080514.

Zhou, X. and Li, Y. (2015) *Atlas of oral microbiology: from healthy microflora to disease*. Amsterdam ; New York : [Hangzhou, China]: Elsevier/AP, Academic Press is an imprint of Elsevier ; Zhejiang University Press.

Zhong, Y. *et al.* (2024) 'Construction methods and biomedical applications of PVA-based hydrogels', *Frontiers in Chemistry*, 12, p. 1376799. Available at: https://doi.org/10.3389/fchem.2024.1376799.

Zhu, J. (2010) 'Bioactive modification of poly(ethylene glycol) hydrogels for tissue engineering', *Biomaterials*, 31(17), pp. 4639–4656. Available at: https://doi.org/10.1016/j.biomaterials.2010.02.044.

Zidan, H.M. *et al.* (2019) 'Characterization and some physical studies of PVA/PVP filled with MWCNTs', *Journal of Materials Research and Technology*, 8(1), pp. 904–913. Available at: https://doi.org/10.1016/j.jmrt.2018.04.023.

Zimbler, D.L. *et al.* (2009) 'Iron acquisition functions expressed by the human pathogen *Acinetobacter baumannii*', *BioMetals*, 22(1), pp. 23–32. Available at: https://doi.org/10.1007/s10534-008-9202-3.

Appendix

Chapter 2 Appendices

A1.1 Release Profiles of SACC from PVA-Borate Hydrogels

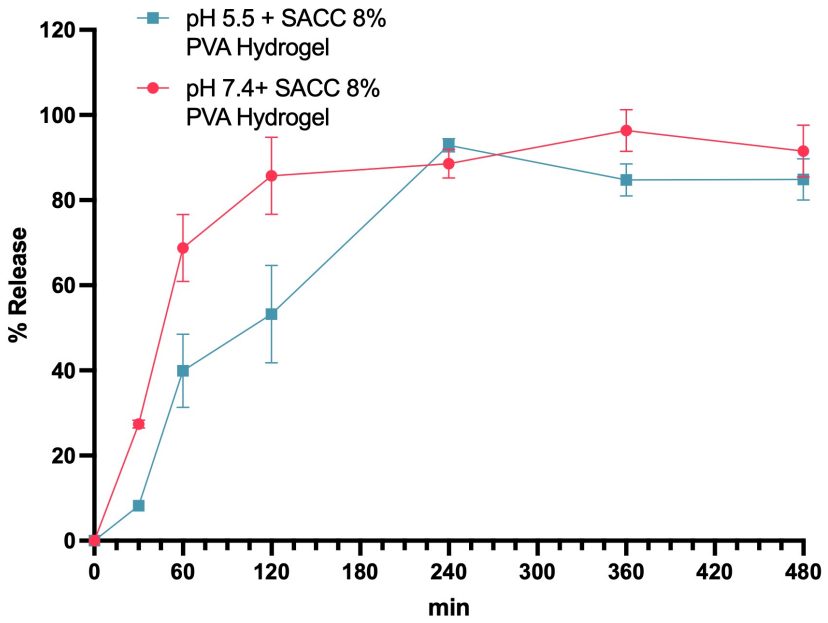

Figure A1.0.1 Release Profiles of SACC from PVA-borate hydrogels. A. Cumulative release (%) of SACC over 480min from 8% SACC-Loaded PVA borate hydrogel. The 8% SACC-loaded PVA borate hydrogel showed faster early-stage release at pH 5.5, while at pH 7.4it demonstrated more controlled release behaviour at later time points. Data are presented as mean ± SD (n = 3).

A1.2 XRD Spectra of the PVA powder and PVA-Hydrogel

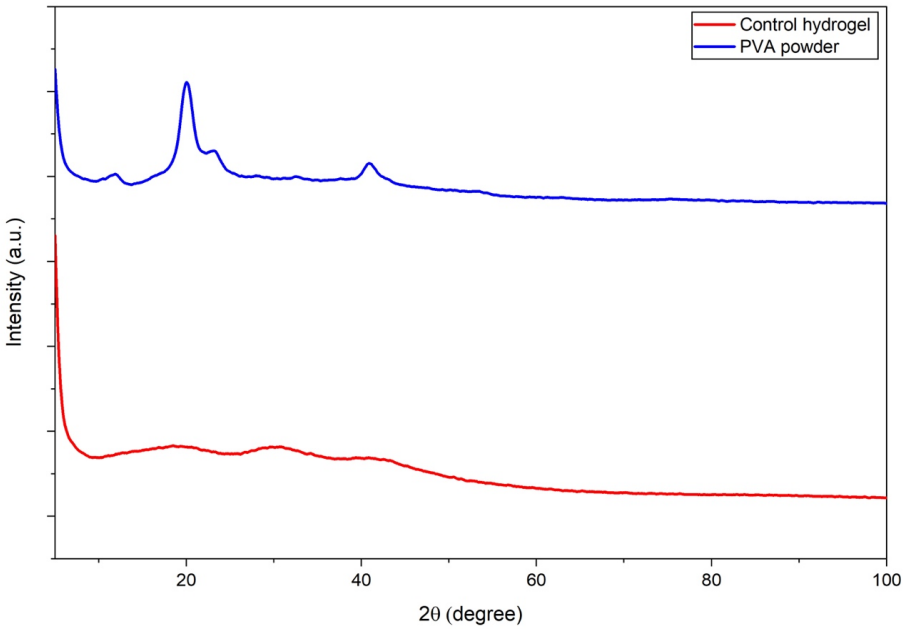

Figure A2.0.2 XRD Spectra of the PVA powder and PVA-Hydrogel

A1.3 Ethics Letter of Approval

College of Health, Medicine and Life Sciences Research Ethics Committee (DLS)
Brunel University of London
Kingston Lane
Uxbridge
UB8 3PH
United Kingdom

www.brunel.ac.uk

21 November 2024

CONDITIONAL LETTER OF APPROVAL

APPROVAL HAS BEEN GRANTED FOR THIS STUDY TO BE CARRIED OUT BETWEEN 21/11/2024 AND 30/09/2025

Applicant (s): Miss Jie Han

Project Title: Testing Artificial Sweetener-Loaded PVA Hydrogel's Effect on Healthy Human

Reference: 47765-MHR-Nov/2024- 53276-3

Dear Miss Jie Han

The Research Ethics Committee has considered the above application recently submitted by you.

The Chair, acting under delegated authority has agreed that there is no objection on ethical grounds to the proposed study. Approval is given on the understanding that the conditions of approval set out below are followed:

PIS - Voluntary Participation and Withdrawal – please remove "you may only withdraw your data up to two weeks after the study. After this point, the data will have been anonymized and cannot be linked back to you for removal." You have already confirmed that participants can withdraw their data by 30th September 2025. The former sentence is contradictory.

Please update the PIS and send in via correspondence for checking before commencing the study. Please also ensure you update any relevant documents with the ethical approval start date.

- **The agreed protocol must be followed. Any changes to the protocol will require prior approval from the Committee by way of an application for an amendment.**

Please note that:

- Research Participant Information Sheets and (where relevant) flyers, posters, and consent forms should include a clear statement that research ethics approval has been obtained from the relevant Research Ethics Committee.
- The Research Participant Information Sheets should include a clear statement that queries should be directed, in the first instance, to the Supervisor (where relevant), or the researcher. Complaints, on the other hand, should be directed, in the first instance, to the Chair of the relevant Research Ethics Committee.
- Approval to proceed with the study is granted subject to any conditions that may appear above.
- The Research Ethics Committee reserves the right to sample and review documentation, including raw data, relevant to the study.
- If your project has been approved to run for a duration longer than 12 months, you will be required to submit an annual progress report to the Research Ethics Committee. You will be contacted about submission of this report before it becomes due.
- You may not undertake any research activity if you are not a registered student of Brunel University or if you cease to become registered, including abeyance or temporary withdrawal. As a deregistered student you would not be insured to undertake research activity. Research activity includes the recruitment of participants, undertaking consent procedures and collection of data. Breach of this requirement constitutes research misconduct and is a disciplinary offence.

Professor Louise Mansfield

Chair of the College of Health, Medicine and Life Sciences Research Ethics Committee (DLS)

Brunel University London

Figure A1.0.3 Ethics Letter of Approval.

A1.4 Medical History Questionnaire for Skin Health Screening

Participant ID: _____
Date: _____

Section 1: General Information

1. **Full Name:** _____
2. **Age:** _____
3. **Gender:** _____

Section 2: Skin Health History

1. **Do you have any current or previous skin conditions?**
   (Examples include eczema, psoriasis, dermatitis, acne, rosacea, etc.)
   - ☐ No
   - ☐ Yes (Please specify): _____
2. **Have you ever been diagnosed with any of the following skin conditions?**
   (Please check all that apply)
   - ☐ Eczema
   - ☐ Psoriasis
   - ☐ Dermatitis
   - ☐ Rosacea
   - ☐ Other (Please specify): _____
3. **Have you experienced any recent skin irritations, rashes, or infections?**
   - ☐ No
   - ☐ Yes (Please specify the affected area and cause, if known):
     _____
4. **Do you have any scars, lesions, or wounds on the skin where the hydrogel will be applied (forearms and Upper arm)?**
   - ☐ No
   - ☐ Yes (Please specify): _____

5. **Do you have any tattoos or piercings on your forearms (or the area where the hydrogel will be applied)?**
    - ☐ No
    - ☐ Yes (Please specify): _____

Section 3: Allergies and Sensitivities

1. **Do you have any known allergies or sensitivities to skin products or materials?**
    - ☐ No
    - ☐ Yes (Please specify): _____
2. **Have you ever experienced an allergic reaction to any of the following substances?**
   (Please check all that apply)
    - ☐ Polyvinyl Alcohol (PVA)
    - ☐ Borax or boron-based compounds
    - ☐ Artificial sweeteners (Acesulfame K, Saccharin, etc.)
    - ☐ Skincare or cosmetic products
    - ☐ Soaps or detergents
    - ☐ Other (Please specify): _____
3. **Have you ever had a reaction to any medical products, dressings, or adhesives applied to your skin (e.g., bandages, wound dressings, or patches)?**
    - ☐ No
    - ☐ Yes (Please specify): _____

Section 4: Medications and Treatments

1. **Are you currently using any medications (oral or topical) to treat a skin condition?**
    - ☐ No
    - ☐ Yes (Please specify): _____
2. **Have you recently used any prescription or over-the-counter skincare products (e.g., topical steroids, acne treatments, moisturizers)?**
    - ☐ No

- ☐ Yes (Please specify): _____

Section 5: Additional Information

1. **Do you have any other medical conditions that may affect your skin health or ability to participate in this study?**
   - ☐ No
   - ☐ Yes (Please specify): _____
2. **Is there anything else you would like to share regarding your skin health that you believe is important for this study?**
   - ☐ No
   - ☐ Yes (Please specify): _____

Consent

I confirm that the above information is accurate and complete to the best of my knowledge. I understand that providing false information may impact my ability to participate in the study. I also understand that this information will be kept confidential and used solely for the purposes of determining my eligibility for this study.

Signature: _____

Date: _____

Chapter 3 Appendices

A2.1 Differentially Expressed Genes of *A. baumannii* in LB broth vs in LCWB medium

Locustag	Gene	logFC	PValue	LCWB_1	LCWB_2	LCWB_3	LB_1	LB_2	LB_3
ABUW_RS20145		-10.585	3.76e-16	62.735	89.094	83.769	0.000	0.158	0.000
ABUW_RS05760	basE	-9.548	1.98e-11	1203.474	3219.328	4524.045	5.684	4.061	2.001
ABUW_RS05765	basF	-8.682	8.11e-15	955.108	1860.782	2206.314	4.344	4.061	3.768
ABUW_RS05725	bauD	-8.681	1.36e-11	184.401	295.665	393.376	0.905	1.002	0.186
ABUW_RS05770	basG	-8.615	2e-13	1611.640	2467.453	3649.919	8.797	5.748	4.932
ABUW_RS05800	basJ	-8.423	1.61e-13	1724.696	4095.582	3830.905	10.245	8.701	9.072
ABUW_RS00710		-8.110	1.32e-09	2928.394	7640.930	6643.811	29.395	21.463	11.166
ABUW_RS05755	basD	-7.849	2.04e-13	2029.982	4790.800	5276.989	20.526	15.873	15.911
ABUW_RS05710	bauF	-7.836	3.25e-09	173.219	589.138	983.965	3.149	1.477	2.838
ABUW_RS05730	bauC	-7.821	2.27e-11	267.377	431.114	410.580	1.412	2.162	1.396
ABUW_RS05715	basA	-7.590	6.44e-10	562.598	2129.707	2230.656	9.702	7.278	8.421
ABUW_RS05750	basC	-7.162	5.47e-14	1307.696	2334.634	2816.287	16.725	12.129	16.097
ABUW_RS05780	barA	-7.151	3.63e-16	3132.029	3753.453	5281.421	28.562	27.528	29.497
ABUW_RS10525		-7.132	1.16e-08	91.250	220.817	197.589	1.122	1.055	1.442
ABUW_RS14485		-6.662	1.19e-11	149.735	61.149	89.629	1.014	0.686	1.210
ABUW_RS05720	basB	-6.600	4.41e-12	1231.095	2139.570	2143.056	23.965	17.666	14.981
ABUW_RS05785	barB	-6.573	3.94e-16	2216.172	2516.439	3186.673	28.309	28.108	26.752
ABUW_RS10640		-6.569	1.77e-08	563.269	2067.681	2138.698	21.177	16.190	12.655
ABUW_RS14490		-6.538	1.61e-13	1036.853	582.234	721.389	8.000	6.856	10.282
ABUW_RS10520		-6.391	2.39e-07	925.362	2461.974	2988.633	30.445	25.524	19.866
ABUW_RS14495		-6.357	8.42e-13	387.031	590.563	765.264	7.494	5.221	8.421
ABUW_RS10630		-6.355	5.28e-10	987.314	1950.095	1990.920	21.105	20.725	18.331
ABUW_RS05790	basH	-6.327	1.68e-13	242.327	216.324	227.340	2.172	2.162	4.234
ABUW_RS05735	bauE	-6.326	1.4e-15	472.801	746.943	738.368	8.724	7.119	8.467
ABUW_RS14160		-6.237	1.9e-07	1227.740	4573.380	4369.054	51.912	48.675	34.149
ABUW_RS20235		-6.133	4.47e-08	1.677	4.274	1.878	0.036	0.000	0.047
ABUW_RS10635		-5.979	1.12e-08	529.274	1404.024	1618.204	22.625	18.932	14.609
ABUW_RS05740	bauB	-5.948	5.87e-14	1672.585	2378.250	2776.769	38.590	39.446	32.521
ABUW_RS10585		-5.816	2.34e-09	275.204	800.202	907.033	13.865	11.707	9.491
ABUW_RS10080		-5.697	3.7e-07	541.910	2285.868	3407.402	48.907	38.339	32.753
ABUW_RS10070		-5.598	1.12e-08	8.051	9.096	16.904	0.471	0.158	0.000
ABUW_RS04720		-5.450	2.59e-06	7.269	7.342	2.404	0.109	0.000	0.233
ABUW_RS10615		-5.423	1.01e-14	136.428	131.723	151.460	3.330	3.164	3.257
ABUW_RS10075		-5.204	1.05e-08	441.602	1324.684	1796.410	34.970	30.956	30.660
ABUW_RS06610	hemP	-5.138	4.25e-09	336.485	922.939	1062.024	24.508	23.678	17.679
ABUW_RS01510		-5.136	2.32e-07	22.142	59.396	34.033	1.520	0.633	0.977
ABUW_RS05745	bauA	-5.131	1.4e-13	1631.992	2023.518	2729.288	66.682	56.322	59.040
ABUW_RS10620		-5.103	9.62e-12	671.628	1231.864	1082.008	30.445	31.483	24.937
ABUW_RS14475		-4.924	3.52e-12	266.594	156.161	137.411	7.168	5.485	5.629
ABUW_RS08385	fumC	-4.911	2.26e-09	1133.135	3638.716	4777.906	105.453	110.481	101.609
ABUW_RS20610		-4.894	2.14e-06	1.006	1.534	2.930	0.145	0.000	0.000
ABUW_RS05795	basI	-4.858	6.52e-10	22.589	13.041	29.150	0.362	1.371	0.651
ABUW_RS10625		-4.844	4.22e-11	836.908	1518.762	1938.555	52.781	52.841	43.919
ABUW_RS06655		-4.801	1.44e-10	159.017	385.416	499.157	14.227	10.283	12.794
ABUW_RS08070		-4.722	2.15e-07	230.586	580.152	373.091	18.571	14.977	11.119
ABUW_RS14500		-4.672	6.02e-07	11.294	29.808	75.505	1.448	1.635	1.582
ABUW_RS14505		-4.543	1.37e-07	12.189	42.300	53.116	2.208	1.371	0.930
ABUW_RS10530		-4.496	4.78e-10	136.316	283.829	354.759	13.141	8.965	12.096
ABUW_RS10610		-4.488	1.57e-12	41.599	57.314	54.018	2.896	2.426	1.396
ABUW_RS20540		-4.438	3.04e-05	8.499	14.904	4.282	0.724	0.105	0.279
ABUW_RS14480		-4.431	1.48e-09	21.694	12.493	24.567	1.014	1.002	0.698

Locustag	Gene	logFC	PValue	LCWB_1	LCWB_2	LCWB_3	LB_1	LB_2	LB_3
ABUW_RS02965		-4.344	1.33e-10	22.924	13.370	11.495	0.615	1.055	0.698
ABUW_RS07805		-4.318	2.6e-07	111.826	446.675	396.606	18.028	14.819	14.934
ABUW_RS14470		-4.308	9.93e-10	53.677	28.164	32.005	1.376	2.162	2.280
ABUW_RS10600		-4.306	1.41e-09	42.606	50.300	26.220	3.149	1.266	1.303
ABUW_RS09310		-4.303	0.00953895	1.230	5.479	3.231	0.217	0.158	0.093
ABUW_RS09530		-4.221	1.74e-05	1.230	1.863	0.751	0.000	0.158	0.047
ABUW_RS00040		-4.202	3.29e-08	29.410	25.095	11.795	1.520	0.738	1.163
ABUW_RS19795		-3.986	0.000275267	2.125	2.740	0.676	0.253	0.000	0.000
ABUW_RS01270		-3.916	1.76e-11	179.481	199.776	146.201	13.105	8.754	12.748
ABUW_RS16655		-3.819	2.67e-09	667.267	1101.784	1641.795	93.760	75.043	72.811
ABUW_RS16845		-3.474	1.52e-05	5.256	52.163	35.386	3.077	2.690	2.559
ABUW_RS01815		-3.420	0.0126835	4.138	0.658	191.729	7.313	5.906	5.443
ABUW_RS15515		-3.394	1.26e-05	294.215	1682.922	1165.552	84.710	99.248	115.148
ABUW_RS10535		-3.359	1.22e-07	7.269	10.520	9.015	0.869	0.738	0.977
ABUW_RS10590		-3.292	3.53e-09	18.563	18.301	17.054	1.412	2.109	2.047
ABUW_RS03435		-3.224	1.59e-07	437.241	1059.155	976.302	103.208	93.975	67.321
ABUW_RS18750		-3.212	3.47e-08	61.504	26.958	32.756	4.597	5.221	3.210
ABUW_RS18705		-3.206	6.87e-11	236.512	170.517	167.463	24.291	21.094	16.702
ABUW_RS13850		-3.159	1.71e-06	38.356	40.766	11.946	3.620	2.848	3.489
ABUW_RS15160	otsB	-3.145	0.0128502	0.447	1.096	0.601	0.145	0.000	0.047
ABUW_RS11865		-3.130	0.0156789	0.335	0.329	0.902	0.000	0.000	0.186
ABUW_RS15520		-3.123	2.79e-05	1189.943	6911.412	4473.784	457.432	479.577	506.047
ABUW_RS06595		-3.102	9.96e-11	187.309	165.366	197.364	22.444	19.670	21.866
ABUW_RS16650		-2.979	2.46e-08	1351.420	2290.252	2399.697	249.351	290.415	226.853
ABUW_RS16645		-2.946	2.91e-08	363.659	545.303	626.802	60.636	84.852	54.015
ABUW_RS10595		-2.896	4.23e-10	181.829	253.364	136.585	27.513	24.153	24.984
ABUW_RS09095		-2.890	0.0241857	1.230	0.110	0.225	0.000	0.000	0.186
ABUW_RS00790		-2.785	1.09e-05	132.961	407.005	392.174	59.767	42.083	33.265
ABUW_RS18710		-2.727	1.14e-11	126.923	126.134	129.072	18.281	20.198	19.261
ABUW_RS02810		-2.691	0.00195921	1.342	0.438	1.352	0.253	0.105	0.093
ABUW_RS17685	FeoB	-2.597	4.9e-08	1300.204	2485.535	2760.316	349.120	414.185	318.553
ABUW_RS17680		-2.568	2.66e-06	48.533	133.915	72.800	13.575	17.455	12.050
ABUW_RS09390		-2.517	0.00645293	0.112	2.411	1.127	0.145	0.158	0.326
ABUW_RS15525		-2.512	0.00128382	327.427	2880.266	1676.204	313.643	291.364	250.906
ABUW_RS07750		-2.510	5.55e-05	24.378	6.246	9.316	2.027	1.846	3.024
ABUW_RS18900		-2.494	0.000300096	5.815	2.849	0.977	0.688	0.580	0.279
ABUW_RS14440		-2.482	9.34e-09	38.916	24.986	28.925	6.842	4.483	5.071
ABUW_RS06600		-2.411	6.74e-09	161.589	83.067	101.950	22.046	19.354	23.634
ABUW_RS17210		-2.398	0.0086265	98.966	48.109	859.927	70.772	62.281	58.714
ABUW_RS20575		-2.336	0.0206091	1.901	0.548	0.676	0.145	0.316	0.140
ABUW_RS18100		-2.307	9.68e-09	924.468	943.432	599.530	175.718	187.211	135.619
ABUW_RS18105		-2.290	6.56e-10	562.039	472.647	376.547	103.570	89.545	95.143
ABUW_RS10295		-2.290	3.16e-08	33.660	58.519	41.997	9.702	8.227	9.398
ABUW_RS01865		-2.254	6.22e-07	1478.790	735.546	534.618	160.623	240.843	174.699
ABUW_RS18395		-2.238	0.0326295	22.365	520.975	21.111	39.857	42.769	36.615
ABUW_RS12395		-2.220	1.16e-05	20.241	8.438	15.026	3.294	3.270	2.791
ABUW_RS08765		-2.212	1.45e-06	319.711	405.032	258.669	79.642	73.513	58.946
ABUW_RS10310		-2.196	0.000190623	38.021	118.134	215.170	28.345	24.469	28.566

Locustag	Gene	logFC	PValue	LCWB_1	LCWB_2	LCWB_3	LB_1	LB_2	LB_3
ABUW_RS11710		-2.186	0.00099404	2.684	8.767	19.684	2.172	2.900	2.140
ABUW_RS13055		-2.181	2.09e-06	182.277	123.943	65.437	30.336	28.214	23.076
ABUW_RS04555		-2.179	4.66e-05	55.801	19.835	15.176	6.190	9.071	4.652
ABUW_RS09395		-2.171	0.00718287	2.013	4.603	0.902	0.362	0.580	0.651
ABUW_RS02145		-2.160	0.000994297	4.585	1.096	3.080	0.471	0.686	0.837
ABUW_RS17690	feoA	-2.152	1.42e-06	28.516	64.985	54.994	11.258	11.180	11.026
ABUW_RS02215		-2.144	1.35e-05	11.071	9.534	5.409	1.846	1.898	2.001
ABUW_RS11715		-2.141	0.00377827	2.237	1.753	2.630	0.145	0.475	0.977
ABUW_RS16540		-2.140	0.000566617	1563.107	3410.447	2663.024	756.993	583.888	391.596
ABUW_RS04520		-2.122	0.000198016	2.348	3.726	2.780	0.941	0.422	0.558
ABUW_RS18825		-2.062	0.00525008	2.348	3.397	0.902	0.796	0.105	0.465
ABUW_RS05915		-2.018	0.00362947	1.118	2.301	1.503	0.362	0.369	0.465
ABUW_RS17505	secE	-2.001	1.9e-05	2847.320	865.077	984.791	361.066	452.629	359.448
ABUW_RS18200		-1.987	0.000203311	877.389	231.337	223.734	106.937	122.241	106.634
ABUW_RS06200		-1.971	0.0116217	0.671	3.836	1.653	0.724	0.211	0.512
ABUW_RS14430	betA	-1.968	3.27e-10	2060.958	2052.997	1766.284	488.891	543.387	470.223
ABUW_RS10605		-1.934	9.5e-06	1621.816	3557.622	2930.709	819.910	697.903	604.678
ABUW_RS14425	betB	-1.921	4.76e-10	2959.370	3151.713	3293.131	769.772	882.794	830.322
ABUW_RS03590		-1.854	1.52e-09	374.059	319.774	284.739	88.945	99.881	81.743
ABUW_RS14345		-1.853	0.000557805	3.131	1.425	2.930	0.507	1.160	0.512
ABUW_RS10305		-1.845	2.09e-05	21.694	33.314	25.844	8.254	7.225	6.932
ABUW_RS11310		-1.828	3.26e-07	42.047	23.232	39.668	9.919	10.020	9.677
ABUW_RS10495		-1.814	0.00980905	5.479	24.657	1.728	2.244	3.533	3.024
ABUW_RS14450		-1.802	1.01e-05	216.048	471.223	237.032	89.850	93.078	82.069
ABUW_RS15105		-1.788	1.6e-05	5139.534	2180.884	1699.419	730.748	980.565	899.597
ABUW_RS04890	ybgC	-1.786	5.18e-09	259.101	186.297	189.926	64.039	60.224	59.877
ABUW_RS03005		-1.780	4.95e-10	2296.016	2866.458	2511.864	699.507	828.792	706.427
ABUW_RS20105		-1.766	0.000176306	30.976	10.849	12.021	4.742	6.856	4.141
ABUW_RS08465		-1.762	2.43e-08	1349.184	1052.470	760.907	311.688	318.945	301.385
ABUW_RS03220		-1.762	6.49e-06	500.199	250.296	258.143	114.503	111.378	71.322
ABUW_RS04085		-1.761	0.00038037	9.393	16.328	7.137	3.149	2.215	4.094
ABUW_RS13330		-1.748	4.15e-05	810.964	314.623	459.564	154.251	171.654	145.994
ABUW_RS08735	cydB	-1.737	6.58e-05	4868.803	4336.673	4093.331	1255.875	1394.118	1338.509
ABUW_RS10315		-1.726	0.0106383	5.927	6.794	38.166	7.059	4.483	4.327
ABUW_RS10170		-1.711	0.0229962	0.112	1.973	0.751	0.326	0.158	0.326
ABUW_RS20335		-1.709	0.00288521	4.809	1.753	2.930	0.507	1.477	1.024
ABUW_RS13745		-1.709	0.000172985	202.853	374.238	413.360	132.169	99.776	71.043
ABUW_RS09490		-1.708	0.0359931	7.716	0.329	0.601	0.905	0.633	0.837
ABUW_RS07630		-1.698	8.55e-05	12.972	18.849	12.697	4.489	3.164	5.909
ABUW_RS14420	betI	-1.690	2.89e-08	279.118	272.213	244.470	73.813	89.176	83.651
ABUW_RS06615		-1.670	1.36e-08	71.121	70.793	57.023	21.322	23.098	18.005
ABUW_RS16105		-1.666	1.09e-06	10.623	9.424	12.772	3.077	3.481	3.908
ABUW_RS20750		-1.650	0.000681771	8.051	3.726	5.710	2.389	1.951	1.117
ABUW_RS15170		-1.640	0.0107243	140.677	19.287	26.370	16.435	21.833	21.169
ABUW_RS08730	cydX	-1.618	0.00172674	5.591	9.424	4.132	1.882	2.637	1.628
ABUW_RS12420		-1.609	3.75e-07	41.376	70.683	81.064	20.490	22.571	20.517
ABUW_RS04140		-1.595	1.68e-08	512.835	411.060	354.910	153.708	140.277	129.012
ABUW_RS05270		-1.592	8.95e-10	336.038	437.580	399.386	137.599	124.931	126.547
ABUW_RS17445		-1.587	3.98e-07	682.364	435.936	401.339	158.342	184.100	163.301
ABUW_RS18095		-1.580	0.000118073	11.965	18.849	8.189	4.670	3.006	5.025
ABUW_RS14415		-1.560	7.06e-07	461.954	467.606	288.195	115.879	152.248	144.784

Locustag	Gene	logFC	PValue	LCWB_1	LCWB_2	LCWB_3	LB_1	LB_2	LB_3
ABUW_RS07865		-1.555	1.88e-05	13.531	8.329	10.218	4.127	3.111	3.536
ABUW_RS06395		-1.533	0.000309444	19.570	8.219	8.640	2.715	4.008	5.816
ABUW_RS17370		-1.516	0.00107679	49.875	10.082	29.526	12.055	9.809	9.258
ABUW_RS01580	rimM	-1.515	2.47e-05	8909.085	4807.348	3098.246	1717.797	2281.552	1882.333
ABUW_RS06415		-1.503	6.19e-07	301.595	568.864	410.430	150.414	152.880	148.599
ABUW_RS05150	rarD	-1.499	1.04e-06	34.890	33.205	25.544	11.838	10.020	11.026
ABUW_RS02315		-1.495	6.15e-06	1301.769	1197.234	718.008	353.319	391.351	396.249
ABUW_RS16100		-1.495	0.0027797	263.351	116.929	46.580	47.532	55.003	48.385
ABUW_RS01870		-1.489	0.000894756	8805.422	3944.682	1955.158	1603.077	2062.594	1573.085
ABUW_RS05075		-1.483	6.67e-06	79.732	80.875	44.401	23.386	23.573	26.054
ABUW_RS05700		-1.480	0.000228413	21.135	30.027	59.577	13.575	13.395	13.213
ABUW_RS11390	ychF	-1.475	2.31e-07	964.613	674.287	635.141	283.524	292.208	242.299
ABUW_RS13235	trmB	-1.473	1.17e-05	206.543	101.806	115.699	49.559	52.155	50.851
ABUW_RS03430		-1.467	4.66e-05	38.021	18.630	21.412	10.353	9.862	7.816
ABUW_RS06080	rodA	-1.461	6.39e-05	148.058	54.793	93.611	38.373	40.185	29.031
ABUW_RS18895		-1.457	0.012203	1.230	1.753	0.751	0.253	0.633	0.465
ABUW_RS20260		-1.452	0.00519921	8.499	2.520	4.658	1.774	2.004	1.908
ABUW_RS04545	ttcA	-1.444	3.17e-06	466.427	265.857	247.099	124.530	129.255	105.936
ABUW_RS04885	tolQ	-1.443	1.23e-07	256.306	176.215	198.040	77.361	77.469	76.998
ABUW_RS04880	tolR	-1.430	9.77e-07	67.655	39.013	48.233	19.223	19.723	18.470
ABUW_RS16095		-1.414	0.000228944	20.576	12.931	7.212	5.249	5.643	4.048
ABUW_RS08690		-1.406	3.92e-05	97.177	42.848	64.911	26.608	22.254	28.287
ABUW_RS11065		-1.404	6.51e-05	88.007	33.205	54.243	21.829	21.516	22.844
ABUW_RS14445		-1.402	7.72e-05	204.866	560.317	333.348	137.563	133.474	144.645
ABUW_RS06045		-1.399	0.000553659	35.225	17.315	12.021	8.145	10.020	6.002
ABUW_RS07795		-1.394	2.52e-07	210.345	233.639	167.387	81.669	72.722	78.022
ABUW_RS01910		-1.383	2.13e-08	622.089	805.024	788.028	256.048	308.134	285.614
ABUW_RS00150		-1.377	2.83e-05	271.179	164.051	141.092	79.642	88.859	53.131
ABUW_RS15960	nreB	-1.376	6.6e-07	43.389	41.314	35.536	14.082	17.139	15.074
ABUW_RS03210		-1.374	3.99e-05	885.776	489.085	344.316	223.395	242.795	196.892
ABUW_RS01605	truB	-1.368	2.53e-05	68.438	28.054	55.070	21.033	19.301	18.377
ABUW_RS15045	pth	-1.353	0.000324515	1257.822	421.251	489.992	268.971	304.126	275.750
ABUW_RS05130		-1.350	3.3e-05	12.413	21.479	24.492	8.073	6.539	8.421
ABUW_RS00510	asd	-1.350	7.68e-08	294.215	289.857	279.931	97.742	123.032	118.358
ABUW_RS07655	prfA	-1.344	2.33e-07	342.636	215.886	273.244	109.218	119.710	98.678
ABUW_RS06605		-1.341	1.21e-06	224.435	136.326	137.186	73.343	62.544	60.389
ABUW_RS04245		-1.338	2.46e-05	684.377	376.101	338.682	205.729	191.694	155.578
ABUW_RS10880		-1.335	1.26e-05	74.700	142.791	80.839	41.522	41.767	34.800
ABUW_RS01660		-1.313	0.000378077	179.928	93.477	61.606	39.459	45.036	49.921
ABUW_RS05405		-1.312	2.59e-05	1277.167	2891.444	2939.349	931.843	965.008	965.848
ABUW_RS16235	dusA	-1.311	0.000319258	93.263	36.492	65.738	25.051	28.899	24.891
ABUW_RS07080	tsaD	-1.310	6.19e-07	174.225	124.162	118.629	52.563	60.488	54.992
ABUW_RS15470		-1.296	2.79e-08	3295.184	2937.690	3403.796	1252.364	1435.146	1238.388
ABUW_RS07310		-1.277	0.000264482	21.806	37.259	28.098	10.896	13.764	11.398
ABUW_RS17240	rimP	-1.272	0.00028119	455.580	160.983	252.884	107.154	149.611	103.377
ABUW_RS12165		-1.271	0.0196566	2.796	1.973	12.321	3.620	2.215	1.628
ABUW_RS18250		-1.271	3.85e-06	34.331	26.082	40.119	15.096	14.502	12.189
ABUW_RS15655		-1.254	0.00152166	12.413	32.547	12.471	5.430	8.912	9.677
ABUW_RS14435	mqo	-1.254	7e-07	2173.678	1826.262	1864.477	847.748	904.257	707.079
ABUW_RS05565	rpmE	-1.249	0.000550413	4912.862	3963.311	1713.167	1272.600	1780.617	1403.271
ABUW_RS08775		-1.245	3.03e-08	300.701	317.253	290.449	126.739	133.896	122.545
ABUW_RS17335		-1.243	0.000374817	73.358	24.219	42.748	19.838	21.200	18.145
ABUW_RS09270		-1.235	0.00437173	5.032	4.164	2.479	2.425	1.055	1.117
ABUW_RS08210		-1.233	1.95e-07	81.857	88.327	71.598	33.811	34.964	33.963
ABUW_RS08740		-1.226	0.000572943	4342.548	4009.119	4233.146	1717.579	1796.859	1863.816
ABUW_RS08725		-1.226	0.000191653	125.805	79.122	96.691	39.097	44.562	45.268
ABUW_RS18220	znuB	-1.226	1.56e-06	179.593	289.199	206.981	98.900	88.332	101.563

Locustag	Gene	logFC	PValue	LCWB_1	LCWB_2	LCWB_3	LB_1	LB_2	LB_3
ABUW_RS16670		-1.224	0.00485181	131.619	417.744	640.099	157.039	167.277	185.679
ABUW_RS08830		-1.221	0.000168274	25.161	13.589	33.057	10.172	8.807	12.096
ABUW_RS17500	nusG	-1.221	0.00407703	3262.083	1037.347	853.165	759.310	826.314	624.730
ABUW_RS10065		-1.219	0.000894005	9.729	12.274	9.466	4.778	4.641	4.001
ABUW_RS04405	rlmE	-1.216	2.22e-07	892.821	677.684	692.915	314.186	322.109	337.907
ABUW_RS07610	pgaC	-1.215	0.00200518	15.544	6.794	5.259	3.656	4.483	3.489
ABUW_RS13640		-1.207	3.99e-07	151.077	117.915	116.149	59.369	57.693	49.595
ABUW_RS03215		-1.198	0.000337281	398.549	175.010	162.880	100.348	117.495	102.912
ABUW_RS08035		-1.197	0.0054893	156.445	266.624	234.853	114.105	102.623	70.252
ABUW_RS01585	trmD	-1.194	0.000508406	6974.938	3516.307	2213.151	1592.470	2114.802	1843.811
ABUW_RS04420		-1.187	0.0144145	14.873	4.055	4.207	2.389	3.375	4.187
ABUW_RS07660	prmC	-1.182	9.52e-06	68.102	44.821	45.378	23.096	25.208	21.308
ABUW_RS18205		-1.178	6.34e-05	188.875	228.817	181.362	86.592	84.219	93.747
ABUW_RS02985		-1.177	0.00177128	20.576	12.055	8.790	5.828	6.486	5.723
ABUW_RS00570		-1.174	4.25e-07	118.759	136.107	142.370	53.758	56.480	65.972
ABUW_RS01755		-1.174	0.00157027	25.049	11.616	13.974	7.711	8.438	6.141
ABUW_RS20285		-1.172	0.0084224	8.499	22.027	6.837	4.525	5.326	6.467
ABUW_RS16240		-1.171	0.0101583	66.760	30.794	45.829	25.160	20.092	18.191
ABUW_RS03850		-1.170	0.00172854	36.120	97.203	47.857	31.169	26.210	22.844
ABUW_RS05665		-1.166	0.0140589	2.796	1.425	3.907	1.484	0.844	1.349
ABUW_RS14405		-1.163	0.000121122	125.357	137.860	58.751	44.889	51.945	46.478
ABUW_RS13105		-1.161	0.000403281	16.327	16.548	16.754	7.783	5.854	8.467
ABUW_RS01050		-1.159	0.00106933	12.301	31.780	41.321	12.453	14.660	11.631
ABUW_RS11780		-1.153	0.000171061	120.213	260.816	290.148	98.321	105.049	98.911
ABUW_RS15915	rho	-1.151	1.56e-05	1953.940	1031.101	1484.249	677.822	732.128	602.213
ABUW_RS16850		-1.151	0.000646313	56.137	134.134	173.698	55.858	49.202	59.272
ABUW_RS01610		-1.149	1.68e-05	46.408	43.177	39.217	20.852	20.356	16.749
ABUW_RS17235	nusA	-1.149	0.000127072	4961.171	3575.155	1946.894	1607.819	1731.151	1389.174
ABUW_RS14740		-1.147	0.000675783	86.889	64.547	39.292	31.639	23.678	30.241
ABUW_RS04025		-1.146	2.37e-06	217.502	343.225	322.153	136.441	125.669	136.968
ABUW_RS13790		-1.144	2.14e-05	49.986	43.835	30.427	17.159	19.829	19.029
ABUW_RS04990		-1.143	0.000225809	155.550	390.348	314.716	124.567	133.105	132.269
ABUW_RS13390		-1.138	0.00132596	4.585	4.164	4.132	2.317	2.057	1.396
ABUW_RS18920	purE	-1.136	1.28e-05	686.837	374.019	514.484	259.052	231.193	226.341
ABUW_RS16405	hisS	-1.135	2.77e-06	1619.356	1289.506	1035.053	585.112	667.474	542.801
ABUW_RS00835		-1.133	2.61e-06	122.897	79.889	99.922	48.038	49.571	40.337
ABUW_RS05400		-1.132	0.00139854	819.127	2378.798	2244.630	765.283	876.149	842.744
ABUW_RS17975		-1.131	0.000370601	76.825	28.712	44.101	22.046	23.678	22.471
ABUW_RS04675	lysA	-1.130	4.49e-06	353.930	252.816	242.817	115.698	149.189	123.150
ABUW_RS07505	mnmG	-1.130	3.27e-05	1604.371	824.968	923.787	511.227	562.003	458.312
ABUW_RS14460		-1.129	0.000308689	23.260	12.712	17.956	7.095	8.121	9.491
ABUW_RS12380		-1.125	0.0194416	3.690	4.164	6.987	2.787	1.635	2.466
ABUW_RS12795		-1.124	0.000845821	174.561	60.053	146.201	61.360	61.173	52.247
ABUW_RS05310		-1.120	4.28e-07	968.192	1308.246	1020.628	500.041	531.153	485.715
ABUW_RS13415		-1.114	0.00207549	3.802	4.274	4.959	1.665	2.109	2.373
ABUW_RS05815		-1.113	0.00109272	33.995	15.671	25.018	8.942	14.239	11.538
ABUW_RS01215		-1.110	4.59e-06	101.203	115.395	143.121	55.279	53.052	58.528
ABUW_RS05460	pstC	-1.109	0.000719757	98.743	45.040	39.443	27.223	32.749	24.611
ABUW_RS08460	uppS	-1.108	1.18e-05	576.241	373.362	308.931	183.393	203.401	196.985
ABUW_RS03225	typA	-1.105	0.000316355	4583.981	2489.261	1894.830	1331.716	1641.078	1197.353
ABUW_RS10985	msbA	-1.101	8.85e-06	606.322	768.203	451.075	276.067	303.124	271.331
ABUW_RS16275		-1.101	4.11e-06	461.731	341.472	329.967	168.261	203.876	156.090
ABUW_RS04090		-1.100	0.00111411	4.026	5.041	3.982	1.991	1.898	2.140
ABUW_RS04755	serC	-1.100	0.000117563	232.599	101.258	167.613	79.352	81.740	72.764
ABUW_RS03110		-1.096	0.00254637	70.786	257.200	224.260	90.212	78.049	90.304
ABUW_RS03205		-1.095	0.000875057	48.533	18.958	26.821	16.290	16.770	10.887

Locustag	Gene	logFC	PValue	LCWB_1	LCWB_2	LCWB_3	LB_1	LB_2	LB_3
ABUW_RS10385	prmB	-1.094	3.1e-05	221.528	115.833	138.388	70.664	78.734	73.323
ABUW_RS15010	ispE	-1.092	4.77e-05	727.653	378.184	413.059	230.635	266.842	214.896
ABUW_RS16995		-1.088	5.28e-05	50.881	30.027	34.484	17.883	19.512	16.795
ABUW_RS05050	lepA	-1.087	4.29e-07	1340.685	1219.371	990.126	539.970	612.102	518.841
ABUW_RS05000	cysT	-1.078	0.00726225	87.113	279.775	328.765	97.851	103.942	128.268
ABUW_RS10165		-1.076	0.00025932	34.331	46.684	35.987	22.444	14.186	18.563
ABUW_RS18620		-1.076	3.41e-05	227.566	194.955	174.900	101.181	97.772	84.302
ABUW_RS10470		-1.075	3.35e-06	55.689	55.341	47.106	25.304	27.159	22.471
ABUW_RS11165	tkt	-1.075	2.39e-05	2234.512	1422.435	1275.841	758.948	876.254	706.241
ABUW_RS07560	cyoE	-1.075	2.24e-05	1341.915	1165.345	727.925	537.400	534.159	464.128
ABUW_RS01885	mlaE	-1.070	4.21e-07	487.451	494.565	382.632	199.719	238.787	211.500
ABUW_RS15340		-1.070	0.000198422	78.390	36.602	63.785	25.558	31.536	28.240
ABUW_RS08400		-1.068	0.00026883	52.670	34.301	25.394	18.064	18.510	16.656
ABUW_RS11020		-1.068	9.06e-06	185.855	146.956	149.732	73.886	76.625	79.650
ABUW_RS18090		-1.067	0.00024999	20.576	24.986	18.482	10.136	10.389	9.910
ABUW_RS15460		-1.066	1.19e-06	6387.738	7407.839	8406.188	3607.329	3885.347	3111.044
ABUW_RS04995	cysW	-1.065	0.00511481	66.313	223.776	207.807	72.220	80.264	85.838
ABUW_RS16715		-1.061	0.00186448	21.247	29.588	14.350	10.534	11.602	8.793
ABUW_RS08235		-1.059	0.000860558	21.135	11.178	12.096	5.937	6.645	8.607
ABUW_RS18930	mpl	-1.058	1.7e-07	313.896	360.869	408.477	175.103	172.656	172.745
ABUW_RS07810		-1.056	0.00022424	53.341	93.587	72.274	32.291	33.962	39.220
ABUW_RS01160	aqpZ	-1.051	1.11e-05	59.715	71.670	65.212	30.191	31.747	32.939
ABUW_RS07375		-1.051	0.0411845	1.006	3.836	1.503	0.833	1.213	0.977
ABUW_RS08480	bamA	-1.050	1.94e-06	2260.232	2723.119	1814.592	1142.676	1129.332	1011.628
ABUW_RS15495		-1.048	9.1e-05	11.183	11.726	10.293	6.118	5.432	4.373
ABUW_RS11380		-1.046	0.00297271	16.438	10.959	15.026	7.566	6.908	6.048
ABUW_RS03020		-1.043	6.5e-06	66.984	58.848	85.271	34.029	32.169	36.475
ABUW_RS06720		-1.041	1.18e-06	260.443	234.187	199.242	101.796	117.600	117.707
ABUW_RS04670		-1.041	3.29e-05	124.239	76.163	125.465	44.129	52.683	61.878
ABUW_RS14170		-1.040	0.00205162	3.802	9.205	9.617	4.127	3.217	3.768
ABUW_RS12735		-1.040	0.0211033	2.348	1.644	3.982	1.412	1.371	1.256
ABUW_RS05985		-1.039	0.00484715	16.998	9.096	13.749	7.602	5.274	6.374
ABUW_RS07700		-1.037	1.62e-05	66.648	52.602	52.590	28.961	28.899	25.775
ABUW_RS00485	aciT	-1.035	0.000101744	395.529	616.754	359.943	199.357	230.402	239.554
ABUW_RS00175		-1.033	4.06e-06	146.492	119.888	136.434	54.989	76.308	65.786
ABUW_RS05255		-1.030	3.76e-05	341.741	346.294	496.753	233.893	181.990	164.371
ABUW_RS14200		-1.029	4.16e-05	1260.841	927.651	682.472	424.345	515.227	467.478
ABUW_RS07605	pgaB	-1.027	0.0106241	9.393	2.959	4.433	2.606	2.795	2.698
ABUW_RS05390		-1.024	0.00011079	45.513	59.615	85.497	32.798	26.104	35.172
ABUW_RS11765		-1.023	0.0195274	2.796	8.000	5.034	2.172	2.637	3.024
ABUW_RS05045		-1.015	1.64e-05	40.257	43.944	49.210	20.707	20.672	24.751
ABUW_RS11775		-1.005	0.000338059	92.816	211.502	153.113	73.270	77.996	76.672
ABUW_RS13375		-1.005	0.000663358	1003.193	540.810	387.065	288.158	374.792	298.827
ABUW_RS15100	rpmF	-1.003	0.00043601	452.673	287.994	697.498	207.141	255.557	255.605
ABUW_RS18480		-1.000	0.0203639	22.477	3.288	17.280	6.951	6.223	8.467
ABUW_RS12145	tgnC	1.002	0.000254806	9.953	4.822	8.189	14.444	14.871	16.888
ABUW_RS15000		1.003	3.74e-05	32.430	32.876	24.492	62.591	51.786	64.669
ABUW_RS16510		1.011	0.00865621	911.719	304.651	280.156	982.451	1144.784	885.267
ABUW_RS00985		1.011	7.94e-05	13.531	8.767	9.842	20.164	24.311	20.099
ABUW_RS08025		1.012	0.0303659	4.809	4.712	1.503	5.901	6.012	9.212
ABUW_RS08920	pcaF	1.013	0.00278509	9.953	4.493	8.565	13.648	17.297	15.911
ABUW_RS15615	add	1.014	0.00709863	4.697	12.602	7.062	18.933	12.393	17.400
ABUW_RS12460		1.015	4.56e-05	34.554	23.561	20.660	55.713	49.255	53.224
ABUW_RS02410		1.018	1.52e-05	67.990	61.807	87.225	160.695	136.743	142.830
ABUW_RS04760		1.019	0.00176077	92.033	127.668	256.941	312.485	307.554	348.980
ABUW_RS18890	dnaK	1.020	0.000842637	3337.230	2887.499	7190.751	9228.939	9622.450	8350.582
ABUW_RS08845		1.021	0.00234759	3.914	3.616	4.057	8.471	7.225	7.863

Locustag	Gene	logFC	PValue	LCWB_1	LCWB_2	LCWB_3	LB_1	LB_2	LB_3
ABUW_RS01005	gabT	1.021	0.000563583	187.421	300.158	429.438	626.272	632.300	605.190
ABUW_RS20510		1.023	0.0211462	8.275	13.808	2.028	18.390	12.235	15.958
ABUW_RS05890		1.023	5.45e-05	31.870	48.876	47.707	105.779	80.949	74.811
ABUW_RS00585		1.024	0.0175119	7.940	6.356	6.311	14.372	15.662	11.678
ABUW_RS06565		1.026	0.000337209	15.544	20.493	36.813	51.188	45.300	54.015
ABUW_RS14640		1.027	0.000282248	8.722	12.055	18.857	26.933	26.051	29.357
ABUW_RS14635		1.030	0.00125125	29.858	63.341	28.023	88.728	74.199	83.232
ABUW_RS10290		1.033	0.000297043	10.735	17.096	9.917	25.160	20.409	30.892
ABUW_RS06280		1.033	0.00506535	14.761	32.438	16.078	45.830	36.546	46.106
ABUW_RS13565		1.034	0.00182605	3.578	7.233	4.583	10.172	8.016	13.073
ABUW_RS14015		1.036	0.0219931	2.125	0.986	1.503	2.715	2.953	3.815
ABUW_RS13590		1.041	0.00382178	39.139	17.753	16.078	56.111	52.788	39.592
ABUW_RS05660	yddG	1.044	0.0318599	2.348	1.534	0.751	2.787	3.902	2.419
ABUW_RS03010		1.048	9.17e-05	7.492	7.233	6.686	15.023	14.660	14.423
ABUW_RS17895		1.050	3.81e-06	22.477	27.068	23.515	52.020	48.833	50.293
ABUW_RS07780		1.056	4.15e-06	2283.268	2231.185	2192.040	4383.618	5207.480	4352.875
ABUW_RS08275		1.060	0.000495452	5.591	7.452	6.762	18.209	10.916	12.003
ABUW_RS13245		1.061	1.76e-05	11.406	17.643	18.106	32.762	29.901	36.336
ABUW_RS14310		1.062	0.0398105	0.671	3.178	0.977	3.692	3.797	2.187
ABUW_RS01765		1.062	0.000233234	5.815	7.342	7.137	16.182	11.180	15.027
ABUW_RS04840		1.064	0.000466261	8.387	9.205	13.899	21.214	23.573	22.239
ABUW_RS04845		1.067	3.32e-05	113.615	90.080	90.831	186.325	195.227	235.042
ABUW_RS01680		1.069	1.25e-05	104.222	139.504	128.921	279.542	224.759	277.798
ABUW_RS07500		1.072	0.0019803	3.019	4.164	2.554	7.638	5.748	6.606
ABUW_RS16140		1.072	0.00429364	1.230	1.425	2.104	3.149	4.008	3.303
ABUW_RS10265		1.073	0.000144825	5.479	8.657	8.414	16.870	13.975	16.935
ABUW_RS15440		1.073	7.26e-05	12.748	24.986	19.984	44.708	37.073	39.825
ABUW_RS09070		1.074	0.0083881	0.895	2.411	1.728	3.910	4.008	2.745
ABUW_RS05685		1.075	0.00240761	4.809	3.945	3.381	9.159	10.125	5.955
ABUW_RS12715		1.077	7.14e-05	9.841	10.520	15.702	27.440	22.676	26.984
ABUW_RS16515		1.077	0.00126483	13.755	13.808	8.865	28.707	20.989	26.007
ABUW_RS10145		1.077	0.0293136	1.342	0.986	0.451	1.774	1.898	1.861
ABUW_RS16940		1.079	0.00272301	3.802	7.890	3.681	10.969	9.914	10.933
ABUW_RS12705		1.081	4.61e-06	206.431	152.216	120.432	359.039	318.470	334.371
ABUW_RS01985		1.083	0.00132109	4.361	1.863	2.179	5.720	5.695	6.002
ABUW_RS09205		1.088	0.0100153	2.460	3.068	2.930	5.901	5.274	6.886
ABUW_RS10685		1.090	3.27e-06	65.866	60.382	86.999	150.848	143.810	160.323
ABUW_RS13285	clpB	1.097	0.0181121	859.496	467.716	2570.615	3191.275	2772.098	2380.750
ABUW_RS04225		1.102	7.61e-05	92.033	58.410	122.761	170.216	205.247	212.942
ABUW_RS14925		1.106	0.00213092	7.828	7.561	2.780	12.453	12.076	13.073
ABUW_RS17125		1.107	0.00287793	3.914	5.699	2.329	9.014	6.750	8.979
ABUW_RS03580		1.113	0.000224354	9.841	10.739	6.311	21.322	18.405	17.400
ABUW_RS08570		1.115	0.00183968	5.368	7.671	4.883	14.118	9.387	14.702
ABUW_RS19995		1.115	0.000273604	12.077	8.986	9.015	21.829	20.198	22.750
ABUW_RS11925		1.117	0.00119481	9.617	22.137	10.067	33.087	27.739	28.799
ABUW_RS12610		1.118	0.000487045	7.940	17.205	8.414	24.182	21.041	26.752
ABUW_RS14215		1.120	0.00580602	2.348	1.753	2.630	5.213	5.063	4.606
ABUW_RS13430		1.122	0.00287891	2.796	1.205	3.005	5.394	4.219	6.002
ABUW_RS18885	grpE	1.123	0.00124726	193.907	167.448	495.251	625.802	607.619	636.594

Locustag	Gene	logFC	PValue	LCWB_1	LCWB_2	LCWB_3	LB_1	LB_2	LB_3
ABUW_RS11475		1.124	6.32e-06	173.778	169.421	152.061	384.705	379.696	314.738
ABUW_RS06500		1.128	0.00770293	4.809	3.178	3.005	8.109	7.014	8.467
ABUW_RS16460		1.129	0.00104659	5.591	8.877	9.842	20.236	14.502	19.029
ABUW_RS11405		1.129	0.00488519	1.789	3.178	2.028	4.272	4.852	6.095
ABUW_RS13650		1.130	8.13e-06	74.364	62.574	49.811	139.843	132.788	134.874
ABUW_RS01810		1.131	1.3e-05	15.879	18.739	15.627	39.640	29.901	40.151
ABUW_RS13605		1.131	0.00851469	1.677	2.082	1.578	4.235	2.426	4.792
ABUW_RS04620		1.133	0.00217695	4.026	7.781	2.855	11.403	9.018	10.654
ABUW_RS10175		1.135	2.87e-05	10.623	9.972	7.513	17.847	20.303	22.983
ABUW_RS14275		1.136	0.00134734	2.684	5.260	7.513	11.005	12.657	11.585
ABUW_RS07450		1.137	0.00440048	7.492	17.534	21.712	34.246	29.848	40.383
ABUW_RS15485		1.142	0.00929389	3.690	4.603	3.231	7.711	7.699	9.724
ABUW_RS03555		1.142	8.57e-06	77.048	95.888	61.380	172.279	161.687	181.911
ABUW_RS07830		1.144	0.00741766	2.125	2.192	1.728	6.046	3.322	3.582
ABUW_RS17655	cpdA	1.145	0.000351989	24.378	31.671	61.606	91.696	75.517	95.840
ABUW_RS01970		1.146	1.85e-05	55.354	34.739	38.466	103.534	94.766	85.465
ABUW_RS05705		1.146	0.000829825	5.144	4.603	12.096	18.571	13.975	17.679
ABUW_RS09425		1.147	0.0225	1.342	1.534	1.878	4.561	4.219	1.908
ABUW_RS07965		1.150	0.0223313	2.125	0.877	3.531	6.046	4.693	4.559
ABUW_RS14045		1.151	7.03e-05	317.587	189.914	176.628	550.323	531.627	435.888
ABUW_RS09145		1.154	5.78e-05	8.611	6.794	5.184	17.123	11.971	15.818
ABUW_RS08245		1.161	1.51e-05	24.154	21.698	16.153	46.627	42.663	48.339
ABUW_RS09640		1.165	0.00689979	1.342	2.630	1.427	3.910	4.377	3.629
ABUW_RS00400	hutG	1.166	0.00103316	12.860	9.863	6.311	19.657	23.995	20.331
ABUW_RS12290		1.166	0.000993224	20.129	11.068	11.194	30.445	36.124	27.729
ABUW_RS09635		1.169	3.13e-05	7.828	8.329	9.015	20.055	17.983	18.796
ABUW_RS18275		1.172	0.0027699	4.809	9.644	3.982	16.652	12.129	11.631
ABUW_RS12295	paaG	1.175	0.00160521	10.064	13.150	7.212	25.884	23.204	18.517
ABUW_RS03575		1.175	0.00201442	5.703	4.164	3.606	7.928	9.756	12.376
ABUW_RS14830		1.178	1.89e-05	33.101	58.081	39.969	109.037	88.068	99.144
ABUW_RS06970		1.179	0.00312388	2.125	1.644	1.953	4.199	4.008	4.792
ABUW_RS11355		1.191	0.00269207	4.809	14.465	16.153	25.413	23.784	33.218
ABUW_RS03495		1.193	0.000262136	4.026	5.479	4.883	8.000	11.549	13.632
ABUW_RS07915		1.193	0.000112236	7.604	12.822	7.513	23.313	20.672	19.215
ABUW_RS15475		1.194	0.00546971	5.256	3.726	2.479	10.028	7.963	7.304
ABUW_RS11590	tauA	1.194	0.00187942	143.920	420.374	351.904	591.230	669.900	835.812
ABUW_RS18995		1.195	0.00186785	2.684	2.849	2.855	7.204	5.010	6.932
ABUW_RS11945		1.196	0.000609901	37.574	44.054	51.088	105.163	102.149	97.608
ABUW_RS07335	uraH	1.196	0.00246546	1.342	2.082	2.179	4.018	4.430	4.699
ABUW_RS04945		1.201	0.03539	0.335	3.616	0.601	2.824	4.008	3.117
ABUW_RS18785		1.202	1.98e-07	46.855	58.958	64.461	141.979	116.809	133.758
ABUW_RS00600		1.205	0.0303069	2.125	0.548	0.376	2.715	2.109	1.582
ABUW_RS00055	erpA	1.210	0.000129405	19.458	33.314	15.927	44.997	50.890	61.784
ABUW_RS05970		1.214	4.28e-05	16.327	10.739	9.842	27.404	28.899	28.519
ABUW_RS12355		1.228	0.000206935	4.249	4.931	6.686	15.711	10.653	11.352
ABUW_RS07645		1.236	0.00060679	3.131	5.808	6.161	13.720	11.233	11.166
ABUW_RS01080		1.239	0.000239453	13.419	17.863	10.067	31.277	28.372	36.801
ABUW_RS08870		1.239	0.0102841	1.230	0.767	1.728	3.548	2.531	3.024
ABUW_RS15745		1.245	0.000731358	6.821	8.877	10.368	19.548	27.475	15.679
ABUW_RS20655		1.255	0.0301463	2.237	0.438	0.526	3.367	2.109	1.535

Locustag	Gene	logFC	PValue	LCWB_1	LCWB_2	LCWB_3	LB_1	LB_2	LB_3
ABUW_RS09630		1.258	1.4e-06	18.787	18.958	17.430	46.952	44.562	40.197
ABUW_RS19800	pqqA	1.260	0.0381168	0.671	0.000	1.503	2.063	2.057	1.768
ABUW_RS18765		1.261	0.000130599	7.604	8.548	17.205	27.006	26.210	28.938
ABUW_RS11605		1.262	6.63e-05	3.578	5.479	5.034	10.353	11.180	12.562
ABUW_RS18135		1.266	0.000775428	7.828	13.370	5.109	17.919	21.358	22.611
ABUW_RS01735	astB	1.268	3.91e-05	265.475	188.708	165.058	506.557	515.174	468.362
ABUW_RS17650		1.271	1.42e-05	17.109	30.903	22.689	56.473	52.736	61.273
ABUW_RS13160	benC	1.281	0.000872632	2.460	1.644	1.352	4.344	3.691	4.839
ABUW_RS04825	rbtA	1.283	0.000193391	25.273	13.479	9.692	42.753	41.028	32.102
ABUW_RS05200		1.286	0.00525622	1.454	0.877	4.583	6.227	5.801	6.467
ABUW_RS13020		1.289	0.00157375	2.125	0.877	1.653	3.548	3.902	4.048
ABUW_RS09325		1.294	0.00682677	2.907	0.548	3.005	6.227	5.326	4.839
ABUW_RS12710		1.300	1.15e-05	59.492	33.862	29.601	102.484	102.254	96.352
ABUW_RS15240		1.305	0.00101154	4.361	2.849	4.357	11.005	10.600	7.258
ABUW_RS00865	acs	1.308	4.9e-06	60.274	73.752	82.567	185.782	158.681	192.658
ABUW_RS03925		1.309	0.000448463	3.690	1.205	2.404	5.466	6.170	6.467
ABUW_RS08645		1.309	0.000925978	4.920	5.589	3.606	8.145	14.344	12.143
ABUW_RS09330		1.311	0.000184095	2.237	3.288	2.329	5.901	5.379	8.049
ABUW_RS11180		1.312	0.00157299	1.789	0.877	1.127	2.932	2.953	3.443
ABUW_RS18010		1.313	1.5e-06	26.056	39.122	30.277	79.678	74.674	82.534
ABUW_RS12280	paaK	1.315	4.96e-05	18.787	11.726	7.889	33.848	33.223	26.705
ABUW_RS12690		1.316	0.029817	2.684	1.534	0.376	3.910	3.691	2.838
ABUW_RS15690		1.320	0.0030851	0.447	2.192	2.930	5.684	3.533	5.443
ABUW_RS18000		1.321	2.94e-05	4.920	7.123	5.409	12.960	13.975	16.563
ABUW_RS11685	mdcA	1.322	0.0154939	1.118	0.219	1.803	3.330	1.846	3.210
ABUW_RS04200		1.324	0.0250957	0.224	2.082	1.728	5.032	2.057	3.117
ABUW_RS14175		1.324	0.00157356	3.578	6.685	5.034	12.308	10.020	15.958
ABUW_RS06145		1.326	0.0418787	0.895	0.877	0.751	1.810	2.795	1.768
ABUW_RS05590		1.329	2.09e-06	276.882	311.007	362.873	768.505	867.869	753.184
ABUW_RS01120		1.334	0.0171017	0.671	2.411	0.451	3.294	2.479	2.466
ABUW_RS08350		1.342	8.72e-07	10.735	11.726	14.199	32.255	28.741	32.660
ABUW_RS11955		1.343	4.24e-05	12.189	13.260	15.702	33.449	36.546	35.126
ABUW_RS12200		1.343	0.00066936	2.460	1.973	3.907	6.733	6.961	8.328
ABUW_RS06065		1.348	0.00735938	1.454	1.534	0.601	3.258	3.217	2.140
ABUW_RS02560		1.353	9.33e-06	25.832	38.355	53.567	111.824	86.803	104.215
ABUW_RS16935		1.353	4.4e-05	4.249	6.685	5.109	13.322	12.657	14.934
ABUW_RS08010		1.363	0.00452649	1.789	3.397	0.526	5.756	3.533	4.141
ABUW_RS16280		1.364	0.0188829	11.518	15.890	9.767	14.661	68.345	12.655
ABUW_RS01375		1.364	7.43e-05	32.094	83.615	60.253	144.694	138.484	170.093
ABUW_RS14295		1.365	0.00554646	4.249	1.096	1.653	6.190	5.748	5.490
ABUW_RS00695		1.366	5.52e-06	8.499	13.589	9.091	30.988	23.784	24.984
ABUW_RS04830		1.371	4.8e-05	13.755	11.726	7.513	31.060	29.426	23.402
ABUW_RS10020		1.373	2.1e-05	5.591	5.918	8.790	16.942	15.135	21.541
ABUW_RS13465		1.373	0.000609139	3.467	3.616	2.179	7.421	6.328	9.584
ABUW_RS14510		1.382	0.00106696	4.026	4.822	3.306	12.417	8.016	10.608
ABUW_RS18445	alr	1.383	0.00855715	210.233	133.257	809.591	910.738	970.546	1133.661
ABUW_RS09105		1.386	0.0161899	1.566	0.877	0.225	2.462	2.426	1.442
ABUW_RS08410		1.388	6.69e-06	6.262	9.753	6.236	19.874	18.088	19.726
ABUW_RS11265		1.394	2.09e-05	2.796	3.945	5.635	9.955	12.973	10.747
ABUW_RS18960		1.399	0.00775345	2.237	0.548	0.826	3.005	2.268	3.862
ABUW_RS16880	hcaR	1.403	4.58e-05	18.451	34.629	18.557	77.723	47.040	63.320
ABUW_RS12055		1.410	9.02e-05	3.690	4.055	2.930	8.869	10.811	8.374

Locustag	Gene	logFC	PValue	LCWB_1	LCWB_2	LCWB_3	LB_1	LB_2	LB_3
ABUW_RS18680	ampD	1.411	3.07e-05	10.623	9.205	5.710	21.141	22.307	23.169
ABUW_RS17430	htpG	1.417	3.05e-06	277.217	230.242	439.881	937.924	871.614	723.362
ABUW_RS08175		1.421	0.000297659	2.796	1.205	3.155	6.552	6.328	6.886
ABUW_RS07270	csuD	1.421	7.49e-05	4.585	5.589	5.109	14.661	13.711	12.562
ABUW_RS17105		1.424	3.98e-05	4.920	8.548	14.049	22.517	27.106	26.565
ABUW_RS18535	prpB	1.424	4.62e-08	68.773	79.012	81.515	202.290	218.905	194.565
ABUW_RS10475		1.430	0.0329086	1.901	0.877	0.075	2.208	1.371	3.210
ABUW_RS11855	katE	1.433	3.64e-06	28.963	35.068	38.917	98.321	94.660	85.838
ABUW_RS18420		1.435	0.000472843	4.473	3.068	2.855	10.860	8.543	8.142
ABUW_RS06760		1.439	0.0300093	0.447	0.548	0.826	1.520	1.055	2.605
ABUW_RS04860		1.439	0.010969	1.006	1.425	1.277	4.272	3.481	2.280
ABUW_RS11880		1.455	0.00557303	0.783	0.438	0.751	2.063	1.898	1.535
ABUW_RS11940		1.455	0.000151195	17.669	19.178	31.028	66.573	63.863	57.737
ABUW_RS05605		1.456	0.00107159	6.710	1.753	2.479	11.295	8.332	9.351
ABUW_RS08065		1.464	0.0049043	0.224	4.493	1.803	4.670	6.328	6.932
ABUW_RS08875		1.475	2.53e-06	45.625	35.944	33.132	111.172	97.033	109.658
ABUW_RS15605		1.476	0.000126163	3.243	2.959	1.803	7.457	5.485	8.561
ABUW_RS14915		1.480	3.36e-05	20.576	18.958	9.015	48.473	43.560	40.942
ABUW_RS13625		1.494	0.000272812	3.243	5.370	3.155	12.815	10.336	9.398
ABUW_RS18515		1.494	0.000116356	16.886	29.150	15.101	63.387	46.513	60.854
ABUW_RS15540		1.501	0.0144699	0.671	1.863	0.301	1.701	2.848	3.024
ABUW_RS02800		1.507	0.0112468	0.112	0.219	0.676	0.905	1.160	1.256
ABUW_RS02305		1.511	0.000864705	47.750	65.423	104.955	164.424	217.692	242.904
ABUW_RS16175		1.512	0.0324471	0.224	0.000	0.902	1.050	1.582	1.256
ABUW_RS06570		1.530	3.88e-07	16.550	19.726	18.857	50.283	47.251	61.878
ABUW_RS17725		1.530	3.93e-06	18.899	20.712	27.272	68.854	56.322	69.228
ABUW_RS17720	GacA	1.535	2.24e-08	160.359	219.393	182.263	549.274	491.021	588.767
ABUW_RS15250		1.538	4.99e-05	19.010	7.014	9.241	36.563	30.165	34.382
ABUW_RS05320		1.540	7.76e-06	5.927	7.561	5.785	17.557	17.297	20.889
ABUW_RS08610		1.541	0.000340275	4.809	13.808	3.907	20.055	21.991	21.680
ABUW_RS15230		1.541	0.00353452	0.559	0.219	1.878	3.294	2.531	2.885
ABUW_RS18525	acnD	1.546	1.78e-07	317.027	281.966	295.332	889.126	903.835	818.551
ABUW_RS00715		1.548	0.00191183	1.006	2.411	1.878	3.584	5.063	7.165
ABUW_RS18440		1.551	1.86e-05	143.585	160.325	318.171	565.310	639.313	622.311
ABUW_RS01825		1.553	0.000174858	35.673	64.437	53.717	168.116	122.663	160.789
ABUW_RS06255		1.556	4.81e-05	1.677	1.973	2.028	5.828	6.117	4.932
ABUW_RS08300	nirD	1.556	9.73e-05	1.006	1.205	0.902	3.113	2.953	2.978
ABUW_RS11270		1.567	0.012406	1.342	0.329	2.028	3.403	2.690	5.676
ABUW_RS05625		1.568	0.0113888	0.895	0.219	1.503	3.186	2.742	2.466
ABUW_RS03860		1.581	0.00534751	1.454	0.548	2.855	5.032	5.432	5.304
ABUW_RS18145		1.595	0.000504005	2.907	1.205	0.977	4.923	4.904	4.839
ABUW_RS09210		1.601	0.00041958	2.796	1.534	2.254	7.602	5.906	6.420
ABUW_RS04345		1.604	9.92e-06	4.920	8.767	4.959	20.779	16.032	19.029
ABUW_RS18425		1.605	1.25e-05	3.019	4.603	3.381	11.910	10.494	10.840
ABUW_RS12540		1.609	0.000198758	5.591	1.425	2.855	10.571	9.071	10.003
ABUW_RS01505	bfr	1.610	1.06e-05	73.246	86.573	35.386	162.722	207.620	222.387
ABUW_RS20185		1.612	0.0194339	0.447	0.219	0.150	0.724	0.949	0.744
ABUW_RS13525		1.614	0.0141654	0.559	1.753	3.982	7.095	6.856	7.118
ABUW_RS11290		1.625	0.00103127	1.677	1.644	1.052	5.394	3.217	4.327
ABUW_RS07190		1.627	0.00830922	0.335	1.534	0.601	3.584	1.898	1.768
ABUW_RS11345		1.627	7.02e-07	49.986	51.506	55.220	184.334	148.925	151.251
ABUW_RS00385	hutH	1.631	1.85e-07	104.222	83.834	97.893	293.877	318.998	272.866

Locustag	Gene	logFC	PValue	LCWB_1	LCWB_2	LCWB_3	LB_1	LB_2	LB_3
ABUW_RS00995		1.631	3.84e-07	103.439	128.655	138.237	383.438	403.269	361.542
ABUW_RS09620		1.634	5.64e-05	4.920	7.233	4.583	22.227	16.770	12.143
ABUW_RS17845	cadR	1.639	1.53e-05	38.580	73.204	33.658	128.440	174.818	147.762
ABUW_RS01090		1.641	0.008634	0.783	0.548	1.202	2.570	3.375	2.466
ABUW_RS08595		1.642	2.71e-06	11.294	8.109	5.860	23.458	24.575	29.403
ABUW_RS18455		1.643	6.86e-05	6.821	4.383	3.832	14.734	14.502	16.888
ABUW_RS12020		1.644	0.000289008	2.460	3.178	1.878	6.299	8.227	8.561
ABUW_RS14515		1.652	0.00109066	0.335	2.520	1.352	4.887	3.639	4.652
ABUW_RS11935		1.653	8.94e-05	53.117	43.506	80.463	223.720	181.938	153.670
ABUW_RS18905		1.661	0.00696836	10.512	31.671	5.184	53.758	42.452	49.642
ABUW_RS04895		1.667	0.000266887	1.789	2.192	0.751	5.503	4.377	4.234
ABUW_RS11835		1.670	0.000730889	2.013	2.301	0.601	5.177	4.483	4.885
ABUW_RS12900		1.680	6.78e-05	2.460	8.438	3.155	16.652	14.239	13.027
ABUW_RS08915		1.680	9.35e-05	3.131	1.096	2.554	7.530	7.594	6.886
ABUW_RS14290		1.688	0.00215575	0.224	0.658	1.202	1.846	2.953	2.698
ABUW_RS17380		1.690	3.7e-06	160.918	145.422	85.497	443.531	418.404	399.599
ABUW_RS07250	csuAB	1.693	2.34e-05	7.604	7.014	5.710	21.865	22.729	20.471
ABUW_RS18405		1.696	7.64e-05	22.142	17.863	18.181	101.579	45.722	40.290
ABUW_RS16520		1.709	5.74e-06	5.591	4.822	2.930	16.870	11.549	13.818
ABUW_RS11470		1.711	0.000245377	34.778	13.150	10.368	82.139	57.165	48.013
ABUW_RS09355		1.713	3.53e-05	6.374	3.068	1.803	11.801	12.340	11.026
ABUW_RS14840		1.732	8.56e-05	4.138	5.260	2.104	10.245	12.446	14.190
ABUW_RS07265	csuC	1.735	0.000220035	1.342	1.315	2.404	6.842	6.381	4.373
ABUW_RS16885		1.735	5.13e-08	14.761	15.452	12.171	50.283	42.083	47.827
ABUW_RS08405		1.740	2.81e-08	23.148	25.534	21.262	68.528	79.420	85.233
ABUW_RS09460		1.745	8.12e-07	42.047	24.438	50.487	124.856	126.407	143.156
ABUW_RS05125		1.747	0.00109457	0.895	0.767	0.301	1.846	1.951	2.419
ABUW_RS14920	cntA	1.747	2.39e-07	21.918	22.794	13.824	68.781	65.550	60.249
ABUW_RS10365		1.755	0.00162924	3.690	2.301	1.052	9.593	6.276	6.374
ABUW_RS18450		1.762	7.91e-07	516.637	920.309	965.709	2290.239	2867.655	2993.151
ABUW_RS10340	lpdA	1.765	0.00303392	1.454	1.315	0.977	3.005	6.012	3.675
ABUW_RS18380		1.773	0.000692643	0.671	2.082	0.601	3.475	3.164	4.280
ABUW_RS13100	xseB	1.774	0.0475195	0.671	0.438	0.000	1.122	1.002	1.210
ABUW_RS18490		1.780	1.45e-06	4.026	2.959	3.982	12.670	12.024	13.259
ABUW_RS00630	hpxO	1.786	0.00109453	0.335	0.438	0.676	1.484	1.477	2.373
ABUW_RS13630		1.798	0.000144711	1.454	2.411	2.028	7.530	7.594	5.490
ABUW_RS12135		1.799	0.0257898	0.112	0.110	0.301	1.122	0.475	0.326
ABUW_RS09400		1.813	5.97e-07	7.157	6.794	8.189	28.273	24.100	25.914
ABUW_RS01300		1.817	9.82e-05	13.531	4.822	16.002	45.251	35.333	42.570
ABUW_RS04935		1.822	1.68e-06	28.963	20.602	21.111	81.886	74.779	92.351
ABUW_RS12060		1.829	0.00197564	0.335	0.658	0.601	2.100	2.531	1.210
ABUW_RS13870		1.834	7.06e-07	27.397	22.684	32.681	78.049	76.678	141.900
ABUW_RS13585		1.852	0.00207781	1.118	0.438	0.376	2.027	1.477	3.117
ABUW_RS18530	prpC	1.864	3.58e-08	92.033	87.998	94.663	366.532	334.080	299.292
ABUW_RS11995		1.872	0.00238751	0.671	0.219	1.352	2.534	3.850	2.791
ABUW_RS14620		1.874	0.00123997	0.112	0.219	0.902	1.665	2.004	1.628
ABUW_RS14940		1.878	3.95e-05	4.697	5.808	3.381	20.743	15.030	14.050
ABUW_RS02300		1.883	0.00438262	0.671	1.315	0.376	2.498	1.793	3.908
ABUW_RS05675		1.885	0.0193062	0.000	1.534	0.075	1.846	1.371	2.140
ABUW_RS07260	csuB	1.885	0.0367541	0.783	0.110	0.000	1.014	0.738	1.117
ABUW_RS15985		1.900	1.12e-05	9.058	10.630	5.935	38.156	26.421	29.171
ABUW_RS05440		1.922	0.00123398	1.901	1.863	0.826	7.566	4.430	4.327

Locustag	Gene	logFC	PValue	LCWB_1	LCWB_2	LCWB_3	LB_1	LB_2	LB_3
ABUW_RS08850		1.923	6.56e-08	19.010	14.685	19.834	80.257	61.384	61.971
ABUW_RS11930		1.925	1.22e-05	41.488	64.766	38.466	222.309	157.099	168.186
ABUW_RS05105		1.930	0.000894277	2.572	1.425	0.451	5.177	5.168	5.304
ABUW_RS08635		1.940	0.000339335	1.901	2.082	3.832	8.833	9.281	13.353
ABUW_RS16505	pta	1.940	0.000339609	133.744	75.615	108.486	461.595	397.837	360.425
ABUW_RS18435		1.944	4.81e-09	242.439	241.419	285.190	977.673	1086.828	895.689
ABUW_RS18360		1.966	0.0354925	0.000	0.767	0.075	0.760	1.107	1.256
ABUW_RS11960		1.969	2.8e-05	22.813	7.890	17.430	69.216	67.027	52.712
ABUW_RS14330		1.973	0.0130568	0.112	0.438	0.150	0.833	0.949	0.930
ABUW_RS11915		1.975	0.00040846	0.447	1.096	3.155	9.050	7.067	4.280
ABUW_RS13490		1.983	2.06e-08	85.883	143.559	120.883	494.466	454.844	436.399
ABUW_RS20220	tgnA	1.992	4.89e-05	0.671	1.973	1.427	5.756	5.590	5.025
ABUW_RS08240		1.993	2.81e-06	4.361	3.068	3.606	19.983	13.922	9.724
ABUW_RS11250		1.995	1.86e-06	3.578	2.849	5.109	16.109	15.399	15.772
ABUW_RS08855		1.997	6.9e-05	0.335	0.877	1.728	3.982	4.113	4.792
ABUW_RS17850		2.002	3.68e-06	5.703	3.178	6.161	18.354	21.569	21.494
ABUW_RS15245		2.009	8.43e-05	9.393	16.219	6.837	74.827	25.840	26.938
ABUW_RS00830	prfB	2.025	0.0476254	0.224	0.000	0.075	0.471	0.475	0.279
ABUW_RS14230		2.029	3.69e-06	2.013	2.520	2.930	10.172	8.385	12.469
ABUW_RS05595		2.042	5.05e-07	9.953	10.849	11.344	38.699	53.105	41.267
ABUW_RS00690		2.065	9.32e-07	22.477	8.548	12.772	58.573	55.689	67.833
ABUW_RS09135	catC	2.071	0.0031059	1.118	0.000	0.451	1.955	2.268	2.326
ABUW_RS10155		2.089	0.00220741	1.230	1.096	0.451	5.611	1.898	3.303
ABUW_RS06715		2.091	3.47e-08	9.505	9.972	9.015	41.884	34.700	44.477
ABUW_RS06405		2.100	6.63e-05	0.559	1.096	0.676	3.439	3.797	2.698
ABUW_RS07785		2.111	3.27e-05	2.907	1.973	1.202	9.159	6.750	9.165
ABUW_RS01250		2.121	2.55e-06	831.428	548.372	485.634	2731.525	2695.790	2686.834
ABUW_RS10355		2.147	0.00171659	1.118	0.219	1.352	4.959	4.430	3.210
ABUW_RS13140		2.149	1.99e-06	3.243	2.849	1.953	10.064	13.342	11.538
ABUW_RS18760		2.159	5.71e-06	2.907	7.561	3.907	17.159	19.987	26.426
ABUW_RS14080		2.166	0.000210496	5.927	2.630	3.306	20.671	15.504	16.144
ABUW_RS05445		2.200	5.69e-05	1.901	0.877	1.052	5.684	6.961	4.699
ABUW_RS10120		2.225	0.000222428	2.796	1.205	0.751	7.602	5.801	7.444
ABUW_RS12105	pobA	2.230	0.000342341	1.342	2.301	0.225	6.299	3.111	6.932
ABUW_RS13275		2.230	0.00438461	0.224	0.329	0.150	1.050	1.266	0.930
ABUW_RS13495		2.235	5.04e-09	68.773	51.834	72.650	305.425	313.829	292.127
ABUW_RS12305	paaE	2.287	1.61e-05	11.406	3.836	11.119	50.464	40.606	39.313
ABUW_RS07255	csuA	2.302	0.0115048	0.559	0.110	0.150	1.267	0.738	1.814
ABUW_RS18540		2.321	3.41e-06	6.933	2.301	5.484	27.947	15.715	30.287
ABUW_RS02230		2.325	1.37e-05	1.677	1.863	1.578	9.593	7.014	8.793
ABUW_RS12300		2.328	8.41e-06	2.013	2.849	6.311	19.874	22.624	17.074
ABUW_RS14910	cntB	2.337	2.62e-08	4.697	5.699	4.808	27.187	24.891	24.518
ABUW_RS16690		2.360	1.25e-05	28.628	28.712	11.420	92.312	117.126	138.410
ABUW_RS00575		2.398	1.52e-06	98.183	43.396	27.197	323.598	304.337	254.582
ABUW_RS10130		2.398	0.0226837	0.112	0.219	0.150	0.869	1.371	0.419
ABUW_RS00875		2.432	0.00643496	0.112	0.329	0.301	1.303	0.527	2.326
ABUW_RS13510		2.449	0.000469908	1.230	0.986	0.225	4.778	2.742	4.559
ABUW_RS11245		2.449	0.000172627	1.454	1.425	0.225	5.792	5.485	4.141
ABUW_RS18030		2.486	8.21e-06	1.677	1.425	1.427	9.448	8.490	7.304
ABUW_RS15545		2.490	1.18e-06	3.355	1.096	1.352	13.756	9.018	8.561
ABUW_RS12325	paaA	2.511	0.00423256	37.462	62.574	8.940	226.146	172.340	213.222
ABUW_RS11300		2.518	6.4e-05	1.230	0.877	0.601	6.046	4.219	4.559

Locustag	Gene	logFC	PValue	LCWB_1	LCWB_2	LCWB_3	LB_1	LB_2	LB_3
ABUW_RS15175	bfr	2.535	8.56e-05	172.436	56.766	32.681	411.059	528.991	568.110
ABUW_RS00350		2.535	5.47e-05	76.601	32.547	20.736	292.683	222.966	229.459
ABUW_RS20225		2.541	2e-05	1.342	0.877	0.301	5.322	4.166	4.001
ABUW_RS06975		2.547	0.000347143	0.335	0.329	0.075	1.086	1.107	1.861
ABUW_RS11235		2.589	1.11e-05	10.176	2.849	2.254	30.228	26.157	31.357
ABUW_RS09455		2.618	1.86e-07	136.316	44.163	109.688	505.434	571.970	705.543
ABUW_RS13505		2.622	1.61e-06	2.013	2.082	1.277	9.412	12.657	10.235
ABUW_RS19925		2.655	0.00307636	0.000	0.548	0.150	0.941	1.793	1.721
ABUW_RS16500		2.672	0.000139327	100.532	25.753	40.119	450.301	287.778	317.483
ABUW_RS12685		2.674	0.00191796	0.447	0.000	0.301	2.136	0.738	1.954
ABUW_RS01110		2.683	0.00148205	0.895	0.000	0.150	2.317	1.107	2.745
ABUW_RS12330	paaZ	2.686	0.00061647	77.496	65.642	23.290	387.022	310.402	364.240
ABUW_RS15500		2.719	0.000196047	0.000	0.219	0.751	2.570	2.268	2.745
ABUW_RS01150		2.730	1.62e-08	4.585	3.836	1.878	19.729	23.362	22.611
ABUW_RS11230		2.751	0.0060845	0.000	0.000	0.301	0.941	0.844	0.884
ABUW_RS11280		2.754	4.4e-06	7.716	2.301	2.179	25.703	25.260	27.961
ABUW_RS12315	paaC	2.760	0.000256392	19.346	15.561	6.386	101.326	84.377	87.280
ABUW_RS09055		2.762	0.00544024	0.224	0.000	0.150	0.543	0.949	1.303
ABUW_RS13910		2.766	0.000285342	0.335	0.000	0.751	3.584	2.320	2.466
ABUW_RS12310	paaD	2.778	4.53e-07	10.064	7.123	7.288	68.202	47.673	50.712
ABUW_RS00910		2.814	0.000126575	120.661	71.231	42.974	593.583	540.276	510.141
ABUW_RS11745		2.837	3.17e-05	0.447	0.767	1.202	5.177	5.590	7.723
ABUW_RS13595	astA	2.839	1.45e-05	16.103	1.753	10.443	85.651	55.478	62.017
ABUW_RS11920		2.844	3.15e-06	8.946	4.055	2.554	48.799	32.116	26.054
ABUW_RS13500		2.847	1.54e-07	16.550	8.109	7.663	86.737	78.840	63.366
ABUW_RS12885		2.853	5.56e-08	11.071	4.164	8.565	69.469	43.296	59.598
ABUW_RS11650	madL	2.895	0.00409355	0.112	0.000	0.150	1.158	0.686	0.326
ABUW_RS09050		2.914	0.0367274	0.224	0.000	0.000	0.615	0.369	0.558
ABUW_RS17065		2.917	0.000107389	17.445	2.630	2.104	36.780	46.724	75.881
ABUW_RS12320	paaB	2.945	2.52e-05	3.914	6.137	0.676	27.947	23.678	25.123
ABUW_RS14270		2.957	0.011578	0.224	0.000	0.150	0.905	1.740	0.558
ABUW_RS18520		3.020	0.0120769	2.684	5.260	2.630	4.996	4.113	75.230
ABUW_RS00905		3.061	0.000227452	15.879	5.151	6.236	87.823	67.080	68.112
ABUW_RS09300		3.128	2.74e-06	2.684	0.877	0.451	12.996	8.121	11.119
ABUW_RS08390		3.135	0.0214836	0.000	0.438	0.000	1.158	1.371	1.024
ABUW_RS09450		3.192	3.48e-06	89.573	26.082	31.479	384.379	427.105	525.215
ABUW_RS20660		3.199	0.000269255	0.112	0.329	0.376	2.896	3.111	2.047
ABUW_RS20685		3.252	0.023779	0.000	0.219	0.000	0.362	0.897	0.837
ABUW_RS00380	hutU	3.320	2.5e-06	110.484	46.355	41.321	697.914	608.727	662.462
ABUW_RS11275		3.325	6.28e-06	1.118	2.082	1.052	16.725	15.557	9.258
ABUW_RS11825		3.350	2.94e-06	9.282	1.644	6.236	51.152	58.062	66.809
ABUW_RS13515		3.416	0.00134654	0.000	0.000	0.376	2.100	1.266	1.814
ABUW_RS12750		3.441	0.000832397	1.006	0.877	0.451	9.666	5.906	8.467
ABUW_RS13600		3.451	7.96e-07	13.978	3.945	2.630	84.492	55.056	75.230
ABUW_RS20630		3.485	0.00327416	0.000	0.110	0.225	1.376	2.215	0.977
ABUW_RS11910		3.615	4.88e-06	0.895	0.658	0.676	12.091	6.803	8.049
ABUW_RS13060		3.747	3.26e-09	1.677	0.767	0.601	12.924	13.289	12.887
ABUW_RS13580		3.760	0.00515	0.000	0.000	0.150	0.724	1.477	0.744
ABUW_RS00325	hppD	3.790	0.000252482	101.091	15.013	13.148	706.602	553.618	503.069
ABUW_RS12115		3.830	1.03e-06	6.710	1.425	0.301	31.314	34.753	43.268
ABUW_RS00345	fahA	3.833	0.000252055	159.688	25.753	26.445	1100.611	939.326	956.217
ABUW_RS04730		3.895	0.00258706	0.000	0.000	0.075	0.615	0.211	0.837

Locustag	Gene	logFC	PValue	LCWB_1	LCWB_2	LCWB_3	LB_1	LB_2	LB_3
ABUW_RS00335		4.244	8.88e-05	20.464	4.493	1.052	184.153	167.066	114.450
ABUW_RS00340	maiA	4.329	0.000207561	34.107	2.301	2.705	304.158	237.521	213.175
ABUW_RS00285		4.427	0.000865593	0.000	0.219	0.000	1.050	1.793	1.814
ABUW_RS15505		7.045	0.00106256	0.000	0.000	0.000	1.339	0.844	0.465
ABUW_RS05670		7.180	0.00425992	0.000	0.000	0.000	0.760	1.160	1.163

A2.2 Differentially Expressed Genes of *A. baumannii* in LB vs in M9 medium

Locustag	Gene	logFC	PValue	M9_1	M9_2	M9_3	LB_1	LB_2	LB_3
ABUW_RS00015	recF	1.709	1.53049e-06	15.912	19.138	18.918	62.410	55.214	58.388
ABUW_RS00025	cybC	1.165	2.2839e-06	78.190	69.298	56.671	170.180	145.287	143.063
ABUW_RS00040		-3.623	2.53873e-07	10.907	14.932	18.330	1.520	0.738	1.163
ABUW_RS00045		-2.869	1.40207e-09	877.114	675.309	732.267	107.299	108.793	96.631
ABUW_RS00050		-2.204	2.29598e-06	32.825	23.343	17.153	6.154	4.008	5.723
ABUW_RS00070	tyrS	1.507	2.97793e-09	142.787	153.651	121.330	402.045	414.449	371.823
ABUW_RS00110		-2.009	5.95907e-10	861.570	669.885	785.911	193.529	197.653	184.609
ABUW_RS00115		-2.753	1.89683e-06	7.798	5.181	10.678	1.593	0.897	0.837
ABUW_RS00120	rsmB	1.066	1.22525e-07	98.581	98.737	92.658	202.724	212.577	192.193
ABUW_RS00155	ppc	1.835	1.88334e-06	675.842	485.028	531.564	2163.645	1973.998	1901.362
ABUW_RS00260		-5.143	4.18257e-11	48.210	28.036	57.932	0.760	2.057	1.117
ABUW_RS00265		1.122	0.000685797	1.370	1.950	1.682	3.439	3.797	3.629
ABUW_RS00270		-4.031	9.07429e-11	413.082	170.778	317.661	18.788	20.514	15.865
ABUW_RS00280		-2.398	1.35082e-07	44.628	19.564	37.248	7.059	6.012	6.095
ABUW_RS00290	purC	1.264	6.92289e-08	116.495	129.211	124.357	266.872	335.135	286.637
ABUW_RS00325	hppD	5.308	2.3881e-05	18.968	13.896	11.183	706.602	553.618	503.069
ABUW_RS00335		4.597	3.94928e-05	8.114	4.693	6.306	184.153	167.066	114.450
ABUW_RS00340	maiA	6.016	2.4843e-05	4.004	4.388	3.111	304.158	237.521	213.175
ABUW_RS00345	fahA	4.654	6.32596e-05	39.833	34.741	44.563	1100.611	939.326	956.217
ABUW_RS00350		4.060	6.71671e-07	13.330	14.810	16.732	292.683	222.966	229.459
ABUW_RS00355		-2.191	0.00204617	44.733	9.203	5.381	3.692	3.375	6.281
ABUW_RS00360	zigA	-2.667	0.00274084	22.867	3.962	1.934	0.869	1.424	2.559
ABUW_RS00370	hutC	1.174	1.09754e-05	35.354	33.461	31.194	73.198	67.027	85.652
ABUW_RS00375		1.227	0.000264145	10.538	14.079	10.006	24.544	27.053	29.776
ABUW_RS00380	hutU	5.338	2.63989e-08	19.916	14.262	14.210	697.914	608.727	662.462
ABUW_RS00385	hutH	3.749	3.53959e-12	27.872	19.199	18.414	293.877	318.998	272.866
ABUW_RS00390		1.706	8.30374e-07	37.251	36.508	34.558	126.594	132.314	94.863
ABUW_RS00395	hutI	1.922	7.59541e-08	19.864	23.404	17.153	77.361	86.855	65.553
ABUW_RS00400	hutG	1.727	1.92403e-05	7.640	7.862	3.279	19.657	23.995	20.331
ABUW_RS00425		1.321	6.39341e-08	16.913	17.127	17.237	46.337	43.560	38.150
ABUW_RS00460	nusB	1.816	6.53724e-09	108.855	100.687	81.139	324.503	360.026	340.001
ABUW_RS00480	serB	1.217	4.26523e-07	96.157	117.021	95.096	234.219	245.062	237.507
ABUW_RS00485	aciT	-2.502	2.05221e-09	945.873	1319.413	1525.914	199.357	230.402	239.554
ABUW_RS00495	dtd	1.015	6.55045e-05	6.797	8.289	10.678	16.182	16.190	19.029
ABUW_RS00515		-1.288	2.76217e-05	482.526	377.698	412.757	155.772	169.756	195.961
ABUW_RS00540		-1.307	8.12637e-07	205.856	180.529	167.238	67.008	78.892	78.022
ABUW_RS00550		-1.630	2.5055e-07	453.178	345.090	412.505	131.010	137.060	123.243
ABUW_RS00575		2.288	2.30099e-06	57.009	61.619	62.136	323.598	304.337	254.582
ABUW_RS00600		1.109	0.0243564	0.948	0.731	1.429	2.715	2.109	1.582
ABUW_RS00605		-1.327	1.09732e-06	69.760	59.425	59.530	25.920	24.522	24.798
ABUW_RS00635		3.491	1.00703e-10	10.222	14.810	8.660	128.114	130.626	122.778
ABUW_RS00645	uraH	-1.272	0.00805697	3.688	3.474	7.063	2.824	1.213	1.442
ABUW_RS00695		2.196	1.34989e-08	5.743	6.461	5.129	30.988	23.784	24.984
ABUW_RS00705	pyrE	1.115	7.35265e-05	34.933	28.219	31.615	66.935	67.449	71.089
ABUW_RS00710		-3.502	3.74837e-06	248.007	256.288	201.376	29.395	21.463	11.166

Locustag	Gene	logFC	PValue	M9_1	M9_2	M9_3	LB_1	LB_2	LB_3
ABUW_RS00770	aceE	1.259	0.000262413	3499.814	2218.647	2028.807	6162.340	6517.537	5857.104
ABUW_RS00780		-1.091	0.00541529	20.654	30.048	26.906	11.367	12.235	12.794
ABUW_RS00785		1.538	4.09954e-06	5.058	5.485	6.811	12.163	21.094	16.888
ABUW_RS00790		-2.175	0.000113557	204.697	215.575	190.865	59.767	42.083	33.265
ABUW_RS00795		3.215	1.53414e-09	16.386	15.420	9.165	113.200	133.421	138.736
ABUW_RS00800		1.549	3.64636e-05	7.482	8.289	11.603	23.530	27.897	27.729
ABUW_RS00805	guaB	1.089	1.65795e-07	813.044	776.849	704.436	1568.903	1721.131	1589.880
ABUW_RS00825		-1.032	0.000722919	2694.937	2017.395	3285.912	1154.694	1353.722	1403.689
ABUW_RS00850		1.065	9.38156e-05	6.428	7.862	8.744	12.670	17.034	18.238
ABUW_RS00865	acs	-1.201	1.04869e-05	535.004	360.815	338.849	185.782	158.681	192.658
ABUW_RS00895		-1.023	0.00313102	402.017	198.692	297.817	168.406	138.273	135.340
ABUW_RS00905		2.157	0.00186641	32.456	6.887	9.669	87.823	67.080	68.112
ABUW_RS00910		2.054	0.00134463	238.365	79.964	76.346	593.583	540.276	510.141
ABUW_RS00915		-2.065	5.74386e-07	43.943	34.558	33.128	11.693	6.856	7.909
ABUW_RS00920		-2.297	4.68696e-12	3871.746	3306.821	3996.738	722.060	798.786	752.859
ABUW_RS00925	omp33-36	4.061	6.339e-10	96.315	214.112	169.004	2370.532	3012.784	2616.443
ABUW_RS00950		-1.329	9.71779e-05	7.376	9.569	8.324	4.054	2.479	3.350
ABUW_RS00965		1.085	1.96303e-06	92.627	96.421	95.180	181.402	230.191	191.448
ABUW_RS00980		2.024	1.59512e-06	1.897	2.499	1.934	8.037	8.807	9.072
ABUW_RS00985		1.465	9.19525e-07	7.271	7.619	8.576	20.164	24.311	20.099
ABUW_RS00990		1.064	0.000156417	5.848	8.106	7.820	15.059	12.076	18.005
ABUW_RS00995		5.209	1.89124e-13	11.065	7.253	12.949	383.438	403.269	361.542
ABUW_RS01005	gabT	6.730	2.69254e-13	7.482	5.363	4.372	626.272	632.300	605.190
ABUW_RS01010		1.049	0.000153313	344.059	252.692	314.129	574.180	678.232	631.942
ABUW_RS01015		-1.203	3.52793e-06	131.775	126.773	123.516	55.641	54.634	55.736
ABUW_RS01020	ycaC	-2.270	1.26707e-09	796.710	680.124	834.090	163.663	150.771	164.650
ABUW_RS01030		1.700	1.66156e-07	351.014	267.747	252.413	990.560	958.575	882.569
ABUW_RS01035		1.632	2.78035e-07	27.398	23.770	17.489	75.225	67.923	70.996
ABUW_RS01050		-1.959	3.80386e-06	41.677	58.084	50.785	12.453	14.660	11.631
ABUW_RS01090		1.611	0.00453126	0.948	1.097	0.589	2.570	3.375	2.466
ABUW_RS01110		1.759	0.00464848	0.474	0.853	0.504	2.317	1.107	2.745
ABUW_RS01140		-1.923	1.43591e-06	742.757	354.842	426.883	142.196	122.610	137.294
ABUW_RS01145		1.828	1.42744e-09	36.777	33.095	39.014	137.816	125.774	122.545
ABUW_RS01150		-1.318	6.84593e-06	46.050	59.547	58.185	19.729	23.362	22.611
ABUW_RS01160	aqpZ	-4.596	2.55964e-14	847.608	596.442	850.738	30.191	31.747	32.939
ABUW_RS01185		1.244	2.45516e-06	10.643	12.129	8.997	24.001	26.526	25.216
ABUW_RS01195		1.546	8.1488e-05	2.582	2.194	2.522	5.539	8.596	7.397
ABUW_RS01205	hisA	1.233	7.01182e-07	95.104	74.052	76.010	148.676	230.824	197.589
ABUW_RS01215		-1.543	6.4164e-08	170.976	154.626	160.596	55.279	53.052	58.528
ABUW_RS01250		4.565	2.65074e-10	140.785	91.301	110.567	2731.525	2695.790	2686.834
ABUW_RS01265		1.097	4.13775e-07	523.834	483.017	408.048	1043.558	1073.855	910.018
ABUW_RS01270		-7.862	3.63378e-15	3097.165	1782.987	3217.217	13.105	8.754	12.748
ABUW_RS01275		1.282	0.000453272	78.296	66.068	54.653	181.583	164.746	138.457
ABUW_RS01285	ettA	1.506	1.62116e-08	795.920	786.601	690.731	1991.365	2353.062	2113.280
ABUW_RS01290		2.881	1.07114e-08	23.868	16.578	15.807	132.458	136.743	147.948
ABUW_RS01300		4.199	2.41086e-08	0.843	4.327	1.513	45.251	35.333	42.570
ABUW_RS01305		4.554	3.29178e-09	0.422	4.084	1.766	57.378	47.620	40.104
ABUW_RS01310		3.358	3.2823e-08	2.371	6.095	2.607	43.549	35.069	35.824
ABUW_RS01315		2.221	2.96274e-11	27.978	37.179	30.606	150.342	148.820	147.389
ABUW_RS01345		-3.424	0.00236966	31.719	28.341	466.653	19.657	12.551	16.330
ABUW_RS01350		2.293	5.98607e-08	53.269	49.551	41.452	251.124	271.166	186.330
ABUW_RS01365	gltX	1.067	1.06874e-06	238.418	233.859	204.150	501.851	489.017	426.397
ABUW_RS01375		2.410	1.07159e-07	28.979	34.253	21.693	144.694	138.484	170.093

Locustag	Gene	logFC	PValue	M9_1	M9_2	M9_3	LB_1	LB_2	LB_3
ABUW_RS01425		2.307	4.23332e-08	86.463	117.996	60.539	425.141	447.831	440.633
ABUW_RS01430		2.885	5.02516e-08	26.713	35.228	14.210	191.429	194.331	181.771
ABUW_RS01435		3.346	1.65803e-09	17.914	20.662	7.567	179.013	157.627	139.992
ABUW_RS01440		2.972	7.61176e-08	28.716	42.542	12.528	231.431	229.769	202.614
ABUW_RS01445	pilQ	3.091	8.66583e-08	94.050	124.152	51.290	773.646	801.634	726.712
ABUW_RS01485		-1.168	3.72373e-05	305.491	242.087	290.250	114.648	124.087	134.223
ABUW_RS01490		-1.300	1.67109e-05	48.368	47.296	57.764	24.363	16.981	20.657
ABUW_RS01495		3.309	2.09612e-06	201.272	170.351	57.176	1357.599	1360.209	1542.984
ABUW_RS01505	bfr	2.128	3.7644e-07	38.568	41.384	56.082	162.722	207.620	222.387
ABUW_RS01510		-5.461	9.46049e-08	61.593	33.156	49.608	1.520	0.633	0.977
ABUW_RS01515		1.323	1.52636e-06	86.094	62.838	51.290	154.070	176.190	172.140
ABUW_RS01530	gmk	1.590	2.63422e-09	67.495	78.441	74.328	211.050	218.431	233.553
ABUW_RS01540		2.865	3.38254e-06	2.951	1.768	1.177	16.833	13.289	14.841
ABUW_RS01545	pilV	2.217	4.30825e-05	10.011	16.273	5.297	49.957	51.312	48.060
ABUW_RS01550		2.197	8.0648e-08	16.597	21.759	11.099	73.777	75.939	78.999
ABUW_RS01555		1.300	6.03838e-05	31.877	49.246	25.897	89.162	92.762	82.534
ABUW_RS01560		1.817	2.89161e-07	189.628	251.169	133.017	697.660	671.799	653.576
ABUW_RS01565		1.774	3.03598e-07	11.539	14.079	11.940	43.187	44.298	41.081
ABUW_RS01570		1.599	3.21528e-07	23.289	32.790	18.246	84.275	72.037	69.740
ABUW_RS01575	rpsP	2.056	5.78541e-08	283.203	269.819	225.339	943.137	1266.023	1028.516
ABUW_RS01580	rimM	1.335	9.40676e-05	721.418	834.872	775.906	1717.797	2281.552	1882.333
ABUW_RS01585	trmD	1.779	9.25064e-06	526.521	604.182	486.244	1592.470	2114.802	1843.811
ABUW_RS01590	rplS	2.347	7.523e-08	338.896	358.743	274.022	1470.220	1873.590	1599.883
ABUW_RS01595		-6.627	7.69246e-05	106.432	1301.006	63.734	5.177	4.588	5.071
ABUW_RS01600		-1.637	0.000625956	5.005	3.047	3.027	1.882	0.316	1.210
ABUW_RS01615		-3.439	3.0582e-08	65.756	53.574	65.079	6.082	5.695	5.164
ABUW_RS01630	serA	1.422	1.1959e-07	462.504	538.114	412.421	1246.282	1398.020	1143.152
ABUW_RS01640		-1.399	2.00733e-06	69.549	53.878	92.490	25.630	27.317	28.752
ABUW_RS01655		-2.567	2.33856e-05	7.535	12.799	16.228	2.172	1.846	2.001
ABUW_RS01670	sodC	-1.081	1.20366e-05	479.364	303.950	397.706	181.474	193.698	183.074
ABUW_RS01680		1.020	2.02204e-05	108.118	151.762	125.870	279.542	224.759	277.798
ABUW_RS01705		1.856	2.29302e-09	40.096	51.562	42.629	170.433	150.666	165.208
ABUW_RS01710		1.106	2.36929e-05	66.072	49.246	44.311	116.711	124.456	103.238
ABUW_RS01715		2.994	2.19653e-12	541.169	513.918	416.372	3610.406	4307.917	3808.771
ABUW_RS01720		2.847	8.34635e-10	97.159	72.894	57.512	543.373	575.925	522.237
ABUW_RS01725	astA	2.748	3.47236e-09	34.090	31.084	19.927	218.652	195.754	160.789
ABUW_RS01730	astD	2.240	4.46164e-09	97.475	109.281	81.727	499.606	463.282	401.134
ABUW_RS01735	astB	2.104	9.60003e-08	143.578	115.375	87.193	506.557	515.174	468.362
ABUW_RS01740	astE	1.261	1.61406e-05	103.270	116.046	116.285	268.899	288.727	246.533
ABUW_RS01750		-1.119	0.0452907	2.529	3.169	1.934	1.303	1.107	1.117
ABUW_RS01755		-1.419	0.000213682	22.182	12.068	25.645	7.711	8.438	6.141
ABUW_RS01760		-1.011	0.00154185	112.175	79.538	95.769	47.604	42.347	52.712
ABUW_RS01790		1.010	0.00396908	3.109	6.095	7.063	10.281	12.867	8.886
ABUW_RS01795	glyS	1.914	1.60813e-09	253.223	250.925	201.796	902.955	972.655	785.891
ABUW_RS01800	glyQ	1.549	5.01132e-08	181.408	172.545	123.852	496.276	479.894	423.140
ABUW_RS01825		1.031	0.00450687	50.423	68.628	102.832	168.116	122.663	160.789
ABUW_RS01835		-1.647	1.55082e-06	608.189	945.920	924.562	239.178	286.354	266.166
ABUW_RS01845	aroE	1.966	8.03133e-07	34.775	28.402	26.654	104.186	112.380	135.386
ABUW_RS01850	hemF	1.593	5.44761e-07	298.272	319.065	279.824	801.086	852.576	1052.662
ABUW_RS01870		1.352	0.00191166	609.981	720.472	722.514	1603.077	2062.594	1573.085
ABUW_RS01910		-1.305	4.61779e-08	709.089	719.497	671.224	256.048	308.134	285.614
ABUW_RS01920		1.961	4.17375e-05	2.266	0.609	1.513	6.480	4.693	6.188
ABUW_RS01935	adeT2	-1.109	3.74009e-05	50.845	48.149	46.581	20.996	24.206	22.378
ABUW_RS01950		-1.636	4.2746e-08	207.279	187.173	237.447	67.189	69.558	66.530
ABUW_RS01960	yihA	1.095	3.77064e-05	63.701	70.335	48.515	127.282	121.819	141.714
ABUW_RS01970		1.516	5.9458e-07	33.721	36.691	28.588	103.534	94.766	85.465
ABUW_RS01990	rpsJ	2.561	5.76554e-08	871.792	985.842	580.584	5052.064	5029.709	4313.003
ABUW_RS01995	rplC	2.509	1.57733e-07	2236.332	2842.150	1665.153	12803.145	13971.975	11624.462
ABUW_RS02000	rplD	2.171	1.29687e-06	1309.796	1637.015	1057.747	6051.168	6890.589	5095.498
ABUW_RS02005	rplW	2.945	1.97589e-08	405.126	544.392	352.050	3581.084	3517.516	2923.690
ABUW_RS02010	rplB	2.117	3.72161e-07	3359.977	3866.267	2685.148	13969.967	15854.794	13159.955
ABUW_RS02015	rpsS	2.292	1.1856e-07	1238.876	1127.791	793.311	4849.521	6090.063	4543.160
ABUW_RS02020	rplV	2.495	4.77578e-08	864.310	1038.257	597.484	4940.711	4970.487	4187.760

Locustag	Gene	logFC	PValue	M9_1	M9_2	M9_3	LB_1	LB_2	LB_3
ABUW_RS02025	rpsC	2.294	4.20017e-08	2664.904	2945.762	1909.999	12212.892	13239.425	11437.759
ABUW_RS02030	rplP	1.680	4.29685e-06	2397.402	3581.211	2397.925	8746.348	9173.090	8928.137
ABUW_RS02035	rpmC	2.239	1.52393e-07	609.348	835.604	597.316	3649.250	2924.346	3069.823
ABUW_RS02040	rpsQ	2.834	3.78131e-09	1468.548	1759.278	997.209	10649.673	10161.882	9313.220
ABUW_RS02045	rplN	2.132	5.09362e-09	1021.587	1022.533	682.575	4245.765	4024.885	3681.248
ABUW_RS02050	rplX	2.671	1.07396e-09	624.891	683.720	369.455	3854.218	3479.072	3358.508
ABUW_RS02055	rplE	2.235	4.22391e-09	1421.707	1462.154	1076.582	6362.132	6703.114	5579.306
ABUW_RS02060	rpsN	1.774	3.13081e-07	880.539	1049.045	824.253	3183.564	3435.934	2800.354
ABUW_RS02065	rpsH	2.086	3.06289e-08	1371.284	1479.646	954.327	5330.629	5805.396	5025.665
ABUW_RS02070	rplF	1.814	1.59304e-07	1972.255	2349.198	1561.228	7034.053	7311.419	6344.820
ABUW_RS02075	rplR	2.161	2.21791e-08	572.940	616.555	411.412	2374.803	2610.939	2174.739
ABUW_RS02080	rpsE	1.845	1.90749e-07	1705.754	1830.588	1425.941	5943.688	6692.198	5187.989
ABUW_RS02085	rpmD	2.440	1.16672e-08	158.963	200.277	155.635	969.383	1007.408	817.156
ABUW_RS02090	rplO	1.406	8.19691e-06	1666.500	1745.443	1536.677	4195.519	5090.460	3832.918
ABUW_RS02095	secY	1.421	1.00369e-05	4830.791	6163.537	4596.493	13659.147	15482.164	12613.897
ABUW_RS02100	rpmJ	1.721	3.99854e-08	373.143	386.109	337.756	1188.759	1262.226	1164.972
ABUW_RS02105	rpsM	2.154	2.09873e-09	1346.731	1313.866	905.980	5381.020	5480.281	5009.986
ABUW_RS02110	rpsK	2.573	6.00624e-09	573.414	480.701	311.943	2533.435	2947.813	2650.685
ABUW_RS02115	rpsD	1.554	2.106e-06	3383.213	3673.426	2720.883	9207.364	10682.910	8813.640
ABUW_RS02120		2.064	3.29672e-08	3674.636	4018.334	2936.636	14202.991	16228.742	14014.795
ABUW_RS02125	rplQ	1.959	1.98503e-07	671.837	792.269	555.864	2461.178	2904.307	2487.570
ABUW_RS02150		-1.660	1.27598e-07	201.799	181.626	169.509	57.342	56.374	61.273
ABUW_RS02155	rrtA	-1.490	3.56716e-06	47.262	41.628	28.672	16.471	12.076	13.306
ABUW_RS02160		-2.097	3.26221e-08	266.448	205.214	182.794	49.848	58.009	45.315
ABUW_RS02165		1.530	3.9935e-06	39.411	41.628	34.558	110.810	106.315	117.149
ABUW_RS02200		1.121	0.0364818	3.319	3.657	4.456	6.335	13.184	5.350
ABUW_RS02205		-4.150	3.78908e-13	7398.009	6084.121	8490.904	455.369	396.255	385.595
ABUW_RS02215		-1.778	9.04507e-05	3.899	6.217	10.258	1.846	1.898	2.001
ABUW_RS02230		1.185	0.0012943	3.056	4.998	3.111	9.593	7.014	8.793
ABUW_RS02240		-1.161	2.52715e-05	262.286	256.471	263.260	119.100	108.372	122.173
ABUW_RS02250		2.217	6.85627e-09	32.298	35.228	34.221	173.293	162.900	136.549
ABUW_RS02265		1.103	0.00123524	11.275	19.564	7.567	24.906	28.003	30.613
ABUW_RS02270	ybeY	1.480	3.66684e-08	52.636	62.228	58.269	163.917	151.509	167.302
ABUW_RS02295		1.128	1.2452e-06	1554.325	1728.255	1210.440	3028.154	3728.247	3063.170
ABUW_RS02305		1.329	0.00220459	46.472	82.829	120.321	164.424	217.692	242.904
ABUW_RS02355		-2.096	2.96685e-05	6.955	5.973	5.886	1.919	1.477	0.930
ABUW_RS02360		-1.693	0.000160738	7.271	6.095	10.510	1.919	1.740	3.629
ABUW_RS02370		1.154	4.34445e-06	5.901	5.485	5.549	12.851	11.971	12.934
ABUW_RS02380		-1.166	2.92458e-05	17.335	21.332	15.891	8.797	8.754	6.793
ABUW_RS02385		-1.143	6.92949e-06	33.668	31.998	35.903	17.014	15.030	13.818
ABUW_RS02390		-1.001	6.48266e-05	24.817	21.332	21.104	10.571	11.602	11.538
ABUW_RS02395		-1.722	1.02471e-05	17.124	12.799	14.798	4.018	5.168	4.466
ABUW_RS02400		-1.341	1.20901e-06	54.849	43.944	37.585	18.354	17.877	17.726
ABUW_RS02415		1.008	0.00170857	17.704	23.343	16.312	39.133	31.694	44.757
ABUW_RS02420	rpsI	2.851	2.5109e-10	180.354	158.771	149.497	1057.170	1378.192	1091.743
ABUW_RS02425	rplM	2.705	1.37312e-10	593.594	735.831	545.606	4213.764	4147.917	3862.507
ABUW_RS02445		1.832	7.71893e-08	9.484	12.799	7.651	38.952	33.540	34.847
ABUW_RS02485		-1.134	7.76817e-05	39.359	49.185	54.485	22.010	21.727	21.262
ABUW_RS02525		2.748	1.83356e-07	83.986	131.222	64.070	647.957	584.890	646.830
ABUW_RS02535		-1.588	4.32399e-06	32.667	59.425	49.272	17.594	13.869	15.353
ABUW_RS02560		1.464	3.30328e-06	31.192	43.152	35.482	111.824	86.803	104.215
ABUW_RS02565		1.169	3.18355e-05	33.141	41.628	30.774	77.578	76.150	83.930
ABUW_RS02590		1.211	8.52887e-06	49.844	50.831	51.206	123.082	102.149	126.314
ABUW_RS02595	radC	2.474	8.09067e-08	3.003	3.962	1.850	20.128	16.032	13.957
ABUW_RS02620	tgt	1.205	6.82011e-07	214.813	203.507	157.905	461.994	463.862	403.088
ABUW_RS02625		1.207	0.000167351	80.403	78.806	56.082	165.111	165.748	167.255
ABUW_RS02630		1.316	0.000514194	15.227	28.951	13.117	56.147	39.657	47.408
ABUW_RS02635	queA	1.130	2.45411e-05	27.925	31.754	26.486	69.505	68.873	50.339
ABUW_RS02645		1.871	7.73638e-06	5.585	6.156	4.709	24.182	20.040	16.330
ABUW_RS02690		1.006	0.047021	1.054	1.036	0.420	1.991	1.160	2.094
ABUW_RS02745		1.587	1.18288e-06	2.898	3.840	3.363	10.643	8.807	10.747
ABUW_RS02775		1.070	0.00479124	1.212	1.768	2.522	3.222	4.008	3.955
ABUW_RS02800		2.330	0.000379673	0.211	0.183	0.252	0.905	1.160	1.256

Locustag	Gene	logFC	PValue	M9_1	M9_2	M9_3	LB_1	LB_2	LB_3
ABUW_RS02810		-1.888	0.0266138	0.790	0.183	0.925	0.253	0.105	0.093
ABUW_RS02875		-1.634	7.36675e-07	179.353	175.227	205.412	60.890	56.585	62.855
ABUW_RS02930		1.543	4.6304e-07	10.643	11.763	10.678	37.251	27.581	31.497
ABUW_RS02935		1.455	1.00935e-06	12.277	14.079	13.873	38.807	32.802	38.383
ABUW_RS02940	aspS	1.943	1.56399e-09	937.601	769.779	579.070	2873.432	3137.820	2783.372
ABUW_RS02950	znuD	-3.153	0.00183098	1439.253	129.455	104.009	65.415	66.236	56.667
ABUW_RS02965		1.831	0.0164132	0.316	0.122	0.168	0.615	1.055	0.698
ABUW_RS02970		-2.123	9.6592e-08	30.928	49.124	38.089	10.317	6.750	9.863
ABUW_RS02985		1.027	0.0112024	2.266	4.632	1.766	5.828	6.486	5.723
ABUW_RS03005		-1.583	2.56829e-09	2240.020	2088.644	2367.319	699.507	828.792	706.427
ABUW_RS03050		-1.693	3.07317e-05	19.495	22.124	12.444	4.416	5.063	7.444
ABUW_RS03065	accD	1.524	6.90862e-09	389.266	360.327	296.472	903.932	1114.461	991.762
ABUW_RS03085		-1.382	9.32524e-06	72.922	74.967	80.130	31.060	25.682	30.567
ABUW_RS03090		-1.106	0.00351608	529.735	379.831	475.146	198.416	192.274	252.767
ABUW_RS03105		-1.374	8.30087e-08	771.209	701.517	669.374	280.628	270.955	274.727
ABUW_RS03110		-1.772	3.13251e-05	268.134	282.801	332.543	90.212	78.049	90.304
ABUW_RS03150		-2.686	5.67375e-11	65.229	51.562	66.677	10.209	9.387	8.840
ABUW_RS03155		-1.324	3.0822e-08	3567.414	3129.583	3535.130	1311.371	1389.319	1385.964
ABUW_RS03160		-1.126	5.80187e-07	5003.242	3881.382	5133.018	1991.438	2396.621	2036.096
ABUW_RS03170		1.099	0.000384415	22.814	35.716	34.810	60.383	81.055	57.969
ABUW_RS03180		-4.552	1.89274e-12	234.835	147.617	196.667	9.774	5.854	8.840
ABUW_RS03210		1.204	0.000166944	84.882	114.157	88.790	223.395	242.795	196.892
ABUW_RS03215		1.450	6.35281e-05	39.569	40.470	37.248	100.348	117.495	102.912
ABUW_RS03220		1.699	1.3495e-05	29.348	30.230	32.035	114.503	111.378	71.322
ABUW_RS03225	typA	2.413	4.61539e-08	270.980	258.117	253.758	1331.716	1641.078	1197.353
ABUW_RS03230	mscL	-1.558	1.93655e-08	300.960	291.395	430.750	115.299	117.337	114.636
ABUW_RS03285		-3.014	4.51933e-11	86.990	67.958	88.202	9.702	9.967	10.421
ABUW_RS03290		-1.739	0.0159907	0.580	0.914	1.177	0.181	0.369	0.233
ABUW_RS03310		-4.567	1.44678e-12	148.636	120.617	158.746	7.457	4.219	6.141
ABUW_RS03315		1.214	1.66861e-07	330.413	353.196	270.154	774.913	778.377	659.252
ABUW_RS03330		4.147	6.09576e-10	0.685	1.097	1.261	18.897	14.713	18.703
ABUW_RS03335	pilG	1.482	1.64773e-05	137.992	195.462	169.172	439.260	480.052	484.366
ABUW_RS03340		2.134	1.30556e-07	92.996	122.689	92.994	413.050	451.311	491.531
ABUW_RS03345		2.878	9.93052e-09	49.001	66.434	36.660	366.279	362.188	392.620
ABUW_RS03350		2.894	3.61241e-08	467.299	539.211	256.701	3253.286	3151.056	2989.150
ABUW_RS03355		2.532	3.46354e-06	346.641	454.615	203.730	2034.336	1975.949	1806.405
ABUW_RS03360		2.429	4.76919e-09	20.391	23.587	16.816	110.666	110.534	107.565
ABUW_RS03365		-1.682	3.98467e-08	40.887	33.948	32.203	12.996	9.809	10.468
ABUW_RS03380		-2.548	3.1483e-06	8.483	6.643	10.426	1.412	1.160	1.721
ABUW_RS03435		-2.411	4.0632e-06	457.393	496.243	453.368	103.208	93.975	67.321
ABUW_RS03460		1.203	0.000734461	15.385	15.542	16.564	42.174	35.544	31.357
ABUW_RS03465		1.573	2.12109e-06	209.650	196.803	181.196	559.663	656.347	532.984
ABUW_RS03470		-2.388	1.95996e-10	58.537	44.431	49.104	9.883	8.754	10.375
ABUW_RS03490		-1.835	1.22328e-07	32.140	37.605	44.731	10.571	9.176	12.189
ABUW_RS03505	gatB	1.713	3.65996e-09	297.271	329.061	245.266	969.890	1017.902	871.589
ABUW_RS03510	gatA	1.417	4.35812e-08	462.873	441.084	313.625	1123.996	1159.181	969.663
ABUW_RS03515	gatC	1.890	1.41027e-08	30.085	30.352	27.158	112.222	102.834	110.123
ABUW_RS03525	mreC	1.310	1.54934e-06	66.599	72.285	64.322	146.106	197.758	160.463
ABUW_RS03535		1.578	0.000272253	6.165	8.655	3.784	17.304	21.200	18.191
ABUW_RS03555		1.331	1.2639e-06	64.913	79.294	60.707	172.279	161.687	181.911
ABUW_RS03560	thrH	1.054	0.000114683	29.084	36.630	29.849	74.175	60.962	63.273
ABUW_RS03570		-2.153	0.00512356	5.638	7.680	48.263	5.430	2.953	4.745
ABUW_RS03605	hchA	-1.574	2.19495e-07	174.559	137.744	164.212	58.356	53.632	47.967
ABUW_RS03650		-1.516	0.000206172	4.953	6.217	4.456	1.339	2.162	2.094

Locustag	Gene	logFC	PValue	M9_1	M9_2	M9_3	LB_1	LB_2	LB_3
ABUW_RS03655		-1.440	0.00280557	6.375	2.438	3.616	1.303	1.951	1.489
ABUW_RS03670		1.266	1.19593e-06	90.362	120.129	98.880	277.623	232.986	233.460
ABUW_RS03675		1.434	1.68328e-05	3.372	5.607	3.111	10.824	12.076	10.142
ABUW_RS03690		-1.298	0.00292233	3.583	2.926	4.793	1.448	1.635	1.442
ABUW_RS03820		1.074	0.00618843	1.739	1.219	1.261	2.136	4.641	2.512
ABUW_RS03860		1.337	0.00748547	1.317	2.682	2.354	5.032	5.432	5.304
ABUW_RS03890		-1.344	7.07429e-06	36.724	33.826	51.878	15.892	14.766	17.354
ABUW_RS04020		-1.603	3.65109e-08	557.292	552.620	573.857	179.447	189.426	185.260
ABUW_RS04025		-1.883	3.31052e-09	466.825	484.723	520.970	136.441	125.669	136.968
ABUW_RS04045		1.815	1.66402e-08	1036.234	1128.827	714.694	3413.656	3362.104	3361.578
ABUW_RS04055		-1.549	1.23101e-05	46.261	49.551	74.076	18.861	16.243	22.704
ABUW_RS04070		-1.028	0.00047088	12.540	8.777	8.408	4.706	5.485	4.559
ABUW_RS04080		-1.058	0.00387319	7.060	6.582	5.802	2.534	3.217	3.722
ABUW_RS04090		-1.252	0.000169016	3.741	4.876	6.054	1.991	1.898	2.140
ABUW_RS04095		1.166	1.3953e-07	664.724	610.033	529.715	1351.988	1460.459	1237.365
ABUW_RS04140		-1.549	2.45559e-08	365.609	411.341	461.692	153.708	140.277	129.012
ABUW_RS04160	rplU	2.483	3.44847e-10	499.597	496.304	394.511	2299.578	2754.696	2720.983
ABUW_RS04165	rpmA	2.402	8.31701e-09	57.642	53.391	53.644	274.836	303.810	292.127
ABUW_RS04170	lolA	1.084	8.37627e-06	70.972	46.138	48.515	118.014	120.764	113.147
ABUW_RS04175		-1.134	0.000354467	170.027	164.012	195.322	84.601	75.676	80.813
ABUW_RS04190		1.577	9.70997e-07	13.067	10.727	13.033	34.282	39.552	36.056
ABUW_RS04225		1.039	0.000130402	82.300	91.545	112.754	170.216	205.247	212.942
ABUW_RS04245		1.908	4.668e-07	48.895	61.375	36.744	205.729	191.694	155.578
ABUW_RS04255	gltA	1.725	3.98157e-09	1080.441	1049.777	731.763	3020.733	3410.621	3030.836
ABUW_RS04270	sdhA	1.628	6.31563e-07	1221.015	1327.397	919.685	3276.419	4217.528	3226.983
ABUW_RS04275		1.379	6.35265e-05	348.959	511.845	400.061	955.880	1308.686	1013.861
ABUW_RS04280		1.338	7.05304e-08	2364.840	2157.881	1880.907	5723.986	5768.059	4694.876
ABUW_RS04285	odhB	1.455	7.17118e-09	1296.202	1294.058	1072.546	3334.231	3643.818	3064.985
ABUW_RS04295	sucC	1.060	1.60675e-06	1926.520	2158.003	1764.706	4126.194	4308.022	3759.967
ABUW_RS04300	sucD	1.699	2.25589e-09	928.907	886.435	705.697	2530.575	3131.544	2524.882
ABUW_RS04310		1.143	2.9684e-06	41.624	39.982	28.083	84.022	77.574	81.557
ABUW_RS04315	trpS	1.006	2.08675e-06	105.641	104.222	91.901	203.738	211.048	191.495
ABUW_RS04320		-1.383	1.26412e-07	444.906	397.811	536.861	180.099	175.188	173.490
ABUW_RS04330		-1.370	6.07818e-08	263.972	240.686	343.978	109.181	106.315	112.729
ABUW_RS04355		-1.632	3.86679e-08	52.636	48.149	51.626	16.001	15.768	17.400
ABUW_RS04365		-1.185	0.000377135	24.079	22.978	35.567	12.779	10.072	13.166
ABUW_RS04375	greA	1.231	2.19231e-05	134.252	140.913	158.914	358.098	342.254	317.809
ABUW_RS04380	carB	1.841	3.39114e-07	649.234	790.928	623.970	2409.991	2800.734	2186.836
ABUW_RS04385	carA	1.347	9.17495e-06	543.698	521.110	364.578	1243.495	1287.381	1106.445
ABUW_RS04390		-1.346	5.97677e-05	70.919	47.906	66.845	20.779	27.739	24.658
ABUW_RS04395		1.095	0.000290776	33.932	40.287	36.491	67.514	87.014	82.023
ABUW_RS04405	rlmE	-1.191	2.89819e-07	644.228	730.285	849.309	314.186	322.109	337.907
ABUW_RS04410	ftsH	-1.247	2.16738e-07	7571.356	8244.684	9791.563	3275.586	3915.459	3600.807
ABUW_RS04425		1.630	0.00466082	1.212	1.219	0.841	2.425	4.693	3.489
ABUW_RS04455		1.368	1.51326e-06	16.913	20.296	16.060	39.024	50.943	47.967
ABUW_RS04470	glpK	1.312	2.10697e-08	52.267	54.793	48.431	130.793	124.772	130.641
ABUW_RS04475	glpD	-2.268	1.78632e-10	133.145	123.847	140.500	29.286	23.204	29.869
ABUW_RS04480		1.492	5.66234e-06	693.545	669.763	528.706	1834.761	2041.289	1445.375
ABUW_RS04485		-3.326	1.08236e-09	62.700	66.678	87.529	7.819	6.170	7.490
ABUW_RS04490		-1.356	3.32675e-05	22.762	21.393	26.149	10.788	9.281	7.211
ABUW_RS04495		-1.170	0.000219522	1701.170	1537.669	1358.003	721.299	689.201	632.640
ABUW_RS04500	groES	2.295	2.22947e-07	102.480	108.610	110.904	595.212	509.953	474.875
ABUW_RS04505	groL	1.452	3.96025e-07	1697.587	1740.140	1627.149	4661.675	5089.880	4100.991
ABUW_RS04520		-2.367	2.24429e-05	3.794	2.621	4.120	0.941	0.422	0.558
ABUW_RS04530		-1.002	1.92878e-05	33.247	31.449	31.867	14.227	15.873	18.191
ABUW_RS04540		1.134	0.000102513	55.903	57.535	35.314	116.060	105.207	106.308
ABUW_RS04610		-1.021	9.17052e-05	212.389	199.850	148.572	86.520	95.821	94.305
ABUW_RS04630		-2.342	6.90347e-08	751.503	471.863	494.568	110.231	109.057	119.661

Locustag	Gene	logFC	PValue	M9_1	M9_2	M9_3	LB_1	LB_2	LB_3
ABUW_RS04635	fdhD	-2.091	9.20592e-07	61.752	48.698	56.671	14.263	13.026	11.864
ABUW_RS04720		-3.969	0.000506868	1.423	2.255	2.270	0.109	0.000	0.233
ABUW_RS04740		-1.514	1.77737e-07	76.979	65.337	78.700	28.562	24.680	24.007
ABUW_RS04760		1.381	0.000117335	98.265	146.825	127.047	312.485	307.554	348.980
ABUW_RS04765		1.178	9.00009e-05	14.121	18.833	14.882	35.911	35.913	36.475
ABUW_RS04785		1.224	0.000321154	5.638	7.070	11.015	18.390	20.092	15.772
ABUW_RS04805	purN	2.407	2.67267e-08	31.613	30.901	22.198	139.264	168.226	144.086
ABUW_RS04810	purM	1.538	5.6144e-07	163.072	176.324	172.283	461.885	555.675	467.850
ABUW_RS04815	cxpE	-1.133	1.39727e-06	807.037	756.493	859.987	359.437	377.534	368.288
ABUW_RS04850		1.440	3.5657e-07	21.602	19.199	21.189	64.546	50.573	52.945
ABUW_RS04855		1.707	1.3374e-08	56.851	70.030	52.215	202.652	193.751	189.075
ABUW_RS04890	ybgC	1.569	5.22194e-08	23.394	20.905	17.489	64.039	60.224	59.877
ABUW_RS04905	ruvA	1.144	1.59454e-07	41.097	37.788	41.789	91.588	87.488	87.466
ABUW_RS04915	purL	1.351	3.08412e-06	455.918	476.678	427.135	1108.719	1312.905	1046.940
ABUW_RS04920		-1.086	0.000113133	58.169	55.097	64.827	29.105	27.423	27.263
ABUW_RS04930		-1.681	4.51285e-06	16.913	12.738	19.339	4.163	5.906	5.257
ABUW_RS04945		-1.145	0.00673212	6.428	8.472	6.895	2.824	4.008	3.117
ABUW_RS04965	queC	1.316	2.71893e-06	114.651	144.021	107.288	304.810	321.793	285.241
ABUW_RS04970	queE	1.058	5.03568e-05	133.567	152.981	129.990	298.511	304.179	264.678
ABUW_RS04980	carO	-4.078	1.33683e-13	7709.559	6058.035	10008.662	427.567	496.611	483.854
ABUW_RS04985		1.016	7.65004e-06	56.430	61.863	58.185	119.426	118.233	119.196
ABUW_RS05010		1.464	0.000859805	140.205	199.119	133.185	375.401	414.080	515.119
ABUW_RS05035	nadB	1.253	1.80013e-07	78.138	74.479	60.455	167.827	173.764	167.116
ABUW_RS05060		1.656	1.89075e-06	16.492	17.614	10.090	40.291	53.105	47.455
ABUW_RS05065	rnc	1.310	2.1962e-05	13.014	18.528	15.303	36.382	35.386	44.291
ABUW_RS05080	recO	1.327	5.62739e-06	10.116	11.275	11.267	26.354	31.589	23.914
ABUW_RS05110		1.081	5.20017e-06	19.758	20.966	19.002	40.581	44.456	41.546
ABUW_RS05115		-2.271	7.21409e-05	6.850	6.461	16.984	2.172	2.215	1.675
ABUW_RS05120		1.468	8.21668e-08	358.812	281.216	249.050	781.791	910.743	768.956
ABUW_RS05125		1.550	0.000831193	0.527	0.853	0.757	1.846	1.951	2.419
ABUW_RS05130		-1.325	3.2033e-05	18.494	20.966	18.414	8.073	6.539	8.421
ABUW_RS05145		-1.532	3.78769e-06	117.444	92.093	112.585	37.757	33.909	39.639
ABUW_RS05150	rarD	-1.343	3.49802e-06	23.289	25.111	35.735	11.838	10.020	11.026
ABUW_RS05155		1.612	3.04549e-06	411.870	382.330	365.587	1186.696	1379.510	980.689
ABUW_RS05160		-1.639	4.32726e-06	28.031	30.109	26.570	10.172	9.440	7.537
ABUW_RS05205		-2.404	4.25691e-10	125.294	97.579	134.615	22.336	20.778	24.332
ABUW_RS05210	wecB	-2.251	7.66839e-09	282.676	199.606	286.887	51.912	52.736	56.946
ABUW_RS05220		-2.500	3.53802e-09	342.373	190.647	256.533	51.477	45.142	42.896
ABUW_RS05225		-2.787	5.84992e-10	159.173	87.522	128.981	20.526	15.979	17.772
ABUW_RS05230		-2.317	2.56619e-08	21.550	19.138	29.429	5.322	3.691	4.839
ABUW_RS05235		-3.656	1.98075e-08	48.895	39.556	69.451	5.394	3.744	3.164
ABUW_RS05245		2.201	3.74212e-08	182.409	191.866	170.602	688.574	890.440	927.139
ABUW_RS05255		1.411	1.08865e-06	73.448	80.940	63.650	233.893	181.990	164.371
ABUW_RS05265		2.004	6.71317e-10	1686.838	1563.511	1182.861	6064.671	6270.260	5444.478
ABUW_RS05285		-2.018	1.31022e-07	22.814	26.634	34.053	7.095	6.328	7.025
ABUW_RS05290		-2.150	0.00076109	1.844	2.926	4.961	0.724	1.002	0.372
ABUW_RS05295		-1.652	1.17522e-07	105.167	179.432	141.762	46.735	44.720	44.105
ABUW_RS05315		1.894	7.85128e-07	7.218	4.754	5.633	19.621	23.256	23.169
ABUW_RS05330		-2.408	6.32213e-08	10.064	7.923	13.705	1.738	1.951	2.233
ABUW_RS05440		1.664	0.00134954	1.159	2.621	1.429	7.566	4.430	4.327
ABUW_RS05445		1.444	0.000525211	2.318	1.828	2.186	5.684	6.961	4.699
ABUW_RS05475	sohB	-1.543	0.000120316	1766.873	2168.730	3298.692	764.632	873.723	844.140
ABUW_RS05490	purB	2.015	6.25783e-10	206.383	250.011	202.301	876.238	933.842	852.095
ABUW_RS05525		2.974	1.33197e-08	3.267	3.901	0.841	24.218	19.723	22.285
ABUW_RS05545		1.073	0.000473841	522.464	494.109	422.931	1025.458	961.791	1042.474
ABUW_RS05555	gloA	1.024	9.51981e-05	18.494	17.553	25.056	39.567	40.976	43.035
ABUW_RS05570		1.356	6.51209e-06	296.744	296.697	201.207	732.160	679.603	623.242
ABUW_RS05585	efp	1.775	1.20093e-08	311.708	411.037	280.749	1126.747	1152.642	1155.854

Locustag	Gene	logFC	PValue	M9_1	M9_2	M9_3	LB_1	LB_2	LB_3
ABUW_RS05645		-1.127	0.0155282	2.213	3.840	2.859	1.122	1.898	1.117
ABUW_RS05655		-1.123	0.0474451	1.581	2.804	2.018	0.941	1.055	0.930
ABUW_RS05660	yddG	1.768	0.00101502	1.581	0.305	0.589	2.787	3.902	2.419
ABUW_RS05665		-1.098	0.0138647	2.318	2.011	4.036	1.484	0.844	1.349
ABUW_RS05695		-1.071	0.000102751	38.937	28.036	33.212	15.856	16.190	15.679
ABUW_RS05700		-1.134	0.002195	27.346	21.576	39.855	13.575	13.395	13.213
ABUW_RS05705		1.717	1.42375e-05	5.216	4.815	5.297	18.571	13.975	17.679
ABUW_RS05710	bauF	-8.895	9.70303e-10	1241.037	1017.047	1383.059	3.149	1.477	2.838
ABUW_RS05715	basA	-7.404	8.1356e-10	1607.489	1295.521	1424.007	9.702	7.278	8.421
ABUW_RS05720	basB	-6.636	4.14341e-12	2345.240	1668.526	1638.752	23.965	17.666	14.981
ABUW_RS05725	bauD	-8.606	1.50475e-11	341.161	196.132	292.352	0.905	1.002	0.186
ABUW_RS05730	bauC	-7.582	3.25831e-11	363.659	245.257	331.282	1.412	2.162	1.396
ABUW_RS05735	bauE	-6.683	7.25677e-16	879.906	816.161	812.313	8.724	7.119	8.467
ABUW_RS05740	bauB	-7.218	6.60658e-15	5860.123	5314.830	5292.100	38.590	39.446	32.521
ABUW_RS05745	bauA	-6.430	1.00067e-14	6207.343	4877.463	4624.576	66.682	56.322	59.040
ABUW_RS05750	basC	-7.401	3.79943e-14	3066.974	2099.553	2460.902	16.725	12.129	16.097
ABUW_RS05755	basD	-7.975	1.71963e-13	4969.257	3946.353	4290.435	20.526	15.873	15.911
ABUW_RS05760	basE	-9.600	1.87863e-11	3415.617	2509.737	3357.045	5.684	4.061	2.001
ABUW_RS05765	basF	-8.455	1.08813e-14	1476.504	1333.492	1478.913	4.344	4.061	3.768
ABUW_RS05770	basG	-8.384	2.68032e-13	2395.242	2064.813	2127.603	8.797	5.748	4.932
ABUW_RS05780	barA	-7.321	2.79486e-16	5168.896	3994.381	4528.807	28.562	27.528	29.497
ABUW_RS05785	barB	-6.701	3.15699e-16	3408.504	2508.701	2741.147	28.309	28.108	26.752
ABUW_RS05790	basH	-7.040	4.36479e-14	362.237	300.659	461.945	2.172	2.162	4.234
ABUW_RS05795	basI	-5.046	2.8355e-10	21.076	26.147	27.579	0.362	1.371	0.651
ABUW_RS05800	basJ	-9.601	4.08204e-14	7351.327	5269.972	9222.498	10.245	8.701	9.072
ABUW_RS05810	hemE	1.504	7.77498e-09	44.891	44.675	47.086	114.503	143.915	129.105
ABUW_RS05815		1.127	0.00210846	6.428	5.485	3.531	8.942	14.239	11.538
ABUW_RS05820		-1.033	8.31028e-05	3012.335	2651.929	3242.357	1181.483	1512.773	1657.155
ABUW_RS05835	folE	1.449	3.68609e-06	20.285	15.664	15.387	40.581	52.103	48.246
ABUW_RS05840	xdhA	-1.395	2.11851e-05	29.717	19.382	26.402	10.209	8.649	9.770
ABUW_RS05845	xdhB	-2.219	9.24165e-10	127.876	104.527	108.045	22.119	24.891	26.193
ABUW_RS05850	xdhC	-1.946	2.95899e-06	17.335	16.395	21.945	3.765	6.856	3.955
ABUW_RS05855		1.295	1.46583e-06	23.921	31.145	21.020	55.858	68.714	62.808
ABUW_RS05885		1.032	3.67952e-05	141.470	154.322	129.738	314.982	278.971	276.169
ABUW_RS05910		-2.998	5.10092e-10	1320.017	991.693	812.229	134.486	122.768	133.897
ABUW_RS05920		2.404	0.00402506	0.263	1.097	0.336	1.520	5.748	2.280
ABUW_RS05940		1.450	1.47206e-07	642.858	662.022	405.021	1487.777	1692.285	1491.667
ABUW_RS05960		1.390	2.48587e-08	659.139	679.393	580.668	1748.422	1800.445	1482.269
ABUW_RS05970		1.126	6.20956e-05	10.011	17.127	11.687	27.404	28.899	28.519
ABUW_RS05975	metF	1.324	0.000112681	117.865	174.556	68.947	280.302	326.697	299.524
ABUW_RS05980	ahcY	1.969	2.51604e-07	607.610	689.145	315.643	2002.769	2266.417	2046.006
ABUW_RS05995		-4.705	6.56262e-12	1133.973	569.564	952.477	32.074	35.807	34.009
ABUW_RS06015		-1.272	1.09856e-06	34.353	43.883	41.873	14.770	17.719	17.261
ABUW_RS06035	rpsB	2.487	3.17276e-10	1267.381	1276.932	994.518	6107.677	7414.833	6316.858
ABUW_RS06040	tsf	2.409	2.02241e-10	829.377	875.098	625.652	3701.958	4791.396	3887.072
ABUW_RS06065		-2.191	7.2354e-07	12.066	15.481	11.940	3.258	3.217	2.140
ABUW_RS06195		-1.927	0.0118906	0.422	0.609	2.438	0.362	0.000	0.372
ABUW_RS06200		-1.471	0.0480667	0.843	1.158	2.607	0.724	0.211	0.512
ABUW_RS06255		1.362	5.95383e-05	1.844	2.621	2.102	5.828	6.117	4.932
ABUW_RS06260		-1.467	6.04188e-06	11.539	11.032	11.687	3.692	4.166	4.559
ABUW_RS06270		-3.819	3.00844e-05	3.530	0.853	3.363	0.362	0.000	0.093
ABUW_RS06275		-2.578	0.000180317	6.217	4.144	10.174	1.122	0.738	1.442
ABUW_RS06280		-1.107	0.00195826	72.079	92.398	113.006	45.830	36.546	46.106
ABUW_RS06285		-1.124	0.0085509	2.055	1.889	1.429	0.977	0.897	0.605
ABUW_RS06305		-1.050	0.0435196	1.159	2.011	1.934	0.652	1.371	0.465
ABUW_RS06390		-1.989	0.0158935	1.423	0.305	1.093	0.362	0.105	0.186
ABUW_RS06395		-1.302	0.00107298	10.222	8.959	11.519	2.715	4.008	5.816
ABUW_RS06405		1.485	0.000279775	1.106	1.707	0.589	3.439	3.797	2.698
ABUW_RS06430		-1.734	1.21977e-05	31.087	36.569	59.530	14.951	11.813	11.073
ABUW_RS06490		2.230	0.0016966	0.000	0.731	0.504	1.774	1.846	1.861
ABUW_RS06495		1.188	5.90452e-05	8.694	10.544	7.231	20.236	17.403	23.030
ABUW_RS06500		-1.468	0.000127003	28.452	20.418	16.060	8.109	7.014	8.467
ABUW_RS06505	glyA	1.600	2.57104e-08	390.742	395.799	301.517	1045.766	1250.677	1002.323
ABUW_RS06525	adeL	-1.582	3.19644e-08	65.650	72.955	91.733	24.653	27.159	25.030

Locustag	Gene	logFC	PValue	M9_1	M9_2	M9_3	LB_1	LB_2	LB_3
ABUW_RS06530		-1.203	0.00296306	3.794	8.045	7.651	3.005	2.162	3.071
ABUW_RS06555		2.969	1.42944e-08	1.106	2.926	1.513	14.625	13.500	15.353
ABUW_RS06560	yegQ	2.570	1.78044e-08	77.506	86.486	34.810	371.202	381.753	432.771
ABUW_RS06575		1.230	9.00956e-06	51.319	64.057	47.506	138.359	140.224	103.936
ABUW_RS06585		-2.065	4.07858e-08	74.660	63.508	58.857	15.313	14.924	16.888
ABUW_RS06590		2.668	7.70959e-06	38.200	40.409	19.675	195.955	205.511	227.598
ABUW_RS06595		-1.689	3.64533e-07	74.660	52.720	79.373	22.444	19.670	21.866
ABUW_RS06600		-1.555	2.00768e-06	55.798	62.838	72.983	22.046	19.354	23.634
ABUW_RS06610	hemP	-6.863	2.17229e-10	2731.398	1952.241	2992.803	24.508	23.678	17.679
ABUW_RS06655		-4.028	1.25451e-09	204.433	211.430	195.322	14.227	10.283	12.794
ABUW_RS06670		-1.129	2.84398e-05	28.979	30.718	44.311	13.937	17.930	15.586
ABUW_RS06695		1.067	1.0565e-07	91.732	101.967	103.000	201.276	211.944	208.057
ABUW_RS06700	thiS	1.620	4.42608e-07	23.236	26.756	17.153	65.741	69.295	72.532
ABUW_RS06715		1.506	1.09126e-06	11.750	13.835	17.405	41.884	34.700	44.477
ABUW_RS06730		-3.382	3.49506e-11	134.410	79.477	148.068	12.344	10.969	11.305
ABUW_RS06750		1.410	1.3131e-05	7.166	4.998	5.297	16.254	16.084	14.516
ABUW_RS06765		-1.659	0.000828659	5.322	4.693	6.306	2.136	1.635	1.256
ABUW_RS06825		1.193	5.8093e-05	5.743	4.205	3.868	10.498	11.338	10.282
ABUW_RS06975		2.932	2.8412e-05	0.105	0.122	0.336	1.086	1.107	1.861
ABUW_RS06980		-1.093	0.000666256	9.958	6.765	13.705	5.032	4.377	4.606
ABUW_RS07065		-1.130	1.58803e-05	80.245	66.556	79.037	33.087	30.270	39.778
ABUW_RS07070		1.690	2.4066e-07	564.194	576.146	617.496	1599.239	2166.694	1904.572
ABUW_RS07075	rpsU	1.892	5.58246e-09	202.062	181.566	184.643	575.664	789.504	744.484
ABUW_RS07140		-1.495	5.6342e-05	15.174	9.752	11.099	4.706	3.586	4.466
ABUW_RS07145		-7.715	1.29348e-12	118.392	60.644	189.352	0.290	0.316	1.163
ABUW_RS07150		-6.410	7.15138e-12	227.616	78.989	164.043	1.810	2.004	1.721
ABUW_RS07155		-6.966	2.89037e-11	189.733	71.127	139.155	0.869	0.791	1.535
ABUW_RS07160		-6.727	3.01022e-12	68.338	34.192	64.911	0.217	0.738	0.698
ABUW_RS07165		-6.288	1.87771e-10	69.023	30.474	85.175	0.724	0.633	0.977
ABUW_RS07170		-4.274	7.05247e-08	8.852	2.560	10.594	0.362	0.211	0.512
ABUW_RS07180		-2.722	4.56404e-06	8.641	8.533	12.360	1.701	0.844	1.768
ABUW_RS07195		-2.622	1.45299e-06	14.121	26.574	15.891	3.765	2.848	2.466
ABUW_RS07280		-1.455	0.021485	1.001	0.549	1.345	0.398	0.105	0.465
ABUW_RS07295	proP	-1.402	7.89638e-07	138.519	96.969	107.456	46.518	43.190	40.104
ABUW_RS07310		-2.617	4.24483e-08	74.924	64.849	80.971	10.896	13.764	11.398
ABUW_RS07320		-1.627	1.19085e-07	44.101	41.933	41.452	13.720	12.551	14.981
ABUW_RS07325		-1.473	8.55944e-08	209.755	184.125	203.982	72.438	71.720	71.229
ABUW_RS07345		-1.454	1.24397e-05	14.648	19.199	15.976	5.358	5.537	7.304
ABUW_RS07375		-1.618	0.00105259	2.371	3.474	3.447	0.833	1.213	0.977
ABUW_RS07380		-2.034	0.000467278	4.110	2.438	1.934	0.615	1.055	0.512
ABUW_RS07390		-1.242	7.46472e-06	25.291	25.903	28.336	9.955	11.338	12.329
ABUW_RS07425		-2.602	1.85124e-10	367.769	238.065	331.534	51.803	49.677	52.852
ABUW_RS07430		-1.708	1.48453e-05	17.598	12.494	24.047	4.489	6.592	5.490
ABUW_RS07435		1.080	0.00214267	5.532	3.596	2.438	9.412	9.703	6.141
ABUW_RS07440		1.680	0.000300805	1.844	0.488	1.682	4.272	3.850	4.699
ABUW_RS07445		-1.007	0.0041882	177.140	188.575	82.652	80.800	75.201	67.414
ABUW_RS07450		-1.893	2.29441e-05	91.679	93.800	203.814	34.246	29.848	40.383
ABUW_RS07460		1.247	1.16367e-06	47.578	55.829	49.524	119.173	134.792	109.007
ABUW_RS07470		1.030	4.23188e-06	253.803	240.686	225.675	465.903	507.580	497.626
ABUW_RS07475	purD	1.100	6.5905e-05	285.785	275.487	230.972	572.442	623.440	503.534
ABUW_RS07500		-4.536	1.26935e-12	176.877	110.073	180.187	7.638	5.748	6.606

Locustag	Gene	logFC	PValue	M9_1	M9_2	M9_3	LB_1	LB_2	LB_3
ABUW_RS07515		-1.886	1.30507e-06	104.851	73.870	87.193	23.784	21.463	26.659
ABUW_RS07520		-2.125	6.27591e-08	16.702	14.932	22.702	3.982	3.322	5.025
ABUW_RS07525		-1.677	4.25715e-05	35.460	23.648	33.801	7.747	12.182	9.305
ABUW_RS07530		-1.501	6.55777e-06	43.416	36.325	40.023	11.838	13.289	17.261
ABUW_RS07535	alr	2.090	1.18422e-08	11.381	13.957	11.940	51.079	52.999	54.759
ABUW_RS07540	dnaB	1.154	8.29269e-06	37.883	43.944	35.482	89.452	85.221	86.582
ABUW_RS07545	rplI	2.685	3.35238e-09	608.453	585.837	489.271	3336.729	4214.311	3275.089
ABUW_RS07550	rpsR	2.328	4.44878e-08	277.197	332.108	274.358	1396.045	1704.941	1335.996
ABUW_RS07555	rpsF	2.164	8.32863e-08	622.415	765.025	605.808	3248.254	3158.439	2527.906
ABUW_RS07565		1.067	1.24773e-05	289.526	205.579	196.835	430.318	571.548	449.287
ABUW_RS07570	cyoC	1.204	3.4952e-07	1095.404	1016.316	875.206	2165.962	2576.871	2138.264
ABUW_RS07580	cyoA	1.191	3.01403e-07	4049.097	4229.581	3132.042	8542.320	9322.807	8181.140
ABUW_RS07600	pgaA	-1.290	0.0106885	3.794	7.984	9.922	2.425	2.479	3.768
ABUW_RS07610	pgaC	-1.419	0.000319305	8.852	12.433	9.669	3.656	4.483	3.489
ABUW_RS07615	pgaD	-1.416	0.0015118	2.424	3.291	1.009	0.760	1.002	0.884
ABUW_RS07620		-3.151	2.84249e-08	20.918	15.664	14.630	2.172	1.688	1.861
ABUW_RS07700		-1.762	1.57979e-08	92.891	79.538	111.660	28.961	28.899	25.775
ABUW_RS07715		1.420	1.54677e-05	7.271	8.045	3.447	15.639	18.668	17.261
ABUW_RS07720	kdpA	1.076	0.000230545	13.910	11.763	7.651	25.268	21.833	24.100
ABUW_RS07725	kdpB	1.256	8.78135e-05	6.639	10.239	8.072	20.453	20.725	18.284
ABUW_RS07740		-1.108	1.44489e-05	22.446	24.684	28.167	11.729	11.549	11.538
ABUW_RS07750		-1.438	0.00858387	3.319	5.851	10.258	2.027	1.846	3.024
ABUW_RS07770		-1.040	1.63713e-06	644.228	609.972	670.972	319.146	309.136	307.945
ABUW_RS07780		2.293	1.39868e-10	1047.826	1064.892	732.267	4383.618	5207.480	4352.875
ABUW_RS07800		2.272	0.000344437	1.054	0.488	0.252	2.968	1.951	4.513
ABUW_RS07805		-3.547	1.91519e-06	179.301	176.141	204.823	18.028	14.819	14.934
ABUW_RS07810		-1.367	1.34166e-05	73.817	120.495	77.523	32.291	33.962	39.220
ABUW_RS07820		-3.164	9.19721e-09	9.642	8.533	14.294	1.267	1.002	1.256
ABUW_RS07825		-1.200	8.68591e-06	79.771	62.107	98.712	29.178	33.804	41.639
ABUW_RS07830		-2.133	5.10374e-07	22.920	16.578	18.246	6.046	3.322	3.582
ABUW_RS07865		-1.129	0.000446488	7.218	9.813	6.642	4.127	3.111	3.536
ABUW_RS07880		1.885	5.46343e-10	72.395	71.797	60.791	215.575	297.692	245.091
ABUW_RS07895	eutC	-1.022	0.0194649	3.056	4.876	4.372	2.063	1.951	1.954
ABUW_RS07935		1.763	8.83663e-07	6.692	3.840	5.381	18.137	17.455	18.749
ABUW_RS07950		-1.218	0.011196	4.110	4.693	2.102	1.267	0.738	2.791
ABUW_RS07955	pepN	1.064	0.00156265	1039.343	1025.275	957.606	2070.790	2042.713	2207.539
ABUW_RS07960		-6.133	7.20482e-12	980.700	438.341	823.244	8.326	12.287	11.492
ABUW_RS07965		-4.747	2.53963e-10	194.686	83.682	135.708	6.046	4.693	4.559
ABUW_RS07970		-4.418	1.11407e-08	329.095	154.383	235.092	11.548	11.813	10.235
ABUW_RS07975		-4.551	8.84859e-12	296.428	179.981	353.563	12.127	12.498	10.747
ABUW_RS07980		-2.669	7.08698e-07	23.605	12.494	25.056	3.403	2.004	4.048
ABUW_RS07985		-2.424	1.52377e-06	15.069	15.847	17.321	3.620	2.109	3.071
ABUW_RS07990		-2.524	3.65713e-08	21.286	17.431	25.140	3.294	3.059	4.699
ABUW_RS08010		3.820	7.95581e-07	0.527	0.305	0.000	5.756	3.533	4.141
ABUW_RS08040		-2.341	1.04283e-09	202.168	133.721	210.877	38.445	40.870	28.519
ABUW_RS08045		-1.655	0.0183649	1.370	1.036	0.504	0.471	0.000	0.419
ABUW_RS08050		-5.480	2.57096e-08	1.686	2.438	2.859	0.072	0.000	0.047
ABUW_RS08060		-1.970	4.13159e-06	6.902	9.935	12.108	2.643	3.059	1.582
ABUW_RS08070		-3.228	9.14287e-06	155.011	172.362	92.154	18.571	14.977	11.119
ABUW_RS08075		-2.613	1.55891e-09	39.622	33.156	33.296	6.082	5.801	5.443
ABUW_RS08085		-6.708	4.01849e-13	14.279	5.973	14.294	0.145	0.105	0.047
ABUW_RS08095		-2.126	4.00833e-08	1103.044	902.342	1236.925	228.535	270.850	243.183
ABUW_RS08110		-1.231	0.000195773	38.358	32.851	62.389	20.309	18.194	18.051
ABUW_RS08125		2.364	2.06665e-06	18.915	18.833	20.432	84.529	102.254	112.450
ABUW_RS08155		-1.914	8.01884e-08	739.964	1359.822	1340.935	267.668	314.831	330.603

Locustag	Gene	logFC	PValue	M9_1	M9_2	M9_3	LB_1	LB_2	LB_3
ABUW_RS08160		-2.660	1.51829e-09	458.394	635.815	785.071	86.882	104.047	106.494
ABUW_RS08165		-1.654	5.67471e-08	137.202	197.839	194.145	52.636	59.328	56.108
ABUW_RS08170		-1.704	5.71757e-07	131.301	151.213	132.429	46.337	40.870	40.058
ABUW_RS08175		1.071	0.00126527	2.793	4.144	2.354	6.552	6.328	6.886
ABUW_RS08185		1.230	1.31357e-07	84.092	87.156	75.001	187.303	196.651	194.193
ABUW_RS08200		-1.036	6.55622e-06	133.830	120.251	103.420	64.220	50.152	59.924
ABUW_RS08240		-1.482	5.46947e-06	34.142	43.517	45.236	19.983	13.922	9.724
ABUW_RS08245		-2.958	2.86345e-11	410.553	322.722	336.495	46.627	42.663	48.339
ABUW_RS08260	accC	2.180	9.32664e-11	751.609	866.444	653.567	3255.495	3832.031	3209.955
ABUW_RS08265	accB	2.223	3.35104e-10	300.485	323.027	209.027	1315.751	1373.076	1199.214
ABUW_RS08270	aroQ	2.832	1.08487e-11	28.241	23.465	25.477	200.154	164.693	185.353
ABUW_RS08275		1.860	1.23255e-06	3.003	4.388	4.120	18.209	10.916	12.003
ABUW_RS08280		-1.139	0.0253608	2.951	3.657	1.513	1.557	0.738	1.396
ABUW_RS08305		-1.281	2.86276e-05	20.496	20.540	26.402	8.833	7.541	11.212
ABUW_RS08310		-1.104	0.000278912	13.646	11.580	18.666	5.973	6.697	7.630
ABUW_RS08315		-1.028	0.000180357	19.811	19.930	20.096	11.150	8.227	9.817
ABUW_RS08320	moaA	-1.972	4.14168e-08	48.000	46.138	49.860	14.263	9.440	12.794
ABUW_RS08380		-2.380	1.00277e-08	341.635	280.607	431.255	56.328	70.877	75.184
ABUW_RS08385	fumC	-4.924	2.19564e-09	3599.660	2896.150	3146.588	105.453	110.481	101.609
ABUW_RS08390		-1.560	0.00995863	3.425	1.158	6.390	1.158	1.371	1.024
ABUW_RS08405		-1.594	4.14047e-08	238.839	199.119	265.698	68.528	79.420	85.233
ABUW_RS08420		1.586	0.00283957	1.054	1.585	1.682	3.511	3.164	6.048
ABUW_RS08445	rimO	1.223	5.28185e-07	128.087	147.252	130.158	334.205	325.853	286.730
ABUW_RS08450	pyrH	1.223	2.58557e-05	125.189	156.394	165.220	366.424	346.947	328.602
ABUW_RS08455	frr	1.472	1.70669e-07	103.587	121.714	98.207	291.705	317.363	288.824
ABUW_RS08470	ispC	1.134	2.98216e-05	99.898	117.265	89.211	216.661	233.197	223.224
ABUW_RS08495	fabZ	1.805	1.19676e-09	86.357	88.619	86.352	314.874	316.941	281.566
ABUW_RS08500	lpxA	1.132	1.19458e-06	154.748	158.100	174.554	372.361	373.632	321.624
ABUW_RS08505		1.346	1.87176e-05	88.728	76.125	49.356	195.918	177.666	172.606
ABUW_RS08530		-3.076	4.8842e-08	44.153	34.923	43.302	5.322	4.588	4.513
ABUW_RS08535		-1.535	0.0261787	0.527	2.255	2.102	0.543	0.844	0.233
ABUW_RS08540		-1.468	3.82009e-06	32.456	23.039	41.789	11.693	10.178	13.073
ABUW_RS08570		-3.396	5.50529e-10	147.951	113.120	142.939	14.118	9.387	14.702
ABUW_RS08575		1.365	0.000352947	6.850	6.643	8.492	20.671	17.561	17.865
ABUW_RS08580		-3.234	1.03953e-06	6.165	3.657	10.174	0.362	1.055	0.744
ABUW_RS08585		-2.046	5.16934e-10	416.243	354.354	442.858	117.689	85.748	90.211
ABUW_RS08590		-4.409	8.07338e-10	40.939	48.210	82.905	2.172	3.533	2.466
ABUW_RS08605		1.527	0.000117346	0.948	1.585	2.522	4.634	5.115	4.094
ABUW_RS08615		3.979	9.68276e-13	7.693	6.461	5.213	107.987	100.356	101.237
ABUW_RS08620		1.347	2.17094e-07	68.601	81.122	68.442	189.185	187.791	178.003
ABUW_RS08625	pfkB	1.781	3.87248e-09	22.920	26.939	21.861	84.058	86.117	76.719
ABUW_RS08630	ptsP	1.528	9.93476e-08	92.417	114.400	97.198	315.670	298.853	261.979
ABUW_RS08645		-2.859	9.76857e-09	66.230	70.274	113.594	8.145	14.344	12.143
ABUW_RS08665		-1.003	2.11967e-05	57.536	57.292	62.052	30.590	26.315	31.218
ABUW_RS08675	grxD	1.796	2.18855e-07	9.642	15.542	14.882	46.409	43.560	48.199
ABUW_RS08685		-1.435	1.78759e-06	189.997	235.871	338.849	103.063	91.760	87.559
ABUW_RS08690		-1.860	1.37982e-06	105.167	76.125	99.216	26.608	22.254	28.287
ABUW_RS08700		-4.664	7.26881e-11	155.696	103.917	236.942	4.851	8.543	6.374
ABUW_RS08705		-2.997	8.18528e-09	38.200	30.169	69.031	5.503	5.537	6.048
ABUW_RS08725		2.237	5.45458e-07	12.329	9.630	4.709	39.097	44.562	45.268
ABUW_RS08730	cydX	1.228	0.0467217	0.474	1.950	0.000	1.882	2.637	1.628
ABUW_RS08735	cydB	1.331	0.000773973	712.882	663.912	207.514	1255.875	1394.118	1338.509
ABUW_RS08740		1.506	8.42168e-05	787.490	845.843	259.560	1717.579	1796.859	1863.816
ABUW_RS08745	cydP	1.873	1.38045e-05	2.213	2.926	1.850	8.000	6.592	11.352
ABUW_RS08775		-1.087	1.84719e-07	259.704	263.663	290.923	126.739	133.896	122.545
ABUW_RS08825	clpA	-1.847	3.32273e-08	1889.638	1536.511	1973.313	486.031	524.508	490.042
ABUW_RS08830		-2.716	6.46309e-09	68.285	60.339	76.178	10.172	8.807	12.096
ABUW_RS08835		-1.954	7.72846e-09	186.835	156.516	145.461	42.644	40.448	43.082

Locustag	Gene	logFC	PValue	M9_1	M9_2	M9_3	LB_1	LB_2	LB_3
ABUW_RS08850		1.826	9.175e-08	15.543	24.501	17.405	80.257	61.384	61.971
ABUW_RS08855		1.368	0.000454957	1.791	1.950	1.093	3.982	4.113	4.792
ABUW_RS08875		2.703	1.14687e-09	20.865	14.201	13.369	111.172	97.033	109.658
ABUW_RS08890	eno	1.394	8.37678e-07	324.670	375.808	339.858	820.779	1053.393	859.865
ABUW_RS08895		-2.258	4.47114e-06	10.274	8.959	9.165	1.303	3.059	1.768
ABUW_RS08925		-1.595	0.000805604	17.598	13.592	8.997	3.620	4.008	5.909
ABUW_RS08935		-1.805	2.94313e-07	23.341	15.298	20.011	5.466	5.168	6.141
ABUW_RS08945	pcaH	-1.290	1.16567e-05	27.978	24.623	20.348	10.498	8.860	10.515
ABUW_RS08950	pcaG	-1.660	8.42259e-08	24.711	22.063	21.693	6.009	8.279	7.537
ABUW_RS08965		-1.544	6.70445e-06	25.818	17.127	20.264	7.023	6.592	8.095
ABUW_RS08970		-2.065	2.11623e-10	250.273	226.180	218.024	48.980	55.161	61.971
ABUW_RS08980		-1.223	0.00173048	6.481	9.325	7.567	3.910	2.109	3.815
ABUW_RS08985		-1.113	0.00621162	4.637	4.876	6.138	2.643	3.164	1.349
ABUW_RS08990		-1.350	0.000222883	9.906	10.300	11.183	4.778	3.217	4.141
ABUW_RS09080		-1.425	0.000534881	4.162	6.156	5.886	2.208	1.898	1.814
ABUW_RS09095		-3.822	0.000490392	1.054	1.097	0.504	0.000	0.000	0.186
ABUW_RS09100		-1.586	6.38317e-05	11.592	9.691	17.069	4.091	4.113	4.420
ABUW_RS09150		2.299	0.000196448	1.739	1.950	1.850	9.195	8.912	9.165
ABUW_RS09180		-1.568	4.08176e-06	12.593	13.531	13.621	3.403	4.061	6.002
ABUW_RS09185		-4.085	1.38354e-11	787.437	499.168	829.634	34.970	48.042	41.825
ABUW_RS09195		-1.937	1.20907e-08	93.312	72.407	83.325	21.431	19.565	24.007
ABUW_RS09205		1.199	0.00331709	3.372	1.950	2.438	5.901	5.274	6.886
ABUW_RS09210		-2.397	8.41383e-08	38.358	24.745	42.798	7.602	5.906	6.420
ABUW_RS09250		-1.053	0.0274541	1.423	1.280	3.195	0.615	1.371	0.791
ABUW_RS09260		-4.069	9.60199e-14	428.888	287.982	421.838	20.164	25.577	22.192
ABUW_RS09265		-5.032	3.38058e-11	65.914	45.285	93.499	2.498	1.213	2.373
ABUW_RS09270		-4.069	2.61033e-10	27.925	20.844	32.203	2.425	1.055	1.117
ABUW_RS09275		-3.277	4.89222e-11	102.164	86.730	99.553	8.543	9.387	11.864
ABUW_RS09285		-1.968	1.27784e-09	410.553	400.919	434.618	106.792	100.883	110.868
ABUW_RS09290		-2.076	3.98523e-09	229.408	184.674	204.655	52.238	47.040	47.455
ABUW_RS09300		3.381	4.36688e-07	1.212	0.975	0.841	12.996	8.121	11.119
ABUW_RS09310		-5.345	0.000535419	0.474	17.370	2.438	0.217	0.158	0.093
ABUW_RS09355		-1.034	0.000500107	27.029	20.966	23.963	11.801	12.340	11.026
ABUW_RS09360		1.585	0.0137285	0.422	0.305	0.420	1.303	1.160	0.977
ABUW_RS09375		-1.456	0.0113248	4.004	2.621	1.598	0.724	1.055	1.396
ABUW_RS09380		-1.659	4.99367e-06	5.743	7.253	8.997	2.208	2.637	2.047
ABUW_RS09395		-2.067	0.00674782	0.948	1.341	4.961	0.362	0.580	0.651
ABUW_RS09400		2.030	9.25987e-08	4.847	7.740	6.727	28.273	24.100	25.914
ABUW_RS09405		1.642	2.88424e-06	8.167	9.325	6.054	26.137	21.516	26.519
ABUW_RS09435	denD	-1.650	0.000288572	7.324	7.558	4.709	2.281	2.004	2.001
ABUW_RS09440		-1.240	8.6758e-05	10.590	13.531	9.501	4.742	4.799	4.745
ABUW_RS09445		-1.275	0.000529551	6.955	5.729	7.315	2.860	2.690	2.652
ABUW_RS09450		1.584	0.00152158	159.279	154.139	132.176	384.379	427.105	525.215
ABUW_RS09465		1.128	0.00421651	5.058	7.740	6.138	13.430	13.975	13.911
ABUW_RS09470		-1.712	0.00115303	3.530	3.352	3.195	1.484	0.211	1.210
ABUW_RS09480		-2.891	5.62114e-08	14.753	16.822	13.873	1.846	2.479	1.861
ABUW_RS09485		-3.088	3.30983e-07	13.488	11.032	13.537	0.760	2.162	1.721
ABUW_RS09490		-2.964	0.000156743	7.376	6.461	4.877	0.905	0.633	0.837
ABUW_RS09495		-2.511	9.10346e-09	29.611	23.709	24.131	4.199	4.113	5.304
ABUW_RS09500		-1.594	0.000427836	7.376	3.779	2.943	1.158	1.846	1.908

Locustag	Gene	logFC	PValue	M9_1	M9_2	M9_3	LB_1	LB_2	LB_3
ABUW_RS09505		-1.485	0.00292029	3.636	2.194	1.513	1.122	0.949	0.605
ABUW_RS09525		-1.209	6.18091e-05	78.085	53.208	74.076	36.128	23.415	29.031
ABUW_RS09545		-1.279	0.000427756	5.480	4.510	7.231	3.005	1.740	2.094
ABUW_RS09555		-1.201	0.000234081	7.798	4.876	8.576	2.679	3.744	2.838
ABUW_RS09570		-1.589	0.00045073	6.165	3.718	6.811	2.172	1.002	2.187
ABUW_RS09575		-1.992	3.70389e-05	5.532	7.923	5.465	1.774	0.791	2.094
ABUW_RS09600	adeA	2.082	1.34883e-08	72.816	61.924	39.602	277.479	249.334	213.919
ABUW_RS09605	adeB	1.057	1.64235e-05	375.989	366.544	325.060	793.484	748.634	679.350
ABUW_RS09615		-1.672	6.13701e-07	78.770	81.244	48.599	21.358	21.358	22.937
ABUW_RS09620		-1.019	0.000920151	44.364	34.314	24.804	22.227	16.770	12.143
ABUW_RS09630		-1.349	2.28787e-07	135.095	114.096	86.016	46.952	44.562	40.197
ABUW_RS09635		-2.002	5.96903e-09	87.885	80.330	59.362	20.055	17.983	18.796
ABUW_RS09640		-1.561	2.43198e-05	13.699	12.616	8.408	3.910	4.377	3.629
ABUW_RS09660		1.140	0.00208251	2.371	1.707	3.363	5.901	5.590	4.466
ABUW_RS09670		2.057	0.00808592	0.422	0.061	0.168	0.833	0.844	1.303
ABUW_RS09680		-1.049	0.000150708	22.446	26.269	27.663	12.489	12.076	12.236
ABUW_RS09685		-1.142	0.0113018	2.108	2.560	3.784	1.195	1.107	1.396
ABUW_RS09695		-1.025	6.42171e-05	163.705	175.593	269.230	85.579	103.836	109.379
ABUW_RS09895		-1.089	0.0255103	1.581	2.011	0.841	0.905	0.633	0.558
ABUW_RS09945		-1.293	0.00660464	1.949	2.133	1.009	0.977	0.475	0.605
ABUW_RS09965		-1.869	1.4547e-06	288.630	322.235	221.303	74.754	83.955	69.275
ABUW_RS09970		-1.550	0.000161891	39.886	46.077	35.062	14.335	18.352	8.793
ABUW_RS09975		-1.957	0.000321007	81.194	102.881	64.238	20.924	28.530	14.702
ABUW_RS09980		-1.352	0.000696826	28.452	33.034	25.140	11.005	11.338	11.678
ABUW_RS09985		-1.726	1.6016e-05	25.818	27.305	19.927	6.516	8.490	7.258
ABUW_RS09995		-2.256	2.06191e-08	473.779	312.178	351.882	88.692	71.509	77.975
ABUW_RS10005		-4.027	6.89468e-08	20.918	9.142	23.795	1.593	0.949	0.605
ABUW_RS10010		-2.545	4.21607e-09	35.144	31.328	40.611	7.240	4.746	6.141
ABUW_RS10015		-1.169	0.000164804	108.592	101.174	96.021	46.301	40.290	49.362
ABUW_RS10025		-4.592	2.66142e-06	6.270	2.011	9.669	0.362	0.316	0.000
ABUW_RS10035		1.447	1.5333e-05	2.845	2.986	2.018	7.747	7.436	6.606
ABUW_RS10060	ppk1	-1.207	0.000291389	186.519	185.222	203.057	84.565	72.564	91.700
ABUW_RS10065		-1.170	0.000938507	8.272	10.788	11.435	4.778	4.641	4.001
ABUW_RS10070		-6.365	6.35791e-10	18.230	14.079	27.579	0.471	0.158	0.000
ABUW_RS10075		-4.471	4.93582e-08	849.030	666.289	628.426	34.970	30.956	30.660
ABUW_RS10080		-5.127	9.2083e-07	1728.621	1262.060	1209.347	48.907	38.339	32.753
ABUW_RS10095	modA	1.046	0.00397475	5.690	8.655	14.630	20.381	17.139	20.703
ABUW_RS10100		-1.954	0.00109677	3.425	4.876	6.054	1.086	0.686	1.814
ABUW_RS10115	antC	-1.281	0.00372713	4.689	5.607	2.522	1.774	2.268	1.396
ABUW_RS10120		1.335	0.00310078	2.266	3.230	2.859	7.602	5.801	7.444
ABUW_RS10150		-1.748	0.000625652	6.692	4.327	12.696	2.172	2.373	2.326
ABUW_RS10155		1.036	0.0329957	1.159	3.291	0.841	5.611	1.898	3.303
ABUW_RS10160		-2.050	1.80559e-08	44.891	51.197	53.812	13.286	12.235	10.561
ABUW_RS10165		-1.639	2.02769e-06	65.282	57.474	49.608	22.444	14.186	18.563
ABUW_RS10195		-2.438	6.7555e-07	288.209	245.988	295.631	43.694	61.595	47.967
ABUW_RS10220		2.650	4.48722e-07	49.001	60.522	78.785	460.401	382.913	335.488
ABUW_RS10230		-1.446	3.22292e-05	60.329	46.747	39.266	18.064	17.561	18.238
ABUW_RS10235		1.332	0.00477966	0.632	0.427	0.673	1.484	1.055	1.768
ABUW_RS10260		1.438	0.00232035	1.633	0.853	1.009	2.715	3.059	4.048
ABUW_RS10270		1.711	0.000322264	1.054	1.341	0.841	3.946	3.428	3.396
ABUW_RS10275	chrA	-1.682	5.51222e-08	34.617	25.659	25.645	8.254	8.912	9.724

Locustag	Gene	logFC	PValue	M9_1	M9_2	M9_3	LB_1	LB_2	LB_3
ABUW_RS10280		1.239	9.49648e-06	12.013	14.810	9.249	29.250	29.585	26.938
ABUW_RS10305		-3.241	1.29323e-08	46.630	62.899	104.093	8.254	7.225	6.932
ABUW_RS10310		-4.380	2.29899e-07	467.509	567.613	661.471	28.345	24.469	28.566
ABUW_RS10315		-4.256	4.16001e-06	65.650	105.014	137.642	7.059	4.483	4.327
ABUW_RS10330		-2.321	6.05676e-10	73.501	70.517	78.785	15.784	14.924	13.818
ABUW_RS10375		-1.550	2.07351e-07	174.822	164.256	132.429	58.899	44.562	57.551
ABUW_RS10400		-1.316	1.04812e-05	166.550	265.492	317.576	94.991	104.469	101.423
ABUW_RS10445		-3.274	1.15563e-07	18.230	10.727	14.210	2.100	0.844	1.349
ABUW_RS10455		-1.206	5.33505e-06	25.396	28.036	30.185	12.091	12.498	11.585
ABUW_RS10460		-2.427	1.17376e-06	5.164	6.887	7.736	0.796	1.688	1.256
ABUW_RS10475		-3.577	2.2669e-08	30.560	16.700	34.978	2.208	1.371	3.210
ABUW_RS10480		-3.359	4.11442e-06	7.535	6.643	12.444	1.195	0.580	0.651
ABUW_RS10500		-1.127	1.76851e-06	134.041	113.852	152.860	53.867	63.916	65.693
ABUW_RS10510		1.587	2.42342e-06	33.668	43.944	54.989	114.575	137.007	145.389
ABUW_RS10520		-3.486	4.22892e-05	313.289	293.040	244.930	30.445	25.524	19.866
ABUW_RS10525		-5.108	5.61572e-07	35.354	44.370	45.909	1.122	1.055	1.442
ABUW_RS10530		-2.830	1.64525e-07	78.928	83.926	81.643	13.141	8.965	12.096
ABUW_RS10535		-2.032	0.000140112	3.477	4.023	3.111	0.869	0.738	0.977
ABUW_RS10540		1.032	0.000285854	40.676	33.522	45.909	74.863	91.496	78.905
ABUW_RS10580	mtlD	-1.497	1.93384e-07	98.160	74.540	71.554	32.146	28.424	26.007
ABUW_RS10585		-6.012	1.6621e-09	841.601	625.027	804.157	13.865	11.707	9.491
ABUW_RS10590		-2.394	3.77538e-07	9.168	7.131	12.949	1.412	2.109	2.047
ABUW_RS10595		-2.400	5.19696e-09	124.978	139.755	140.500	27.513	24.153	24.984
ABUW_RS10600		-3.820	7.19936e-09	24.342	25.781	34.810	3.149	1.266	1.303
ABUW_RS10605		-1.539	0.000104663	2076.157	2102.296	1989.372	819.910	697.903	604.678
ABUW_RS10610		-4.494	1.4046e-12	51.108	49.795	52.887	2.896	2.426	1.396
ABUW_RS10615		-5.337	1.2174e-14	143.156	120.190	132.092	3.330	3.164	3.257
ABUW_RS10620		-5.636	2.97488e-12	1528.086	1250.480	1541.974	30.445	31.483	24.937
ABUW_RS10625		-5.302	1.45282e-11	2344.028	1701.682	1854.842	52.781	52.841	43.919
ABUW_RS10630		-6.527	4.02687e-10	1979.631	1742.334	1829.954	21.105	20.725	18.331
ABUW_RS10635		-6.102	9.2069e-09	1490.993	1114.931	1262.907	22.625	18.932	14.609
ABUW_RS10640		-6.580	1.74361e-08	1865.296	1378.045	1561.565	21.177	16.190	12.655
ABUW_RS10645	ybaK	-1.001	0.000251533	12.909	18.406	21.609	9.231	7.647	9.258
ABUW_RS10650		-1.519	0.000231207	29.506	38.458	67.434	13.213	16.981	16.842
ABUW_RS10660		-3.275	7.0635e-10	42.836	66.373	92.742	6.661	6.803	7.304
ABUW_RS10665		-3.075	3.31257e-11	118.129	179.798	203.394	18.426	21.727	19.354
ABUW_RS10670		-1.899	3.38894e-08	11.697	11.519	12.780	3.620	2.848	3.071
ABUW_RS10685		1.243	5.9336e-07	75.293	58.632	58.100	150.848	143.810	160.323
ABUW_RS10730	fdx	1.785	6.5897e-08	10.380	11.093	11.435	43.730	33.065	36.243
ABUW_RS10760		-1.995	4.37254e-08	38.041	46.382	38.762	10.933	10.020	9.910
ABUW_RS10765	rraA	-1.492	3.053e-06	48.895	54.000	66.593	18.209	21.411	20.564
ABUW_RS10770		-1.948	4.00205e-07	22.182	25.964	29.849	6.046	6.012	8.095
ABUW_RS10775	rpsT	3.795	5.61687e-09	1.686	1.828	2.607	24.834	29.479	28.799
ABUW_RS10800		-1.013	0.000102648	123.345	102.759	87.697	51.333	52.736	51.596
ABUW_RS10805		-1.832	7.18971e-09	248.850	222.523	250.732	70.628	64.970	67.088
ABUW_RS10810		-1.702	1.58637e-08	259.072	231.178	233.327	72.727	77.363	72.346
ABUW_RS10815		-1.130	3.22945e-06	507.026	424.811	411.159	220.137	201.028	192.332
ABUW_RS10875		-1.212	7.67065e-05	6.744	8.533	7.231	3.548	3.375	2.745
ABUW_RS10880		-1.287	1.78814e-05	83.091	102.333	102.916	41.522	41.767	34.800
ABUW_RS10890		-1.512	6.61018e-08	165.654	136.707	212.054	61.686	60.382	58.063

Locustag	Gene	logFC	PValue	M9_1	M9_2	M9_3	LB_1	LB_2	LB_3
ABUW_RS10895		-1.633	1.76095e-08	940.130	700.481	1081.038	289.642	296.638	291.197
ABUW_RS10900	rpsA	1.688	4.45431e-08	5320.588	5849.531	5127.048	15976.609	19297.267	17248.850
ABUW_RS10940	gspJ	1.160	0.000487208	4.320	3.657	4.036	10.245	7.119	9.398
ABUW_RS10965		1.715	3.19482e-06	6.270	7.436	4.456	16.471	22.096	22.053
ABUW_RS10970		1.482	3.03228e-06	7.376	11.397	11.687	28.743	26.210	29.310
ABUW_RS10975	kdsB	1.099	8.41951e-07	51.372	64.910	53.056	106.828	130.837	125.337
ABUW_RS10980	lpxK	1.444	5.04514e-07	22.340	23.343	14.210	54.446	53.579	56.202
ABUW_RS10995		2.290	1.011e-10	17.019	24.257	18.246	94.303	95.557	101.516
ABUW_RS11000		1.145	2.02274e-07	66.283	62.046	57.428	132.820	139.327	139.015
ABUW_RS11035	fba	1.003	9.86499e-07	1057.047	982.916	882.605	1766.378	2215.685	1876.192
ABUW_RS11045		2.360	1.34047e-09	70.814	92.581	61.548	383.040	417.191	355.726
ABUW_RS11055		1.385	2.66112e-05	10.274	14.201	7.736	28.852	24.522	31.497
ABUW_RS11060		1.462	3.06414e-08	35.196	48.942	42.041	116.132	118.075	113.287
ABUW_RS11065		-1.543	2.13072e-05	49.422	66.617	77.271	21.829	21.516	22.844
ABUW_RS11070		1.428	0.00195888	1.581	1.402	1.850	5.611	2.953	4.094
ABUW_RS11075	sstT	1.209	3.11544e-07	148.846	174.008	144.873	377.103	374.950	329.207
ABUW_RS11080		1.065	6.90742e-06	29.664	28.768	27.074	60.926	67.765	50.526
ABUW_RS11085		1.648	1.52846e-07	10.011	9.691	9.838	33.703	30.850	28.054
ABUW_RS11090		-1.502	8.14118e-07	128.403	137.500	178.085	52.165	51.523	52.898
ABUW_RS11105	gcvH	1.077	4.69818e-06	17.598	16.700	12.780	32.762	33.593	33.637
ABUW_RS11115	putP	2.877	3.0586e-11	261.495	223.193	237.615	1724.458	1971.203	1609.560
ABUW_RS11120		1.043	0.0172227	0.738	1.707	2.102	3.367	2.637	2.838
ABUW_RS11125	putA	7.123	2.17724e-13	31.087	30.657	29.176	4265.096	4473.823	3944.158
ABUW_RS11140		-1.130	0.00210453	7.851	5.851	11.519	3.475	3.797	4.094
ABUW_RS11155		-1.859	1.16922e-07	252.328	190.098	307.739	64.039	69.822	72.811
ABUW_RS11160		-1.271	8.90122e-06	74.133	64.179	80.718	28.454	30.376	31.916
ABUW_RS11205	ruvC	1.024	0.000393915	11.644	11.946	21.525	27.838	30.534	32.102
ABUW_RS11220	bioB	1.345	2.35493e-07	245.900	245.013	257.626	653.857	665.312	582.347
ABUW_RS11230		1.378	0.0386709	0.211	0.366	0.504	0.941	0.844	0.884
ABUW_RS11235		2.206	2.44007e-05	5.901	9.508	3.195	30.228	26.157	31.357
ABUW_RS11240		2.473	0.000118263	0.632	0.914	0.504	3.946	4.430	3.350
ABUW_RS11250		1.056	0.000447316	6.270	6.765	10.090	16.109	15.399	15.772
ABUW_RS11270		-2.183	2.01288e-05	18.230	10.483	25.393	3.403	2.690	5.676
ABUW_RS11275		2.725	1.00373e-05	2.845	1.524	1.766	16.725	15.557	9.258
ABUW_RS11280		4.343	4.48807e-08	1.054	0.731	2.354	25.703	25.260	27.961
ABUW_RS11290		1.459	0.000903353	1.317	2.072	1.345	5.394	3.217	4.327
ABUW_RS11305		-1.596	0.000385897	4.953	4.998	5.886	2.462	1.002	1.535
ABUW_RS11310		1.122	0.000366417	4.689	4.571	4.288	9.919	10.020	9.677
ABUW_RS11315		1.277	2.84769e-07	164.758	176.324	192.883	392.995	472.985	428.072
ABUW_RS11325		1.368	0.0303242	0.527	1.036	0.673	1.339	2.531	2.047
ABUW_RS11330		-3.509	2.64747e-12	560.400	506.116	491.710	41.160	52.472	43.361
ABUW_RS11335		-3.663	9.17072e-11	512.980	399.456	403.592	33.558	36.915	33.451
ABUW_RS11340		-3.380	9.74962e-11	855.827	659.950	587.395	67.189	66.025	68.856
ABUW_RS11345		-2.593	1.09959e-09	1177.019	840.175	907.662	184.334	148.925	151.251
ABUW_RS11390	ychF	1.163	4.81681e-06	111.595	142.498	111.072	283.524	292.208	242.299
ABUW_RS11395		-1.966	0.000517125	5.480	10.605	12.108	2.425	2.057	2.559
ABUW_RS11410		1.381	9.6092e-05	3.477	2.804	5.549	10.788	8.807	10.328
ABUW_RS11425		-1.150	2.06205e-05	35.565	29.743	29.008	16.182	11.707	14.516
ABUW_RS11450		-1.358	6.41789e-06	71.236	64.666	70.292	29.178	25.577	25.588
ABUW_RS11455		-1.224	0.000128176	167.867	130.186	122.255	63.243	55.372	61.366
ABUW_RS11475		1.520	1.43549e-07	143.525	143.107	89.042	384.705	379.696	314.738
ABUW_RS11515		-1.787	3.30829e-05	4.320	4.693	5.802	1.086	1.688	1.535
ABUW_RS11525	arsB	-1.625	0.00043144	2.951	4.998	3.700	1.701	1.160	0.791
ABUW_RS11545		-1.847	4.44451e-08	109.593	73.565	73.908	23.277	22.571	25.682
ABUW_RS11575	tauD	1.120	0.0122437	132.776	90.752	92.322	205.692	206.934	274.867
ABUW_RS11590	tauA	2.079	1.07376e-05	153.694	181.809	160.596	591.230	669.900	835.812

Locustag	Gene	logFC	PValue	M9_1	M9_2	M9_3	LB_1	LB_2	LB_3
ABUW_RS11600		-1.019	0.0261548	2.424	3.901	2.186	1.738	1.055	1.349
ABUW_RS11615		2.764	7.13223e-07	2.213	1.219	3.195	14.661	12.709	16.284
ABUW_RS11620		-2.169	1.56094e-09	879.854	555.241	957.102	175.863	180.883	175.258
ABUW_RS11625	cydB	-2.404	1.83894e-09	796.921	535.859	1013.436	143.825	151.298	148.227
ABUW_RS11645	madM	-1.263	0.000261863	7.482	8.045	5.381	3.403	3.111	2.233
ABUW_RS11650	madL	-1.229	0.00616663	2.108	1.889	1.177	1.158	0.686	0.326
ABUW_RS11665	mdcE	-1.046	0.0016523	9.221	8.716	6.727	3.837	3.797	4.420
ABUW_RS11690		-1.631	6.87381e-06	29.980	33.522	27.495	9.014	11.127	9.351
ABUW_RS11725	yfcF	-1.595	3.91402e-06	49.264	34.497	34.558	14.191	14.450	10.608
ABUW_RS11730	yghU	-2.160	2.34617e-10	182.831	157.369	186.998	41.305	40.554	36.056
ABUW_RS11785		1.442	0.000254454	12.487	12.251	10.258	31.096	27.528	36.940
ABUW_RS11795		1.601	0.000862403	9.537	9.935	10.426	23.965	28.319	38.383
ABUW_RS11800		-1.033	0.00201362	7.324	6.826	14.462	3.801	5.115	4.839
ABUW_RS11810		-1.228	0.000883523	10.116	6.156	8.997	2.860	3.639	4.373
ABUW_RS11815		-1.076	5.42093e-05	20.391	27.122	25.729	10.969	11.338	12.376
ABUW_RS11825		2.903	6.76297e-06	5.532	7.680	10.762	51.152	58.062	66.809
ABUW_RS11845		-2.972	0.0421597	0.685	0.000	0.925	0.000	0.000	0.186
ABUW_RS11850		-7.287	2.12352e-12	298.694	144.509	310.430	2.063	1.635	1.024
ABUW_RS11855	katE	-4.957	2.3181e-13	3698.135	1880.505	3081.089	98.321	94.660	85.838
ABUW_RS11860		-6.957	4.70795e-12	448.120	155.053	451.350	3.765	2.848	1.721
ABUW_RS11865		-6.437	1.37291e-09	7.640	3.108	6.306	0.000	0.000	0.186
ABUW_RS11870		-7.326	3.66619e-12	150.374	64.605	196.835	1.014	0.633	0.837
ABUW_RS11875	surA1	-7.131	8.10215e-13	134.093	56.134	170.434	0.977	0.897	0.651
ABUW_RS11880		-1.094	0.0016388	4.057	3.047	4.877	2.063	1.898	1.535
ABUW_RS11885		-2.966	4.67631e-06	7.113	2.133	6.642	1.014	0.422	0.465
ABUW_RS11895		-1.893	0.000379618	2.529	3.962	1.345	0.760	0.897	0.512
ABUW_RS11905		1.068	0.00764412	1.475	1.707	2.018	3.258	3.059	4.420
ABUW_RS11910		1.023	0.0116367	5.638	4.754	2.607	12.091	6.803	8.049
ABUW_RS11920		1.089	0.00601522	20.075	14.689	15.471	48.799	32.116	26.054
ABUW_RS11925		1.701	1.88164e-05	9.695	10.117	7.567	33.087	27.739	28.799
ABUW_RS11930		2.517	5.3052e-07	38.252	36.325	20.516	222.309	157.099	168.186
ABUW_RS11935		2.036	9.57923e-06	64.281	39.373	32.035	223.720	181.938	153.670
ABUW_RS11940		1.018	0.00255111	34.459	34.375	23.711	66.573	63.863	57.737
ABUW_RS11955		1.657	3.2238e-06	11.434	10.605	11.267	33.449	36.546	35.126
ABUW_RS11960		1.594	0.000165857	20.812	16.761	25.309	69.216	67.027	52.712
ABUW_RS11970		-1.863	2.63234e-06	27.925	19.077	16.648	6.227	4.535	6.746
ABUW_RS11990		-1.059	0.00289441	6.850	4.023	4.036	2.643	2.268	2.326
ABUW_RS11995		-1.148	0.00303705	6.692	5.729	7.820	2.534	3.850	2.791
ABUW_RS12000		-2.058	7.07762e-07	11.170	8.594	7.904	2.208	1.846	2.605
ABUW_RS12005		-1.803	2.68684e-07	27.240	21.149	17.153	7.059	5.643	6.095
ABUW_RS12040		-2.690	1.88516e-08	20.285	13.896	20.852	2.027	3.902	2.745
ABUW_RS12060		1.709	0.00107321	0.896	0.366	0.420	2.100	2.531	1.210
ABUW_RS12105	pobA	1.874	0.000411234	1.844	1.036	1.598	6.299	3.111	6.932
ABUW_RS12110	pobR	1.254	0.00882449	5.216	1.158	2.354	8.905	4.641	7.816
ABUW_RS12115		4.411	1.49378e-07	1.159	1.341	2.943	31.314	34.753	43.268
ABUW_RS12140		-1.464	0.00759645	2.160	2.682	1.261	1.158	0.527	0.465
ABUW_RS12180		-3.080	1.45612e-08	145.158	67.165	103.589	11.620	13.395	12.422
ABUW_RS12185		-2.702	1.45057e-09	371.247	228.191	303.619	48.762	43.560	46.385
ABUW_RS12190		-2.470	4.7469e-08	19.495	15.481	15.135	3.729	3.006	2.233
ABUW_RS12195		-2.303	1.18442e-10	49.106	39.982	46.665	8.362	8.701	10.468
ABUW_RS12200		-2.056	2.56043e-07	33.141	33.034	25.056	6.733	6.961	8.328
ABUW_RS12205		-1.209	0.000280426	19.495	23.160	22.534	8.833	8.385	10.933
ABUW_RS12210		-2.148	0.00520028	0.843	0.792	0.757	0.253	0.105	0.140

Locustag	Gene	logFC	PValue	M9_1	M9_2	M9_3	LB_1	LB_2	LB_3
ABUW_RS12245		-2.164	3.0804e-05	8.061	3.901	11.099	1.882	1.424	1.675
ABUW_RS12285	pcaF	1.543	0.000147561	16.176	8.777	7.399	31.748	35.227	29.078
ABUW_RS12290		2.148	2.17424e-06	7.113	4.937	9.501	30.445	36.124	27.729
ABUW_RS12295	paaG	2.460	1.21497e-06	5.638	3.047	3.363	25.884	23.204	18.517
ABUW_RS12300		4.287	2.16566e-08	1.106	1.158	0.673	19.874	22.624	17.074
ABUW_RS12305	paaE	3.687	9.99972e-08	5.690	2.316	1.598	50.464	40.606	39.313
ABUW_RS12310	paaD	3.950	7.79365e-09	4.953	2.377	3.279	68.202	47.673	50.712
ABUW_RS12315	paaC	4.050	1.0193e-05	11.065	2.011	2.607	101.326	84.377	87.280
ABUW_RS12320	paaB	4.475	4.65258e-07	2.055	0.488	0.673	27.947	23.678	25.123
ABUW_RS12325	paaA	3.923	0.000239515	22.287	10.483	6.642	226.146	172.340	213.222
ABUW_RS12330	paaZ	4.632	9.4829e-06	25.870	10.422	5.381	387.022	310.402	364.240
ABUW_RS12335		-1.684	3.39983e-07	212.073	181.687	220.462	62.338	61.912	66.809
ABUW_RS12360	abaF	-1.669	0.00102897	3.530	4.388	2.691	1.376	1.002	0.930
ABUW_RS12405		-1.395	6.96628e-05	295.480	182.114	360.879	100.928	104.311	113.334
ABUW_RS12420		-2.820	1.59318e-10	146.633	166.511	135.540	20.490	22.571	20.517
ABUW_RS12430		-1.151	1.92248e-06	109.909	118.971	132.849	60.347	49.993	52.340
ABUW_RS12515	tssF	-1.712	0.00774996	91.363	18.224	23.291	15.385	14.133	11.352
ABUW_RS12525		-1.032	0.000120723	313.552	292.857	387.448	151.464	176.981	157.346
ABUW_RS12590	uca	-1.098	0.000277965	21.286	28.158	22.366	9.774	10.442	13.399
ABUW_RS12600		-1.595	0.0359449	0.527	0.609	0.673	0.109	0.316	0.186
ABUW_RS12605		-5.090	9.45744e-11	188.152	64.788	175.899	4.091	4.008	4.466
ABUW_RS12625		1.373	3.83547e-06	32.562	26.574	18.078	68.962	66.500	65.972
ABUW_RS12630		-2.056	2.75725e-05	6.112	5.607	6.054	1.593	1.371	1.256
ABUW_RS12640		-1.692	2.9257e-06	39.728	34.619	46.245	11.946	12.815	12.515
ABUW_RS12700		-1.788	4.91849e-06	28.768	35.594	72.310	13.611	11.602	13.957
ABUW_RS12715		-1.012	5.19949e-05	54.797	47.235	53.644	27.440	22.676	26.984
ABUW_RS12720		-1.005	0.00513583	7.376	5.059	8.660	3.548	3.691	3.164
ABUW_RS12725		-4.331	2.03743e-10	124.083	70.091	168.163	7.168	5.010	5.629
ABUW_RS12730		-1.390	2.73029e-07	33.036	29.865	34.894	11.620	13.342	12.376
ABUW_RS12750		1.847	0.0084392	2.424	1.280	3.195	9.666	5.906	8.467
ABUW_RS12765		-1.726	7.46186e-06	11.750	14.506	22.618	4.163	4.693	5.769
ABUW_RS12790	fdxA	1.445	0.000415644	4.268	4.266	9.165	14.878	15.610	16.144
ABUW_RS12800		1.158	1.56143e-05	15.965	24.075	22.113	48.799	49.519	39.871
ABUW_RS12805		-1.379	0.000197333	1061.420	451.202	643.225	258.075	267.211	303.526
ABUW_RS12815		1.004	0.00984978	1.475	1.463	2.186	4.127	2.637	3.117
ABUW_RS12885		1.631	1.66326e-05	13.278	25.172	17.321	69.469	43.296	59.598
ABUW_RS12900		-2.361	8.64222e-08	83.986	69.177	72.983	16.652	14.239	13.027
ABUW_RS12935		2.792	5.29113e-08	24.500	26.695	26.233	162.650	202.083	171.303
ABUW_RS12940		3.339	1.72562e-07	0.211	0.792	0.925	5.430	6.908	6.095
ABUW_RS12965		-2.550	0.0101919	0.527	0.609	0.841	0.072	0.158	0.093
ABUW_RS12975		-4.257	1.96109e-09	50.371	30.352	57.007	3.439	1.002	2.466
ABUW_RS12980		-2.949	1.70527e-05	2.845	1.768	2.691	0.326	0.475	0.140
ABUW_RS13000		-1.465	0.000426205	5.058	8.106	10.426	3.258	2.057	2.931
ABUW_RS13005		-2.075	0.000400425	2.529	1.524	4.877	0.941	0.211	0.744
ABUW_RS13010		-5.866	1.22693e-08	35.144	17.066	72.815	0.905	0.580	0.558
ABUW_RS13030		-3.232	2.96214e-07	11.908	5.546	10.847	0.941	0.475	1.535
ABUW_RS13035		-6.313	4.75427e-06	3.530	1.524	3.700	0.000	0.000	0.093
ABUW_RS13040		-4.377	2.00762e-08	5.585	3.596	11.856	0.652	0.000	0.186
ABUW_RS13060		-1.096	5.23831e-05	24.079	26.452	33.380	12.924	13.289	12.887
ABUW_RS13085		2.576	0.00012614	1.054	0.427	0.841	3.258	6.697	4.373
ABUW_RS13095	xseA	-1.528	1.39118e-06	42.783	38.580	38.930	13.430	10.758	17.493
ABUW_RS13100	xseB	-1.043	0.0432583	2.898	1.950	1.934	1.122	1.002	1.210
ABUW_RS13105		-2.481	2.84871e-08	30.770	36.508	57.428	7.783	5.854	8.467
ABUW_RS13110		-5.229	0.000927747	747.604	18.406	26.906	9.629	4.746	6.513
ABUW_RS13115		-3.412	3.1063e-08	9.695	11.885	13.958	1.303	1.213	0.744

Locustag	Gene	logFC	PValue	M9_1	M9_2	M9_3	LB_1	LB_2	LB_3
ABUW_RS13120		-3.832	1.14516e-07	23.921	10.056	23.459	1.014	1.582	1.489
ABUW_RS13140		3.288	1.34519e-08	1.212	1.280	1.009	10.064	13.342	11.538
ABUW_RS13155	benB	2.216	0.00483707	0.422	0.000	0.168	1.303	0.791	0.837
ABUW_RS13175		-2.978	6.63228e-08	9.168	7.253	7.483	1.158	1.055	0.791
ABUW_RS13180		-1.669	0.00927597	1.423	2.743	2.018	1.050	0.264	0.465
ABUW_RS13200		-2.980	2.70517e-08	80.983	67.226	83.493	10.788	7.383	11.026
ABUW_RS13220		-3.467	3.71742e-12	1336.509	874.001	1428.043	99.154	120.132	109.844
ABUW_RS13230		-1.428	0.00030334	6.428	7.680	7.567	2.172	2.848	3.071
ABUW_RS13235	trmB	1.101	0.000331423	19.390	30.291	21.357	49.559	52.155	50.851
ABUW_RS13250		-5.852	7.4871e-13	3462.879	1776.587	3597.182	50.029	54.476	48.478
ABUW_RS13255		1.900	3.90838e-09	72.658	55.890	52.215	225.132	247.857	202.754
ABUW_RS13260		1.484	6.67829e-08	89.255	92.459	68.527	232.662	246.381	221.689
ABUW_RS13270	rlmKL	1.030	1.33264e-07	139.889	136.707	134.531	283.017	283.296	273.517
ABUW_RS13275		-1.781	4.50942e-05	3.583	2.255	5.633	1.050	1.266	0.930
ABUW_RS13280		-1.287	0.000452083	28.979	27.244	58.016	15.675	15.610	15.120
ABUW_RS13315		-1.076	1.32329e-06	588.694	405.734	528.453	229.947	259.037	233.646
ABUW_RS13325		1.005	0.000336514	460.713	484.540	468.251	851.875	1081.712	904.249
ABUW_RS13340	alaS	1.643	2.20451e-07	317.767	364.960	283.103	1037.911	1093.419	884.756
ABUW_RS13345		1.587	2.5512e-07	353.859	466.743	326.405	1141.988	1233.907	1069.876
ABUW_RS13355	rnhB	2.028	7.4054e-09	6.481	7.680	6.390	28.888	26.895	28.194
ABUW_RS13360		2.033	5.58409e-08	11.592	7.192	5.802	31.531	38.761	32.428
ABUW_RS13370		2.304	5.52663e-08	37.356	32.546	30.942	145.454	189.584	164.092
ABUW_RS13380		-3.134	9.93152e-09	16.860	17.614	24.384	2.498	1.635	2.419
ABUW_RS13385		-1.431	0.0444016	4.110	5.242	43.807	6.082	5.695	7.025
ABUW_RS13390		-1.089	0.00113309	4.637	4.876	2.607	2.317	2.057	1.396
ABUW_RS13395		-1.716	0.00196913	1.949	3.047	2.438	0.833	0.369	0.977
ABUW_RS13450		-1.909	2.71476e-08	150.427	138.841	195.238	38.554	41.925	48.478
ABUW_RS13455		-1.270	0.013299	2.266	5.729	2.102	1.665	0.738	1.721
ABUW_RS13460		-1.243	6.31385e-05	21.655	22.185	16.060	11.041	8.332	5.862
ABUW_RS13485	mhpT	-1.822	1.20488e-05	15.438	10.361	11.435	2.534	3.955	4.234
ABUW_RS13520		-2.250	0.00021576	5.216	2.621	3.027	1.086	0.844	0.326
ABUW_RS13525		-2.753	9.35403e-06	70.972	45.650	24.636	7.095	6.856	7.118
ABUW_RS13590		1.081	0.0024743	27.872	19.016	23.207	56.111	52.788	39.592
ABUW_RS13595	astA	3.643	1.18494e-06	3.477	7.314	5.633	85.651	55.478	62.017
ABUW_RS13600		3.759	2.15339e-07	5.638	5.973	4.036	84.492	55.056	75.230
ABUW_RS13610		3.870	4.2442e-09	9.010	6.948	4.540	107.118	98.932	100.167
ABUW_RS13615		2.325	9.5276e-08	8.483	5.424	5.633	32.038	35.386	31.823
ABUW_RS13645		1.262	7.07518e-06	9.168	7.131	6.222	18.173	18.036	18.424
ABUW_RS13675		-1.007	0.00978735	7.745	7.680	18.246	6.480	4.430	5.257
ABUW_RS13690		1.584	0.0498095	0.211	0.000	0.504	0.398	0.686	0.930
ABUW_RS13705		1.398	7.44724e-05	154.326	133.782	115.780	225.168	254.449	586.115
ABUW_RS13715		-2.382	0.00133102	74.186	95.872	594.878	47.133	49.097	49.967
ABUW_RS13720	argG	2.228	2.67045e-09	191.630	187.112	145.629	803.403	910.111	744.810
ABUW_RS13745		-1.023	0.00892201	254.857	199.180	161.521	132.169	99.776	71.043
ABUW_RS13755		-2.142	8.73991e-09	77.242	60.705	75.926	15.892	15.082	17.447
ABUW_RS13760		-3.055	2.158e-11	610.086	634.413	703.680	90.647	70.455	73.090
ABUW_RS13765		-2.756	1.40041e-05	13.699	25.233	37.164	3.475	4.061	3.629
ABUW_RS13770		-1.344	3.89599e-05	9.958	8.228	6.727	3.439	3.639	2.838
ABUW_RS13775		-2.854	1.22108e-07	6.850	8.228	11.351	1.484	0.897	1.117
ABUW_RS13800		1.034	1.94305e-05	16.386	16.639	17.069	37.721	38.181	26.612
ABUW_RS13815		2.394	2.20051e-07	140.574	157.978	90.976	698.312	693.737	658.879
ABUW_RS13835		1.811	2.43869e-05	4.637	2.743	4.120	14.263	12.393	13.725

Locustag	Gene	logFC	PValue	M9_1	M9_2	M9_3	LB_1	LB_2	LB_3
ABUW_RS13850		-1.300	0.0111237	4.320	10.727	10.090	3.620	2.848	3.489
ABUW_RS13855		2.601	4.17604e-07	1.686	1.646	3.111	10.136	14.608	13.073
ABUW_RS13870		2.618	7.5603e-09	17.651	16.700	13.705	78.049	76.678	141.900
ABUW_RS13900		-3.516	0.0105062	26.819	24.257	1262.570	31.893	42.663	40.104
ABUW_RS13950	nth	1.291	0.000464808	3.899	6.765	3.111	12.851	12.709	8.607
ABUW_RS13955	adk	1.181	8.97106e-07	199.112	208.810	218.276	446.789	513.697	458.824
ABUW_RS13975	rsmD	1.982	3.31266e-06	2.371	4.754	2.607	14.299	12.762	11.538
ABUW_RS13980		-1.242	3.83155e-07	90.414	79.782	77.271	32.182	35.649	36.940
ABUW_RS14015		-1.046	0.00276601	6.270	8.228	4.793	2.715	2.953	3.815
ABUW_RS14020		1.649	0.0133298	0.685	0.731	1.429	2.534	3.322	2.698
ABUW_RS14025		-2.283	2.88592e-09	167.340	113.059	192.883	34.716	33.329	29.078
ABUW_RS14030		-1.225	5.03353e-05	700.553	575.232	607.658	257.858	280.817	267.376
ABUW_RS14045		1.212	3.97258e-05	255.910	217.708	181.196	550.323	531.627	435.888
ABUW_RS14050		1.332	0.000558918	3.846	2.255	3.952	7.349	7.910	9.956
ABUW_RS14065	cysD	1.228	6.95474e-05	158.383	162.245	158.746	337.536	401.581	384.292
ABUW_RS14080		3.343	3.29997e-06	2.002	1.036	2.186	20.671	15.504	16.144
ABUW_RS14085		-1.246	0.0359446	3.688	1.219	1.850	1.231	0.949	0.698
ABUW_RS14090	rubA	1.261	3.2091e-05	23.183	18.711	13.958	49.269	43.771	41.872
ABUW_RS14110		1.828	0.000317071	0.738	0.609	0.336	2.281	2.215	1.814
ABUW_RS14130		-1.267	4.75656e-06	101.953	110.621	118.471	47.604	41.819	48.013
ABUW_RS14155		1.287	4.25825e-06	13.857	21.941	15.639	41.450	42.188	41.919
ABUW_RS14160		-4.318	4.55078e-06	859.832	979.808	849.225	51.912	48.675	34.149
ABUW_RS14170		-1.430	5.78408e-05	8.641	11.215	10.426	4.127	3.217	3.768
ABUW_RS14175		1.406	0.000589171	4.531	7.558	1.934	12.308	10.020	15.958
ABUW_RS14190		1.883	5.74533e-09	79.666	87.705	63.734	312.485	279.604	261.467
ABUW_RS14205	metH	1.221	8.96072e-06	121.817	144.265	114.519	301.516	323.058	263.003
ABUW_RS14230		1.086	0.000486843	5.638	4.205	4.709	10.172	8.385	12.469
ABUW_RS14240		-2.083	1.57981e-08	244.108	143.473	225.843	46.952	50.732	47.129
ABUW_RS14250		-1.083	0.00415402	6.955	5.912	11.940	3.946	4.852	2.698
ABUW_RS14265		-1.162	8.1093e-06	41.466	29.621	27.579	16.327	14.819	13.027
ABUW_RS14285		-1.110	0.0017051	4.847	6.278	6.727	2.932	2.795	2.419
ABUW_RS14305		-1.047	0.000712433	10.432	10.544	8.829	4.344	5.326	4.885
ABUW_RS14330		1.396	0.0243936	0.316	0.609	0.000	0.833	0.949	0.930
ABUW_RS14355		-1.073	1.42731e-05	46.103	36.447	37.921	17.919	19.038	20.424
ABUW_RS14360	pgaD	1.022	0.000134064	14.700	25.720	16.984	40.400	38.128	38.104
ABUW_RS14380		4.171	4.47548e-07	0.369	0.366	0.504	8.688	6.697	6.606
ABUW_RS14420	betI	2.273	9.71223e-10	20.918	15.847	13.873	73.813	89.176	83.651
ABUW_RS14425	betB	2.805	2.66085e-12	130.036	121.958	103.000	769.772	882.794	830.322
ABUW_RS14430	betA	3.619	9.44396e-14	41.993	39.921	40.275	488.891	543.387	470.223
ABUW_RS14440		-2.125	7.0526e-08	20.338	28.463	23.627	6.842	4.483	5.071
ABUW_RS14445		2.385	2.53795e-07	30.823	30.474	17.741	137.563	133.474	144.645
ABUW_RS14450		1.590	5.26279e-05	33.089	38.885	15.303	89.850	93.078	82.069
ABUW_RS14460		-2.366	2.60713e-08	40.149	44.614	42.377	7.095	8.121	9.491
ABUW_RS14470		-2.971	2.25599e-07	17.019	10.300	17.741	1.376	2.162	2.280
ABUW_RS14475		-3.462	3.97895e-10	67.758	50.282	85.343	7.168	5.485	5.629
ABUW_RS14480		-2.390	2.09973e-05	4.584	4.449	5.465	1.014	1.002	0.698
ABUW_RS14485		-5.375	2.68653e-10	39.253	31.206	52.971	1.014	0.686	1.210
ABUW_RS14490		-6.391	2.09518e-13	783.064	469.608	861.753	8.000	6.856	10.282
ABUW_RS14495		-4.528	5.55852e-11	156.434	137.926	196.499	7.494	5.221	8.421
ABUW_RS14500		-4.621	6.42953e-07	44.733	33.034	36.744	1.448	1.635	1.582
ABUW_RS14505		-5.190	2.10909e-08	54.480	50.100	65.920	2.208	1.371	0.930
ABUW_RS14585	fic	1.178	3.57046e-06	34.775	46.443	37.753	96.909	85.062	87.140
ABUW_RS14610		2.096	0.00647153	0.158	0.670	0.000	0.724	1.898	1.396
ABUW_RS14620		1.122	0.00914144	0.948	0.670	0.757	1.665	2.004	1.628

Locustag	Gene	logFC	PValue	M9_1	M9_2	M9_3	LB_1	LB_2	LB_3
ABUW_RS14640		1.254	2.97999e-05	13.594	10.910	9.753	26.933	26.051	29.357
ABUW_RS14675		-1.242	4.68609e-06	117.233	94.226	127.300	44.310	50.468	48.385
ABUW_RS14685		-2.195	3.48139e-08	51.266	38.458	38.593	8.399	9.492	10.235
ABUW_RS14695		1.442	7.66738e-06	25.554	31.267	16.816	67.225	60.646	73.462
ABUW_RS14700		1.556	2.55693e-07	39.095	52.477	34.137	128.549	118.708	123.057
ABUW_RS14710		2.850	1.61351e-08	60.908	63.752	38.005	404.796	405.431	366.287
ABUW_RS14715		2.764	1.22763e-07	69.391	73.199	40.780	447.875	416.400	385.688
ABUW_RS14740		3.285	4.0637e-08	1.686	4.327	2.859	31.639	23.678	30.241
ABUW_RS14750		-1.574	0.000699375	5.269	2.499	7.483	2.027	1.688	1.210
ABUW_RS14760		-1.472	7.30655e-07	356.125	225.570	286.550	104.801	106.737	101.470
ABUW_RS14765	dut	1.504	6.75629e-07	14.068	19.138	15.723	36.997	53.790	48.199
ABUW_RS14770	rep	1.198	4.75549e-06	60.118	45.650	39.855	105.779	126.671	102.633
ABUW_RS14775		-1.065	2.49902e-05	3927.596	3176.818	3666.465	1684.311	1657.110	1805.707
ABUW_RS14850	tuf	1.398	5.24189e-08	9288.227	8710.209	6456.884	20945.556	23237.564	20271.172
ABUW_RS14855	fusA	2.057	2.12786e-08	9039.482	9888.770	6694.751	36314.572	38059.795	32236.425
ABUW_RS14860	rpsG	2.366	4.93543e-09	1700.537	1674.681	1142.838	7756.728	8290.613	7253.814
ABUW_RS14865	rpsL	2.342	5.13408e-09	1256.791	1224.211	970.975	5629.212	6581.664	5288.528
ABUW_RS14870		-1.380	1.16798e-05	525.467	398.542	550.987	193.601	178.510	194.379
ABUW_RS14875		2.538	2.9796e-11	450.544	368.373	325.228	2110.792	2395.461	2142.126
ABUW_RS14880	hemJ	1.125	9.92363e-06	86.884	89.533	100.478	183.900	234.832	184.795
ABUW_RS14940		1.027	0.00301146	8.799	10.056	5.297	20.743	15.030	14.050
ABUW_RS14945		1.448	0.0287536	1.054	2.194	2.270	2.860	10.020	2.187
ABUW_RS14975	pgeF	1.452	1.57353e-05	15.701	8.472	16.228	31.603	36.757	41.825
ABUW_RS15005	lolB	1.128	4.27735e-05	17.809	21.393	15.387	42.065	39.341	38.336
ABUW_RS15010	ispE	1.677	3.50253e-07	65.914	78.380	78.532	230.635	266.842	214.896
ABUW_RS15035		2.147	6.15159e-07	529.577	557.922	423.688	2101.850	2595.329	1995.946
ABUW_RS15040	rplY	2.572	1.29222e-08	69.233	77.770	54.317	404.760	430.164	364.193
ABUW_RS15045	pth	1.033	0.0031138	105.536	158.222	151.263	268.971	304.126	275.750
ABUW_RS15050	panD	1.794	6.03162e-06	26.977	38.580	33.212	114.141	122.083	105.890
ABUW_RS15055		-1.075	0.000330526	18.968	16.090	16.396	7.240	8.121	9.165
ABUW_RS15060		-1.954	6.7086e-08	296.534	204.787	252.077	63.858	66.183	64.390
ABUW_RS15080	lysM	-2.926	1.25446e-10	1640.630	1324.776	1983.571	221.693	197.653	231.738
ABUW_RS15085	acpP	2.410	3.38455e-10	28.399	20.052	21.945	109.290	147.396	118.823
ABUW_RS15090	fabG	2.389	1.40419e-11	319.137	310.776	287.643	1507.760	1716.016	1583.460
ABUW_RS15095	fabD	2.121	2.30756e-10	248.534	232.214	223.909	992.877	1124.692	948.913
ABUW_RS15100	rpmF	1.213	7.44558e-05	107.222	88.314	114.351	207.141	255.557	255.605
ABUW_RS15125	scpB	1.098	0.000931415	10.274	16.151	7.399	23.856	26.473	22.890
ABUW_RS15130	rluB	1.283	4.02623e-08	95.104	89.107	91.229	211.086	239.841	219.642
ABUW_RS15135	bioD	2.076	1.96664e-07	9.695	14.810	14.042	55.749	54.318	51.596
ABUW_RS15140	bioC	2.309	8.04467e-09	7.218	13.104	10.174	54.337	51.997	44.198
ABUW_RS15145		2.767	2.32947e-10	18.388	18.650	12.192	120.983	116.282	100.493
ABUW_RS15150	bioA	2.281	5.75435e-10	32.983	34.497	31.194	160.080	167.435	152.461
ABUW_RS15160	otsB	-7.723	1.61345e-11	17.651	7.375	26.486	0.145	0.000	0.047
ABUW_RS15165		-6.695	3.9023e-11	685.431	224.169	607.995	4.887	6.276	3.536
ABUW_RS15175	bfr	3.064	1.48908e-05	51.530	49.856	79.457	411.059	528.991	568.110
ABUW_RS15180	ligA	1.021	0.000319143	61.804	55.158	48.851	109.037	123.349	104.773
ABUW_RS15190	smc	1.332	4.0537e-08	79.824	103.491	87.529	233.965	219.222	228.435
ABUW_RS15205		1.601	2.99277e-06	39.464	47.479	32.287	127.716	107.844	126.919
ABUW_RS15210		1.672	2.47631e-05	23.183	24.197	19.927	74.646	67.080	73.229
ABUW_RS15230		-2.506	1.14946e-07	19.548	17.614	12.444	3.294	2.531	2.885
ABUW_RS15235		-1.362	9.39032e-06	100.794	83.256	73.067	33.232	33.329	33.591
ABUW_RS15240		-1.965	1.09787e-06	41.677	37.666	33.380	11.005	10.600	7.258
ABUW_RS15250		-1.293	9.92821e-05	95.209	89.168	63.229	36.563	30.165	34.382
ABUW_RS15260		-1.121	1.41733e-05	161.123	191.439	237.531	81.090	91.918	98.213
ABUW_RS15270		2.189	8.92223e-09	13.014	16.395	11.771	62.084	64.917	61.505
ABUW_RS15280		-2.909	5.33681e-09	38.937	30.413	63.482	6.046	4.799	6.653
ABUW_RS15305		-1.651	9.9038e-08	113.071	79.599	109.811	33.594	32.380	30.287
ABUW_RS15330		-6.326	2.87828e-13	9426.588	5823.567	11392.478	103.751	119.973	108.402
ABUW_RS15335		-5.097	2.0152e-11	157.382	68.445	150.338	3.873	4.166	2.931
ABUW_RS15355		1.488	0.000221413	3.214	5.120	5.045	12.634	11.180	13.166
ABUW_RS15360		1.771	1.05329e-06	4.584	3.901	6.558	19.042	17.034	14.283
ABUW_RS15385	nuoK	1.059	2.91047e-06	196.688	203.080	144.368	413.883	374.053	346.840
ABUW_RS15390	nuoJ	1.244	8.59337e-06	308.916	285.787	178.758	598.181	684.930	550.152
ABUW_RS15395	nuoI	1.790	4.24305e-08	404.230	389.400	223.909	1152.667	1257.744	1111.144
ABUW_RS15400	nuoH	1.119	7.6062e-06	885.491	1014.122	717.889	1876.899	2060.854	1747.877

Locustag	Gene	logFC	PValue	M9_1	M9_2	M9_3	LB_1	LB_2	LB_3
ABUW_RS15405	nuoG	1.864	1.12681e-08	1759.391	1926.643	1103.236	5886.889	6153.398	5400.978
ABUW_RS15410	nuoF	2.046	1.53255e-08	747.973	824.999	473.968	2558.848	3503.963	2392.892
ABUW_RS15415	nuoE	1.924	4.34426e-09	178.089	204.482	134.194	647.703	705.760	608.726
ABUW_RS15420	nuoC	1.878	2.00131e-09	1005.411	1015.280	694.767	3231.747	3665.914	3088.619
ABUW_RS15425		1.358	8.03427e-05	316.081	344.298	704.520	1178.804	1270.927	1045.032
ABUW_RS15430	ndhC	1.014	6.07896e-06	494.434	515.198	416.120	921.019	1077.230	880.755
ABUW_RS15475		-3.586	1.98853e-09	125.716	80.208	99.469	10.028	7.963	7.304
ABUW_RS15490		-1.085	0.00772806	2.108	3.413	5.129	2.244	1.213	1.210
ABUW_RS15500		3.402	1.00838e-05	0.263	0.000	0.504	2.570	2.268	2.745
ABUW_RS15515		-4.088	2.28015e-06	1883.684	2414.657	787.341	84.710	99.248	115.148
ABUW_RS15520		-3.529	9.29647e-06	7064.541	7145.417	2451.401	457.432	479.577	506.047
ABUW_RS15525		-3.684	7.72147e-05	4420.976	5013.439	1563.246	313.643	291.364	250.906
ABUW_RS15550		-1.273	3.88333e-06	126.506	85.511	89.042	41.341	42.610	40.802
ABUW_RS15555		-1.452	0.000714049	3.003	3.291	5.213	1.557	1.318	1.163
ABUW_RS15580	tcuA	-1.336	0.00446866	1.897	4.266	7.736	1.412	2.162	1.721
ABUW_RS15605		1.238	0.000240342	3.477	2.804	2.775	7.457	5.485	8.561
ABUW_RS15610		-3.953	8.23196e-13	86.726	106.294	104.850	7.059	6.117	5.955
ABUW_RS15615	add	-2.147	1.42756e-06	96.052	45.772	74.749	18.933	12.393	17.400
ABUW_RS15655		-1.793	3.54047e-05	21.866	26.817	34.305	5.430	8.912	9.677
ABUW_RS15660		-2.235	2.19293e-07	29.717	37.118	27.327	6.589	5.379	8.002
ABUW_RS15690		1.753	0.000204355	1.528	1.341	1.513	5.684	3.533	5.443
ABUW_RS15700		-1.441	1.95636e-09	374.724	381.903	434.534	142.522	151.351	144.784
ABUW_RS15730		-1.141	5.71456e-06	346.483	305.108	324.219	150.704	148.662	143.109
ABUW_RS15755		-3.220	2.54745e-11	849.979	671.835	597.484	82.320	70.718	74.393
ABUW_RS15790	hpf	-2.388	4.05999e-08	141.259	116.716	209.868	29.323	25.471	34.428
ABUW_RS15830	gigA	1.170	2.55252e-06	97.475	105.563	99.216	215.503	214.001	250.720
ABUW_RS15875		-1.226	1.98143e-06	185.413	172.058	214.661	81.415	83.059	80.022
ABUW_RS15880	polA	1.091	9.11026e-08	249.430	252.022	219.958	518.720	516.809	501.487
ABUW_RS15895	tilS	1.184	0.00288421	17.704	30.109	27.579	57.740	52.155	60.761
ABUW_RS15900		1.536	1.13087e-07	156.908	143.838	149.413	415.693	464.811	425.466
ABUW_RS15950	rplT	1.515	1.88629e-05	503.707	481.737	464.551	1018.037	1772.548	1354.234
ABUW_RS15955	rpmI	2.177	3.00061e-07	95.209	88.680	73.319	270.383	385.813	508.559
ABUW_RS15980	thrS	1.181	5.14633e-08	727.372	701.822	671.560	1579.872	1656.794	1526.467
ABUW_RS15995		1.208	2.20338e-05	13.488	16.761	17.069	34.029	35.597	39.360
ABUW_RS16005	panC	1.151	8.61014e-07	123.240	153.773	116.117	291.416	313.249	268.958
ABUW_RS16010	panB	1.388	3.82835e-08	142.682	157.430	115.949	350.351	389.083	350.562
ABUW_RS16015	folK	1.916	1.27989e-06	11.802	16.029	11.267	51.984	44.351	51.642
ABUW_RS16035		-1.244	0.000435804	18.388	16.029	22.198	7.602	9.809	6.467
ABUW_RS16045	rlmD	1.251	5.51788e-08	74.660	77.770	76.262	177.709	185.102	181.399
ABUW_RS16065		-1.981	0.00861267	33.299	68.567	377.863	37.033	36.493	47.269
ABUW_RS16070		-1.204	5.74687e-05	96.790	149.202	130.243	50.753	50.521	61.924
ABUW_RS16090		-2.756	1.25327e-07	397.486	381.172	363.233	51.731	63.968	53.457
ABUW_RS16095		-3.428	1.63208e-09	51.583	53.513	55.914	5.249	5.643	4.048
ABUW_RS16100		-3.061	4.92967e-06	519.988	369.835	369.119	47.532	55.003	48.385
ABUW_RS16105		-1.224	3.83675e-05	8.430	8.350	7.483	3.077	3.481	3.908
ABUW_RS16110		1.451	0.0355764	0.790	0.061	1.261	2.751	1.846	0.698
ABUW_RS16120		-2.991	0.00120014	377.569	177.787	2037.299	113.562	100.409	111.752
ABUW_RS16130		-1.073	0.000130043	50.529	50.161	70.629	26.608	29.216	25.449
ABUW_RS16140		-2.684	1.53952e-09	25.080	16.456	25.477	3.149	4.008	3.303
ABUW_RS16155		-4.064	6.89467e-13	448.489	283.959	436.804	21.648	22.835	25.449
ABUW_RS16230		-3.415	0.00617807	364.766	11.641	14.378	15.711	10.916	10.003
ABUW_RS16240		-2.957	2.78971e-06	293.583	78.197	121.246	25.160	20.092	18.191
ABUW_RS16255	acnA	-2.133	1.89724e-09	1727.198	1334.528	1266.606	304.303	320.896	361.681
ABUW_RS16270		1.068	0.000171245	7.429	11.946	12.612	26.390	22.413	17.447
ABUW_RS16280		-4.139	1.10615e-06	590.644	510.992	568.897	14.661	68.345	12.655
ABUW_RS16285		-2.827	9.03368e-09	37.620	46.808	68.358	6.733	6.117	8.561
ABUW_RS16295		-1.041	0.0480762	77.558	70.639	93.331	43.224	35.807	38.057
ABUW_RS16315		1.693	0.000563409	3.583	3.352	2.018	9.485	9.545	10.747

Locustag	Gene	logFC	PValue	M9_1	M9_2	M9_3	LB_1	LB_2	LB_3
ABUW_RS16350		2.262	2.91895e-11	199.481	183.699	159.839	890.972	922.082	793.056
ABUW_RS16375	grxC	1.334	8.40627e-06	148.320	157.186	167.575	381.085	397.943	413.230
ABUW_RS16380	secB	1.668	6.53397e-08	101.268	138.170	137.726	401.430	404.851	391.503
ABUW_RS16430	ndk	1.895	1.36343e-09	234.413	231.787	235.429	795.294	977.612	836.510
ABUW_RS16440		-2.680	1.59677e-08	65.440	39.799	61.800	9.231	8.438	8.328
ABUW_RS16445		-2.146	0.000201802	18.125	15.176	11.015	4.235	1.635	4.001
ABUW_RS16465		-2.234	1.63611e-07	321.666	260.372	218.528	72.619	50.890	46.478
ABUW_RS16480		-1.382	0.00876607	2080.214	451.384	415.111	409.249	375.952	345.630
ABUW_RS16500		1.213	0.0245777	197.057	127.870	129.990	450.301	287.778	317.483
ABUW_RS16510		3.245	1.79971e-07	100.004	130.674	86.688	982.451	1144.784	885.267
ABUW_RS16515		1.188	0.000422124	7.008	11.032	15.891	28.707	20.989	26.007
ABUW_RS16535	tig	1.924	2.74958e-09	535.373	588.823	498.436	1880.953	2366.193	1911.132
ABUW_RS16540		1.647	0.00386423	170.449	240.747	141.846	756.993	583.888	391.596
ABUW_RS16545		1.441	3.65058e-08	33.141	38.458	29.849	101.398	83.164	91.188
ABUW_RS16580		-2.482	6.44024e-05	3.372	2.804	4.709	0.579	0.316	0.977
ABUW_RS16595		1.021	0.00402441	5.111	5.059	2.438	11.403	8.965	5.816
ABUW_RS16630		1.015	2.37945e-06	24.448	25.842	24.468	51.658	53.843	45.687
ABUW_RS16645		-2.207	1.00252e-06	319.770	283.837	316.483	60.636	84.852	54.015
ABUW_RS16650		-2.417	3.19387e-07	1475.924	1326.056	1291.242	249.351	290.415	226.853
ABUW_RS16655		-3.563	6.19383e-09	1115.900	991.205	750.093	93.760	75.043	72.811
ABUW_RS16670		-2.524	9.53238e-06	896.819	987.731	1047.910	157.039	167.277	185.679
ABUW_RS16675	rpmB	1.710	7.98299e-08	683.587	729.492	638.684	2257.513	2289.199	2165.853
ABUW_RS16680	rpmG	3.067	1.191e-09	7.956	7.253	5.970	54.953	71.509	52.991
ABUW_RS16715		-2.839	1.95626e-08	71.762	47.418	102.748	10.534	11.602	8.793
ABUW_RS16720		2.331	2.11185e-08	8.430	9.691	7.147	46.084	41.608	40.244
ABUW_RS16750		1.018	3.49082e-06	60.224	71.249	63.734	134.015	137.956	123.243
ABUW_RS16770	gltP	1.133	0.00038085	220.556	218.013	216.594	518.575	586.947	331.626
ABUW_RS16775		-1.076	0.000585507	71.815	60.522	82.652	37.106	32.116	32.521
ABUW_RS16785		3.014	5.53579e-10	11.381	17.370	8.240	120.874	92.235	88.490
ABUW_RS16790		3.254	7.88398e-07	64.333	91.484	41.620	684.592	571.759	632.547
ABUW_RS16795		1.247	4.55432e-07	72.658	68.323	72.562	182.886	155.043	168.698
ABUW_RS16800	truA	1.368	1.00522e-07	25.396	25.659	22.786	68.456	61.753	60.621
ABUW_RS16810	infA	2.343	8.38399e-09	24.658	21.454	24.552	103.462	145.867	109.239
ABUW_RS16815		-2.428	4.34494e-06	49.528	31.510	63.061	10.245	7.594	8.700
ABUW_RS16840	leuC	-1.280	3.50591e-08	263.550	278.047	251.909	104.620	115.702	106.541
ABUW_RS16845		-4.354	1.05824e-06	49.580	49.124	73.487	3.077	2.690	2.559
ABUW_RS16850		-1.567	3.00918e-05	170.765	155.297	161.100	55.858	49.202	59.272
ABUW_RS16890		-2.007	1.57304e-09	157.856	154.017	164.716	38.409	37.495	42.616
ABUW_RS16895		-1.160	0.000291678	16.176	15.481	22.870	8.905	6.592	8.607
ABUW_RS16935		1.190	8.1432e-05	5.532	6.521	5.886	13.322	12.657	14.934
ABUW_RS16945	hemW	1.255	5.59954e-06	73.817	86.059	76.262	171.664	185.577	206.289
ABUW_RS16950		-1.466	8.38168e-06	16.650	10.239	17.993	5.792	5.010	5.304
ABUW_RS16980		2.040	1.46914e-09	18.915	20.052	23.795	87.244	81.318	88.536
ABUW_RS17000		1.903	9.17069e-07	4.320	4.815	3.279	15.603	17.772	13.771
ABUW_RS17020		1.520	7.86447e-06	17.387	23.282	9.922	48.002	43.401	55.271
ABUW_RS17045	tusA	1.001	0.0096699	1.475	2.804	3.531	4.887	5.063	5.118
ABUW_RS17065		2.020	0.00110993	10.222	13.165	16.228	36.780	46.724	75.881
ABUW_RS17100		-1.871	1.60565e-08	162.914	127.992	149.749	39.857	34.700	45.827
ABUW_RS17105		-1.771	7.52729e-07	89.413	74.296	96.189	22.517	27.106	26.565
ABUW_RS17120	rpsO	1.525	2.14417e-07	917.684	707.307	641.291	2025.032	2339.614	2158.177
ABUW_RS17125		-1.272	0.000118591	25.765	17.980	15.891	9.014	6.750	8.979
ABUW_RS17145		-1.326	9.08678e-08	145.211	120.008	161.353	60.781	50.415	58.714
ABUW_RS17195		-1.275	1.4029e-07	1707.808	1386.883	1315.458	606.072	641.897	574.298
ABUW_RS17225		1.715	8.66835e-07	24.290	22.307	21.525	63.641	87.488	73.136
ABUW_RS17230	infB	1.350	8.45842e-06	2055.345	2307.327	1938.923	4963.517	5986.332	5108.711
ABUW_RS17240	rimP	1.146	0.000804225	55.218	56.316	50.953	107.154	149.611	103.377

Locustag	Gene	logFC	PValue	M9_1	M9_2	M9_3	LB_1	LB_2	LB_3
ABUW_RS17265	tpiA	1.625	1.67888e-07	62.173	59.425	63.061	185.854	195.544	188.191
ABUW_RS17270	pilB	2.736	6.28436e-08	104.693	128.662	53.056	610.996	648.806	653.343
ABUW_RS17275		2.301	5.4329e-07	87.516	107.026	42.713	384.524	394.093	394.620
ABUW_RS17285	coaE	1.626	3.61761e-08	36.355	37.240	30.269	112.005	101.621	107.565
ABUW_RS17295	rlmB	1.021	2.17086e-05	56.430	51.623	51.626	87.859	122.399	114.124
ABUW_RS17300		1.709	1.52158e-09	44.206	39.982	48.179	138.830	141.542	151.902
ABUW_RS17310	recN	1.360	4.19559e-07	102.059	88.497	73.656	246.925	212.894	219.130
ABUW_RS17320	ruvX	1.049	5.68516e-05	165.812	161.940	163.287	337.970	318.470	359.494
ABUW_RS17370		1.195	0.0132126	4.320	6.339	2.691	12.055	9.809	9.258
ABUW_RS17395		-2.054	1.06666e-07	34.827	24.379	36.155	8.000	6.908	7.956
ABUW_RS17400		-2.774	3.33992e-08	48.737	26.513	70.208	6.444	7.858	6.932
ABUW_RS17410		-2.686	4.52191e-09	31.719	35.228	42.461	5.720	4.746	6.420
ABUW_RS17420		-1.368	3.33227e-05	635.640	405.429	643.897	241.133	202.399	209.034
ABUW_RS17430	htpG	1.436	2.57148e-06	303.436	293.101	339.942	937.924	871.614	723.362
ABUW_RS17440		2.927	3.0006e-08	476.941	645.140	192.463	3157.354	3092.942	3752.849
ABUW_RS17445		1.220	1.11038e-05	73.923	78.441	64.575	158.342	184.100	163.301
ABUW_RS17450		-1.193	0.000142786	60.750	69.055	88.706	30.300	27.528	37.545
ABUW_RS17460		-1.614	8.97529e-05	6.533	4.571	4.288	1.955	1.793	1.303
ABUW_RS17465		1.572	0.00527685	0.685	0.914	0.336	2.534	1.582	1.814
ABUW_RS17480	rplL	2.379	1.68025e-08	444.642	529.642	439.663	2171.609	2816.080	2368.141
ABUW_RS17485	rplJ	2.801	1.67639e-10	1507.538	1630.189	1127.283	9322.627	10204.862	10195.789
ABUW_RS17490	rplA	1.882	1.38342e-06	1323.337	1593.986	1276.612	4535.842	6141.269	4781.830
ABUW_RS17495	rplK	2.255	8.35391e-08	827.586	982.368	732.520	3634.806	4608.246	3892.888
ABUW_RS17515	tuf	3.019	1.57552e-09	907.568	1056.176	712.760	7615.473	7684.365	6395.997
ABUW_RS17590		1.811	2.0921e-07	16.123	19.199	10.678	49.885	53.263	59.737
ABUW_RS17600		-1.244	1.19465e-06	127.718	116.594	115.360	49.848	43.771	58.249
ABUW_RS17615		1.509	6.9363e-07	11.486	12.251	10.426	32.400	35.280	29.915
ABUW_RS17630		-1.001	6.77366e-05	13.488	13.957	15.471	6.154	8.069	7.258
ABUW_RS17645	thiC	-2.139	2.1712e-08	481.999	441.328	325.985	96.403	88.859	98.353
ABUW_RS17665	gluQRS	1.461	7.0122e-06	42.415	42.786	28.588	108.204	101.569	104.680
ABUW_RS17680		-2.352	6.95973e-06	63.227	67.226	89.379	13.575	17.455	12.050
ABUW_RS17685		-2.473	9.02665e-08	2031.477	1922.071	2051.845	349.120	414.185	318.553
ABUW_RS17690		-2.079	1.94836e-06	51.846	40.896	48.683	11.258	11.180	11.026
ABUW_RS17695	xerD	1.332	4.3041e-05	23.815	24.501	19.171	62.591	51.734	56.062
ABUW_RS17715	pbpG	-1.207	6.52273e-07	1556.117	1371.950	1585.360	595.538	670.111	689.632
ABUW_RS17730		2.781	1.12238e-07	42.678	66.982	30.185	327.001	279.710	357.727
ABUW_RS17805		2.035	1.42238e-06	3.741	7.619	7.483	28.888	19.459	27.403
ABUW_RS17810		1.497	5.62218e-06	35.144	38.276	23.459	87.787	83.217	103.656
ABUW_RS17855	arsC	1.291	0.000242687	5.480	2.804	4.372	10.896	10.811	9.444
ABUW_RS17860		1.390	7.06269e-06	7.745	8.350	6.811	22.698	18.985	18.563
ABUW_RS17875	arsH	1.125	1.69714e-06	25.343	24.136	19.002	51.260	51.575	47.129
ABUW_RS17925		-5.501	3.01106e-13	96.842	112.328	92.490	1.882	3.111	1.768
ABUW_RS17930		-4.383	1.31804e-12	55.429	71.371	61.380	3.873	2.057	2.885
ABUW_RS17945	ppa	2.041	7.71335e-11	123.714	123.421	110.567	459.242	505.892	508.001
ABUW_RS17980		1.241	0.000122706	3.267	5.059	4.540	9.050	9.281	11.864
ABUW_RS18010		1.450	3.62858e-07	30.349	24.684	31.783	79.678	74.674	82.534
ABUW_RS18015		-2.984	6.94107e-07	56.272	46.260	45.152	7.313	5.274	5.955
ABUW_RS18030		1.039	0.00333229	2.108	5.181	5.381	9.448	8.490	7.304
ABUW_RS18045		-1.204	0.000578423	15.649	11.336	13.958	6.661	3.744	7.211
ABUW_RS18090		-3.097	2.28378e-10	65.282	81.244	114.603	10.136	10.389	9.910
ABUW_RS18095		-2.218	1.27767e-06	19.231	15.542	25.309	4.670	3.006	5.025
ABUW_RS18100		-2.560	2.41595e-09	1140.348	743.328	1057.327	175.718	187.211	135.619
ABUW_RS18105		-2.492	2.02447e-10	558.240	420.118	644.486	103.570	89.545	95.143
ABUW_RS18115		3.263	9.70784e-11	40.623	44.492	25.309	387.637	352.643	324.927
ABUW_RS18120	dprA	3.320	1.94034e-10	11.592	16.029	6.727	126.123	108.424	113.334
ABUW_RS18125		1.720	1.11163e-05	18.283	17.980	13.958	56.944	47.409	61.924
ABUW_RS18140		1.140	3.04698e-05	40.834	38.215	39.350	88.330	82.373	90.304
ABUW_RS18165	atpD	1.217	3.46852e-07	5926.511	5741.713	4326.170	11355.659	14230.907	11591.104
ABUW_RS18170	atpG	1.043	9.4771e-06	4522.929	5341.952	3277.924	9210.332	9275.239	8601.209
ABUW_RS18175	atpA	1.309	5.44337e-07	6430.112	6519.659	4353.497	14021.553	15668.532	13180.333

Locustag	Gene	logFC	PValue	M9_1	M9_2	M9_3	LB_1	LB_2	LB_3
ABUW_RS18180		1.562	7.70766e-08	1406.954	1504.330	934.904	3825.982	4041.180	3491.428
ABUW_RS18185		1.532	2.51213e-07	1461.804	1347.327	826.523	3323.154	3770.541	3421.269
ABUW_RS18195	atpB	1.120	4.43419e-05	2264.837	2425.262	1702.486	4626.814	5179.689	4086.197
ABUW_RS18205		-1.389	1.0075e-05	350.645	183.882	157.569	86.592	84.219	93.747
ABUW_RS18210		1.091	2.99271e-05	51.951	43.334	29.092	93.543	75.043	97.562
ABUW_RS18225		-1.357	1.32738e-06	37.409	43.395	42.125	13.503	16.875	17.679
ABUW_RS18250		-1.967	9.27883e-09	57.484	50.831	55.242	15.096	14.502	12.189
ABUW_RS18275		1.093	0.00286953	7.482	6.034	5.297	16.652	12.129	11.631
ABUW_RS18290		-2.359	3.94509e-07	16.439	11.215	16.060	3.005	3.111	2.373
ABUW_RS18380		1.045	0.00790003	1.423	2.133	1.766	3.475	3.164	4.280
ABUW_RS18390		-1.293	0.000114898	19.442	13.165	10.594	6.806	5.221	5.676
ABUW_RS18405		1.232	0.00103765	31.087	30.413	18.078	101.579	45.722	40.290
ABUW_RS18410		-1.700	5.18334e-06	16.228	17.431	12.360	5.068	4.852	4.280
ABUW_RS18415	mmsB	-1.180	0.0297429	6.586	2.560	3.700	2.896	1.424	1.256
ABUW_RS18420		-1.221	0.000218001	27.767	23.221	12.864	10.860	8.543	8.142
ABUW_RS18435		4.839	3.14107e-14	38.516	36.569	27.999	977.673	1086.828	895.689
ABUW_RS18440		5.022	1.50679e-11	25.238	14.932	15.639	565.310	639.313	622.311
ABUW_RS18445	alr	3.551	4.65386e-06	96.632	69.116	91.481	910.738	970.546	1133.661
ABUW_RS18450		3.420	1.64142e-10	241.632	202.471	317.913	2290.239	2867.655	2993.151
ABUW_RS18455		1.634	3.71401e-05	5.427	4.998	4.288	14.734	14.502	16.888
ABUW_RS18460		-2.510	0.00262124	92.627	9.447	9.753	5.792	5.959	8.235
ABUW_RS18465		-1.962	0.0338395	504.971	43.091	27.495	51.296	45.827	51.177
ABUW_RS18470		-1.817	8.88779e-09	205.276	150.543	186.661	44.454	55.056	54.527
ABUW_RS18475		-2.436	1.80593e-09	154.748	133.904	179.010	27.006	30.112	29.310
ABUW_RS18480		1.003	0.0345272	3.161	4.266	3.363	6.951	6.223	8.467
ABUW_RS18485		-2.230	1.74636e-07	14.753	16.700	18.834	3.910	1.951	4.652
ABUW_RS18505		1.835	0.00791032	0.422	0.183	1.093	2.534	1.055	1.768
ABUW_RS18535	prpB	1.125	8.86802e-07	107.749	91.545	82.652	202.290	218.905	194.565
ABUW_RS18540		1.922	1.16992e-05	6.270	6.826	6.474	27.947	15.715	30.287
ABUW_RS18545		1.554	8.29729e-08	542.381	473.204	313.877	1345.327	1331.415	1227.594
ABUW_RS18550	dld	2.049	2.0691e-06	30.191	23.526	30.017	108.457	121.397	116.497
ABUW_RS18555	lldD	2.145	3.47411e-07	71.130	66.190	56.671	253.441	330.441	275.564
ABUW_RS18560	lldR	3.078	2.87715e-08	13.805	10.178	10.847	101.652	105.840	88.164
ABUW_RS18565	lldP	3.848	9.65144e-09	37.040	31.571	31.951	514.810	488.859	446.170
ABUW_RS18640	wecB	1.024	1.00846e-06	1288.615	1425.585	1026.217	2734.566	2468.869	2401.732
ABUW_RS18665		1.286	2.81755e-06	165.285	147.008	111.745	332.721	354.700	347.584
ABUW_RS18670		1.040	0.000120033	33.774	26.878	33.549	65.342	65.445	62.855
ABUW_RS18700	rph	1.077	5.66798e-07	72.974	62.899	67.349	126.558	158.470	143.993
ABUW_RS18705		-2.681	7.60057e-10	154.115	114.339	130.495	24.291	21.094	16.702
ABUW_RS18710		-2.673	1.44169e-11	127.086	120.617	120.237	18.281	20.198	19.261
ABUW_RS18755	argA	1.051	5.17598e-06	33.668	34.923	33.212	75.768	62.755	72.346
ABUW_RS18760		2.250	1.88892e-06	3.319	5.424	4.709	17.159	19.987	26.426
ABUW_RS18765		1.208	0.000142848	13.172	10.788	11.519	27.006	26.210	28.938
ABUW_RS18770	ssuD	1.101	0.000225366	16.755	15.969	16.060	29.467	34.278	41.081
ABUW_RS18785		1.401	2.32519e-08	50.898	48.698	49.020	141.979	116.809	133.758
ABUW_RS18805	ileS	1.227	1.05011e-07	788.175	749.362	607.658	1668.383	1783.254	1570.433
ABUW_RS18820		-1.393	1.74272e-05	150.638	94.226	160.428	55.387	46.566	52.154
ABUW_RS18870		-1.600	9.90742e-07	31.297	20.479	34.810	8.073	9.703	10.794
ABUW_RS18875		-1.321	2.03553e-05	53.216	66.007	68.611	22.951	27.897	24.332
ABUW_RS18885	grpE	1.586	5.10137e-05	177.246	228.313	217.351	625.802	607.619	636.594
ABUW_RS18890	dnaK	1.444	2.92896e-05	3264.347	3482.779	3251.270	9228.939	9622.450	8350.582
ABUW_RS18895		-1.588	0.00323555	1.106	1.036	1.934	0.253	0.633	0.465
ABUW_RS18900		-1.413	0.0280046	1.317	1.707	1.177	0.688	0.580	0.279
ABUW_RS18940		1.560	5.49218e-07	5.058	5.303	7.736	19.114	18.194	15.120
ABUW_RS18955		1.916	7.03118e-07	11.434	12.373	8.156	40.364	42.610	38.801
ABUW_RS18960		1.401	0.00364662	1.423	1.158	0.757	3.005	2.268	3.862

Locustag	Gene	logFC	PValue	M9_1	M9_2	M9_3	LB_1	LB_2	LB_3
ABUW_RS18975	hpt	1.156	0.000392653	10.064	11.215	20.936	25.956	31.483	35.126
ABUW_RS18980		-3.664	1.77186e-10	206.067	114.827	209.027	14.191	15.557	12.050
ABUW_RS19005	yidC	1.543	1.94652e-07	679.530	779.592	602.361	1836.535	2281.921	1889.498
ABUW_RS19010	yidD	1.968	6.8435e-08	40.676	49.673	36.744	164.062	182.676	151.204
ABUW_RS19015	rnpA	1.718	1.38439e-07	111.016	107.026	96.946	313.643	393.882	329.207
ABUW_RS19020	rpmH	1.816	3.12459e-07	42.467	45.650	41.957	158.994	161.318	137.898
ABUW_RS19720		-4.241	3.75529e-11	16192.224	11041.671	13673.782	666.600	777.217	719.129
ABUW_RS19795		-2.912	0.00814111	0.263	1.036	1.345	0.253	0.000	0.000
ABUW_RS19800	pqqA	1.630	0.00690699	0.948	0.427	0.420	2.063	2.057	1.768
ABUW_RS20090		-3.565	7.98725e-10	5.901	4.998	6.138	0.290	0.369	0.791
ABUW_RS20105		-2.152	1.46977e-05	19.600	20.783	29.513	4.742	6.856	4.141
ABUW_RS20110		1.685	9.10627e-07	32.878	29.072	25.729	94.049	98.141	90.630
ABUW_RS20115		1.001	0.000631017	27.662	34.923	29.260	74.284	52.261	57.039
ABUW_RS20125		-1.258	0.00115623	8.061	3.901	8.408	2.643	2.900	2.931
ABUW_RS20145		-11.317	6.90193e-17	115.284	100.931	176.067	0.000	0.158	0.000
ABUW_RS20155		-2.202	0.000972604	2.424	0.731	3.531	0.109	0.527	0.837
ABUW_RS20185		1.614	0.00867276	0.105	0.244	0.504	0.724	0.949	0.744
ABUW_RS20200		-1.875	0.000660851	2.951	1.646	3.868	0.796	0.475	0.930
ABUW_RS20205		-2.306	7.32682e-07	41.255	24.806	54.317	6.878	9.440	8.049
ABUW_RS20220	tgnA	1.280	0.000602405	2.476	2.377	1.766	5.756	5.590	5.025
ABUW_RS20225		1.783	8.80361e-05	1.317	1.280	1.345	5.322	4.166	4.001
ABUW_RS20235		-4.690	2.85463e-05	0.474	1.707	0.589	0.036	0.000	0.047
ABUW_RS20265		2.395	0.00294556	0.211	0.853	0.841	4.778	1.529	2.885
ABUW_RS20270		-1.830	0.00468092	1.212	0.488	2.018	0.109	0.422	0.512
ABUW_RS20295		-4.582	3.58003e-09	7.324	4.876	9.585	0.434	0.211	0.186
ABUW_RS20305		-2.708	1.71702e-07	11.750	13.226	13.621	2.425	1.371	1.954
ABUW_RS20445		1.062	0.0302458	2.371	0.853	1.850	2.968	4.166	3.675
ABUW_RS20475		-6.756	1.4501e-08	3.741	2.926	5.381	0.000	0.105	0.000
ABUW_RS20510		-1.247	0.00244211	37.304	29.499	44.563	18.390	12.235	15.958
ABUW_RS20540		-5.138	2.32398e-06	8.167	14.750	21.525	0.724	0.105	0.279
ABUW_RS20665		2.570	0.00179634	0.158	0.427	0.420	3.511	0.844	1.070
ABUW_RS20695		-2.205	0.00102081	1.159	1.707	2.018	0.398	0.316	0.279
ABUW_RS20705		-7.156	2.75748e-12	1782.153	572.855	1687.267	7.566	10.969	9.956
ABUW_RS20715		2.205	4.85658e-08	65.650	73.870	39.014	276.429	276.493	273.052
ABUW_RS20735		-4.277	0.0261381	0.053	0.122	2.438	0.000	0.105	0.000
ABUW_RS20750		-2.084	2.88982e-05	6.270	7.253	10.426	2.389	1.951	1.117
ABUW_RS20790		-1.605	3.86807e-05	5.690	7.862	6.895	2.968	1.898	1.675

2.3 Differentially Expressed Genes of *A. baumannii* in M9 Succinate medium vs in LCWB medium

Locustag	Gene	logFC	PValue	LCWB_1	LCWB_2	LCWB_3	M9_1	M9_2	M9_3
ABUW_RS00015	recF	-1.340	3.33e-05	61.281	24.876	49.961	15.912	19.138	18.918
ABUW_RS00025	cybC	-1.040	9.58e-06	130.389	129.093	160.776	78.190	69.298	56.671
ABUW_RS00035	abc-f	-1.705	8.74e-10	351.917	274.734	337.329	98.160	107.818	89.547
ABUW_RS00045		3.495	1.29e-10	74.812	89.204	39.668	877.114	675.309	732.267
ABUW_RS00050		2.229	6.42e-06	7.604	5.699	3.005	32.825	23.343	17.153
ABUW_RS00070	tyrS	-1.413	7.62e-09	380.545	358.129	374.443	142.787	153.651	121.330
ABUW_RS00105		-1.297	1.04e-06	55.242	56.985	45.528	23.447	16.761	23.963
ABUW_RS00110		2.124	2.93e-10	168.075	201.311	162.279	861.570	669.885	785.911
ABUW_RS00115		2.114	0.000102321	1.006	2.740	1.653	7.798	5.181	10.678
ABUW_RS00120	rsmB	-1.349	5.01e-09	255.747	236.050	247.325	98.581	98.737	92.658
ABUW_RS00150		-1.142	0.000197949	271.179	164.051	141.092	94.261	94.897	71.385
ABUW_RS00180	dnaJ	-1.100	2.57e-05	276.882	286.460	493.748	155.433	183.577	154.458
ABUW_RS00245	mutY	-1.037	1.53e-06	76.713	64.766	82.792	36.935	36.508	35.903
ABUW_RS00260		4.869	3.42e-10	1.006	1.534	1.878	48.210	28.036	57.932
ABUW_RS00270		4.620	3.02e-11	11.406	14.027	11.344	413.082	170.778	317.661
ABUW_RS00280		2.924	5.1e-08	4.920	4.383	4.132	44.628	19.564	37.248
ABUW_RS00285		5.261	5.83e-05	0.000	0.219	0.000	3.267	2.316	2.438
ABUW_RS00350		-1.525	0.00519206	76.601	32.547	20.736	13.330	14.810	16.732
ABUW_RS00355		1.650	0.0165665	6.933	4.274	7.889	44.733	9.203	5.381
ABUW_RS00380	hutU	-2.018	0.000442422	110.484	46.355	41.321	19.916	14.262	14.210
ABUW_RS00385	hutH	-2.119	9.89e-09	104.222	83.834	97.893	27.872	19.199	18.414
ABUW_RS00390		-1.293	2.5e-05	112.385	85.806	68.142	37.251	36.508	34.558
ABUW_RS00425		-1.354	5.89e-08	46.632	43.177	41.396	16.913	17.127	17.237
ABUW_RS00460	nusB	-1.327	4.5e-07	251.945	185.859	291.876	108.855	100.687	81.139
ABUW_RS00480	serB	-1.368	9.57e-08	219.068	319.774	257.242	96.157	117.021	95.096
ABUW_RS00485	aciT	1.466	2.01e-06	395.529	616.754	359.943	945.873	1319.413	1525.914
ABUW_RS00515		1.109	0.000135814	146.269	166.353	276.475	482.526	377.698	412.757
ABUW_RS00540		1.400	3.99e-07	56.920	62.684	89.629	205.856	180.529	167.238
ABUW_RS00550		1.372	2.27e-06	115.181	130.518	221.105	453.178	345.090	412.505
ABUW_RS00555		1.028	7.74e-05	78.614	87.889	151.836	251.485	212.466	187.166
ABUW_RS00585		1.288	0.00452042	7.940	6.356	6.311	11.117	13.043	26.822
ABUW_RS00605		1.107	1.29e-05	33.883	21.260	32.305	69.760	59.425	59.530
ABUW_RS00630	hpxO	1.337	0.0161832	0.335	0.438	0.676	1.054	1.524	1.345
ABUW_RS00635		-3.461	1.22e-10	174.113	107.066	93.085	10.222	14.810	8.660
ABUW_RS00690		1.492	4.78e-05	22.477	8.548	12.772	33.352	32.851	56.923
ABUW_RS00705	pyrE	-1.567	1.66e-06	132.738	66.738	81.891	34.933	28.219	31.615
ABUW_RS00710		-4.608	2.1e-07	2928.394	7640.930	6643.811	248.007	256.288	201.376
ABUW_RS00770	aceE	-1.280	0.000224679	4010.424	5761.300	9037.422	3499.814	2218.647	2028.807
ABUW_RS00785		-1.550	6.05e-06	18.787	17.424	14.350	5.058	5.485	6.811
ABUW_RS00795		-3.088	2.85e-09	83.758	156.599	112.318	16.386	15.420	9.165
ABUW_RS00800		-2.442	1.57e-07	38.133	46.574	61.531	7.482	8.289	11.603
ABUW_RS00805	guaB	-1.101	1.43e-07	1675.381	1450.599	1796.861	813.044	776.849	704.436
ABUW_RS00820	recJ	-1.318	2.21e-07	161.030	126.244	175.727	62.436	58.937	64.575
ABUW_RS00825		1.062	0.000565286	688.290	1448.736	1692.732	2694.937	2017.395	3285.912
ABUW_RS00830	prfB	2.449	0.0173184	0.224	0.000	0.075	0.474	0.366	0.925
ABUW_RS00840		-1.078	9.11e-05	109.366	52.163	66.114	34.406	37.910	35.314
ABUW_RS00850		-1.225	3e-05	18.787	13.808	20.510	6.428	7.862	8.744
ABUW_RS00865	acs	2.509	1.04e-09	60.274	73.752	82.567	535.004	360.815	338.849
ABUW_RS00875		2.678	0.00328028	0.112	0.329	0.301	1.633	2.682	0.420
ABUW_RS00915		3.028	2.52e-08	2.348	7.014	4.357	43.943	34.558	33.128
ABUW_RS00920		1.848	1.06e-10	991.451	1065.621	1048.125	3871.746	3306.821	3996.738
ABUW_RS00925	omp33-36	-3.487	4.11e-09	2629.147	1559.966	1184.184	96.315	214.112	169.004
ABUW_RS00950		1.286	0.000416608	2.460	3.726	3.982	7.376	9.569	8.324
ABUW_RS00965		-2.030	4.43e-10	432.991	407.662	320.801	92.627	96.421	95.180
ABUW_RS00980		-1.420	0.00029951	5.256	5.479	6.161	1.897	2.499	1.934
ABUW_RS00995		-3.578	2.96e-11	103.439	128.655	138.237	11.065	7.253	12.949
ABUW_RS01005	gabT	-5.709	2.07e-12	187.421	300.158	429.438	7.482	5.363	4.372
ABUW_RS01015		1.634	9.86e-08	28.851	46.136	47.707	131.775	126.773	123.516
ABUW_RS01020	ycaC	2.096	3.93e-09	135.533	169.640	234.403	796.710	680.124	834.090
ABUW_RS01030		-2.037	1.57e-08	783.902	1445.558	1346.913	351.014	267.747	252.413
ABUW_RS01035		-2.064	1.33e-08	68.997	96.108	123.136	27.398	23.770	17.489
ABUW_RS01060		-1.221	2.22e-06	39.139	41.314	38.166	17.335	17.127	16.312
ABUW_RS01075		1.093	5.13e-05	9.617	15.013	16.453	32.035	28.890	27.411
ABUW_RS01120		1.622	0.00541747	0.671	2.411	0.451	2.740	3.779	3.784
ABUW_RS01140		1.643	9.43e-06	102.768	176.654	208.258	742.757	354.842	426.883
ABUW_RS01145		-1.751	2.89e-09	98.743	135.997	131.175	36.777	33.095	39.014
ABUW_RS01150		4.048	4.04e-11	4.585	3.836	1.878	46.050	59.547	58.185
ABUW_RS01160	aqpZ	3.545	7.58e-13	59.715	71.670	65.212	847.608	596.442	850.738
ABUW_RS01170		1.236	0.0320733	0.895	0.877	0.751	1.528	2.804	1.513
ABUW_RS01180		-1.234	3.12e-07	146.716	167.229	211.413	72.869	71.493	79.289
ABUW_RS01185		-1.489	3.22e-07	25.608	25.862	37.640	10.643	12.129	8.997
ABUW_RS01195		-1.531	0.000183122	3.914	9.205	7.813	2.582	2.194	2.522
ABUW_RS01205	hisA	-1.466	7.71e-08	228.685	229.913	219.227	95.104	74.052	76.010
ABUW_RS01245		1.428	4.09e-05	4.138	6.685	5.935	19.390	12.190	13.537
ABUW_RS01250		-2.443	5.33e-07	831.428	548.372	485.634	140.785	91.301	110.567
ABUW_RS01265		-1.663	1.46e-09	1555.838	1600.185	1324.901	523.834	483.017	408.048
ABUW_RS01270		3.947	9.29e-12	179.481	199.776	146.201	3097.165	1782.987	3217.217
ABUW_RS01275		-1.538	8.33e-05	284.933	124.929	169.416	78.296	66.068	54.653
ABUW_RS01285	ettA	-1.948	4.6e-10	3482.828	2957.087	2331.555	795.920	786.601	690.731
ABUW_RS01290		-2.577	5.01e-08	74.141	160.435	103.453	23.868	16.578	15.807
ABUW_RS01300		-2.383	7.47e-05	13.531	4.822	16.002	0.843	4.327	1.513
ABUW_RS01305		-4.072	2.04e-08	25.385	34.629	43.349	0.422	4.084	1.766
ABUW_RS01310		-2.679	1.01e-06	14.202	35.396	22.088	2.371	6.095	2.607
ABUW_RS01315		-1.843	4.86e-10	110.261	126.901	106.608	27.978	37.179	30.606
ABUW_RS01330		1.689	1.07e-06	17.557	21.917	13.749	47.894	54.122	68.695
ABUW_RS01345		4.316	0.000885941	6.933	11.397	8.039	31.719	28.341	466.653
ABUW_RS01350		-2.763	5.49e-09	479.511	231.009	271.366	53.269	49.551	41.452
ABUW_RS01365	gltX	-1.073	1.02e-06	556.783	442.511	424.479	238.418	233.859	204.150
ABUW_RS01370		1.437	8.81e-06	66.760	69.697	39.743	132.987	123.908	218.781
ABUW_RS01375		-1.046	0.00116763	32.094	83.615	60.253	28.979	34.253	21.693
ABUW_RS01400	murF	-1.001	2.4e-06	413.310	326.787	347.472	188.627	186.441	168.079
ABUW_RS01410		-1.057	0.000382824	18.675	24.328	27.046	7.113	14.323	12.696
ABUW_RS01425		-2.436	2.14e-08	326.868	577.960	531.688	86.463	117.996	60.539
ABUW_RS01430		-3.101	2.11e-08	141.796	279.446	237.333	26.713	35.228	14.210
ABUW_RS01435		-3.120	4.44e-09	96.953	161.860	148.530	17.914	20.662	7.567
ABUW_RS01440		-3.162	3.66e-08	182.500	327.555	247.250	28.716	42.542	12.528
ABUW_RS01445	pilQ	-3.003	1.23e-07	449.541	1028.690	688.558	94.050	124.152	51.290
ABUW_RS01480		1.166	7.1e-05	91.027	198.790	210.887	415.663	332.047	377.527
ABUW_RS01485		1.881	1.49e-07	45.849	75.505	105.106	305.491	242.087	290.250

Locustag	Gene	logFC	PValue	LCWB_1	LCWB_2	LCWB_3	M9_1	M9_2	M9_3
ABUW_RS01490		1.957	2.6e-07	10.959	9.424	18.331	48.368	47.296	57.764
ABUW_RS01495		-2.710	1.51e-05	510.263	1410.928	892.758	201.272	170.351	57.176
ABUW_RS01500		-1.022	2.32e-05	120.437	80.327	79.411	40.781	48.393	48.767
ABUW_RS01530	gmk	-1.496	6.61e-09	235.059	182.023	203.975	67.495	78.441	74.328
ABUW_RS01540		-3.541	2.25e-07	18.116	42.410	12.471	2.951	1.768	1.177
ABUW_RS01545	pilV	-2.841	3.12e-06	61.728	121.312	47.932	10.011	16.273	5.297
ABUW_RS01550		-2.326	4.28e-08	77.384	88.656	83.994	16.597	21.759	11.099
ABUW_RS01555		-1.986	4.67e-07	142.243	159.777	123.662	31.877	49.246	25.897
ABUW_RS01575	rpsP	-2.700	1.64e-09	2442.844	1448.407	1168.933	283.203	269.819	225.339
ABUW_RS01580	rimM	-2.850	1.29e-08	8909.085	4807.348	3098.246	721.418	834.872	775.906
ABUW_RS01585	trmD	-2.974	1.97e-08	6974.938	3516.307	2213.151	526.521	604.182	486.244
ABUW_RS01590	rplS	-2.465	4.06e-08	2771.837	1467.694	1127.687	338.896	358.743	274.022
ABUW_RS01595		5.061	0.000430509	23.260	16.219	5.785	106.432	1301.006	63.734
ABUW_RS01600		2.114	0.000587221	1.230	0.877	0.601	5.005	3.047	3.027
ABUW_RS01605	truB	-1.951	5.82e-07	68.438	28.054	55.070	12.540	12.068	14.798
ABUW_RS01610		-2.014	2.73e-08	46.408	43.177	39.217	9.853	8.472	13.873
ABUW_RS01615		3.099	2.31e-07	14.537	4.055	3.681	65.756	53.574	65.079
ABUW_RS01620		-1.116	1.99e-05	37.126	31.671	56.272	19.653	18.345	20.096
ABUW_RS01630	serA	-1.589	2.76e-08	1714.632	1212.796	1323.173	462.504	538.114	412.421
ABUW_RS01640		1.343	4.58e-06	23.260	34.410	27.272	69.549	53.878	92.490
ABUW_RS01655		2.141	0.000391451	1.118	6.466	1.052	7.535	12.799	16.228
ABUW_RS01660		-1.335	0.000351326	179.928	93.477	61.606	31.087	45.468	56.335
ABUW_RS01665	yccS	1.317	1.33e-05	24.825	26.520	28.098	66.757	68.201	63.313
ABUW_RS01670	sodC	1.040	1.96e-05	142.243	206.352	225.162	479.364	303.950	397.706
ABUW_RS01690		1.268	0.000922285	11.183	17.643	6.236	25.080	22.002	35.987
ABUW_RS01700		1.067	0.000134464	12.413	17.205	26.971	38.358	40.775	41.284
ABUW_RS01705		-1.647	1.32e-08	122.114	175.339	123.587	40.096	51.562	42.629
ABUW_RS01710		-1.311	3.54e-06	147.499	113.313	136.209	66.072	49.246	44.311
ABUW_RS01715		-3.161	1.06e-12	4913.980	4656.557	3593.422	541.169	513.918	416.372
ABUW_RS01720		-1.959	1.18e-07	332.571	205.585	348.599	97.159	72.894	57.512
ABUW_RS01725	astA	-2.117	1.17e-07	158.234	87.669	125.766	34.090	31.084	19.927
ABUW_RS01730	astD	-1.264	7.06e-06	256.641	254.351	183.240	97.475	109.281	81.727
ABUW_RS01760		1.980	2.76e-06	11.071	28.821	32.230	112.175	79.538	95.769
ABUW_RS01765		1.359	1.83e-05	5.815	7.342	7.137	18.968	14.018	19.423
ABUW_RS01795	glyS	-1.786	4.24e-09	900.760	860.475	675.185	253.223	250.925	201.796
ABUW_RS01800	glyQ	-1.792	7.11e-09	568.972	485.688	601.258	181.408	172.545	123.852
ABUW_RS01815		-3.524	0.0129773	4.138	0.658	191.729	6.797	5.668	4.793
ABUW_RS01820		-1.387	0.00246307	9.617	4.055	10.443	3.161	3.840	2.186
ABUW_RS01835		2.066	9.7e-08	138.105	166.133	286.392	608.189	945.920	924.562
ABUW_RS01845	aroE	-1.688	5.55e-06	89.908	61.807	137.561	34.775	28.402	26.654
ABUW_RS01850	hemF	-1.196	1.69e-05	577.583	835.160	642.879	298.272	319.065	279.824
ABUW_RS01865		-2.137	1.19e-06	1478.790	735.546	534.618	197.531	186.807	240.474
ABUW_RS01870		-2.840	1.85e-06	8805.422	3944.682	1955.158	609.981	720.472	722.514
ABUW_RS01905		-1.235	1.32e-05	35.673	24.438	47.632	16.123	15.603	14.210
ABUW_RS01920		-1.928	0.000118543	8.275	4.493	4.583	2.266	0.609	1.513
ABUW_RS01935	adeT2	1.124	4.66e-05	15.879	19.178	30.953	50.845	48.149	46.581
ABUW_RS01965		-1.016	0.000123277	25.496	34.081	41.922	16.334	20.662	13.201
ABUW_RS01990	rpsJ	-2.719	2.73e-08	8213.749	4582.914	3264.056	871.792	985.842	580.584
ABUW_RS01995	rplC	-2.682	6.99e-08	22137.681	13136.154	7994.782	2236.332	2842.150	1665.153
ABUW_RS02000	rplD	-2.489	2.54e-07	11528.726	7058.368	3890.708	1309.796	1637.015	1057.747
ABUW_RS02005	rplW	-2.529	1.31e-07	3743.719	2256.609	1513.324	405.126	544.392	352.050
ABUW_RS02010	rplB	-2.000	7.44e-07	19134.364	13038.512	7474.513	3359.977	3866.267	2685.148
ABUW_RS02015	rpsS	-1.837	1.79e-06	5556.310	3349.078	2387.150	1238.876	1127.791	793.311
ABUW_RS02020	rplV	-2.059	5.21e-07	5000.087	3085.632	2338.241	864.310	1038.257	597.484
ABUW_RS02025	rpsC	-1.923	3.91e-07	12921.969	9346.976	6252.539	2664.904	2945.762	1909.999
ABUW_RS02030	rplP	-1.929	8.31e-07	13687.084	11746.156	6475.522	2397.402	3581.211	2397.925
ABUW_RS02035	rpmC	-1.948	8.53e-07	3267.451	2977.470	1635.634	609.348	835.604	597.316
ABUW_RS02040	rpsQ	-2.189	1.03e-07	8446.348	6275.700	4542.828	1468.548	1759.278	997.209
ABUW_RS02045	rplN	-1.938	1.83e-08	4374.866	3343.708	2732.518	1021.587	1022.533	682.575
ABUW_RS02050	rplX	-2.093	2.69e-08	2965.856	2220.883	1975.894	624.891	683.720	369.455
ABUW_RS02055	rplE	-1.951	2.57e-08	6678.263	4757.267	3884.472	1421.707	1462.154	1076.582
ABUW_RS02060	rpsN	-1.904	1.28e-07	4575.706	3510.171	2220.664	880.539	1049.045	824.253
ABUW_RS02065	rpsH	-2.020	4.66e-08	6909.743	4851.730	3678.769	1371.284	1479.646	954.327
ABUW_RS02070	rplF	-2.178	1.49e-08	11188.439	9492.835	5933.767	1972.255	2349.198	1561.228
ABUW_RS02075	rplR	-1.924	1.01e-07	2635.073	2080.503	1361.413	572.940	616.555	411.412
ABUW_RS02080	rpsE	-1.919	1.16e-07	8218.446	6589.556	3955.844	1705.754	1830.588	1425.941
ABUW_RS02085	rpmD	-2.043	1.18e-07	963.495	706.067	453.028	158.963	200.277	155.635
ABUW_RS02090	rplO	-1.780	4.87e-07	7609.776	6013.678	3372.618	1666.500	1745.443	1536.677
ABUW_RS02095	secY	-1.963	2.05e-07	26680.510	21314.497	12811.605	4830.791	6163.537	4596.493
ABUW_RS02100	rpmJ	-1.745	3.36e-08	1522.067	1290.493	864.886	373.143	386.109	337.756
ABUW_RS02105	rpsM	-2.018	5.09e-09	6082.900	4386.316	3975.378	1346.731	1313.866	905.980
ABUW_RS02110	rpsK	-2.087	9.01e-08	2702.952	1680.621	1425.048	573.414	480.701	311.943
ABUW_RS02115	rpsD	-1.884	1.94e-07	16350.226	12229.982	7510.725	3383.213	3673.426	2720.883
ABUW_RS02120		-2.089	2.82e-08	20614.608	14506.425	10099.747	3674.636	4018.334	2936.636
ABUW_RS02125	rplQ	-2.044	1.16e-07	3848.724	2759.173	1722.033	671.837	792.269	555.864
ABUW_RS02130		1.391	2.51e-06	33.101	60.711	42.523	124.030	103.491	129.990
ABUW_RS02140		-1.165	0.0145094	4.361	2.301	5.560	1.475	0.853	3.700
ABUW_RS02145		-1.126	0.0410186	4.585	1.096	3.080	1.054	1.585	1.429
ABUW_RS02150		2.190	4.47e-09	49.427	46.246	26.370	201.799	181.626	169.509
ABUW_RS02155	rrtA	2.348	4.2e-08	8.722	9.315	5.560	47.262	41.628	28.672
ABUW_RS02160		2.551	3.4e-09	45.178	40.657	26.596	266.448	205.214	182.794
ABUW_RS02165		-1.365	1.64e-05	73.693	72.875	150.333	39.411	41.628	34.558
ABUW_RS02205		3.931	7.67e-13	473.920	376.540	589.312	7398.009	6084.121	8490.904
ABUW_RS02230		1.140	0.0166263	1.677	1.863	1.578	3.056	4.998	3.111
ABUW_RS02235		-1.070	0.00717667	8.163	6.246	5.409	3.583	2.986	2.607
ABUW_RS02250		-2.815	2.77e-10	303.049	183.338	229.669	32.298	35.228	34.221
ABUW_RS02295		-1.400	7.61e-08	3989.401	4349.385	3521.899	1554.325	1728.255	1210.440
ABUW_RS02300		1.808	0.00781411	0.671	1.315	0.376	2.108	1.585	4.540
ABUW_RS02355		2.552	4.33e-05	2.460	0.767	0.301	6.955	5.973	5.886
ABUW_RS02360		2.668	2.06e-05	1.230	0.329	1.878	7.271	6.095	10.510
ABUW_RS02395		1.243	0.000526351	8.387	2.959	7.363	17.124	12.799	14.798
ABUW_RS02420	rpsI	-2.190	8.66e-09	1039.649	633.301	558.059	180.354	158.771	149.497
ABUW_RS02425	rplM	-2.613	2.19e-10	5104.197	3413.515	2957.830	593.594	735.831	545.606
ABUW_RS02440		-1.470	2.02e-09	138.665	144.654	151.160	47.736	55.463	53.728
ABUW_RS02445		-1.246	1.6e-05	18.563	29.260	23.741	9.484	12.799	7.651
ABUW_RS02525		-2.897	9.8e-08	355.496	926.555	801.777	83.986	131.222	64.070
ABUW_RS02535		1.698	3.48e-06	13.419	10.630	18.857	32.667	59.425	49.272
ABUW_RS02565		-1.452	2.87e-06	132.290	66.738	90.380	33.141	41.628	30.774
ABUW_RS02570		-1.044	0.000776224	71.681	35.835	75.730	36.724	31.998	19.759
ABUW_RS02595	radC	-3.333	1.27e-09	28.628	26.739	35.461	3.003	3.962	1.850
ABUW_RS02605	secF	-1.007	1.11e-06	802.241	1040.197	805.759	422.724	447.240	447.399
ABUW_RS02610	secD	-1.128	6.69e-07	2129.395	2771.008	2377.534	1109.472	1256.880	962.987
ABUW_RS02615	yajC	-1.392	1.66e-08	309.647	347.280	298.938	120.921	136.646	106.447
ABUW_RS02620	tgt	-1.693	7.52e-09	717.701	580.590	566.398	214.813	203.507	157.905
ABUW_RS02635	queA	-1.913	3.74e-08	127.706	92.601	104.805	27.925	31.754	26.486
ABUW_RS02645		-2.303	7.69e-07	43.053	20.931	18.632	5.585	6.156	4.709
ABUW_RS02650		1.158	0.00487027	2.460	3.178	4.583	8.114	4.632	11.183

Locustag	Gene	logFC	PValue	LCWB_1	LCWB_2	LCWB_3	M9_1	M9_2	M9_3
ABUW_RS02740		-1.059	2.45e-05	84.317	134.901	165.209	61.277	61.009	62.557
ABUW_RS02745		-1.527	4.09e-06	7.828	9.644	11.269	2.898	3.840	3.363
ABUW_RS02775		-1.130	0.00629187	4.920	3.616	3.231	1.212	1.768	2.522
ABUW_RS02875		2.235	1.81e-08	30.640	55.999	32.606	179.353	175.227	205.412
ABUW_RS02915	ghy	-1.163	2.13e-06	46.184	62.245	55.971	22.551	29.804	20.936
ABUW_RS02930		-1.083	5.06e-05	26.391	17.643	25.920	10.643	11.763	10.678
ABUW_RS02935		-1.668	2.12e-07	43.836	29.588	53.567	12.277	14.079	13.873
ABUW_RS02940	aspS	-1.651	1.46e-08	2410.303	2199.952	2573.170	937.601	769.779	579.070
ABUW_RS02950	znuD	2.112	0.0167961	117.082	138.298	132.077	1439.253	129.455	104.009
ABUW_RS02960		-1.422	2.12e-07	47.191	54.684	44.552	18.125	20.844	15.387
ABUW_RS02965		-6.174	4.74e-11	22.924	13.370	11.495	0.316	0.122	0.168
ABUW_RS02970		1.298	4.5e-05	10.735	20.383	16.754	30.928	49.124	38.089
ABUW_RS02975		1.316	6.36e-06	134.527	181.695	259.946	362.237	507.701	567.719
ABUW_RS02980		1.331	3.93e-05	386.136	544.317	765.340	882.066	1587.647	1800.273
ABUW_RS02985		-2.204	1.22e-05	20.576	12.055	8.790	2.266	4.632	1.766
ABUW_RS03025		-1.063	4.73e-06	506.126	512.208	362.122	197.478	266.345	196.331
ABUW_RS03050		2.035	1.58e-05	2.237	7.342	3.832	19.495	22.124	12.444
ABUW_RS03060	trpA	-1.457	2.81e-09	1870.741	1470.872	1515.127	590.433	595.284	583.443
ABUW_RS03065	accD	-1.991	1.64e-10	1284.213	1389.888	1486.203	389.266	360.327	296.472
ABUW_RS03070	folC	-1.320	7.04e-09	323.849	311.336	327.337	129.562	127.321	128.645
ABUW_RS03090		1.441	0.000454629	69.668	249.858	189.926	529.735	379.831	475.146
ABUW_RS03125		-1.457	9.34e-08	106.011	88.656	135.307	40.044	43.030	37.164
ABUW_RS03135		1.127	1.39e-05	44.171	47.013	61.681	125.874	117.509	91.229
ABUW_RS03150		3.315	1.2e-11	5.703	7.452	5.409	65.229	51.562	66.677
ABUW_RS03165		-1.190	3.05e-05	433.774	233.091	271.516	123.819	165.902	121.162
ABUW_RS03180		4.249	7.5e-12	9.729	11.178	9.617	234.835	147.617	196.667
ABUW_RS03205		-1.266	0.000302832	48.533	18.958	26.821	11.486	13.652	14.042
ABUW_RS03210		-2.577	2.36e-08	885.776	489.085	344.316	84.882	114.157	88.790
ABUW_RS03215		-2.647	5.44e-08	398.549	175.010	162.880	39.569	40.470	37.248
ABUW_RS03220		-3.461	2.11e-09	500.199	250.296	258.143	29.348	30.230	32.035
ABUW_RS03225	typA	-3.518	3.79e-10	4583.981	2489.261	1894.830	270.980	258.117	253.758
ABUW_RS03275		-1.229	2.61e-06	100.308	146.079	144.097	67.389	52.720	46.161
ABUW_RS03285		3.873	6.37e-12	6.262	6.685	3.982	86.990	67.958	88.202
ABUW_RS03290		2.118	0.0248622	0.000	0.329	0.225	0.580	0.914	1.177
ABUW_RS03295		1.087	0.0075656	3.690	1.315	2.705	3.636	6.034	7.147
ABUW_RS03310		4.669	2.68e-12	6.039	4.383	6.236	148.636	120.617	158.746
ABUW_RS03315		-1.298	6.9e-08	739.060	850.393	757.075	330.413	353.196	270.154
ABUW_RS03330		-3.696	7.18e-09	9.282	14.465	14.350	0.685	1.097	1.261
ABUW_RS03335	pilG	-2.356	6.29e-08	531.398	1225.179	815.451	137.992	195.462	169.172
ABUW_RS03340		-2.274	5.95e-08	303.385	629.575	560.012	92.996	122.689	92.994
ABUW_RS03345		-3.021	5.45e-09	247.136	502.345	487.963	49.001	66.434	36.660
ABUW_RS03350		-2.862	4.16e-08	1785.082	3909.066	3491.622	467.299	539.211	256.701
ABUW_RS03355		-2.753	1.41e-06	1623.829	3034.784	2121.193	346.641	454.615	203.730
ABUW_RS03360		-2.322	9.78e-09	89.461	128.874	87.300	20.391	23.587	16.816
ABUW_RS03365		2.216	3.27e-09	6.598	8.986	7.513	40.887	33.948	32.203
ABUW_RS03370		1.443	0.00011317	2.237	1.863	4.282	7.903	8.655	7.315
ABUW_RS03375	dapE	-1.196	5.71e-07	142.802	103.888	152.888	60.329	55.646	58.521
ABUW_RS03380		2.977	6.97e-06	2.796	0.219	0.451	8.483	6.643	10.426
ABUW_RS03430		-2.364	4.37e-07	38.021	18.630	21.412	4.637	5.912	4.456
ABUW_RS03460		-1.775	1.71e-05	87.001	35.616	40.344	15.385	15.542	16.564
ABUW_RS03465		-1.618	1.54e-06	766.122	697.957	341.086	209.650	196.803	181.196
ABUW_RS03470		2.386	4.69e-10	8.946	11.068	9.166	58.537	44.431	49.104
ABUW_RS03475		-1.086	8.87e-05	121.443	235.063	258.895	96.474	93.251	100.562
ABUW_RS03490		1.326	1.02e-05	11.854	18.630	15.026	32.140	37.605	44.731
ABUW_RS03495		1.588	1.24e-05	4.026	5.479	4.883	17.177	13.348	12.612
ABUW_RS03505	gatB	-1.799	1.88e-09	1066.151	1139.701	829.124	297.271	329.061	245.266
ABUW_RS03510	gatA	-1.781	1.91e-09	1411.359	1347.587	1426.400	462.873	441.084	313.625
ABUW_RS03515	gatC	-1.706	6.35e-08	111.938	66.738	107.359	30.085	30.352	27.158
ABUW_RS03520		-1.516	3.02e-08	942.472	716.149	665.794	262.707	279.814	270.238
ABUW_RS03525	mreC	-2.251	1.24e-09	419.908	265.528	282.335	66.599	72.285	64.322
ABUW_RS03530	mreD	-1.980	1.6e-07	88.231	62.136	38.391	16.123	16.273	15.135
ABUW_RS03535		-1.898	5.51e-05	41.040	17.863	12.772	6.165	8.655	3.784
ABUW_RS03570		1.951	0.0146842	2.572	6.027	6.386	5.638	7.680	48.263
ABUW_RS03580		1.241	8.26e-05	9.841	10.739	6.311	23.763	18.467	20.180
ABUW_RS03590		-1.304	1.82e-07	374.059	319.774	284.739	121.817	122.080	152.440
ABUW_RS03605	hchA	1.151	1.13e-05	65.530	56.218	92.183	174.559	137.744	164.212
ABUW_RS03615		1.496	0.0237808	0.224	1.534	0.601	1.159	2.621	3.027
ABUW_RS03640		1.610	9.43e-07	6.150	7.671	9.166	23.973	20.722	26.570
ABUW_RS03650		1.720	0.000351416	1.566	2.740	0.751	4.953	6.217	4.456
ABUW_RS03655		2.441	0.000451381	0.224	2.082	0.225	6.375	2.438	3.616
ABUW_RS03670		-1.176	3.14e-06	280.237	235.283	183.991	90.362	120.129	98.880
ABUW_RS03690		1.362	0.00678947	0.447	2.520	1.352	3.583	2.926	4.793
ABUW_RS03710		2.674	0.0159859	0.224	0.110	0.150	0.000	1.889	1.513
ABUW_RS03845		3.146	0.0309823	0.000	0.000	0.150	0.369	0.670	0.925
ABUW_RS03925		1.176	0.00153936	3.690	1.205	2.404	6.217	5.303	4.793
ABUW_RS03975		1.065	0.00200481	6.262	3.507	6.686	11.117	9.691	14.462
ABUW_RS03980		1.316	3.38e-05	9.505	9.205	7.438	20.759	15.359	28.924
ABUW_RS04030		-1.334	9.47e-07	115.069	81.204	81.966	38.726	40.348	30.858
ABUW_RS04040		1.054	0.00862159	4.138	7.561	2.705	5.322	11.824	12.276
ABUW_RS04055		1.049	0.000748002	16.662	39.122	26.070	46.261	49.551	74.076
ABUW_RS04095		-1.167	1.39e-07	1498.472	1320.958	1233.243	664.724	610.033	529.715
ABUW_RS04100		1.712	3.33e-06	2.125	3.397	4.733	10.907	10.971	13.117
ABUW_RS04160	rplU	-2.006	6.28e-09	2412.763	1796.673	1376.740	499.597	496.304	394.511
ABUW_RS04165	rpmA	-2.002	9.59e-08	295.109	240.104	125.991	57.642	53.391	53.644
ABUW_RS04175		1.382	5.84e-05	32.206	84.382	85.722	170.027	164.012	195.322
ABUW_RS04185	cysG	-1.481	6.01e-08	385.689	240.543	284.739	107.696	114.339	104.093
ABUW_RS04190		-1.877	1.22e-07	59.380	30.794	45.077	13.067	10.727	13.033
ABUW_RS04205		-1.456	1.71e-05	301.148	147.723	130.349	69.339	70.091	71.385
ABUW_RS04215		1.205	9.86e-06	59.044	80.546	118.929	176.297	209.785	212.390
ABUW_RS04245		-3.246	4.85e-10	684.377	376.101	338.682	48.895	61.375	36.744
ABUW_RS04255	gltA	-1.302	1.8e-07	2287.294	2244.992	2523.509	1080.441	1049.777	731.763
ABUW_RS04260	sdhC	-1.514	6.3e-06	1169.143	637.466	600.356	260.652	354.537	226.936
ABUW_RS04265	sdhD	-1.251	9.48e-05	1337.777	843.598	510.953	336.367	441.084	353.563
ABUW_RS04270	sdhA	-1.307	8.83e-06	3798.737	2762.570	2023.601	1221.015	1327.397	919.685
ABUW_RS04275		-1.095	0.000582205	1175.070	1049.621	469.481	348.959	511.845	400.061
ABUW_RS04315	trpS	-1.414	2.51e-08	302.714	220.708	281.133	105.641	104.222	91.901
ABUW_RS04345		1.224	0.000243941	4.920	8.767	4.959	10.854	16.761	15.639
ABUW_RS04350		1.502	9.5e-06	12.077	12.931	7.363	28.821	25.659	36.071
ABUW_RS04355		2.465	4.21e-10	8.499	7.452	11.269	52.636	48.149	51.626
ABUW_RS04365		2.114	2.92e-06	3.131	10.849	5.184	24.079	22.978	35.567
ABUW_RS04375	greA	-1.186	3.38e-05	469.894	302.459	216.071	134.252	140.913	158.914
ABUW_RS04380	carB	-2.009	1.13e-07	3911.570	2694.955	1706.030	649.234	790.928	623.970
ABUW_RS04385	carA	-2.269	1.39e-08	3134.042	1673.169	2084.831	543.698	521.110	364.578
ABUW_RS04390		2.149	5.54e-07	12.860	7.671	20.435	70.919	47.906	66.845
ABUW_RS04395		-1.065	0.000417959	118.871	53.917	59.502	33.932	40.287	36.491
ABUW_RS04400	yhbY	-1.116	4.39e-05	216.943	115.504	115.323	59.012	70.091	77.439
ABUW_RS04420		-1.860	0.00148689	14.873	4.055	4.207	1.370	1.768	3.363

Locustag	Gene	logFC	PValue	LCWB_1	LCWB_2	LCWB_3	M9_1	M9_2	M9_3
ABUW_RS04425		-2.327	0.000283507	8.946	2.520	5.484	1.212	1.219	0.841
ABUW_RS04450	folD	-1.461	1.41e-08	912.949	815.215	667.221	269.820	298.891	301.349
ABUW_RS04455		-1.956	1.51e-08	86.889	55.780	64.686	16.913	20.296	16.060
ABUW_RS04475	glpD	2.427	1.07e-10	22.701	26.191	24.943	133.145	123.847	140.500
ABUW_RS04480		-2.225	4.08e-08	4169.777	2624.491	2051.474	693.545	669.763	528.706
ABUW_RS04485		2.890	1.22e-08	9.170	13.479	6.987	62.700	66.678	87.529
ABUW_RS04490		1.489	2.84e-05	7.045	10.192	7.813	22.762	21.393	26.149
ABUW_RS04495		1.734	3.36e-06	496.956	529.961	355.886	1701.170	1537.669	1358.003
ABUW_RS04500	groES	-1.534	2.58e-05	218.061	194.626	518.015	102.480	108.610	110.904
ABUW_RS04510		-1.582	0.00150432	6.262	4.383	4.658	1.897	1.524	1.598
ABUW_RS04540		-1.538	3.69e-06	117.753	119.888	195.110	55.903	57.535	35.314
ABUW_RS04545	ttcA	-1.958	7.61e-08	466.427	265.857	247.099	90.362	74.235	87.361
ABUW_RS04555		-1.196	0.00665024	55.801	19.835	15.176	10.590	12.068	16.900
ABUW_RS04570		1.479	1.19e-05	3.690	8.548	8.189	19.548	20.966	17.153
ABUW_RS04610		1.020	0.000101145	60.386	95.121	120.357	212.389	199.850	148.572
ABUW_RS04615		1.546	4.4e-08	36.344	57.643	44.176	127.613	151.213	124.357
ABUW_RS04630		2.736	1.08e-08	56.025	92.929	108.336	751.503	471.863	494.568
ABUW_RS04635	fdhD	1.438	7.76e-05	12.860	14.246	33.282	61.752	48.698	56.671
ABUW_RS04670		-1.177	9.05e-06	124.239	76.163	125.465	49.738	49.064	45.404
ABUW_RS04695	xerA	1.058	0.000269505	7.940	17.205	12.697	25.027	27.427	26.486
ABUW_RS04710	gyrA	-1.015	1.32e-06	1595.984	1462.434	1424.597	812.359	697.982	707.463
ABUW_RS04720		-1.480	0.0128486	7.269	7.342	2.404	1.423	2.255	2.270
ABUW_RS04730		3.844	0.00397806	0.000	0.000	0.075	0.527	0.549	0.589
ABUW_RS04740		1.085	1.33e-05	26.838	37.369	39.593	76.979	65.337	78.700
ABUW_RS04745		1.630	2.99e-08	22.365	24.109	31.404	78.138	75.149	89.295
ABUW_RS04750		1.336	1.42e-07	27.957	28.931	33.883	83.038	79.903	66.677
ABUW_RS04755	serC	-1.142	8.5e-05	232.599	101.258	167.613	73.501	76.429	77.355
ABUW_RS04780	lolD	-1.074	4.89e-06	97.065	107.943	86.999	53.005	49.185	35.987
ABUW_RS04785		-2.108	7.93e-07	33.883	38.794	27.798	5.638	7.070	11.015
ABUW_RS04805	purN	-3.092	1.02e-09	363.323	175.887	186.846	31.613	30.901	22.198
ABUW_RS04810	purM	-2.202	5.18e-09	1115.690	624.863	613.729	163.072	176.324	172.283
ABUW_RS04825	rbtA	1.782	5.54e-06	25.273	13.479	9.692	58.537	56.438	48.683
ABUW_RS04830		2.049	3.81e-07	13.755	11.726	7.513	49.053	48.393	36.576
ABUW_RS04835		1.547	1.39e-06	7.269	7.452	10.218	20.865	27.549	25.645
ABUW_RS04840		1.737	2.26e-06	8.387	9.205	13.899	28.874	29.987	48.599
ABUW_RS04845		1.621	2.18e-07	113.615	90.080	90.831	226.879	303.219	376.097
ABUW_RS04850		-1.733	3.51e-08	84.317	58.519	63.409	21.602	19.199	21.189
ABUW_RS04855		-1.979	1.84e-09	282.249	189.366	235.004	56.851	70.030	52.215
ABUW_RS04875	tolA	-1.462	1.84e-05	117.977	58.519	63.184	29.559	26.817	30.438
ABUW_RS04880	tolR	-1.448	1.02e-06	67.655	39.013	48.233	20.285	16.273	20.180
ABUW_RS04885	tolQ	-1.217	1.13e-06	256.306	176.215	198.040	92.206	77.405	101.655
ABUW_RS04890	ybgC	-3.355	1.24e-12	259.101	186.297	189.926	23.394	20.905	17.489
ABUW_RS04895		1.450	0.00140762	1.789	2.192	0.751	5.216	3.230	3.616
ABUW_RS04900	ruvB	-1.164	2.46e-07	222.758	226.406	269.864	108.381	110.073	102.496
ABUW_RS04905	ruvA	-1.377	1.41e-08	95.276	98.409	119.230	41.097	37.788	41.789
ABUW_RS04915	purL	-1.803	8.3e-08	2213.712	1388.025	1142.863	455.918	476.678	427.135
ABUW_RS04920		1.351	1.71e-05	27.733	29.479	13.448	58.169	55.097	64.827
ABUW_RS04930		2.148	1.29e-06	5.032	2.959	3.155	16.913	12.738	19.339
ABUW_RS04935		1.700	4.12e-06	28.963	20.602	21.111	44.101	94.348	90.976
ABUW_RS04945		2.346	0.000187406	0.335	3.616	0.601	6.428	8.472	6.895
ABUW_RS04965	queC	-1.850	3.64e-08	606.546	378.293	335.451	114.651	144.021	107.288
ABUW_RS04970	queE	-1.968	2.67e-08	778.311	454.127	398.635	133.567	152.981	129.990
ABUW_RS04975	dapD	-1.396	8.71e-08	1156.171	946.062	778.637	330.097	370.445	393.923
ABUW_RS04980	carO	3.392	1.48e-12	772.272	806.996	686.304	7709.559	6058.035	10008.662
ABUW_RS04985		-1.561	3.34e-08	136.652	204.817	179.258	56.430	61.863	58.185
ABUW_RS04990		-1.796	1.79e-06	155.550	390.348	314.716	89.255	91.423	66.845
ABUW_RS04995	cysW	-1.712	0.000113074	66.313	223.776	207.807	55.903	61.375	34.389
ABUW_RS05000	cysT	-1.413	0.00111131	87.113	279.775	328.765	80.035	116.168	65.079
ABUW_RS05005		-1.202	0.00424646	66.537	219.940	242.892	67.811	104.222	58.185
ABUW_RS05010		-1.539	0.000579064	178.027	711.327	484.207	140.205	199.119	133.185
ABUW_RS05025	tmk	-1.194	1.58e-07	54.124	51.396	62.958	24.658	24.075	25.056
ABUW_RS05035	nadB	-1.235	2.34e-07	165.503	144.216	192.180	78.138	74.479	60.455
ABUW_RS05040		1.589	8.81e-07	91.138	200.215	140.491	463.452	391.533	444.203
ABUW_RS05050	lepA	-1.755	6.35e-10	1340.685	1219.371	990.126	327.462	372.212	352.134
ABUW_RS05055	lepB	-1.265	3.23e-07	278.783	296.432	202.247	95.683	109.463	118.303
ABUW_RS05060		-1.892	4.18e-07	61.952	58.081	46.054	16.492	17.614	10.090
ABUW_RS05065	rnc	-1.606	2.43e-06	63.965	47.341	31.930	13.014	18.528	15.303
ABUW_RS05070	era	-1.229	1.67e-07	857.707	645.575	671.729	271.348	337.959	318.333
ABUW_RS05075		-1.488	7.55e-06	79.732	80.875	44.401	17.651	26.452	29.092
ABUW_RS05080	recO	-1.572	8.89e-07	41.599	25.095	30.427	10.116	11.275	11.267
ABUW_RS05085	pdxJ	-1.255	1.53e-08	249.261	250.844	226.138	91.521	110.256	102.411
ABUW_RS05090		-1.666	3.17e-08	102.545	79.012	84.220	26.819	34.863	21.693
ABUW_RS05105		1.465	0.0111284	2.572	1.425	0.451	3.425	2.133	6.222
ABUW_RS05115		3.590	1.61e-05	2.237	0.219	0.225	6.850	6.461	16.984
ABUW_RS05120		-1.569	3.44e-08	1029.920	814.886	794.790	358.812	281.216	249.050
ABUW_RS05145		2.059	1.49e-07	17.892	19.287	38.992	117.444	92.093	112.585
ABUW_RS05155		-1.902	4.12e-07	2174.349	1140.907	1020.703	411.870	382.330	365.587
ABUW_RS05160		1.211	0.000187517	19.010	10.739	7.588	28.031	30.109	26.570
ABUW_RS05165		1.257	0.000214141	3.802	3.726	2.780	7.851	7.740	8.744
ABUW_RS05170	cgtA	-1.561	1.56e-09	1010.686	879.652	745.280	284.257	299.257	309.841
ABUW_RS05175	proB	-1.554	1.43e-07	1044.681	854.228	585.481	276.143	277.194	292.688
ABUW_RS05200		1.555	0.00135946	1.454	0.877	4.583	5.480	7.984	9.165
ABUW_RS05205		2.534	3.37e-10	18.899	23.561	19.308	125.294	97.579	134.615
ABUW_RS05210	wecB	2.286	7.52e-09	37.574	51.287	68.067	282.676	199.606	286.887
ABUW_RS05220		2.887	7.07e-10	30.417	34.301	41.621	342.373	190.647	256.533
ABUW_RS05225		2.689	1.45e-09	17.445	17.534	22.914	159.173	87.522	128.981
ABUW_RS05230		3.314	2.76e-09	1.566	2.192	3.005	21.550	19.138	29.429
ABUW_RS05235		4.022	2.83e-08	3.243	4.164	2.479	48.895	39.556	69.451
ABUW_RS05245		-1.966	1.62e-07	639.982	456.648	1031.296	182.409	191.866	170.602
ABUW_RS05255		-2.441	7.86e-10	341.741	346.294	496.753	73.448	80.940	63.650
ABUW_RS05265		-1.766	3.85e-09	4268.631	5242.845	5572.546	1686.838	1563.511	1182.861
ABUW_RS05270		-1.250	2.69e-08	336.038	437.580	399.386	160.333	167.730	165.305
ABUW_RS05275	icd	1.268	1.24e-06	104.222	126.244	139.139	348.011	263.297	279.403
ABUW_RS05285		1.567	5.51e-06	8.051	8.548	11.119	22.814	26.634	34.053
ABUW_RS05290		1.579	0.0147783	1.566	1.205	0.526	1.844	2.926	4.961
ABUW_RS05295		1.235	5.16e-06	55.578	70.026	55.671	105.167	179.432	141.762
ABUW_RS05315		-1.906	1.1e-06	25.273	27.616	14.350	7.218	4.754	5.633
ABUW_RS05325		1.232	1.59e-06	53.565	61.916	56.347	142.313	120.556	140.669
ABUW_RS05330		1.769	7.74e-06	2.460	3.726	3.005	10.064	7.923	13.705
ABUW_RS05345	csy1	1.047	1.93e-05	60.945	87.779	67.541	149.584	147.800	149.329
ABUW_RS05365	thiE	-1.133	4.89e-06	67.879	70.026	92.033	36.039	41.994	26.654
ABUW_RS05395	fabR	-1.221	0.000233652	55.130	28.712	71.673	19.179	27.244	20.600
ABUW_RS05405		-1.021	0.000328229	1277.167	2891.444	2939.349	1192.826	1094.513	1216.073
ABUW_RS05435		1.099	9.24e-05	16.438	10.630	15.777	37.620	26.208	28.083
ABUW_RS05490	purB	-1.695	6.99e-09	813.648	749.902	569.929	206.383	250.011	202.301
ABUW_RS05500	mnmA	-1.208	2.77e-07	331.565	234.077	237.483	121.554	115.436	110.315
ABUW_RS05515	dacC	-1.320	2.62e-07	294.998	220.160	201.045	93.734	104.770	88.034

Locustag	Gene	logFC	PValue	LCWB_1	LCWB_2	LCWB_3	M9_1	M9_2	M9_3
ABUW_RS05525		-3.044	1.36e-08	21.023	26.191	22.464	3.267	3.901	0.841
ABUW_RS05565	rpmE	-2.239	1.24e-06	4912.862	3963.311	1713.167	488.058	819.330	936.754
ABUW_RS05570		-1.840	1.55e-07	656.755	1152.304	1036.555	296.744	296.697	201.207
ABUW_RS05580	epmB	-1.264	1.88e-07	68.997	55.232	64.536	24.658	28.768	25.140
ABUW_RS05585	efp	-2.472	1.29e-10	1788.996	2227.568	1553.443	311.708	411.037	280.749
ABUW_RS05590		2.322	1.44e-09	276.882	311.007	362.873	1984.742	1338.733	1431.322
ABUW_RS05595		2.938	3.77e-09	9.953	10.849	11.344	111.701	62.899	72.310
ABUW_RS05610		1.209	0.000644605	8.499	7.233	3.606	11.434	16.334	15.807
ABUW_RS05625		1.500	0.0189305	0.895	0.219	1.503	1.739	2.499	4.204
ABUW_RS05670		7.403	0.0030886	0.000	0.000	0.000	2.213	0.914	0.000
ABUW_RS05675		2.046	0.0134368	0.000	1.534	0.075	1.791	2.986	1.093
ABUW_RS05685		1.036	0.003872	4.809	3.945	3.381	8.219	6.095	10.510
ABUW_RS05710	bauF	1.058	0.026464	173.219	589.138	983.965	1241.037	1017.047	1383.059
ABUW_RS05740	bauB	1.270	1.37e-05	1672.585	2378.250	2776.769	5860.123	5314.830	5292.100
ABUW_RS05745	bauA	1.299	5.71e-06	1631.992	2023.518	2729.288	6207.343	4877.463	4624.576
ABUW_RS05800	basJ	1.178	0.00058857	1724.696	4095.582	3830.905	7351.327	5269.972	9222.498
ABUW_RS05810	hemE	-2.155	4.89e-11	212.246	167.668	228.242	44.891	44.675	47.086
ABUW_RS05815		-2.240	1.82e-06	33.995	15.671	25.018	6.428	5.485	3.531
ABUW_RS05820		1.143	2.89e-05	1236.463	1506.817	1290.642	3012.335	2651.929	3242.357
ABUW_RS05835	folE	-1.878	1.57e-07	80.179	41.533	67.766	20.285	15.664	15.387
ABUW_RS05840	xdhA	1.750	4.61e-06	5.256	11.616	5.860	29.717	19.382	26.402
ABUW_RS05845	xdhB	2.253	1.13e-09	17.669	25.753	27.647	127.876	104.527	108.045
ABUW_RS05850	xdhC	1.958	8.85e-06	6.262	3.836	4.282	17.335	16.395	21.945
ABUW_RS05855		-1.211	4e-06	62.064	46.136	68.067	23.921	31.145	21.020
ABUW_RS05860	trpC	-1.012	5.75e-06	243.558	188.051	171.069	87.727	117.874	93.078
ABUW_RS05880		-1.285	3.1e-06	69.668	106.847	126.818	36.672	46.626	41.536
ABUW_RS05900		-1.022	0.000161557	20.800	24.986	29.075	11.434	16.334	8.997
ABUW_RS05910		3.139	3.04e-10	83.646	151.887	119.080	1320.017	991.693	812.229
ABUW_RS05920		-2.562	0.00435987	7.045	2.082	1.653	0.263	1.097	0.336
ABUW_RS05960		-1.644	2.47e-09	1884.160	2302.197	1812.713	659.139	679.393	580.668
ABUW_RS05980	ahcY	-1.258	4.76e-05	1309.709	1544.186	1004.550	607.610	689.145	315.643
ABUW_RS05990		1.075	0.00653247	7.381	3.288	7.137	18.072	7.375	12.360
ABUW_RS05995		4.089	3.97e-11	39.475	41.095	74.453	1133.973	569.564	952.477
ABUW_RS06035	rpsB	-2.239	1.32e-09	7131.383	5278.571	4297.757	1267.381	1276.932	994.518
ABUW_RS06040	tsf	-2.042	1.96e-09	3805.111	3127.494	2667.532	829.377	875.098	625.652
ABUW_RS06045		-2.299	8.72e-06	35.225	17.315	12.021	2.845	4.754	5.633
ABUW_RS06065		3.540	6.19e-08	1.454	1.534	0.601	12.066	15.481	11.940
ABUW_RS06080	rodA	-1.445	7.76e-05	148.058	54.793	93.611	41.572	37.666	29.176
ABUW_RS06130		1.582	0.0116827	0.224	0.219	0.676	1.370	1.097	1.261
ABUW_RS06145		1.675	0.0129334	0.895	0.877	0.751	2.266	2.133	3.868
ABUW_RS06245		1.179	0.0360906	0.671	0.438	0.902	1.212	1.280	2.522
ABUW_RS06250		1.343	0.00328689	1.006	1.205	1.052	2.793	2.377	3.195
ABUW_RS06260		1.331	5.26e-05	4.361	4.164	4.959	11.539	11.032	11.687
ABUW_RS06270		1.915	0.0100567	1.566	0.219	0.376	3.530	0.853	3.363
ABUW_RS06275		2.102	0.00263264	0.783	1.863	1.878	6.217	4.144	10.174
ABUW_RS06280		2.140	5.38e-06	14.761	32.438	16.078	72.079	92.398	113.006
ABUW_RS06390		2.517	0.0240078	0.112	0.438	0.000	1.423	0.305	1.093
ABUW_RS06450		-3.196	0.0163369	1.230	0.000	0.676	0.158	0.000	0.000
ABUW_RS06480		1.563	0.0192931	2.013	0.658	0.301	3.899	1.219	2.859
ABUW_RS06495		-1.275	3.82e-05	18.451	16.328	29.000	8.694	10.544	7.231
ABUW_RS06500		2.596	1.56e-06	4.809	3.178	3.005	28.452	20.418	16.060
ABUW_RS06505	glyA	-2.034	9.69e-10	1757.349	1255.425	1443.379	390.742	395.799	301.517
ABUW_RS06525	adeL	1.405	2.16e-07	25.273	34.849	26.821	65.650	72.955	91.733
ABUW_RS06530		1.092	0.0120971	4.026	0.986	3.756	3.794	8.045	7.651
ABUW_RS06535		1.321	0.00334597	1.230	1.096	1.427	2.845	3.413	3.363
ABUW_RS06550	abeS	-1.341	0.00689486	7.604	3.945	6.912	1.581	3.596	2.186
ABUW_RS06555		-3.812	3.78e-10	26.056	24.876	27.046	1.106	2.926	1.513
ABUW_RS06560	yegQ	-3.330	6.37e-10	813.312	563.604	631.234	77.506	86.486	34.810
ABUW_RS06575		-1.668	2.24e-07	218.956	159.887	139.965	51.319	64.057	47.506
ABUW_RS06585		1.919	1.68e-07	11.071	17.753	22.689	74.660	63.508	58.857
ABUW_RS06590		-2.557	1.24e-05	84.876	241.091	255.739	38.200	40.409	19.675
ABUW_RS06595		-1.413	2.47e-06	187.309	165.366	197.364	74.660	52.720	79.373
ABUW_RS06610	hemP	1.725	0.000265604	336.485	922.939	1062.024	2731.398	1952.241	2992.803
ABUW_RS06645		-1.330	1.68e-06	367.014	259.501	230.721	119.867	108.671	112.165
ABUW_RS06650		1.369	0.000151034	28.628	11.068	13.974	51.056	51.136	34.810
ABUW_RS06665		-1.327	6.27e-07	683.146	1048.854	1155.560	391.848	434.258	325.060
ABUW_RS06695		-1.382	3.05e-09	260.443	270.022	242.817	91.732	101.967	103.000
ABUW_RS06700	thiS	-1.513	1.24e-06	68.102	44.711	79.336	23.236	26.756	17.153
ABUW_RS06720		-1.868	4.89e-10	260.443	234.187	199.242	60.065	62.350	67.686
ABUW_RS06730		2.490	2.54e-09	18.563	19.945	25.469	134.410	79.477	148.068
ABUW_RS06750		-1.299	5.7e-05	19.010	10.849	13.673	7.166	4.998	5.297
ABUW_RS06760		1.422	0.0388454	0.447	0.548	0.826	1.475	1.341	2.522
ABUW_RS06765		1.333	0.00953475	0.447	3.945	2.028	5.322	4.693	6.306
ABUW_RS06870		1.284	0.00107613	2.684	2.630	4.207	10.116	8.350	4.961
ABUW_RS06965		1.112	0.00297554	1.789	4.493	7.663	9.747	10.666	11.435
ABUW_RS06970		1.444	0.000655104	2.125	1.644	1.953	3.688	5.546	6.727
ABUW_RS07065		1.405	1.75e-06	20.800	30.027	33.958	80.245	66.556	79.037
ABUW_RS07070		-2.195	7.91e-09	3812.827	1991.409	2244.705	564.194	576.146	617.496
ABUW_RS07075	rpsU	-1.918	4.7e-09	915.633	631.767	601.633	202.062	181.566	184.643
ABUW_RS07080	tsaD	-1.617	4.48e-08	174.225	124.162	118.629	42.099	52.538	41.032
ABUW_RS07140		1.595	9.75e-05	3.019	4.493	4.357	15.174	9.752	11.099
ABUW_RS07145		8.702	5.02e-12	0.335	0.329	0.225	118.392	60.644	189.352
ABUW_RS07150		6.668	1.78e-11	1.006	0.877	2.404	227.616	78.989	164.043
ABUW_RS07155		7.074	1.05e-10	0.335	1.315	1.202	189.733	71.127	139.155
ABUW_RS07160		6.120	3.25e-11	1.006	0.438	0.902	68.338	34.192	64.911
ABUW_RS07165		5.300	2.73e-09	0.895	1.753	1.878	69.023	30.474	85.175
ABUW_RS07170		5.749	3.75e-07	0.000	0.219	0.150	8.852	2.560	10.594
ABUW_RS07180		3.555	4.62e-06	0.000	1.096	1.202	8.641	8.533	12.360
ABUW_RS07190		1.907	0.00297931	0.335	1.534	0.601	2.160	2.438	4.877
ABUW_RS07195		2.717	4.7e-06	5.256	2.192	1.578	14.121	26.574	15.891
ABUW_RS07250	csuAB	1.392	0.000231514	7.604	7.014	5.710	13.172	14.079	26.318
ABUW_RS07260	csuB	2.336	0.0100616	0.783	0.110	0.000	2.266	1.036	0.336
ABUW_RS07265	csuC	1.207	0.00736388	1.342	1.315	2.404	4.320	4.144	3.700
ABUW_RS07275	csuE	1.026	0.0131971	2.684	1.096	2.329	3.688	5.120	3.784
ABUW_RS07295	proP	1.987	1.29e-08	30.081	34.629	22.313	138.519	96.969	107.456
ABUW_RS07310		1.340	0.000107325	21.806	37.259	28.098	74.924	64.849	80.971
ABUW_RS07335	uraH	1.874	2.82e-05	1.342	2.082	2.179	6.955	8.350	5.465
ABUW_RS07345		1.200	0.00019094	7.157	4.603	9.466	14.648	19.199	15.976
ABUW_RS07380		1.181	0.0298396	0.671	2.520	0.826	4.110	2.438	1.934
ABUW_RS07385		1.270	0.000107373	5.368	9.534	11.194	23.815	21.637	18.330
ABUW_RS07390		1.208	2.04e-05	11.294	14.685	8.790	25.291	25.903	28.336
ABUW_RS07395		1.323	0.000317449	6.150	8.548	4.658	15.596	14.932	17.153
ABUW_RS07425		2.771	9.8e-11	36.008	42.848	57.774	367.769	238.065	331.534
ABUW_RS07430		2.260	2.91e-06	1.566	4.493	4.808	17.598	12.494	24.047
ABUW_RS07435		-1.775	2.19e-05	9.393	15.890	15.401	5.532	3.596	2.438
ABUW_RS07440		-1.056	0.0271701	4.585	1.973	2.028	1.844	0.488	1.682
ABUW_RS07450		3.030	1.92e-07	7.492	17.534	21.712	91.679	93.800	203.814

Locustag	Gene	logFC	PValue	LCWB_1	LCWB_2	LCWB_3	M9_1	M9_2	M9_3
ABUW_RS07460		-1.543	7.84e-08	183.171	145.093	118.103	47.578	55.829	49.524
ABUW_RS07465		-1.475	2.61e-08	485.438	362.622	350.702	130.827	157.369	142.939
ABUW_RS07485	fis	-1.226	0.00084116	151.189	52.273	60.178	42.573	33.217	36.407
ABUW_RS07495	prmA	-1.438	3.57e-08	336.932	388.923	278.954	105.062	132.014	133.858
ABUW_RS07500		5.608	4.28e-13	3.019	4.164	2.554	176.877	110.073	180.187
ABUW_RS07505	mnmG	-1.644	4e-07	1604.371	824.968	923.787	353.122	354.842	365.083
ABUW_RS07515		1.842	2.42e-06	20.576	17.863	34.860	104.851	73.870	87.193
ABUW_RS07520		1.586	5.41e-06	7.828	5.151	5.184	16.702	14.932	22.702
ABUW_RS07525		1.298	0.000724235	16.327	4.712	16.228	35.460	23.648	33.801
ABUW_RS07530		1.713	2.76e-06	13.531	7.233	15.326	43.416	36.325	40.023
ABUW_RS07535	alr	-1.898	5.61e-08	55.913	30.136	52.665	11.381	13.957	11.940
ABUW_RS07540	dnaB	-1.429	6.67e-07	141.572	79.122	95.790	37.883	43.944	35.482
ABUW_RS07545	rplI	-2.268	3.02e-08	3969.608	2290.142	1848.775	608.453	585.837	489.271
ABUW_RS07550	rpsR	-2.384	3.31e-08	2322.631	1280.959	1009.208	277.197	332.108	274.358
ABUW_RS07555	rpsF	-2.434	1.85e-08	5121.865	3399.817	2253.270	622.415	765.025	605.808
ABUW_RS07560	cyoE	-1.488	4.67e-07	1341.915	1165.345	727.925	375.514	427.188	350.200
ABUW_RS07570	cyoC	-1.182	4.46e-07	2542.929	2005.984	2228.027	1095.404	1016.316	875.206
ABUW_RS07575	cyoB	-1.138	3.57e-07	19851.841	18566.721	15481.916	8392.251	8592.761	7508.577
ABUW_RS07580	cyoA	-1.438	2.45e-08	11136.775	9818.089	9953.621	4049.097	4229.581	3132.042
ABUW_RS07615	pgaD	1.597	0.0030671	0.783	0.877	0.676	2.424	3.291	1.009
ABUW_RS07620		3.865	3.69e-08	1.901	0.000	1.503	20.918	15.664	14.630
ABUW_RS07630		-1.055	0.00491227	12.972	18.849	12.697	9.168	4.144	7.988
ABUW_RS07645		1.215	0.000832935	3.131	5.808	6.161	13.488	11.519	10.510
ABUW_RS07655	prfA	-1.513	5.17e-08	342.636	215.886	273.244	92.153	101.479	97.787
ABUW_RS07660	prmC	-1.790	7.97e-08	68.102	44.821	45.378	11.802	17.736	16.312
ABUW_RS07690		1.400	0.0173417	0.783	4.712	1.653	7.745	7.375	2.691
ABUW_RS07710	folB	-1.047	1.18e-05	46.408	52.054	68.367	28.083	28.158	24.636
ABUW_RS07715		-1.673	3.09e-06	19.234	21.260	20.811	7.271	8.045	3.447
ABUW_RS07720	kdpA	-1.054	0.000383233	15.432	26.082	28.173	13.910	11.763	7.651
ABUW_RS07750		-1.072	0.0245119	24.378	6.246	9.316	3.319	5.851	10.258
ABUW_RS07765		1.103	2.49e-06	117.865	116.491	176.553	299.010	277.925	307.234
ABUW_RS07775		-1.037	7.02e-05	22.701	26.739	31.028	10.432	15.603	13.453
ABUW_RS07780		-1.237	5.94e-07	2283.268	2231.185	2192.040	1047.826	1064.892	732.267
ABUW_RS07785		2.296	1.38e-05	2.907	1.973	1.202	11.644	7.619	9.249
ABUW_RS07790		1.618	2.44e-06	9.393	5.260	8.715	27.188	23.404	21.441
ABUW_RS07795		-2.202	6.15e-10	210.345	233.639	167.387	39.464	53.878	39.266
ABUW_RS07800		-2.224	0.00103739	4.138	1.863	3.155	1.054	0.488	0.252
ABUW_RS07820		2.347	1.11e-06	2.460	1.425	2.329	9.642	8.533	14.294
ABUW_RS07825		1.325	3.75e-06	27.286	37.150	31.479	79.771	62.107	98.712
ABUW_RS07830		3.277	3.53e-08	2.125	2.192	1.728	22.920	16.578	18.246
ABUW_RS07870	nfsB	1.285	4.83e-07	29.522	38.246	32.606	79.824	83.926	80.718
ABUW_RS07880		-1.586	6.62e-09	194.130	213.475	208.258	72.395	71.797	60.791
ABUW_RS07895	eutC	1.797	0.00284425	2.684	0.548	0.526	3.056	4.876	4.372
ABUW_RS07900		1.065	0.0134515	1.789	0.986	3.231	5.269	4.571	3.279
ABUW_RS07905	eat	1.518	0.0180638	1.677	0.548	0.301	2.055	2.316	2.354
ABUW_RS07915		1.445	1.49e-05	7.604	12.822	7.513	27.240	27.914	19.843
ABUW_RS07935		-1.463	1.63e-05	13.419	18.191	12.772	6.692	3.840	5.381
ABUW_RS07950		1.964	0.00271995	1.230	0.438	1.127	4.110	4.693	2.102
ABUW_RS07960		6.324	7.98e-12	14.537	5.479	8.189	980.700	438.341	823.244
ABUW_RS07965		5.897	1.06e-10	2.125	0.877	3.531	194.686	83.682	135.708
ABUW_RS07970		4.434	1.75e-08	21.582	4.164	8.039	329.095	154.383	235.092
ABUW_RS07975		4.351	2.26e-11	12.413	9.315	18.256	296.428	179.981	353.563
ABUW_RS07980		2.940	1.25e-06	1.118	3.068	3.456	23.605	12.494	25.056
ABUW_RS07985		1.484	0.000407539	4.249	3.616	8.640	15.069	15.847	17.321
ABUW_RS07990		2.264	4.53e-07	6.262	2.082	4.808	21.286	17.431	25.140
ABUW_RS08010		-2.457	0.00237004	1.789	3.397	0.526	0.527	0.305	0.000
ABUW_RS08035		-2.016	9.07e-05	156.445	266.624	234.853	62.542	69.847	29.513
ABUW_RS08040		2.295	1.79e-09	34.331	40.766	36.287	202.168	133.721	210.877
ABUW_RS08050		3.517	1.95e-05	0.447	0.110	0.075	1.686	2.438	2.859
ABUW_RS08060		1.631	0.000100611	4.026	2.301	2.930	6.902	9.935	12.108
ABUW_RS08065		1.606	0.0028471	0.224	4.493	1.803	5.585	5.729	8.660
ABUW_RS08070		-1.494	0.0041189	230.586	580.152	373.091	155.011	172.362	92.154
ABUW_RS08075		2.589	5.68e-09	8.722	5.479	3.907	39.622	33.156	33.296
ABUW_RS08085		6.107	3.82e-11	0.112	0.219	0.150	14.279	5.973	14.294
ABUW_RS08095		1.988	9.88e-08	168.969	328.650	318.998	1103.044	902.342	1236.925
ABUW_RS08110		1.456	6.1e-05	12.972	22.575	13.223	38.358	32.851	62.389
ABUW_RS08120		1.090	0.0206183	0.895	1.315	2.780	3.109	4.571	3.784
ABUW_RS08125		-1.903	2.73e-05	34.331	60.382	120.883	18.915	18.833	20.432
ABUW_RS08155		2.057	3.27e-08	212.134	285.364	328.614	739.964	1359.822	1340.935
ABUW_RS08160		2.722	1.24e-09	65.754	92.601	125.541	458.394	635.815	785.071
ABUW_RS08165		1.676	5.78e-08	43.053	55.232	66.639	137.202	197.839	194.145
ABUW_RS08170		2.281	2e-08	25.944	19.287	39.292	131.301	151.213	132.429
ABUW_RS08190		-1.001	0.000212684	27.286	21.369	19.684	10.643	10.422	13.117
ABUW_RS08195		1.320	8.53e-05	3.690	4.164	6.987	15.122	11.336	11.603
ABUW_RS08210		-1.073	1.29e-06	81.857	88.327	71.598	32.351	40.957	41.705
ABUW_RS08235		-1.120	0.000732824	21.135	11.178	12.096	5.638	5.973	8.997
ABUW_RS08240		3.475	9.97e-10	4.361	3.068	3.606	34.142	43.517	45.236
ABUW_RS08245		4.119	6.01e-13	24.154	21.698	16.153	410.553	322.722	336.495
ABUW_RS08260	accC	-2.357	3.15e-11	3941.428	4353.440	3341.890	751.609	866.444	653.567
ABUW_RS08265	accB	-2.799	1.4e-11	1832.832	2222.308	1743.745	300.485	323.027	209.027
ABUW_RS08270	aroQ	-2.461	8.52e-11	162.819	110.902	151.535	28.241	23.465	25.477
ABUW_RS08280		1.849	0.00802943	1.566	0.438	0.451	2.951	3.657	1.513
ABUW_RS08285		6.866	0.0275213	0.000	0.000	0.000	0.105	1.768	0.589
ABUW_RS08300	nirD	2.281	6.95e-07	1.006	1.205	0.902	4.531	4.876	5.718
ABUW_RS08305		1.157	0.00016064	13.419	10.411	6.837	20.496	20.540	26.402
ABUW_RS08310		1.562	2.89e-05	7.269	3.726	3.982	13.646	11.580	18.666
ABUW_RS08315		1.082	0.000213822	6.598	9.424	11.795	19.811	19.930	20.096
ABUW_RS08320	moaA	2.647	2.79e-09	7.381	8.548	7.137	48.000	46.138	49.860
ABUW_RS08325		1.082	0.0061106	2.237	1.096	3.231	4.268	6.461	3.700
ABUW_RS08380		2.582	4.08e-09	39.027	54.355	81.515	341.635	280.607	431.255
ABUW_RS08390		4.695	0.000228436	0.000	0.438	0.000	3.425	1.158	6.390
ABUW_RS08400		-1.912	7.25e-07	52.670	34.301	25.394	8.746	8.777	12.444
ABUW_RS08405		3.333	3.04e-12	23.148	25.534	21.262	238.839	199.119	265.698
ABUW_RS08420		-1.194	0.0338231	1.566	1.753	5.635	1.054	1.585	1.682
ABUW_RS08425	argF	-1.059	4.97e-05	246.241	148.490	210.286	74.818	124.822	90.724
ABUW_RS08445	rimO	-1.979	8.05e-10	655.861	440.758	502.238	128.087	147.252	130.158
ABUW_RS08450	pyrH	-2.105	3.46e-08	845.406	667.931	408.326	125.189	156.394	165.220
ABUW_RS08455	frr	-1.867	7.28e-09	495.167	379.389	306.602	103.587	121.714	98.207
ABUW_RS08460	uppS	-1.779	3.32e-08	576.241	373.362	308.931	129.299	126.102	110.904
ABUW_RS08465		-1.681	4.63e-08	1349.184	1052.470	760.907	286.417	363.984	335.906
ABUW_RS08470	ispC	-1.914	5.14e-08	555.553	297.857	302.920	99.898	117.265	89.211
ABUW_RS08495	fabZ	-2.158	9.92e-11	459.270	309.582	397.508	86.357	88.619	86.352
ABUW_RS08500	lpxA	-1.901	1.17e-09	769.812	526.893	523.048	154.748	158.100	174.554
ABUW_RS08505		-1.029	0.000316461	179.705	95.998	162.429	88.728	76.125	49.356
ABUW_RS08530		2.375	1.98e-06	5.144	12.822	5.935	44.153	34.923	43.302
ABUW_RS08535		1.996	0.0275767	0.000	0.877	0.301	0.527	2.255	2.102
ABUW_RS08540		2.256	6.59e-08	6.262	6.137	7.663	32.456	23.039	41.789

Locustag	Gene	logFC	PValue	LCWB_1	LCWB_2	LCWB_3	M9_1	M9_2	M9_3
ABUW_RS08545		1.324	0.00458809	1.677	2.849	1.878	7.482	3.962	4.120
ABUW_RS08570		4.511	5.15e-11	5.368	7.671	4.883	147.951	113.120	142.939
ABUW_RS08575		-2.251	1.62e-06	50.098	38.136	16.829	6.850	6.643	8.492
ABUW_RS08580		3.838	3.9e-06	0.447	0.658	0.301	6.165	3.657	10.174
ABUW_RS08585		1.671	9.17e-09	113.056	121.532	146.126	416.243	354.354	442.858
ABUW_RS08590		5.015	1.23e-09	1.342	3.726	0.601	40.939	48.210	82.905
ABUW_RS08605		-1.056	0.00823224	3.355	4.274	2.554	0.948	1.585	2.522
ABUW_RS08610		1.298	0.00177031	4.809	13.808	3.907	19.653	15.969	18.162
ABUW_RS08615		-4.130	6.18e-13	145.710	97.751	100.673	7.693	6.461	5.213
ABUW_RS08620		-1.682	1.15e-08	300.589	198.681	201.196	68.601	81.122	68.442
ABUW_RS08625	pfkB	-1.164	1.5e-06	60.274	56.875	44.251	22.920	26.939	21.861
ABUW_RS08630	ptsP	-1.506	1.24e-07	279.342	233.748	350.026	92.417	114.400	97.198
ABUW_RS08635		2.062	0.000216748	1.901	2.082	3.832	4.531	14.018	16.396
ABUW_RS08645		4.168	3.84e-10	4.920	5.589	3.606	66.230	70.274	113.594
ABUW_RS08655	brnQ	-1.661	3.86e-09	511.829	491.935	390.821	147.793	161.087	131.924
ABUW_RS08675	grxD	-1.476	3.55e-06	48.085	29.479	33.432	9.642	15.542	14.882
ABUW_RS08685		1.485	1.33e-06	73.582	106.189	93.010	189.997	235.871	338.849
ABUW_RS08700		5.089	6.99e-11	6.374	5.260	3.306	155.696	103.917	236.942
ABUW_RS08705		2.561	1.22e-07	9.393	5.370	8.264	38.200	30.169	69.031
ABUW_RS08715		1.154	2.86e-05	20.576	28.273	23.741	50.687	40.531	70.797
ABUW_RS08725		-3.463	1.79e-09	125.805	79.122	96.691	12.329	9.630	4.709
ABUW_RS08730	cydX	-2.846	5.8e-05	5.591	9.424	4.132	0.474	1.950	0.000
ABUW_RS08735	cydB	-3.068	1.26e-07	4868.803	4336.673	4093.331	712.882	663.912	207.514
ABUW_RS08740		-2.732	9.59e-08	4342.548	4009.119	4233.146	787.490	845.843	259.560
ABUW_RS08745	cydP	-2.308	1.61e-06	14.090	13.808	7.813	2.213	2.926	1.850
ABUW_RS08765		-3.189	2.05e-08	319.711	405.032	258.669	31.087	41.750	34.978
ABUW_RS08805		1.841	2.53e-07	15.544	12.602	9.842	48.632	49.003	36.744
ABUW_RS08825	clpA	1.481	5.87e-07	427.959	692.149	813.272	1889.638	1536.511	1973.313
ABUW_RS08830		1.495	1.14e-05	25.161	13.589	33.057	68.285	60.339	76.178
ABUW_RS08870		1.174	0.0179507	1.230	0.767	1.728	1.897	4.327	2.607
ABUW_RS08875		-1.229	3.81e-05	45.625	35.944	33.132	20.865	14.201	13.369
ABUW_RS08880		-1.010	8.87e-06	2205.102	1454.763	1488.381	860.675	862.055	834.090
ABUW_RS08885	kdsA	-1.422	6.35e-07	751.584	438.895	484.733	221.030	227.094	176.403
ABUW_RS08890	eno	-1.656	9.3e-08	1407.557	1109.675	761.884	324.670	375.808	339.858
ABUW_RS08895		2.072	4.91e-05	3.690	2.630	0.902	10.274	8.959	9.165
ABUW_RS08910		1.264	0.00330596	7.828	1.973	4.282	15.122	10.178	7.736
ABUW_RS08915		2.145	5.46e-06	3.131	1.096	2.554	11.012	9.630	9.669
ABUW_RS08920	pcaF	1.953	3.6e-06	9.953	4.493	8.565	33.458	33.339	22.450
ABUW_RS08925		1.985	0.00042638	4.920	3.068	2.554	17.598	13.592	8.997
ABUW_RS08930	pcaD	1.657	0.000794598	3.578	0.548	2.104	8.641	5.485	5.213
ABUW_RS08935		2.305	7.31e-08	5.256	3.397	3.381	23.341	15.298	20.011
ABUW_RS08940	pcaC	1.094	0.0117569	5.256	1.973	2.479	9.326	4.998	5.633
ABUW_RS08945	pcaH	2.112	1.3e-07	5.591	8.109	3.681	27.978	24.623	20.348
ABUW_RS08950	pcaG	2.595	1.57e-09	3.914	3.288	4.057	24.711	22.063	21.693
ABUW_RS08960		1.627	5.16e-05	4.361	3.397	2.630	13.383	10.422	7.147
ABUW_RS08965		2.028	1.04e-06	5.368	4.603	5.484	25.818	17.127	20.264
ABUW_RS08970		1.888	8.8e-10	56.920	75.067	55.896	250.273	226.180	218.024
ABUW_RS08985		1.038	0.0202997	4.138	1.534	2.028	4.637	4.876	6.138
ABUW_RS08990		1.512	0.000256956	4.585	2.411	3.907	9.906	10.300	11.183
ABUW_RS09045		1.863	0.00225906	1.118	0.877	0.225	2.582	1.585	3.447
ABUW_RS09050		3.227	0.0214733	0.224	0.000	0.000	0.316	1.219	0.420
ABUW_RS09055		2.506	0.0162119	0.224	0.000	0.150	0.632	1.341	0.168
ABUW_RS09065		1.615	0.00934138	1.566	0.438	0.451	1.949	2.316	3.027
ABUW_RS09070		1.731	0.000135032	0.895	2.411	1.728	5.901	6.521	4.204
ABUW_RS09075		1.329	0.0180667	0.783	2.301	0.676	2.898	4.327	1.513
ABUW_RS09080		1.524	0.00125277	3.243	1.973	0.751	4.162	6.156	5.886
ABUW_RS09105		2.022	0.000902989	1.566	0.877	0.225	3.056	4.266	2.438
ABUW_RS09110	pcaD	1.717	0.0088126	1.118	0.986	1.052	2.318	6.339	1.513
ABUW_RS09120		1.262	0.00117155	1.342	2.520	2.705	6.165	4.571	5.381
ABUW_RS09135	catC	1.492	0.0398531	1.118	0.000	0.451	0.948	1.828	1.682
ABUW_RS09150		-2.452	0.00016801	5.479	21.479	4.282	1.739	1.950	1.850
ABUW_RS09165	abaQ	1.190	0.036005	0.447	0.548	0.751	1.054	1.463	1.766
ABUW_RS09170	araD1	1.482	0.0153677	0.224	1.096	1.052	2.529	1.646	2.859
ABUW_RS09180		1.784	3.93e-06	3.467	4.493	3.606	12.593	13.531	13.621
ABUW_RS09185		3.099	4.94e-10	77.160	79.998	89.629	787.437	499.168	829.634
ABUW_RS09190		1.514	3.28e-06	3.690	6.356	5.109	16.334	14.323	12.528
ABUW_RS09195		1.881	2.71e-08	18.451	20.054	28.549	93.312	72.407	83.325
ABUW_RS09210		3.998	1.73e-09	2.796	1.534	2.254	38.358	24.745	42.798
ABUW_RS09250		2.146	0.00300246	0.559	0.219	0.451	1.423	1.280	3.195
ABUW_RS09255		1.557	6.64e-05	2.460	2.630	3.606	8.272	9.447	8.492
ABUW_RS09260		4.698	2.58e-14	14.090	15.780	14.049	428.888	287.982	421.838
ABUW_RS09265		5.363	9.09e-11	2.125	0.658	2.028	65.914	45.285	93.499
ABUW_RS09270		2.834	4.54e-08	5.032	4.164	2.479	27.925	20.844	32.203
ABUW_RS09275		2.485	2.67e-09	23.595	12.164	15.927	102.164	86.730	99.553
ABUW_RS09285		1.326	2.75e-07	141.572	169.750	185.418	410.553	400.919	434.618
ABUW_RS09290		1.525	2.68e-07	66.201	80.656	68.292	229.408	184.674	204.655
ABUW_RS09325		1.092	0.0236932	2.907	0.548	3.005	4.847	4.388	5.129
ABUW_RS09330		1.215	0.000520489	2.237	3.288	2.329	6.112	5.912	6.054
ABUW_RS09345		-1.076	0.00154002	11.406	6.685	12.997	4.268	6.095	4.540
ABUW_RS09355		2.747	7.15e-08	6.374	3.068	1.803	27.029	20.966	23.963
ABUW_RS09375		1.787	0.0127682	1.118	0.000	1.202	4.004	2.621	1.598
ABUW_RS09390		-1.659	0.0479522	0.112	2.411	1.127	0.263	0.792	0.000
ABUW_RS09405		-1.326	5.57e-05	24.490	21.589	14.199	8.167	9.325	6.054
ABUW_RS09425		1.014	0.0493015	1.342	1.534	1.878	4.479	1.341	4.036
ABUW_RS09440		1.298	0.000169201	6.150	5.260	2.780	10.590	13.531	9.501
ABUW_RS09445		2.223	2.63e-05	2.572	0.986	0.902	6.955	5.729	7.315
ABUW_RS09450		1.608	0.00172077	89.573	26.082	31.479	159.279	154.139	132.176
ABUW_RS09455		2.376	6.06e-07	136.316	44.163	109.688	431.049	556.399	520.466
ABUW_RS09465		-1.432	0.00085186	30.752	7.781	12.997	5.058	7.740	6.138
ABUW_RS09470		2.188	0.00124555	0.447	1.205	0.601	3.530	3.352	3.195
ABUW_RS09475	iaaH	1.223	0.0428591	1.118	0.548	0.826	2.371	1.280	2.186
ABUW_RS09480		2.895	3.52e-07	1.901	3.178	1.277	14.753	16.822	13.873
ABUW_RS09485		2.618	8.1e-06	3.019	1.753	1.578	13.488	11.032	13.537
ABUW_RS09490		1.256	0.0455684	7.716	0.329	0.601	7.376	6.461	4.877
ABUW_RS09495		2.142	1.91e-07	8.946	5.370	3.756	29.611	23.709	24.131
ABUW_RS09500		2.026	0.000359763	0.895	1.973	0.826	7.376	3.779	2.943
ABUW_RS09505		1.432	0.0116464	0.224	0.548	1.728	3.636	2.194	1.513
ABUW_RS09525		1.984	3.69e-07	15.879	18.630	17.355	78.085	53.208	74.076
ABUW_RS09530		-2.229	0.00235443	1.230	1.863	0.751	0.105	0.244	0.504
ABUW_RS09555		1.086	0.00149552	2.348	3.288	4.057	7.798	4.876	8.576
ABUW_RS09570		1.803	0.000763569	3.019	0.767	1.127	6.165	3.718	6.811
ABUW_RS09575		1.811	0.00037469	1.454	1.425	2.329	5.532	7.923	5.465
ABUW_RS09585		1.354	0.0342036	0.671	0.438	0.826	1.265	1.585	2.522
ABUW_RS09600	adeA	-2.456	1.5e-09	359.857	341.582	259.496	72.816	61.924	39.602
ABUW_RS09605	adeB	-1.585	1.15e-07	1047.588	1284.465	871.121	375.989	366.544	325.060
ABUW_RS09610	adeC	-1.481	3.04e-07	248.925	280.432	239.061	100.478	88.132	86.436
ABUW_RS09615		2.670	3.65e-09	11.183	8.438	12.922	78.770	81.244	48.599

Locustag	Gene	logFC	PValue	LCWB_1	LCWB_2	LCWB_3	M9_1	M9_2	M9_3
ABUW_RS09620		2.653	1.31e-07	4.920	7.233	4.583	44.364	34.314	24.804
ABUW_RS09630		2.607	5.79e-11	18.787	18.958	17.430	135.095	114.096	86.016
ABUW_RS09635		3.172	3.76e-11	7.828	8.329	9.015	87.885	80.330	59.362
ABUW_RS09640		2.726	5.88e-07	1.342	2.630	1.427	13.699	12.616	8.408
ABUW_RS09670		-2.291	0.00714867	0.224	1.096	1.878	0.422	0.061	0.168
ABUW_RS09680		1.759	1.5e-06	9.729	7.342	5.785	22.446	26.269	27.663
ABUW_RS09685		1.239	0.0199324	0.895	1.753	0.902	2.108	2.560	3.784
ABUW_RS09965		1.638	7.53e-06	122.114	66.081	79.562	288.630	322.235	221.303
ABUW_RS09970		1.667	0.000137874	19.458	5.808	12.922	39.886	46.077	35.062
ABUW_RS09975		1.280	0.008222	67.319	14.575	21.412	81.194	102.881	64.238
ABUW_RS09980		1.001	0.00870066	26.726	7.123	10.142	28.452	33.034	25.140
ABUW_RS09985		1.514	0.000126927	9.841	10.739	5.635	25.818	27.305	19.927
ABUW_RS09995		2.517	5.78e-09	43.389	71.670	83.093	473.779	312.178	351.882
ABUW_RS10000		1.395	1.8e-05	5.591	9.315	11.795	19.073	24.806	28.083
ABUW_RS10005		4.957	1.62e-07	0.335	0.110	1.052	20.918	9.142	23.795
ABUW_RS10010		2.504	1.61e-08	7.604	7.561	4.132	35.144	31.328	40.611
ABUW_RS10015		1.303	6.86e-05	22.365	49.533	51.463	108.592	101.174	96.021
ABUW_RS10020		1.343	3.16e-05	5.591	5.918	8.790	21.286	13.896	17.237
ABUW_RS10025		9.702	7.54e-06	0.000	0.000	0.000	6.270	2.011	9.669
ABUW_RS10060	ppk1	1.512	3.52e-05	43.165	46.903	109.914	186.519	185.222	203.057
ABUW_RS10115	antC	1.948	0.000946989	0.559	0.658	1.878	4.689	5.607	2.522
ABUW_RS10130		3.430	0.000830464	0.112	0.219	0.150	0.790	3.169	1.429
ABUW_RS10145		1.468	0.00473187	1.342	0.986	0.451	2.213	2.011	3.195
ABUW_RS10150		2.166	0.000526367	0.447	3.726	1.127	6.692	4.327	12.696
ABUW_RS10160		1.311	6.71e-06	17.669	17.643	24.567	44.891	51.197	53.812
ABUW_RS10170		-2.588	0.00683695	0.112	1.973	0.751	0.105	0.122	0.252
ABUW_RS10190		1.621	0.00642262	5.479	5.479	7.288	19.495	18.345	19.087
ABUW_RS10195		1.923	1.13e-05	84.652	48.328	85.422	288.209	245.988	295.631
ABUW_RS10220		-2.911	1.49e-07	265.475	549.358	597.050	49.001	60.522	78.785
ABUW_RS10225		-1.041	0.00902851	66.648	17.643	28.699	18.705	19.991	15.723
ABUW_RS10230		2.095	1.06e-06	15.656	10.849	8.339	60.329	46.747	39.266
ABUW_RS10275	chrA	1.005	4.27e-05	12.413	15.123	15.251	34.617	25.659	25.645
ABUW_RS10290		1.234	5.3e-05	10.735	17.096	9.917	24.658	29.743	33.885
ABUW_RS10295		-3.108	1.35e-09	33.660	58.519	41.997	4.426	5.303	5.970
ABUW_RS10305		1.396	0.000185034	21.694	33.314	25.844	46.630	62.899	104.093
ABUW_RS10310		2.184	0.000163647	38.021	118.134	215.170	467.509	567.613	661.471
ABUW_RS10315		2.530	0.000360812	5.927	6.794	38.166	65.650	105.014	137.642
ABUW_RS10330		2.304	1.2e-09	13.307	13.370	18.031	73.501	70.517	78.785
ABUW_RS10335		1.430	0.0386885	0.783	0.438	0.601	1.475	2.194	1.177
ABUW_RS10340	lpdA	2.259	0.000325482	1.454	1.315	0.977	7.008	5.242	5.129
ABUW_RS10345		1.430	0.00122068	2.907	4.931	2.028	11.434	7.070	6.895
ABUW_RS10350		1.546	0.00886959	4.138	0.438	1.953	8.852	5.546	3.952
ABUW_RS10355		2.214	0.00159665	1.118	0.219	1.352	5.638	2.743	4.877
ABUW_RS10365		2.650	2.19e-05	3.690	2.301	1.052	20.285	9.630	11.435
ABUW_RS10375		1.020	3.48e-05	58.373	87.889	86.173	174.822	164.256	132.429
ABUW_RS10380	aroC	-1.677	2.18e-08	328.210	286.788	202.323	81.931	90.996	82.484
ABUW_RS10385	prmB	-1.336	3.43e-06	221.528	115.833	138.388	60.224	59.669	68.611
ABUW_RS10445		4.734	7.52e-08	0.335	0.000	1.052	18.230	10.727	14.210
ABUW_RS10455		1.312	4.07e-06	8.499	12.055	12.772	25.396	28.036	30.185
ABUW_RS10460		2.240	1.7e-05	1.789	1.096	1.277	5.164	6.887	7.736
ABUW_RS10465		-1.055	0.000323213	16.998	16.328	21.787	7.956	11.885	6.642
ABUW_RS10475		5.006	1.17e-08	1.901	0.877	0.075	30.560	16.700	34.978
ABUW_RS10480		2.346	0.000336765	1.789	3.836	0.075	7.535	6.643	12.444
ABUW_RS10495		-1.884	0.0107973	5.479	24.657	1.728	1.949	4.084	2.186
ABUW_RS10500		1.009	7.78e-06	53.453	70.026	75.204	134.041	113.852	152.860
ABUW_RS10510		-1.251	4.11e-05	150.406	91.505	73.326	33.668	43.944	54.989
ABUW_RS10520		-2.905	0.000158447	925.362	2461.974	2988.633	313.289	293.040	244.930
ABUW_RS10525		-2.024	0.000432783	91.250	220.817	197.589	35.354	44.370	45.909
ABUW_RS10530		-1.666	4.28e-05	136.316	283.829	354.759	78.928	83.926	81.643
ABUW_RS10535		-1.327	0.000876134	7.269	10.520	9.015	3.477	4.023	3.111
ABUW_RS10540		-1.950	2.18e-07	137.323	220.269	106.458	40.676	33.522	45.909
ABUW_RS10550		-1.412	0.000576003	10.959	6.246	6.010	3.109	2.316	3.195
ABUW_RS10555		1.211	0.00533255	4.249	4.164	7.062	13.488	9.508	13.958
ABUW_RS10580	mtlD	1.528	2.14e-07	30.640	23.999	30.052	98.160	74.540	71.554
ABUW_RS10650		1.698	0.000128904	6.150	15.342	19.158	29.506	38.458	67.434
ABUW_RS10660		3.741	4.62e-10	7.045	3.616	4.508	42.836	66.373	92.742
ABUW_RS10665		2.866	1.21e-10	23.372	24.986	20.510	118.129	179.798	203.394
ABUW_RS10670		2.181	4.15e-08	1.901	3.068	2.855	11.697	11.519	12.780
ABUW_RS10730	fdx	-1.599	4.01e-07	31.759	41.533	26.671	10.380	11.093	11.435
ABUW_RS10760		2.028	7.8e-08	7.045	10.082	12.622	38.041	46.382	38.762
ABUW_RS10765	rraA	1.300	2.15e-05	16.998	33.314	18.707	48.895	54.000	66.593
ABUW_RS10770		1.619	7.31e-06	5.032	7.890	11.720	22.182	25.964	29.849
ABUW_RS10775	rpsT	-3.371	4.94e-08	31.982	16.767	13.824	1.686	1.828	2.607
ABUW_RS10790		1.205	0.00132861	2.348	2.630	2.179	5.005	5.303	6.222
ABUW_RS10795		1.669	4.94e-06	8.499	6.356	3.982	16.808	19.869	21.945
ABUW_RS10860		1.050	1.64e-06	265.252	294.350	305.324	624.470	552.437	613.712
ABUW_RS10865	zapE	-1.032	4.86e-07	673.865	737.299	821.912	356.705	374.772	360.794
ABUW_RS10875		1.627	2.06e-05	2.684	2.192	2.404	6.744	8.533	7.231
ABUW_RS10890		1.555	5.58e-08	58.038	68.053	49.134	165.654	136.707	212.054
ABUW_RS10895		1.540	4.03e-08	270.843	297.199	367.531	940.130	700.481	1081.038
ABUW_RS10900	rpsA	-1.715	3.63e-08	22642.018	18103.389	12751.126	5320.588	5849.531	5127.048
ABUW_RS10965		-1.005	0.0016313	13.084	15.671	8.715	6.270	7.436	4.456
ABUW_RS10970		-1.699	7.14e-07	42.270	27.397	28.624	7.376	11.397	11.687
ABUW_RS10980	lpxK	-1.653	1e-07	67.096	65.204	57.774	22.340	23.343	14.210
ABUW_RS10990		-1.736	1.26e-08	95.947	88.984	96.916	33.141	23.221	28.167
ABUW_RS10995		-3.177	1e-12	168.410	173.476	196.688	17.019	24.257	18.246
ABUW_RS11000		-1.404	1.35e-08	146.381	163.065	182.338	66.283	62.046	57.428
ABUW_RS11005		-1.361	3.28e-07	105.564	88.984	105.256	30.296	37.544	49.440
ABUW_RS11010	rsmG	-1.291	1.82e-08	124.798	112.217	131.401	48.685	48.576	53.476
ABUW_RS11015	murU	-1.379	2.34e-08	98.631	97.313	79.261	38.990	31.876	34.726
ABUW_RS11035	fba	-1.114	2.56e-07	2168.646	2264.718	1894.754	1057.047	982.916	882.605
ABUW_RS11045		-2.800	1.34e-10	639.646	534.016	395.705	70.814	92.581	61.548
ABUW_RS11055		-1.531	1.09e-05	32.094	21.150	40.119	10.274	14.201	7.736
ABUW_RS11060		-1.858	1.17e-09	154.991	149.257	152.812	35.196	48.942	42.041
ABUW_RS11075	sstT	-1.481	2.13e-08	496.956	424.100	384.886	148.846	174.008	144.873
ABUW_RS11080		-1.348	4.23e-07	88.343	62.903	66.940	29.664	28.768	27.074
ABUW_RS11085		-1.250	8.15e-06	28.739	18.739	22.914	10.011	9.691	9.838
ABUW_RS11115	putP	-3.483	2.38e-12	2460.625	3293.846	2325.094	261.495	223.193	237.615
ABUW_RS11120		-1.394	0.0041883	1.789	3.616	5.484	0.738	1.707	2.102
ABUW_RS11125	putA	-7.159	2.06e-13	2402.475	5613.139	4992.174	31.087	30.657	29.176
ABUW_RS11135	trmA	-1.306	9.07e-07	103.998	67.177	81.365	29.137	37.666	35.398
ABUW_RS11140		1.260	0.00250141	4.697	3.945	2.104	7.851	5.851	11.519
ABUW_RS11150		1.621	5.81e-05	10.064	16.657	5.484	25.818	30.535	40.780
ABUW_RS11155		2.156	2.07e-08	38.245	54.684	74.453	252.328	190.098	307.739
ABUW_RS11160		1.034	0.000103647	22.813	40.985	42.598	74.133	64.179	80.718
ABUW_RS11165	tkt	-1.321	2.2e-06	2234.512	1422.435	1275.841	635.640	682.745	655.921
ABUW_RS11170	metK	-1.161	2.57e-07	1375.463	1312.958	1072.768	528.576	582.789	570.074

Locustag	Gene	logFC	PValue	LCWB_1	LCWB_2	LCWB_3	M9_1	M9_2	M9_3
ABUW_RS11180		1.484	0.000653531	1.789	0.877	1.127	3.056	3.047	4.624
ABUW_RS11220	bioB	-1.805	4.6e-09	709.426	1136.962	769.171	245.900	245.013	257.626
ABUW_RS11240		-1.696	0.0115306	5.032	0.877	1.277	0.632	0.914	0.504
ABUW_RS11245		2.115	0.00110724	1.454	1.425	0.225	3.372	6.095	2.607
ABUW_RS11260		1.130	0.0052293	3.578	1.644	3.606	6.112	5.546	8.324
ABUW_RS11265		1.180	0.00017043	2.796	3.945	5.635	8.852	10.666	9.417
ABUW_RS11270		3.750	9.33e-07	1.342	0.329	2.028	18.230	10.483	25.393
ABUW_RS11280		-1.589	0.0134511	7.716	2.301	2.179	1.054	0.731	2.354
ABUW_RS11300		3.307	1.57e-06	1.230	0.877	0.601	9.747	7.801	8.240
ABUW_RS11305		2.082	0.000275351	1.677	1.973	0.376	4.953	4.998	5.886
ABUW_RS11310		-2.950	1.78e-09	42.047	23.232	39.668	4.689	4.571	4.288
ABUW_RS11315		-1.137	1.3e-06	419.908	442.511	312.161	164.758	176.324	192.883
ABUW_RS11330		4.272	2.88e-13	24.714	24.219	31.329	560.400	506.116	491.710
ABUW_RS11335		4.478	1.12e-11	18.451	15.671	24.417	512.980	399.456	403.592
ABUW_RS11340		4.336	5.37e-12	33.324	28.164	42.147	855.827	659.950	587.395
ABUW_RS11345		4.221	2.4e-12	49.986	51.506	55.220	1177.019	840.175	907.662
ABUW_RS11350		-1.117	2.43e-05	97.401	144.874	184.517	61.119	67.958	68.190
ABUW_RS11365		-1.073	0.00330838	8.387	22.356	29.000	9.642	9.447	9.753
ABUW_RS11370		-1.153	0.00205754	7.045	12.383	14.650	6.533	4.998	3.700
ABUW_RS11390	ychF	-2.638	9.79e-11	964.613	674.287	635.141	111.595	142.498	111.072
ABUW_RS11395		1.821	0.00263929	1.230	4.822	1.953	5.480	10.605	12.108
ABUW_RS11400		1.456	0.000118763	2.796	2.301	1.352	5.480	4.998	6.727
ABUW_RS11410		-1.103	0.00158842	10.847	5.041	8.790	3.477	2.804	5.549
ABUW_RS11425		1.630	8.21e-07	9.505	9.644	11.194	35.565	29.743	29.008
ABUW_RS11440	dapC	-1.368	3.61e-08	417.783	480.209	399.085	156.170	198.936	147.311
ABUW_RS11450		1.819	3.04e-07	17.445	13.041	27.122	71.236	64.666	70.292
ABUW_RS11455		1.657	6.18e-06	22.701	45.698	63.935	167.867	130.186	122.255
ABUW_RS11460	msrB	1.624	5.43e-05	13.866	46.684	44.927	132.987	92.642	101.402
ABUW_RS11470		1.196	0.00483698	34.778	13.150	10.368	48.685	44.614	37.669
ABUW_RS11485		-1.423	4.02e-07	97.177	57.423	83.994	27.714	33.461	27.747
ABUW_RS11490	cysE	-1.127	2.5e-06	138.105	112.984	108.336	61.699	53.086	49.440
ABUW_RS11510		1.578	0.0113029	0.224	0.877	0.676	1.106	2.316	2.186
ABUW_RS11515		1.287	0.00179793	0.895	2.630	2.329	4.320	4.693	5.802
ABUW_RS11540		1.923	0.0102205	0.783	0.219	0.376	1.897	1.341	1.934
ABUW_RS11545		2.198	7.67e-09	16.103	16.876	22.689	109.593	73.565	73.908
ABUW_RS11550		1.128	0.00202639	2.237	7.890	4.057	12.277	8.045	10.342
ABUW_RS11570		1.592	0.0274346	0.112	0.548	0.601	0.896	2.133	1.009
ABUW_RS11575	tauD	-1.118	0.0126332	65.866	268.268	350.777	132.776	90.752	92.322
ABUW_RS11615		-2.647	2.29e-06	18.787	16.219	6.311	2.213	1.219	3.195
ABUW_RS11620		2.621	1.3e-10	138.217	131.066	119.756	879.854	555.241	957.102
ABUW_RS11625	cydB	2.558	8.68e-10	143.026	117.586	137.561	796.921	535.859	1013.436
ABUW_RS11645	madM	1.190	0.00131287	3.578	3.288	2.554	7.482	8.045	5.381
ABUW_RS11650	madL	4.124	3.4e-05	0.112	0.000	0.150	2.108	1.889	1.177
ABUW_RS11655	mdcH	1.460	0.0170122	0.447	2.192	0.601	4.584	1.950	1.598
ABUW_RS11665	mdcE	1.986	3.14e-05	3.914	0.877	1.653	9.221	8.716	6.727
ABUW_RS11680		1.482	0.0125881	1.342	1.205	0.451	3.899	1.707	2.018
ABUW_RS11685	mdcA	1.677	0.00338088	1.118	0.219	1.803	3.741	2.986	4.288
ABUW_RS11710		-2.266	0.00122801	2.684	8.767	19.684	2.371	2.377	1.934
ABUW_RS11715		-1.882	0.0111616	2.237	1.753	2.630	1.159	0.366	0.084
ABUW_RS11725	yfcF	1.943	8.51e-07	10.400	9.972	10.443	49.264	34.497	34.558
ABUW_RS11730	yghU	1.482	4.69e-08	53.788	60.492	73.927	182.831	157.369	186.998
ABUW_RS11745		2.191	0.000922587	0.447	0.767	1.202	4.795	2.682	4.288
ABUW_RS11750	epsC	1.250	0.00107411	3.131	8.219	10.443	16.070	22.490	14.630
ABUW_RS11765		-1.144	0.0151321	2.796	8.000	5.034	0.843	3.413	3.195
ABUW_RS11775		-1.162	8.73e-05	92.816	211.502	153.113	70.972	72.407	60.875
ABUW_RS11780		-1.725	2.29e-06	120.213	260.816	290.148	75.082	69.055	58.857
ABUW_RS11785		-1.270	0.00101962	13.195	34.301	36.663	12.487	12.251	10.258
ABUW_RS11790		-1.144	0.0252589	11.294	69.368	58.150	16.228	28.890	17.909
ABUW_RS11795		-1.175	0.0106835	7.716	37.040	22.539	9.537	9.935	10.426
ABUW_RS11800		1.527	0.000266735	4.249	2.411	3.080	7.324	6.826	14.462
ABUW_RS11805		1.112	0.0364036	2.460	2.520	0.451	2.266	4.205	4.624
ABUW_RS11810		1.624	0.000307516	4.026	1.096	3.005	10.116	6.156	8.997
ABUW_RS11815		1.002	0.000197558	12.972	13.918	9.917	20.391	27.122	25.729
ABUW_RS11835		2.087	8.16e-05	2.013	2.301	0.601	4.162	6.461	9.417
ABUW_RS11850		8.613	2.98e-12	0.112	0.877	0.826	298.694	144.509	310.430
ABUW_RS11855	katE	6.390	1.46e-14	28.963	35.068	38.917	3698.135	1880.505	3081.089
ABUW_RS11860		7.062	9.97e-12	2.796	2.740	2.404	448.120	155.053	451.350
ABUW_RS11865		3.307	3.4e-06	0.335	0.329	0.902	7.640	3.108	6.306
ABUW_RS11870		7.403	1.53e-11	1.230	0.877	0.451	150.374	64.605	196.835
ABUW_RS11875	surA1	7.763	3.08e-12	0.671	0.877	0.225	134.093	56.134	170.434
ABUW_RS11880		2.549	1.43e-05	0.783	0.438	0.751	4.057	3.047	4.877
ABUW_RS11885		3.758	1.24e-05	0.112	0.767	0.301	7.113	2.133	6.642
ABUW_RS11905		-1.215	0.00575201	2.907	5.260	3.756	1.475	1.707	2.018
ABUW_RS11910		2.592	0.00053881	0.895	0.658	0.676	5.638	4.754	2.607
ABUW_RS11915		1.413	0.00915838	0.447	1.096	3.155	6.165	4.084	3.363
ABUW_RS11920		1.756	0.000742823	8.946	4.055	2.554	20.075	14.689	15.471
ABUW_RS11945		1.008	0.00253528	37.574	44.054	51.088	111.174	91.484	64.407
ABUW_RS11950		1.117	0.00146707	19.681	21.041	25.769	56.430	47.113	41.116
ABUW_RS11970		2.412	5.72e-07	2.125	3.616	5.785	27.925	19.077	16.648
ABUW_RS11985	dcaP	1.046	0.0301121	1.118	0.658	0.601	1.423	1.646	1.766
ABUW_RS11990		1.420	0.00125766	3.131	0.877	1.728	6.850	4.023	4.036
ABUW_RS11995		3.020	1e-05	0.671	0.219	1.352	6.692	5.729	7.820
ABUW_RS12000		2.364	1.17e-06	1.454	1.534	2.254	11.170	8.594	7.904
ABUW_RS12005		2.499	2.49e-08	4.361	3.288	3.982	27.240	21.149	17.153
ABUW_RS12020		2.257	7.88e-06	2.460	3.178	1.878	14.279	13.470	6.811
ABUW_RS12025		1.818	4.28e-06	5.591	4.931	5.334	22.393	16.395	16.984
ABUW_RS12030		-1.030	0.000222642	22.365	16.109	15.627	7.587	9.691	9.165
ABUW_RS12040		2.562	1.51e-07	2.348	3.945	3.005	20.285	13.896	20.852
ABUW_RS12145	tgnC	1.150	7.05e-05	9.953	4.822	8.189	18.547	16.273	16.228
ABUW_RS12165		-1.845	0.00409531	2.796	1.973	12.321	1.686	1.889	1.513
ABUW_RS12180		2.736	9.38e-08	8.611	17.205	20.961	145.158	67.165	103.589
ABUW_RS12185		2.432	6.73e-09	37.014	56.985	72.575	371.247	228.191	303.619
ABUW_RS12190		2.756	8.7e-08	3.355	2.301	1.953	19.495	15.481	15.135
ABUW_RS12195		2.982	1.42e-11	6.374	5.370	5.484	49.106	39.982	46.665
ABUW_RS12200		3.400	3.94e-09	2.460	1.973	3.907	33.141	33.034	25.056
ABUW_RS12205		1.417	0.000136294	4.809	13.808	6.085	19.495	23.160	22.534
ABUW_RS12210		4.380	0.00200349	0.000	0.110	0.000	0.843	0.792	0.757
ABUW_RS12245		2.834	2.38e-05	0.112	2.082	0.977	8.061	3.901	11.099
ABUW_RS12295	paaG	-1.285	0.00255579	10.064	13.150	7.212	5.638	3.047	3.363
ABUW_RS12300		-1.959	0.00185014	2.013	2.849	6.311	1.106	1.158	0.673
ABUW_RS12305	paaE	-1.400	0.00683188	11.406	3.836	11.119	5.690	2.316	1.598
ABUW_RS12310	paaD	-1.172	0.0110335	10.064	7.123	7.288	4.953	2.377	3.279
ABUW_RS12330	paaZ	-1.946	0.00766882	77.496	65.642	23.290	25.870	10.422	5.381
ABUW_RS12335		1.756	2.4e-07	57.367	60.053	64.235	212.073	181.687	220.462
ABUW_RS12355		1.242	0.000219556	4.249	4.931	6.686	13.857	13.226	11.015
ABUW_RS12360	abaF	1.643	0.00434805	0.447	1.644	1.277	3.530	4.388	2.691
ABUW_RS12395		-1.438	0.00082924	20.241	8.438	15.026	4.268	3.474	8.997

Locustag	Gene	logFC	PValue	LCWB_1	LCWB_2	LCWB_3	M9_1	M9_2	M9_3
ABUW_RS12405		1.555	2.46e-05	49.763	117.367	117.427	295.480	182.114	360.879
ABUW_RS12420		1.212	8.67e-06	41.376	70.683	81.064	146.633	166.511	135.540
ABUW_RS12515	tssF	1.697	0.011184	25.944	11.397	5.259	91.363	18.224	23.291
ABUW_RS12520	tssE	1.022	0.0360092	17.780	4.164	3.456	12.645	20.235	16.900
ABUW_RS12525		1.429	3.76e-06	171.989	118.354	79.637	313.552	292.857	387.448
ABUW_RS12530	tssC	1.245	4.63e-05	107.800	74.409	46.580	174.453	167.182	198.685
ABUW_RS12535	tssB	1.131	0.000861598	20.129	10.192	11.119	29.980	27.183	32.876
ABUW_RS12540		2.011	1.83e-05	5.591	1.425	2.855	11.802	14.628	12.864
ABUW_RS12565	atzF	1.180	0.0198075	0.671	1.205	2.705	3.846	2.743	4.877
ABUW_RS12585		-1.393	0.000619553	12.636	14.027	12.471	3.319	8.472	2.859
ABUW_RS12605		4.797	3.96e-10	5.144	5.808	4.583	188.152	64.788	175.899
ABUW_RS12610		1.162	0.000374452	7.940	17.205	8.414	29.506	23.648	20.768
ABUW_RS12630		1.406	0.00208011	2.684	1.753	2.254	6.112	5.607	6.054
ABUW_RS12635		1.011	0.0292687	1.677	0.767	2.179	2.476	3.169	4.372
ABUW_RS12640		1.203	0.000173135	25.832	15.342	11.795	39.728	34.619	46.245
ABUW_RS12650		1.041	0.000345639	11.965	10.849	14.350	30.085	27.183	19.339
ABUW_RS12685		3.396	0.000114588	0.447	0.000	0.301	2.845	3.230	2.018
ABUW_RS12700		2.233	8.63e-07	10.400	9.424	9.091	28.768	35.594	72.310
ABUW_RS12705		1.521	5.99e-08	206.431	152.216	120.432	437.740	495.694	439.663
ABUW_RS12710		2.143	2.14e-08	59.492	33.862	29.601	157.224	173.337	209.952
ABUW_RS12715		2.088	1.76e-08	9.841	10.520	15.702	54.797	47.235	53.644
ABUW_RS12720		1.727	0.000346231	3.355	0.658	2.254	7.376	5.059	8.660
ABUW_RS12725		3.599	2.99e-09	10.064	8.109	11.420	124.083	70.091	168.163
ABUW_RS12730		2.163	2.78e-09	6.710	8.329	6.837	33.036	29.865	34.894
ABUW_RS12735		-1.631	0.00298506	2.348	1.644	3.982	0.316	1.585	0.841
ABUW_RS12765		2.014	5.35e-06	4.249	3.507	4.132	11.750	14.506	22.618
ABUW_RS12770		-1.098	0.00765623	4.138	4.822	5.710	2.740	2.072	2.018
ABUW_RS12790	fdxA	-1.297	0.00166517	22.924	10.849	9.015	4.268	4.266	9.165
ABUW_RS12800		-1.389	2.1e-06	62.064	44.602	55.595	15.965	24.075	22.113
ABUW_RS12805		2.063	2.94e-06	99.973	236.707	179.333	1061.420	451.202	643.225
ABUW_RS12885		1.221	0.00115736	11.071	4.164	8.565	13.278	25.172	17.321
ABUW_RS12890		1.173	1.72e-05	16.662	30.246	22.388	51.319	48.942	56.082
ABUW_RS12900		4.041	5.19e-10	2.460	8.438	3.155	83.986	69.177	72.983
ABUW_RS12935		-2.661	1.02e-07	106.459	101.806	279.405	24.500	26.695	26.233
ABUW_RS12940		-3.282	5.21e-07	5.144	3.945	8.039	0.211	0.792	0.925
ABUW_RS12950		1.293	0.0427212	1.454	0.986	0.150	1.897	1.707	2.186
ABUW_RS12975		4.420	6.79e-09	2.796	2.520	1.352	50.371	30.352	57.007
ABUW_RS12980		4.572	2.5e-05	0.112	0.000	0.150	2.845	1.768	2.691
ABUW_RS13000		2.022	0.000134659	2.572	1.644	1.578	5.058	8.106	10.426
ABUW_RS13005		2.463	0.000875495	0.671	0.219	0.601	2.529	1.524	4.877
ABUW_RS13010		6.140	6.92e-08	1.342	0.329	0.225	35.144	17.066	72.815
ABUW_RS13020		1.039	0.0107494	2.125	0.877	1.653	2.793	2.926	4.120
ABUW_RS13030		2.989	4.61e-06	1.454	0.986	1.127	11.908	5.546	10.847
ABUW_RS13035		8.694	5.56e-05	0.000	0.000	0.000	3.530	1.524	3.700
ABUW_RS13040		4.686	4.42e-07	0.447	0.329	0.075	5.585	3.596	11.856
ABUW_RS13055		-1.422	0.000203139	182.277	123.943	65.437	42.994	34.741	61.043
ABUW_RS13060		4.843	3.75e-11	1.677	0.767	0.601	24.079	26.452	33.380
ABUW_RS13085		-3.091	2.31e-05	12.525	4.055	4.132	1.054	0.427	0.841
ABUW_RS13095	xseA	2.502	9.4e-09	7.045	7.671	6.611	42.783	38.580	38.930
ABUW_RS13100	xseB	2.817	0.00157496	0.671	0.438	0.000	2.898	1.950	1.934
ABUW_RS13105		1.320	6.2e-05	16.327	16.548	16.754	30.770	36.508	57.428
ABUW_RS13110		4.008	0.00432115	19.234	12.602	17.505	747.604	18.406	26.906
ABUW_RS13115		3.483	2.49e-07	0.224	1.425	1.352	9.695	11.885	13.958
ABUW_RS13120		4.488	2.97e-07	2.013	0.877	0.000	23.921	10.056	23.459
ABUW_RS13140		-1.139	0.0137949	3.243	2.849	1.953	1.212	1.280	1.009
ABUW_RS13155	benB	-2.403	0.00544096	1.342	0.767	1.277	0.422	0.000	0.168
ABUW_RS13175		3.795	1.24e-07	0.671	0.110	0.826	9.168	7.253	7.483
ABUW_RS13180		1.607	0.0312031	0.224	0.767	0.902	1.423	2.743	2.018
ABUW_RS13200		3.030	4.52e-08	3.802	12.274	11.795	80.983	67.226	83.493
ABUW_RS13220		3.648	2.1e-12	86.665	98.847	104.504	1336.509	874.001	1428.043
ABUW_RS13230		1.063	0.00672788	3.243	6.027	1.578	6.428	7.680	7.567
ABUW_RS13235	trmB	-2.575	1.62e-08	206.543	101.806	115.699	19.390	30.291	21.357
ABUW_RS13250		6.195	4.51e-13	46.743	36.602	37.414	3462.879	1776.587	3597.182
ABUW_RS13255		-1.916	3.66e-09	262.792	206.133	214.644	72.658	55.890	52.215
ABUW_RS13260		-2.051	8.07e-10	367.685	281.309	389.394	89.255	92.459	68.527
ABUW_RS13270	rlmKL	-1.639	2.04e-10	454.797	406.347	419.220	139.889	136.707	134.531
ABUW_RS13275		4.011	1.01e-06	0.224	0.329	0.150	3.583	2.255	5.633
ABUW_RS13280		1.658	7.53e-05	10.064	14.137	11.720	28.979	27.244	58.016
ABUW_RS13285	clpB	1.263	0.00831496	859.496	467.716	2570.615	3290.481	2938.692	3131.538
ABUW_RS13295		1.695	0.0128111	0.447	0.658	0.751	1.475	2.377	2.522
ABUW_RS13325		-1.647	1.64e-06	1966.688	1472.516	988.548	460.713	484.540	468.251
ABUW_RS13330		-1.053	0.00352559	810.964	314.623	459.564	222.716	255.557	285.541
ABUW_RS13340	alaS	-2.007	1.62e-08	1761.040	1060.909	1060.371	317.767	364.960	283.103
ABUW_RS13345		-1.889	2.63e-08	1903.730	1270.438	1076.674	353.859	466.743	326.405
ABUW_RS13355	rnhB	-2.204	3.04e-09	38.580	27.725	28.850	6.481	7.680	6.390
ABUW_RS13360		-1.554	2.92e-06	28.068	22.684	22.989	11.592	7.192	5.802
ABUW_RS13370		-2.528	1.75e-08	298.800	162.407	122.460	37.356	32.546	30.942
ABUW_RS13375		-1.737	2.28e-06	1003.193	540.810	387.065	191.103	191.317	196.667
ABUW_RS13380		3.391	3.18e-08	2.460	2.630	0.826	16.860	17.614	24.384
ABUW_RS13395		2.012	0.00357307	0.112	1.096	0.601	1.949	3.047	2.438
ABUW_RS13415		-1.037	0.0048954	3.802	4.274	4.959	1.739	2.743	1.934
ABUW_RS13440		1.403	0.000251922	1.789	1.315	1.427	3.741	4.327	3.868
ABUW_RS13450		1.796	7.45e-08	37.350	40.547	60.779	150.427	138.841	195.238
ABUW_RS13460		1.641	9.69e-06	8.722	6.137	4.808	21.655	22.185	16.060
ABUW_RS13485	mhpT	2.262	6.85e-06	3.578	3.068	1.503	15.438	10.361	11.435
ABUW_RS13490		1.601	3.43e-07	85.883	143.559	120.883	448.383	332.230	281.926
ABUW_RS13495		1.898	4.59e-08	68.773	51.834	72.650	317.240	240.503	162.866
ABUW_RS13500		2.882	1.36e-07	16.550	8.109	7.663	114.599	73.199	45.825
ABUW_RS13505		2.909	4.19e-07	2.013	2.082	1.277	12.909	11.458	15.051
ABUW_RS13510		2.993	4.75e-05	1.230	0.986	0.225	7.113	7.801	2.354
ABUW_RS13515		4.278	5.73e-05	0.000	0.000	0.376	4.215	3.901	1.009
ABUW_RS13520		3.134	0.000208964	0.559	0.438	0.301	5.216	2.621	3.027
ABUW_RS13525		4.368	5e-07	0.559	1.753	3.982	70.972	45.650	24.636
ABUW_RS13550		1.166	0.00269449	4.026	2.630	1.427	6.165	4.815	6.390
ABUW_RS13580		3.032	0.0396882	0.000	0.000	0.150	0.632	0.549	0.504
ABUW_RS13585		1.493	0.0151086	1.118	0.438	0.376	1.581	1.463	2.270
ABUW_RS13610		-3.060	1.07e-07	26.615	85.697	62.207	9.010	6.948	4.540
ABUW_RS13615		-1.530	3e-05	15.320	18.411	22.989	8.483	5.424	5.633
ABUW_RS13630		1.041	0.018462	1.454	2.411	2.028	5.058	3.657	3.279
ABUW_RS13640		-1.433	4.65e-08	151.077	117.915	116.149	43.152	52.477	46.918
ABUW_RS13650		2.091	2.77e-09	74.364	62.574	49.811	266.185	249.218	278.478
ABUW_RS13685		1.082	0.000140439	198.044	114.189	125.541	314.343	314.250	297.061
ABUW_RS13690		-2.357	0.00632141	1.901	0.438	1.052	0.211	0.000	0.504
ABUW_RS13715		2.766	0.000535685	37.014	40.218	34.935	74.186	95.872	594.878
ABUW_RS13720	argG	-2.117	5.4e-09	1013.481	654.342	609.297	191.630	187.112	145.629
ABUW_RS13735	rnt	-1.164	1.76e-06	187.980	173.476	205.628	99.424	92.581	60.623
ABUW_RS13755		2.879	4.57e-10	11.965	9.424	7.964	77.242	60.705	75.926

Locustag	Gene	logFC	PValue	LCWB_1	LCWB_2	LCWB_3	M9_1	M9_2	M9_3
ABUW_RS13760		3.682	2.26e-12	64.300	43.506	44.326	610.086	634.413	703.680
ABUW_RS13765		3.336	1.07e-05	1.342	5.370	1.127	13.699	25.233	37.164
ABUW_RS13770		1.873	7.56e-06	2.460	2.959	1.653	9.958	8.228	6.727
ABUW_RS13775		2.515	3.28e-06	1.006	2.740	0.977	6.850	8.228	11.351
ABUW_RS13800		-1.313	1.37e-06	48.756	40.328	35.686	16.386	16.639	17.069
ABUW_RS13815		-1.966	2.41e-06	275.652	662.780	585.556	140.574	157.978	90.976
ABUW_RS13820	nudC	-1.043	2.68e-05	94.046	115.176	163.255	57.536	67.104	56.419
ABUW_RS13835		-1.938	1.77e-05	8.722	22.794	12.847	4.637	2.743	4.120
ABUW_RS13840	rsmI	-1.131	2.75e-05	21.806	20.602	24.342	8.746	10.483	11.519
ABUW_RS13850		-1.859	0.000319058	38.356	40.766	11.946	4.320	10.727	10.090
ABUW_RS13855		-3.056	5.76e-08	13.307	13.479	24.041	1.686	1.646	3.111
ABUW_RS13900		3.751	0.00848335	36.344	25.862	34.935	26.819	24.257	1262.570
ABUW_RS13910		2.651	0.000652676	0.335	0.000	0.751	2.687	2.011	3.279
ABUW_RS13920	lon	1.223	0.000682637	1147.673	1158.331	3112.070	3660.831	3937.760	5057.428
ABUW_RS13925	rlmH	-1.092	7.09e-05	25.273	16.000	27.347	10.907	12.190	9.081
ABUW_RS13945		-1.350	0.00216724	40.257	11.068	16.078	9.642	9.752	6.474
ABUW_RS13950	nth	-1.228	0.00121686	15.097	8.438	9.466	3.899	6.765	3.111
ABUW_RS13955	adk	-1.475	5.03e-08	576.464	688.095	476.018	199.112	208.810	218.276
ABUW_RS13970	mrdA	-1.674	9.88e-09	256.194	181.804	180.610	64.175	70.213	59.193
ABUW_RS13975	rsmD	-1.189	0.0018298	6.710	10.411	5.560	2.371	4.754	2.607
ABUW_RS13980		1.145	1.4e-06	32.430	39.670	39.668	90.414	79.782	77.271
ABUW_RS13990		1.311	2e-06	9.505	13.918	13.598	34.511	30.779	26.822
ABUW_RS13995	ureE	1.230	8.64e-07	14.314	15.123	15.251	33.510	35.594	35.903
ABUW_RS14015		2.081	5.5e-05	2.125	0.986	1.503	6.270	8.228	4.793
ABUW_RS14020		-2.615	0.000382278	8.834	1.863	5.860	0.685	0.731	1.429
ABUW_RS14025		2.264	4.43e-09	31.982	41.095	25.844	167.340	113.059	192.883
ABUW_RS14030		2.132	7.72e-08	114.175	149.805	165.359	700.553	575.232	607.658
ABUW_RS14050		-1.802	3.77e-05	13.084	14.465	7.889	3.846	2.255	3.952
ABUW_RS14060	cysN	-1.499	7e-06	723.516	1381.559	1003.123	376.305	421.154	302.190
ABUW_RS14065	cysD	-1.132	0.000162094	266.594	456.976	327.563	158.383	162.245	158.746
ABUW_RS14075	lysS	-1.794	9.89e-07	653.401	337.308	491.344	134.041	140.974	152.608
ABUW_RS14085		2.174	0.010453	1.118	0.000	0.451	3.688	1.219	1.850
ABUW_RS14110		-1.755	0.00136428	2.013	1.863	2.104	0.738	0.609	0.336
ABUW_RS14130		1.258	6.3e-06	32.541	41.205	63.634	101.953	110.621	118.471
ABUW_RS14135		1.469	4.02e-06	7.604	8.657	10.894	28.452	21.759	25.813
ABUW_RS14145		-1.106	1.13e-05	255.523	425.744	321.778	137.834	142.680	185.989
ABUW_RS14160		-1.919	0.0027126	1227.740	4573.380	4369.054	859.832	979.808	849.225
ABUW_RS14200		-1.063	2.95e-05	1260.841	927.651	682.472	401.279	451.141	521.895
ABUW_RS14205	metH	-1.777	8.74e-08	579.595	421.470	304.498	121.817	144.265	114.519
ABUW_RS14210		1.542	3.72e-05	4.026	4.164	3.606	11.328	12.982	9.669
ABUW_RS14215		1.118	0.0071032	2.348	1.753	2.630	5.954	4.754	3.952
ABUW_RS14220		1.325	7.45e-05	4.361	7.014	4.808	13.120	13.043	14.210
ABUW_RS14225		1.388	0.000357585	6.262	2.301	4.057	14.648	8.228	9.753
ABUW_RS14240		2.561	1.38e-09	24.714	35.177	43.425	244.108	143.473	225.843
ABUW_RS14255		-1.171	4.35e-07	219.179	199.996	213.442	85.040	88.010	108.297
ABUW_RS14275		1.152	0.00138583	2.684	5.260	7.513	9.273	15.176	11.183
ABUW_RS14285		1.642	0.000327682	1.677	2.192	1.803	4.847	6.278	6.727
ABUW_RS14290		2.062	0.000361016	0.224	0.658	1.202	3.952	2.621	2.859
ABUW_RS14295		1.531	0.0026819	4.249	1.096	1.653	6.955	7.375	5.045
ABUW_RS14300		1.698	2.13e-06	4.138	6.137	5.409	16.650	14.750	19.927
ABUW_RS14305		1.077	0.00138401	5.927	5.041	3.531	10.432	10.544	8.829
ABUW_RS14310		1.386	0.0100754	0.671	3.178	0.977	4.426	4.571	2.943
ABUW_RS14345		-1.605	0.00251944	3.131	1.425	2.930	0.580	1.036	0.925
ABUW_RS14360	pgaD	-1.164	4.21e-05	49.092	48.328	31.930	14.700	25.720	16.984
ABUW_RS14375		-1.513	9.87e-06	40.257	19.726	22.839	8.694	9.874	10.426
ABUW_RS14380		-4.746	7.71e-08	17.221	7.781	8.414	0.369	0.366	0.504
ABUW_RS14395		1.219	0.0189873	4.585	1.425	3.606	9.379	3.291	10.174
ABUW_RS14410		-1.004	1.99e-05	689.632	625.192	403.518	303.278	254.948	298.070
ABUW_RS14415		-2.359	3.56e-09	461.954	467.606	288.195	75.293	64.544	97.703
ABUW_RS14420	betI	-3.963	4.36e-13	279.118	272.213	244.470	20.918	15.847	13.873
ABUW_RS14425	betB	-4.726	2.67e-15	2959.370	3151.713	3293.131	130.036	121.958	103.000
ABUW_RS14430	betA	-5.588	3.7e-16	2060.958	2052.997	1766.284	41.993	39.921	40.275
ABUW_RS14435	mqo	-1.153	2.01e-06	2173.678	1826.262	1864.477	873.373	930.683	833.670
ABUW_RS14445		-3.786	7.24e-10	204.866	560.317	333.348	30.823	30.474	17.741
ABUW_RS14450		-3.391	6.23e-09	216.048	471.223	237.032	33.089	38.885	15.303
ABUW_RS14460		1.238	7.04e-05	23.260	12.712	17.956	40.149	44.614	42.377
ABUW_RS14470		-1.337	0.000247467	53.677	28.164	32.005	17.019	10.300	17.741
ABUW_RS14475		-1.463	8.68e-06	266.594	156.161	137.411	67.758	50.282	85.343
ABUW_RS14480		-2.041	4.71e-06	21.694	12.493	24.567	4.584	4.449	5.465
ABUW_RS14485		-1.287	0.000306998	149.735	61.149	89.629	39.253	31.206	52.971
ABUW_RS14495		-1.830	2.2e-06	387.031	590.563	765.264	156.434	137.926	196.499
ABUW_RS14515		1.756	0.000761873	0.335	2.520	1.352	6.112	4.327	3.531
ABUW_RS14570		1.303	9.56e-06	11.518	10.301	11.119	21.813	28.341	31.531
ABUW_RS14610		-1.851	0.0320715	0.671	1.534	1.052	0.158	0.670	0.000
ABUW_RS14645	ggt	1.217	0.000770148	78.055	81.971	151.084	350.540	200.277	174.301
ABUW_RS14650		-1.027	1.23e-05	88.007	62.793	72.650	34.090	37.971	37.585
ABUW_RS14675		1.046	3.9e-05	64.300	41.753	57.849	117.233	94.226	127.300
ABUW_RS14685		2.170	9.3e-08	7.940	13.260	7.663	51.266	38.458	38.593
ABUW_RS14695		-1.022	0.000349522	36.679	46.574	66.489	25.554	31.267	16.816
ABUW_RS14700		-1.169	9.8e-06	69.220	103.450	110.214	39.095	52.477	34.137
ABUW_RS14710		-2.964	9.99e-09	232.487	549.577	491.043	60.908	63.752	38.005
ABUW_RS14715		-3.023	4.16e-08	263.686	647.767	583.602	69.391	73.199	40.780
ABUW_RS14740		-4.432	6.39e-10	86.889	64.547	39.292	1.686	4.327	2.859
ABUW_RS14750		1.772	0.00125244	2.460	1.096	0.977	5.269	2.499	7.483
ABUW_RS14760		1.484	7.34e-07	101.203	83.615	125.165	356.125	225.570	286.550
ABUW_RS14765	dut	-2.092	9.27e-09	81.969	71.341	55.746	14.068	19.138	15.723
ABUW_RS14770	rep	-1.655	8.45e-08	173.666	135.449	150.784	60.118	45.650	39.855
ABUW_RS14775		1.509	3.94e-07	855.023	1621.006	1307.245	3927.596	3176.818	3666.465
ABUW_RS14805		-1.309	7.75e-06	73.134	42.848	59.051	25.554	23.465	21.441
ABUW_RS14830		1.562	6.5e-07	33.101	58.081	39.969	145.790	116.351	124.609
ABUW_RS14835	rimI	-1.143	0.010695	5.144	2.192	3.381	1.370	1.341	2.270
ABUW_RS14840		1.788	6.96e-05	4.138	5.260	2.104	16.966	10.178	10.762
ABUW_RS14850	tuf	-1.369	6.94e-08	21978.441	21960.730	19238.143	9288.227	8710.209	6456.884
ABUW_RS14855	fusA	-1.874	7.19e-08	41548.704	29852.613	22518.652	9039.482	9888.770	6694.751
ABUW_RS14860	rpsG	-1.931	7.1e-08	8023.756	4674.638	4534.864	1700.537	1674.681	1142.838
ABUW_RS14865	rpsL	-1.816	1.43e-07	5749.770	3287.600	3116.127	1256.791	1224.211	970.975
ABUW_RS14870		1.439	7.64e-06	105.228	189.256	248.301	525.467	398.542	550.987
ABUW_RS14875		-2.468	4.41e-11	1743.818	2431.180	2158.908	450.544	368.373	325.228
ABUW_RS14880	hemJ	-1.747	4.04e-08	264.581	412.703	251.908	86.884	89.533	100.478
ABUW_RS14890		1.284	0.0446214	0.895	3.726	1.427	2.002	6.765	5.970
ABUW_RS14910	cntB	2.426	1.7e-08	4.697	5.699	4.808	32.298	27.366	21.441
ABUW_RS14915		1.400	6.57e-05	20.576	18.958	9.015	52.267	41.262	31.867
ABUW_RS14920	cntA	1.652	5.32e-07	21.918	22.794	13.824	67.389	64.605	49.776
ABUW_RS14925		1.077	0.00303901	7.828	7.561	2.780	12.118	11.397	13.453
ABUW_RS14935		1.070	0.00230774	2.237	1.425	3.681	6.428	4.449	5.213
ABUW_RS14975	pgeF	-1.292	7.43e-05	37.126	28.602	32.831	15.701	8.472	16.228
ABUW_RS15000		1.249	3.06e-06	32.430	32.876	24.492	58.854	81.427	72.394

Locustag	Gene	logFC	PValue	LCWB_1	LCWB_2	LCWB_3	M9_1	M9_2	M9_3
ABUW_RS15010	ispE	-2.769	4.7e-10	727.653	378.184	413.059	65.914	78.380	78.532
ABUW_RS15035		-2.898	1.51e-08	6168.224	2489.042	2606.827	529.577	557.922	423.688
ABUW_RS15040	rplY	-2.455	2.44e-08	565.058	283.172	257.993	69.233	77.770	54.317
ABUW_RS15045	pth	-2.386	7.94e-07	1257.822	421.251	489.992	105.536	158.222	151.263
ABUW_RS15050	panD	-2.106	9.54e-07	229.020	89.204	107.359	26.977	38.580	33.212
ABUW_RS15060		1.693	4.71e-07	52.111	83.615	96.691	296.534	204.787	252.077
ABUW_RS15080	lysM	2.178	6.6e-09	306.851	414.566	372.264	1640.630	1324.776	1983.571
ABUW_RS15085	acpP	-2.071	3.18e-09	97.401	115.724	83.994	28.399	20.052	21.945
ABUW_RS15090	fabG	-2.803	1.51e-12	2218.409	2402.140	1784.615	319.137	310.776	287.643
ABUW_RS15095	fabD	-2.679	9e-12	1850.948	1367.532	1294.248	248.534	232.214	223.909
ABUW_RS15100	rpmF	-2.216	6.1e-08	452.673	287.994	697.498	107.222	88.314	114.351
ABUW_RS15105		-1.994	4.79e-06	5139.534	2180.884	1699.419	638.591	724.129	902.112
ABUW_RS15130	rluB	-1.326	2.7e-08	232.934	223.009	234.853	95.104	89.107	91.229
ABUW_RS15135	bioD	-2.750	5.08e-09	67.319	123.285	67.691	9.695	14.810	14.042
ABUW_RS15140	bioC	-2.968	2.66e-10	94.158	78.354	65.588	7.218	13.104	10.174
ABUW_RS15145		-3.318	2e-11	142.914	216.543	135.833	18.388	18.650	12.192
ABUW_RS15150	bioA	-2.561	1.21e-10	170.982	243.940	168.139	32.983	34.497	31.194
ABUW_RS15160	otsB	4.578	6.64e-09	0.447	1.096	0.601	17.651	7.375	26.486
ABUW_RS15165		6.623	7.4e-11	3.578	3.507	7.663	685.431	224.169	607.995
ABUW_RS15170		-1.947	0.0044338	140.677	19.287	26.370	14.121	17.187	16.732
ABUW_RS15180	ligA	-1.180	8.26e-05	125.469	107.614	142.820	61.804	55.158	48.851
ABUW_RS15190	smc	-1.215	1.47e-07	196.367	205.365	226.890	79.824	103.491	87.529
ABUW_RS15195		1.233	0.00323487	5.479	2.849	5.635	9.484	12.312	11.687
ABUW_RS15210		-1.602	4.41e-05	37.014	50.629	115.473	23.183	24.197	19.927
ABUW_RS15225		-1.784	2.77e-05	52.111	15.123	41.697	12.118	9.813	9.585
ABUW_RS15230		4.047	1.02e-08	0.559	0.219	1.878	19.548	17.614	12.444
ABUW_RS15235		2.314	2.56e-08	24.154	12.274	15.552	100.794	83.256	73.067
ABUW_RS15240		3.270	1.25e-08	4.361	2.849	4.357	41.677	37.666	33.380
ABUW_RS15245		2.659	3.84e-06	9.393	16.219	6.837	80.456	64.240	56.251
ABUW_RS15250		2.831	2.58e-08	19.010	7.014	9.241	95.209	89.168	63.229
ABUW_RS15255	dcd	-1.387	1.81e-07	286.611	264.761	364.000	103.112	115.375	132.092
ABUW_RS15270		-1.435	3.21e-06	32.653	47.232	32.155	13.014	16.395	11.771
ABUW_RS15280		3.668	1.64e-09	4.138	3.945	2.554	38.937	30.413	63.482
ABUW_RS15285	metG	-1.334	1.94e-08	807.385	682.615	784.047	314.448	320.833	266.791
ABUW_RS15295		-1.366	5.08e-05	40.593	21.917	20.585	8.641	11.397	12.192
ABUW_RS15305		1.731	7.52e-08	21.806	35.506	33.508	113.071	79.599	109.811
ABUW_RS15310		1.525	1.07e-06	25.496	47.013	57.474	130.036	122.263	124.020
ABUW_RS15320		-1.497	0.000568799	37.685	9.644	20.210	6.165	7.984	10.006
ABUW_RS15330		5.657	1.04e-12	194.130	139.723	193.908	9426.588	5823.567	11392.478
ABUW_RS15335		5.288	4.03e-11	2.125	2.959	4.207	157.382	68.445	150.338
ABUW_RS15340		-1.157	0.000104243	78.390	36.602	63.785	21.708	31.084	27.579
ABUW_RS15355		-1.122	0.00451061	14.985	6.794	7.363	3.214	5.120	5.045
ABUW_RS15360		-1.850	9.66e-07	21.359	20.164	12.396	4.584	3.901	6.558
ABUW_RS15365	upp	-1.155	0.0105916	249.932	307.829	194.359	92.364	110.256	135.371
ABUW_RS15390	nuoJ	-1.023	7.5e-05	589.995	488.866	494.349	308.916	285.787	178.758
ABUW_RS15395	nuoI	-1.330	1.92e-06	919.659	801.846	838.290	404.230	389.400	223.909
ABUW_RS15400	nuoH	-1.079	1.16e-05	2057.603	2057.161	1417.460	885.491	1014.122	717.889
ABUW_RS15405	nuoG	-1.416	4.22e-07	4612.497	4068.953	4100.167	1759.391	1926.643	1103.236
ABUW_RS15410	nuoF	-1.493	9.01e-07	2139.683	1956.451	1666.587	747.973	824.999	473.968
ABUW_RS15415	nuoE	-1.477	1.55e-07	528.267	522.619	389.544	178.089	204.482	134.194
ABUW_RS15420	nuoC	-1.423	8.73e-08	2741.420	2269.759	2273.029	1005.411	1015.280	694.767
ABUW_RS15430	ndhC	-1.082	2.82e-06	1192.850	1031.539	794.414	494.434	515.198	416.120
ABUW_RS15440		1.315	7.91e-06	12.748	24.986	19.984	52.109	43.700	48.095
ABUW_RS15460		-1.377	4.24e-08	6387.738	7407.839	8406.188	3165.608	2643.701	2740.054
ABUW_RS15470		-1.533	2.72e-09	3295.184	2937.690	3403.796	1262.639	1068.183	998.722
ABUW_RS15475		4.780	2.87e-10	5.256	3.726	2.479	125.716	80.208	99.469
ABUW_RS15490		1.649	0.0022049	1.342	0.767	1.127	2.108	3.413	5.129
ABUW_RS15505		7.593	0.000294431	0.000	0.000	0.000	1.739	1.219	0.925
ABUW_RS15540		1.912	0.00281983	0.671	1.863	0.301	1.949	3.596	4.709
ABUW_RS15545		2.263	5.74e-06	3.355	1.096	1.352	10.169	8.350	8.324
ABUW_RS15550		1.758	9.95e-08	24.937	29.479	34.334	126.506	85.511	89.042
ABUW_RS15555		1.515	0.00211127	0.895	1.425	1.503	3.003	3.291	5.213
ABUW_RS15595		1.752	0.021261	0.000	1.973	0.376	1.317	4.327	1.850
ABUW_RS15600		1.263	0.000231424	9.505	25.205	13.148	42.151	36.752	35.146
ABUW_RS15610		3.790	3.14e-12	6.710	7.561	7.212	86.726	106.294	104.850
ABUW_RS15615	add	3.161	3.83e-08	4.697	12.602	7.062	96.052	45.772	74.749
ABUW_RS15660		2.657	1.05e-07	4.473	7.561	3.306	29.717	37.118	27.327
ABUW_RS15705		-1.823	0.0471968	30.976	13.698	25.694	7.060	5.607	7.315
ABUW_RS15710	tsaB	-1.145	2.92e-06	78.949	50.191	70.546	26.871	31.754	31.867
ABUW_RS15715		1.016	0.00118826	24.378	67.944	42.448	77.558	90.874	104.261
ABUW_RS15730		1.421	4.24e-07	98.743	137.750	127.719	346.483	305.108	324.219
ABUW_RS15745		1.035	0.00369411	6.821	8.877	10.368	21.550	15.176	17.153
ABUW_RS15755		4.163	1.19e-12	45.290	44.492	29.150	849.979	671.835	597.484
ABUW_RS15760		-1.251	0.00277106	10.959	8.657	8.414	1.633	5.181	5.297
ABUW_RS15775	hisG	-1.395	2.33e-07	344.425	293.583	221.105	113.387	112.023	100.898
ABUW_RS15780	murA	-1.128	3.12e-07	1117.927	828.694	960.525	449.490	473.874	406.367
ABUW_RS15790	hpf	2.803	8.03e-09	16.662	24.547	25.394	141.259	116.716	209.868
ABUW_RS15795		1.210	0.000982961	59.156	130.299	96.541	172.662	208.870	281.001
ABUW_RS15880	polA	-1.299	8.45e-09	559.690	643.602	572.333	249.430	252.022	219.958
ABUW_RS15895	tilS	-1.039	0.00797524	47.973	63.670	43.049	17.704	30.109	27.579
ABUW_RS15900		-1.561	9.41e-08	393.405	591.220	344.542	156.908	143.838	149.413
ABUW_RS15915	rho	-1.303	3.75e-06	1953.940	1031.101	1484.249	570.200	658.975	582.602
ABUW_RS15920		-1.454	5.67e-09	1898.362	1914.479	1544.202	697.602	626.611	630.613
ABUW_RS15930	pheT	-1.062	6.67e-07	1246.639	1312.410	1074.871	600.496	594.065	545.858
ABUW_RS15935	pheS	-1.391	5.15e-08	368.915	305.747	430.414	147.002	146.337	127.888
ABUW_RS15950	rplT	-2.384	8.6e-08	3797.395	2206.418	1566.516	503.707	481.737	464.551
ABUW_RS15955	rpmI	-2.545	4.31e-08	718.819	410.731	373.692	95.209	88.680	73.319
ABUW_RS15960	nreB	-1.881	1.71e-08	43.389	41.314	35.536	13.436	9.447	9.417
ABUW_RS15975	infC	-1.217	1.16e-07	1913.011	2025.490	1616.852	829.957	818.355	740.760
ABUW_RS15980	thrS	-1.705	3.03e-10	1966.576	2481.700	2402.101	727.372	701.822	671.560
ABUW_RS15985		1.427	0.000286191	9.058	10.630	5.935	21.602	24.684	21.357
ABUW_RS16005	panC	-1.553	1.7e-08	351.917	391.992	409.604	123.240	153.773	116.117
ABUW_RS16010	panB	-1.320	7.83e-08	301.372	347.609	390.220	142.682	157.430	115.949
ABUW_RS16015	folK	-1.909	1.61e-06	45.178	28.821	72.199	11.802	16.029	11.267
ABUW_RS16035		1.103	0.00201414	4.138	10.411	11.194	18.388	16.029	22.198
ABUW_RS16050		-1.103	2.55e-05	130.389	73.642	90.005	44.944	54.305	37.248
ABUW_RS16065		3.124	0.000641393	14.985	14.356	24.642	33.299	68.567	377.863
ABUW_RS16070		1.407	1.29e-05	33.995	38.684	68.067	96.790	149.202	130.243
ABUW_RS16075		1.177	7.51e-06	60.163	111.888	78.360	186.519	193.511	185.905
ABUW_RS16090		1.854	1.35e-05	175.567	89.313	52.440	397.486	381.172	363.233
ABUW_RS16095		2.014	1.48e-06	20.576	12.931	7.212	51.583	53.513	55.914
ABUW_RS16100		1.567	0.00181536	263.351	116.929	46.580	519.988	369.835	369.119
ABUW_RS16120		2.895	0.00154028	83.758	136.874	127.269	377.569	177.787	2037.299
ABUW_RS16130		1.111	0.00012494	16.998	34.958	27.046	50.529	50.161	70.629
ABUW_RS16135		1.239	3.01e-06	27.845	32.986	44.326	96.684	69.847	82.989
ABUW_RS16140		3.757	3.09e-10	1.230	1.425	2.104	25.080	16.456	25.477
ABUW_RS16155		4.310	4.68e-13	16.327	18.411	23.741	448.489	283.959	436.804

Locustag	Gene	logFC	PValue	LCWB_1	LCWB_2	LCWB_3	M9_1	M9_2	M9_3
ABUW_RS16230		2.867	0.0167439	22.924	18.301	13.223	364.766	11.641	14.378
ABUW_RS16235	dusA	-1.945	7.12e-06	93.263	36.492	65.738	18.968	16.700	14.882
ABUW_RS16240		1.786	0.000385666	66.760	30.794	45.829	293.583	78.197	121.246
ABUW_RS16255	acnA	1.880	1.07e-08	311.101	425.963	438.378	1727.198	1334.528	1266.606
ABUW_RS16275		-2.037	1.41e-09	461.731	341.472	329.967	90.572	86.120	99.469
ABUW_RS16280		5.503	1.2e-07	11.518	15.890	9.767	590.644	510.992	568.897
ABUW_RS16285		3.814	1.19e-09	4.809	3.068	3.080	37.620	46.808	68.358
ABUW_RS16295		1.539	0.00848998	31.535	26.191	25.469	77.558	70.639	93.331
ABUW_RS16315		-1.279	0.00908237	2.013	9.315	10.368	3.583	3.352	2.018
ABUW_RS16320	leuS	-1.313	3.79e-08	1476.889	1654.211	1569.220	670.573	692.984	528.537
ABUW_RS16340		-1.038	8.85e-06	255.635	182.900	161.452	100.741	101.235	89.715
ABUW_RS16350		-2.600	4.17e-12	1204.145	1112.743	976.452	199.481	183.699	159.839
ABUW_RS16360	orn	-1.045	1.55e-05	73.134	47.013	55.520	28.136	27.610	29.345
ABUW_RS16365	rsgA	-1.111	7.91e-06	164.161	98.190	176.478	65.756	73.504	64.070
ABUW_RS16380	secB	-1.179	5.4e-06	239.420	236.378	376.922	101.268	138.170	137.726
ABUW_RS16390	der	-1.281	7.36e-06	395.641	187.941	286.918	112.702	118.850	126.711
ABUW_RS16400		-1.409	7.91e-09	247.136	213.365	195.937	74.871	91.910	80.382
ABUW_RS16405	hisS	-1.379	2.43e-07	1619.356	1289.506	1035.053	452.704	562.981	500.790
ABUW_RS16430	ndk	-2.053	4.53e-10	1104.620	986.170	820.860	234.413	231.787	235.429
ABUW_RS16435	iscX	-1.311	2.65e-07	187.533	127.888	153.564	59.855	61.192	68.022
ABUW_RS16440		2.689	3.6e-08	10.064	8.877	7.212	65.440	39.799	61.800
ABUW_RS16445		2.107	0.000678973	4.361	2.082	3.832	18.125	15.176	11.015
ABUW_RS16465		3.229	2.32e-09	34.219	34.191	17.806	321.666	260.372	218.528
ABUW_RS16475		1.248	0.00271276	535.200	610.836	579.545	1658.017	1227.015	1212.962
ABUW_RS16480		1.484	0.00581531	357.173	401.416	295.633	2080.214	451.384	415.111
ABUW_RS16500		1.459	0.0110119	100.532	25.753	40.119	197.057	127.870	129.990
ABUW_RS16505	pta	1.074	0.019308	133.744	75.615	108.486	282.097	194.609	192.295
ABUW_RS16510		-2.235	1.11e-05	911.719	304.651	280.156	100.004	130.674	86.688
ABUW_RS16520		1.890	1.86e-06	5.591	4.822	2.930	15.543	14.506	18.246
ABUW_RS16535	tig	-2.316	2.15e-10	3299.880	2519.069	2260.558	535.373	588.823	498.436
ABUW_RS16540		-3.787	4.11e-06	1563.107	3410.447	2663.024	170.449	240.747	141.846
ABUW_RS16545		-1.681	4.79e-09	108.695	105.861	111.191	33.141	38.458	29.849
ABUW_RS16550	leuA	1.337	3.72e-07	336.373	320.103	511.929	985.021	1033.016	934.988
ABUW_RS16580		1.231	0.0184868	1.342	2.301	1.052	3.372	2.804	4.709
ABUW_RS16625	thyA	-1.385	4.36e-07	440.260	335.226	533.792	178.616	179.554	143.107
ABUW_RS16630		-1.326	8.66e-08	67.655	61.369	58.676	24.448	25.842	24.468
ABUW_RS16640	msrA	-1.034	1.94e-05	191.670	301.692	291.050	125.611	149.019	108.381
ABUW_RS16660	purU	-1.078	2.08e-06	166.286	123.723	167.913	69.023	72.712	75.337
ABUW_RS16670		1.300	0.00315791	131.619	417.744	640.099	896.819	987.731	1047.910
ABUW_RS16675	rpmB	-2.473	5.73e-10	5180.574	3458.665	2756.785	683.587	729.492	638.684
ABUW_RS16680	rpmG	-2.643	1.2e-08	64.300	30.575	39.067	7.956	7.253	5.970
ABUW_RS16690		1.603	0.000597188	28.628	28.712	11.420	57.168	56.195	93.078
ABUW_RS16715		1.778	7.07e-06	21.247	29.588	14.350	71.762	47.418	102.748
ABUW_RS16720		-2.630	4.72e-09	36.903	72.218	48.533	8.430	9.691	7.147
ABUW_RS16750		-1.807	1.77e-09	262.456	197.366	223.284	60.224	71.249	63.734
ABUW_RS16770	gltP	-1.263	0.000138594	785.132	417.087	370.987	220.556	218.013	216.594
ABUW_RS16775		1.255	0.000181859	16.103	26.410	46.204	71.815	60.522	82.652
ABUW_RS16780	asd	-1.048	1.38e-06	965.284	935.870	937.160	483.790	459.552	429.153
ABUW_RS16785		-2.355	1.93e-08	66.984	56.437	67.541	11.381	17.370	8.240
ABUW_RS16790		-2.662	6.59e-06	268.607	496.428	487.362	64.333	91.484	41.620
ABUW_RS16795		-1.344	1.81e-07	175.008	147.175	219.527	72.658	68.323	72.562
ABUW_RS16800	truA	-1.603	1.32e-08	74.476	59.834	89.854	25.396	25.659	22.786
ABUW_RS16810	infA	-2.106	3.91e-08	131.955	79.889	92.559	24.658	21.454	24.552
ABUW_RS16815		3.306	5.22e-07	1.342	10.192	3.306	49.528	31.510	63.061
ABUW_RS16835	leuD	1.424	7.42e-06	8.611	16.219	13.448	34.775	39.373	28.672
ABUW_RS16840	leuC	1.497	4.64e-09	86.330	104.217	90.606	263.550	278.047	251.909
ABUW_RS16870	katG	1.202	2.71e-06	310.094	372.595	436.274	1028.595	893.992	651.885
ABUW_RS16885		2.564	2.07e-10	14.761	15.452	12.171	80.930	86.303	82.064
ABUW_RS16890		2.177	7.11e-10	32.206	40.876	32.456	157.856	154.017	164.716
ABUW_RS16915		-1.468	1.87e-07	1458.550	1494.653	1824.809	655.451	593.455	478.257
ABUW_RS16980		-1.890	4.96e-09	58.373	80.437	92.484	18.915	20.052	23.795
ABUW_RS16995		-2.018	5.52e-08	50.881	30.027	34.484	9.063	9.874	9.501
ABUW_RS17000		-1.934	1.22e-06	19.570	10.959	17.430	4.320	4.815	3.279
ABUW_RS17020		-1.622	4.37e-06	50.098	52.821	54.393	17.387	23.282	9.922
ABUW_RS17060		1.047	0.00471459	8.722	9.644	5.334	12.013	16.639	19.759
ABUW_RS17100		1.947	1.26e-08	28.180	47.889	38.166	162.914	127.992	149.749
ABUW_RS17105		3.195	1.07e-09	4.920	8.548	14.049	89.413	74.296	96.189
ABUW_RS17115	pnp	-1.373	2.64e-07	5754.802	5573.359	3730.157	2126.317	2002.401	1684.324
ABUW_RS17120	rpsO	-1.377	7.89e-07	2435.575	1546.377	1906.399	917.684	707.307	641.291
ABUW_RS17125		2.379	6.73e-07	3.914	5.699	2.329	25.765	17.980	15.891
ABUW_RS17145		2.122	2.09e-10	28.404	33.424	35.837	145.211	120.008	161.353
ABUW_RS17190		1.302	4.62e-06	64.636	126.244	91.207	205.856	230.751	258.972
ABUW_RS17210		-1.999	0.0212803	98.966	48.109	859.927	87.042	87.766	77.944
ABUW_RS17225		-1.519	4.55e-06	85.771	69.149	41.621	24.290	22.307	21.525
ABUW_RS17230	infB	-1.926	1.09e-07	10945.776	8162.563	4835.380	2055.345	2307.327	1938.923
ABUW_RS17235	nusA	-2.107	1.17e-07	4961.171	3575.155	1946.894	752.820	853.523	826.355
ABUW_RS17240	rimP	-2.418	2.69e-07	455.580	160.983	252.884	55.218	56.316	50.953
ABUW_RS17265	tpiA	-2.129	4.73e-09	350.463	190.900	266.483	62.173	59.425	63.061
ABUW_RS17270	pilB	-2.515	1.81e-07	353.818	683.163	604.488	104.693	128.662	53.056
ABUW_RS17275		-2.413	3.11e-07	273.080	483.058	511.253	87.516	107.026	42.713
ABUW_RS17285	coaE	-1.495	1.26e-07	74.029	96.875	121.784	36.355	37.240	30.269
ABUW_RS17290		-1.194	1.61e-06	121.891	93.258	94.137	38.305	41.689	55.494
ABUW_RS17295	rlmB	-1.485	2.39e-07	191.223	112.655	143.572	56.430	51.623	51.626
ABUW_RS17325		-1.080	6.96e-05	40.257	33.753	34.334	13.594	16.029	22.029
ABUW_RS17330		-2.038	0.00679326	6.710	2.959	2.404	0.000	0.792	2.522
ABUW_RS17335		-2.087	2.46e-06	73.358	24.219	42.748	12.224	8.289	12.528
ABUW_RS17360		1.662	1.79e-06	8.722	7.233	9.391	19.231	29.255	32.708
ABUW_RS17370		-2.711	8.92e-06	49.875	10.082	29.526	4.320	6.339	2.691
ABUW_RS17380		1.326	5.59e-05	160.918	145.422	85.497	226.879	457.906	295.379
ABUW_RS17385	fadB	1.223	1.27e-06	941.241	1140.578	1271.709	1912.084	2907.852	3011.217
ABUW_RS17390	fadA	1.308	1.42e-07	392.846	427.936	564.745	1029.806	1163.263	1238.271
ABUW_RS17395		2.647	1.83e-08	4.249	7.014	4.132	34.827	24.379	36.155
ABUW_RS17400		2.601	1.66e-07	9.170	7.342	7.438	48.737	26.513	70.208
ABUW_RS17410		3.421	1.24e-09	2.460	4.603	3.155	31.719	35.228	42.461
ABUW_RS17420		2.062	3.03e-07	72.352	161.640	168.740	635.640	405.429	643.897
ABUW_RS17435		1.467	0.000685486	25.161	4.603	17.881	49.053	31.267	52.131
ABUW_RS17440		-2.843	4.3e-08	3072.650	3674.770	2695.179	476.941	645.140	192.463
ABUW_RS17445		-2.806	2.37e-10	682.364	435.936	401.339	73.923	78.441	64.575
ABUW_RS17450		1.202	0.000167474	17.221	32.109	44.476	60.750	69.055	88.706
ABUW_RS17460		1.975	9.77e-05	1.566	1.753	0.826	6.533	4.571	4.288
ABUW_RS17465		-1.816	0.00347433	2.572	2.192	2.404	0.685	0.914	0.336
ABUW_RS17480	rplL	-2.001	1.56e-07	2541.251	1968.505	1152.705	444.642	529.642	439.663
ABUW_RS17485	rplJ	-2.293	2.45e-09	9005.367	6249.070	5654.813	1507.538	1630.189	1127.283
ABUW_RS17490	rplA	-2.046	5.05e-07	8709.139	5362.295	3244.147	1323.337	1593.986	1276.612
ABUW_RS17495	rplK	-2.162	1.42e-07	5702.244	3392.584	2287.228	827.586	982.368	732.520
ABUW_RS17500	nusG	-2.187	2.99e-05	3262.083	1037.347	853.165	305.280	399.395	426.799
ABUW_RS17505	secE	-2.175	7.92e-06	2847.320	865.077	984.791	281.517	357.707	401.238

Locustag	Gene	logFC	PValue	LCWB_1	LCWB_2	LCWB_3	M9_1	M9_2	M9_3
ABUW_RS17515	tuf	-3.127	1.01e-09	11612.148	6724.457	5044.614	907.568	1056.176	712.760
ABUW_RS17590		-1.859	1.75e-07	49.875	44.711	73.101	16.123	19.199	10.678
ABUW_RS17600		2.165	1.24e-09	24.490	28.383	27.272	127.718	116.594	115.360
ABUW_RS17610	argH	-1.033	2.84e-07	620.412	635.493	694.944	343.269	330.158	280.076
ABUW_RS17615		-1.412	2.25e-06	22.365	39.013	29.826	11.486	12.251	10.426
ABUW_RS17645	thiC	2.955	3.84e-10	35.002	70.793	55.295	481.999	441.328	325.985
ABUW_RS17660	dksA	-1.005	3.14e-06	386.695	252.159	323.205	161.808	153.224	164.464
ABUW_RS17665	gluQRS	-1.114	0.000149295	98.183	48.876	99.696	42.415	42.786	28.588
ABUW_RS17675	murD	-1.115	4.5e-06	234.052	178.626	234.853	123.925	88.071	86.772
ABUW_RS17695	xerD	-1.020	0.000703502	27.845	48.218	60.479	23.815	24.501	19.171
ABUW_RS17700		-1.065	8.32e-08	295.445	320.979	295.182	138.151	151.579	146.050
ABUW_RS17710	thrC	-1.237	3.18e-08	1428.916	1392.956	1556.899	629.107	656.903	571.419
ABUW_RS17715	pbpG	1.202	7e-07	499.304	772.367	690.210	1556.117	1371.950	1585.360
ABUW_RS17730		-2.884	7.35e-08	191.223	420.265	423.728	42.678	66.982	30.185
ABUW_RS17805		-1.111	0.00165813	9.953	18.958	11.344	3.741	7.619	7.483
ABUW_RS17815		1.105	8.04e-05	44.730	69.259	102.326	150.691	159.319	157.737
ABUW_RS17820		-1.111	2.28e-05	137.882	130.079	78.735	58.274	50.648	51.122
ABUW_RS17825		-1.151	0.000363108	55.466	39.670	23.365	19.758	18.711	14.126
ABUW_RS17845	cadR	1.012	0.00164978	38.580	73.204	33.658	106.590	100.565	84.502
ABUW_RS17850		1.288	0.000619326	5.703	3.178	6.161	10.801	10.910	16.060
ABUW_RS17895		1.095	2.45e-06	22.477	27.068	23.515	46.735	56.134	53.224
ABUW_RS17925		5.473	1.15e-12	3.019	2.411	1.578	96.842	112.328	92.490
ABUW_RS17930		4.622	3.37e-12	3.355	2.411	2.028	55.429	71.371	61.380
ABUW_RS17945	ppa	-1.771	5.99e-10	414.428	430.456	376.922	123.714	123.421	110.567
ABUW_RS17975		-1.416	4.95e-05	76.825	28.712	44.101	20.865	16.334	18.666
ABUW_RS17980		-1.346	9.05e-05	12.972	8.219	11.194	3.267	5.059	4.540
ABUW_RS18015		2.972	1.87e-06	2.684	13.260	3.456	56.272	46.260	45.152
ABUW_RS18020		-1.267	0.00288772	306.851	72.656	109.012	60.329	61.497	81.139
ABUW_RS18030		1.447	0.00407357	1.677	1.425	1.427	2.108	5.181	5.381
ABUW_RS18045		1.119	0.00206666	5.815	3.616	8.865	15.649	11.336	13.958
ABUW_RS18090		2.030	7.28e-08	20.576	24.986	18.482	65.282	81.244	114.603
ABUW_RS18115		-3.163	1.51e-10	258.207	407.882	328.089	40.623	44.492	25.309
ABUW_RS18120	dprA	-3.199	3.53e-10	98.183	119.340	102.401	11.592	16.029	6.727
ABUW_RS18150		1.192	0.00458622	71.569	113.313	117.126	136.991	120.556	435.375
ABUW_RS18160		-1.281	7.12e-07	5264.779	5944.200	4245.166	1997.334	2601.220	1761.259
ABUW_RS18165	atpD	-1.092	1.37e-06	12114.248	11456.300	10533.242	5926.511	5741.713	4326.170
ABUW_RS18170	atpG	-1.352	3.98e-07	12019.084	11761.060	9769.480	4522.929	5341.952	3277.924
ABUW_RS18175	atpA	-1.170	2.2e-06	14757.485	12975.281	11207.299	6430.112	6519.659	4353.497
ABUW_RS18180		-1.463	1.83e-07	4060.970	3354.777	3185.922	1406.954	1504.330	934.904
ABUW_RS18185		-1.414	6.99e-07	3764.854	3023.058	2901.108	1461.804	1347.327	826.523
ABUW_RS18190	atpE	-1.269	5.41e-06	3352.103	3280.258	1842.840	1151.518	1305.821	1059.009
ABUW_RS18195	atpB	-1.495	1.62e-06	8202.902	5331.611	4485.654	2264.837	2425.262	1702.486
ABUW_RS18200		-2.892	6.45e-06	877.389	231.337	223.734	72.184	53.635	53.224
ABUW_RS18220	znuB	-1.009	1.61e-05	179.593	289.199	206.981	125.294	108.245	101.907
ABUW_RS18280	guaA	-1.630	3.15e-07	2369.374	1335.533	1401.307	580.527	524.705	544.429
ABUW_RS18290		1.936	1.19e-05	2.796	5.699	3.080	16.439	11.215	16.060
ABUW_RS18390		2.110	3.38e-06	3.578	3.726	2.930	19.442	13.165	10.594
ABUW_RS18395		-2.435	0.0237972	22.365	520.975	21.111	43.416	33.339	26.738
ABUW_RS18410		2.343	8.09e-07	2.907	4.274	2.179	16.228	17.431	12.360
ABUW_RS18420		2.656	2.84e-07	4.473	3.068	2.855	27.767	23.221	12.864
ABUW_RS18425		1.619	1.36e-05	3.019	4.603	3.381	12.593	12.616	8.072
ABUW_RS18430		-1.090	0.000101582	352.588	284.268	165.810	144.315	117.204	114.856
ABUW_RS18435		-2.895	2.9e-11	242.439	241.419	285.190	38.516	36.569	27.999
ABUW_RS18440		-3.471	1.65e-09	143.585	160.325	318.171	25.238	14.932	15.639
ABUW_RS18445	alr	-2.168	0.000391993	210.233	133.257	809.591	96.632	69.116	91.481
ABUW_RS18450		-1.658	1.74e-06	516.637	920.309	965.709	241.632	202.471	317.913
ABUW_RS18460		2.452	0.00491292	5.479	9.096	6.311	92.627	9.447	9.753
ABUW_RS18465		1.839	0.0459164	30.081	56.875	73.626	504.971	43.091	27.495
ABUW_RS18470		2.253	6.42e-10	33.883	38.355	41.321	205.276	150.543	186.661
ABUW_RS18475		2.569	1.27e-09	21.247	24.109	32.831	154.748	133.904	179.010
ABUW_RS18480		-2.003	0.000284687	22.477	3.288	17.280	3.161	4.266	3.363
ABUW_RS18485		2.167	1.04e-06	3.467	5.041	2.855	14.753	16.700	18.834
ABUW_RS18490		1.908	6.8e-07	4.026	2.959	3.982	14.489	13.652	13.285
ABUW_RS18515		1.819	1.48e-05	16.886	29.150	15.101	54.849	73.443	86.184
ABUW_RS18520		2.952	0.0142928	2.684	5.260	2.630	24.395	30.291	25.561
ABUW_RS18525	acnD	1.394	6.75e-07	317.027	281.966	295.332	986.865	771.913	590.506
ABUW_RS18530	prpC	1.290	3.94e-06	92.033	87.998	94.663	282.518	228.862	159.839
ABUW_RS18550	dld	-2.319	4.94e-07	181.829	125.148	111.041	30.191	23.526	30.017
ABUW_RS18555	lldD	-2.773	1.38e-08	441.378	487.003	399.311	71.130	66.190	56.671
ABUW_RS18560	lldR	-2.756	1.35e-07	88.902	79.998	67.992	13.805	10.178	10.847
ABUW_RS18565	lldP	-4.088	4.78e-09	652.059	561.193	499.833	37.040	31.571	31.951
ABUW_RS18620		-1.102	2.75e-05	227.566	194.955	174.900	76.030	86.852	115.780
ABUW_RS18635	wecC	-1.016	6.37e-07	3310.280	3737.563	3643.308	1876.044	1922.254	1486.732
ABUW_RS18640	wecB	-1.083	4.92e-07	2534.765	2822.076	2569.488	1288.615	1425.585	1026.217
ABUW_RS18660		-1.094	7.91e-07	1028.466	1019.156	797.495	445.591	470.766	416.372
ABUW_RS18685	nadC	-1.540	2.67e-07	165.056	100.272	170.092	48.210	58.145	43.302
ABUW_RS18700	rph	-1.533	5.08e-09	195.249	208.105	184.893	72.974	62.899	67.349
ABUW_RS18750		-3.236	5.32e-08	61.504	26.958	32.756	3.319	5.120	4.456
ABUW_RS18805	ileS	-1.170	1.98e-07	1467.048	1563.911	1796.786	788.175	749.362	607.658
ABUW_RS18815		-1.299	1.07e-06	450.324	493.469	406.899	143.788	242.453	162.698
ABUW_RS18820		1.824	9.82e-07	23.819	36.931	52.741	150.638	94.226	160.428
ABUW_RS18825		-1.645	0.0229264	2.348	3.397	0.902	0.158	1.097	0.841
ABUW_RS18865		3.113	0.0125733	0.335	0.110	0.000	1.739	0.305	1.429
ABUW_RS18870		1.990	1.97e-07	6.933	7.123	7.588	31.297	20.479	34.810
ABUW_RS18900		-1.080	0.0432495	5.815	2.849	0.977	1.317	1.707	1.177
ABUW_RS18915		-1.177	1.88e-05	488.569	231.118	376.246	174.664	160.112	149.749
ABUW_RS18920	purE	-1.107	1.75e-05	686.837	374.019	514.484	231.199	287.921	212.138
ABUW_RS18930	mpl	-1.226	2.4e-08	313.896	360.869	408.477	156.961	158.283	147.984
ABUW_RS18940		-2.525	7.3e-10	37.574	34.191	30.953	5.058	5.303	7.736
ABUW_RS18950		-1.282	0.000169041	33.772	25.315	33.132	14.858	8.655	14.546
ABUW_RS18955		-2.175	1.63e-07	51.999	38.794	54.619	11.434	12.373	8.156
ABUW_RS18965	guaD	-1.155	5.66e-07	127.482	164.928	175.501	76.821	68.079	65.247
ABUW_RS18975	hpt	-1.318	0.000135844	44.730	26.849	32.080	10.064	11.215	20.936
ABUW_RS18980		4.313	5.01e-11	5.591	10.192	10.518	206.067	114.827	209.027
ABUW_RS19000	mnmE	-1.442	1.78e-06	134.303	73.204	95.790	40.518	40.165	30.522
ABUW_RS19005	yidC	-1.923	1.07e-08	3424.119	2429.975	1963.948	679.530	779.592	602.361
ABUW_RS19010	yidD	-2.532	2.49e-09	350.687	201.530	184.592	40.676	49.673	36.744
ABUW_RS19015	rnpA	-2.178	6.09e-09	666.149	399.005	362.197	111.016	107.026	96.946
ABUW_RS19020	rpmH	-2.145	3.82e-08	267.824	169.750	138.838	42.467	45.650	41.957
ABUW_RS19650		1.170	1.2e-05	99.078	66.738	64.010	165.654	158.344	192.463
ABUW_RS19705		-1.084	0.000362939	13.866	15.890	15.401	5.164	9.630	6.558
ABUW_RS19720		3.726	1.88e-10	1443.341	621.795	1027.014	16192.224	11041.671	13673.782
ABUW_RS19925		1.957	0.0412736	0.000	0.548	0.150	0.896	0.914	0.841
ABUW_RS20090		4.273	5.48e-09	0.224	0.219	0.376	5.901	4.998	6.138
ABUW_RS20100		-1.207	0.0028987	5.368	2.411	4.508	1.949	1.280	2.186
ABUW_RS20110		-1.614	1.77e-06	124.686	79.998	65.137	32.878	29.072	25.729
ABUW_RS20125		1.675	0.000483009	3.914	1.534	1.202	8.061	3.901	8.408

Locustag	Gene	logFC	PValue	LCWB_1	LCWB_2	LCWB_3	M9_1	M9_2	M9_3
ABUW_RS20155		2.733	0.0018048	0.000	0.219	0.601	2.424	0.731	3.531
ABUW_RS20200		2.237	0.00125557	1.006	0.767	0.150	2.951	1.646	3.868
ABUW_RS20205		2.566	5.6e-07	8.946	3.178	7.889	41.255	24.806	54.317
ABUW_RS20235		-1.443	0.00296275	1.677	4.274	1.878	0.474	1.707	0.589
ABUW_RS20260		-2.334	0.000450164	8.499	2.520	4.658	0.527	0.427	2.522
ABUW_RS20265		-1.814	0.0417821	3.243	2.630	0.902	0.211	0.853	0.841
ABUW_RS20270		3.137	0.00195558	0.224	0.000	0.150	1.212	0.488	2.018
ABUW_RS20285		-1.116	0.0139077	8.499	22.027	6.837	3.477	5.607	8.324
ABUW_RS20295		4.464	1.15e-07	0.447	0.000	0.451	7.324	4.876	9.585
ABUW_RS20305		2.309	4.63e-06	3.914	3.288	1.052	11.750	13.226	13.621
ABUW_RS20335		-2.325	0.000816283	4.809	1.753	2.930	0.369	0.488	1.177
ABUW_RS20380		1.090	2.85e-05	27.509	23.013	41.471	68.654	62.899	65.836
ABUW_RS20390		1.213	0.00707062	1.677	5.370	1.352	5.269	6.643	6.811
ABUW_RS20475		9.138	4.05e-07	0.000	0.000	0.000	3.741	2.926	5.381
ABUW_RS20510		2.270	2.94e-05	8.275	13.808	2.028	37.304	29.499	44.563
ABUW_RS20565		1.016	0.0340013	2.796	0.986	1.127	2.740	4.510	2.186
ABUW_RS20610		-2.784	0.000273777	1.006	1.534	2.930	0.105	0.427	0.336
ABUW_RS20630		4.321	0.000221337	0.000	0.110	0.225	1.949	1.280	5.381
ABUW_RS20640		-2.544	0.0260348	0.447	3.507	0.225	0.316	0.000	0.336
ABUW_RS20660		3.113	0.000519065	0.112	0.329	0.376	2.793	1.707	3.195
ABUW_RS20665		-1.909	0.0402743	1.454	1.205	1.052	0.158	0.427	0.420
ABUW_RS20695		3.948	0.000440502	0.112	0.219	0.000	1.159	1.707	2.018
ABUW_RS20705		6.694	7.03e-12	10.847	16.438	11.870	1782.153	572.855	1687.267
ABUW_RS20715		-2.150	6.98e-08	181.382	263.227	349.801	65.650	73.870	39.014
ABUW_RS20790		1.013	0.00457055	3.914	3.178	3.080	5.690	7.862	6.895

2.4 Enrichment Analysis (GSEA) of *A. baumannii* in LCWB medium vs in LB Broth Up Regulated

ClassID	Class	Description	Single_list
P	COG	METABOLISM; Inorganic ion transport and metabolism	0;22/108;0.00014;ABUW_RS00790,ABUW_RS01270,ABUW_RS04990,ABUW_RS04995,ABUW_RS05000,ABUW_RS05460,ABUW_RS05725,ABUW_RS05730,ABUW_RS05735,ABUW_RS05740,ABUW_RS05745,ABUW_RS08070,ABUW_RS08765,ABUW_RS10305,ABUW_RS10520,ABUW_RS11380,ABUW_RS13790,ABUW_RS14200,ABUW_RS15170,ABUW_RS16540,ABUW_RS17210,ABUW_RS18220
COG3433	eggNOG_COG	isochorismatase activity	9;2/2;0.00000;ABUW_RS05765,ABUW_RS10075
COG4264	eggNOG_COG	IucA IucC family	9;2/2;0.00000;ABUW_RS10620,ABUW_RS10625
COG4773	eggNOG_COG	Receptor	9;2/2;0.00000;ABUW_RS08070,ABUW_RS10520
COG0697	eggNOG_COG	spore germination	0;2/8;0.03031;ABUW_RS07865,ABUW_RS16105
COG1132	eggNOG_COG	(ABC) transporter	2;3/4;0.00010;ABUW_RS05780,ABUW_RS05785,ABUW_RS10985
COG1020	eggNOG_COG	D-alanine [D-alanyl carrier protein] ligase activity	2;3/5;0.00042;ABUW_RS05715,ABUW_RS05720,ABUW_RS05755
COG2233	eggNOG_COG	PERMEase	2;2/3;0.00083;ABUW_RS00150,ABUW_RS03220
COG0834	eggNOG_COG	ABC-type amino acid transport signal transduction systems periplasmic component domain	2;2/3;0.00083;ABUW_RS11775,ABUW_RS11780
COG4774	eggNOG_COG	siderophore transport	9;4/4;0.00000;ABUW_RS00790,ABUW_RS05745,ABUW_RS08765,ABUW_RS16540
COG1535	eggNOG_COG	isochorismatase	9;2/2;0.00000;ABUW_RS05765,ABUW_RS10075
GO:0005315	GO	inorganic phosphate transmembrane transporter activity	1; 2/ 4;5.5e-03;ABUW_RS05460,ABUW_RS14200
GO:0019285	GO	glycine betaine biosynthetic process from choline	1; 3/ 5;8.9e-04;ABUW_RS14420,ABUW_RS14425,ABUW_RS14430
GO:0004748	GO	ribonucleoside-diphosphate reductase activity, thioredoxin disulfide as acceptor	9; 2/ 2;0.0e+00;ABUW_RS15460,ABUW_RS15470
GO:0006212	GO	uracil catabolic process	9; 2/ 2;0.0e+00;ABUW_RS00150,ABUW_RS15515
GO:0016765	GO	transferase activity, transferring alkyl or aryl (other than methyl) groups	1; 3/ 6;2.0e-03;ABUW_RS03020,ABUW_RS05765,ABUW_RS10075
GO:0015419	GO	ABC-type sulfate transporter activity	2; 3/ 4;2.3e-04;ABUW_RS04990,ABUW_RS04995,ABUW_RS05000
GO:0006811	GO	monoatomic ion transport	0; 5/ 17;5.4e-03;ABUW_RS05725,ABUW_RS05730,ABUW_RS05735,ABUW_RS14505,ABUW_RS15655
GO:0097216	GO	guanosine tetraphosphate binding	1; 4/ 10;2.3e-03;ABUW_RS03225,ABUW_RS05050,ABUW_RS16275,ABUW_RS18930
GO:0006353	GO	DNA-templated transcription termination	2; 3/ 4;2.3e-04;ABUW_RS15915,ABUW_RS17235,ABUW_RS17500
GO:0036009	GO	protein-glutamine N-methyltransferase activity	9; 2/ 2;0.0e+00;ABUW_RS07660,ABUW_RS10385
GO:0055072	GO	iron ion homeostasis	9;15/ 18;4.4e-15;ABUW_RS00790,ABUW_RS05725,ABUW_RS05730,ABUW_RS05735,ABUW_RS05740,ABUW_RS05745,ABUW_RS08035,ABUW_RS08070,ABUW_RS08765,ABUW_RS10520,ABUW_RS10605,ABUW_RS14160,ABUW_RS14505,ABUW_RS16540,ABUW_RS17685
GO:0009263	GO	deoxyribonucleotide biosynthetic process	9; 2/ 2;0.0e+00;ABUW_RS15460,ABUW_RS15470
GO:0016881	GO	acid-amino acid ligase activity	3; 4/ 5;2.2e-05;ABUW_RS10620,ABUW_RS10625,ABUW_RS10640,ABUW_RS18930
GO:0019904	GO	protein domain specific binding	9; 2/ 2;0.0e+00;ABUW_RS00790,ABUW_RS17235
GO:0000027	GO	ribosomal large subunit assembly	1; 2/ 3;2.0e-03;ABUW_RS01870,ABUW_RS03225
GO:0031564	GO	transcription antitermination	2; 3/ 4;2.3e-04;ABUW_RS01865,ABUW_RS17235,ABUW_RS17500
GO:0009254	GO	peptidoglycan turnover	0; 2/ 8;4.9e-02;ABUW_RS11020,ABUW_RS18930
GO:0047527	GO	2,3-dihydroxybenzoate-serine ligase activity	9; 2/ 2;0.0e+00;ABUW_RS05765,ABUW_RS10075
GO:0009239	GO	enterobactin biosynthetic process	9; 3/ 3;0.0e+00;ABUW_RS05765,ABUW_RS05800,ABUW_RS10075
GO:0016874	GO	ligase activity	0; 4/ 11;3.8e-03;ABUW_RS05715,ABUW_RS05720,ABUW_RS05755,ABUW_RS05760
GO:1902495	GO	transmembrane transporter complex	1; 3/ 6;2.0e-03;ABUW_RS00790,ABUW_RS08070,ABUW_RS10520
GO:0006749	GO	glutathione metabolic process	0; 2/ 6;2.1e-02;ABUW_RS10310,ABUW_RS10315
GO:0071281	GO	cellular response to iron ion	9; 2/ 2;0.0e+00;ABUW_RS10080,ABUW_RS14475
GO:0018364	GO	peptidyl-glutamine methylation	9; 2/ 2;0.0e+00;ABUW_RS07660,ABUW_RS10385
GO:0042274	GO	ribosomal small subunit biogenesis	1; 2/ 4;5.5e-03;ABUW_RS01580,ABUW_RS17240
GO:0043022	GO	ribosome binding	1; 4/ 8;8.4e-04;ABUW_RS01580,ABUW_RS03225,ABUW_RS05050,ABUW_RS11390
GO:0019752	GO	carboxylic acid metabolic process	0; 2/ 8;4.9e-02;ABUW_RS05720,ABUW_RS05770
GO:0071555	GO	cell wall organization	0; 8/ 47;3.3e-02;ABUW_RS03590,ABUW_RS04555,ABUW_RS05255,ABUW_RS06080,ABUW_RS07375,ABUW_RS08460,ABUW_RS11020,ABUW_RS18930
GO:0031177	GO	phosphopantetheine binding	1; 3/ 7;4.1e-03;ABUW_RS05720,ABUW_RS05765,ABUW_RS10075
GO:0010468	GO	regulation of gene expression	0; 2/ 5;1.2e-02;ABUW_RS06720,ABUW_RS13055
GO:0019646	GO	aerobic electron transport chain	0; 3/ 10;1.6e-02;ABUW_RS08730,ABUW_RS08735,ABUW_RS08740
GO:0009252	GO	peptidoglycan biosynthetic process	0; 6/ 35;5.0e-02;ABUW_RS03590,ABUW_RS05255,ABUW_RS06080,ABUW_RS08460,ABUW_RS11020,ABUW_RS18930
GO:1901576	GO	organic substance biosynthetic process	1; 2/ 3;2.0e-03;ABUW_RS05715,ABUW_RS05755
GO:0006119	GO	oxidative phosphorylation	9; 2/ 2;0.0e+00;ABUW_RS08730,ABUW_RS08735
GO:0070069	GO	cytochrome complex	1; 3/ 5;8.9e-04;ABUW_RS08730,ABUW_RS08735,ABUW_RS08740
GO:0019867	GO	outer membrane	9; 2/ 2;0.0e+00;ABUW_RS08730,ABUW_RS14160
GO:0140359	GO	ABC-type transporter activity	1; 3/ 6;2.0e-03;ABUW_RS05780,ABUW_RS05785,ABUW_RS10985
GO:0043708	GO	cell adhesion involved in biofilm formation	0; 2/ 6;2.1e-02;ABUW_RS07605,ABUW_RS07610

ClassID	Class	Description	Single_list
GO:0009279	GO	cell outer membrane	1;17/ 62;1.0e-05;ABUW_RS00710,ABUW_RS00790,ABUW_RS04555,ABUW_RS05745,ABUW_RS07605,ABUW_RS08035,ABUW_RS08070,ABUW_RS08480,ABUW_RS08765,ABUW_RS08775,ABUW_RS10520,ABUW_RS10605,ABUW_RS13745,ABUW_RS14160,ABUW_RS14485,ABUW_RS14495,ABUW_RS16540
GO:0042254	GO	ribosome biogenesis	1; 3/ 5;8.9e-04;ABUW_RS01865,ABUW_RS15105,ABUW_RS17235
GO:0032784	GO	regulation of DNA-templated transcription elongation	1; 2/ 4;5.5e-03;ABUW_RS17235,ABUW_RS17500
GO:0000270	GO	peptidoglycan metabolic process	0; 2/ 6;2.1e-02;ABUW_RS04555,ABUW_RS05255
GO:0005525	GO	GTP binding	0; 8/ 40;1.2e-02;ABUW_RS03020,ABUW_RS03205,ABUW_RS03225,ABUW_RS05050,ABUW_RS05130,ABUW_RS11390,ABUW_RS16275,ABUW_RS17685
GO:0019290	GO	siderophore biosynthetic process	4; 5/ 6;2.1e-06;ABUW_RS05760,ABUW_RS10080,ABUW_RS10620,ABUW_RS10625,ABUW_RS10640
GO:0003676	GO	nucleic acid binding	0; 5/ 17;5.4e-03;ABUW_RS03215,ABUW_RS06720,ABUW_RS07660,ABUW_RS10385,ABUW_RS13055
GO:0016149	GO	translation release factor activity, codon specific	9; 2/ 2;0.0e+00;ABUW_RS07655,ABUW_RS16275
GO:0050313	GO	sulfur dioxygenase activity	1; 2/ 4;5.5e-03;ABUW_RS10310,ABUW_RS10315
GO:0001000	GO	bacterial-type RNA polymerase core enzyme binding	9; 2/ 2;0.0e+00;ABUW_RS14505,ABUW_RS17235
GO:0008908	GO	isochorismatase activity	9; 2/ 2;0.0e+00;ABUW_RS05765,ABUW_RS10075
GO:0015344	GO	siderophore uptake transmembrane transporter activity	6;11/ 15;2.6e-10;ABUW_RS00710,ABUW_RS00790,ABUW_RS05745,ABUW_RS08035,ABUW_RS08070,ABUW_RS08765,ABUW_RS10520,ABUW_RS10605,ABUW_RS13745,ABUW_RS14160,ABUW_RS16540
GO:0043190	GO	ATP-binding cassette (ABC) transporter complex	0; 3/ 14;5.0e-02;ABUW_RS01885,ABUW_RS04990,ABUW_RS18220
GO:0045727	GO	positive regulation of translation	9; 2/ 2;0.0e+00;ABUW_RS01870,ABUW_RS05050
GO:0006740	GO	NADPH regeneration	1; 2/ 3;2.0e-03;ABUW_RS16095,ABUW_RS16100
GO:0038023	GO	signaling receptor activity	8;11/ 14;5.8e-11;ABUW_RS00710,ABUW_RS00790,ABUW_RS05745,ABUW_RS08035,ABUW_RS08070,ABUW_RS08765,ABUW_RS10520,ABUW_RS10605,ABUW_RS13745,ABUW_RS14160,ABUW_RS16540
GO:0019289	GO	rhizobactin 1021 biosynthetic process	9; 3/ 3;0.0e+00;ABUW_RS05750,ABUW_RS10635,ABUW_RS10640
GO:0005886	GO	plasma membrane	0;71/518;1.2e-05;ABUW_RS00150,ABUW_RS00510,ABUW_RS00570,ABUW_RS01050,ABUW_RS01160,ABUW_RS01270,ABUW_RS01610,ABUW_RS01660,ABUW_RS01885,ABUW_RS03110,ABUW_RS03210,ABUW_RS03220,ABUW_RS03590,ABUW_RS04140,ABUW_RS04880,ABUW_RS04885,ABUW_RS04995,ABUW_RS05000,ABUW_RS05050,ABUW_RS05130,ABUW_RS05150,ABUW_RS05255,ABUW_RS05405,ABUW_RS05460,ABUW_RS05725,ABUW_RS05730,ABUW_RS05735,ABUW_RS05740,ABUW_RS05765,ABUW_RS05780,ABUW_RS05785,ABUW_RS05815,ABUW_RS06080,ABUW_RS06605,ABUW_RS07560,ABUW_RS07610,ABUW_RS07795,ABUW_RS07865,ABUW_RS08465,ABUW_RS08730,ABUW_RS08735,ABUW_RS08740,ABUW_RS08830,ABUW_RS10075,ABUW_RS10165,ABUW_RS10305,ABUW_RS10630,ABUW_RS10985,ABUW_RS11380,ABUW_RS11710,ABUW_RS11715,ABUW_RS11765,ABUW_RS11775,ABUW_RS13375,ABUW_RS13640,ABUW_RS13790,ABUW_RS14200,ABUW_RS14415,ABUW_RS14450,ABUW_RS15655,ABUW_RS15960,ABUW_RS16095,ABUW_RS16105,ABUW_RS16650,ABUW_RS17210,ABUW_RS17445,ABUW_RS17505,ABUW_RS17685,ABUW_RS17975,ABUW_RS18220,ABUW_RS18705
GO:0015675	GO	nickel cation transport	1; 2/ 3;2.0e-03;ABUW_RS00710,ABUW_RS13745
GO:0003723	GO	RNA binding	0; 8/ 39;1.1e-02;ABUW_RS01605,ABUW_RS01865,ABUW_RS01870,ABUW_RS02315,ABUW_RS05270,ABUW_RS13055,ABUW_RS15915,ABUW_RS17235
GO:0008802	GO	betaine-aldehyde dehydrogenase activity	1; 2/ 4;5.5e-03;ABUW_RS14425,ABUW_RS14430
GO:0006829	GO	zinc ion transport	1; 3/ 5;8.9e-04;ABUW_RS00710,ABUW_RS13745,ABUW_RS18220
IPR039261	IPR	Ferredoxin-NADP reductase (FNR), nucleotide-binding domain	0; 3/12;2.2e-02;ABUW_RS03435,ABUW_RS05400,ABUW_RS18710
IPR036640	IPR	ABC transporter type 1, transmembrane domain superfamily	1; 3/ 6;1.6e-03;ABUW_RS05780,ABUW_RS05785,ABUW_RS10985
IPR029021	IPR	Protein-tyrosine phosphatase-like	1; 2/ 3;1.6e-03;ABUW_RS10310,ABUW_RS10315
IPR039426	IPR	TonB-dependent receptor-like	1; 4/ 9;1.4e-03;ABUW_RS08035,ABUW_RS10605,ABUW_RS14160,ABUW_RS14495
IPR006043	IPR	Nucleobase cation symporter 2 family	2; 3/ 4;2.2e-04;ABUW_RS00150,ABUW_RS03220,ABUW_RS13375
IPR010071	IPR	Amino acid adenylation domain	1; 3/ 6;1.6e-03;ABUW_RS05715,ABUW_RS05720,ABUW_RS05755
IPR006042	IPR	Xanthine/uracil permease	1; 2/ 3;1.6e-03;ABUW_RS00150,ABUW_RS03220
IPR010917	IPR	TonB-dependent receptor, conserved site	3; 7/11;1.4e-06;ABUW_RS00790,ABUW_RS05745,ABUW_RS08070,ABUW_RS08765,ABUW_RS10520,ABUW_RS10605,ABUW_RS14160
IPR001638	IPR	Solute-binding protein family 3/N-terminal domain of MltF	0; 3/11;1.7e-02;ABUW_RS04555,ABUW_RS11775,ABUW_RS11780
IPR001433	IPR	Oxidoreductase FAD/NAD(P)-binding	0; 3/12;2.2e-02;ABUW_RS03435,ABUW_RS05400,ABUW_RS18710
IPR010105	IPR	TonB-dependent siderophore receptor	8;11/14;4.5e-11;ABUW_RS00710,ABUW_RS00790,ABUW_RS05745,ABUW_RS08035,ABUW_RS08070,ABUW_RS08765,ABUW_RS10520,ABUW_RS10605,ABUW_RS13745,ABUW_RS14160,ABUW_RS16540
IPR012910	IPR	TonB-dependent receptor, plug domain	5;12/19;6.2e-10;ABUW_RS00710,ABUW_RS00790,ABUW_RS05745,ABUW_RS08035,ABUW_RS08070,ABUW_RS08765,ABUW_RS10520,ABUW_RS10605,ABUW_RS13745,ABUW_RS14160,ABUW_RS14495,ABUW_RS16540
IPR044528	IPR	Persulfide dioxygenase-like, MBL-fold metallo-hydrolase domain	1; 2/ 4;4.6e-03;ABUW_RS10310,ABUW_RS10315
IPR037066	IPR	TonB-dependent receptor, plug domain superfamily	5;12/19;6.2e-10;ABUW_RS00710,ABUW_RS00790,ABUW_RS05745,ABUW_RS08035,ABUW_RS08070,ABUW_RS08765,ABUW_RS10520,ABUW

ClassID	Class	Description	Single_list
			RS10605,ABUW_RS13745,ABUW_RS14160,ABUW_RS14495,ABUW_RS16540
IPR005939	IPR	Beta-lactamase hydrolase-like protein, phosphatase-like domain	1; 2/ 3;1.6e-03;ABUW_RS10310,ABUW_RS10315
IPR011527	IPR	ABC transporter type 1, transmembrane domain	1; 3/ 5;9.3e-04;ABUW_RS05780,ABUW_RS05785,ABUW_RS10985
IPR000795	IPR	Translational (tr)-type GTP-binding domain	0; 3/ 8;5.3e-03;ABUW_RS03225,ABUW_RS05050,ABUW_RS16275
IPR025110	IPR	AMP-binding enzyme, C-terminal domain	0; 4/14;8.4e-03;ABUW_RS05715,ABUW_RS05720,ABUW_RS05755,ABUW_RS05760
IPR005804	IPR	Fatty acid desaturase domain	1; 2/ 3;1.6e-03;ABUW_RS05405,ABUW_RS18705
IPR002052	IPR	DNA methylase, N-6 adenine-specific, conserved site	1; 4/ 8;7.7e-04;ABUW_RS02315,ABUW_RS03215,ABUW_RS07660,ABUW_RS10385
IPR002059	IPR	Cold-shock protein, DNA-binding	1; 2/ 4;4.6e-03;ABUW_RS06720,ABUW_RS13055
IPR036736	IPR	ACP-like superfamily	1; 4/ 9;1.4e-03;ABUW_RS05720,ABUW_RS05760,ABUW_RS05765,ABUW_RS10075
IPR009000	IPR	Translation protein, beta-barrel domain superfamily	0; 3/10;1.3e-02;ABUW_RS01580,ABUW_RS03225,ABUW_RS16275
IPR031157	IPR	Tr-type G domain, conserved site	1; 3/ 7;3.4e-03;ABUW_RS03225,ABUW_RS05050,ABUW_RS16275
IPR036380	IPR	Isochorismatase-like superfamily	0; 2/ 6;1.7e-02;ABUW_RS05765,ABUW_RS10075
IPR000873	IPR	AMP-dependent synthetase/ligase domain	0; 4/16;1.5e-02;ABUW_RS05715,ABUW_RS05720,ABUW_RS05755,ABUW_RS05760
IPR000531	IPR	TonB-dependent receptor-like, beta-barrel	5;12/19;6.2e-10;ABUW_RS00710,ABUW_RS00790,ABUW_RS05745,ABUW_RS08035,ABUW_RS08070,ABUW_RS08765,ABUW_RS10520,ABUW_RS10605,ABUW_RS13745,ABUW_RS14160,ABUW_RS14495,ABUW_RS16540
IPR007848	IPR	Methyltransferase small domain	9; 2/ 2;0.0e+00;ABUW_RS03215,ABUW_RS10385
IPR009081	IPR	Phosphopantetheine binding ACP domain	1; 4/ 9;1.4e-03;ABUW_RS05720,ABUW_RS05760,ABUW_RS05765,ABUW_RS10075
IPR006073	IPR	GTP binding domain	0; 2/ 8;3.6e-02;ABUW_RS11390,ABUW_RS17685
IPR035647	IPR	EF-G domain III/V-like	1; 3/ 6;1.6e-03;ABUW_RS03225,ABUW_RS05050,ABUW_RS16275
IPR029063	IPR	S-adenosyl-L-methionine-dependent methyltransferase superfamily	0; 7/36;1.5e-02;ABUW_RS02315,ABUW_RS03215,ABUW_RS04405,ABUW_RS07375,ABUW_RS07660,ABUW_RS10385,ABUW_RS13235
IPR022770	IPR	Aerobactin siderophore biosynthesis IucA/IucC-like, C-terminal	9; 3/ 3;0.0e+00;ABUW_RS10620,ABUW_RS10625,ABUW_RS10640
IPR005667	IPR	Sulphate ABC transporter permease protein 2	9; 2/ 2;0.0e+00;ABUW_RS04995,ABUW_RS05000
IPR003439	IPR	ABC transporter-like, ATP-binding domain	0; 6/33;2.7e-02;ABUW_RS04990,ABUW_RS05735,ABUW_RS05780,ABUW_RS05785,ABUW_RS10985,ABUW_RS11380
IPR011129	IPR	Cold shock domain	1; 3/ 6;1.6e-03;ABUW_RS06720,ABUW_RS13055,ABUW_RS15915
IPR018313	IPR	Solute-binding protein family 3, conserved site	1; 2/ 4;4.6e-03;ABUW_RS11775,ABUW_RS11780
IPR004516	IPR	Histidine-tRNA ligase/ATP phosphoribosyltransferase regulatory subunit	9; 2/ 2;0.0e+00;ABUW_RS13330,ABUW_RS16405
IPR007310	IPR	Aerobactin siderophore biosynthesis, IucA/IucC, N-terminal	9; 3/ 3;0.0e+00;ABUW_RS10620,ABUW_RS10625,ABUW_RS10640
IPR016291	IPR	Isochorismatase	9; 2/ 2;0.0e+00;ABUW_RS05765,ABUW_RS10075
IPR045851	IPR	AMP-binding enzyme, C-terminal domain superfamily	0; 4/16;1.5e-02;ABUW_RS05715,ABUW_RS05720,ABUW_RS05755,ABUW_RS05760
IPR017938	IPR	Riboflavin synthase-like beta-barrel	0; 3/13;2.9e-02;ABUW_RS03435,ABUW_RS05400,ABUW_RS18710
IPR012156	IPR	Cold shock, CspA	1; 2/ 4;4.6e-03;ABUW_RS06720,ABUW_RS13055
IPR012171	IPR	Fatty acid desaturase	9; 2/ 2;0.0e+00;ABUW_RS05405,ABUW_RS18705
IPR004161	IPR	Translation elongation factor EFTu-like, domain 2	1; 3/ 6;1.6e-03;ABUW_RS03225,ABUW_RS05050,ABUW_RS16275
IPR037294	IPR	ABC transporter, BtuC-like	9; 3/ 3;0.0e+00;ABUW_RS05725,ABUW_RS05730,ABUW_RS18220
IPR010916	IPR	TonB box, conserved site	2; 5/ 9;1.0e-04;ABUW_RS00790,ABUW_RS05745,ABUW_RS08070,ABUW_RS10520,ABUW_RS10605
IPR036942	IPR	TonB-dependent receptor-like, beta-barrel domain superfamily	5;12/19;6.2e-10;ABUW_RS00710,ABUW_RS00790,ABUW_RS05745,ABUW_RS08035,ABUW_RS08070,ABUW_RS08765,ABUW_RS10520,ABUW_RS10605,ABUW_RS13745,ABUW_RS14160,ABUW_RS14495,ABUW_RS16540
IPR000522	IPR	ABC transporter, permease protein, BtuC-like	9; 2/ 2;0.0e+00;ABUW_RS05725,ABUW_RS05730
IPR023213	IPR	Chloramphenicol acetyltransferase-like domain superfamily	0; 3/ 9;8.4e-03;ABUW_RS05715,ABUW_RS05720,ABUW_RS05755
IPR042099	IPR	ANL, N-terminal domain	0; 3/12;2.2e-02;ABUW_RS05715,ABUW_RS05755,ABUW_RS05760
IPR035906	IPR	MetI-like superfamily	0; 4/22;4.7e-02;ABUW_RS04995,ABUW_RS05000,ABUW_RS05460,ABUW_RS13790
IPR002898	IPR	MotA/TolQ/ExbB proton channel	1; 2/ 4;4.6e-03;ABUW_RS04885,ABUW_RS16650
IPR000515	IPR	ABC transporter type 1, transmembrane domain MetI-like	0; 4/22;4.7e-02;ABUW_RS04995,ABUW_RS05000,ABUW_RS05460,ABUW_RS13790
IPR004556	IPR	Methyltransferase HemK-like	9; 2/ 2;0.0e+00;ABUW_RS07660,ABUW_RS10385
IPR005225	IPR	Small GTP-binding protein domain	0; 3/11;1.7e-02;ABUW_RS03225,ABUW_RS05050,ABUW_RS16275
IPR025700	IPR	L-lysine 6-monooxygenase/L-ornithine 5-monooxygenase	9; 2/ 2;0.0e+00;ABUW_RS05750,ABUW_RS10635
IPR001242	IPR	Condensation domain	1; 3/ 6;1.6e-03;ABUW_RS05715,ABUW_RS05720,ABUW_RS05755
IPR000640	IPR	Elongation factor EFG, domain V-like	1; 2/ 3;1.6e-03;ABUW_RS03225,ABUW_RS05050
IPR019844	IPR	Cold-shock (CSD) domain	1; 2/ 3;1.6e-03;ABUW_RS06720,ABUW_RS13055
IPR041715	IPR	Class II Histidinyl-tRNA synthetase (HisRS)-like catalytic core domain	9; 2/ 2;0.0e+00;ABUW_RS13330,ABUW_RS16405
IPR037455	IPR	Aerobactin siderophore biosynthesis, IucA/IucC-like	9; 3/ 3;0.0e+00;ABUW_RS10620,ABUW_RS10625,ABUW_RS10640
IPR001031	IPR	Thioesterase	1; 2/ 4;4.6e-03;ABUW_RS05720,ABUW_RS05790
IPR002781	IPR	Transmembrane protein TauE-like	1; 2/ 4;4.6e-03;ABUW_RS01610,ABUW_RS10305
IPR020845	IPR	AMP-binding, conserved site	0; 4/14;8.4e-03;ABUW_RS05715,ABUW_RS05720,ABUW_RS05755,ABUW_RS05760
IPR000868	IPR	Isochorismatase-like	0; 2/ 6;1.7e-02;ABUW_RS05765,ABUW_RS10075
IPR031043	IPR	Putative histamine N-monooxygenase	9; 2/ 2;0.0e+00;ABUW_RS05750,ABUW_RS10635
00564 Glycerophos	KEGG	ko00564	0;5/15;0.00167;ABUW_RS00510,ABUW_RS04140,ABUW_RS04520,ABUW_RS08465,ABUW_RS08775

ClassID	Class	Description	Single_list
pholipid metabolism [PATH:ko00564]			
01053 Biosynthesis of siderophore group nonribosomal peptides [PATH:ko01053]	KEGG	ko01053	1;3/ 5;0.00077;ABUW_RS05720,ABUW_RS05765,ABUW_RS10075
01040 Biosynthesis of unsaturated fatty acids [PATH:ko01040]	KEGG	ko01040	1;2/ 4;0.00528;ABUW_RS05405,ABUW_RS18705
00997 Biosynthesis of various other secondary metabolites [PATH:ko00997]	KEGG	ko00997	9;3/ 3;0.00000;ABUW_RS06655,ABUW_RS10620,ABUW_RS10625
00930 Caprolactam degradation [PATH:ko00930]	KEGG	ko00930	9;2/ 2;0.00000;ABUW_RS13390,ABUW_RS13415
Methyltransferase	KEYWORDS	keyword	0; 3/ 8;1.6e-02;ABUW_RS07660,ABUW_RS10385,ABUW_RS13235
Ligase	KEYWORDS	keyword	1; 4/ 7;6.1e-04;ABUW_RS05715,ABUW_RS05720,ABUW_RS05755,ABUW_RS05760
Cell inner membrane	KEYWORDS	keyword	0;32/186;1.7e-04;ABUW_RS00150,ABUW_RS00570,ABUW_RS01050,ABUW_RS01160,ABUW_RS01885,ABUW_RS03220,ABUW_RS04995,ABUW_RS05000,ABUW_RS05050,ABUW_RS05130,ABUW_RS05725,ABUW_RS05730,ABUW_RS05740,ABUW_RS06080,ABUW_RS07560,ABUW_RS07610,ABUW_RS07795,ABUW_RS08465,ABUW_RS08740,ABUW_RS08830,ABUW_RS11765,ABUW_RS13375,ABUW_RS13790,ABUW_RS14200,ABUW_RS14415,ABUW_RS15655,ABUW_RS16095,ABUW_RS16650,ABUW_RS17505,ABUW_RS17685,ABUW_RS17975,ABUW_RS18220
Cell membrane	KEYWORDS	keyword	0;17/115;3.1e-02;ABUW_RS00510,ABUW_RS01270,ABUW_RS01610,ABUW_RS03110,ABUW_RS05150,ABUW_RS05405,ABUW_RS05460,ABUW_RS05815,ABUW_RS07865,ABUW_RS10165,ABUW_RS10305,ABUW_RS10630,ABUW_RS11710,ABUW_RS11715,ABUW_RS16105,ABUW_RS17445,ABUW_RS18705
Cell outer membrane	KEYWORDS	keyword	2;12/ 29;3.6e-06;ABUW_RS00710,ABUW_RS04555,ABUW_RS05745,ABUW_RS07605,ABUW_RS08035,ABUW_RS08480,ABUW_RS08765,ABUW_RS10605,ABUW_RS13745,ABUW_RS14485,ABUW_RS14495,ABUW_RS16540
Calcium	KEYWORDS	keyword	0; 2/ 6;4.0e-02;ABUW_RS08775,ABUW_RS11165
operon_1089	operons	NZ_CP008706.1;ID=gene-ABUW_RS11775;Name=ABUW_RS11775;gbkey=Gene;gene_biotype=protein_coding;locus_tag=ABUW_RS11775;old_locus_tag=ABUW_2420	0; 2/ 5;5.3e-03;ABUW_RS11775,ABUW_RS11780
operon_1433	operons	NZ_CP008706.1;ID=gene-ABUW_RS15100;Name=rpmF;gbkey=Gene;gene=rpmF;gene_biotype=protein_coding;locus_tag=ABUW_RS15100;old_locus_tag=ABUW_3110	9; 2/ 2;0.0e+00;ABUW_RS15100,ABUW_RS15105
operon_0980	operons	NZ_CP008706.1;ID=gene-ABUW_RS10520;Name=ABUW_RS10520;gbkey=Gene;gene_biotype=protein_coding;locus_tag=ABUW_RS10520;old_locus_tag=ABUW_2165	2; 4/ 6;3.5e-05;ABUW_RS10520,ABUW_RS10525,ABUW_RS10530,ABUW_RS10535
operon_1081	operons	NZ_CP008706.1;ID=gene-ABUW_RS11710;Name=ABUW_RS11710;gbkey=Gene;gene_biotype=protein_coding;locus_tag=ABUW_RS11710;old_locus_tag=ABUW_2407	9; 2/ 2;0.0e+00;ABUW_RS11710,ABUW_RS11715
operon_1664	operons	NZ_CP008706.1;ID=gene-ABUW_RS17680;Name=ABUW_RS17680;gbkey=Gene;gene_biotype=protein_coding;locus_tag=ABUW_RS17680;old_locus_tag=ABUW_3631	9; 3/ 3;0.0e+00;ABUW_RS17680,ABUW_RS17685,ABUW_RS17690
operon_0854	operons	NZ_CP008706.1;ID=gene-ABUW_RS09310;Name=ABUW_RS09310;gbkey=Gene;gene_biotype=protein_coding;locus_tag=ABUW_RS09310;old_locus_tag=ABUW_1912	0; 2/ 6;9.6e-03;ABUW_RS09310,ABUW_RS20750
operon_0955	operons	NZ_CP008706.1;ID=gene-ABUW_RS10310;Name=ABUW_RS10310;gbkey=Gene;gene_biotype=protein_coding;locus_tag=ABUW_RS10310;old_locus_tag=ABUW_2122	9; 2/ 2;0.0e+00;ABUW_RS10310,ABUW_RS10315
operon_1370	operons	NZ_CP008706.1;ID=gene-ABUW_RS14445;Name=ABUW_RS14445;gbkey=Gene;gene_biotype=protein_coding;locus_tag=ABUW_RS14445;old_locus_tag=ABUW_2975	9; 2/ 2;0.0e+00;ABUW_RS14445,ABUW_RS14450
operon_0463	operons	NZ_CP008706.1;ID=gene-ABUW_RS05050;Name=lepA;gbkey=Gene;gene=lepA;gene_biotype=protein_coding;locus_tag=ABUW_RS05050;old_locus_tag=ABUW_1029	0; 2/ 9;3.1e-02;ABUW_RS05050,ABUW_RS05075

ClassID	Class	Description	Single_list
operon_0982	operons	NZ_CP008706.1;ID=gene-ABUW_RS10585;Name=ABUW_RS10585;gbkey=Gene;gene_biotype=protein_coding;locus_tag=ABUW_RS10585;old_locus_tag=ABUW_2178	9;12/12;0.0e+00;ABUW_RS10585,ABUW_RS10590,ABUW_RS10595,ABUW_RS10600,ABUW_RS10605,ABUW_RS10610,ABUW_RS10615,ABUW_RS10620,ABUW_RS10625,ABUW_RS10630,ABUW_RS10635,ABUW_RS10640
operon_1653	operons	NZ_CP008706.1;ID=gene-ABUW_RS17490;Name=rplA;gbkey=Gene;gene=rplA;gene_biotype=protein_coding;locus_tag=ABUW_RS17490;old_locus_tag=ABUW_3593	0; 2/ 6;9.6e-03;ABUW_RS17500,ABUW_RS17505
operon_1572	operons	NZ_CP008706.1;ID=gene-ABUW_RS16645;Name=ABUW_RS16645;gbkey=Gene;gene_biotype=protein_coding;locus_tag=ABUW_RS16645;old_locus_tag=ABUW_3424	9; 3/ 3;0.0e+00;ABUW_RS16645,ABUW_RS16650,ABUW_RS16655
operon_1367	operons	NZ_CP008706.1;ID=gene-ABUW_RS14405;Name=ABUW_RS14405;gbkey=Gene;gene_biotype=protein_coding;locus_tag=ABUW_RS14405;old_locus_tag=ABUW_2967	2; 2/ 3;7.4e-04;ABUW_RS14405,ABUW_RS14415
operon_0537	operons	NZ_CP008706.1;ID=gene-ABUW_RS05760;Name=basE;gbkey=Gene;gene=basE;gene_biotype=protein_coding;locus_tag=ABUW_RS05760;old_locus_tag=ABUW_1180	9; 9/ 9;0.0e+00;ABUW_RS05760,ABUW_RS05765,ABUW_RS05770,ABUW_RS05780,ABUW_RS05785,ABUW_RS05790,ABUW_RS05795,ABUW_RS05800,ABUW_RS20145
operon_0322	operons	NZ_CP008706.1;ID=gene-ABUW_RS03430;Name=ABUW_RS03430;gbkey=Gene;gene_biotype=protein_coding;locus_tag=ABUW_RS03430;old_locus_tag=ABUW_0697	9; 2/ 2;0.0e+00;ABUW_RS03430,ABUW_RS03435
operon_1751	operons	NZ_CP008706.1;ID=gene-ABUW_RS18705;Name=ABUW_RS18705;gbkey=Gene;gene_biotype=protein_coding;locus_tag=ABUW_RS18705;old_locus_tag=ABUW_3842	9; 2/ 2;0.0e+00;ABUW_RS18705,ABUW_RS18710
operon_0305	operons	NZ_CP008706.1;ID=gene-ABUW_RS03210;Name=ABUW_RS03210;gbkey=Gene;gene_biotype=protein_coding;locus_tag=ABUW_RS03210;old_locus_tag=ABUW_0652	9; 3/ 3;0.0e+00;ABUW_RS03210,ABUW_RS03215,ABUW_RS03220
operon_0431	operons	NZ_CP008706.1;ID=gene-ABUW_RS04665;Name=ABUW_RS04665;gbkey=Gene;gene_biotype=protein_coding;locus_tag=ABUW_RS04665;old_locus_tag=ABUW_0951	0; 2/ 5;5.3e-03;ABUW_RS04670,ABUW_RS04675
operon_0673	operons	NZ_CP008706.1;ID=gene-ABUW_RS07600;Name=pgaA;gbkey=Gene;gene=pgaA;gene_biotype=protein_coding;locus_tag=ABUW_RS07600;old_locus_tag=ABUW_1557	1; 2/ 4;2.4e-03;ABUW_RS07605,ABUW_RS07610
operon_1050	operons	NZ_CP008706.1;ID=gene-ABUW_RS11355;Name=ABUW_RS11355;gbkey=Gene;gene_biotype=protein_coding;locus_tag=ABUW_RS11355;old_locus_tag=ABUW_2335	0; 2/ 8;2.3e-02;ABUW_RS11380,ABUW_RS11390
operon_1589	operons	NZ_CP008706.1;ID=gene-ABUW_RS16845;Name=ABUW_RS16845;gbkey=Gene;gene_biotype=protein_coding;locus_tag=ABUW_RS16845;old_locus_tag=ABUW_3464	9; 2/ 2;0.0e+00;ABUW_RS16845,ABUW_RS16850
operon_0497	operons	NZ_CP008706.1;ID=gene-ABUW_RS05400;Name=ABUW_RS05400;gbkey=Gene;gene_biotype=protein_coding;locus_tag=ABUW_RS05400;old_locus_tag=ABUW_1104	9; 2/ 2;0.0e+00;ABUW_RS05400,ABUW_RS05405
operon_1368	operons	NZ_CP008706.1;ID=gene-ABUW_RS14420;Name=betI;gbkey=Gene;gene=betI;gene_biotype=protein_coding;locus_tag=ABUW_RS14420;old_locus_tag=ABUW_2970	9; 3/ 3;0.0e+00;ABUW_RS14420,ABUW_RS14425,ABUW_RS14430
operon_0774	operons	NZ_CP008706.1;ID=gene-ABUW_RS08445;Name=rimO;gbkey=Gene;gene=rimO;gene_biotype=protein_coding;locus_tag=ABUW_RS08445;old_locus_tag=ABUW_1734	0; 3/12;1.3e-02;ABUW_RS08460,ABUW_RS08465,ABUW_RS08480
operon_1369	operons	NZ_CP008706.1;ID=gene-ABUW_RS14435;Name=mqo;gbkey=Gene;gene=mqo;gene_biotype=protein_coding;locus_tag=ABUW_RS14435;old_locus_tag=ABUW_2973	9; 2/ 2;0.0e+00;ABUW_RS14435,ABUW_RS14440
operon_0371	operons	NZ_CP008706.1;ID=gene-ABUW_RS04080;Name=ABUW_RS04080;gbkey=Gene;gene_biotype=protein_coding;locus_tag=ABUW_RS04080;old_locus_tag=ABUW_0833	2; 2/ 3;7.4e-04;ABUW_RS04085,ABUW_RS04090
operon_0536	operons	NZ_CP008706.1;ID=gene-ABUW_RS05750;Name=basC;gbkey=Gene;gene=basC;gene_biotype=protein_coding;locus_tag=ABUW_RS05750;old_locus_tag=ABUW_1178	9; 2/ 2;0.0e+00;ABUW_RS05750,ABUW_RS05755
operon_0399	operons	NZ_CP008706.1;ID=gene-ABUW_RS04405;Name=rlmE;gbkey=Gene;gene=rlmE;gene_biotype=protein_coding;locus_tag=ABUW_RS04405;old_locus_tag=ABUW_0898	1; 2/ 4;2.4e-03;ABUW_RS04405,ABUW_RS04420
operon_1703	operons	NZ_CP008706.1;ID=gene-ABUW_RS18095;Name=ABUW_RS18095;gbkey=Gene;gene_biotype=protein_coding;locus_tag=ABUW_RS18095;old_locus_tag=ABUW_3718	3; 3/ 4;7.0e-05;ABUW_RS18095,ABUW_RS18100,ABUW_RS18105
operon_1521	operons	NZ_CP008706.1;ID=gene-ABUW_RS16090;Name=ABUW_RS16090;gbkey=Gene;gene_biotype=protein_coding;locus_tag=ABUW_RS16090;old_locus_tag=ABUW_3312	2; 2/ 3;7.4e-04;ABUW_RS16095,ABUW_RS16100
operon_1464	operons	NZ_CP008706.1;ID=gene-ABUW_RS15460;Name=ABUW_RS15460;gbkey=Gene;gene_biotype=protein_coding;locus_tag=ABUW_RS15460;old_locus_tag=ABUW_3183	2; 2/ 3;7.4e-04;ABUW_RS15460,ABUW_RS15470
operon_0459	operons	NZ_CP008706.1;ID=gene-ABUW_RS04985;Name=ABUW_RS04985;gbkey=Gene;gene_biotype=protein_coding;locus_tag=ABUW_RS04985;old_locus_tag=ABUW_1016	1; 3/ 6;7.4e-04;ABUW_RS04990,ABUW_RS04995,ABUW_RS05000
operon_0806	operons	NZ_CP008706.1;ID=gene-ABUW_RS08725;Name=ABUW_RS08725;gbkey=Gene;ge	4; 4/ 5;6.5e-06;ABUW_RS08725,ABUW_RS08730,ABUW_RS08735,ABUW_RS08740

ClassID	Class	Description	Single_list
		ne_biotype=protein_coding;locus_tag=ABUW_RS08725;old_locus_tag=ABUW_1792	
operon_1472	operons	NZ_CP008706.1;ID=gene-ABUW_RS15520;Name=ABUW_RS15520;gbkey=Gene;gene_biotype=protein_coding;locus_tag=ABUW_RS15520;old_locus_tag=ABUW_3197	9; 2/ 2;0.0e+00;ABUW_RS15520,ABUW_RS15525
operon_1374	operons	NZ_CP008706.1;ID=gene-ABUW_RS14495;Name=ABUW_RS14495;gbkey=Gene;gene_biotype=protein_coding;locus_tag=ABUW_RS14495;old_locus_tag=ABUW_2985	3; 3/ 4;7.0e-05;ABUW_RS14495,ABUW_RS14500,ABUW_RS14505
operon_0450	operons	NZ_CP008706.1;ID=gene-ABUW_RS04865;Name=pal;gbkey=Gene;gene=pal;gene_biotype=protein_coding;locus_tag=ABUW_RS04865;old_locus_tag=ABUW_0992	1; 3/ 6;7.4e-04;ABUW_RS04880,ABUW_RS04885,ABUW_RS04890
operon_0535	operons	NZ_CP008706.1;ID=gene-ABUW_RS05725;Name=bauD;gbkey=Gene;gene=bauD;gene_biotype=protein_coding;locus_tag=ABUW_RS05725;old_locus_tag=ABUW_1173	9; 5/ 5;0.0e+00;ABUW_RS05725,ABUW_RS05730,ABUW_RS05735,ABUW_RS05740,ABUW_RS05745
operon_0930	operons	NZ_CP008706.1;ID=gene-ABUW_RS10075;Name=ABUW_RS10075;gbkey=Gene;gene_biotype=protein_coding;locus_tag=ABUW_RS10075;old_locus_tag=ABUW_2075	9; 2/ 2;0.0e+00;ABUW_RS10075,ABUW_RS10080
operon_0678	operons	NZ_CP008706.1;ID=gene-ABUW_RS07655;Name=prfA;gbkey=Gene;gene=prfA;gene_biotype=protein_coding;locus_tag=ABUW_RS07655;old_locus_tag=ABUW_1567	9; 2/ 2;0.0e+00;ABUW_RS07655,ABUW_RS07660
operon_1770	operons	NZ_CP008706.1;ID=gene-ABUW_RS18895;Name=ABUW_RS18895;gbkey=Gene;gene_biotype=protein_coding;locus_tag=ABUW_RS18895;old_locus_tag=ABUW_3880	2; 2/ 3;7.4e-04;ABUW_RS18895,ABUW_RS18900
operon_0862	operons	NZ_CP008706.1;ID=gene-ABUW_RS09390;Name=ABUW_RS09390;gbkey=Gene;gene_biotype=protein_coding;locus_tag=ABUW_RS09390;old_locus_tag=ABUW_1928	9; 2/ 2;0.0e+00;ABUW_RS09390,ABUW_RS09395
operon_0197	operons	NZ_CP008706.1;ID=gene-ABUW_RS01870;Name=ABUW_RS01870;gbkey=Gene;gene_biotype=protein_coding;locus_tag=ABUW_RS01870;old_locus_tag=ABUW_0381	1; 3/ 7;1.6e-03;ABUW_RS01870,ABUW_RS01885,ABUW_RS20105
operon_0595	operons	NZ_CP008706.1;ID=gene-ABUW_RS06590;Name=ABUW_RS06590;gbkey=Gene;gene_biotype=protein_coding;locus_tag=ABUW_RS06590;old_locus_tag=ABUW_1351	3; 3/ 4;7.0e-05;ABUW_RS06595,ABUW_RS06600,ABUW_RS06605
operon_1373	operons	NZ_CP008706.1;ID=gene-ABUW_RS14470;Name=ABUW_RS14470;gbkey=Gene;gene_biotype=protein_coding;locus_tag=ABUW_RS14470;old_locus_tag=ABUW_2980	9; 5/ 5;0.0e+00;ABUW_RS14470,ABUW_RS14475,ABUW_RS14480,ABUW_RS14485,ABUW_RS14490
operon_0169	operons	NZ_CP008706.1;ID=gene-ABUW_RS01605;Name=truB;gbkey=Gene;gene=truB;gene_biotype=protein_coding;locus_tag=ABUW_RS01605;old_locus_tag=ABUW_0326	9; 2/ 2;0.0e+00;ABUW_RS01605,ABUW_RS01610
operon_0166	operons	NZ_CP008706.1;ID=gene-ABUW_RS01540;Name=ABUW_RS01540;gbkey=Gene;gene_biotype=protein_coding;locus_tag=ABUW_RS01540;old_locus_tag=ABUW_0313	0; 2/10;4.1e-02;ABUW_RS01580,ABUW_RS01585
operon_1628	operons	NZ_CP008706.1;ID=gene-ABUW_RS17225;Name=ABUW_RS17225;gbkey=Gene;gene_biotype=protein_coding;locus_tag=ABUW_RS17225;old_locus_tag=ABUW_3540	1; 2/ 4;2.4e-03;ABUW_RS17235,ABUW_RS17240
PF13434	Pfam	L-lysine 6-monooxygenase/L-ornithine 5-monooxygenase	9; 2/ 2;0.0e+00;ABUW_RS05750,ABUW_RS10635
PF00005	Pfam	ABC transporter	0; 6/33;2.3e-02;ABUW_RS04990,ABUW_RS05735,ABUW_RS05780,ABUW_RS05785,ABUW_RS10985,ABUW_RS11380
PF00860	Pfam	Permease family	2; 3/ 4;1.9e-04;ABUW_RS00150,ABUW_RS03220,ABUW_RS13375
PF01032	Pfam	FecCD transport family	9; 2/ 2;0.0e+00;ABUW_RS05725,ABUW_RS05730
PF00487	Pfam	Fatty acid desaturase	1; 2/ 3;1.4e-03;ABUW_RS05405,ABUW_RS18705
PF00664	Pfam	ABC transporter transmembrane region	1; 2/ 4;3.7e-03;ABUW_RS05780,ABUW_RS10985
PF00550	Pfam	Phosphopantetheine attachment site	1; 4/ 9;1.3e-03;ABUW_RS05720,ABUW_RS05760,ABUW_RS05765,ABUW_RS10075
PF00313	Pfam	'Cold-shock' DNA-binding domain	1; 2/ 4;3.7e-03;ABUW_RS06720,ABUW_RS13055
PF00497	Pfam	Bacterial extracellular solute-binding proteins, family 3	1; 3/ 6;1.4e-03;ABUW_RS04555,ABUW_RS11775,ABUW_RS11780
PF00593	Pfam	TonB dependent receptor	5;12/19;5.5e-10;ABUW_RS00710,ABUW_RS00790,ABUW_RS05745,ABUW_RS08035,ABUW_RS08070,ABUW_RS08765,ABUW_RS10520,ABUW_RS10605,ABUW_RS13745,ABUW_RS14160,ABUW_RS14495,ABUW_RS16540
PF06276	Pfam	Ferric iron reductase FhuF-like transporter	9; 3/ 3;0.0e+00;ABUW_RS10620,ABUW_RS10625,ABUW_RS10640
PF00501	Pfam	AMP-binding enzyme	0; 4/16;1.2e-02;ABUW_RS05715,ABUW_RS05720,ABUW_RS05755,ABUW_RS05760
PF00009	Pfam	Elongation factor Tu GTP binding domain	0; 3/ 8;4.1e-03;ABUW_RS03225,ABUW_RS05050,ABUW_RS16275
PF00528	Pfam	Binding-protein-dependent transport system inner membrane component	0; 4/22;4.1e-02;ABUW_RS04995,ABUW_RS05000,ABUW_RS05460,ABUW_RS13790
PF00857	Pfam	Isochorismatase family	0; 2/ 6;1.4e-02;ABUW_RS05765,ABUW_RS10075
PF13193	Pfam	AMP-binding enzyme C-terminal domain	0; 4/14;6.5e-03;ABUW_RS05715,ABUW_RS05720,ABUW_RS05755,ABUW_RS05760
PF00975	Pfam	Thioesterase domain	1; 2/ 4;3.7e-03;ABUW_RS05720,ABUW_RS05790
PF00175	Pfam	Oxidoreductase NAD-binding domain	0; 3/12;1.9e-02;ABUW_RS03435,ABUW_RS05400,ABUW_RS18710
PF04273	Pfam	Beta-lactamase hydrolase-like protein, phosphatase-like domain	1; 2/ 3;1.4e-03;ABUW_RS10310,ABUW_RS10315
PF05175	Pfam	Methyltransferase small domain	9; 2/ 2;0.0e+00;ABUW_RS03215,ABUW_RS10385
PF01925	Pfam	Sulfite exporter TauE/SafE	1; 2/ 4;3.7e-03;ABUW_RS01610,ABUW_RS10305

ClassID	Class	Description	Single_list
PF13393	Pfam	Histidyl-tRNA synthetase	9; 2/ 2;0.0e+00;ABUW_RS13330,ABUW_RS16405
PF04183	Pfam	IucA / IucC family	9; 3/ 3;0.0e+00;ABUW_RS10620,ABUW_RS10625,ABUW_RS10640
PF00679	Pfam	Elongation factor G C-terminus	1; 2/ 3;1.4e-03;ABUW_RS03225,ABUW_RS05050
PF03144	Pfam	Elongation factor Tu domain 2	1; 3/ 6;1.4e-03;ABUW_RS03225,ABUW_RS05050,ABUW_RS16275
PF07715	Pfam	TonB-dependent Receptor Plug Domain	5;12/19;5.5e-10;ABUW_RS00710,ABUW_RS00790,ABUW_RS05745,ABUW_RS08035,ABUW_RS08070,ABUW_RS08765,ABUW_RS10520,ABUW_RS10605,ABUW_RS13745,ABUW_RS14160,ABUW_RS14495,ABUW_RS16540
PF01618	Pfam	MotA/TolQ/ExbB proton channel family	1; 2/ 4;3.7e-03;ABUW_RS04885,ABUW_RS16650
PF00668	Pfam	Condensation domain	1; 3/ 6;1.4e-03;ABUW_RS05715,ABUW_RS05720,ABUW_RS05755

2.5 Enrichment Analysis (GSEA) of LCWB vs LB Down Regulated

ClassID	Class	Description	Single_list
IPR006176	IPR	3-hydroxyacyl-CoA dehydrogenase, NAD binding	0; 2/ 5;0.01060;ABUW_RS12020,ABUW_RS12290
K	COG	INFORMATION STORAGE AND PROCESSING; Transcription	0;25/138;0.00197;ABUW_RS00875,ABUW_RS01110,ABUW_RS02230,ABUW_RS05440,ABUW_RS05605,ABUW_RS06565,ABUW_RS07645,ABUW_RS09145,ABUW_RS10130,ABUW_RS10155,ABUW_RS10175,ABUW_RS11925,ABUW_RS11955,ABUW_RS14230,ABUW_RS14940,ABUW_RS15605,ABUW_RS16880,ABUW_RS16935,ABUW_RS17105,ABUW_RS17720,ABUW_RS17845,ABUW_RS18135,ABUW_RS18540,ABUW_RS18785,ABUW_RS20220
I	COG	METABOLISM; Lipid transport and metabolism	0;19/85;0.00094;ABUW_RS00865,ABUW_RS04935,ABUW_RS08915,ABUW_RS08920,ABUW_RS11930,ABUW_RS11935,ABUW_RS11940,ABUW_RS11945,ABUW_RS11995,ABUW_RS12020,ABUW_RS12290,ABUW_RS12295,ABUW_RS12300,ABUW_RS13490,ABUW_RS13505,ABUW_RS14295,ABUW_RS14925,ABUW_RS18405,ABUW_RS20225
COG2207	eggNOG_COG	Transcriptional regulator	0; 2/ 8;0.0450;ABUW_RS10155,ABUW_RS10290
COG1473	eggNOG_COG	amidohydrolase	9; 2/ 2;0.0000;ABUW_RS04895,ABUW_RS09300
COG1113	eggNOG_COG	amino acid transport	0; 4/10;0.0059;ABUW_RS00350,ABUW_RS00995,ABUW_RS13590,ABUW_RS18435
COG1309	eggNOG_COG	transcriptional regulator	0; 3/13;0.0431;ABUW_RS11925,ABUW_RS18135,ABUW_RS18785
COG1018	eggNOG_COG	Is involved in NO detoxification in an aerobic process, termed nitric oxide dioxygenase (NOD) reaction that utilizes O(2) and NAD(P)H to convert NO to nitrate, which protects the bacterium from various noxious nitrogen compounds. Therefore, plays a central role in the inducible response to nitrosative stress	0; 2/ 5;0.0122;ABUW_RS01970,ABUW_RS12305
COG1522	eggNOG_COG	sequence-specific DNA binding	0; 2/ 5;0.0122;ABUW_RS00875,ABUW_RS05440
COG1804	eggNOG_COG	L-carnitine dehydratase bile acid-inducible protein F	1; 2/ 4;0.0072;ABUW_RS12055,ABUW_RS12200
COG0789	eggNOG_COG	Transcriptional regulator	1; 2/ 3;0.0043;ABUW_RS17105,ABUW_RS17845
COG0654	eggNOG_COG	COG0654 2-polyprenyl-6-methoxyphenol hydroxylase and related FAD-dependent oxidoreductases	0; 2/ 5;0.0122;ABUW_RS00630,ABUW_RS12105
COG2267	eggNOG_COG	carboxylic ester hydrolase activity	0; 2/ 5;0.0122;ABUW_RS14295,ABUW_RS20225
COG1012	eggNOG_COG	belongs to the aldehyde dehydrogenase family	0; 5/15;0.0061;ABUW_RS12145,ABUW_RS12330,ABUW_RS12355,ABUW_RS13495,ABUW_RS14915
COG1024	eggNOG_COG	Enoyl-CoA hydratase	1; 5/11;0.0021;ABUW_RS04935,ABUW_RS11940,ABUW_RS12295,ABUW_RS12300,ABUW_RS13490
COG1853	eggNOG_COG	conserved protein domain typically associated with flavoprotein oxygenases, DIM6 NTAB family	0; 2/ 6;0.0211;ABUW_RS10130,ABUW_RS20220
COG0446	eggNOG_COG	pyridine nucleotide-disulphide oxidoreductase	1; 2/ 4;0.0072;ABUW_RS08850,ABUW_RS14310
COG0715	eggNOG_COG	COG0715 ABC-type nitrate sulfonate bicarbonate transport systems periplasmic components	1; 2/ 4;0.0072;ABUW_RS18760,ABUW_RS18765
COG1250	eggNOG_COG	3-hydroxyacyl-CoA dehydrogenase	1; 2/ 3;0.0043;ABUW_RS12020,ABUW_RS12290
COG0583	eggNOG_COG	DNA-binding transcription factor activity	0;10/42;0.0061;ABUW_RS05605,ABUW_RS07645,ABUW_RS09145,ABUW_RS10175,ABUW_RS11955,ABUW_RS14230,ABUW_RS14940,ABUW_RS15605,ABUW_RS16880,ABUW_RS16935
COG3396	eggNOG_COG	Phenylacetate-CoA oxygenase	9; 2/ 2;0.0000;ABUW_RS12315,ABUW_RS12325
GO:0036382	GO	flavin reductase (NADH) activity	1; 2/ 3;3.3e-03;ABUW_RS10130,ABUW_RS20220
GO:0030435	GO	sporulation resulting in formation of a cellular spore	0; 3/ 10;1.6e-02;ABUW_RS11930,ABUW_RS13505,ABUW_RS18405
GO:0071949	GO	FAD binding	0; 4/ 11;6.3e-03;ABUW_RS00630,ABUW_RS01970,ABUW_RS08850,ABUW_RS12105
GO:0006351	GO	DNA-templated transcription	0; 8/ 24;1.4e-03;ABUW_RS05605,ABUW_RS07645,ABUW_RS10685,ABUW_RS11955,ABUW_RS14230,ABUW_RS14940,ABUW_RS15605,ABUW_RS16935
GO:0019679	GO	propionate metabolic process, methylcitrate cycle	1; 2/ 3;3.3e-03;ABUW_RS18525,ABUW_RS18530
GO:0031956	GO	medium-chain fatty acid-CoA ligase activity	1; 2/ 3;3.3e-03;ABUW_RS11920,ABUW_RS15985
GO:0030976	GO	thiamine pyrophosphate binding	0; 2/ 5;1.2e-02;ABUW_RS05445,ABUW_RS14275
GO:0043565	GO	sequence-specific DNA binding	1;17/ 51;3.7e-06;ABUW_RS00875,ABUW_RS01080,ABUW_RS02230,ABUW_RS05440,ABUW_RS05605,ABUW_RS07645,ABUW_RS10120,ABUW_RS10290,ABUW_RS11955,ABUW_RS13605,ABUW_RS14230,ABUW_RS14940,ABUW_RS15545,ABUW_RS15605,ABUW_RS16935,ABUW_RS18455,ABUW_RS18540
GO:0032991	GO	protein-containing complex	0; 2/ 6;2.0e-02;ABUW_RS07335,ABUW_RS14915
GO:0016709	GO	oxidoreductase activity, acting on paired donors, with incorporation or reduction of molecular oxygen, NAD(P)H as one donor, and incorporation of one atom of oxygen	0; 4/ 12;6.3e-03;ABUW_RS00630,ABUW_RS09620,ABUW_RS14910,ABUW_RS14920
GO:0004322	GO	ferroxidase activity	9; 2/ 2;0.0e+00;ABUW_RS01505,ABUW_RS15175
GO:0008199	GO	ferric iron binding	0; 2/ 5;1.2e-02;ABUW_RS01505,ABUW_RS15175
GO:0045893	GO	positive regulation of DNA-templated transcription	0; 7/ 22;2.9e-03;ABUW_RS01080,ABUW_RS09205,ABUW_RS10155,ABUW_RS13430,ABUW_RS14940,ABUW_RS16880,ABUW_RS17845
GO:0042945	GO	D-serine transmembrane transporter activity	1; 2/ 4;6.3e-03;ABUW_RS13590,ABUW_RS18435
GO:0001761	GO	beta-alanine transmembrane transporter activity	1; 2/ 4;6.3e-03;ABUW_RS13590,ABUW_RS18435
GO:0008860	GO	ferredoxin-NAD+ reductase activity	1; 2/ 3;3.3e-03;ABUW_RS13160,ABUW_RS14310
GO:0033539	GO	fatty acid beta-oxidation using acyl-CoA dehydrogenase	0; 3/ 13;3.8e-02;ABUW_RS11930,ABUW_RS13505,ABUW_RS18405
GO:0003987	GO	acetate-CoA ligase activity	1; 2/ 4;6.3e-03;ABUW_RS00865,ABUW_RS15985
GO:0016810	GO	hydrolase activity, acting on carbon-nitrogen (but not peptide) bonds	0; 2/ 5;1.2e-02;ABUW_RS14295,ABUW_RS20225
GO:0062077	GO	phenylacetyl-CoA 1,2-epoxidase complex	9; 4/ 4;0.0e+00;ABUW_RS12305,ABUW_RS12315,ABUW_RS12320,ABUW_RS12325
GO:0042944	GO	D-alanine transmembrane transporter activity	1; 2/ 4;6.3e-03;ABUW_RS13590,ABUW_RS18435
GO:0006826	GO	iron ion transport	1; 2/ 3;3.3e-03;ABUW_RS01505,ABUW_RS15175

ClassID	Class	Description	Single_list
GO:0042952	GO	beta-ketoadipate pathway	0; 4/ 19;3.8e-02;ABUW_RS08915,ABUW_RS08920,ABUW_RS09135,ABUW_RS11995
GO:0033103	GO	protein secretion by the type VI secretion system	2; 3/ 4;8.4e-04;ABUW_RS00575,ABUW_RS12705,ABUW_RS12710
GO:0015293	GO	symporter activity	0; 4/ 20;4.5e-02;ABUW_RS00910,ABUW_RS13590,ABUW_RS14045,ABUW_RS18435
GO:0019556	GO	histidine catabolic process to glutamate and formamide	1; 3/ 5;2.2e-03;ABUW_RS00380,ABUW_RS00385,ABUW_RS00400
GO:0019629	GO	propionate catabolic process, 2-methylcitrate cycle	2; 3/ 4;8.4e-04;ABUW_RS07780,ABUW_RS18525,ABUW_RS18535
GO:0004300	GO	enoyl-CoA hydratase activity	1; 5/ 10;9.4e-04;ABUW_RS04935,ABUW_RS11940,ABUW_RS12295,ABUW_RS12300,ABUW_RS12330
GO:0009437	GO	carnitine metabolic process	1; 2/ 3;3.3e-03;ABUW_RS14910,ABUW_RS14920
GO:0140662	GO	ATP-dependent protein folding chaperone	0; 2/ 6;2.0e-02;ABUW_RS17430,ABUW_RS18890
GO:0045892	GO	negative regulation of DNA-templated transcription	0; 5/ 26;4.0e-02;ABUW_RS14940,ABUW_RS16880,ABUW_RS18135,ABUW_RS18785,ABUW_RS18995
GO:0016655	GO	oxidoreductase activity, acting on NAD(P)H, quinone or similar compound as acceptor	0; 2/ 7;3.1e-02;ABUW_RS04200,ABUW_RS12115
GO:0008691	GO	3-hydroxybutyryl-CoA dehydrogenase activity	9; 2/ 2;0.0e+00;ABUW_RS12020,ABUW_RS12290
GO:0019545	GO	arginine catabolic process to succinate	0; 3/ 7;6.3e-03;ABUW_RS01735,ABUW_RS13595,ABUW_RS13600
GO:0033104	GO	type VI protein secretion system complex	1; 2/ 4;6.3e-03;ABUW_RS00575,ABUW_RS12710
GO:0042942	GO	D-serine transport	1; 2/ 4;6.3e-03;ABUW_RS13590,ABUW_RS18435
GO:0006593	GO	ornithine catabolic process	0; 2/ 5;1.2e-02;ABUW_RS13565,ABUW_RS13600
GO:0003857	GO	3-hydroxyacyl-CoA dehydrogenase activity	1; 2/ 4;6.3e-03;ABUW_RS12020,ABUW_RS12290
GO:0019544	GO	arginine catabolic process to glutamate	0; 3/ 7;6.3e-03;ABUW_RS01735,ABUW_RS13595,ABUW_RS13600
GO:0006790	GO	sulfur compound metabolic process	0; 3/ 8;7.4e-03;ABUW_RS11590,ABUW_RS18760,ABUW_RS18765
GO:0003700	GO	DNA-binding transcription factor activity	0;25/120;2.6e-04;ABUW_RS01080,ABUW_RS02230,ABUW_RS05605,ABUW_RS06565,ABUW_RS07645,ABUW_RS08350,ABUW_RS08610,ABUW_RS09145,ABUW_RS09205,ABUW_RS10120,ABUW_RS10175,ABUW_RS10290,ABUW_RS11925,ABUW_RS11955,ABUW_RS13430,ABUW_RS13565,ABUW_RS14230,ABUW_RS14940,ABUW_RS15545,ABUW_RS15605,ABUW_RS16880,ABUW_RS16935,ABUW_RS17845,ABUW_RS18135,ABUW_RS18540
GO:0051537	GO	2 iron, 2 sulfur cluster binding	0; 8/ 34;6.3e-03;ABUW_RS00055,ABUW_RS05625,ABUW_RS12305,ABUW_RS13160,ABUW_RS13465,ABUW_RS14910,ABUW_RS14920,ABUW_RS18960
GO:0006572	GO	tyrosine catabolic process	2; 3/ 4;8.4e-04;ABUW_RS00325,ABUW_RS00340,ABUW_RS12060
GO:0006635	GO	fatty acid beta-oxidation	1; 6/ 14;9.8e-04;ABUW_RS04935,ABUW_RS11940,ABUW_RS12020,ABUW_RS12290,ABUW_RS12295,ABUW_RS12300
GO:0008718	GO	D-amino-acid dehydrogenase activity	1; 2/ 3;3.3e-03;ABUW_RS08405,ABUW_RS18450
GO:0016836	GO	hydro-lyase activity	1; 3/ 5;2.2e-03;ABUW_RS00345,ABUW_RS09425,ABUW_RS18525
GO:0009411	GO	response to UV	0; 2/ 5;1.2e-02;ABUW_RS05605,ABUW_RS15605
GO:0016620	GO	oxidoreductase activity, acting on the aldehyde or oxo group of donors, NAD or NADP as acceptor	1; 2/ 4;6.3e-03;ABUW_RS12145,ABUW_RS12330
GO:0042597	GO	periplasmic space	0; 7/ 32;1.2e-02;ABUW_RS01375,ABUW_RS07335,ABUW_RS09105,ABUW_RS11475,ABUW_RS13140,ABUW_RS18760,ABUW_RS18765
GO:0009450	GO	gamma-aminobutyric acid catabolic process	1; 3/ 5;2.2e-03;ABUW_RS00995,ABUW_RS01005,ABUW_RS14915
GO:0018489	GO	vanillate monooxygenase activity	9; 2/ 2;0.0e+00;ABUW_RS13465,ABUW_RS18960
GO:0016853	GO	isomerase activity	0; 3/ 8;7.4e-03;ABUW_RS04935,ABUW_RS06570,ABUW_RS12295
GO:0008126	GO	acetylesterase activity	1; 2/ 4;6.3e-03;ABUW_RS14925,ABUW_RS17125
GO:0006101	GO	citrate metabolic process	0; 2/ 5;1.2e-02;ABUW_RS14045,ABUW_RS18525
GO:0003995	GO	acyl-CoA dehydrogenase activity	0; 4/ 14;1.2e-02;ABUW_RS11930,ABUW_RS12060,ABUW_RS13505,ABUW_RS18405
GO:0042959	GO	alkanesulfonate transmembrane transporter activity	0; 3/ 8;7.4e-03;ABUW_RS11590,ABUW_RS18760,ABUW_RS18765
GO:0009447	GO	putrescine catabolic process	1; 2/ 4;6.3e-03;ABUW_RS01005,ABUW_RS13630
GO:0006144	GO	purine nucleobase metabolic process	0; 2/ 5;1.2e-02;ABUW_RS00630,ABUW_RS07335
GO:0003994	GO	aconitate hydratase activity	1; 2/ 3;3.3e-03;ABUW_RS07780,ABUW_RS18525
GO:0042941	GO	D-alanine transport	1; 2/ 4;6.3e-03;ABUW_RS13590,ABUW_RS18435
GO:0070403	GO	NAD+ binding	0; 2/ 7;3.1e-02;ABUW_RS12020,ABUW_RS12290
GO:0015187	GO	glycine transmembrane transporter activity	1; 2/ 4;6.3e-03;ABUW_RS13590,ABUW_RS18435
GO:0050660	GO	flavin adenine dinucleotide binding	0;14/ 70;5.1e-03;ABUW_RS08300,ABUW_RS09620,ABUW_RS10265,ABUW_RS10340,ABUW_RS11355,ABUW_RS11930,ABUW_RS12060,ABUW_RS12305,ABUW_RS13160,ABUW_RS13505,ABUW_RS14275,ABUW_RS14310,ABUW_RS14910,ABUW_RS18405
GO:0042802	GO	identical protein binding	0; 9/ 52;2.8e-02;ABUW_RS04935,ABUW_RS06145,ABUW_RS10685,ABUW_RS12295,ABUW_RS12300,ABUW_RS12330,ABUW_RS14230,ABUW_RS14515,ABUW_RS16510
GO:0019439	GO	aromatic compound catabolic process	0; 6/ 26;1.2e-02;ABUW_RS05625,ABUW_RS09145,ABUW_RS10120,ABUW_RS10130,ABUW_RS10145,ABUW_RS13510
GO:0042918	GO	alkanesulfonate transport	0; 3/ 8;7.4e-03;ABUW_RS11590,ABUW_RS18760,ABUW_RS18765
GO:1902494	GO	catalytic complex	1; 3/ 5;2.2e-03;ABUW_RS04935,ABUW_RS12295,ABUW_RS12300
GO:0042626	GO	ATPase-coupled transmembrane transporter activity	0; 2/ 6;2.0e-02;ABUW_RS18760,ABUW_RS18765

ClassID	Class	Description	Single_list
GO:0006085	GO	acetyl-CoA biosynthetic process	1; 2/ 4;6.3e-03;ABUW_RS16500,ABUW_RS16505
GO:0010438	GO	cellular response to sulfur starvation	0; 3/ 7;6.3e-03;ABUW_RS11590,ABUW_RS18760,ABUW_RS18765
GO:0006559	GO	L-phenylalanine catabolic process	0; 3/ 7;6.3e-03;ABUW_RS00325,ABUW_RS00340,ABUW_RS12060
GO:0015180	GO	L-alanine transmembrane transporter activity	1; 2/ 4;6.3e-03;ABUW_RS13590,ABUW_RS18435
GO:0006879	GO	intracellular iron ion homeostasis	1; 2/ 4;6.3e-03;ABUW_RS01505,ABUW_RS15175
GO:0047569	GO	3-oxoadipate CoA-transferase activity	0; 2/ 6;2.0e-02;ABUW_RS08915,ABUW_RS11995
GO:0047780	GO	citrate dehydratase activity	1; 2/ 3;3.3e-03;ABUW_RS07780,ABUW_RS18525
GO:0016740	GO	transferase activity	0; 4/ 18;3.1e-02;ABUW_RS01985,ABUW_RS11685,ABUW_RS11935,ABUW_RS12055
GO:0015816	GO	glycine transport	1; 2/ 4;6.3e-03;ABUW_RS13590,ABUW_RS18435
GO:0001762	GO	beta-alanine transport	1; 2/ 4;6.3e-03;ABUW_RS13590,ABUW_RS18435
GO:0015808	GO	L-alanine transport	1; 2/ 4;6.3e-03;ABUW_RS13590,ABUW_RS18435
GO:0019557	GO	histidine catabolic process to glutamate and formate	1; 3/ 5;2.2e-03;ABUW_RS00380,ABUW_RS00385,ABUW_RS00400
GO:0046274	GO	lignin catabolic process	1; 2/ 4;6.3e-03;ABUW_RS13465,ABUW_RS18960
GO:0016627	GO	oxidoreductase activity, acting on the CH-CH group of donors	0; 2/ 5;1.2e-02;ABUW_RS10265,ABUW_RS11355
GO:0010124	GO	phenylacetate catabolic process	7;12/ 16;2.4e-10;ABUW_RS04935,ABUW_RS12020,ABUW_RS12280,ABUW_RS12290,ABUW_RS12295,ABUW_RS12300,ABUW_RS12305,ABUW_RS12310,ABUW_RS12315,ABUW_RS12320,ABUW_RS12325,ABUW_RS12330
IPR002563	IPR	Flavin reductase like domain	0; 2/ 6;0.01802;ABUW_RS10130,ABUW_RS20220
IPR001041	IPR	2Fe-2S ferredoxin-type iron-sulfur binding domain	0; 3/ 11;0.01935;ABUW_RS12305,ABUW_RS13160,ABUW_RS14910
IPR015590	IPR	Aldehyde dehydrogenase domain	0; 6/ 25;0.01037;ABUW_RS12145,ABUW_RS12330,ABUW_RS12355,ABUW_RS13495,ABUW_RS14915,ABUW_RS18420
IPR018060	IPR	DNA binding HTH domain, AraC-type	1; 8/ 20;0.00056;ABUW_RS01080,ABUW_RS02230,ABUW_RS10120,ABUW_RS10155,ABUW_RS10290,ABUW_RS13430,ABUW_RS13565,ABUW_RS15545
IPR006091	IPR	Acyl-CoA oxidase/dehydrogenase, middle domain	0; 5/ 21;0.01407;ABUW_RS11355,ABUW_RS11930,ABUW_RS12060,ABUW_RS13505,ABUW_RS18405
IPR018376	IPR	Enoyl-CoA hydratase/isomerase, conserved site	0; 3/ 8;0.00722;ABUW_RS11940,ABUW_RS12300,ABUW_RS13490
IPR046373	IPR	Acyl-CoA oxidase/dehydrogenase, middle domain superfamily	0; 5/ 24;0.02482;ABUW_RS11355,ABUW_RS11930,ABUW_RS12060,ABUW_RS13505,ABUW_RS18405
IPR032687	IPR	HTH-type transcriptional regulator AraC-type, N-terminal	1; 3/ 5;0.00281;ABUW_RS13430,ABUW_RS13565,ABUW_RS15545
IPR031325	IPR	RHS repeat	1; 2/ 3;0.00281;ABUW_RS12690,ABUW_RS12705
IPR006531	IPR	Gp5/Type VI secretion system Vgr protein, OB-fold domain	1; 2/ 3;0.00281;ABUW_RS00575,ABUW_RS12710
IPR036010	IPR	2Fe-2S ferredoxin-like superfamily	0; 3/ 11;0.01935;ABUW_RS12305,ABUW_RS13160,ABUW_RS14910
IPR009040	IPR	Ferritin-like diiron domain	9; 2/ 2;0.00000;ABUW_RS01505,ABUW_RS15175
IPR007814	IPR	1,2-phenylacetyl-CoA epoxidase, subunit A/C	9; 2/ 2;0.00000;ABUW_RS12315,ABUW_RS12325
IPR011991	IPR	ArsR-like helix-turn-helix domain	0; 5/ 16;0.00531;ABUW_RS01110,ABUW_RS05440,ABUW_RS13020,ABUW_RS13605,ABUW_RS18455
IPR016161	IPR	Aldehyde/histidinol dehydrogenase	0; 6/ 26;0.01127;ABUW_RS12145,ABUW_RS12330,ABUW_RS12355,ABUW_RS13495,ABUW_RS14915,ABUW_RS18420
IPR004360	IPR	Glyoxalase/fosfomycin resistance/dioxygenase domain	1; 2/ 4;0.00585;ABUW_RS00325,ABUW_RS00335
IPR036264	IPR	Bacterial exopeptidase dimerisation domain	1; 2/ 4;0.00585;ABUW_RS04895,ABUW_RS09300
IPR037923	IPR	Transcription regulator HTH-like	0; 2/ 6;0.01802;ABUW_RS01080,ABUW_RS10120
IPR012000	IPR	Thiamine pyrophosphate enzyme, central domain	1; 2/ 3;0.00281;ABUW_RS05445,ABUW_RS14275
IPR014748	IPR	Enoyl-CoA hydratase, C-terminal	1; 4/ 9;0.00281;ABUW_RS04935,ABUW_RS11940,ABUW_RS12295,ABUW_RS12300
IPR001663	IPR	Aromatic-ring-hydroxylating dioxygenase, alpha subunit	0; 2/ 5;0.01060;ABUW_RS05625,ABUW_RS14920
IPR011650	IPR	Peptidase M20, dimerisation domain	0; 2/ 5;0.01060;ABUW_RS04895,ABUW_RS09300
IPR015879	IPR	Aromatic-ring-hydroxylating dioxygenase, alpha subunit, C-terminal domain	0; 2/ 5;0.01060;ABUW_RS05625,ABUW_RS14920
IPR003673	IPR	CoA-transferase family III	1; 2/ 4;0.00585;ABUW_RS12055,ABUW_RS12200
IPR000847	IPR	Transcription regulator HTH, LysR	0;10/ 54;0.01284;ABUW_RS05605,ABUW_RS07645,ABUW_RS09145,ABUW_RS10175,ABUW_RS11955,ABUW_RS14230,ABUW_RS14940,ABUW_RS15605,ABUW_RS16880,ABUW_RS16935
IPR006089	IPR	Acyl-CoA dehydrogenase, conserved site	0; 4/ 14;0.01060;ABUW_RS11930,ABUW_RS12060,ABUW_RS13505,ABUW_RS18405
IPR006076	IPR	FAD dependent oxidoreductase	0; 3/ 10;0.01407;ABUW_RS08405,ABUW_RS09630,ABUW_RS18450
IPR036188	IPR	FAD/NAD(P)-binding domain superfamily	0;11/ 57;0.00852;ABUW_RS00630,ABUW_RS08300,ABUW_RS08405,ABUW_RS08850,ABUW_RS09620,ABUW_RS09630,ABUW_RS10265,ABUW_RS10340,ABUW_RS12105,ABUW_RS14310,ABUW_RS18450
IPR037026	IPR	Vgr protein, OB-fold domain superfamily	1; 2/ 3;0.00281;ABUW_RS00575,ABUW_RS12710
IPR016156	IPR	FAD/NAD-linked reductase, dimerisation domain superfamily	0; 3/ 7;0.00531;ABUW_RS08300,ABUW_RS10340,ABUW_RS14310
IPR017439	IPR	Amidohydrolase	1; 2/ 3;0.00281;ABUW_RS04895,ABUW_RS09300
IPR011234	IPR	Fumarylacetoacetase-like, C-terminal	1; 2/ 3;0.00281;ABUW_RS00345,ABUW_RS09425
IPR006058	IPR	2Fe-2S ferredoxin, iron-sulphur binding site	0; 3/ 7;0.00531;ABUW_RS12305,ABUW_RS13160,ABUW_RS14910
IPR004841	IPR	Amino acid permease/ SLC12A domain	0; 5/ 16;0.00531;ABUW_RS00350,ABUW_RS00995,ABUW_RS13590,ABUW_RS13630,ABUW_RS18435

ClassID	Class	Description	Single_list
IPR000485	IPR	AsnC-type HTH domain	1; 5/ 12;0.00281;ABUW_RS00875,ABUW_RS05440,ABUW_RS13605,ABUW_RS18455,ABUW_RS18540
IPR023606	IPR	CoA-transferase family III domain 1 superfamily	1; 2/ 4;0.00585;ABUW_RS12055,ABUW_RS12200
IPR001826	IPR	RHS protein	1; 2/ 3;0.00281;ABUW_RS12690,ABUW_RS12705
IPR001753	IPR	Enoyl-CoA hydratase/isomerase	0; 5/ 13;0.00281;ABUW_RS04935,ABUW_RS11940,ABUW_RS12295,ABUW_RS12300,ABUW_RS13490
IPR039261	IPR	Ferredoxin-NADP reductase (FNR), nucleotide-binding domain	0; 4/ 12;0.00585;ABUW_RS01970,ABUW_RS12305,ABUW_RS13160,ABUW_RS14910
IPR017941	IPR	Rieske [2Fe-2S] iron-sulphur domain	0; 4/ 10;0.00364;ABUW_RS05625,ABUW_RS13465,ABUW_RS14920,ABUW_RS18960
IPR019887	IPR	Transcription regulator AsnC/Lrp, ligand binding domain	0; 4/ 11;0.00531;ABUW_RS00875,ABUW_RS05440,ABUW_RS13605,ABUW_RS18455
IPR002938	IPR	FAD-binding domain	0; 2/ 5;0.01060;ABUW_RS00630,ABUW_RS12105
IPR036250	IPR	Acyl-CoA dehydrogenase-like, C-terminal	0; 5/ 24;0.02482;ABUW_RS11355,ABUW_RS11930,ABUW_RS12060,ABUW_RS13505,ABUW_RS18405
IPR044043	IPR	Vanillate O-demethylase oxygenase-like, C-terminal catalytic domain	1; 2/ 3;0.00281;ABUW_RS13465,ABUW_RS18960
IPR016162	IPR	Aldehyde dehydrogenase, N-terminal	0; 6/ 25;0.01037;ABUW_RS12145,ABUW_RS12330,ABUW_RS12355,ABUW_RS13495,ABUW_RS14915,ABUW_RS18420
IPR045851	IPR	AMP-binding enzyme, C-terminal domain superfamily	0; 5/ 16;0.00531;ABUW_RS00865,ABUW_RS11920,ABUW_RS12280,ABUW_RS15985,ABUW_RS18360
IPR017927	IPR	FAD-binding domain, ferredoxin reductase-type	0; 4/ 11;0.00531;ABUW_RS01970,ABUW_RS12305,ABUW_RS13160,ABUW_RS14910
IPR001709	IPR	Flavoprotein pyridine nucleotide cytochrome reductase	0; 2/ 5;0.01060;ABUW_RS12305,ABUW_RS13160
IPR009057	IPR	Homeobox-like domain superfamily	0;11/ 42;0.00281;ABUW_RS01080,ABUW_RS02230,ABUW_RS10120,ABUW_RS10155,ABUW_RS10290,ABUW_RS11925,ABUW_RS13430,ABUW_RS13565,ABUW_RS15545,ABUW_RS18135,ABUW_RS18785
IPR020845	IPR	AMP-binding, conserved site	0; 4/ 14;0.01060;ABUW_RS00865,ABUW_RS11920,ABUW_RS15985,ABUW_RS18360
IPR019888	IPR	Transcription regulator AsnC-like	0; 4/ 11;0.00531;ABUW_RS00875,ABUW_RS05440,ABUW_RS13605,ABUW_RS18455
IPR036388	IPR	Winged helix-like DNA-binding domain superfamily	0;21/136;0.00932;ABUW_RS00875,ABUW_RS01110,ABUW_RS05440,ABUW_RS05605,ABUW_RS06565,ABUW_RS07645,ABUW_RS08350,ABUW_RS08610,ABUW_RS09145,ABUW_RS10130,ABUW_RS10175,ABUW_RS11955,ABUW_RS13020,ABUW_RS13605,ABUW_RS14230,ABUW_RS14940,ABUW_RS15605,ABUW_RS16880,ABUW_RS16935,ABUW_RS18455,ABUW_RS18540
IPR002024	IPR	Bacterioferritin	9; 2/ 2;0.00000;ABUW_RS01505,ABUW_RS15175
IPR017938	IPR	Riboflavin synthase-like beta-barrel	0; 4/ 13;0.00852;ABUW_RS01970,ABUW_RS12305,ABUW_RS13160,ABUW_RS14910
IPR000399	IPR	TPP-binding enzyme, conserved site	1; 2/ 3;0.00281;ABUW_RS05445,ABUW_RS14275
IPR009100	IPR	Acyl-CoA dehydrogenase/oxidase, N-terminal and middle domain superfamily	0; 5/ 24;0.02482;ABUW_RS11355,ABUW_RS11930,ABUW_RS12060,ABUW_RS13505,ABUW_RS18405
IPR011766	IPR	Thiamine pyrophosphate enzyme, TPP-binding	1; 2/ 3;0.00281;ABUW_RS05445,ABUW_RS14275
IPR008331	IPR	Ferritin/DPS protein domain	9; 2/ 2;0.00000;ABUW_RS01505,ABUW_RS15175
IPR019885	IPR	Transcription regulator HTH, AsnC-type, conserved site	0; 2/ 8;0.03928;ABUW_RS05440,ABUW_RS18455
IPR010067	IPR	Aliphatic sulfonates-binding protein	1; 2/ 3;0.00281;ABUW_RS18760,ABUW_RS18765
IPR023080	IPR	D-amino acid dehydrogenase DadA	1; 2/ 3;0.00281;ABUW_RS08405,ABUW_RS18450
IPR005119	IPR	LysR, substrate-binding	0;10/ 52;0.01060;ABUW_RS05605,ABUW_RS07645,ABUW_RS09145,ABUW_RS10175,ABUW_RS11955,ABUW_RS14230,ABUW_RS14940,ABUW_RS15605,ABUW_RS16880,ABUW_RS16935
IPR025110	IPR	AMP-binding enzyme, C-terminal domain	0; 4/ 14;0.01060;ABUW_RS00865,ABUW_RS11920,ABUW_RS15985,ABUW_RS18360
IPR006180	IPR	3-hydroxyacyl-CoA dehydrogenase, conserved site	1; 2/ 4;0.00585;ABUW_RS12020,ABUW_RS12290
IPR037523	IPR	Vicinal oxygen chelate (VOC) domain	1; 2/ 4;0.00585;ABUW_RS00325,ABUW_RS00335
IPR028244	IPR	Putative type VI secretion system, Rhs element associated Vgr domain	1; 2/ 3;0.00281;ABUW_RS00575,ABUW_RS12710
IPR006533	IPR	Type VI secretion system, RhsGE-associated Vgr protein	1; 2/ 3;0.00281;ABUW_RS00575,ABUW_RS12710
IPR012349	IPR	FMN-binding split barrel	0; 2/ 7;0.02726;ABUW_RS10130,ABUW_RS20220
IPR011968	IPR	Phenylacetate degradation probable enoyl-CoA hydratase PaaB	1; 2/ 3;0.00281;ABUW_RS04935,ABUW_RS12295
IPR036922	IPR	Rieske [2Fe-2S] iron-sulphur domain superfamily	0; 4/ 10;0.00364;ABUW_RS05625,ABUW_RS13465,ABUW_RS14920,ABUW_RS18960
IPR006108	IPR	3-hydroxyacyl-CoA dehydrogenase, C-terminal	0; 2/ 5;0.01060;ABUW_RS12020,ABUW_RS12290
IPR004840	IPR	Amino acid permease, conserved site	0; 4/ 15;0.01338;ABUW_RS00350,ABUW_RS00995,ABUW_RS13590,ABUW_RS18435
IPR045351	IPR	Domain of unknown function DUF6531	1; 2/ 3;0.00281;ABUW_RS12690,ABUW_RS12705
IPR017847	IPR	Type VI secretion system, RhsGE-associated Vgr family subset	1; 2/ 3;0.00281;ABUW_RS00575,ABUW_RS12710
IPR029045	IPR	ClpP/crotonase-like domain superfamily	0; 6/ 24;0.00852;ABUW_RS04935,ABUW_RS11935,ABUW_RS11940,ABUW_RS12295,ABUW_RS12300,ABUW_RS13490
IPR015931	IPR	Aconitase/3-isopropylmalate dehydratase large subunit, alpha/beta/alpha, subdomain 1/3	1; 2/ 4;0.00585;ABUW_RS07780,ABUW_RS18525

ClassID	Class	Description	Single_list
IPR016163	IPR	Aldehyde dehydrogenase, C-terminal	0; 6/ 25;0.01037;ABUW_RS12145,ABUW_RS12330,ABUW_RS12355,ABUW_RS13495,ABUW_RS14915,ABUW_RS18420
IPR029035	IPR	DHS-like NAD/FAD-binding domain superfamily	0; 2/ 6;0.01802;ABUW_RS05445,ABUW_RS14275
IPR011967	IPR	3-hydroxyacyl-CoA dehydrogenase PaaC	9; 2/ 2;0.00000;ABUW_RS12020,ABUW_RS12290
IPR015928	IPR	Aconitase/3-isopropylmalate dehydratase, swivel	1; 2/ 4;0.00585;ABUW_RS07780,ABUW_RS18525
IPR036663	IPR	Fumarylacetoacetase-like, C-terminal domain superfamily	1; 2/ 3;0.00281;ABUW_RS00345,ABUW_RS09425
IPR022385	IPR	Rhs repeat-associated core	1; 2/ 3;0.00281;ABUW_RS12690,ABUW_RS12705
IPR000873	IPR	AMP-dependent synthetase/ligase domain	0; 5/ 16;0.00531;ABUW_RS00865,ABUW_RS11920,ABUW_RS12280,ABUW_RS15985,ABUW_RS18360
IPR042099	IPR	ANL, N-terminal domain	0; 4/ 12;0.00585;ABUW_RS00865,ABUW_RS12280,ABUW_RS15985,ABUW_RS18360
IPR018062	IPR	HTH domain AraC-type, conserved site	0; 4/ 11;0.00531;ABUW_RS01080,ABUW_RS02230,ABUW_RS10120,ABUW_RS10290
IPR015168	IPR	SsuA/THI5-like	1; 2/ 3;0.00281;ABUW_RS18760,ABUW_RS18765
IPR004165	IPR	Coenzyme A transferase family I	0; 2/ 8;0.03928;ABUW_RS08915,ABUW_RS11995
IPR020449	IPR	Transcription regulator HTH, AraC- type	0; 5/ 14;0.00318;ABUW_RS01080,ABUW_RS02230,ABUW_RS10290,ABUW_RS13565,ABUW_RS15545
IPR009078	IPR	Ferritin-like superfamily	1; 4/ 7;0.00164;ABUW_RS01505,ABUW_RS12315,ABUW_RS12325,ABUW_RS15175
IPR029061	IPR	Thiamin diphosphate-binding fold	0; 4/ 11;0.00531;ABUW_RS05445,ABUW_RS10355,ABUW_RS14215,ABUW_RS14275
IPR018769	IPR	Type VI secretion system spike protein VgrG2, domain of unknown function DUF2345	1; 2/ 3;0.00281;ABUW_RS00575,ABUW_RS12710
IPR009075	IPR	Acyl-CoA dehydrogenase/oxidase C-terminal	0; 4/ 20;0.03946;ABUW_RS11930,ABUW_RS12060,ABUW_RS13505,ABUW_RS18405
IPR001433	IPR	Oxidoreductase FAD/NAD(P)-binding	0; 4/ 12;0.00585;ABUW_RS01970,ABUW_RS12305,ABUW_RS13160,ABUW_RS14910
IPR002577	IPR	Helix-turn-helix, HxlR type	0; 2/ 8;0.03928;ABUW_RS01110,ABUW_RS13020
IPR001638	IPR	Solute-binding protein family 3/N-terminal domain of MltF	0; 4/ 11;0.00531;ABUW_RS11345,ABUW_RS11590,ABUW_RS18760,ABUW_RS18765
IPR011008	IPR	Dimeric alpha-beta barrel	0; 5/ 16;0.00531;ABUW_RS00875,ABUW_RS05440,ABUW_RS09135,ABUW_RS13605,ABUW_RS18455
IPR013786	IPR	Acyl-CoA dehydrogenase/oxidase, N-terminal	0; 5/ 24;0.02482;ABUW_RS11355,ABUW_RS11930,ABUW_RS12060,ABUW_RS13505,ABUW_RS18405
IPR012001	IPR	Thiamine pyrophosphate enzyme, N-terminal TPP-binding domain	1; 2/ 3;0.00281;ABUW_RS05445,ABUW_RS14275
IPR029068	IPR	Glyoxalase/Bleomycin resistance protein/Dihydroxybiphenyl dioxygenase	1; 2/ 4;0.00585;ABUW_RS00325,ABUW_RS00335
IPR015881	IPR	Aromatic-ring-hydroxylating dioxygenase, 2Fe-2S-binding site	1; 4/ 7;0.00164;ABUW_RS05625,ABUW_RS13465,ABUW_RS14920,ABUW_RS18960
IPR005814	IPR	Aminotransferase class-III	0; 2/ 8;0.03928;ABUW_RS01005,ABUW_RS13600
IPR037171	IPR	NagB/RpiA transferase-like	0; 4/ 12;0.00585;ABUW_RS01250,ABUW_RS08915,ABUW_RS11685,ABUW_RS11995
IPR036008	IPR	Aconitase, iron-sulfur domain	1; 2/ 4;0.00585;ABUW_RS07780,ABUW_RS18525
IPR006530	IPR	YD repeat	1; 2/ 3;0.00281;ABUW_RS12690,ABUW_RS12705
IPR041040	IPR	3-hydroxybutyryl-CoA dehydrogenase reduced Rossmann-fold domain	9; 2/ 2;0.00000;ABUW_RS12020,ABUW_RS12290
IPR037069	IPR	Acyl-CoA dehydrogenase/oxidase, N-terminal domain superfamily	0; 5/ 24;0.02482;ABUW_RS11355,ABUW_RS11930,ABUW_RS12060,ABUW_RS13505,ABUW_RS18405
IPR012347	IPR	Ferritin-like	2; 4/ 6;0.00063;ABUW_RS01505,ABUW_RS12315,ABUW_RS12325,ABUW_RS15175
IPR002933	IPR	Peptidase M20	0; 2/ 5;0.01060;ABUW_RS04895,ABUW_RS09300
IPR008333	IPR	Flavoprotein pyridine nucleotide cytochrome reductase-like, FAD-binding domain	1; 4/ 8;0.00281;ABUW_RS01970,ABUW_RS12305,ABUW_RS13160,ABUW_RS14910
IPR036390	IPR	Winged helix DNA-binding domain superfamily	0;21/113;0.00281;ABUW_RS00875,ABUW_RS01110,ABUW_RS05440,ABUW_RS05605,ABUW_RS06565,ABUW_RS07645,ABUW_RS08350,ABUW_RS08610,ABUW_RS09145,ABUW_RS10130,ABUW_RS10175,ABUW_RS11955,ABUW_RS13020,ABUW_RS13605,ABUW_RS14230,ABUW_RS14940,ABUW_RS15605,ABUW_RS16880,ABUW_RS16935,ABUW_RS18455,ABUW_RS18540
IPR001030	IPR	Aconitase/3-isopropylmalate dehydratase large subunit, alpha/beta/alpha domain	1; 2/ 4;0.00585;ABUW_RS07780,ABUW_RS18525
IPR000551	IPR	MerR-type HTH domain	0; 2/ 6;0.01802;ABUW_RS09205,ABUW_RS17845
IPR044855	IPR	CoA-transferase family III domain 3 superfamily	1; 2/ 4;0.00585;ABUW_RS12055,ABUW_RS12200
00650 Butanoate metabolism [PATH:ko00650]	KEGG	ko00650	0; 6/23;7.5e-03;ABUW_RS00340,ABUW_RS00865,ABUW_RS12020,ABUW_RS12290,ABUW_RS14275,ABUW_RS14915
00330 Arginine and proline metabolism [PATH:ko00330]	KEGG	ko00330	0; 4/15;1.8e-02;ABUW_RS01735,ABUW_RS09630,ABUW_RS13595,ABUW_RS13600
02026 Biofilm	KEGG	ko02026	0; 2/ 7;4.2e-02;ABUW_RS05605,ABUW_RS15605

ClassID	Class	Description	Single_list
formation - Escherichia coli [PATH:ko02026]			
00920 Sulfur metabolism [PATH:ko00920]	KEGG	ko00920	0; 8/34;6.7e-03;ABUW_RS01375,ABUW_RS03555,ABUW_RS09455,ABUW_RS11590,ABUW_RS11605,ABUW_RS11745,ABUW_RS18760,ABUW_RS18765
00640 Propanoate metabolism [PATH:ko00640]	KEGG	ko00640	1; 6/13;2.1e-04;ABUW_RS01005,ABUW_RS12300,ABUW_RS18420,ABUW_RS18525,ABUW_RS18530,ABUW_RS18535
00360 Phenylalanine metabolism [PATH:ko00360]	KEGG	ko00360	5;10/14;3.8e-09;ABUW_RS04935,ABUW_RS12280,ABUW_RS12295,ABUW_RS12305,ABUW_RS12310,ABUW_RS12315,ABUW_RS12320,ABUW_RS12325,ABUW_RS12330,ABUW_RS18450
DNA-binding	KEYWORDS	keyword	0;16/83;0.020;ABUW_RS00875,ABUW_RS01110,ABUW_RS07645,ABUW_RS07915,ABUW_RS10155,ABUW_RS10175,ABUW_RS11925,ABUW_RS11955,ABUW_RS13020,ABUW_RS13605,ABUW_RS14230,ABUW_RS15545,ABUW_RS16935,ABUW_RS17845,ABUW_RS18540,ABUW_RS18785
2Fe-2S	KEYWORDS	keyword	0; 7/30;0.023;ABUW_RS05625,ABUW_RS12305,ABUW_RS13160,ABUW_RS13465,ABUW_RS14910,ABUW_RS14920,ABUW_RS18960
Activator	KEYWORDS	keyword	0;13/68;0.023;ABUW_RS01080,ABUW_RS02230,ABUW_RS05440,ABUW_RS05605,ABUW_RS09205,ABUW_RS10120,ABUW_RS13430,ABUW_RS13565,ABUW_RS14940,ABUW_RS15605,ABUW_RS16880,ABUW_RS17720,ABUW_RS18455
Aromatic hydrocarbons catabolism	KEYWORDS	keyword	0; 6/27;0.037;ABUW_RS08915,ABUW_RS09135,ABUW_RS11995,ABUW_RS12105,ABUW_RS13510,ABUW_RS14310
3D-structure	KEYWORDS	keyword	0;46/359;0.023;ABUW_RS00325,ABUW_RS00575,ABUW_RS01005,ABUW_RS01375,ABUW_RS01505,ABUW_RS01680,ABUW_RS01970,ABUW_RS02410,ABUW_RS04935,ABUW_RS05890,ABUW_RS05970,ABUW_RS06145,ABUW_RS07335,ABUW_RS08610,ABUW_RS08850,ABUW_RS09105,ABUW_RS09145,ABUW_RS09425,ABUW_RS10130,ABUW_RS10145,ABUW_RS10290,ABUW_RS10685,ABUW_RS11475,ABUW_RS11590,ABUW_RS11605,ABUW_RS11930,ABUW_RS11935,ABUW_RS11945,ABUW_RS12020,ABUW_RS12290,ABUW_RS12295,ABUW_RS12300,ABUW_RS12315,ABUW_RS12325,ABUW_RS12330,ABUW_RS13490,ABUW_RS13505,ABUW_RS13525,ABUW_RS14175,ABUW_RS14515,ABUW_RS14915,ABUW_RS18275,ABUW_RS18405,ABUW_RS18535,ABUW_RS18760,ABUW_RS18765
operon_0854	operons	NZ_CP008706.1;ID=gene-ABUW_RS09310;Name=ABUW_RS09310;gbkey=Gene;gene_biotype=protein_coding;locus_tag=ABUW_RS09310;old_locus_tag=ABUW_1912	0;2/ 6;1.6e-02;ABUW_RS09325,ABUW_RS09330
operon_0039	operons	NZ_CP008706.1;ID=gene-ABUW_RS00335;Name=ABUW_RS00335;gbkey=Gene;gene_biotype=protein_coding;locus_tag=ABUW_RS00335;old_locus_tag=ABUW_0068	9;3/ 3;0.0e+00;ABUW_RS00335,ABUW_RS00340,ABUW_RS00345
operon_1417	operons	NZ_CP008706.1;ID=gene-ABUW_RS14910;Name=cntB;gbkey=Gene;gene=cntB;gene_biotype=protein_coding;locus_tag=ABUW_RS14910;old_locus_tag=ABUW_3072	2;4/ 6;1.0e-04;ABUW_RS14910,ABUW_RS14915,ABUW_RS14920,ABUW_RS14925
operon_1273	operons	NZ_CP008706.1;ID=gene-ABUW_RS13580;Name=ABUW_RS13580;gbkey=Gene;gene_biotype=protein_coding;locus_tag=ABUW_RS13580;old_locus_tag=ABUW_2796	9;2/ 2;0.0e+00;ABUW_RS13580,ABUW_RS13585
operon_1036	operons	NZ_CP008706.1;ID=gene-ABUW_RS11265;Name=ABUW_RS11265;gbkey=Gene;gene_biotype=protein_coding;locus_tag=ABUW_RS11265;old_locus_tag=ABUW_2316	9;2/ 2;0.0e+00;ABUW_RS11265,ABUW_RS11270
operon_1275	operons	NZ_CP008706.1;ID=gene-ABUW_RS13595;Name=astA;gbkey=Gene;gene=astA;gene_biotype=protein_coding;locus_tag=ABUW_RS13595;old_locus_tag=ABUW_2799	9;2/ 2;0.0e+00;ABUW_RS13595,ABUW_RS13600
operon_1357	operons	NZ_CP008706.1;ID=gene-ABUW_RS14275;Name=ABUW_RS14275;gbkey=Gene;gene_biotype=protein_coding;locus_tag=ABUW_RS14275;old_locus_tag=ABUW_2941	1;5/13;1.3e-03;ABUW_RS14275,ABUW_RS14290,ABUW_RS14295,ABUW_RS14310,ABUW_RS14330
operon_1668	operons	NZ_CP008706.1;ID=gene-ABUW_RS17720;Name=ABUW_RS17720;gbkey=Gene;gene_biotype=protein_coding;locus_tag=ABUW_RS17720;old_locus_tag=ABUW_3639	1;2/ 3;1.3e-03;ABUW_RS17720,ABUW_RS17725
operon_1109	operons	NZ_CP008706.1;ID=gene-ABUW_RS11930;Name=ABUW_RS11930;gbkey=Gene;gene_biotype=protein_coding;locus_tag=ABUW_RS11930;old_locus_tag=ABUW_2452	3;4/ 5;2.0e-05;ABUW_RS11930,ABUW_RS11935,ABUW_RS11940,ABUW_RS11945
operon_1108	operons	NZ_CP008706.1;ID=gene-ABUW_RS11915;Name=ABUW_RS11915;gbkey=Gene;gene_biotype=protein_coding;locus_tag=ABUW_RS11915;old_locus_tag=ABUW_2449	9;3/ 3;0.0e+00;ABUW_RS11915,ABUW_RS11920,ABUW_RS11925
operon_0887	operons	NZ_CP008706.1;ID=gene-ABUW_RS09630;Name=ABUW_RS09630;gbkey=Gene;gene_biotype=protein_coding;locus_tag=ABUW_RS09630;old_locus_tag=ABUW_1980	9;3/ 3;0.0e+00;ABUW_RS09630,ABUW_RS09635,ABUW_RS09640

ClassID	Class	Description	Single_list
operon_0642	operons	NZ_CP008706.1;ID=gene-ABUW_RS07250;Name=csuAB;gbkey=Gene;gene=csuAB;gene_biotype=protein_coding;locus_tag=ABUW_RS07250;old_locus_tag=ABUW_1487	4;5/ 6;2.0e-06;ABUW_RS07250,ABUW_RS07255,ABUW_RS07260,ABUW_RS07265,ABUW_RS07270
operon_1033	operons	NZ_CP008706.1;ID=gene-ABUW_RS11235;Name=ABUW_RS11235;gbkey=Gene;gene_biotype=protein_coding;locus_tag=ABUW_RS11235;old_locus_tag=ABUW_2310	2;3/ 4;1.8e-04;ABUW_RS11235,ABUW_RS11245,ABUW_RS11250
operon_1173	operons	NZ_CP008706.1;ID=gene-ABUW_RS12680;Name=ABUW_RS12680;gbkey=Gene;gene_biotype=protein_coding;locus_tag=ABUW_RS12680;old_locus_tag=ABUW_2611	1;2/ 3;1.3e-03;ABUW_RS12685,ABUW_RS12690
operon_0816	operons	NZ_CP008706.1;ID=gene-ABUW_RS08850;Name=ABUW_RS08850;gbkey=Gene;gene_biotype=protein_coding;locus_tag=ABUW_RS08850;old_locus_tag=ABUW_1819	1;2/ 4;4.5e-03;ABUW_RS08850,ABUW_RS08855
operon_1731	operons	NZ_CP008706.1;ID=gene-ABUW_RS18440;Name=ABUW_RS18440;gbkey=Gene;gene_biotype=protein_coding;locus_tag=ABUW_RS18440;old_locus_tag=ABUW_3787	9;3/ 3;0.0e+00;ABUW_RS18440,ABUW_RS18445,ABUW_RS18450
operon_1127	operons	NZ_CP008706.1;ID=gene-ABUW_RS12125;Name=ABUW_RS12125;gbkey=Gene;gene_biotype=protein_coding;locus_tag=ABUW_RS12125;old_locus_tag=ABUW_2491	1;4/10;1.9e-03;ABUW_RS12135,ABUW_RS12145,ABUW_RS20220,ABUW_RS20225
operon_0447	operons	NZ_CP008706.1;ID=gene-ABUW_RS04835;Name=ABUW_RS04835;gbkey=Gene;gene_biotype=protein_coding;locus_tag=ABUW_RS04835;old_locus_tag=ABUW_0986	1;2/ 3;1.3e-03;ABUW_RS04840,ABUW_RS04845
operon_1265	operons	NZ_CP008706.1;ID=gene-ABUW_RS13490;Name=ABUW_RS13490;gbkey=Gene;gene_biotype=protein_coding;locus_tag=ABUW_RS13490;old_locus_tag=ABUW_2778	6;7/ 8;2.1e-08;ABUW_RS13490,ABUW_RS13495,ABUW_RS13500,ABUW_RS13505,ABUW_RS13510,ABUW_RS13515,ABUW_RS13525
operon_1727	operons	NZ_CP008706.1;ID=gene-ABUW_RS18390;Name=ABUW_RS18390;gbkey=Gene;gene_biotype=protein_coding;locus_tag=ABUW_RS18390;old_locus_tag=ABUW_3777	0;2/ 7;2.6e-02;ABUW_RS18405,ABUW_RS18420
operon_0957	operons	NZ_CP008706.1;ID=gene-ABUW_RS10330;Name=ABUW_RS10330;gbkey=Gene;gene_biotype=protein_coding;locus_tag=ABUW_RS10330;old_locus_tag=ABUW_2126	0;2/ 6;1.6e-02;ABUW_RS10340,ABUW_RS10355
operon_0868	operons	NZ_CP008706.1;ID=gene-ABUW_RS09450;Name=ABUW_RS09450;gbkey=Gene;gene_biotype=protein_coding;locus_tag=ABUW_RS09450;old_locus_tag=ABUW_1942	2;3/ 4;1.8e-04;ABUW_RS09450,ABUW_RS09455,ABUW_RS09460
operon_1446	operons	NZ_CP008706.1;ID=gene-ABUW_RS15235;Name=ABUW_RS15235;gbkey=Gene;gene_biotype=protein_coding;locus_tag=ABUW_RS15235;old_locus_tag=ABUW_3138	1;2/ 3;1.3e-03;ABUW_RS15240,ABUW_RS15245
operon_0514	operons	NZ_CP008706.1;ID=gene-ABUW_RS05590;Name=ABUW_RS05590;gbkey=Gene;gene_biotype=protein_coding;locus_tag=ABUW_RS05590;old_locus_tag=ABUW_1142	9;2/ 2;0.0e+00;ABUW_RS05590,ABUW_RS05595
operon_1140	operons	NZ_CP008706.1;ID=gene-ABUW_RS12265;Name=ABUW_RS12265;gbkey=Gene;gene_biotype=protein_coding;locus_tag=ABUW_RS12265;old_locus_tag=ABUW_2523	5;9/13;3.9e-08;ABUW_RS12280,ABUW_RS12290,ABUW_RS12295,ABUW_RS12300,ABUW_RS12305,ABUW_RS12310,ABUW_RS12315,ABUW_RS12320,ABUW_RS12325
operon_0828	operons	NZ_CP008706.1;ID=gene-ABUW_RS09040;Name=ABUW_RS09040;gbkey=Gene;gene_biotype=protein_coding;locus_tag=ABUW_RS09040;old_locus_tag=ABUW_1857	0;3/ 9;9.3e-03;ABUW_RS09050,ABUW_RS09055,ABUW_RS09070
operon_1385	operons	NZ_CP008706.1;ID=gene-ABUW_RS14635;Name=ABUW_RS14635;gbkey=Gene;gene_biotype=protein_coding;locus_tag=ABUW_RS14635;old_locus_tag=ABUW_3016	9;2/ 2;0.0e+00;ABUW_RS14635,ABUW_RS14640
operon_0446	operons	NZ_CP008706.1;ID=gene-ABUW_RS04825;Name=rbtA;gbkey=Gene;gene=rbtA;gene_biotype=protein_coding;locus_tag=ABUW_RS04825;old_locus_tag=ABUW_0984	9;2/ 2;0.0e+00;ABUW_RS04825,ABUW_RS04830
operon_1559	operons	NZ_CP008706.1;ID=gene-ABUW_RS16500;Name=ABUW_RS16500;gbkey=Gene;gene_biotype=protein_coding;locus_tag=ABUW_RS16500;old_locus_tag=ABUW_3395	9;2/ 2;0.0e+00;ABUW_RS16500,ABUW_RS16505
operon_0935	operons	NZ_CP008706.1;ID=gene-ABUW_RS10125;Name=ABUW_RS10125;gbkey=Gene;gene_biotype=protein_coding;locus_tag=ABUW_RS10125;old_locus_tag=ABUW_2085	0;2/ 5;9.3e-03;ABUW_RS10130,ABUW_RS10145
operon_1174	operons	NZ_CP008706.1;ID=gene-ABUW_RS12700;Name=ABUW_RS12700;gbkey=Gene;gene_biotype=protein_coding;locus_tag=ABUW_RS12700;old_locus_tag=ABUW_2616	1;2/ 3;1.3e-03;ABUW_RS12705,ABUW_RS12710
operon_0044	operons	NZ_CP008706.1;ID=gene-ABUW_RS00380;Name=hutU;gbkey=Gene;gene=hutU;gene_biotype=protein_coding;locus_tag=ABUW_RS00380;old_locus_tag=ABUW_0077	1;3/ 5;7.9e-04;ABUW_RS00380,ABUW_RS00385,ABUW_RS00400
operon_1757	operons	NZ_CP008706.1;ID=gene-ABUW_RS18760;Name=ABUW_RS18760;gbkey=Gene;gene_biotype=protein_coding;locus_tag=ABUW_RS18760;old_locus_tag=ABUW_3853	0;2/ 5;9.3e-03;ABUW_RS18760,ABUW_RS18765
operon_1739	operons	NZ_CP008706.1;ID=gene-ABUW_RS18515;Name=ABUW_RS18515;gbkey=Gene;gene_biotype=protein_coding;locus_tag=ABUW_RS18515;old_locus_tag=ABUW_3805	9;6/ 6;0.0e+00;ABUW_RS18515,ABUW_RS18520,ABUW_RS18525,ABUW_RS18530,ABUW_RS18535,ABUW_RS18540
operon_1317	operons	NZ_CP008706.1;ID=gene-ABUW_RS13980;Name=ABUW_RS13980;gbkey=Gene;gene	0;2/ 8;3.8e-02;ABUW_RS14015,ABUW_RS20660

ClassID	Class	Description	Single_list
		_biotype=protein_coding;locus_tag=ABUW_RS13980;old_locus_tag=ABUW_2878	
operon_0098	operons	NZ_CP008706.1;ID=gene-ABUW_RS00905;Name=ABUW_RS00905;gbkey=Gene;gene_biotype=protein_coding;locus_tag=ABUW_RS00905;old_locus_tag=ABUW_0183	9;2/ 2;0.0e+00;ABUW_RS00905,ABUW_RS00910
operon_1560	operons	NZ_CP008706.1;ID=gene-ABUW_RS16510;Name=ABUW_RS16510;gbkey=Gene;gene_biotype=protein_coding;locus_tag=ABUW_RS16510;old_locus_tag=ABUW_3397	9;2/ 2;0.0e+00;ABUW_RS16510,ABUW_RS16515
operon_1469	operons	NZ_CP008706.1;ID=gene-ABUW_RS15495;Name=ABUW_RS15495;gbkey=Gene;gene_biotype=protein_coding;locus_tag=ABUW_RS15495;old_locus_tag=ABUW_3191	1;2/ 3;1.3e-03;ABUW_RS15500,ABUW_RS15505
operon_0061	operons	NZ_CP008706.1;ID=gene-ABUW_RS00575;Name=ABUW_RS00575;gbkey=Gene;gene_biotype=protein_coding;locus_tag=ABUW_RS00575;old_locus_tag=ABUW_0116	1;3/ 6;1.6e-03;ABUW_RS00575,ABUW_RS00585,ABUW_RS00600
operon_1679	operons	NZ_CP008706.1;ID=gene-ABUW_RS17895;Name=ABUW_RS17895;gbkey=Gene;gene_biotype=protein_coding;locus_tag=ABUW_RS17895;old_locus_tag=ABUW_3675	0;2/ 5;9.3e-03;ABUW_RS17895,ABUW_RS19995
PF10106	Pfam	Uncharacterized protein conserved in bacteria (DUF2345)	1; 2/ 3;0.00203;ABUW_RS00575,ABUW_RS12710
PF00970	Pfam	Oxidoreductase FAD-binding domain	1; 4/ 8;0.00203;ABUW_RS01970,ABUW_RS12305,ABUW_RS13160,ABUW_RS14910
PF02737	Pfam	3-hydroxyacyl-CoA dehydrogenase, NAD binding domain	0; 2/ 5;0.00931;ABUW_RS12020,ABUW_RS12290
PF04717	Pfam	Type VI secretion system/phage-baseplate injector OB domain	1; 2/ 3;0.00203;ABUW_RS00575,ABUW_RS12710
PF00501	Pfam	AMP-binding enzyme	0; 5/16;0.00466;ABUW_RS00865,ABUW_RS11920,ABUW_RS12280,ABUW_RS15985,ABUW_RS18360
PF07687	Pfam	Peptidase dimerisation domain	0; 2/ 5;0.00931;ABUW_RS04895,ABUW_RS09300
PF00111	Pfam	2Fe-2S iron-sulfur cluster binding domain	0; 3/ 9;0.00931;ABUW_RS12305,ABUW_RS13160,ABUW_RS14910
PF05138	Pfam	Phenylacetic acid catabolic protein	9; 2/ 2;0.00000;ABUW_RS12315,ABUW_RS12325
PF00903	Pfam	Glyoxalase/Bleomycin resistance protein/Dioxygenase superfamily	1; 2/ 4;0.00564;ABUW_RS00325,ABUW_RS00335
PF01613	Pfam	Flavin reductase like domain	0; 2/ 6;0.01572;ABUW_RS10130,ABUW_RS20220
PF02515	Pfam	CoA-transferase family III	1; 2/ 4;0.00564;ABUW_RS12055,ABUW_RS12200
PF00175	Pfam	Oxidoreductase NAD-binding domain	0; 4/12;0.00564;ABUW_RS01970,ABUW_RS12305,ABUW_RS13160,ABUW_RS14910
PF00441	Pfam	Acyl-CoA dehydrogenase, C-terminal domain	0; 4/20;0.03464;ABUW_RS11930,ABUW_RS12060,ABUW_RS13505,ABUW_RS18405
PF02776	Pfam	Thiamine pyrophosphate enzyme, N-terminal TPP binding domain	1; 2/ 3;0.00203;ABUW_RS05445,ABUW_RS14275
PF00355	Pfam	Rieske [2Fe-2S] domain	1; 4/ 9;0.00203;ABUW_RS05625,ABUW_RS13465,ABUW_RS14920,ABUW_RS18960
PF02775	Pfam	Thiamine pyrophosphate enzyme, C-terminal TPP binding domain	1; 2/ 3;0.00203;ABUW_RS05445,ABUW_RS14275
PF20148	Pfam	Domain of unknown function (DUF6531)	1; 2/ 3;0.00203;ABUW_RS12690,ABUW_RS12705
PF01494	Pfam	FAD binding domain	0; 2/ 5;0.00931;ABUW_RS00630,ABUW_RS12105
PF18321	Pfam	3-hydroxybutyryl-CoA dehydrogenase reduced Rossmann-fold domain	9; 2/ 2;0.00000;ABUW_RS12020,ABUW_RS12290
PF03466	Pfam	LysR substrate binding domain	0;10/52;0.00931;ABUW_RS05605,ABUW_RS07645,ABUW_RS09145,ABUW_RS10175,ABUW_RS11955,ABUW_RS14230,ABUW_RS14940,ABUW_RS15605,ABUW_RS16880,ABUW_RS16935
PF13296	Pfam	Putative type VI secretion system Rhs element Vgr	1; 2/ 3;0.00203;ABUW_RS00575,ABUW_RS12710
PF09084	Pfam	NMT1/THI5 like	1; 2/ 3;0.00203;ABUW_RS18760,ABUW_RS18765
PF02770	Pfam	Acyl-CoA dehydrogenase, middle domain	0; 5/21;0.01206;ABUW_RS11355,ABUW_RS11930,ABUW_RS12060,ABUW_RS13505,ABUW_RS18405
PF00171	Pfam	Aldehyde dehydrogenase family	0; 6/25;0.00931;ABUW_RS12145,ABUW_RS12330,ABUW_RS12355,ABUW_RS13495,ABUW_RS14915,ABUW_RS18420
PF19112	Pfam	Vanillate O-demethylase oxygenase C-terminal domain	1; 2/ 3;0.00203;ABUW_RS13465,ABUW_RS18960
PF00330	Pfam	Aconitase family (aconitate hydratase)	1; 2/ 4;0.00564;ABUW_RS07780,ABUW_RS18525
PF12833	Pfam	Helix-turn-helix domain	1; 8/20;0.00035;ABUW_RS01080,ABUW_RS02230,ABUW_RS10120,ABUW_RS10155,ABUW_RS10290,ABUW_RS13430,ABUW_RS13565,ABUW_RS15545
PF05593	Pfam	RHS Repeat	1; 2/ 3;0.00203;ABUW_RS12690,ABUW_RS12705
PF12697	Pfam	Alpha/beta hydrolase family	0; 2/ 5;0.00931;ABUW_RS14295,ABUW_RS20225
PF00205	Pfam	Thiamine pyrophosphate enzyme, central domain	1; 2/ 3;0.00203;ABUW_RS05445,ABUW_RS14275
PF02771	Pfam	Acyl-CoA dehydrogenase, N-terminal domain	0; 5/24;0.02252;ABUW_RS11355,ABUW_RS11930,ABUW_RS12060,ABUW_RS13505,ABUW_RS18405
PF01266	Pfam	FAD dependent oxidoreductase	0; 3/10;0.01206;ABUW_RS08405,ABUW_RS09630,ABUW_RS18450
PF00324	Pfam	Amino acid permease	0; 5/16;0.00466;ABUW_RS00350,ABUW_RS00995,ABUW_RS13590,ABUW_RS13630,ABUW_RS18435
PF00848	Pfam	Ring hydroxylating alpha subunit (catalytic domain)	0; 2/ 5;0.00931;ABUW_RS05625,ABUW_RS14920
PF13193	Pfam	AMP-binding enzyme C-terminal domain	0; 4/14;0.00931;ABUW_RS00865,ABUW_RS11920,ABUW_RS15985,ABUW_RS18360
PF01144	Pfam	Coenzyme A transferase	0; 2/ 8;0.03464;ABUW_RS08915,ABUW_RS11995
PF03527	Pfam	RHS protein	1; 2/ 3;0.00203;ABUW_RS12690,ABUW_RS12705
PF01638	Pfam	HxlR-like helix-turn-helix	0; 2/ 8;0.03464;ABUW_RS01110,ABUW_RS13020
PF00126	Pfam	Bacterial regulatory helix-turn-helix protein, lysR family	0;10/54;0.01109;ABUW_RS05605,ABUW_RS07645,ABUW_RS09145,ABUW_RS10175,ABUW_RS11955,ABUW_RS14230,ABUW_RS14940,ABUW_RS15605,ABUW_RS16880,ABUW_RS16935
PF00202	Pfam	Aminotransferase class-III	0; 2/ 8;0.03464;ABUW_RS01005,ABUW_RS13600

ClassID	Class	Description	Single_list
PF01037	Pfam	Lrp/AsnC ligand binding domain	0; 4/11;0.00456;ABUW_RS00875,ABUW_RS05440,ABUW_RS13605,ABUW_RS18455
PF00725	Pfam	3-hydroxyacyl-CoA dehydrogenase, C-terminal domain	0; 2/ 5;0.00931;ABUW_RS12020,ABUW_RS12290
PF00378	Pfam	Enoyl-CoA hydratase/isomerase	1; 5/13;0.00203;ABUW_RS04935,ABUW_RS11940,ABUW_RS12295,ABUW_RS12300,ABUW_RS13490
PF12625	Pfam	Arabinose-binding domain of AraC transcription regulator, N-term	1; 3/ 5;0.00203;ABUW_RS13430,ABUW_RS13565,ABUW_RS15545
PF00210	Pfam	Ferritin-like domain	9; 2/ 2;0.00000;ABUW_RS01505,ABUW_RS15175
PF01557	Pfam	Fumarylacetoacetate (FAA) hydrolase family	1; 2/ 3;0.00203;ABUW_RS00345,ABUW_RS09425
PF01546	Pfam	Peptidase family M20/M25/M40	0; 2/ 5;0.00931;ABUW_RS04895,ABUW_RS09300
PF07992	Pfam	Pyridine nucleotide-disulphide oxidoreductase	0; 4/22;0.04962;ABUW_RS08300,ABUW_RS08850,ABUW_RS10340,ABUW_RS14310

2.6 Enrichment Analysis (GSEA) of *A. baumannii* in LCWB medium vs M9 medium Up Regulated

ClassID	Class	Description	Single_list
GO:0019843	GO	rRNA binding	9; 37/ 40;5.8e-20;ABUW_RS01285,ABUW_RS01995,ABUW_RS02000,ABUW_RS02005,ABUW_RS02010,ABUW_RS02015,ABUW_RS02020,ABUW_RS02030,ABUW_RS02040,ABUW_RS02045,ABUW_RS02050,ABUW_RS02055,ABUW_RS02060,ABUW_RS02065,ABUW_RS02070,ABUW_RS02075,ABUW_RS02080,ABUW_RS02090,ABUW_RS02105,ABUW_RS02110,ABUW_RS02115,ABUW_RS03225,ABUW_RS04160,ABUW_RS05065,ABUW_RS05565,ABUW_RS07545,ABUW_RS07550,ABUW_RS07555,ABUW_RS10775,ABUW_RS14860,ABUW_RS14865,ABUW_RS15950,ABUW_RS16365,ABUW_RS16810,ABUW_RS16915,ABUW_RS17120,ABUW_RS17490
IPR004498	IPR	Ribosomal protein L11 methyltransferase	9; 2/ 2;0.0e+00;ABUW_RS04455,ABUW_RS07495
GO:0046686	GO	response to cadmium ion	0; 2/ 3;3.9e-02;ABUW_RS01310,ABUW_RS01315
Allosteric enzyme	KEYWORDS	keyword	1; 4/ 6;2.4e-02;ABUW_RS04255,ABUW_RS13345,ABUW_RS15365,ABUW_RS15460
operon_1314	operons	NZ_CP008706.1;ID=gene-ABUW_RS13945;Name=ABUW_RS13945;gbkey=Gene;gene_biotype=protein_coding;locus_tag=ABUW_RS13945;old_locus_tag=ABUW_2870	9; 2/ 2;0.0e+00;ABUW_RS13945,ABUW_RS13950
GO:0006541	GO	glutamine metabolic process	0; 7/ 14;3.7e-02;ABUW_RS04380,ABUW_RS04385,ABUW_RS04915,ABUW_RS05880,ABUW_RS08880,ABUW_RS14255,ABUW_RS18280
PF02875	Pfam	Mur ligase family, glutamate ligase domain	1; 4/ 6;0.0112;ABUW_RS01400,ABUW_RS03070,ABUW_RS17675,ABUW_RS18930
IPR036615	IPR	Mur ligase, C-terminal domain superfamily	1; 4/ 6;1.2e-02;ABUW_RS01400,ABUW_RS03070,ABUW_RS17675,ABUW_RS18930
GO:0003735	GO	structural constituent of ribosome	9; 54/ 55;6.1e-33;ABUW_RS01265,ABUW_RS01575,ABUW_RS01590,ABUW_RS01990,ABUW_RS01995,ABUW_RS02000,ABUW_RS02005,ABUW_RS02010,ABUW_RS02015,ABUW_RS02020,ABUW_RS02030,ABUW_RS02035,ABUW_RS02040,ABUW_RS02045,ABUW_RS02050,ABUW_RS02055,ABUW_RS02060,ABUW_RS02065,ABUW_RS02070,ABUW_RS02075,ABUW_RS02080,ABUW_RS02085,ABUW_RS02090,ABUW_RS02100,ABUW_RS02105,ABUW_RS02110,ABUW_RS02115,ABUW_RS02125,ABUW_RS02420,ABUW_RS02425,ABUW_RS04160,ABUW_RS04165,ABUW_RS05565,ABUW_RS06035,ABUW_RS07075,ABUW_RS07545,ABUW_RS07550,ABUW_RS07555,ABUW_RS10775,ABUW_RS10900,ABUW_RS14860,ABUW_RS14865,ABUW_RS15040,ABUW_RS15100,ABUW_RS15950,ABUW_RS15955,ABUW_RS16675,ABUW_RS16680,ABUW_RS17120,ABUW_RS17480,ABUW_RS17485,ABUW_RS17490,ABUW_RS17495,ABUW_RS19020
IPR009051	IPR	Alpha-helical ferredoxin	1; 2/ 3;2.9e-02;ABUW_RS04275,ABUW_RS16995
IPR006194	IPR	Glycine-tRNA synthetase, heterodimeric	9; 2/ 2;0.0e+00;ABUW_RS01795,ABUW_RS01800
PF05157	Pfam	Type II secretion system (T2SS), protein E, N-terminal domain	9; 2/ 2;0.0000;ABUW_RS06590,ABUW_RS17270
IPR011332	IPR	Zinc-binding ribosomal protein	9; 2/ 2;0.0e+00;ABUW_RS15100,ABUW_RS16680
IPR003651	IPR	Endonuclease III-like, iron-sulphur cluster loop motif	9; 2/ 2;0.0e+00;ABUW_RS00245,ABUW_RS13950
GO:0006402	GO	mRNA catabolic process	0; 2/ 3;3.9e-02;ABUW_RS16915,ABUW_RS17115
GO:0030632	GO	D-alanine biosynthetic process	0; 2/ 3;3.9e-02;ABUW_RS07535,ABUW_RS18445
IPR022813	IPR	Protein-export membrane protein SecD/SecF, archaeal and bacterial	9; 2/ 2;0.0e+00;ABUW_RS02605,ABUW_RS02610
operon_1461	operons	NZ_CP008706.1;ID=gene-ABUW_RS15360;Name=ABUW_RS15360;gbkey=Gene;gene_biotype=protein_coding;locus_tag=ABUW_RS15360;old_locus_tag=ABUW_3163	3;10/15;2.6e-05;ABUW_RS15360,ABUW_RS15365,ABUW_RS15390,ABUW_RS15395,ABUW_RS15400,ABUW_RS15405,ABUW_RS15410,ABUW_RS15415,ABUW_RS15420,ABUW_RS15430
03008 Ribosome biogenesis in eukaryotes [PATH:ko03008]	KEGG	ko03008	9; 2/ 2;0.0e+00;ABUW_RS05065,ABUW_RS16360
IPR002052	IPR	DNA methylase, N-6 adenine-specific, conserved site	2; 6/ 8;1.3e-03;ABUW_RS03215,ABUW_RS03670,ABUW_RS07660,ABUW_RS10385,ABUW_RS13270,ABUW_RS13975
IPR022645	IPR	Protein-export membrane protein SecD/SecF, bacterial	9; 2/ 2;0.0e+00;ABUW_RS02605,ABUW_RS02610
GO:0045333	GO	cellular respiration	9; 2/ 2;0.0e+00;ABUW_RS15405,ABUW_RS15410
IPR006131	IPR	Aspartate/ornithine carbamoyltransferase, Asp/Orn-binding domain	9; 2/ 2;0.0e+00;ABUW_RS08425,ABUW_RS13260
GO:0045261	GO	proton-transporting ATP synthase complex, catalytic core F(1)	9; 5/ 5;0.0e+00;ABUW_RS18160,ABUW_RS18165,ABUW_RS18170,ABUW_RS18175,ABUW_RS18180
operon_1370	operons	NZ_CP008706.1;ID=gene-ABUW_RS14445;Name=ABUW_RS14445;gbkey=Gene;gene_biotype=protein_coding;locus_tag=ABUW_RS14445;old_locus_tag=ABUW_2975	9; 2/ 2;0.0e+00;ABUW_RS14445,ABUW_RS14450
operon_1653	operons	NZ_CP008706.1;ID=gene-ABUW_RS17490;Name=rplA;gbkey=Gene;gene=rplA;gene_biotype=protein_coding;locus_tag=ABUW_RS17490;old_locus_tag=ABUW_3593	3; 5/ 6;1.3e-04;ABUW_RS17490,ABUW_RS17495,ABUW_RS17500,ABUW_RS17505,ABUW_RS17515
IPR034408	IPR	Sulphate/thiosulphate-binding site	9; 2/ 2;0.0e+00;ABUW_RS01375,ABUW_RS05010
PF00749	Pfam	tRNA synthetases class I (E and Q), catalytic domain	1; 2/ 3;0.0266;ABUW_RS01365,ABUW_RS17665
operon_1081	operons	NZ_CP008706.1;ID=gene-ABUW_RS11710;Name=ABUW_RS11710;gbkey=Gene;gene_biotype=protein_coding;locus_tag=ABUW_RS11710;old_locus_tag=ABUW_2407	9; 2/ 2;0.0e+00;ABUW_RS11710,ABUW_RS11715
GO:0019867	GO	outer membrane	9; 2/ 2;0.0e+00;ABUW_RS08730,ABUW_RS14160

ClassID	Class	Description	Single_list
PF02910	Pfam	Fumarate reductase flavoprotein C-term	1; 2/ 3;0.0266;ABUW_RS04270,ABUW_RS05035
IPR034804	IPR	Fumarate reductase/succinate dehydrogenase, transmembrane subunit	9; 2/ 2;0.0e+00;ABUW_RS04260,ABUW_RS04265
IPR004101	IPR	Mur ligase, C-terminal	1; 4/ 6;1.2e-02;ABUW_RS01400,ABUW_RS03070,ABUW_RS17675,ABUW_RS18930
operon_1008	operons	NZ_CP008706.1;ID=gene-ABUW_RS11035;Name=fba;gbkey=Gene;gene=fba;gene_biotype=protein_coding;locus_tag=ABUW_RS11035;old_locus_tag=ABUW_2269	1; 2/ 3;1.1e-02;ABUW_RS11035,ABUW_RS11045
PF06968	Pfam	Biotin and Thiamin Synthesis associated domain	9; 2/ 2;0.0000;ABUW_RS11220,ABUW_RS15150
COG1686	eggNOG_COG	Belongs to the peptidase S11 family	9;2/ 2;0.0000;ABUW_RS05255,ABUW_RS05515
IPR034704	IPR	L28p-like	1; 2/ 3;2.9e-02;ABUW_RS05565,ABUW_RS16675
IPR003697	IPR	Nucleoside triphosphate pyrophosphatase Maf-like protein	9; 2/ 2;0.0e+00;ABUW_RS03535,ABUW_RS11055
PF02463	Pfam	RecF/RecN/SMC N terminal domain	1; 2/ 3;0.0266;ABUW_RS00015,ABUW_RS15190
operon_1316	operons	NZ_CP008706.1;ID=gene-ABUW_RS13970;Name=mrdA;gbkey=Gene;gene=mrdA;gene_biotype=protein_coding;locus_tag=ABUW_RS13970;old_locus_tag=ABUW_2876	9; 2/ 2;0.0e+00;ABUW_RS13970,ABUW_RS13975
PF00456	Pfam	Transketolase, thiamine diphosphate binding domain	1; 2/ 3;0.0266;ABUW_RS00770,ABUW_RS11165
PF01171	Pfam	PP-loop family	9; 2/ 2;0.0000;ABUW_RS04545,ABUW_RS15895
COG2804	eggNOG_COG	Type II secretory pathway, ATPase PulE Tfp pilus assembly pathway, ATPase PilB	9;2/ 2;0.0000;ABUW_RS06590,ABUW_RS17270
IPR029063	IPR	S-adenosyl-L-methionine-dependent methyltransferase superfamily	1;17/ 36;3.9e-03;ABUW_RS00120,ABUW_RS00425,ABUW_RS02565,ABUW_RS03215,ABUW_RS03670,ABUW_RS04455,ABUW_RS07495,ABUW_RS07660,ABUW_RS10385,ABUW_RS11010,ABUW_RS11135,ABUW_RS12800,ABUW_RS13235,ABUW_RS13270,ABUW_RS13975,ABUW_RS15140,ABUW_RS15705
GO:0006400	GO	tRNA modification	3; 7/ 8;8.3e-05;ABUW_RS04245,ABUW_RS05500,ABUW_RS06560,ABUW_RS08445,ABUW_RS15895,ABUW_RS17665,ABUW_RS19000
IPR011257	IPR	DNA glycosylase	1; 2/ 3;2.9e-02;ABUW_RS00245,ABUW_RS13950
operon_0169	operons	NZ_CP008706.1;ID=gene-ABUW_RS01605;Name=truB;gbkey=Gene;gene=truB;gene_biotype=protein_coding;locus_tag=ABUW_RS01605;old_locus_tag=ABUW_0326	9; 2/ 2;0.0e+00;ABUW_RS01605,ABUW_RS01610
IPR000640	IPR	Elongation factor EFG, domain V-like	9; 3/ 3;0.0e+00;ABUW_RS03225,ABUW_RS05050,ABUW_RS14855
IPR003156	IPR	DHHA1 domain	9; 2/ 2;0.0e+00;ABUW_RS00820,ABUW_RS13340
PF00185	Pfam	Aspartate/ornithine carbamoyltransferase, Asp/Orn binding domain	9; 2/ 2;0.0000;ABUW_RS08425,ABUW_RS13260
operon_0387	operons	NZ_CP008706.1;ID=gene-ABUW_RS04260;Name=sdhC;gbkey=Gene;gene=sdhC;gene_biotype=protein_coding;locus_tag=ABUW_RS04260;old_locus_tag=ABUW_0868	9; 4/ 4;0.0e+00;ABUW_RS04260,ABUW_RS04265,ABUW_RS04270,ABUW_RS04275
GO:0045727	GO	positive regulation of translation	9; 2/ 2;0.0e+00;ABUW_RS01870,ABUW_RS05050
PF00593	Pfam	TonB dependent receptor	1;10/19;0.0069;ABUW_RS00710,ABUW_RS03025,ABUW_RS08035,ABUW_RS08070,ABUW_RS08765,ABUW_RS10225,ABUW_RS10520,ABUW_RS14160,ABUW_RS14495,ABUW_RS16540
GO:0015291	GO	secondary active transmembrane transporter activity	9; 2/ 2;0.0e+00;ABUW_RS00995,ABUW_RS12770
J	COG	INFORMATION STORAGE AND PROCESSING; Translation, ribosomal structure and biogenesis	3;25/45;1.2e-06;ABUW_RS00070,ABUW_RS00850,ABUW_RS01580,ABUW_RS01605,ABUW_RS02420,ABUW_RS03505,ABUW_RS03515,ABUW_RS04095,ABUW_RS04190,ABUW_RS04850,ABUW_RS05070,ABUW_RS05270,ABUW_RS06035,ABUW_RS11390,ABUW_RS13235,ABUW_RS15225,ABUW_RS15930,ABUW_RS16235,ABUW_RS16275,ABUW_RS16915,ABUW_RS17295,ABUW_RS17665,ABUW_RS18440,ABUW_RS18480,ABUW_RS18805
PF03725	Pfam	3' exoribonuclease family, domain 2	9; 2/ 2;0.0000;ABUW_RS17115,ABUW_RS18700
operon_1631	operons	NZ_CP008706.1;ID=gene-ABUW_RS17290;Name=ABUW_RS17290;gbkey=Gene;gene_biotype=protein_coding;locus_tag=ABUW_RS17290;old_locus_tag=ABUW_3553	0; 2/ 4;3.2e-02;ABUW_RS17290,ABUW_RS17295
PF00579	Pfam	tRNA synthetases class I (W and Y)	9; 2/ 2;0.0000;ABUW_RS00070,ABUW_RS04315
operon_0884	operons	NZ_CP008706.1;ID=gene-ABUW_RS09600;Name=adeA;gbkey=Gene;gene=adeA;gene_biotype=protein_coding;locus_tag=ABUW_RS09600;old_locus_tag=ABUW_1974	9; 3/ 3;0.0e+00;ABUW_RS09600,ABUW_RS09605,ABUW_RS09610
GO:0008784	GO	alanine racemase activity	0; 2/ 3;3.9e-02;ABUW_RS07535,ABUW_RS18445
operon_0206	operons	NZ_CP008706.1;ID=gene-ABUW_RS01990;Name=rpsJ;gbkey=Gene;gene=rpsJ;gene_biotype=protein_coding;locus_tag=ABUW_RS01990;old_locus_tag=ABUW_0405	9; 7/ 7;0.0e+00;ABUW_RS01990,ABUW_RS01995,ABUW_RS02000,ABUW_RS02005,ABUW_RS02010,ABUW_RS02015,ABUW_RS02020
GO:0043952	GO	protein transport by the Sec complex	1; 5/ 7;5.9e-03;ABUW_RS02095,ABUW_RS02605,ABUW_RS02610,ABUW_RS02615,ABUW_RS17505
IPR006043	IPR	Nucleobase cation symporter 2 family	1; 3/ 4;1.1e-02;ABUW_RS00150,ABUW_RS03220,ABUW_RS13375
GO:0017004	GO	cytochrome complex assembly	0; 2/ 3;3.9e-02;ABUW_RS04260,ABUW_RS04265
GO:0009117	GO	nucleotide metabolic process	0; 3/ 5;3.9e-02;ABUW_RS03535,ABUW_RS11055,ABUW_RS13370
IPR002547	IPR	tRNA-binding domain	1; 2/ 3;2.9e-02;ABUW_RS15285,ABUW_RS15930
IPR012947	IPR	Threonyl/alanyl tRNA synthetase, SAD	9; 2/ 2;0.0e+00;ABUW_RS13340,ABUW_RS15980
operon_0207	operons	NZ_CP008706.1;ID=gene-ABUW_RS02030;Name=rplP;gbkey=Gene;gene=rplP;gene_biotype=protein_coding;locus_tag=ABUW_RS02030;old_locus_tag=ABUW_0413	9;20/20;0.0e+00;ABUW_RS02030,ABUW_RS02035,ABUW_RS02040,ABUW_RS02045,ABUW_RS02050,ABUW_RS02055,ABUW_RS02060,ABUW_RS02065,ABUW_RS02070,ABUW_RS02075,ABUW_RS02080,ABUW_RS02085,ABUW_RS02090,ABUW_RS02095,ABUW_RS02100,ABUW_RS02105,ABUW_RS02110,ABUW_RS02115,ABUW_RS02120,ABUW_RS02125
IPR027408	IPR	PNPase/RNase PH domain superfamily	9; 2/ 2;0.0e+00;ABUW_RS17115,ABUW_RS18700
GO:0070469	GO	respirasome	9; 2/ 2;0.0e+00;ABUW_RS07575,ABUW_RS07580
COG4773	eggNOG_COG	Receptor	9;2/ 2;0.0000;ABUW_RS08070,ABUW_RS10520
GO:0015940	GO	pantothenate biosynthetic process	9; 3/ 3;0.0e+00;ABUW_RS15050,ABUW_RS16005,ABUW_RS16010

ClassID	Class	Description	Single_list
Methyltransferase	KEYWORDS	keyword	1; 5/ 8;2.4e-02;ABUW_RS04850,ABUW_RS07660,ABUW_RS10385,ABUW_RS11135,ABUW_RS13235
operon_0149	operons	NZ_CP008706.1;ID=gene-ABUW_RS01300;Name=ABUW_RS01300;gbkey=Gene;gene_biotype=protein_coding;locus_tag=ABUW_RS01300;old_locus_tag=ABUW_0265	2; 4/ 5;6.1e-04;ABUW_RS01300,ABUW_RS01305,ABUW_RS01310,ABUW_RS01315
operon_1409	operons	NZ_CP008706.1;ID=gene-ABUW_RS14850;Name=tuf;gbkey=Gene;gene=tuf;gene_biotype=protein_coding;locus_tag=ABUW_RS14850;old_locus_tag=ABUW_3060	9; 2/ 2;0.0e+00;ABUW_RS14850,ABUW_RS14855
PF00696	Pfam	Amino acid kinase family	0; 3/ 5;0.0266;ABUW_RS05175,ABUW_RS08450,ABUW_RS13345
IPR036676	IPR	PurM-like, C-terminal domain superfamily	1; 2/ 3;2.9e-02;ABUW_RS04810,ABUW_RS04915
IPR036974	IPR	PUA domain superfamily	9; 2/ 2;0.0e+00;ABUW_RS01605,ABUW_RS05175
operon_0289	operons	NZ_CP008706.1;ID=gene-ABUW_RS03060;Name=trpA;gbkey=Gene;gene=trpA;gene_biotype=protein_coding;locus_tag=ABUW_RS03060;old_locus_tag=ABUW_0622	1; 3/ 4;2.8e-03;ABUW_RS03060,ABUW_RS03065,ABUW_RS03070
IPR036901	IPR	Aspartate/ornithine carbamoyltransferase superfamily	9; 2/ 2;0.0e+00;ABUW_RS08425,ABUW_RS13260
operon_0595	operons	NZ_CP008706.1;ID=gene-ABUW_RS06590;Name=ABUW_RS06590;gbkey=Gene;gene_biotype=protein_coding;locus_tag=ABUW_RS06590;old_locus_tag=ABUW_1351	0; 2/ 4;3.2e-02;ABUW_RS06590,ABUW_RS06595
IPR001269	IPR	tRNA-dihydrouridine synthase	1; 2/ 3;2.9e-02;ABUW_RS15225,ABUW_RS16235
operon_0315	operons	NZ_CP008706.1;ID=gene-ABUW_RS03315;Name=ABUW_RS03315;gbkey=Gene;gene_biotype=protein_coding;locus_tag=ABUW_RS03315;old_locus_tag=ABUW_0674	0; 2/ 4;3.2e-02;ABUW_RS03315,ABUW_RS03330
operon_1250	operons	NZ_CP008706.1;ID=gene-ABUW_RS13340;Name=alaS;gbkey=Gene;gene=alaS;gene_biotype=protein_coding;locus_tag=ABUW_RS13340;old_locus_tag=ABUW_2748	9; 2/ 2;0.0e+00;ABUW_RS13340,ABUW_RS13345
operon_0182	operons	NZ_CP008706.1;ID=gene-ABUW_RS01715;Name=ABUW_RS01715;gbkey=Gene;gene_biotype=protein_coding;locus_tag=ABUW_RS01715;old_locus_tag=ABUW_0350	1; 4/ 6;2.8e-03;ABUW_RS01715,ABUW_RS01720,ABUW_RS01725,ABUW_RS01730
operon_0274	operons	NZ_CP008706.1;ID=gene-ABUW_RS02930;Name=ABUW_RS02930;gbkey=Gene;gene_biotype=protein_coding;locus_tag=ABUW_RS02930;old_locus_tag=ABUW_0596	9; 3/ 3;0.0e+00;ABUW_RS02930,ABUW_RS02935,ABUW_RS02940
operon_0790	operons	NZ_CP008706.1;ID=gene-ABUW_RS08620;Name=ABUW_RS08620;gbkey=Gene;gene_biotype=protein_coding;locus_tag=ABUW_RS08620;old_locus_tag=ABUW_1770	9; 3/ 3;0.0e+00;ABUW_RS08620,ABUW_RS08625,ABUW_RS08630
operon_0714	operons	NZ_CP008706.1;ID=gene-ABUW_RS07960;Name=ABUW_RS07960;gbkey=Gene;gene_biotype=protein_coding;locus_tag=ABUW_RS07960;old_locus_tag=ABUW_1631	0; 2/ 4;3.2e-02;ABUW_RS07960,ABUW_RS07965
IPR017911	IPR	MacB, ATP-binding domain	1; 2/ 3;2.9e-02;ABUW_RS04780,ABUW_RS16340
IPR009094	IPR	Disulphide bond isomerase DsbC/G, N-terminal domain superfamily	1; 2/ 3;2.9e-02;ABUW_RS03275,ABUW_RS17700
operon_1628	operons	NZ_CP008706.1;ID=gene-ABUW_RS17225;Name=ABUW_RS17225;gbkey=Gene;gene_biotype=protein_coding;locus_tag=ABUW_RS17225;old_locus_tag=ABUW_3540	9; 4/ 4;0.0e+00;ABUW_RS17225,ABUW_RS17230,ABUW_RS17235,ABUW_RS17240
GO:0008271	GO	secondary active sulfate transmembrane transporter activity	9; 2/ 2;0.0e+00;ABUW_RS08575,ABUW_RS17820
PF00814	Pfam	tRNA N6-adenosine threonylcarbamoyltransferase	9; 2/ 2;0.0000;ABUW_RS07080,ABUW_RS15710
COG0566	eggNOG_COG	Belongs to the class IV-like SAM-binding methyltransferase superfamily. RNA methyltransferase TrmH family	9;2/ 2;0.0000;ABUW_RS04850,ABUW_RS17295
GO:0003729	GO	mRNA binding	1; 3/ 4;1.4e-02;ABUW_RS01265,ABUW_RS07780,ABUW_RS10900
PF03144	Pfam	Elongation factor Tu domain 2	9; 6/ 6;0.0000;ABUW_RS03225,ABUW_RS05050,ABUW_RS14850,ABUW_RS14855,ABUW_RS16275,ABUW_RS17515
operon_1432	operons	NZ_CP008706.1;ID=gene-ABUW_RS15085;Name=acpP;gbkey=Gene;gene=acpP;gene_biotype=protein_coding;locus_tag=ABUW_RS15085;old_locus_tag=ABUW_3107	9; 3/ 3;0.0e+00;ABUW_RS15085,ABUW_RS15090,ABUW_RS15095
PF12848	Pfam	ABC transporter	1; 3/ 4;0.0100;ABUW_RS00035,ABUW_RS01285,ABUW_RS16750
IPR035996	IPR	Tetrapyrrole methylase superfamily	9; 2/ 2;0.0e+00;ABUW_RS04185,ABUW_RS13840
IPR035587	IPR	DUS-like, FMN-binding domain	1; 2/ 3;2.9e-02;ABUW_RS15225,ABUW_RS16235
GO:0016879	GO	ligase activity, forming carbon-nitrogen bonds	9; 2/ 2;0.0e+00;ABUW_RS04965,ABUW_RS15895
IPR037167	IPR	D-Ala-D-Ala carboxypeptidase, C-terminal domain superfamily	9; 2/ 2;0.0e+00;ABUW_RS05255,ABUW_RS05515
operon_0210	operons	NZ_CP008706.1;ID=gene-ABUW_RS02140;Name=ABUW_RS02140;gbkey=Gene;gene_biotype=protein_coding;locus_tag=ABUW_RS02140;old_locus_tag=ABUW_0435	9; 2/ 2;0.0e+00;ABUW_RS02140,ABUW_RS02145
PF07943	Pfam	Penicillin-binding protein 5, C-terminal domain	9; 2/ 2;0.0000;ABUW_RS05255,ABUW_RS05515
IPR004154	IPR	Anticodon-binding	9; 3/ 3;0.0e+00;ABUW_RS03315,ABUW_RS15980,ABUW_RS16405
IPR012340	IPR	Nucleic acid-binding, OB-fold	4;23/ 34;1.3e-07;ABUW_RS01265,ABUW_RS02010,ABUW_RS02040,ABUW_RS02940,ABUW_RS04905,ABUW_RS05080,ABUW_RS05585,ABUW_RS06720,ABUW_RS08445,ABUW_RS10900,ABUW_RS13055,ABUW_RS14075,ABUW_RS14865,ABUW_RS15180,ABUW_RS15285,ABUW_RS15360,ABUW_RS15915,ABUW_RS15930,ABUW_RS16365,ABUW_RS16810,ABUW_RS16915,ABUW_RS17115,ABUW_RS17235
operon_0156	operons	NZ_CP008706.1;ID=gene-ABUW_RS01425;Name=ABUW_RS01425;gbkey=Gene;gene_biotype=protein_coding;locus_tag=ABUW_RS01425;old_locus_tag=ABUW_0290	1; 5/ 8;2.3e-03;ABUW_RS01425,ABUW_RS01430,ABUW_RS01435,ABUW_RS01440,ABUW_RS01445
operon_1583	operons	NZ_CP008706.1;ID=gene-ABUW_RS16780;Name=asd;gbkey=Gene;gene=asd;gene_bio	9; 5/ 5;0.0e+00;ABUW_RS16780,ABUW_RS16785,ABUW_RS16790,ABUW_RS16795,ABUW_RS16800

ClassID	Class	Description	Single_list
		type=protein_coding;locus_tag=ABUW_RS16780;old_locus_tag=ABUW_3451	
IPR035647	IPR	EF-G domain III/V-like	1; 4/ 6;1.2e-02;ABUW_RS03225,ABUW_RS05050,ABUW_RS14855,ABUW_RS16275
IPR004160	IPR	Translation elongation factor EFTu/EF1A, C-terminal	9; 2/ 2;0.0e+00;ABUW_RS14850,ABUW_RS17515
Aminoacyl-tRNA synthetase	KEYWORDS	keyword	6;18/ 22;3.1e-08;ABUW_RS00070,ABUW_RS01365,ABUW_RS01795,ABUW_RS01800,ABUW_RS02940,ABUW_RS03315,ABUW_RS04095,ABUW_RS04315,ABUW_RS13340,ABUW_RS14075,ABUW_RS15285,ABUW_RS15930,ABUW_RS15935,ABUW_RS15980,ABUW_RS16320,ABUW_RS16405,ABUW_RS17665,ABUW_RS18805
GO:0003333	GO	amino acid transmembrane transport	9; 4/ 4;0.0e+00;ABUW_RS00390,ABUW_RS01350,ABUW_RS01710,ABUW_RS03210
IPR001482	IPR	Type II/IV secretion system protein	1; 4/ 5;3.2e-03;ABUW_RS06590,ABUW_RS14710,ABUW_RS14715,ABUW_RS17270
PF02355	Pfam	Protein export membrane protein	9; 2/ 2;0.0000;ABUW_RS02605,ABUW_RS02610
GO:0000049	GO	tRNA binding	6; 22/ 29;1.1e-08;ABUW_RS01285,ABUW_RS01365,ABUW_RS01990,ABUW_RS02030,ABUW_RS02055,ABUW_RS02105,ABUW_RS03225,ABUW_RS04545,ABUW_RS05500,ABUW_RS13340,ABUW_RS14860,ABUW_RS14865,ABUW_RS15225,ABUW_RS15285,ABUW_RS15930,ABUW_RS15935,ABUW_RS15980,ABUW_RS16235,ABUW_RS17490,ABUW_RS18700,ABUW_RS18805,ABUW_RS19015
GO:0009055	GO	electron transfer activity	0; 12/ 26;2.1e-02;ABUW_RS00795,ABUW_RS04260,ABUW_RS04265,ABUW_RS04275,ABUW_RS07570,ABUW_RS07575,ABUW_RS07580,ABUW_RS08735,ABUW_RS08740,ABUW_RS10730,ABUW_RS12790,ABUW_RS13945
GO:0042254	GO	ribosome biogenesis	9; 5/ 5;0.0e+00;ABUW_RS01865,ABUW_RS05170,ABUW_RS15105,ABUW_RS16390,ABUW_RS17235
IPR002684	IPR	Biotin synthase/Biotin biosynthesis bifunctional protein BioAB	9; 2/ 2;0.0e+00;ABUW_RS11220,ABUW_RS15150
operon_1089	operons	NZ_CP008706.1;ID=gene-ABUW_RS11775;Name=ABUW_RS11775;gbkey=Gene;gene_biotype=protein_coding;locus_tag=ABUW_RS11775;old_locus_tag=ABUW_2420	9; 5/ 5;0.0e+00;ABUW_RS11775,ABUW_RS11780,ABUW_RS11785,ABUW_RS11790,ABUW_RS11795
operon_1633	operons	NZ_CP008706.1;ID=gene-ABUW_RS17325;Name=ABUW_RS17325;gbkey=Gene;gene_biotype=protein_coding;locus_tag=ABUW_RS17325;old_locus_tag=ABUW_3560	9; 3/ 3;0.0e+00;ABUW_RS17325,ABUW_RS17330,ABUW_RS17335
GO:0070043	GO	rRNA (guanine-N7-)-methyltransferase activity	9; 2/ 2;0.0e+00;ABUW_RS11010,ABUW_RS13270
IPR000878	IPR	Tetrapyrrole methylase	9; 2/ 2;0.0e+00;ABUW_RS04185,ABUW_RS13840
IPR031167	IPR	OBG-type guanine nucleotide-binding (G) domain	9; 2/ 2;0.0e+00;ABUW_RS05170,ABUW_RS11390
operon_0334	operons	NZ_CP008706.1;ID=gene-ABUW_RS03505;Name=gatB;gbkey=Gene;gene=gatB;gene_biotype=protein_coding;locus_tag=ABUW_RS03505;old_locus_tag=ABUW_0712	9; 3/ 3;0.0e+00;ABUW_RS03505,ABUW_RS03510,ABUW_RS03515
IPR022646	IPR	Protein-export membrane protein SecD/SecF/SecDF, conserved site	9; 2/ 2;0.0e+00;ABUW_RS02605,ABUW_RS02610
IPR012907	IPR	Peptidase S11, D-Ala-D-Ala carboxypeptidase A, C-terminal	9; 2/ 2;0.0e+00;ABUW_RS05255,ABUW_RS05515
operon_1784	operons	NZ_CP008706.1;ID=gene-ABUW_RS19000;Name=mnmE;gbkey=Gene;gene=mnmE;gene_biotype=protein_coding;locus_tag=ABUW_RS19000;old_locus_tag=ABUW_3902	9; 5/ 5;0.0e+00;ABUW_RS19000,ABUW_RS19005,ABUW_RS19010,ABUW_RS19015,ABUW_RS19020
IPR001986	IPR	Enolpyruvate transferase domain	9; 2/ 2;0.0e+00;ABUW_RS06665,ABUW_RS15780
PF00324	Pfam	Amino acid permease	1; 9/16;0.0051;ABUW_RS00350,ABUW_RS00390,ABUW_RS00995,ABUW_RS01350,ABUW_RS01710,ABUW_RS03210,ABUW_RS13640,ABUW_RS18430,ABUW_RS18435
operon_1608	operons	NZ_CP008706.1;ID=gene-ABUW_RS16990;Name=ABUW_RS16990;gbkey=Gene;gene_biotype=protein_coding;locus_tag=ABUW_RS16990;old_locus_tag=ABUW_3493	1; 2/ 3;1.1e-02;ABUW_RS16995,ABUW_RS17000
operon_0755	operons	NZ_CP008706.1;ID=gene-ABUW_RS08260;Name=accC;gbkey=Gene;gene=accC;gene_biotype=protein_coding;locus_tag=ABUW_RS08260;old_locus_tag=ABUW_1696	9; 3/ 3;0.0e+00;ABUW_RS08260,ABUW_RS08265,ABUW_RS08270
GO:0005524	GO	ATP binding	1;100/289;9.4e-04;ABUW_RS00015,ABUW_RS00035,ABUW_RS00070,ABUW_RS00180,ABUW_RS01180,ABUW_RS01285,ABUW_RS01365,ABUW_RS01400,ABUW_RS01425,ABUW_RS01530,ABUW_RS01795,ABUW_RS01800,ABUW_RS01870,ABUW_RS02940,ABUW_RS03065,ABUW_RS03070,ABUW_RS03315,ABUW_RS03355,ABUW_RS03505,ABUW_RS03510,ABUW_RS03515,ABUW_RS03520,ABUW_RS04095,ABUW_RS04315,ABUW_RS04380,ABUW_RS04385,ABUW_RS04500,ABUW_RS04510,ABUW_RS04545,ABUW_RS04710,ABUW_RS04780,ABUW_RS04810,ABUW_RS04900,ABUW_RS04905,ABUW_RS04915,ABUW_RS04965,ABUW_RS04990,ABUW_RS05025,ABUW_RS05175,ABUW_RS05500,ABUW_RS06590,ABUW_RS07465,ABUW_RS07540,ABUW_RS08260,ABUW_RS08450,ABUW_RS08625,ABUW_RS08880,ABUW_RS10865,ABUW_RS10980,ABUW_RS11045,ABUW_RS11170,ABUW_RS11390,ABUW_RS11785,ABUW_RS13340,ABUW_RS13345,ABUW_RS13720,ABUW_RS13955,ABUW_RS14060,ABUW_RS14065,ABUW_RS14075,ABUW_RS14700,ABUW_RS14710,ABUW_RS14715,ABUW_RS14770,ABUW_RS15010,ABUW_RS15035,ABUW_RS15135,ABUW_RS15190,ABUW_RS15210,ABUW_RS15285,ABUW_RS15460,ABUW_RS15775,ABUW_RS15895,ABUW_RS15900,ABUW_RS15915,ABUW_RS15930,ABUW_RS15935,ABUW_RS15980,ABUW_RS16005,ABUW_RS16015,ABUW_RS16320,ABUW_RS16340,ABUW_RS16405,ABUW_RS16430,ABUW_RS16750,ABUW_RS17270,ABUW_RS17285,ABUW_RS17665,ABUW_RS17675,ABUW_RS17730,ABUW_RS18160,ABUW_RS18165,ABUW_RS18170,ABUW_RS18175,ABUW_RS182

ClassID	Class	Description	Single_list
			80,ABUW_RS18660,ABUW_RS18805,ABUW_RS18915,ABUW_RS18930,ABUW_RS18955
GO:0070069	GO	cytochrome complex	0; 3/ 5;3.9e-02;ABUW_RS08730,ABUW_RS08735,ABUW_RS08740
GO:0031564	GO	transcription antitermination	9; 4/ 4;0.0e+00;ABUW_RS00460,ABUW_RS01865,ABUW_RS17235,ABUW_RS17500
GO:0009317	GO	acetyl-CoA carboxylase complex	9; 3/ 3;0.0e+00;ABUW_RS03065,ABUW_RS08265,ABUW_RS15900
operon_1436	operons	NZ_CP008706.1;ID=gene-ABUW_RS15135;Name=bioD;gbkey=Gene;gene=bioD;gene_biotype=protein_coding;locus_tag=ABUW_RS15135;old_locus_tag=ABUW_3117	2; 4/ 5;6.1e-04;ABUW_RS15135,ABUW_RS15140,ABUW_RS15145,ABUW_RS15150
IPR029028	IPR	Alpha/beta knot methyltransferases	3; 7/ 8;5.8e-05;ABUW_RS00850,ABUW_RS01585,ABUW_RS04190,ABUW_RS04850,ABUW_RS11485,ABUW_RS13925,ABUW_RS17295
operon_1662	operons	NZ_CP008706.1;ID=gene-ABUW_RS17660;Name=dksA;gbkey=Gene;gene=dksA;gene_biotype=protein_coding;locus_tag=ABUW_RS17660;old_locus_tag=ABUW_3627	9; 2/ 2;0.0e+00;ABUW_RS17660,ABUW_RS17665
IPR027417	IPR	P-loop containing nucleoside triphosphate hydrolase	0;49/147;2.7e-02;ABUW_RS00015,ABUW_RS00035,ABUW_RS01285,ABUW_RS01530,ABUW_RS01870,ABUW_RS03225,ABUW_RS04780,ABUW_RS04900,ABUW_RS04990,ABUW_RS05025,ABUW_RS05050,ABUW_RS05070,ABUW_RS05170,ABUW_RS06590,ABUW_RS07465,ABUW_RS07540,ABUW_RS08880,ABUW_RS10865,ABUW_RS10970,ABUW_RS10980,ABUW_RS11005,ABUW_RS11390,ABUW_RS11785,ABUW_RS13325,ABUW_RS13955,ABUW_RS14060,ABUW_RS14700,ABUW_RS14710,ABUW_RS14715,ABUW_RS14770,ABUW_RS14850,ABUW_RS14855,ABUW_RS15135,ABUW_RS15190,ABUW_RS15915,ABUW_RS16275,ABUW_RS16340,ABUW_RS16365,ABUW_RS16390,ABUW_RS16750,ABUW_RS17230,ABUW_RS17270,ABUW_RS17285,ABUW_RS17515,ABUW_RS17730,ABUW_RS18165,ABUW_RS18175,ABUW_RS18660,ABUW_RS19000
operon_1006	operons	NZ_CP008706.1;ID=gene-ABUW_RS10935;Name=gspK;gbkey=Gene;gene=gspK;gene_biotype=protein_coding;locus_tag=ABUW_RS10935;old_locus_tag=ABUW_2249	1; 9/18;1.7e-03;ABUW_RS10965,ABUW_RS10970,ABUW_RS10980,ABUW_RS10990,ABUW_RS10995,ABUW_RS11000,ABUW_RS11005,ABUW_RS11010,ABUW_RS11015
GO:1902358	GO	sulfate transmembrane transport	9; 3/ 3;0.0e+00;ABUW_RS01375,ABUW_RS05000,ABUW_RS05010
GO:0015453	GO	oxidoreduction-driven active transmembrane transporter activity	1; 3/ 4;1.4e-02;ABUW_RS07570,ABUW_RS07575,ABUW_RS07580
operon_0187	operons	NZ_CP008706.1;ID=gene-ABUW_RS01785;Name=ABUW_RS01785;gbkey=Gene;gene_biotype=protein_coding;locus_tag=ABUW_RS01785;old_locus_tag=ABUW_0364	0; 2/ 4;3.2e-02;ABUW_RS01795,ABUW_RS01800
operon_0239	operons	NZ_CP008706.1;ID=gene-ABUW_RS02420;Name=rpsI;gbkey=Gene;gene=rpsI;gene_biotype=protein_coding;locus_tag=ABUW_RS02420;old_locus_tag=ABUW_0493	9; 2/ 2;0.0e+00;ABUW_RS02420,ABUW_RS02425
PF08264	Pfam	Anticodon-binding domain of tRNA ligase	9; 3/ 3;0.0000;ABUW_RS04095,ABUW_RS16320,ABUW_RS18805
IPR015847	IPR	Exoribonuclease, phosphorolytic domain 2	9; 2/ 2;0.0e+00;ABUW_RS17115,ABUW_RS18700
operon_0171	operons	NZ_CP008706.1;ID=gene-ABUW_RS01620;Name=ABUW_RS01620;gbkey=Gene;gene_biotype=protein_coding;locus_tag=ABUW_RS01620;old_locus_tag=ABUW_0329	1; 2/ 3;1.1e-02;ABUW_RS01620,ABUW_RS01630
GO:0009319	GO	cytochrome o ubiquinol oxidase complex	1; 3/ 4;1.4e-02;ABUW_RS07570,ABUW_RS07575,ABUW_RS07580
PF00679	Pfam	Elongation factor G C-terminus	9; 3/ 3;0.0000;ABUW_RS03225,ABUW_RS05050,ABUW_RS14855
GO:0015078	GO	proton transmembrane transporter activity	0; 2/ 3;3.9e-02;ABUW_RS07575,ABUW_RS07580
operon_1571	operons	NZ_CP008706.1;ID=gene-ABUW_RS16610;Name=lgt;gbkey=Gene;gene=lgt;gene_biotype=protein_coding;locus_tag=ABUW_RS16610;old_locus_tag=ABUW_3417	0; 3/ 7;3.8e-02;ABUW_RS16625,ABUW_RS16630,ABUW_RS16640
IPR011129	IPR	Cold shock domain	1; 4/ 6;1.2e-02;ABUW_RS06720,ABUW_RS13055,ABUW_RS15360,ABUW_RS15915
IPR009006	IPR	Alanine racemase/group IV decarboxylase, C-terminal	1; 2/ 3;2.9e-02;ABUW_RS07535,ABUW_RS18445
GO:0004748	GO	ribonucleoside-diphosphate reductase activity, thioredoxin disulfide as acceptor	9; 2/ 2;0.0e+00;ABUW_RS15460,ABUW_RS15470
operon_1464	operons	NZ_CP008706.1;ID=gene-ABUW_RS15460;Name=ABUW_RS15460;gbkey=Gene;gene_biotype=protein_coding;locus_tag=ABUW_RS15460;old_locus_tag=ABUW_3183	1; 2/ 3;1.1e-02;ABUW_RS15460,ABUW_RS15470
GO:0010468	GO	regulation of gene expression	0; 3/ 5;3.9e-02;ABUW_RS06720,ABUW_RS13055,ABUW_RS17660
Exonuclease	KEYWORDS	keyword	1; 3/ 4;2.4e-02;ABUW_RS00820,ABUW_RS13735,ABUW_RS14695
GO:0097216	GO	guanosine tetraphosphate binding	4; 9/ 10;5.9e-06;ABUW_RS03070,ABUW_RS03225,ABUW_RS05050,ABUW_RS14850,ABUW_RS14855,ABUW_RS16275,ABUW_RS17515,ABUW_RS17660,ABUW_RS18930
operon_1009	operons	NZ_CP008706.1;ID=gene-ABUW_RS11050;Name=ABUW_RS11050;gbkey=Gene;gene_biotype=protein_coding;locus_tag=ABUW_RS11050;old_locus_tag=ABUW_2272	1; 2/ 3;1.1e-02;ABUW_RS11055,ABUW_RS11060
operon_1704	operons	NZ_CP008706.1;ID=gene-ABUW_RS18115;Name=ABUW_RS18115;gbkey=Gene;gene_biotype=protein_coding;locus_tag=ABUW_RS18115;old_locus_tag=ABUW_3722	1; 2/ 3;1.1e-02;ABUW_RS18115,ABUW_RS18120
IPR000795	IPR	Translational (tr)-type GTP-binding domain	9; 8/ 8;0.0e+00;ABUW_RS03225,ABUW_RS05050,ABUW_RS14060,ABUW_RS14850,ABUW_RS14855,ABUW_RS16275,ABUW_RS17230,ABUW_RS17515
GO:0003723	GO	RNA binding	2; 22/ 39;5.2e-05;ABUW_RS00070,ABUW_RS00120,ABUW_RS00460,ABUW_RS01605,ABUW_RS01865,ABUW_RS01870,ABUW_RS04190,ABUW

ClassID	Class	Description	Single_list
			_RS04400,ABUW_RS04850,ABUW_RS05175,ABUW_RS05270,ABUW_RS11485,ABUW_RS13055,ABUW_RS13270,ABUW_RS13355,ABUW_RS15130,ABUW_RS15915,ABUW_RS16800,ABUW_RS17115,ABUW_RS17235,ABUW_RS17295,ABUW_RS18480
GO:0015806	GO	S-methylmethionine transport	9; 2/ 2;0.0e+00;ABUW_RS01350,ABUW_RS01710
IPR018163	IPR	Threonyl/alanyl tRNA synthetase, class II-like, putative editing domain superfamily	9; 2/ 2;0.0e+00;ABUW_RS13340,ABUW_RS15980
COG0765	eggNOG_COG	amino acid transport	0;2/ 4;0.0444;ABUW_RS11790,ABUW_RS11795
operon_1688	operons	NZ_CP008706.1;ID=gene-ABUW_RS17970;Name=ABUW_RS17970;gbkey=Gene;gene_biotype=protein_coding;locus_tag=ABUW_RS17970;old_locus_tag=ABUW_3691	0; 2/ 4;3.2e-02;ABUW_RS17975,ABUW_RS17980
operon_1509	operons	NZ_CP008706.1;ID=gene-ABUW_RS15925;Name=ABUW_RS15925;gbkey=Gene;gene_biotype=protein_coding;locus_tag=ABUW_RS15925;old_locus_tag=ABUW_3279	1; 2/ 3;1.1e-02;ABUW_RS15930,ABUW_RS15935
operon_1778	operons	NZ_CP008706.1;ID=gene-ABUW_RS18950;Name=ABUW_RS18950;gbkey=Gene;gene_biotype=protein_coding;locus_tag=ABUW_RS18950;old_locus_tag=ABUW_3892	9; 2/ 2;0.0e+00;ABUW_RS18950,ABUW_RS18955
GO:1990904	GO	ribonucleoprotein complex	9; 38/ 40;9.9e-22;ABUW_RS01575,ABUW_RS01590,ABUW_RS01990,ABUW_RS01995,ABUW_RS02000,ABUW_RS02005,ABUW_RS02030,ABUW_RS02035,ABUW_RS02040,ABUW_RS02050,ABUW_RS02055,ABUW_RS02060,ABUW_RS02065,ABUW_RS02070,ABUW_RS02075,ABUW_RS02100,ABUW_RS02105,ABUW_RS02110,ABUW_RS02125,ABUW_RS02420,ABUW_RS02425,ABUW_RS04160,ABUW_RS04165,ABUW_RS05565,ABUW_RS07075,ABUW_RS07545,ABUW_RS07550,ABUW_RS07555,ABUW_RS10775,ABUW_RS15040,ABUW_RS15950,ABUW_RS15955,ABUW_RS16675,ABUW_RS16680,ABUW_RS17120,ABUW_RS17480,ABUW_RS17495,ABUW_RS19020
GO:0042274	GO	ribosomal small subunit biogenesis	9; 4/ 4;0.0e+00;ABUW_RS01580,ABUW_RS05070,ABUW_RS16365,ABUW_RS17240
operon_1707	operons	NZ_CP008706.1;ID=gene-ABUW_RS18160;Name=ABUW_RS18160;gbkey=Gene;gene_biotype=protein_coding;locus_tag=ABUW_RS18160;old_locus_tag=ABUW_3731	9; 9/ 9;0.0e+00;ABUW_RS18160,ABUW_RS18165,ABUW_RS18170,ABUW_RS18175,ABUW_RS18180,ABUW_RS18185,ABUW_RS18190,ABUW_RS18195,ABUW_RS18200
PF02574	Pfam	Homocysteine S-methyltransferase	9; 2/ 2;0.0000;ABUW_RS14205,ABUW_RS14445
operon_0189	operons	NZ_CP008706.1;ID=gene-ABUW_RS01810;Name=ABUW_RS01810;gbkey=Gene;gene_biotype=protein_coding;locus_tag=ABUW_RS01810;old_locus_tag=ABUW_0369	1; 2/ 3;1.1e-02;ABUW_RS01815,ABUW_RS01820
GO:0005840	GO	ribosome	9; 39/ 41;2.5e-22;ABUW_RS01575,ABUW_RS01580,ABUW_RS01590,ABUW_RS01990,ABUW_RS01995,ABUW_RS02000,ABUW_RS02005,ABUW_RS02030,ABUW_RS02035,ABUW_RS02040,ABUW_RS02050,ABUW_RS02055,ABUW_RS02060,ABUW_RS02065,ABUW_RS02070,ABUW_RS02075,ABUW_RS02100,ABUW_RS02105,ABUW_RS02110,ABUW_RS02125,ABUW_RS02420,ABUW_RS02425,ABUW_RS04160,ABUW_RS04165,ABUW_RS05565,ABUW_RS07075,ABUW_RS07545,ABUW_RS07550,ABUW_RS07555,ABUW_RS10775,ABUW_RS15040,ABUW_RS15950,ABUW_RS15955,ABUW_RS16675,ABUW_RS16680,ABUW_RS17120,ABUW_RS17480,ABUW_RS17495,ABUW_RS19020
GO:0004820	GO	glycine-tRNA ligase activity	9; 2/ 2;0.0e+00;ABUW_RS01795,ABUW_RS01800
IPR012156	IPR	Cold shock, CspA	1; 3/ 4;1.1e-02;ABUW_RS06720,ABUW_RS13055,ABUW_RS15360
operon_0512	operons	NZ_CP008706.1;ID=gene-ABUW_RS05570;Name=ABUW_RS05570;gbkey=Gene;gene_biotype=protein_coding;locus_tag=ABUW_RS05570;old_locus_tag=ABUW_1138	1; 2/ 3;1.1e-02;ABUW_RS05570,ABUW_RS05580
GO:0006730	GO	one-carbon metabolic process	9; 6/ 6;0.0e+00;ABUW_RS03070,ABUW_RS05835,ABUW_RS05980,ABUW_RS11170,ABUW_RS16630,ABUW_RS16660
GO:0006226	GO	dUMP biosynthetic process	9; 2/ 2;0.0e+00;ABUW_RS14765,ABUW_RS15255
GO:0036009	GO	protein-glutamine N-methyltransferase activity	9; 2/ 2;0.0e+00;ABUW_RS07660,ABUW_RS10385
GO:0044205	GO	'de novo' UMP biosynthetic process	0; 4/ 7;3.9e-02;ABUW_RS00705,ABUW_RS04380,ABUW_RS04385,ABUW_RS13260
IPR005225	IPR	Small GTP-binding protein domain	9;11/ 11;0.0e+00;ABUW_RS03225,ABUW_RS05050,ABUW_RS05070,ABUW_RS14060,ABUW_RS14850,ABUW_RS14855,ABUW_RS16275,ABUW_RS16390,ABUW_RS17230,ABUW_RS17515,ABUW_RS19000
operon_0475	operons	NZ_CP008706.1;ID=gene-ABUW_RS05170;Name=cgtA;gbkey=Gene;gene=cgtA;gene_biotype=protein_coding;locus_tag=ABUW_RS05170;old_locus_tag=ABUW_1053	9; 2/ 2;0.0e+00;ABUW_RS05170,ABUW_RS05175
GO:0006099	GO	tricarboxylic acid cycle	0; 11/ 23;1.9e-02;ABUW_RS02295,ABUW_RS04255,ABUW_RS04260,ABUW_RS04265,ABUW_RS04270,ABUW_RS04275,ABUW_RS05265,ABUW_RS07780,ABUW_RS10220,ABUW_RS14435,ABUW_RS16510
COG0833	eggNOG_COG	amino acid	9;3/ 3;0.0000;ABUW_RS01350,ABUW_RS01710,ABUW_RS03210
IPR011063	IPR	tRNA(Ile)-lysidine/2-thiocytidine synthase, N-terminal	9; 2/ 2;0.0e+00;ABUW_RS04545,ABUW_RS15895
IPR013155	IPR	Methionyl/Valyl/Leucyl/Isoleucyl-tRNA synthetase, anticodon-binding	9; 3/ 3;0.0e+00;ABUW_RS04095,ABUW_RS16320,ABUW_RS18805
IPR000821	IPR	Alanine racemase	9; 2/ 2;0.0e+00;ABUW_RS07535,ABUW_RS18445
operon_0258	operons	NZ_CP008706.1;ID=gene-ABUW_RS02605;Name=secF;gbkey=Gene;gene=secF;gene_biotype=protein_coding;locus_tag=ABUW_RS02605;old_locus_tag=ABUW_0530	9; 4/ 4;0.0e+00;ABUW_RS02605,ABUW_RS02610,ABUW_RS02615,ABUW_RS02620
IPR010978	IPR	Class I and II aminoacyl-tRNA synthetase, tRNA-binding arm	1; 2/ 3;2.9e-02;ABUW_RS04095,ABUW_RS15935
PF07973	Pfam	Threonyl and Alanyl tRNA synthetase second additional domain	9; 2/ 2;0.0000;ABUW_RS13340,ABUW_RS15980

ClassID	Class	Description	Single_list
operon_0376	operons	NZ_CP008706.1;ID=gene-ABUW_RS04160;Name=rplU;gbkey=Gene;gene=rplU;gene_biotype=protein_coding;locus_tag=ABUW_RS04160;old_locus_tag=ABUW_0848	9; 2/ 2;0.0e+00;ABUW_RS04160,ABUW_RS04165
PF00730	Pfam	HhH-GPD superfamily base excision DNA repair protein	9; 2/ 2;0.0000;ABUW_RS00245,ABUW_RS13950
IPR018496	IPR	Pseudouridine synthase, RsuA/RluB/E/F, conserved site	1; 2/ 3;2.9e-02;ABUW_RS05270,ABUW_RS15130
Amino-acid transport	KEYWORDS	keyword	1;23/ 51;4.9e-03;ABUW_RS00350,ABUW_RS00390,ABUW_RS00995,ABUW_RS01620,ABUW_RS03210,ABUW_RS04205,ABUW_RS07460,ABUW_RS07465,ABUW_RS08655,ABUW_RS11075,ABUW_RS11115,ABUW_RS11370,ABUW_RS11775,ABUW_RS11785,ABUW_RS11790,ABUW_RS11795,ABUW_RS12770,ABUW_RS13640,ABUW_RS13855,ABUW_RS14450,ABUW_RS16770,ABUW_RS18430,ABUW_RS18435
PF01584	Pfam	CheW-like domain	9; 2/ 2;0.0000;ABUW_RS03345,ABUW_RS03355
PF00152	Pfam	tRNA synthetases class II (D, K and N)	1; 2/ 3;0.0266;ABUW_RS02940,ABUW_RS14075
operon_0980	operons	NZ_CP008706.1;ID=gene-ABUW_RS10520;Name=ABUW_RS10520;gbkey=Gene;gene_biotype=protein_coding;locus_tag=ABUW_RS10520;old_locus_tag=ABUW_2165	3; 5/ 6;1.3e-04;ABUW_RS10520,ABUW_RS10525,ABUW_RS10530,ABUW_RS10535,ABUW_RS10540
operon_0450	operons	NZ_CP008706.1;ID=gene-ABUW_RS04865;Name=pal;gbkey=Gene;gene=pal;gene_biotype=protein_coding;locus_tag=ABUW_RS04865;old_locus_tag=ABUW_0992	1; 4/ 6;2.8e-03;ABUW_RS04875,ABUW_RS04880,ABUW_RS04885,ABUW_RS04890
PF00590	Pfam	Tetrapyrrole (Corrin/Porphyrin) Methylases	9; 2/ 2;0.0000;ABUW_RS04185,ABUW_RS13840
operon_0590	operons	NZ_CP008706.1;ID=gene-ABUW_RS06555;Name=ABUW_RS06555;gbkey=Gene;gene_biotype=protein_coding;locus_tag=ABUW_RS06555;old_locus_tag=ABUW_1344	1; 2/ 3;1.1e-02;ABUW_RS06555,ABUW_RS06560
PF10576	Pfam	Iron-sulfur binding domain of endonuclease III	9; 2/ 2;0.0000;ABUW_RS00245,ABUW_RS13950
operon_1433	operons	NZ_CP008706.1;ID=gene-ABUW_RS15100;Name=rpmF;gbkey=Gene;gene=rpmF;gene_biotype=protein_coding;locus_tag=ABUW_RS15100;old_locus_tag=ABUW_3110	9; 2/ 2;0.0e+00;ABUW_RS15100,ABUW_RS15105
GO:0015171	GO	amino acid transmembrane transporter activity	0; 7/ 13;2.1e-02;ABUW_RS00390,ABUW_RS01350,ABUW_RS01710,ABUW_RS03210,ABUW_RS11075,ABUW_RS11765,ABUW_RS13855
IPR033704	IPR	dUTPase, trimeric	9; 2/ 2;0.0e+00;ABUW_RS14765,ABUW_RS15255
GO:0044208	GO	'de novo' AMP biosynthetic process	9; 2/ 2;0.0e+00;ABUW_RS05490,ABUW_RS13325
IPR009080	IPR	Aminoacyl-tRNA synthetase, class Ia, anticodon-binding	1; 4/ 6;1.2e-02;ABUW_RS04095,ABUW_RS15285,ABUW_RS16320,ABUW_RS18805
COG1651	eggNOG_COG	Required for disulfide bond formation in some periplasmic proteins. Acts by transferring its disulfide bond to other proteins and is reduced in the process	1;2/ 3;0.0150;ABUW_RS03275,ABUW_RS17700
IPR020103	IPR	Pseudouridine synthase, catalytic domain superfamily	0; 5/ 10;3.8e-02;ABUW_RS01605,ABUW_RS05270,ABUW_RS15130,ABUW_RS16800,ABUW_RS18480
IPR041715	IPR	Class II Histidinyl-tRNA synthetase (HisRS)-like catalytic core domain	9; 2/ 2;0.0e+00;ABUW_RS13330,ABUW_RS16405
IPR036565	IPR	Mur-like, catalytic domain superfamily	1; 4/ 6;1.2e-02;ABUW_RS01400,ABUW_RS03070,ABUW_RS17675,ABUW_RS18930
GO:0043683	GO	type IV pilus assembly	1; 4/ 5;4.3e-03;ABUW_RS01425,ABUW_RS01430,ABUW_RS01435,ABUW_RS01445
operon_0396	operons	NZ_CP008706.1;ID=gene-ABUW_RS04365;Name=ABUW_RS04365;gbkey=Gene;gene_biotype=protein_coding;locus_tag=ABUW_RS04365;old_locus_tag=ABUW_0890	1; 3/ 5;1.1e-02;ABUW_RS04375,ABUW_RS04380,ABUW_RS04385
IPR017900	IPR	4Fe-4S ferredoxin, iron-sulphur binding, conserved site	2; 6/ 8;1.3e-03;ABUW_RS04275,ABUW_RS06555,ABUW_RS12790,ABUW_RS13945,ABUW_RS15395,ABUW_RS16995
operon_0085	operons	NZ_CP008706.1;ID=gene-ABUW_RS00795;Name=ABUW_RS00795;gbkey=Gene;gene_biotype=protein_coding;locus_tag=ABUW_RS00795;old_locus_tag=ABUW_0160	1; 4/ 6;2.8e-03;ABUW_RS00795,ABUW_RS00800,ABUW_RS00805,ABUW_RS00820
GO:0004781	GO	sulfate adenylyltransferase (ATP) activity	9; 2/ 2;0.0e+00;ABUW_RS14060,ABUW_RS14065
GO:0016682	GO	oxidoreductase activity, acting on diphenols and related substances as donors, oxygen as acceptor	0; 3/ 5;3.9e-02;ABUW_RS07575,ABUW_RS07580,ABUW_RS08735
IPR003395	IPR	RecF/RecN/SMC, N-terminal	1; 2/ 3;2.9e-02;ABUW_RS00015,ABUW_RS15190
IPR006132	IPR	Aspartate/ornithine carbamoyltransferase, carbamoyl-P binding	9; 2/ 2;0.0e+00;ABUW_RS08425,ABUW_RS13260
Cytoplasm	KEYWORDS	keyword	2;65/153;8.0e-06;ABUW_RS00120,ABUW_RS00380,ABUW_RS00385,ABUW_RS00850,ABUW_RS01850,ABUW_RS02250,ABUW_RS02565,ABUW_RS02635,ABUW_RS03215,ABUW_RS03225,ABUW_RS03535,ABUW_RS04190,ABUW_RS04455,ABUW_RS04480,ABUW_RS05035,ABUW_RS05065,ABUW_RS05085,ABUW_RS05170,ABUW_RS05395,ABUW_RS05585,ABUW_RS05810,ABUW_RS05900,ABUW_RS05980,ABUW_RS06040,ABUW_RS06695,ABUW_RS07495,ABUW_RS07505,ABUW_RS07655,ABUW_RS07880,ABUW_RS08455,ABUW_RS08495,ABUW_RS08630,ABUW_RS08885,ABUW_RS08890,ABUW_RS11010,ABUW_RS11055,ABUW_RS11315,ABUW_RS11855,ABUW_RS13270,ABUW_RS13325,ABUW_RS13355,ABUW_RS13840,ABUW_RS13925,ABUW_RS14850,ABUW_RS14855,ABUW_RS15045,ABUW_RS15085,ABUW_RS15705,ABUW_RS15975,ABUW_RS16010,ABUW_RS16275,ABUW_RS16360,ABUW_RS16365,ABUW_RS16625,ABUW_RS16810,ABUW_RS17115,ABUW_RS17225,ABUW_RS17230,ABUW_RS17240,ABUW_RS17265,ABUW_RS17295,ABUW_RS17515,ABUW_RS17945,ABUW_RS18640,ABUW_RS19000
PF05175	Pfam	Methyltransferase small domain	9; 2/ 2;0.0000;ABUW_RS03215,ABUW_RS10385
GO:0140330	GO	xenobiotic detoxification by transmembrane export across the cell outer membrane	0; 3/ 5;3.9e-02;ABUW_RS09600,ABUW_RS09605,ABUW_RS14650

ClassID	Class	Description	Single_list
IPR046346	IPR	Aminoacid dehydrogenase-like, N-terminal domain superfamily	1; 4/ 6;1.2e-02;ABUW_RS01715,ABUW_RS01845,ABUW_RS04450,ABUW_RS05960
IPR036121	IPR	ATPase, F1/V1/A1 complex, alpha/beta subunit, N-terminal domain superfamily	9; 2/ 2;0.0e+00;ABUW_RS18165,ABUW_RS18175
GO:0006189	GO	'de novo' IMP biosynthetic process	1; 7/ 12;1.3e-02;ABUW_RS04805,ABUW_RS04810,ABUW_RS04915,ABUW_RS05490,ABUW_RS16660,ABUW_RS18915,ABUW_RS18920
PF00633	Pfam	Helix-hairpin-helix motif	9; 2/ 2;0.0000;ABUW_RS00245,ABUW_RS13950
IPR000905	IPR	Gcp-like domain	9; 2/ 2;0.0e+00;ABUW_RS07080,ABUW_RS15710
IPR006195	IPR	Aminoacyl-tRNA synthetase, class II	2; 6/ 8;1.3e-03;ABUW_RS02940,ABUW_RS03315,ABUW_RS14075,ABUW_RS15935,ABUW_RS15980,ABUW_RS16405
operon_1731	operons	NZ_CP008706.1;ID=gene-ABUW_RS18440;Name=ABUW_RS18440;gbkey=Gene;gene_biotype=protein_coding;locus_tag=ABUW_RS18440;old_locus_tag=ABUW_3787	9; 3/ 3;0.0e+00;ABUW_RS18440,ABUW_RS18445,ABUW_RS18450
COG0424	eggNOG_COG	maF-like protein	9;2/ 2;0.0000;ABUW_RS03535,ABUW_RS11055
IPR037257	IPR	Type II secretion system protein GspE, N-terminal superfamily	1; 2/ 3;2.9e-02;ABUW_RS06590,ABUW_RS17270
operon_0670	operons	NZ_CP008706.1;ID=gene-ABUW_RS07560;Name=cyoE;gbkey=Gene;gene=cyoE;gene_biotype=protein_coding;locus_tag=ABUW_RS07560;old_locus_tag=ABUW_1549	2; 4/ 5;6.1e-04;ABUW_RS07560,ABUW_RS07570,ABUW_RS07575,ABUW_RS07580
IPR008991	IPR	Translation protein SH3-like domain superfamily	9; 5/ 5;0.0e+00;ABUW_RS01590,ABUW_RS02010,ABUW_RS02050,ABUW_RS05585,ABUW_RS17500
IPR008948	IPR	L-Aspartase-like	1; 4/ 6;1.2e-02;ABUW_RS00385,ABUW_RS05490,ABUW_RS10220,ABUW_RS17610
operon_1549	operons	NZ_CP008706.1;ID=gene-ABUW_RS16365;Name=rsgA;gbkey=Gene;gene=rsgA;gene_biotype=protein_coding;locus_tag=ABUW_RS16365;old_locus_tag=ABUW_3368	0; 2/ 4;3.2e-02;ABUW_RS16365,ABUW_RS16380
operon_1772	operons	NZ_CP008706.1;ID=gene-ABUW_RS18915;Name=ABUW_RS18915;gbkey=Gene;gene_biotype=protein_coding;locus_tag=ABUW_RS18915;old_locus_tag=ABUW_3885	9; 2/ 2;0.0e+00;ABUW_RS18915,ABUW_RS18920
IPR002300	IPR	Aminoacyl-tRNA synthetase, class Ia	9; 3/ 3;0.0e+00;ABUW_RS04095,ABUW_RS16320,ABUW_RS18805
GO:0009060	GO	aerobic respiration	1; 7/ 11;5.7e-03;ABUW_RS04260,ABUW_RS04265,ABUW_RS04275,ABUW_RS07570,ABUW_RS07575,ABUW_RS07580,ABUW_RS15410
GO:0004826	GO	phenylalanine-tRNA ligase activity	9; 2/ 2;0.0e+00;ABUW_RS15930,ABUW_RS15935
operon_1657	operons	NZ_CP008706.1;ID=gene-ABUW_RS17610;Name=argH;gbkey=Gene;gene=argH;gene_biotype=protein_coding;locus_tag=ABUW_RS17610;old_locus_tag=ABUW_3617	9; 2/ 2;0.0e+00;ABUW_RS17610,ABUW_RS17615
IPR010994	IPR	RuvA domain 2-like	0; 4/ 7;2.9e-02;ABUW_RS01265,ABUW_RS02595,ABUW_RS04905,ABUW_RS15180
COG1136	eggNOG_COG	(ABC) transporter	9;2/ 2;0.0000;ABUW_RS04780,ABUW_RS16340
GO:0009007	GO	site-specific DNA-methyltransferase (adenine-specific) activity	0; 2/ 3;3.9e-02;ABUW_RS03670,ABUW_RS10385
IPR003265	IPR	HhH-GPD domain	9; 2/ 2;0.0e+00;ABUW_RS00245,ABUW_RS13950
IPR036942	IPR	TonB-dependent receptor-like, beta-barrel domain superfamily	1;10/ 19;7.5e-03;ABUW_RS00710,ABUW_RS03025,ABUW_RS08035,ABUW_RS08070,ABUW_RS08765,ABUW_RS10225,ABUW_RS10520,ABUW_RS14160,ABUW_RS14495,ABUW_RS16540
GO:0050380	GO	undecaprenyl-diphosphatase activity	9; 2/ 2;0.0e+00;ABUW_RS03590,ABUW_RS18940
PF08245	Pfam	Mur ligase middle domain	1; 4/ 6;0.0112;ABUW_RS01400,ABUW_RS03070,ABUW_RS17675,ABUW_RS18930
IPR002305	IPR	Aminoacyl-tRNA synthetase, class Ic	9; 2/ 2;0.0e+00;ABUW_RS00070,ABUW_RS04315
IPR045864	IPR	Class II Aminoacyl-tRNA synthetase/Biotinyl protein ligase (BPL) and lipoyl protein ligase (LPL)	3;10/ 13;4.4e-05;ABUW_RS01800,ABUW_RS02940,ABUW_RS03315,ABUW_RS13330,ABUW_RS13340,ABUW_RS14075,ABUW_RS15930,ABUW_RS15935,ABUW_RS15980,ABUW_RS16405
IPR014722	IPR	Ribosomal protein L2, domain 2	9; 4/ 4;0.0e+00;ABUW_RS02010,ABUW_RS02050,ABUW_RS05585,ABUW_RS17500
IPR020094	IPR	Pseudouridine synthase TruA/RsuA/RluB/E/F, N-terminal	1; 3/ 4;1.1e-02;ABUW_RS05270,ABUW_RS15130,ABUW_RS16800
PF00254	Pfam	FKBP-type peptidyl-prolyl cis-trans isomerase	1; 4/ 6;0.0112;ABUW_RS05245,ABUW_RS14375,ABUW_RS16535,ABUW_RS18815
GO:0015450	GO	protein-transporting ATPase activity	0; 2/ 3;3.9e-02;ABUW_RS02605,ABUW_RS02610
PF02769	Pfam	AIR synthase related protein, C-terminal domain	1; 2/ 3;0.0266;ABUW_RS04810,ABUW_RS04915
IPR006027	IPR	NusB/RsmB/TIM44	9; 2/ 2;0.0e+00;ABUW_RS00120,ABUW_RS00460
IPR020058	IPR	Glutamyl/glutaminyl-tRNA synthetase, class Ib, catalytic domain	1; 2/ 3;2.9e-02;ABUW_RS01365,ABUW_RS17665
GO:0004088	GO	carbamoyl-phosphate synthase (glutamine-hydrolyzing) activity	9; 2/ 2;0.0e+00;ABUW_RS04380,ABUW_RS04385
IPR000362	IPR	Fumarate lyase family	0; 3/ 5;2.9e-02;ABUW_RS05490,ABUW_RS10220,ABUW_RS17610
operon_0806	operons	NZ_CP008706.1;ID=gene-ABUW_RS08725;Name=ABUW_RS08725;gbkey=Gene;gene_biotype=protein_coding;locus_tag=ABUW_RS08725;old_locus_tag=ABUW_1792	9; 5/ 5;0.0e+00;ABUW_RS08725,ABUW_RS08730,ABUW_RS08735,ABUW_RS08740,ABUW_RS08745
PF00437	Pfam	Type II/IV secretion system protein	2; 4/ 5;0.0030;ABUW_RS06590,ABUW_RS14710,ABUW_RS14715,ABUW_RS17270
Methylation	KEYWORDS	keyword	9; 3/ 3;0.0e+00;ABUW_RS01995,ABUW_RS14865,ABUW_RS17495
IPR006042	IPR	Xanthine/uracil permease	1; 2/ 3;2.9e-02;ABUW_RS00150,ABUW_RS03220

ClassID	Class	Description	Single_list
IPR015946	IPR	K homology domain-like, alpha/beta	1; 4/ 6;1.2e-02;ABUW_RS05070,ABUW_RS16390,ABUW_RS17225,ABUW_RS17235
PF01168	Pfam	Alanine racemase, N-terminal domain	1; 2/ 3;0.0266;ABUW_RS07535,ABUW_RS18445
IPR002645	IPR	STAS domain	1; 3/ 4;1.1e-02;ABUW_RS08575,ABUW_RS14255,ABUW_RS17820
IPR042092	IPR	Pseudouridine synthase, RsuA/RluB/E/F, catalytic domain	1; 2/ 3;2.9e-02;ABUW_RS05270,ABUW_RS15130
operon_0166	operons	NZ_CP008706.1;ID=gene-ABUW_RS01540;Name=ABUW_RS01540;gbkey=Gene;gene_biotype=protein_coding;locus_tag=ABUW_RS01540;old_locus_tag=ABUW_0313	2; 7/10;1.6e-04;ABUW_RS01540,ABUW_RS01545,ABUW_RS01550,ABUW_RS01555,ABUW_RS01575,ABUW_RS01580,ABUW_RS01585
COG0488	eggNOG_COG	(ABC) transporter	1;3/ 4;0.0049;ABUW_RS00035,ABUW_RS01285,ABUW_RS16750
IPR023170	IPR	Helix-hairpin-helix, base-excision DNA repair, C-terminal	9; 2/ 2;0.0e+00;ABUW_RS00245,ABUW_RS13950
00240 Pyrimidine metabolism [PATH:ko00240]	KEGG	ko00240	1;12/18;5.7e-03;ABUW_RS00705,ABUW_RS04380,ABUW_RS04385,ABUW_RS05025,ABUW_RS08450,ABUW_RS08880,ABUW_RS13260,ABUW_RS14765,ABUW_RS15255,ABUW_RS15365,ABUW_RS16005,ABUW_RS16625
IPR010918	IPR	PurM-like, C-terminal domain	1; 2/ 3;2.9e-02;ABUW_RS04810,ABUW_RS04915
IPR018517	IPR	tRNA-dihydrouridine synthase, conserved site	1; 2/ 3;2.9e-02;ABUW_RS15225,ABUW_RS16235
IPR000531	IPR	TonB-dependent receptor-like, beta-barrel	1;10/ 19;7.5e-03;ABUW_RS00710,ABUW_RS03025,ABUW_RS08035,ABUW_RS08070,ABUW_RS08765,ABUW_RS10225,ABUW_RS10520,ABUW_RS14160,ABUW_RS14495,ABUW_RS16540
operon_1325	operons	NZ_CP008706.1;ID=gene-ABUW_RS14060;Name=cysN;gbkey=Gene;gene=cysN;gene_biotype=protein_coding;locus_tag=ABUW_RS14060;old_locus_tag=ABUW_2895	9; 3/ 3;0.0e+00;ABUW_RS14060,ABUW_RS14065,ABUW_RS20285
IPR003789	IPR	Aspartyl/glutamyl-tRNA amidotransferase subunit B-like	9; 2/ 2;0.0e+00;ABUW_RS03505,ABUW_RS07070
IPR002545	IPR	CheW-like domain	9; 2/ 2;0.0e+00;ABUW_RS03345,ABUW_RS03355
IPR029062	IPR	Class I glutamine amidotransferase-like	0; 6/ 11;2.0e-02;ABUW_RS04385,ABUW_RS04915,ABUW_RS05880,ABUW_RS08880,ABUW_RS11855,ABUW_RS18280
GO:0070180	GO	large ribosomal subunit rRNA binding	9; 2/ 2;0.0e+00;ABUW_RS17485,ABUW_RS17495
GO:0019285	GO	glycine betaine biosynthetic process from choline	0; 3/ 5;3.9e-02;ABUW_RS14420,ABUW_RS14425,ABUW_RS14430
operon_0398	operons	NZ_CP008706.1;ID=gene-ABUW_RS04395;Name=ABUW_RS04395;gbkey=Gene;gene_biotype=protein_coding;locus_tag=ABUW_RS04395;old_locus_tag=ABUW_0896	9; 2/ 2;0.0e+00;ABUW_RS04395,ABUW_RS04400
IPR031157	IPR	Tr-type G domain, conserved site	9; 7/ 7;0.0e+00;ABUW_RS03225,ABUW_RS05050,ABUW_RS14060,ABUW_RS14850,ABUW_RS14855,ABUW_RS16275,ABUW_RS17515
GO:0006235	GO	dTTP biosynthetic process	9; 2/ 2;0.0e+00;ABUW_RS05025,ABUW_RS16625
IPR037099	IPR	Fumarate reductase/succinate dehydrogenase flavoprotein-like, C-terminal domain superfamily	1; 2/ 3;2.9e-02;ABUW_RS04270,ABUW_RS05035
IPR020612	IPR	Methylthiotransferase, conserved site	1; 2/ 3;2.9e-02;ABUW_RS08445,ABUW_RS18020
operon_0327	operons	NZ_CP008706.1;ID=gene-ABUW_RS03465;Name=ABUW_RS03465;gbkey=Gene;gene_biotype=protein_coding;locus_tag=ABUW_RS03465;old_locus_tag=ABUW_0704	9; 2/ 2;0.0e+00;ABUW_RS03465,ABUW_RS20110
operon_1426	operons	NZ_CP008706.1;ID=gene-ABUW_RS15000;Name=ABUW_RS15000;gbkey=Gene;gene_biotype=protein_coding;locus_tag=ABUW_RS15000;old_locus_tag=ABUW_3090	0; 5/11;1.6e-02;ABUW_RS15010,ABUW_RS15035,ABUW_RS15040,ABUW_RS15045,ABUW_RS15050
IPR007831	IPR	Type II secretion system protein GspE, N-terminal	9; 2/ 2;0.0e+00;ABUW_RS06590,ABUW_RS17270
IPR019844	IPR	Cold-shock (CSD) domain	9; 3/ 3;0.0e+00;ABUW_RS06720,ABUW_RS13055,ABUW_RS15360
operon_1099	operons	NZ_CP008706.1;ID=gene-ABUW_RS11855;Name=katE;gbkey=Gene;gene=katE;gene_biotype=protein_coding;locus_tag=ABUW_RS11855;old_locus_tag=ABUW_2436	9; 2/ 2;0.0e+00;ABUW_RS11855,ABUW_RS11860
GO:0019516	GO	lactate oxidation	9; 2/ 2;0.0e+00;ABUW_RS18550,ABUW_RS18555
operon_1402	operons	NZ_CP008706.1;ID=gene-ABUW_RS14765;Name=dut;gbkey=Gene;gene=dut;gene_biotype=protein_coding;locus_tag=ABUW_RS14765;old_locus_tag=ABUW_3042	9; 2/ 2;0.0e+00;ABUW_RS14765,ABUW_RS14770
IPR004840	IPR	Amino acid permease, conserved site	1; 9/ 15;2.8e-03;ABUW_RS00350,ABUW_RS00390,ABUW_RS00995,ABUW_RS01350,ABUW_RS01710,ABUW_RS03210,ABUW_RS13640,ABUW_RS18430,ABUW_RS18435
PF00575	Pfam	S1 RNA binding domain	1; 4/ 6;0.0112;ABUW_RS01265,ABUW_RS10900,ABUW_RS16915,ABUW_RS17115
PF00842	Pfam	Alanine racemase, C-terminal domain	9; 2/ 2;0.0000;ABUW_RS07535,ABUW_RS18445
operon_0254	operons	NZ_CP008706.1;ID=gene-ABUW_RS02565;Name=ABUW_RS02565;gbkey=Gene;gene_biotype=protein_coding;locus_tag=ABUW_RS02565;old_locus_tag=ABUW_0522	0; 2/ 4;3.2e-02;ABUW_RS02565,ABUW_RS02570
GO:0006119	GO	oxidative phosphorylation	9; 2/ 2;0.0e+00;ABUW_RS08730,ABUW_RS08735
IPR036393	IPR	Acetylglutamate kinase-like superfamily	0; 3/ 5;2.9e-02;ABUW_RS05175,ABUW_RS08450,ABUW_RS13345
operon_1563	operons	NZ_CP008706.1;ID=gene-ABUW_RS16540;Name=ABUW_RS16540;gbkey=Gene;gene_biotype=protein_coding;locus_tag=ABUW_RS16540;old_locus_tag=ABUW_3403	9; 2/ 2;0.0e+00;ABUW_RS16540,ABUW_RS16545
IPR001179	IPR	FKBP-type peptidyl-prolyl cis-trans isomerase domain	1; 4/ 6;1.2e-02;ABUW_RS05245,ABUW_RS14375,ABUW_RS16535,ABUW_RS18815
IPR005474	IPR	Transketolase, N-terminal	1; 2/ 3;2.9e-02;ABUW_RS00770,ABUW_RS11165
GO:0005737	GO	cytoplasm	3;172/447;1.8e-10;ABUW_RS00015,ABUW_RS00070,ABUW_RS00180,ABUW_RS00380,ABUW_RS00385,ABUW_RS00850,ABUW_RS01205,ABUW_RS01285,ABUW_RS01365,ABUW_RS01400,ABUW_RS01425,ABUW_RS01530,ABUW_RS01575,ABUW_RS01580,ABUW_RS01585,ABUW_RS01795,ABUW_RS01800,ABUW_RS01850,ABUW_RS018

ClassID	Class	Description	Single_list
			65,ABUW_RS02015,ABUW_RS02060,ABUW_RS02075,ABUW_RS02085,ABUW_RS02090,ABUW_RS02120,ABUW_RS02140,ABUW_RS02250,ABUW_RS02565,ABUW_RS02635,ABUW_RS02940,ABUW_RS03070,ABUW_RS03215,ABUW_RS03225,ABUW_RS03315,ABUW_RS03520,ABUW_RS03535,ABUW_RS04095,ABUW_RS04160,ABUW_RS04190,ABUW_RS04255,ABUW_RS04315,ABUW_RS04380,ABUW_RS04455,ABUW_RS04480,ABUW_RS04500,ABUW_RS04545,ABUW_RS04710,ABUW_RS04755,ABUW_RS04805,ABUW_RS04810,ABUW_RS04850,ABUW_RS04855,ABUW_RS04915,ABUW_RS04975,ABUW_RS05035,ABUW_RS05065,ABUW_RS05070,ABUW_RS05085,ABUW_RS05120,ABUW_RS05170,ABUW_RS05175,ABUW_RS05245,ABUW_RS05265,ABUW_RS05395,ABUW_RS05500,ABUW_RS05810,ABUW_RS05900,ABUW_RS05980,ABUW_RS06040,ABUW_RS06505,ABUW_RS06555,ABUW_RS06590,ABUW_RS06665,ABUW_RS06695,ABUW_RS07080,ABUW_RS07495,ABUW_RS07505,ABUW_RS07655,ABUW_RS07880,ABUW_RS08265,ABUW_RS08425,ABUW_RS08445,ABUW_RS08450,ABUW_RS08455,ABUW_RS08495,ABUW_RS08500,ABUW_RS08630,ABUW_RS08885,ABUW_RS10865,ABUW_RS11010,ABUW_RS11045,ABUW_RS11055,ABUW_RS11170,ABUW_RS11315,ABUW_RS11390,ABUW_RS11485,ABUW_RS11490,ABUW_RS11855,ABUW_RS13270,ABUW_RS13325,ABUW_RS13330,ABUW_RS13340,ABUW_RS13345,ABUW_RS13355,ABUW_RS13720,ABUW_RS13840,ABUW_RS13925,ABUW_RS13955,ABUW_RS14075,ABUW_RS14710,ABUW_RS14715,ABUW_RS14835,ABUW_RS14850,ABUW_RS14855,ABUW_RS14875,ABUW_RS15035,ABUW_RS15045,ABUW_RS15050,ABUW_RS15085,ABUW_RS15135,ABUW_RS15150,ABUW_RS15190,ABUW_RS15210,ABUW_RS15285,ABUW_RS15360,ABUW_RS15705,ABUW_RS15710,ABUW_RS15760,ABUW_RS15775,ABUW_RS15780,ABUW_RS15895,ABUW_RS15930,ABUW_RS15935,ABUW_RS15975,ABUW_RS15980,ABUW_RS16005,ABUW_RS16010,ABUW_RS16275,ABUW_RS16320,ABUW_RS16360,ABUW_RS16365,ABUW_RS16380,ABUW_RS16405,ABUW_RS16430,ABUW_RS16535,ABUW_RS16625,ABUW_RS16680,ABUW_RS16750,ABUW_RS16810,ABUW_RS16915,ABUW_RS17115,ABUW_RS17120,ABUW_RS17225,ABUW_RS17230,ABUW_RS17240,ABUW_RS17265,ABUW_RS17270,ABUW_RS17285,ABUW_RS17295,ABUW_RS17515,ABUW_RS17610,ABUW_RS17660,ABUW_RS17675,ABUW_RS17695,ABUW_RS17710,ABUW_RS17730,ABUW_RS17945,ABUW_RS18640,ABUW_RS18685,ABUW_RS18805,ABUW_RS18930,ABUW_RS19000
IPR018950	IPR	Disulphide bond isomerase, DsbC/G, N-terminal	1; 2/ 3;2.9e-02;ABUW_RS03275,ABUW_RS17700
IPR009000	IPR	Translation protein, beta-barrel domain superfamily	9;10/ 10;0.0e+00;ABUW_RS01580,ABUW_RS01995,ABUW_RS03225,ABUW_RS13340,ABUW_RS14060,ABUW_RS14850,ABUW_RS14855,ABUW_RS16275,ABUW_RS17230,ABUW_RS17515
IPR022761	IPR	Fumarate lyase, N-terminal	0; 3/ 5;2.9e-02;ABUW_RS05490,ABUW_RS10220,ABUW_RS17610
Pyrimidine biosynthesis	KEYWORDS	keyword	9; 2/ 2;0.0e+00;ABUW_RS13255,ABUW_RS13260
PF01740	Pfam	STAS domain	1; 2/ 3;0.0266;ABUW_RS08575,ABUW_RS17820
IPR010722	IPR	Biotin and thiamin synthesis-associated domain	9; 2/ 2;0.0e+00;ABUW_RS11220,ABUW_RS15150
IPR017896	IPR	4Fe-4S ferredoxin-type, iron-sulphur binding domain	1; 6/ 10;1.1e-02;ABUW_RS04275,ABUW_RS06555,ABUW_RS12790,ABUW_RS13945,ABUW_RS15395,ABUW_RS16995
operon_1652	operons	NZ_CP008706.1;ID=gene-ABUW_RS17480;Name=rplL;gbkey=Gene;gene=rplL;gene_biotype=protein_coding;locus_tag=ABUW_RS17480;old_locus_tag=ABUW_3591	9; 2/ 2;0.0e+00;ABUW_RS17480,ABUW_RS17485
GO:0005525	GO	GTP binding	1; 19/ 40;3.6e-03;ABUW_RS03205,ABUW_RS03225,ABUW_RS04480,ABUW_RS05050,ABUW_RS05070,ABUW_RS05170,ABUW_RS05835,ABUW_RS11390,ABUW_RS13325,ABUW_RS14060,ABUW_RS14850,ABUW_RS14855,ABUW_RS15365,ABUW_RS16275,ABUW_RS16365,ABUW_RS16390,ABUW_RS17230,ABUW_RS17515,ABUW_RS19000
operon_1742	operons	NZ_CP008706.1;ID=gene-ABUW_RS18555;Name=lldD;gbkey=Gene;gene=lldD;gene_biotype=protein_coding;locus_tag=ABUW_RS18555;old_locus_tag=ABUW_3812	9; 3/ 3;0.0e+00;ABUW_RS18555,ABUW_RS18560,ABUW_RS18565
COG1113	eggNOG_COG	amino acid transport	0;5/10;0.0150;ABUW_RS00350,ABUW_RS00995,ABUW_RS13640,ABUW_RS18430,ABUW_RS18435
PF00860	Pfam	Permease family	1; 3/ 4;0.0100;ABUW_RS00150,ABUW_RS03220,ABUW_RS13375
IPR011547	IPR	SLC26A/SulP transporter domain	1; 2/ 3;2.9e-02;ABUW_RS08575,ABUW_RS17820
GO:0032259	GO	methylation	0; 8/ 17;3.9e-02;ABUW_RS00850,ABUW_RS04185,ABUW_RS12800,ABUW_RS14205,ABUW_RS14445,ABUW_RS15140,ABUW_RS16625,ABUW_RS20715
IPR036477	IPR	Formyl transferase, N-terminal domain superfamily	1; 2/ 3;2.9e-02;ABUW_RS04805,ABUW_RS16660
PF07549	Pfam	SecD/SecF GG Motif	9; 2/ 2;0.0000;ABUW_RS02605,ABUW_RS02610
IPR036157	IPR	dUTPase-like superfamily	9; 2/ 2;0.0e+00;ABUW_RS14765,ABUW_RS15255
PF01127	Pfam	Succinate dehydrogenase/Fumarate reductase transmembrane subunit	9; 2/ 2;0.0000;ABUW_RS04260,ABUW_RS04265
GO:0002161	GO	aminoacyl-tRNA editing activity	1; 4/ 5;4.3e-03;ABUW_RS03315,ABUW_RS04095,ABUW_RS16320,ABUW_RS18805
GO:0022904	GO	respiratory electron transport chain	0; 5/ 9;3.5e-02;ABUW_RS04275,ABUW_RS07575,ABUW_RS15410,ABUW_RS15420,ABUW_RS18550
PF02729	Pfam	Aspartate/ornithine carbamoyltransferase, carbamoyl-P binding domain	9; 2/ 2;0.0000;ABUW_RS08425,ABUW_RS13260
IPR011079	IPR	Alanine racemase, C-terminal	9; 2/ 2;0.0e+00;ABUW_RS07535,ABUW_RS18445
operon_1277	operons	NZ_CP008706.1;ID=gene-ABUW_RS13610;Name=ABUW_RS13610;gbkey=Gene;gene_biotype=protein_coding;locus_tag=ABUW_RS13610;old_locus_tag=ABUW_2802	0; 2/ 4;3.2e-02;ABUW_RS13610,ABUW_RS13615
PF00916	Pfam	Sulfate permease family	1; 2/ 3;0.0266;ABUW_RS08575,ABUW_RS17820

ClassID	Class	Description	Single_list
IPR006321	IPR	Pilus retraction protein PilT/PilU	9; 2/ 2;0.0e+00;ABUW_RS14710,ABUW_RS14715
00051 Fructose and mannose metabolism [PATH:ko00051]	KEGG	ko00051	9; 2/ 2;0.0e+00;ABUW_RS08620,ABUW_RS08630
GO:0006564	GO	L-serine biosynthetic process	1; 3/ 4;1.4e-02;ABUW_RS00480,ABUW_RS01630,ABUW_RS04755
IPR014776	IPR	Tetrapyrrole methylase, subdomain 2	9; 2/ 2;0.0e+00;ABUW_RS04185,ABUW_RS13840
GO:0009986	GO	cell surface	9; 2/ 2;0.0e+00;ABUW_RS08890,ABUW_RS11780
GO:0046933	GO	proton-transporting ATP synthase activity, rotational mechanism	9; 8/ 8;0.0e+00;ABUW_RS18160,ABUW_RS18165,ABUW_RS18170,ABUW_RS18175,ABUW_RS18180,ABUW_RS18185,ABUW_RS18190,ABUW_RS18195
GO:0015419	GO	ABC-type sulfate transporter activity	1; 3/ 4;1.4e-02;ABUW_RS04990,ABUW_RS04995,ABUW_RS05000
IPR003029	IPR	S1 domain	1; 5/ 7;4.4e-03;ABUW_RS01265,ABUW_RS10900,ABUW_RS16915,ABUW_RS17115,ABUW_RS17235
GO:0016149	GO	translation release factor activity, codon specific	9; 2/ 2;0.0e+00;ABUW_RS07655,ABUW_RS16275
operon_0114	operons	NZ_CP008706.1;ID=gene-ABUW_RS01030;Name=ABUW_RS01030;gbkey=Gene;gene_biotype=protein_coding;locus_tag=ABUW_RS01030;old_locus_tag=ABUW_0208	1; 2/ 3;1.1e-02;ABUW_RS01030,ABUW_RS01035
IPR009008	IPR	Valyl/Leucyl/Isoleucyl-tRNA synthetase, editing domain	9; 3/ 3;0.0e+00;ABUW_RS04095,ABUW_RS16320,ABUW_RS18805
operon_0335	operons	NZ_CP008706.1;ID=gene-ABUW_RS03520;Name=ABUW_RS03520;gbkey=Gene;gene_biotype=protein_coding;locus_tag=ABUW_RS03520;old_locus_tag=ABUW_0715	1; 4/ 6;2.8e-03;ABUW_RS03520,ABUW_RS03525,ABUW_RS03530,ABUW_RS03535
IPR005824	IPR	KOW	9; 2/ 2;0.0e+00;ABUW_RS02050,ABUW_RS17500
IPR020557	IPR	Fumarate lyase, conserved site	1; 4/ 6;1.2e-02;ABUW_RS05490,ABUW_RS10220,ABUW_RS16510,ABUW_RS17610
IPR000957	IPR	Sulphate/thiosulphate-binding, conserved site	9; 2/ 2;0.0e+00;ABUW_RS01375,ABUW_RS05010
GO:0006166	GO	purine ribonucleoside salvage	9; 2/ 2;0.0e+00;ABUW_RS02250,ABUW_RS18975
operon_0463	operons	NZ_CP008706.1;ID=gene-ABUW_RS05050;Name=lepA;gbkey=Gene;gene=lepA;gene_biotype=protein_coding;locus_tag=ABUW_RS05050;old_locus_tag=ABUW_1029	9; 9/ 9;0.0e+00;ABUW_RS05050,ABUW_RS05055,ABUW_RS05060,ABUW_RS05065,ABUW_RS05070,ABUW_RS05075,ABUW_RS05080,ABUW_RS05085,ABUW_RS05090
PF00588	Pfam	SpoU rRNA Methylase family	9; 4/ 4;0.0000;ABUW_RS04190,ABUW_RS04850,ABUW_RS11485,ABUW_RS17295
PF00587	Pfam	tRNA synthetase class II core domain (G, H, P, S and T)	1; 2/ 3;0.0266;ABUW_RS03315,ABUW_RS15980
PF00133	Pfam	tRNA synthetases class I (I, L, M and V)	9; 3/ 3;0.0000;ABUW_RS04095,ABUW_RS16320,ABUW_RS18805
GO:0045272	GO	plasma membrane respiratory chain complex I	0; 3/ 5;3.9e-02;ABUW_RS15405,ABUW_RS15410,ABUW_RS15415
GO:0035796	GO	ATP-binding cassette (ABC) transporter complex, transmembrane substrate-binding subunit-containing	9; 2/ 2;0.0e+00;ABUW_RS05000,ABUW_RS05010
GO:0015934	GO	large ribosomal subunit	9; 8/ 8;0.0e+00;ABUW_RS02010,ABUW_RS02020,ABUW_RS02045,ABUW_RS02085,ABUW_RS02090,ABUW_RS15100,ABUW_RS17485,ABUW_RS17490
operon_0507	operons	NZ_CP008706.1;ID=gene-ABUW_RS05485;Name=ABUW_RS05485;gbkey=Gene;gene_biotype=protein_coding;locus_tag=ABUW_RS05485;old_locus_tag=ABUW_1121	0; 4/ 9;2.6e-02;ABUW_RS05490,ABUW_RS05500,ABUW_RS05515,ABUW_RS05525
PF00275	Pfam	EPSP synthase (3-phosphoshikimate 1-carboxyvinyltransferase)	9; 2/ 2;0.0000;ABUW_RS06665,ABUW_RS15780
operon_1373	operons	NZ_CP008706.1;ID=gene-ABUW_RS14470;Name=ABUW_RS14470;gbkey=Gene;gene_biotype=protein_coding;locus_tag=ABUW_RS14470;old_locus_tag=ABUW_2980	2; 4/ 5;6.1e-04;ABUW_RS14470,ABUW_RS14475,ABUW_RS14480,ABUW_RS14485
IPR000194	IPR	ATPase, F1/V1/A1 complex, alpha/beta subunit, nucleotide-binding domain	9; 3/ 3;0.0e+00;ABUW_RS15915,ABUW_RS18165,ABUW_RS18175
00190 Oxidative phosphorylation [PATH:ko00190]	KEGG	ko00190	2;25/39;1.3e-04;ABUW_RS03535,ABUW_RS07560,ABUW_RS07570,ABUW_RS07575,ABUW_RS07580,ABUW_RS08730,ABUW_RS08735,ABUW_RS08740,ABUW_RS15390,ABUW_RS15395,ABUW_RS15400,ABUW_RS15405,ABUW_RS15410,ABUW_RS15415,ABUW_RS15420,ABUW_RS15430,ABUW_RS17945,ABUW_RS18160,ABUW_RS18165,ABUW_RS18170,ABUW_RS18175,ABUW_RS18180,ABUW_RS18185,ABUW_RS18190,ABUW_RS18195
PF00006	Pfam	ATP synthase alpha/beta family, nucleotide-binding domain	9; 3/ 3;0.0000;ABUW_RS15915,ABUW_RS18165,ABUW_RS18175
GO:0003743	GO	translation initiation factor activity	9; 3/ 3;0.0e+00;ABUW_RS15975,ABUW_RS16810,ABUW_RS17230
PF00768	Pfam	D-alanyl-D-alanine carboxypeptidase	1; 2/ 3;0.0266;ABUW_RS05255,ABUW_RS05515
operon_1665	operons	NZ_CP008706.1;ID=gene-ABUW_RS17695;Name=xerD;gbkey=Gene;gene=xerD;gene_biotype=protein_coding;locus_tag=ABUW_RS17695;old_locus_tag=ABUW_3634	9; 2/ 2;0.0e+00;ABUW_RS17695,ABUW_RS17700
IPR000748	IPR	Pseudouridine synthase, RsuA/RluB/E/F	1; 2/ 3;2.9e-02;ABUW_RS05270,ABUW_RS15130
GO:0048039	GO	ubiquinone binding	0; 2/ 3;3.9e-02;ABUW_RS04260,ABUW_RS07575
GO:0009252	GO	peptidoglycan biosynthetic process	0; 14/ 35;4.8e-02;ABUW_RS01400,ABUW_RS03520,ABUW_RS03530,ABUW_RS03590,ABUW_RS05255,ABUW_RS05515,ABUW_RS06080,ABUW_RS08460,ABUW_RS11015,ABUW_RS13970,ABUW_RS15780,ABUW_RS17675,ABUW_RS18930,ABUW_RS18940
GO:0043107	GO	type IV pilus-dependent motility	1; 5/ 8;1.6e-02;ABUW_RS01425,ABUW_RS01430,ABUW_RS01435,ABUW_RS14710,ABUW_RS14715
PF02272	Pfam	DHHA1 domain	9; 2/ 2;0.0000;ABUW_RS00820,ABUW_RS13340
GO:0043022	GO	ribosome binding	3; 7/ 8;8.3e-05;ABUW_RS01285,ABUW_RS01580,ABUW_RS03225,ABUW_RS05050,ABUW_RS11390,ABUW_RS16750,ABUW_RS16810
IPR009019	IPR	K homology domain superfamily, prokaryotic type	9; 2/ 2;0.0e+00;ABUW_RS05070,ABUW_RS17235

ClassID	Class	Description	Single_list
GO:0016597	GO	amino acid binding	0; 2/ 3;3.9e-02;ABUW_RS08425,ABUW_RS13260
IPR015413	IPR	Methionyl/Leucyl tRNA synthetase	9; 2/ 2;0.0e+00;ABUW_RS15285,ABUW_RS16320
operon_1239	operons	NZ_CP008706.1;ID=gene-ABUW_RS13255;Name=ABUW_RS13255;gbkey=Gene;gene_biotype=protein_coding;locus_tag=ABUW_RS13255;old_locus_tag=ABUW_2731	1; 2/ 3;1.1e-02;ABUW_RS13255,ABUW_RS13260
IPR002314	IPR	Aminoacyl-tRNA synthetase, class II (G/ P/ S/T)	1; 2/ 3;2.9e-02;ABUW_RS03315,ABUW_RS15980
GO:0045263	GO	proton-transporting ATP synthase complex, coupling factor F(o)	9; 3/ 3;0.0e+00;ABUW_RS18185,ABUW_RS18190,ABUW_RS18195
GO:0044096	GO	type IV pilus	9; 4/ 4;0.0e+00;ABUW_RS01425,ABUW_RS01430,ABUW_RS01435,ABUW_RS14710
IPR000701	IPR	Succinate dehydrogenase/fumarate reductase type B, transmembrane subunit	9; 2/ 2;0.0e+00;ABUW_RS04260,ABUW_RS04265
00970 Aminoacyl-tRNA biosynthesis [PATH:ko00970]	KEGG	ko00970	3;15/19;6.6e-05;ABUW_RS00070,ABUW_RS01795,ABUW_RS01800,ABUW_RS02940,ABUW_RS03315,ABUW_RS04095,ABUW_RS04315,ABUW_RS13340,ABUW_RS14075,ABUW_RS15930,ABUW_RS15935,ABUW_RS15980,ABUW_RS16320,ABUW_RS16405,ABUW_RS18805
PF00551	Pfam	Formyl transferase	1; 2/ 3;0.0266;ABUW_RS04805,ABUW_RS16660
IPR009001	IPR	Translation elongation factor EF1A/initiation factor IF2gamma, C-terminal	9; 3/ 3;0.0e+00;ABUW_RS14060,ABUW_RS14850,ABUW_RS17515
operon_0135	operons	NZ_CP008706.1;ID=gene-ABUW_RS01180;Name=ABUW_RS01180;gbkey=Gene;gene_biotype=protein_coding;locus_tag=ABUW_RS01180;old_locus_tag=ABUW_0241	1; 2/ 3;1.1e-02;ABUW_RS01180,ABUW_RS01185
PF13393	Pfam	Histidyl-tRNA synthetase	9; 2/ 2;0.0000;ABUW_RS13330,ABUW_RS16405
operon_0457	operons	NZ_CP008706.1;ID=gene-ABUW_RS04945;Name=ABUW_RS04945;gbkey=Gene;gene_biotype=protein_coding;locus_tag=ABUW_RS04945;old_locus_tag=ABUW_1008	0; 3/ 7;3.8e-02;ABUW_RS04965,ABUW_RS04970,ABUW_RS04975
operon_1188	operons	NZ_CP008706.1;ID=gene-ABUW_RS12790;Name=fdxA;gbkey=Gene;gene=fdxA;gene_biotype=protein_coding;locus_tag=ABUW_RS12790;old_locus_tag=ABUW_2636	1; 2/ 3;1.1e-02;ABUW_RS12790,ABUW_RS12800
GO:0022900	GO	electron transport chain	9; 2/ 2;0.0e+00;ABUW_RS04270,ABUW_RS10730
operon_1101	operons	NZ_CP008706.1;ID=gene-ABUW_RS11870;Name=ABUW_RS11870;gbkey=Gene;gene_biotype=protein_coding;locus_tag=ABUW_RS11870;old_locus_tag=ABUW_2439	9; 2/ 2;0.0e+00;ABUW_RS11870,ABUW_RS11875
IPR004364	IPR	Aminoacyl-tRNA synthetase, class II (D/K/N)	1; 2/ 3;2.9e-02;ABUW_RS02940,ABUW_RS14075
operon_1248	operons	NZ_CP008706.1;ID=gene-ABUW_RS13315;Name=ABUW_RS13315;gbkey=Gene;gene_biotype=protein_coding;locus_tag=ABUW_RS13315;old_locus_tag=ABUW_2743	0; 2/ 4;3.2e-02;ABUW_RS13325,ABUW_RS13330
operon_0622	operons	NZ_CP008706.1;ID=gene-ABUW_RS07070;Name=ABUW_RS07070;gbkey=Gene;gene_biotype=protein_coding;locus_tag=ABUW_RS07070;old_locus_tag=ABUW_1451	9; 2/ 2;0.0e+00;ABUW_RS07070,ABUW_RS07075
operon_0441	operons	NZ_CP008706.1;ID=gene-ABUW_RS04775;Name=ABUW_RS04775;gbkey=Gene;gene_biotype=protein_coding;locus_tag=ABUW_RS04775;old_locus_tag=ABUW_0974	1; 2/ 3;1.1e-02;ABUW_RS04780,ABUW_RS04785
PF00037	Pfam	4Fe-4S binding domain	1; 2/ 3;0.0266;ABUW_RS06555,ABUW_RS12790
IPR018044	IPR	Peptidase S11, D-alanyl-D-alanine carboxypeptidase A	1; 2/ 3;2.9e-02;ABUW_RS05255,ABUW_RS05515
IPR036345	IPR	Exoribonuclease, PH domain 2 superfamily	9; 2/ 2;0.0e+00;ABUW_RS17115,ABUW_RS18700
PF01336	Pfam	OB-fold nucleic acid binding domain	1; 2/ 3;0.0266;ABUW_RS02940,ABUW_RS14075
GO:0006605	GO	protein targeting	0; 3/ 5;3.9e-02;ABUW_RS02605,ABUW_RS02610,ABUW_RS17505
IPR014729	IPR	Rossmann-like alpha/beta/alpha sandwich fold	1;16/ 31;1.4e-03;ABUW_RS00070,ABUW_RS01365,ABUW_RS04095,ABUW_RS04315,ABUW_RS04545,ABUW_RS04965,ABUW_RS05500,ABUW_RS13720,ABUW_RS14065,ABUW_RS15285,ABUW_RS15895,ABUW_RS16005,ABUW_RS16320,ABUW_RS17665,ABUW_RS18280,ABUW_RS18805
IPR001967	IPR	Peptidase S11, D-alanyl-D-alanine carboxypeptidase A, N-terminal	1; 2/ 3;2.9e-02;ABUW_RS05255,ABUW_RS05515
operon_1630	operons	NZ_CP008706.1;ID=gene-ABUW_RS17270;Name=pilB;gbkey=Gene;gene=pilB;gene_biotype=protein_coding;locus_tag=ABUW_RS17270;old_locus_tag=ABUW_3549	9; 4/ 4;0.0e+00;ABUW_RS17270,ABUW_RS17275,ABUW_RS17285,ABUW_RS20715
IPR036621	IPR	Anticodon-binding domain superfamily	9; 3/ 3;0.0e+00;ABUW_RS03315,ABUW_RS15980,ABUW_RS16405
GO:0051538	GO	3 iron, 4 sulfur cluster binding	0; 2/ 3;3.9e-02;ABUW_RS04275,ABUW_RS12790
GO:0050566	GO	asparaginyl-tRNA synthase (glutamine-hydrolyzing) activity	9; 2/ 2;0.0e+00;ABUW_RS03505,ABUW_RS03515
GO:0019646	GO	aerobic electron transport chain	1; 6/ 10;1.4e-02;ABUW_RS07570,ABUW_RS07575,ABUW_RS07580,ABUW_RS08730,ABUW_RS08735,ABUW_RS08740
GO:0008177	GO	succinate dehydrogenase (ubiquinone) activity	9; 3/ 3;0.0e+00;ABUW_RS04260,ABUW_RS04270,ABUW_RS04275
GO:0006364	GO	rRNA processing	1; 7/ 10;2.1e-03;ABUW_RS00850,ABUW_RS01580,ABUW_RS05065,ABUW_RS05270,ABUW_RS16915,ABUW_RS18480,ABUW_RS18700
Phosphoprotein	KEYWORDS	keyword	9; 2/ 2;0.0e+00;ABUW_RS03335,ABUW_RS03340
GO:0009486	GO	cytochrome bo3 ubiquinol oxidase activity	1; 3/ 4;1.4e-02;ABUW_RS07570,ABUW_RS07575,ABUW_RS07580
IPR001902	IPR	SLC26A/SulP transporter	1; 2/ 3;2.9e-02;ABUW_RS08575,ABUW_RS17820
operon_0678	operons	NZ_CP008706.1;ID=gene-ABUW_RS07655;Name=prfA;gbkey=Gene;gene=prfA;gene_biotype=protein_coding;locus_tag=ABUW_RS07655;old_locus_tag=ABUW_1567	9; 2/ 2;0.0e+00;ABUW_RS07655,ABUW_RS07660
IPR010105	IPR	TonB-dependent siderophore receptor	1; 8/ 14;7.2e-03;ABUW_RS00710,ABUW_RS08035,ABUW_RS08070,ABUW_RS08765,ABUW_RS10225,ABUW_RS10520,ABUW_RS14160,ABUW_RS16540

ClassID	Class	Description	Single_list
IPR004841	IPR	Amino acid permease/ SLC12A domain	1; 9/ 16;5.6e-03;ABUW_RS00350,ABUW_RS00390,ABUW_RS00995,ABUW_RS01350,ABUW_RS01710,ABUW_RS03210,ABUW_RS13640,ABUW_RS18430,ABUW_RS18435
GO:0018364	GO	peptidyl-glutamine methylation	9; 2/ 2;0.0e+00;ABUW_RS07660,ABUW_RS10385
operon_0316	operons	NZ_CP008706.1;ID=gene-ABUW_RS03335;Name=pilG;gbkey=Gene;gene=pilG;gene_biotype=protein_coding;locus_tag=ABUW_RS03335;old_locus_tag=ABUW_0678	9; 6/ 6;0.0e+00;ABUW_RS03335,ABUW_RS03340,ABUW_RS03345,ABUW_RS03350,ABUW_RS03355,ABUW_RS03360
GO:0004076	GO	biotin synthase activity	9; 2/ 2;0.0e+00;ABUW_RS11220,ABUW_RS15150
IPR017926	IPR	Glutamine amidotransferase	0; 4/ 7;2.9e-02;ABUW_RS04385,ABUW_RS05880,ABUW_RS08880,ABUW_RS18280
operon_0044	operons	NZ_CP008706.1;ID=gene-ABUW_RS00380;Name=hutU;gbkey=Gene;gene=hutU;gene_biotype=protein_coding;locus_tag=ABUW_RS00380;old_locus_tag=ABUW_0077	1; 3/ 5;1.1e-02;ABUW_RS00380,ABUW_RS00385,ABUW_RS00390
PF00156	Pfam	Phosphoribosyl transferase domain	1; 3/ 4;0.0100;ABUW_RS00705,ABUW_RS01920,ABUW_RS18975
IPR015939	IPR	Fumarate reductase/succinate dehydrogenase flavoprotein-like, C-terminal	1; 2/ 3;2.9e-02;ABUW_RS04270,ABUW_RS05035
GO:0003924	GO	GTPase activity	2; 12/ 18;2.1e-04;ABUW_RS03225,ABUW_RS05050,ABUW_RS05070,ABUW_RS05170,ABUW_RS14060,ABUW_RS14850,ABUW_RS14855,ABUW_RS16275,ABUW_RS16365,ABUW_RS17230,ABUW_RS17515,ABUW_RS19000
operon_1298	operons	NZ_CP008706.1;ID=gene-ABUW_RS13810;Name=dnaQ;gbkey=Gene;gene=dnaQ;gene_biotype=protein_coding;locus_tag=ABUW_RS13810;old_locus_tag=ABUW_2841	1; 2/ 3;1.1e-02;ABUW_RS13815,ABUW_RS13820
GO:0031522	GO	cell envelope Sec protein transport complex	9; 2/ 2;0.0e+00;ABUW_RS02095,ABUW_RS02615
GO:0006426	GO	glycyl-tRNA aminoacylation	9; 2/ 2;0.0e+00;ABUW_RS01795,ABUW_RS01800
IPR001608	IPR	Alanine racemase, N-terminal	1; 2/ 3;2.9e-02;ABUW_RS07535,ABUW_RS18445
operon_0539	operons	NZ_CP008706.1;ID=gene-ABUW_RS05810;Name=hemE;gbkey=Gene;gene=hemE;gene_biotype=protein_coding;locus_tag=ABUW_RS05810;old_locus_tag=ABUW_1190	0; 2/ 4;3.2e-02;ABUW_RS05810,ABUW_RS05815
GO:0015344	GO	siderophore uptake transmembrane transporter activity	0; 8/ 15;1.7e-02;ABUW_RS00710,ABUW_RS08035,ABUW_RS08070,ABUW_RS08765,ABUW_RS10225,ABUW_RS10520,ABUW_RS14160,ABUW_RS16540
operon_1575	operons	NZ_CP008706.1;ID=gene-ABUW_RS16675;Name=rpmB;gbkey=Gene;gene=rpmB;gene_biotype=protein_coding;locus_tag=ABUW_RS16675;old_locus_tag=ABUW_3430	1; 2/ 3;1.1e-02;ABUW_RS16675,ABUW_RS16680
operon_0452	operons	NZ_CP008706.1;ID=gene-ABUW_RS04900;Name=ruvB;gbkey=Gene;gene=ruvB;gene_biotype=protein_coding;locus_tag=ABUW_RS04900;old_locus_tag=ABUW_0999	1; 2/ 3;1.1e-02;ABUW_RS04900,ABUW_RS04905
PF08032	Pfam	RNA 2'-O ribose methyltransferase substrate binding	9; 2/ 2;0.0000;ABUW_RS04850,ABUW_RS17295
PF01138	Pfam	3' exoribonuclease family, domain 1	9; 2/ 2;0.0000;ABUW_RS17115,ABUW_RS18700
COG0659	eggNOG_COG	secondary active sulfate transmembrane transporter activity	1;2/ 3;0.0150;ABUW_RS08575,ABUW_RS17820
COG0834	eggNOG_COG	ABC-type amino acid transport signal transduction systems periplasmic component domain	1;2/ 3;0.0150;ABUW_RS11775,ABUW_RS11780
IPR004556	IPR	Methyltransferase HemK-like	9; 2/ 2;0.0e+00;ABUW_RS07660,ABUW_RS10385
GO:0006424	GO	glutamyl-tRNA aminoacylation	0; 2/ 3;3.9e-02;ABUW_RS01365,ABUW_RS17665
GO:0065002	GO	intracellular protein transmembrane transport	0; 3/ 5;3.9e-02;ABUW_RS02605,ABUW_RS02610,ABUW_RS17505
operon_1440	operons	NZ_CP008706.1;ID=gene-ABUW_RS15180;Name=ligA;gbkey=Gene;gene=ligA;gene_biotype=protein_coding;locus_tag=ABUW_RS15180;old_locus_tag=ABUW_3127	0; 2/ 4;3.2e-02;ABUW_RS15180,ABUW_RS15190
PF00467	Pfam	KOW motif	9; 2/ 2;0.0000;ABUW_RS02050,ABUW_RS17500
GO:0030420	GO	establishment of competence for transformation	0; 2/ 3;3.9e-02;ABUW_RS01920,ABUW_RS04785
U	COG	CELLULAR PROCESSES AND SIGNALING; Intracellular trafficking, secretion, and vesicular transport	0; 5/ 9;2.6e-02;ABUW_RS02615,ABUW_RS05055,ABUW_RS10995,ABUW_RS17980,ABUW_RS19005
operon_0668	operons	NZ_CP008706.1;ID=gene-ABUW_RS07535;Name=alr;gbkey=Gene;gene=alr;gene_biotype=protein_coding;locus_tag=ABUW_RS07535;old_locus_tag=ABUW_1544	9; 2/ 2;0.0e+00;ABUW_RS07535,ABUW_RS07540
IPR004516	IPR	Histidine-tRNA ligase/ATP phosphoribosyltransferase regulatory subunit	9; 2/ 2;0.0e+00;ABUW_RS13330,ABUW_RS16405
IPR001412	IPR	Aminoacyl-tRNA synthetase, class I, conserved site	3; 7/ 8;5.8e-05;ABUW_RS00070,ABUW_RS01365,ABUW_RS04095,ABUW_RS04315,ABUW_RS15285,ABUW_RS16320,ABUW_RS18805
operon_1511	operons	NZ_CP008706.1;ID=gene-ABUW_RS15950;Name=rplT;gbkey=Gene;gene=rplT;gene_biotype=protein_coding;locus_tag=ABUW_RS15950;old_locus_tag=ABUW_3284	9; 2/ 2;0.0e+00;ABUW_RS15950,ABUW_RS15955
IPR029064	IPR	50S ribosomal protein L30e-like	9; 2/ 2;0.0e+00;ABUW_RS04850,ABUW_RS17295
Cadmium resistance	KEYWORDS	keyword	9; 2/ 2;0.0e+00;ABUW_RS01310,ABUW_RS01315
IPR006073	IPR	GTP binding domain	1; 5/ 8;1.2e-02;ABUW_RS05070,ABUW_RS05170,ABUW_RS11390,ABUW_RS16390,ABUW_RS19000
GO:0003676	GO	nucleic acid binding	2; 12/ 17;7.9e-05;ABUW_RS00820,ABUW_RS02940,ABUW_RS03215,ABUW_RS06720,ABUW_RS07660,ABUW_RS10385,ABUW_RS13055,ABUW_RS13735,ABUW_RS13835,ABUW_RS13975,ABUW_RS14075,ABUW_RS16360
IPR041709	IPR	Elongation factor Tu (EF-Tu), GTP-binding domain	9; 2/ 2;0.0e+00;ABUW_RS14850,ABUW_RS17515
GO:0050567	GO	glutaminyl-tRNA synthase (glutamine-hydrolyzing) activity	1; 3/ 4;1.4e-02;ABUW_RS03505,ABUW_RS03510,ABUW_RS03515
IPR001537	IPR	tRNA/rRNA methyltransferase, SpoU type	9; 4/ 4;0.0e+00;ABUW_RS04190,ABUW_RS04850,ABUW_RS11485,ABUW_RS17295

ClassID	Class	Description	Single_list
GO:0015295	GO	solute:proton symporter activity	1; 3/ 4;1.4e-02;ABUW_RS04205,ABUW_RS13375,ABUW_RS18565
operon_1413	operons	NZ_CP008706.1;ID=gene-ABUW_RS14875;Name=ABUW_RS14875;gbkey=Gene;gene_biotype=protein_coding;locus_tag=ABUW_RS14875;old_locus_tag=ABUW_3065	9; 2/ 2;0.0e+00;ABUW_RS14875,ABUW_RS14880
IPR029001	IPR	Inosine triphosphate pyrophosphatase-like	1; 2/ 3;2.9e-02;ABUW_RS03535,ABUW_RS11055
IPR005669	IPR	Thiosulphate/Sulfate-binding protein	9; 2/ 2;0.0e+00;ABUW_RS01375,ABUW_RS05010
IPR000445	IPR	Helix-hairpin-helix motif	9; 2/ 2;0.0e+00;ABUW_RS00245,ABUW_RS13950
IPR032781	IPR	ABC-transporter extension domain	1; 3/ 4;1.1e-02;ABUW_RS00035,ABUW_RS01285,ABUW_RS16750
PF00313	Pfam	'Cold-shock' DNA-binding domain	1; 3/ 4;0.0100;ABUW_RS06720,ABUW_RS13055,ABUW_RS15360
IPR002059	IPR	Cold-shock protein, DNA-binding	1; 3/ 4;1.1e-02;ABUW_RS06720,ABUW_RS13055,ABUW_RS15360
GO:0008173	GO	RNA methyltransferase activity	9; 2/ 2;0.0e+00;ABUW_RS04850,ABUW_RS11485
GO:0031119	GO	tRNA pseudouridine synthesis	9; 2/ 2;0.0e+00;ABUW_RS01605,ABUW_RS16800
GO:0032784	GO	regulation of DNA-templated transcription elongation	1; 3/ 4;1.4e-02;ABUW_RS04375,ABUW_RS17235,ABUW_RS17500
IPR004035	IPR	Endonuclease III, iron-sulphur binding site	9; 2/ 2;0.0e+00;ABUW_RS00245,ABUW_RS13950
GO:0015826	GO	threonine transport	0; 3/ 5;3.9e-02;ABUW_RS11075,ABUW_RS11765,ABUW_RS12770
operon_1252	operons	NZ_CP008706.1;ID=gene-ABUW_RS13355;Name=rnhB;gbkey=Gene;gene=rnhB;gene_biotype=protein_coding;locus_tag=ABUW_RS13355;old_locus_tag=ABUW_2751	9; 2/ 2;0.0e+00;ABUW_RS13355,ABUW_RS13360
COG0042	eggNOG_COG	Catalyzes the synthesis of 5,6-dihydrouridine (D), a modified base found in the D-loop of most tRNAs, via the reduction of the C5-C6 double bond in target uridines	9;2/ 2;0.0000;ABUW_RS15225,ABUW_RS16235
IPR036589	IPR	Homocysteine-binding domain superfamily	9; 2/ 2;0.0e+00;ABUW_RS14205,ABUW_RS14445
IPR013123	IPR	RNA 2-O ribose methyltransferase, substrate binding	9; 2/ 2;0.0e+00;ABUW_RS04850,ABUW_RS17295
IPR036968	IPR	Enolpyruvate transferase domain superfamily	9; 2/ 2;0.0e+00;ABUW_RS06665,ABUW_RS15780
IPR029057	IPR	Phosphoribosyltransferase-like	2; 6/ 8;1.3e-03;ABUW_RS00705,ABUW_RS01920,ABUW_RS02250,ABUW_RS15035,ABUW_RS15365,ABUW_RS18975
IPR036921	IPR	PurM-like, N-terminal domain superfamily	1; 2/ 3;2.9e-02;ABUW_RS04810,ABUW_RS04915
IPR022967	IPR	RNA-binding domain, S1	2; 6/ 8;1.3e-03;ABUW_RS01265,ABUW_RS10900,ABUW_RS16810,ABUW_RS16915,ABUW_RS17115,ABUW_RS17235
GO:0008276	GO	protein methyltransferase activity	9; 2/ 2;0.0e+00;ABUW_RS04455,ABUW_RS07495
IPR014777	IPR	Tetrapyrrole methylase, subdomain 1	9; 2/ 2;0.0e+00;ABUW_RS04185,ABUW_RS13840
operon_0629	operons	NZ_CP008706.1;ID=gene-ABUW_RS07150;Name=ABUW_RS07150;gbkey=Gene;gene_biotype=protein_coding;locus_tag=ABUW_RS07150;old_locus_tag=ABUW_1467	1; 3/ 4;2.8e-03;ABUW_RS07150,ABUW_RS07155,ABUW_RS07160
operon_0661	operons	NZ_CP008706.1;ID=gene-ABUW_RS07460;Name=ABUW_RS07460;gbkey=Gene;gene_biotype=protein_coding;locus_tag=ABUW_RS07460;old_locus_tag=ABUW_1528	1; 2/ 3;1.1e-02;ABUW_RS07460,ABUW_RS07465
IPR020003	IPR	ATPase, alpha/beta subunit, nucleotide-binding domain, active site	9; 2/ 2;0.0e+00;ABUW_RS18165,ABUW_RS18175
GO:0016743	GO	carboxyl- or carbamoyltransferase activity	9; 2/ 2;0.0e+00;ABUW_RS03065,ABUW_RS15900
operon_0459	operons	NZ_CP008706.1;ID=gene-ABUW_RS04985;Name=ABUW_RS04985;gbkey=Gene;gene_biotype=protein_coding;locus_tag=ABUW_RS04985;old_locus_tag=ABUW_1016	9; 6/ 6;0.0e+00;ABUW_RS04985,ABUW_RS04990,ABUW_RS04995,ABUW_RS05000,ABUW_RS05005,ABUW_RS05010
IPR006130	IPR	Aspartate/ornithine carbamoyltransferase	9; 2/ 2;0.0e+00;ABUW_RS08425,ABUW_RS13260
PF02874	Pfam	ATP synthase alpha/beta family, beta-barrel domain	9; 2/ 2;0.0000;ABUW_RS18165,ABUW_RS18175
PF03143	Pfam	Elongation factor Tu C-terminal domain	9; 2/ 2;0.0000;ABUW_RS14850,ABUW_RS17515
IPR004541	IPR	Translation elongation factor EFTu/EF1A, bacterial/organelle	9; 2/ 2;0.0e+00;ABUW_RS14850,ABUW_RS17515
GO:0009378	GO	four-way junction helicase activity	9; 2/ 2;0.0e+00;ABUW_RS04900,ABUW_RS04905
operon_0448	operons	NZ_CP008706.1;ID=gene-ABUW_RS04850;Name=ABUW_RS04850;gbkey=Gene;gene_biotype=protein_coding;locus_tag=ABUW_RS04850;old_locus_tag=ABUW_0989	9; 2/ 2;0.0e+00;ABUW_RS04850,ABUW_RS04855
IPR000924	IPR	Glutamyl/glutaminyl-tRNA synthetase	1; 2/ 3;2.9e-02;ABUW_RS01365,ABUW_RS17665
IPR012677	IPR	Nucleotide-binding alpha-beta plait domain superfamily	1; 2/ 3;2.9e-02;ABUW_RS01870,ABUW_RS02005
operon_1254	operons	NZ_CP008706.1;ID=gene-ABUW_RS13370;Name=ABUW_RS13370;gbkey=Gene;gene_biotype=protein_coding;locus_tag=ABUW_RS13370;old_locus_tag=ABUW_2754	9; 2/ 2;0.0e+00;ABUW_RS13370,ABUW_RS13375
GO:0006401	GO	RNA catabolic process	0; 2/ 3;3.9e-02;ABUW_RS01870,ABUW_RS13355
IPR004100	IPR	ATPase, F1/V1/A1 complex, alpha/beta subunit, N-terminal domain	9; 2/ 2;0.0e+00;ABUW_RS18165,ABUW_RS18175
operon_0819	operons	NZ_CP008706.1;ID=gene-ABUW_RS08880;Name=ABUW_RS08880;gbkey=Gene;gene_biotype=protein_coding;locus_tag=ABUW_RS08880;old_locus_tag=ABUW_1825	9; 3/ 3;0.0e+00;ABUW_RS08880,ABUW_RS08885,ABUW_RS08890
operon_1368	operons	NZ_CP008706.1;ID=gene-ABUW_RS14420;Name=betI;gbkey=Gene;gene=betI;gene_biotype=protein_coding;locus_tag=ABUW_RS14420;old_locus_tag=ABUW_2970	9; 3/ 3;0.0e+00;ABUW_RS14420,ABUW_RS14425,ABUW_RS14430
03010 Ribosome [PATH:ko03010]	KEGG	ko03010	9;53/53;0.0e+00;ABUW_RS01575,ABUW_RS01590,ABUW_RS01990,ABUW_RS01995,ABUW_RS02000,ABUW_RS02005,ABUW_RS02010,ABUW_RS02015,ABUW_RS02020,ABUW_RS02030,ABUW_RS02035,ABUW_RS02040,ABUW_RS02045,ABUW_RS02050,ABUW_RS02055,ABUW_RS02060,ABUW_RS02065,ABUW_RS02070,ABUW_RS02075,ABUW_RS02080,ABUW_RS02085,ABUW_RS02090,ABUW_RS02100,ABUW_RS02105,ABUW_RS02110,ABUW_RS02115,ABUW_RS02125,ABUW_RS02420,ABUW_RS02425,ABUW_RS04160,ABUW_RS04165,ABUW_RS05565,ABUW_RS06035,ABUW_RS07075,ABUW_RS07545,ABUW_RS07550,ABUW_RS07555,ABUW_RS10775,ABUW_RS10900,ABUW_RS14860,ABUW_RS14865,ABUW_RS15040,ABUW_RS15100,ABUW_RS15950,ABUW_RS15955,ABUW_RS16675,ABUW_RS16680,ABUW_RS17120,ABUW_RS17480,ABUW_RS17485,ABUW_RS17490,ABUW_RS17495,ABUW_RS19020

ClassID	Class	Description	Single_list
GO:0046961	GO	proton-transporting ATPase activity, rotational mechanism	9; 2/ 2;0.0e+00;ABUW_RS18165,ABUW_RS18175
IPR033720	IPR	Elongation factor Tu, domain 2	9; 2/ 2;0.0e+00;ABUW_RS14850,ABUW_RS17515
GO:2001295	GO	malonyl-CoA biosynthetic process	1; 4/ 5;4.3e-03;ABUW_RS03065,ABUW_RS08260,ABUW_RS08265,ABUW_RS15900
GO:0009088	GO	threonine biosynthetic process	1; 4/ 6;1.7e-02;ABUW_RS01180,ABUW_RS13345,ABUW_RS16780,ABUW_RS17710
GO:0006396	GO	RNA processing	9; 3/ 3;0.0e+00;ABUW_RS03205,ABUW_RS04850,ABUW_RS17115
GO:0003989	GO	acetyl-CoA carboxylase activity	1; 4/ 5;4.3e-03;ABUW_RS03065,ABUW_RS08260,ABUW_RS08265,ABUW_RS15900
operon_0543	operons	NZ_CP008706.1;ID=gene-ABUW_RS05855;Name=ABUW_RS05855;gbkey=Gene;gene_biotype=protein_coding;locus_tag=ABUW_RS05855;old_locus_tag=ABUW_1199	1; 2/ 3;1.1e-02;ABUW_RS05855,ABUW_RS05860
operon_0305	operons	NZ_CP008706.1;ID=gene-ABUW_RS03210;Name=ABUW_RS03210;gbkey=Gene;gene_biotype=protein_coding;locus_tag=ABUW_RS03210;old_locus_tag=ABUW_0652	9; 3/ 3;0.0e+00;ABUW_RS03210,ABUW_RS03215,ABUW_RS03220
GO:0048038	GO	quinone binding	0; 9/ 17;1.4e-02;ABUW_RS15390,ABUW_RS15395,ABUW_RS15400,ABUW_RS15405,ABUW_RS15410,ABUW_RS15415,ABUW_RS15420,ABUW_RS15430,ABUW_RS18550
GO:0015935	GO	small ribosomal subunit	9; 6/ 6;0.0e+00;ABUW_RS02015,ABUW_RS02080,ABUW_RS02115,ABUW_RS06035,ABUW_RS14860,ABUW_RS14865
operon_0774	operons	NZ_CP008706.1;ID=gene-ABUW_RS08445;Name=rimO;gbkey=Gene;gene=rimO;gene_biotype=protein_coding;locus_tag=ABUW_RS08445;old_locus_tag=ABUW_1734	2; 8/12;1.3e-04;ABUW_RS08445,ABUW_RS08450,ABUW_RS08455,ABUW_RS08460,ABUW_RS08465,ABUW_RS08470,ABUW_RS08495,ABUW_RS08500
operon_0684	operons	NZ_CP008706.1;ID=gene-ABUW_RS07700;Name=ABUW_RS07700;gbkey=Gene;gene_biotype=protein_coding;locus_tag=ABUW_RS07700;old_locus_tag=ABUW_1576	0; 2/ 4;3.2e-02;ABUW_RS07710,ABUW_RS07715
GO:0006412	GO	translation	9; 59/ 64;1.1e-30;ABUW_RS01265,ABUW_RS01285,ABUW_RS01575,ABUW_RS01590,ABUW_RS01990,ABUW_RS01995,ABUW_RS02000,ABUW_RS02005,ABUW_RS02010,ABUW_RS02015,ABUW_RS02020,ABUW_RS02030,ABUW_RS02035,ABUW_RS02040,ABUW_RS02045,ABUW_RS02050,ABUW_RS02055,ABUW_RS02060,ABUW_RS02065,ABUW_RS02070,ABUW_RS02075,ABUW_RS02080,ABUW_RS02085,ABUW_RS02090,ABUW_RS02100,ABUW_RS02105,ABUW_RS02110,ABUW_RS02115,ABUW_RS02125,ABUW_RS02420,ABUW_RS02425,ABUW_RS03505,ABUW_RS03510,ABUW_RS03515,ABUW_RS04160,ABUW_RS04165,ABUW_RS05565,ABUW_RS06035,ABUW_RS07075,ABUW_RS07545,ABUW_RS07550,ABUW_RS07555,ABUW_RS10775,ABUW_RS10900,ABUW_RS14860,ABUW_RS14865,ABUW_RS15040,ABUW_RS15045,ABUW_RS15100,ABUW_RS15950,ABUW_RS15955,ABUW_RS16675,ABUW_RS16680,ABUW_RS17120,ABUW_RS17480,ABUW_RS17485,ABUW_RS17490,ABUW_RS17495,ABUW_RS19020
operon_0001	operons	NZ_CP008706.1;ID=gene-ABUW_RS00010;Name=dnaN;gbkey=Gene;gene=dnaN;gene_biotype=protein_coding;locus_tag=ABUW_RS00010;old_locus_tag=ABUW_0002	0; 2/ 4;3.2e-02;ABUW_RS00015,ABUW_RS00025
COG2233	eggNOG_COG	PERMEase	1;2/ 3;0.0150;ABUW_RS00150,ABUW_RS03220
GO:0038023	GO	signaling receptor activity	1; 8/ 14;1.0e-02;ABUW_RS00710,ABUW_RS08035,ABUW_RS08070,ABUW_RS08765,ABUW_RS10225,ABUW_RS10520,ABUW_RS14160,ABUW_RS16540
IPR002376	IPR	Formyl transferase, N-terminal	1; 2/ 3;2.9e-02;ABUW_RS04805,ABUW_RS16660
IPR015956	IPR	Penicillin-binding protein, C-terminal domain superfamily	9; 2/ 2;0.0e+00;ABUW_RS05255,ABUW_RS05515
GO:0106029	GO	tRNA pseudouridine synthase activity	1; 3/ 4;1.4e-02;ABUW_RS01605,ABUW_RS16800,ABUW_RS18480
GO:0009263	GO	deoxyribonucleotide biosynthetic process	9; 2/ 2;0.0e+00;ABUW_RS15460,ABUW_RS15470
PF07715	Pfam	TonB-dependent Receptor Plug Domain	1;10/19;0.0069;ABUW_RS00710,ABUW_RS03025,ABUW_RS08035,ABUW_RS08070,ABUW_RS08765,ABUW_RS10225,ABUW_RS10520,ABUW_RS14160,ABUW_RS14495,ABUW_RS16540
IPR036061	IPR	CheW-like domain superfamily	9; 2/ 2;0.0e+00;ABUW_RS03345,ABUW_RS03355
IPR029054	IPR	dUTPase-like	9; 2/ 2;0.0e+00;ABUW_RS14765,ABUW_RS15255
GO:0000175	GO	3'-5'-RNA exonuclease activity	9; 2/ 2;0.0e+00;ABUW_RS16360,ABUW_RS18700
operon_0962	operons	NZ_CP008706.1;ID=gene-ABUW_RS10380;Name=aroC;gbkey=Gene;gene=aroC;gene_biotype=protein_coding;locus_tag=ABUW_RS10380;old_locus_tag=ABUW_2136	9; 2/ 2;0.0e+00;ABUW_RS10380,ABUW_RS10385
IPR012910	IPR	TonB-dependent receptor, plug domain	1;10/ 19;7.5e-03;ABUW_RS00710,ABUW_RS03025,ABUW_RS08035,ABUW_RS08070,ABUW_RS08765,ABUW_RS10225,ABUW_RS10520,ABUW_RS14160,ABUW_RS14495,ABUW_RS16540
GO:0008033	GO	tRNA processing	0; 7/ 13;2.1e-02;ABUW_RS03205,ABUW_RS05065,ABUW_RS11485,ABUW_RS13735,ABUW_RS16915,ABUW_RS18480,ABUW_RS18700
F	COG	METABOLISM; Nucleotide transport and metabolism	0;15/35;9.2e-03;ABUW_RS00150,ABUW_RS01530,ABUW_RS03220,ABUW_RS04385,ABUW_RS04805,ABUW_RS04965,ABUW_RS13325,ABUW_RS13370,ABUW_RS13375,ABUW_RS15035,ABUW_RS15470,ABUW_RS15775,ABUW_RS16660,ABUW_RS18915,ABUW_RS18965
PF09334	Pfam	tRNA synthetases class I (M)	9; 2/ 2;0.0000;ABUW_RS15285,ABUW_RS16320
IPR023168	IPR	Aspartyl/glutamyl-tRNA(Asn/Gln) amidotransferase, C-terminal, domain 2	9; 2/ 2;0.0e+00;ABUW_RS03505,ABUW_RS07070
PF02545	Pfam	Maf-like protein	9; 2/ 2;0.0000;ABUW_RS03535,ABUW_RS11055
GO:0006353	GO	DNA-templated transcription termination	9; 4/ 4;0.0e+00;ABUW_RS00460,ABUW_RS15915,ABUW_RS17235,ABUW_RS17500

ClassID	Class	Description	Single_list
IPR010917	IPR	TonB-dependent receptor, conserved site	0; 6/ 11;2.0e-02;ABUW_RS03025,ABUW_RS08070,ABUW_RS08765,ABUW_RS10225,ABUW_RS10520,ABUW_RS14160
GO:0016706	GO	2-oxoglutarate-dependent dioxygenase activity	9; 2/ 2;0.0e+00;ABUW_RS11060,ABUW_RS16545
Ribonucleoprotein	KEYWORDS	keyword	9;46/ 47;6.0e-28;ABUW_RS01575,ABUW_RS01590,ABUW_RS01990,ABUW_RS02000,ABUW_RS02005,ABUW_RS02010,ABUW_RS02015,ABUW_RS02020,ABUW_RS02030,ABUW_RS02035,ABUW_RS02040,ABUW_RS02045,ABUW_RS02050,ABUW_RS02055,ABUW_RS02060,ABUW_RS02065,ABUW_RS02070,ABUW_RS02075,ABUW_RS02080,ABUW_RS02085,ABUW_RS02090,ABUW_RS02100,ABUW_RS02105,ABUW_RS02110,ABUW_RS02115,ABUW_RS02125,ABUW_RS02420,ABUW_RS02425,ABUW_RS04160,ABUW_RS04165,ABUW_RS07075,ABUW_RS07545,ABUW_RS07550,ABUW_RS07555,ABUW_RS10775,ABUW_RS14860,ABUW_RS15040,ABUW_RS15100,ABUW_RS15950,ABUW_RS15955,ABUW_RS16675,ABUW_RS16680,ABUW_RS17120,ABUW_RS17480,ABUW_RS17485,ABUW_RS19020
IPR003726	IPR	Homocysteine-binding domain	9; 2/ 2;0.0e+00;ABUW_RS14205,ABUW_RS14445
IPR014717	IPR	Translation elongation factor EF1B/ribosomal protein S6	9; 2/ 2;0.0e+00;ABUW_RS01435,ABUW_RS07555
GO:0000027	GO	ribosomal large subunit assembly	9; 3/ 3;0.0e+00;ABUW_RS01870,ABUW_RS03225,ABUW_RS15950
IPR013792	IPR	RNA 3'-terminal phosphate cyclase/enolpyruvate transferase, alpha/beta	9; 2/ 2;0.0e+00;ABUW_RS06665,ABUW_RS15780
operon_1012	operons	NZ_CP008706.1;ID=gene-ABUW_RS11075;Name=sstT;gbkey=Gene;gene=sstT;gene_biotype=protein_coding;locus_tag=ABUW_RS11075;old_locus_tag=ABUW_2277	9; 3/ 3;0.0e+00;ABUW_RS11075,ABUW_RS11080,ABUW_RS11085
GO:0009307	GO	DNA restriction-modification system	0; 2/ 3;3.9e-02;ABUW_RS00425,ABUW_RS03670
GO:0002098	GO	tRNA wobble uridine modification	9; 2/ 2;0.0e+00;ABUW_RS06560,ABUW_RS07505
GO:0003746	GO	translation elongation factor activity	9; 6/ 6;0.0e+00;ABUW_RS05050,ABUW_RS05585,ABUW_RS06040,ABUW_RS14850,ABUW_RS14855,ABUW_RS17515
operon_0444	operons	NZ_CP008706.1;ID=gene-ABUW_RS04805;Name=purN;gbkey=Gene;gene=purN;gene_biotype=protein_coding;locus_tag=ABUW_RS04805;old_locus_tag=ABUW_0980	9; 2/ 2;0.0e+00;ABUW_RS04805,ABUW_RS04810
COG4774	eggNOG_COG	siderophore transport	0;2/ 4;0.0444;ABUW_RS08765,ABUW_RS16540
IPR033954	IPR	Disulphide bond isomerase, DsbC/G	1; 2/ 3;2.9e-02;ABUW_RS03275,ABUW_RS17700
operon_1367	operons	NZ_CP008706.1;ID=gene-ABUW_RS14405;Name=ABUW_RS14405;gbkey=Gene;gene_biotype=protein_coding;locus_tag=ABUW_RS14405;old_locus_tag=ABUW_2967	1; 2/ 3;1.1e-02;ABUW_RS14410,ABUW_RS14415
GO:0070814	GO	hydrogen sulfide biosynthetic process	0; 2/ 3;3.9e-02;ABUW_RS14060,ABUW_RS14065
GO:0051536	GO	iron-sulfur cluster binding	9; 2/ 2;0.0e+00;ABUW_RS00800,ABUW_RS04275
operon_0669	operons	NZ_CP008706.1;ID=gene-ABUW_RS07545;Name=rplI;gbkey=Gene;gene=rplI;gene_biotype=protein_coding;locus_tag=ABUW_RS07545;old_locus_tag=ABUW_1546	9; 3/ 3;0.0e+00;ABUW_RS07545,ABUW_RS07550,ABUW_RS07555
operon_1362	operons	NZ_CP008706.1;ID=gene-ABUW_RS14375;Name=ABUW_RS14375;gbkey=Gene;gene_biotype=protein_coding;locus_tag=ABUW_RS14375;old_locus_tag=ABUW_2961	9; 2/ 2;0.0e+00;ABUW_RS14375,ABUW_RS14380
IPR013221	IPR	Mur ligase, central	1; 4/ 6;1.2e-02;ABUW_RS01400,ABUW_RS03070,ABUW_RS17675,ABUW_RS18930
operon_0561	operons	NZ_CP008706.1;ID=gene-ABUW_RS06035;Name=rpsB;gbkey=Gene;gene=rpsB;gene_biotype=protein_coding;locus_tag=ABUW_RS06035;old_locus_tag=ABUW_1235	0; 3/ 6;2.3e-02;ABUW_RS06035,ABUW_RS06040,ABUW_RS06045
IPR000836	IPR	Phosphoribosyltransferase domain	2; 6/ 8;1.3e-03;ABUW_RS00705,ABUW_RS01920,ABUW_RS02250,ABUW_RS15035,ABUW_RS15365,ABUW_RS18975
PF00009	Pfam	Elongation factor Tu GTP binding domain	9; 8/ 8;0.0000;ABUW_RS03225,ABUW_RS05050,ABUW_RS14060,ABUW_RS14850,ABUW_RS14855,ABUW_RS16275,ABUW_RS17230,ABUW_RS17515
IPR018045	IPR	Sulphate anion transporter, conserved site	9; 2/ 2;0.0e+00;ABUW_RS08575,ABUW_RS17820
IPR029026	IPR	tRNA (guanine-N1-)-methyltransferase, N-terminal	3; 7/ 8;5.8e-05;ABUW_RS00850,ABUW_RS01585,ABUW_RS04190,ABUW_RS04850,ABUW_RS11485,ABUW_RS13925,ABUW_RS17295
GO:0008360	GO	regulation of cell shape	0; 15/ 36;3.5e-02;ABUW_RS01400,ABUW_RS03520,ABUW_RS03525,ABUW_RS03530,ABUW_RS03590,ABUW_RS05255,ABUW_RS05515,ABUW_RS06080,ABUW_RS08460,ABUW_RS11015,ABUW_RS13970,ABUW_RS15780,ABUW_RS17675,ABUW_RS18930,ABUW_RS18940
IPR005667	IPR	Sulphate ABC transporter permease protein 2	9; 2/ 2;0.0e+00;ABUW_RS04995,ABUW_RS05000
operon_0481	operons	NZ_CP008706.1;ID=gene-ABUW_RS05240;Name=ABUW_RS05240;gbkey=Gene;gene_biotype=protein_coding;locus_tag=ABUW_RS05240;old_locus_tag=ABUW_1067	0; 2/ 4;3.2e-02;ABUW_RS05245,ABUW_RS05255
IPR037118	IPR	Valyl-tRNA synthetase, tRNA-binding arm superfamily	9; 2/ 2;0.0e+00;ABUW_RS04095,ABUW_RS16750
IPR036513	IPR	STAS domain superfamily	1; 3/ 4;1.1e-02;ABUW_RS08575,ABUW_RS14255,ABUW_RS17820
GO:0015709	GO	thiosulfate transport	9; 2/ 2;0.0e+00;ABUW_RS05000,ABUW_RS05010
PF01926	Pfam	50S ribosome-binding GTPase	1; 5/ 7;0.0041;ABUW_RS05070,ABUW_RS05170,ABUW_RS11390,ABUW_RS16390,ABUW_RS19000
IPR004161	IPR	Translation elongation factor EFTu-like, domain 2	9; 6/ 6;0.0e+00;ABUW_RS03225,ABUW_RS05050,ABUW_RS14850,ABUW_RS14855,ABUW_RS16275,ABUW_RS17515
GO:0006432	GO	phenylalanyl-tRNA aminoacylation	9; 2/ 2;0.0e+00;ABUW_RS15930,ABUW_RS15935
IPR004036	IPR	Endonuclease III-like, conserved site-2	9; 2/ 2;0.0e+00;ABUW_RS00245,ABUW_RS13950
IPR036397	IPR	Ribonuclease H superfamily	0; 5/ 10;3.8e-02;ABUW_RS13355,ABUW_RS13735,ABUW_RS15880,ABUW_RS16050,ABUW_RS16360

ClassID	Class	Description	Single_list
PF00206	Pfam	Lyase	0; 3/ 5;0.0266;ABUW_RS05490,ABUW_RS10220,ABUW_RS17610
IPR037066	IPR	TonB-dependent receptor, plug domain superfamily	1;10/ 19;7.5e-03;ABUW_RS00710,ABUW_RS03025,ABUW_RS08035,ABUW_RS08070,ABUW_RS08765,ABUW_RS10225,ABUW_RS10520,ABUW_RS14160,ABUW_RS14495,ABUW_RS16540
GO:0004129	GO	cytochrome-c oxidase activity	9; 3/ 3;0.0e+00;ABUW_RS07570,ABUW_RS07575,ABUW_RS07580
PF00117	Pfam	Glutamine amidotransferase class-I	0; 4/ 7;0.0266;ABUW_RS04385,ABUW_RS05880,ABUW_RS08880,ABUW_RS18280
PF13098	Pfam	Thioredoxin-like domain	1; 2/ 3;0.0266;ABUW_RS03275,ABUW_RS17700
PF03129	Pfam	Anticodon binding domain	9; 3/ 3;0.0000;ABUW_RS03315,ABUW_RS15980,ABUW_RS16405
GO:0046656	GO	folic acid biosynthetic process	0; 3/ 5;3.9e-02;ABUW_RS03070,ABUW_RS15760,ABUW_RS16015
operon_1514	operons	NZ_CP008706.1;ID=gene-ABUW_RS15975;Name=infC;gbkey=Gene;gene=infC;gene_biotype=protein_coding;locus_tag=ABUW_RS15975	9; 2/ 2;0.0e+00;ABUW_RS15975,ABUW_RS15980
GO:0001522	GO	pseudouridine synthesis	0; 2/ 3;3.9e-02;ABUW_RS05270,ABUW_RS18480
operon_1394	operons	NZ_CP008706.1;ID=gene-ABUW_RS14695;Name=ABUW_RS14695;gbkey=Gene;gene_biotype=protein_coding;locus_tag=ABUW_RS14695;old_locus_tag=ABUW_3028	9; 2/ 2;0.0e+00;ABUW_RS14695,ABUW_RS14700
GO:0046654	GO	tetrahydrofolate biosynthetic process	1; 5/ 7;5.9e-03;ABUW_RS03070,ABUW_RS05835,ABUW_RS15760,ABUW_RS16015,ABUW_RS16630
operon_1396	operons	NZ_CP008706.1;ID=gene-ABUW_RS14710;Name=ABUW_RS14710;gbkey=Gene;gene_biotype=protein_coding;locus_tag=ABUW_RS14710;old_locus_tag=ABUW_3031	9; 2/ 2;0.0e+00;ABUW_RS14710,ABUW_RS14715
IPR001048	IPR	Aspartate/glutamate/uridylate kinase	0; 3/ 5;2.9e-02;ABUW_RS05175,ABUW_RS08450,ABUW_RS13345
GO:0004527	GO	exonuclease activity	0; 2/ 3;3.9e-02;ABUW_RS14700,ABUW_RS16050
IPR001247	IPR	Exoribonuclease, phosphorolytic domain 1	9; 2/ 2;0.0e+00;ABUW_RS17115,ABUW_RS18700
GO:0000413	GO	protein peptidyl-prolyl isomerization	0; 2/ 3;3.9e-02;ABUW_RS07880,ABUW_RS14375
IPR007848	IPR	Methyltransferase small domain	9; 2/ 2;0.0e+00;ABUW_RS03215,ABUW_RS10385
GO:0044210	GO	'de novo' CTP biosynthetic process	9; 2/ 2;0.0e+00;ABUW_RS08450,ABUW_RS08880
PF01029	Pfam	NusB family	9; 2/ 2;0.0000;ABUW_RS00120,ABUW_RS00460
PF01207	Pfam	Dihydrouridine synthase (Dus)	1; 2/ 3;0.0266;ABUW_RS15225,ABUW_RS16235
IPR035926	IPR	NusB-like superfamily	9; 2/ 2;0.0e+00;ABUW_RS00120,ABUW_RS00460
IPR024083	IPR	Fumarase/histidase, N-terminal	1; 4/ 6;1.2e-02;ABUW_RS00385,ABUW_RS05490,ABUW_RS10220,ABUW_RS17610
PF00692	Pfam	dUTPase	9; 2/ 2;0.0000;ABUW_RS14765,ABUW_RS15255
PF01588	Pfam	Putative tRNA binding domain	1; 2/ 3;0.0266;ABUW_RS15285,ABUW_RS15930
IPR004365	IPR	OB-fold nucleic acid binding domain, AA-tRNA synthetase-type	1; 2/ 3;2.9e-02;ABUW_RS02940,ABUW_RS14075
IPR012337	IPR	Ribonuclease H-like superfamily	0; 6/ 12;2.9e-02;ABUW_RS01265,ABUW_RS13355,ABUW_RS13735,ABUW_RS15880,ABUW_RS16050,ABUW_RS16360
GO:0000100	GO	S-methylmethionine transmembrane transporter activity	9; 2/ 2;0.0e+00;ABUW_RS01350,ABUW_RS01710
GO:0009246	GO	enterobacterial common antigen biosynthetic process	0; 2/ 3;3.9e-02;ABUW_RS18635,ABUW_RS18640
PF10411	Pfam	Disulfide bond isomerase protein N-terminus	1; 2/ 3;0.0266;ABUW_RS03275,ABUW_RS17700

2.7 Enrichment Analysis (GSEA) of *A. baumannii* in LCWB Medium vs M9 Medium Down Regulated

ClassID	Class	Description	Single_list
GO:0000721	GO	(R,R)-butanediol dehydrogenase activity	9; 2/ 2;0.0e+00;ABUW_RS10330,ABUW_RS15610
G	COG	METABOLISM; Carbohydrate transport and metabolism	1;16/35;5.2e-04;ABUW_RS00270,ABUW_RS03380,ABUW_RS08935,ABUW_RS08970,ABUW_RS09555,ABUW_RS12190,ABUW_RS13550,ABUW_RS14210,ABUW_RS14215,ABUW_RS14220,ABUW_RS14305,ABUW_RS14760,ABUW_RS15160,ABUW_RS15165,ABUW_RS16075,ABUW_RS16480
I	COG	METABOLISM; Lipid transport and metabolism	3;38/85;7.4e-08;ABUW_RS00865,ABUW_RS01835,ABUW_RS02975,ABUW_RS02980,ABUW_RS04485,ABUW_RS04935,ABUW_RS05995,ABUW_RS06650,ABUW_RS07690,ABUW_RS08155,ABUW_RS08165,ABUW_RS08910,ABUW_RS08915,ABUW_RS08920,ABUW_RS09120,ABUW_RS09445,ABUW_RS10015,ABUW_RS10190,ABUW_RS10195,ABUW_RS10660,ABUW_RS10665,ABUW_RS11655,ABUW_RS11945,ABUW_RS11970,ABUW_RS11990,ABUW_RS11995,ABUW_RS12020,ABUW_RS12025,ABUW_RS12730,ABUW_RS13490,ABUW_RS13505,ABUW_RS14295,ABUW_RS14925,ABUW_RS15600,ABUW_RS16065,ABUW_RS16070,ABUW_RS16465,ABUW_RS18410
COG1250	eggNOG_COG	3-hydroxyacyl-CoA dehydrogenase	1; 2/ 3;0.01420;ABUW_RS12020,ABUW_RS12730
COG2057	eggNOG_COG	Acyl CoA acetate 3-ketoacid CoA transferase beta subunit	9; 3/ 3;0.00000;ABUW_RS08915,ABUW_RS09120,ABUW_RS11990
COG1788	eggNOG_COG	Acyl CoA acetate 3-ketoacid CoA transferase, alpha subunit	1; 2/ 3;0.01420;ABUW_RS08910,ABUW_RS11995
COG1960	eggNOG_COG	acyl-CoA dehydrogenase activity	1;10/18;0.00028;ABUW_RS01835,ABUW_RS02975,ABUW_RS02980,ABUW_RS05995,ABUW_RS06650,ABUW_RS10660,ABUW_RS10665,ABUW_RS11970,ABUW_RS13505,ABUW_RS15600
COG1063	eggNOG_COG	alcohol dehydrogenase	9; 3/ 3;0.00000;ABUW_RS10330,ABUW_RS12605,ABUW_RS15610
COG0765	eggNOG_COG	amino acid transport	0; 2/ 4;0.03420;ABUW_RS11335,ABUW_RS11340
COG0386	eggNOG_COG	Belongs to the glutathione peroxidase family	9; 2/ 2;0.00000;ABUW_RS11455,ABUW_RS18150
COG0183	eggNOG_COG	Belongs to the thiolase family	0; 4/ 8;0.01664;ABUW_RS08155,ABUW_RS08920,ABUW_RS10195,ABUW_RS12025
COG0753	eggNOG_COG	catalase activity	9; 2/ 2;0.00000;ABUW_RS10000,ABUW_RS12185
COG0329	eggNOG_COG	Catalyzes the condensation of (S)-aspartate-beta- semialdehyde (S)-ASA and pyruvate to 4-hydroxy- tetrahydrodipicolinate (HTPA)	0; 2/ 4;0.03420;ABUW_RS14515,ABUW_RS17930
COG0119	eggNOG_COG	Catalyzes the condensation of the acetyl group of acetyl-CoA with 3-methyl-2-oxobutanoate (2-oxoisovalerate) to form 3-carboxy-3-hydroxy-4-methylpentanoate (2-isopropylmalate)	9; 2/ 2;0.00000;ABUW_RS12195,ABUW_RS16550
COG0365	eggNOG_COG	Catalyzes the conversion of acetate into acetyl-CoA (AcCoA), an essential intermediate at the junction of anabolic and catabolic pathways. AcsA undergoes a two-step reaction. In the first half reaction, AcsA combines acetate with ATP to form acetyl-adenylate (AcAMP) intermediate. In the second half reaction, it can then transfer the acetyl group from AcAMP to the sulfhydryl group of CoA, forming the product AcCoA	9; 3/ 3;0.00000;ABUW_RS00865,ABUW_RS07690,ABUW_RS18410
COG2885	eggNOG_COG	chlorophyll binding	1; 2/ 3;0.01420;ABUW_RS13250,ABUW_RS14775
COG1680	eggNOG_COG	COG1680 Beta-lactamase class C and other penicillin binding	9; 2/ 2;0.00000;ABUW_RS08170,ABUW_RS17125
COG2084	eggNOG_COG	Dehydrogenase	9; 2/ 2;0.00000;ABUW_RS09445,ABUW_RS16070
COG0625	eggNOG_COG	glutathione transferase activity	0; 3/ 6;0.02432;ABUW_RS11725,ABUW_RS11730,ABUW_RS16890
COG1335	eggNOG_COG	isochorismatase	0; 2/ 4;0.03420;ABUW_RS01020,ABUW_RS09275
COG1804	eggNOG_COG	L-carnitine dehydratase bile acid-inducible protein F	0; 2/ 4;0.03420;ABUW_RS03150,ABUW_RS12200
COG2271	eggNOG_COG	Major facilitator Superfamily	9; 5/ 5;0.00000;ABUW_RS08935,ABUW_RS12190,ABUW_RS13550,ABUW_RS14220,ABUW_RS14305
COG0243	eggNOG_COG	molybdopterin cofactor binding	9; 2/ 2;0.00000;ABUW_RS04630,ABUW_RS08305
COG1902	eggNOG_COG	pentaerythritol trinitrate reductase activity	0; 3/ 6;0.02432;ABUW_RS09190,ABUW_RS09255,ABUW_RS13715
COG3485	eggNOG_COG	protocatechuate 3,4-dioxygenase	9; 2/ 2;0.00000;ABUW_RS08945,ABUW_RS08950
COG0446	eggNOG_COG	pyridine nucleotide-disulphide oxidoreductase	1; 3/ 4;0.00347;ABUW_RS09190,ABUW_RS13715,ABUW_RS14310
COG0745	eggNOG_COG	RESPONSE REGULATOR receiver	0; 3/ 7;0.03956;ABUW_RS04055,ABUW_RS07395,ABUW_RS08285
COG0542	eggNOG_COG	response to heat	9; 2/ 2;0.00000;ABUW_RS08825,ABUW_RS13285
COG1028	eggNOG_COG	Short-chain dehydrogenase reductase Sdr	0; 6/15;0.02432;ABUW_RS08160,ABUW_RS09070,ABUW_RS10160,ABUW_RS11850,ABUW_RS14225,ABUW_RS14290
COG0789	eggNOG_COG	Transcriptional regulator	1; 2/ 3;0.01420;ABUW_RS17105,ABUW_RS17845
COG0668	eggNOG_COG	transmembrane transport	9; 2/ 2;0.00000;ABUW_RS08040,ABUW_RS15330
GO:0003857	GO	3-hydroxyacyl-CoA dehydrogenase activity	1; 3/ 4;2.9e-03;ABUW_RS03135,ABUW_RS12020,ABUW_RS17385
GO:0008692	GO	3-hydroxybutyryl-CoA epimerase activity	9; 2/ 2;0.0e+00;ABUW_RS03135,ABUW_RS17385
GO:0003861	GO	3-isopropylmalate dehydratase activity	9; 2/ 2;0.0e+00;ABUW_RS16835,ABUW_RS16840

ClassID	Class	Description	Single_list
GO:0047569	GO	3-oxoadipate CoA-transferase activity	3; 5/ 6;1.1e-04;ABUW_RS08910,ABUW_RS08915,ABUW_RS09120,ABUW_RS11990,ABUW_RS11995
GO:0047570	GO	3-oxoadipate enol-lactonase activity	9; 2/ 2;0.0e+00;ABUW_RS08930,ABUW_RS09110
GO:0033812	GO	3-oxoadipyl-CoA thiolase activity	0; 2/ 4;3.5e-02;ABUW_RS08920,ABUW_RS12025
GO:0019380	GO	3-phenylpropionate catabolic process	9; 2/ 2;0.0e+00;ABUW_RS14310,ABUW_RS16465
GO:0046279	GO	3,4-dihydroxybenzoate biosynthetic process	1; 2/ 3;1.2e-02;ABUW_RS08960,ABUW_RS08970
GO:0019619	GO	3,4-dihydroxybenzoate catabolic process	1; 4/ 6;2.9e-03;ABUW_RS08920,ABUW_RS08925,ABUW_RS08945,ABUW_RS12025
GO:0003987	GO	acetate-CoA ligase activity	9; 4/ 4;0.0e+00;ABUW_RS00865,ABUW_RS07690,ABUW_RS15985,ABUW_RS18410
GO:0045150	GO	acetoin catabolic process	1; 3/ 4;2.9e-03;ABUW_RS10335,ABUW_RS10350,ABUW_RS10355
GO:0006085	GO	acetyl-CoA biosynthetic process	9; 4/ 4;0.0e+00;ABUW_RS07690,ABUW_RS16500,ABUW_RS16505,ABUW_RS18410
GO:0003988	GO	acetyl-CoA C-acyltransferase activity	9; 2/ 2;0.0e+00;ABUW_RS08155,ABUW_RS17390
GO:0008126	GO	acetylesterase activity	1; 3/ 4;2.9e-03;ABUW_RS08170,ABUW_RS14925,ABUW_RS17125
GO:0003994	GO	aconitate hydratase activity	1; 2/ 3;1.2e-02;ABUW_RS16255,ABUW_RS18525
GO:0003995	GO	acyl-CoA dehydrogenase activity	0; 6/14;1.2e-02;ABUW_RS05995,ABUW_RS06650,ABUW_RS10660,ABUW_RS12005,ABUW_RS13505,ABUW_RS15600
GO:0042121	GO	alginic acid biosynthetic process	1; 2/ 3;1.2e-02;ABUW_RS14760,ABUW_RS17600
GO:0006520	GO	amino acid metabolic process	0; 2/ 4;3.5e-02;ABUW_RS07895,ABUW_RS07900
GO:0019439	GO	aromatic compound catabolic process	0;10/26;6.4e-03;ABUW_RS05625,ABUW_RS05845,ABUW_RS09080,ABUW_RS09570,ABUW_RS10115,ABUW_RS10130,ABUW_RS10145,ABUW_RS12190,ABUW_RS13510,ABUW_RS14220
GO:0042952	GO	beta-ketoadipate pathway	5;14/19;1.9e-08;ABUW_RS08910,ABUW_RS08915,ABUW_RS08920,ABUW_RS08925,ABUW_RS08930,ABUW_RS08940,ABUW_RS08945,ABUW_RS08950,ABUW_RS09110,ABUW_RS09120,ABUW_RS09135,ABUW_RS11990,ABUW_RS11995,ABUW_RS12025
GO:0045227	GO	capsule polysaccharide biosynthetic process	0; 2/ 4;3.5e-02;ABUW_RS05210,ABUW_RS16440
GO:0009437	GO	carnitine metabolic process	1; 2/ 3;1.2e-02;ABUW_RS14910,ABUW_RS14920
GO:0004096	GO	catalase activity	9; 3/ 3;0.0e+00;ABUW_RS11855,ABUW_RS12185,ABUW_RS16870
GO:0034605	GO	cellular response to heat	1; 3/ 4;2.9e-03;ABUW_RS08825,ABUW_RS13285,ABUW_RS13920
GO:0061077	GO	chaperone-mediated protein folding	0; 2/ 4;3.5e-02;ABUW_RS07065,ABUW_RS09970
GO:0015109	GO	chromate transmembrane transporter activity	9; 2/ 2;0.0e+00;ABUW_RS10275,ABUW_RS11515
GO:0047780	GO	citrate dehydratase activity	1; 2/ 3;1.2e-02;ABUW_RS16255,ABUW_RS18525
GO:0031419	GO	cobalamin binding	1; 2/ 3;1.2e-02;ABUW_RS07895,ABUW_RS07900
GO:0071111	GO	cyclic-guanylate-specific phosphodiesterase activity	0; 2/ 4;3.5e-02;ABUW_RS11805,ABUW_RS16295
GO:0008851	GO	ethanolamine ammonia-lyase activity	9; 2/ 2;0.0e+00;ABUW_RS07895,ABUW_RS07900
GO:0009350	GO	ethanolamine ammonia-lyase complex	9; 2/ 2;0.0e+00;ABUW_RS07895,ABUW_RS07900
GO:0046336	GO	ethanolamine catabolic process	9; 2/ 2;0.0e+00;ABUW_RS07895,ABUW_RS07900
GO:0031471	GO	ethanolamine degradation polyhedral organelle	9; 2/ 2;0.0e+00;ABUW_RS07895,ABUW_RS07900
GO:0005576	GO	extracellular region	0; 8/19;6.4e-03;ABUW_RS01595,ABUW_RS05145,ABUW_RS05275,ABUW_RS08170,ABUW_RS08570,ABUW_RS14645,ABUW_RS17125,ABUW_RS19650
GO:0006635	GO	fatty acid beta-oxidation	0; 6/14;1.2e-02;ABUW_RS03135,ABUW_RS04935,ABUW_RS08155,ABUW_RS12020,ABUW_RS17385,ABUW_RS17390
GO:0033539	GO	fatty acid beta-oxidation using acyl-CoA dehydrogenase	0; 5/13;3.1e-02;ABUW_RS05995,ABUW_RS06650,ABUW_RS10660,ABUW_RS13505,ABUW_RS15600
GO:0006631	GO	fatty acid metabolic process	0; 4/11;5.0e-02;ABUW_RS08165,ABUW_RS11920,ABUW_RS12730,ABUW_RS15985
GO:0008860	GO	ferredoxin-NAD+ reductase activity	1; 2/ 3;1.2e-02;ABUW_RS10115,ABUW_RS14310
GO:0015473	GO	fimbrial usher porin activity	9; 3/ 3;0.0e+00;ABUW_RS07970,ABUW_RS09975,ABUW_RS11245
GO:0050660	GO	flavin adenine dinucleotide binding	0;22/70;2.8e-03;ABUW_RS01835,ABUW_RS02130,ABUW_RS02975,ABUW_RS02980,ABUW_RS05995,ABUW_RS06650,ABUW_RS08300,ABUW_RS09045,ABUW_RS09075,ABUW_RS09620,ABUW_RS10115,ABUW_RS10340,ABUW_RS10660,ABUW_RS10665,ABUW_RS10875,ABUW_RS11970,ABUW_RS12005,ABUW_RS13505,ABUW_RS14275,ABUW_RS14310,ABUW_RS14910,ABUW_RS15600
GO:0036382	GO	flavin reductase (NADH) activity	1; 2/ 3;1.2e-02;ABUW_RS09080,ABUW_RS10130
GO:0008863	GO	formate dehydrogenase (NAD+) activity	9; 2/ 2;0.0e+00;ABUW_RS04630,ABUW_RS08315
GO:0006749	GO	glutathione metabolic process	1; 4/ 6;2.9e-03;ABUW_RS08990,ABUW_RS10310,ABUW_RS10315,ABUW_RS11725

ClassID	Class	Description	Single_list
GO:0004602	GO	glutathione peroxidase activity	9; 2/ 2;0.0e+00;ABUW_RS11455,ABUW_RS18150
GO:0006071	GO	glycerol metabolic process	0; 3/ 7;3.6e-02;ABUW_RS04475,ABUW_RS04490,ABUW_RS11745
GO:0046503	GO	glycerolipid catabolic process	9; 2/ 2;0.0e+00;ABUW_RS08170,ABUW_RS17125
GO:0006097	GO	glyoxylate cycle	1; 3/ 4;2.9e-03;ABUW_RS05275,ABUW_RS10860,ABUW_RS14030
GO:0020037	GO	heme binding	0; 7/16;7.4e-03;ABUW_RS08300,ABUW_RS10000,ABUW_RS11620,ABUW_RS11855,ABUW_RS12180,ABUW_RS12185,ABUW_RS16870
GO:0042744	GO	hydrogen peroxide catabolic process	1; 2/ 3;1.2e-02;ABUW_RS11855,ABUW_RS16870
GO:0016787	GO	hydrolase activity	0;12/33;5.6e-03;ABUW_RS01020,ABUW_RS04895,ABUW_RS08990,ABUW_RS09275,ABUW_RS09525,ABUW_RS09555,ABUW_RS09575,ABUW_RS09615,ABUW_RS10310,ABUW_RS10315,ABUW_RS15550,ABUW_RS16440
GO:0004419	GO	hydroxymethylglutaryl-CoA lyase activity	9; 2/ 2;0.0e+00;ABUW_RS11950,ABUW_RS12195
GO:0030350	GO	iron-responsive element binding	9; 2/ 2;0.0e+00;ABUW_RS16255,ABUW_RS18525
GO:0140009	GO	L-aspartate import across plasma membrane	9; 3/ 3;0.0e+00;ABUW_RS11330,ABUW_RS11335,ABUW_RS11340
GO:0098712	GO	L-glutamate import across plasma membrane	9; 3/ 3;0.0e+00;ABUW_RS11330,ABUW_RS11335,ABUW_RS11340
GO:0009098	GO	leucine biosynthetic process	0; 3/ 6;2.2e-02;ABUW_RS16550,ABUW_RS16835,ABUW_RS16840
GO:0006629	GO	lipid metabolic process	0; 3/ 6;2.2e-02;ABUW_RS10670,ABUW_RS12195,ABUW_RS14750
GO:0008381	GO	mechanosensitive monoatomic ion channel activity	0; 2/ 4;3.5e-02;ABUW_RS08040,ABUW_RS15330
GO:0031956	GO	medium-chain fatty acid-CoA ligase activity	1; 2/ 3;1.2e-02;ABUW_RS11920,ABUW_RS15985
GO:0045121	GO	membrane raft	9; 3/ 3;0.0e+00;ABUW_RS07690,ABUW_RS16070,ABUW_RS18410
GO:0006777	GO	Mo-molybdopterin cofactor biosynthetic process	0; 3/ 7;3.6e-02;ABUW_RS04635,ABUW_RS08310,ABUW_RS08320
GO:0030151	GO	molybdenum ion binding	0; 2/ 4;3.5e-02;ABUW_RS04630,ABUW_RS05845
GO:0043546	GO	molybdopterin cofactor binding	9; 3/ 3;0.0e+00;ABUW_RS04630,ABUW_RS08305,ABUW_RS08315
GO:0004499	GO	N,N-dimethylaniline monooxygenase activity	0; 3/ 6;2.2e-02;ABUW_RS02130,ABUW_RS09620,ABUW_RS10875
GO:0008750	GO	NAD(P)+ transhydrogenase (AB-specific) activity	9; 2/ 2;0.0e+00;ABUW_RS16090,ABUW_RS16100
GO:0070403	GO	NAD+ binding	2; 5/ 7;6.3e-04;ABUW_RS03135,ABUW_RS12020,ABUW_RS12730,ABUW_RS16100,ABUW_RS17385
GO:0070404	GO	NADH binding	1; 2/ 3;1.2e-02;ABUW_RS00630,ABUW_RS16100
GO:0050661	GO	NADP binding	0;11/33;1.3e-02;ABUW_RS02130,ABUW_RS08300,ABUW_RS09070,ABUW_RS09255,ABUW_RS09445,ABUW_RS09620,ABUW_RS10875,ABUW_RS14285,ABUW_RS14915,ABUW_RS16070,ABUW_RS16090
GO:0006740	GO	NADPH regeneration	9; 3/ 3;0.0e+00;ABUW_RS16090,ABUW_RS16095,ABUW_RS16100
GO:0016151	GO	nickel cation binding	0; 3/ 7;3.6e-02;ABUW_RS13990,ABUW_RS13995,ABUW_RS14015
GO:0042128	GO	nitrate assimilation	0; 3/ 7;3.6e-02;ABUW_RS08280,ABUW_RS08300,ABUW_RS08305
GO:0016491	GO	oxidoreductase activity	0;21/64;1.9e-03;ABUW_RS01075,ABUW_RS04610,ABUW_RS05840,ABUW_RS05845,ABUW_RS07425,ABUW_RS07870,ABUW_RS08305,ABUW_RS09075,ABUW_RS09190,ABUW_RS09195,ABUW_RS09260,ABUW_RS09630,ABUW_RS10350,ABUW_RS11850,ABUW_RS12020,ABUW_RS12040,ABUW_RS12605,ABUW_RS13440,ABUW_RS14225,ABUW_RS14290,ABUW_RS16135
GO:0016709	GO	oxidoreductase activity, acting on paired donors, with incorporation or reduction of molecular oxygen, NAD(P)H as one donor, and incorporation of one atom of oxygen	0; 5/12;2.0e-02;ABUW_RS00630,ABUW_RS09620,ABUW_RS10875,ABUW_RS14910,ABUW_RS14920
GO:0016620	GO	oxidoreductase activity, acting on the aldehyde or oxo group of donors, NAD or NADP as acceptor	0; 2/ 4;3.5e-02;ABUW_RS10770,ABUW_RS12145
GO:0052890	GO	oxidoreductase activity, acting on the CH-CH group of donors, with a flavin as acceptor	9; 4/ 4;0.0e+00;ABUW_RS01835,ABUW_RS02975,ABUW_RS02980,ABUW_RS11970
GO:1990204	GO	oxidoreductase complex	9; 2/ 2;0.0e+00;ABUW_RS05845,ABUW_RS08305
GO:0042597	GO	periplasmic space	0;11/32;1.2e-02;ABUW_RS01670,ABUW_RS05040,ABUW_RS05845,ABUW_RS07170,ABUW_RS07335,ABUW_RS09105,ABUW_RS11155,ABUW_RS14240,ABUW_RS16135,ABUW_RS17715,ABUW_RS18150
GO:0004601	GO	peroxidase activity	0; 3/ 7;3.6e-02;ABUW_RS11725,ABUW_RS11730,ABUW_RS12185
GO:0009297	GO	pilus assembly	1; 3/ 5;1.1e-02;ABUW_RS07970,ABUW_RS09975,ABUW_RS11245
GO:0042619	GO	poly-hydroxybutyrate biosynthetic process	9; 2/ 2;0.0e+00;ABUW_RS07195,ABUW_RS10455
GO:2000147	GO	positive regulation of cell motility	1; 2/ 3;1.2e-02;ABUW_RS11805,ABUW_RS17600
GO:0019679	GO	propionate metabolic process, methylcitrate cycle	9; 3/ 3;0.0e+00;ABUW_RS16255,ABUW_RS18525,ABUW_RS18530
GO:0006515	GO	protein quality control for misfolded or incompletely synthesized proteins	9; 2/ 2;0.0e+00;ABUW_RS08825,ABUW_RS13920
GO:0030091	GO	protein repair	0; 2/ 4;3.5e-02;ABUW_RS03605,ABUW_RS11460

ClassID	Class	Description	Single_list
GO:0033103	GO	protein secretion by the type VI secretion system	1; 3/ 4;2.9e-03;ABUW_RS12705,ABUW_RS12710,ABUW_RS13685
GO:0018578	GO	protocatechuate 3,4-dioxygenase activity	9; 2/ 2;0.0e+00;ABUW_RS08945,ABUW_RS08950
GO:0019630	GO	quinate metabolic process	1; 2/ 3;1.2e-02;ABUW_RS08960,ABUW_RS08970
GO:0008876	GO	quinoprotein glucose dehydrogenase activity	9; 2/ 2;0.0e+00;ABUW_RS08585,ABUW_RS09285
GO:0006417	GO	regulation of translation	0; 2/ 4;3.5e-02;ABUW_RS10895,ABUW_RS15790
GO:0006970	GO	response to osmotic stress	9; 2/ 2;0.0e+00;ABUW_RS08040,ABUW_RS15160
GO:0006979	GO	response to oxidative stress	1; 7/13;1.6e-03;ABUW_RS08825,ABUW_RS11455,ABUW_RS11460,ABUW_RS11855,ABUW_RS12185,ABUW_RS16255,ABUW_RS16870
GO:0030435	GO	sporulation resulting in formation of a cellular spore	1; 5/10;8.3e-03;ABUW_RS06650,ABUW_RS13505,ABUW_RS15330,ABUW_RS15600,ABUW_RS19650
GO:0050313	GO	sulfur dioxygenase activity	1; 3/ 4;2.9e-03;ABUW_RS08990,ABUW_RS10310,ABUW_RS10315
GO:0097351	GO	toxin sequestering activity	9; 2/ 2;0.0e+00;ABUW_RS05670,ABUW_RS12705
GO:0005992	GO	trehalose biosynthetic process	9; 2/ 2;0.0e+00;ABUW_RS15160,ABUW_RS15165
GO:0004806	GO	triglyceride lipase activity	1; 3/ 4;2.9e-03;ABUW_RS01595,ABUW_RS08170,ABUW_RS17125
GO:0033104	GO	type VI protein secretion system complex	0; 2/ 4;3.5e-02;ABUW_RS12710,ABUW_RS13685
GO:0050547	GO	vanillin synthase activity	9; 2/ 2;0.0e+00;ABUW_RS13490,ABUW_RS16065
IPR036010	IPR	2Fe-2S ferredoxin-like superfamily	0; 4/11;0.04733;ABUW_RS05840,ABUW_RS09075,ABUW_RS10115,ABUW_RS14910
IPR001041	IPR	2Fe-2S ferredoxin-type iron-sulfur binding domain	0; 4/11;0.04733;ABUW_RS05840,ABUW_RS09075,ABUW_RS10115,ABUW_RS14910
IPR006058	IPR	2Fe-2S ferredoxin, iron-sulphur binding site	1; 4/ 7;0.00797;ABUW_RS05840,ABUW_RS09075,ABUW_RS10115,ABUW_RS14910
IPR006108	IPR	3-hydroxyacyl-CoA dehydrogenase, C-terminal	2; 4/ 5;0.00079;ABUW_RS03135,ABUW_RS12020,ABUW_RS12730,ABUW_RS17385
IPR006180	IPR	3-hydroxyacyl-CoA dehydrogenase, conserved site	1; 3/ 4;0.00348;ABUW_RS03135,ABUW_RS12020,ABUW_RS17385
IPR006176	IPR	3-hydroxyacyl-CoA dehydrogenase, NAD binding	2; 4/ 5;0.00079;ABUW_RS03135,ABUW_RS12020,ABUW_RS12730,ABUW_RS17385
IPR029154	IPR	3-hydroxyisobutyrate dehydrogenase-like, NAD-binding domain	1; 2/ 3;0.01223;ABUW_RS09445,ABUW_RS16070
IPR015815	IPR	3-hydroxyisobutyrate dehydrogenase-related	1; 2/ 3;0.01223;ABUW_RS09445,ABUW_RS16070
IPR002204	IPR	3-hydroxyisobutyrate dehydrogenase-related, conserved site	1; 2/ 3;0.01223;ABUW_RS09445,ABUW_RS16070
IPR012792	IPR	3-oxoacid CoA-transferase, subunit A	0; 2/ 4;0.03289;ABUW_RS08910,ABUW_RS11995
IPR012791	IPR	3-oxoacid CoA-transferase, subunit B	1; 3/ 4;0.00348;ABUW_RS08915,ABUW_RS09120,ABUW_RS11990
IPR026968	IPR	3-oxoadipate enol-lactonase 1/2	9; 2/ 2;0.00000;ABUW_RS08930,ABUW_RS09110
IPR008927	IPR	6-phosphogluconate dehydrogenase-like, C-terminal domain superfamily	0; 6/15;0.01752;ABUW_RS03135,ABUW_RS09445,ABUW_RS12020,ABUW_RS12730,ABUW_RS16070,ABUW_RS17385
IPR013328	IPR	6-phosphogluconate dehydrogenase, domain 2	1; 3/ 5;0.01211;ABUW_RS09445,ABUW_RS12730,ABUW_RS16070
IPR006115	IPR	6-phosphogluconate dehydrogenase, NADP-binding	1; 2/ 3;0.01223;ABUW_RS09445,ABUW_RS16070
IPR043429	IPR	ABC transporter membrane protein permease protein ArtM/GltK/GlnP/TcyL/YhdX-like	0; 2/ 4;0.03289;ABUW_RS11335,ABUW_RS11340
IPR025878	IPR	Acetyl-CoA dehydrogenase-like C-terminal domain	9; 4/ 4;0.00000;ABUW_RS01835,ABUW_RS02975,ABUW_RS02980,ABUW_RS11970
IPR000573	IPR	Aconitase A/isopropylmalate dehydratase small subunit, swivel domain	9; 3/ 3;0.00000;ABUW_RS16255,ABUW_RS16835,ABUW_RS18525
IPR018136	IPR	Aconitase family, 4Fe-4S cluster binding site	1; 2/ 3;0.01223;ABUW_RS16255,ABUW_RS16840
IPR036008	IPR	Aconitase, iron-sulfur domain	1; 3/ 4;0.00348;ABUW_RS16255,ABUW_RS16840,ABUW_RS18525
IPR001030	IPR	Aconitase/3-isopropylmalate dehydratase large subunit, alpha/beta/alpha domain	1; 3/ 4;0.00348;ABUW_RS16255,ABUW_RS16840,ABUW_RS18525
IPR015931	IPR	Aconitase/3-isopropylmalate dehydratase large subunit, alpha/beta/alpha, subdomain 1/3	1; 3/ 4;0.00348;ABUW_RS16255,ABUW_RS16840,ABUW_RS18525
IPR015928	IPR	Aconitase/3-isopropylmalate dehydratase, swivel	1; 3/ 4;0.00348;ABUW_RS16255,ABUW_RS16835,ABUW_RS18525
IPR006249	IPR	Aconitase/Iron-responsive element-binding protein 2	9; 2/ 2;0.00000;ABUW_RS16255,ABUW_RS18525
IPR036250	IPR	Acyl-CoA dehydrogenase-like, C-terminal	1;12/24;0.00021;ABUW_RS01835,ABUW_RS02975,ABUW_RS02980,ABUW_RS05995,ABUW_RS06650,ABUW_RS09045,ABUW_RS10660,ABUW_RS10665,ABUW_RS11970,ABUW_RS12005,ABUW_RS13505,ABUW_RS15600
IPR006089	IPR	Acyl-CoA dehydrogenase, conserved site	0; 6/14;0.01223;ABUW_RS06650,ABUW_RS10660,ABUW_RS10665,ABUW_RS12005,ABUW_RS13505,ABUW_RS15600
IPR009075	IPR	Acyl-CoA dehydrogenase/oxidase C-terminal	2;11/20;0.00013;ABUW_RS01835,ABUW_RS02975,ABUW_RS02980,ABUW_RS05995,ABUW_RS06650,ABUW_RS10660,ABUW_RS10665,ABUW_RS11970,ABUW_RS12005,ABUW_RS13505,ABUW_RS15600
IPR013786	IPR	Acyl-CoA dehydrogenase/oxidase, N-terminal	1;12/24;0.00021;ABUW_RS01835,ABUW_RS02975,ABUW_RS02980,ABUW_RS05995,ABUW_RS06650,ABUW_RS09045,ABUW_RS10660,ABUW_RS10665,ABUW_RS11970,ABUW_RS12005,ABUW_RS13505,ABUW_RS15600
IPR009100	IPR	Acyl-CoA dehydrogenase/oxidase, N-terminal and middle domain superfamily	1;12/24;0.00021;ABUW_RS01835,ABUW_RS02975,ABUW_RS02980,ABUW_RS05995,ABUW_RS06650,ABUW_RS09045,ABUW_RS10660,ABUW_RS10665,ABUW_RS11970,ABUW_RS12005,ABUW_RS13505,ABUW_RS15600
IPR037069	IPR	Acyl-CoA dehydrogenase/oxidase, N-terminal domain superfamily	1;12/24;0.00021;ABUW_RS01835,ABUW_RS02975,ABUW_RS02980,ABUW_RS05995,ABUW_RS06650,ABUW_RS09045,ABUW_RS10660,ABUW_RS10665,ABUW_RS11970,ABUW_RS12005,ABUW_RS13505,ABUW_RS15600
IPR006091	IPR	Acyl-CoA oxidase/dehydrogenase, middle domain	1;10/21;0.00115;ABUW_RS01835,ABUW_RS02975,ABUW_RS02980,ABUW_RS06650,ABUW_RS10660,ABUW_RS10665,ABUW_RS11970,ABUW_RS12005,ABUW_RS13505,ABUW_RS15600
IPR046373	IPR	Acyl-CoA oxidase/dehydrogenase, middle domain superfamily	1;12/24;0.00021;ABUW_RS01835,ABUW_RS02975,ABUW_RS02980,ABUW_RS05995,ABUW_RS06650,ABUW_RS09045,ABUW_RS10660,ABUW_RS10665,ABUW_RS11970,ABUW_RS12005,ABUW_RS13505,ABUW_RS15600
IPR013149	IPR	Alcohol dehydrogenase-like, C-terminal	0; 3/ 7;0.03496;ABUW_RS10330,ABUW_RS12605,ABUW_RS15610
IPR002328	IPR	Alcohol dehydrogenase, zinc-type, conserved site	1; 3/ 5;0.01211;ABUW_RS10330,ABUW_RS12605,ABUW_RS15610

ClassID	Class	Description	Single_list
IPR015590	IPR	Aldehyde dehydrogenase domain	0; 8/25;0.03289;ABUW_RS05435,ABUW_RS12145,ABUW_RS12355,ABUW_RS13495, ABUW_RS14915,ABUW_RS16475,ABUW_RS16670,ABUW_RS18420
IPR016163	IPR	Aldehyde dehydrogenase, C-terminal	0; 8/25;0.03289;ABUW_RS05435,ABUW_RS12145,ABUW_RS12355,ABUW_RS13495, ABUW_RS14915,ABUW_RS16475,ABUW_RS16670,ABUW_RS18420
IPR016162	IPR	Aldehyde dehydrogenase, N-terminal	0; 8/25;0.03289;ABUW_RS05435,ABUW_RS12145,ABUW_RS12355,ABUW_RS13495, ABUW_RS14915,ABUW_RS16475,ABUW_RS16670,ABUW_RS18420
IPR016161	IPR	Aldehyde/histidinol dehydrogenase	0; 8/26;0.04145;ABUW_RS05435,ABUW_RS12145,ABUW_RS12355,ABUW_RS13495, ABUW_RS14915,ABUW_RS16475,ABUW_RS16670,ABUW_RS18420
IPR029058	IPR	Alpha/Beta hydrolase fold	1;15/35;0.00040;ABUW_RS01595,ABUW_RS02535,ABUW_RS07195,ABUW_RS08930,ABUW_RS09110,ABUW_RS09185,ABUW_RS09555,ABUW_RS09575,ABUW_RS09615,ABUW_RS10145,ABUW_RS10455,ABUW_RS13525,ABUW_RS14295,ABUW_RS14925,ABUW_RS16465
IPR000073	IPR	Alpha/beta hydrolase fold-1	1; 9/19;0.00207;ABUW_RS01595,ABUW_RS02535,ABUW_RS07195,ABUW_RS08930, ABUW_RS09110,ABUW_RS09185,ABUW_RS10455,ABUW_RS14295,ABUW_RS16465
IPR036928	IPR	Amidase signature (AS) superfamily	0; 2/ 4;0.03289;ABUW_RS09475,ABUW_RS12565
IPR023631	IPR	Amidase signature domain	0; 2/ 4;0.03289;ABUW_RS09475,ABUW_RS12565
IPR017439	IPR	Amidohydrolase	1; 2/ 3;0.01223;ABUW_RS04895,ABUW_RS15550
IPR010065	IPR	Amino acid ABC transporter, permease protein, 3-TM domain	0; 3/ 6;0.02162;ABUW_RS06535,ABUW_RS11335,ABUW_RS11340
IPR025110	IPR	AMP-binding enzyme, C-terminal domain	0; 5/14;0.03800;ABUW_RS00865,ABUW_RS07690,ABUW_RS11920,ABUW_RS15985, ABUW_RS18410
IPR020845	IPR	AMP-binding, conserved site	0; 5/14;0.03800;ABUW_RS00865,ABUW_RS07690,ABUW_RS11920,ABUW_RS15985, ABUW_RS18410
IPR023271	IPR	Aquaporin-like	9; 2/ 2;0.00000;ABUW_RS00280,ABUW_RS01160
IPR009010	IPR	Aspartate decarboxylase-like domain superfamily	1; 3/ 5;0.01211;ABUW_RS04630,ABUW_RS08305,ABUW_RS08315
IPR036264	IPR	Bacterial exopeptidase dimerisation domain	0; 2/ 4;0.03289;ABUW_RS04895,ABUW_RS15550
IPR012793	IPR	Beta-ketoadipyl CoA thiolase	0; 2/ 4;0.03289;ABUW_RS08920,ABUW_RS12025
IPR005939	IPR	Beta-lactamase hydrolase-like protein, phosphatase-like domain	1; 2/ 3;0.01223;ABUW_RS10310,ABUW_RS10315
IPR001466	IPR	Beta-lactamase-related	1; 2/ 3;0.01223;ABUW_RS08170,ABUW_RS17125
IPR011614	IPR	Catalase core domain	9; 2/ 2;0.00000;ABUW_RS11855,ABUW_RS12185
IPR020835	IPR	Catalase superfamily	9; 3/ 3;0.00000;ABUW_RS10000,ABUW_RS11855,ABUW_RS12185
IPR018028	IPR	Catalase, mono-functional, haem-containing	9; 2/ 2;0.00000;ABUW_RS11855,ABUW_RS12185
IPR003370	IPR	Chromate transporter	9; 2/ 2;0.00000;ABUW_RS10275,ABUW_RS11515
IPR014047	IPR	Chromate transporter, long chain	9; 2/ 2;0.00000;ABUW_RS10275,ABUW_RS11515
IPR019489	IPR	Clp ATPase, C-terminal	0; 2/ 4;0.03289;ABUW_RS08825,ABUW_RS13285
IPR004176	IPR	Clp, repeat (R) domain	1; 2/ 3;0.01223;ABUW_RS08825,ABUW_RS13285
IPR036628	IPR	Clp, N-terminal domain superfamily	1; 2/ 3;0.01223;ABUW_RS08825,ABUW_RS13285
IPR001270	IPR	ClpA/B family	0; 2/ 4;0.03289;ABUW_RS08825,ABUW_RS13285
IPR018368	IPR	ClpA/B, conserved site 1	1; 2/ 3;0.01223;ABUW_RS08825,ABUW_RS13285
IPR028299	IPR	ClpA/B, conserved site 2	9; 2/ 2;0.00000;ABUW_RS08825,ABUW_RS13285
IPR041546	IPR	ClpA/ClpB, AAA lid domain	1; 2/ 3;0.01223;ABUW_RS08825,ABUW_RS13285
IPR003673	IPR	CoA-transferase family III	0; 2/ 4;0.03289;ABUW_RS03150,ABUW_RS12200
IPR023606	IPR	CoA-transferase family III domain 1 superfamily	0; 2/ 4;0.03289;ABUW_RS03150,ABUW_RS12200
IPR044855	IPR	CoA-transferase family III domain 3 superfamily	0; 2/ 4;0.03289;ABUW_RS03150,ABUW_RS12200
IPR004164	IPR	Coenzyme A transferase active site	1; 3/ 4;0.00348;ABUW_RS08915,ABUW_RS09120,ABUW_RS11990
IPR004163	IPR	Coenzyme A transferase binding site	0; 2/ 4;0.03289;ABUW_RS08910,ABUW_RS11995
IPR004165	IPR	Coenzyme A transferase family I	1; 5/ 8;0.00248;ABUW_RS08910,ABUW_RS08915,ABUW_RS09120,ABUW_RS11990,ABUW_RS11995
IPR001753	IPR	Enoyl-CoA hydratase/isomerase	0; 5/13;0.03121;ABUW_RS03135,ABUW_RS04935,ABUW_RS13490,ABUW_RS16065, ABUW_RS17385
IPR000639	IPR	Epoxide hydrolase-like	0; 2/ 4;0.03289;ABUW_RS09185,ABUW_RS16465
IPR016156	IPR	FAD/NAD-linked reductase, dimerisation domain superfamily	0; 3/ 7;0.03496;ABUW_RS08300,ABUW_RS10340,ABUW_RS14310
IPR018030	IPR	Fimbrial membrane usher, conserved site	9; 3/ 3;0.00000;ABUW_RS07970,ABUW_RS09975,ABUW_RS11245
IPR020946	IPR	Flavin monooxygenase-like	0; 3/ 6;0.02162;ABUW_RS02130,ABUW_RS09620,ABUW_RS10875
IPR012938	IPR	Glucose/Sorbosone dehydrogenase	9; 5/ 5;0.00000;ABUW_RS00270,ABUW_RS07425,ABUW_RS08585,ABUW_RS09260,ABUW_RS09285
IPR000889	IPR	Glutathione peroxidase	9; 2/ 2;0.00000;ABUW_RS11455,ABUW_RS18150
IPR029759	IPR	Glutathione peroxidase active site	9; 2/ 2;0.00000;ABUW_RS11455,ABUW_RS18150
IPR029760	IPR	Glutathione peroxidase conserved site	9; 2/ 2;0.00000;ABUW_RS11455,ABUW_RS18150
IPR040079	IPR	Glutathione transferase family	1; 3/ 5;0.01211;ABUW_RS11725,ABUW_RS11730,ABUW_RS16890
IPR039567	IPR	Glycine zipper domain	9; 2/ 2;0.00000;ABUW_RS13250,ABUW_RS14775
IPR006531	IPR	Gp5/Type VI secretion system Vgr protein, OB-fold domain	1; 2/ 3;0.01223;ABUW_RS12710,ABUW_RS13685
IPR043594	IPR	HMG-CoA lyase	9; 2/ 2;0.00000;ABUW_RS11950,ABUW_RS12195
IPR000627	IPR	Intradiol ring-cleavage dioxygenase, C-terminal	1; 2/ 3;0.01223;ABUW_RS08945,ABUW_RS08950
IPR015889	IPR	Intradiol ring-cleavage dioxygenase, core	1; 2/ 3;0.01223;ABUW_RS08945,ABUW_RS08950
IPR019818	IPR	Isocitrate/isopropylmalate dehydrogenase, conserved site	1; 2/ 3;0.01223;ABUW_RS05275,ABUW_RS14935
IPR024084	IPR	Isopropylmalate dehydrogenase-like domain	1; 2/ 3;0.01223;ABUW_RS05275,ABUW_RS14935
IPR018392	IPR	LysM domain	0; 2/ 4;0.03289;ABUW_RS15080,ABUW_RS19650
IPR036779	IPR	LysM domain superfamily	0; 2/ 4;0.03289;ABUW_RS15080,ABUW_RS19650
IPR011701	IPR	Major facilitator superfamily	0;16/47;0.00468;ABUW_RS04920,ABUW_RS08935,ABUW_RS09355,ABUW_RS09440,ABUW_RS09485,ABUW_RS10150,ABUW_RS12000,ABUW_RS12190,ABUW_RS13175,ABUW_RS13460,ABUW_RS13485,ABUW_RS13550,ABUW_RS14220,ABUW_RS14305,ABUW_RS15595,ABUW_RS18390
IPR020846	IPR	Major facilitator superfamily domain	1;19/53;0.00117;ABUW_RS04920,ABUW_RS07295,ABUW_RS08935,ABUW_RS09355,ABUW_RS09440,ABUW_RS09485,ABUW_RS10150,ABUW_RS10230,ABUW_RS12000,ABUW_RS12190,ABUW_RS12360,ABUW_RS13175,ABUW_RS13460,ABUW_RS13485,ABUW_RS13550,ABUW_RS14220,ABUW_RS14305,ABUW_RS15595, ABUW_RS18390
IPR004746	IPR	Major facilitator superfamily, aromatic acid:H+ symporter family	2; 6/ 8;0.00019;ABUW_RS08935,ABUW_RS10150,ABUW_RS12000,ABUW_RS13175,ABUW_RS13460,ABUW_RS15595
IPR005828	IPR	Major facilitator, sugar transporter-like	0; 4/ 8;0.01225;ABUW_RS07295,ABUW_RS10230,ABUW_RS12360,ABUW_RS18390

ClassID	Class	Description	Single_list
IPR039562	IPR	Membrane fusion protein, biotin-lipoyl like domain	0; 3/ 6;0.02162;ABUW_RS04745,ABUW_RS09480,ABUW_RS15310
IPR013216	IPR	Methyltransferase type 11	1; 2/ 3;0.01223;ABUW_RS01700,ABUW_RS10460
IPR036259	IPR	MFS transporter superfamily	1;20/56;0.00094;ABUW_RS04920,ABUW_RS05290,ABUW_RS07295,ABUW_RS08935,ABUW_RS09355,ABUW_RS09440,ABUW_RS09485,ABUW_RS10150,ABUW_RS10230,ABUW_RS12000,ABUW_RS12190,ABUW_RS12360,ABUW_RS13175,ABUW_RS13460,ABUW_RS13485,ABUW_RS13550,ABUW_RS14220,ABUW_RS14305,ABUW_RS15595,ABUW_RS18390
IPR004736	IPR	MFS transporter, metabolite:H symporter	0; 3/ 6;0.02162;ABUW_RS07295,ABUW_RS10230,ABUW_RS18390
IPR006657	IPR	Molybdopterin dinucleotide-binding domain	9; 3/ 3;0.00000;ABUW_RS04630,ABUW_RS08305,ABUW_RS08315
IPR006656	IPR	Molybdopterin oxidoreductase	1; 3/ 4;0.00348;ABUW_RS04630,ABUW_RS08305,ABUW_RS08315
IPR006963	IPR	Molybdopterin oxidoreductase, 4Fe-4S domain	1; 2/ 3;0.01223;ABUW_RS08305,ABUW_RS08315
IPR027467	IPR	Molybdopterin oxidoreductase, molybdopterin cofactor binding site	9; 2/ 2;0.00000;ABUW_RS08305,ABUW_RS08315
IPR016040	IPR	NAD(P)-binding domain	1; 2/ 3;0.01223;ABUW_RS08380,ABUW_RS10770
IPR036291	IPR	NAD(P)-binding domain superfamily	0;27/93;0.00439;ABUW_RS03135,ABUW_RS04615,ABUW_RS08160,ABUW_RS08380,ABUW_RS09070,ABUW_RS09195,ABUW_RS09290,ABUW_RS09445,ABUW_RS09570,ABUW_RS10160,ABUW_RS10330,ABUW_RS10335,ABUW_RS10770,ABUW_RS11850,ABUW_RS12020,ABUW_RS12605,ABUW_RS12730,ABUW_RS13440,ABUW_RS14225,ABUW_RS14285,ABUW_RS14290,ABUW_RS14675,ABUW_RS15610,ABUW_RS16035,ABUW_RS16070,ABUW_RS16100,ABUW_RS17385
IPR037171	IPR	NagB/RpiA transferase-like	1; 6/12;0.00532;ABUW_RS08910,ABUW_RS08915,ABUW_RS09120,ABUW_RS11685,ABUW_RS11990,ABUW_RS11995
IPR029479	IPR	Nitroreductase	0; 2/ 4;0.03289;ABUW_RS04610,ABUW_RS07870
IPR000415	IPR	Nitroreductase-like	0; 2/ 4;0.03289;ABUW_RS04610,ABUW_RS07870
IPR000015	IPR	Outer membrane usher protein	9; 3/ 3;0.00000;ABUW_RS07970,ABUW_RS09975,ABUW_RS11245
IPR042186	IPR	Outer membrane usher protein FimD, plug domain	9; 3/ 3;0.00000;ABUW_RS07970,ABUW_RS09975,ABUW_RS11245
IPR025949	IPR	PapC-like, C-terminal domain	9; 3/ 3;0.00000;ABUW_RS07970,ABUW_RS09975,ABUW_RS11245
IPR043142	IPR	PapC-like, C-terminal domain superfamily	9; 3/ 3;0.00000;ABUW_RS07970,ABUW_RS09975,ABUW_RS11245
IPR025885	IPR	PapC, N-terminal domain	9; 3/ 3;0.00000;ABUW_RS07970,ABUW_RS09975,ABUW_RS11245
IPR037224	IPR	PapC, N-terminal domain superfamily	9; 3/ 3;0.00000;ABUW_RS07970,ABUW_RS09975,ABUW_RS11245
IPR044528	IPR	Persulfide dioxygenase-like, MBL-fold metallo-hydrolase domain	1; 3/ 4;0.00348;ABUW_RS08990,ABUW_RS10310,ABUW_RS10315
IPR010125	IPR	Poly(R)-hydroxyalkanoic acid synthase, class III, PhaC subunit	9; 2/ 2;0.00000;ABUW_RS07195,ABUW_RS10455
IPR019893	IPR	PQQ-dependent dehydrogenase, s-GDH family	9; 2/ 2;0.00000;ABUW_RS08585,ABUW_RS09285
IPR029021	IPR	Protein-tyrosine phosphatase-like	1; 2/ 3;0.01223;ABUW_RS10310,ABUW_RS10315
IPR028244	IPR	Putative type VI secretion system, Rhs element associated Vgr domain	1; 2/ 3;0.01223;ABUW_RS12710,ABUW_RS13685
IPR000891	IPR	Pyruvate carboxyltransferase	9; 3/ 3;0.00000;ABUW_RS11950,ABUW_RS12195,ABUW_RS16550
IPR020625	IPR	Schiff base-forming aldolase, active site	0; 2/ 4;0.03289;ABUW_RS14515,ABUW_RS17930
IPR020624	IPR	Schiff base-forming aldolase, conserved site	0; 2/ 4;0.03289;ABUW_RS14515,ABUW_RS17930
IPR022742	IPR	Serine aminopeptidase, S33	9; 3/ 3;0.00000;ABUW_RS09110,ABUW_RS09575,ABUW_RS09615
IPR002347	IPR	Short-chain dehydrogenase/reductase SDR	0;12/35;0.01187;ABUW_RS04615,ABUW_RS08160,ABUW_RS09070,ABUW_RS09195,ABUW_RS09570,ABUW_RS10160,ABUW_RS10335,ABUW_RS11850,ABUW_RS13440,ABUW_RS14225,ABUW_RS14290,ABUW_RS16035
IPR020904	IPR	Short-chain dehydrogenase/reductase, conserved site	0;10/27;0.01066;ABUW_RS04615,ABUW_RS08160,ABUW_RS09070,ABUW_RS10160,ABUW_RS10335,ABUW_RS11850,ABUW_RS13440,ABUW_RS14225,ABUW_RS14290,ABUW_RS16035
IPR011042	IPR	Six-bladed beta-propeller, TolB-like	3; 6/ 7;0.00003;ABUW_RS00270,ABUW_RS07425,ABUW_RS08585,ABUW_RS09260,ABUW_RS09285,ABUW_RS09375
IPR011041	IPR	Soluble quinoprotein glucose/sorbosone dehydrogenase	9; 5/ 5;0.00000;ABUW_RS00270,ABUW_RS07425,ABUW_RS08585,ABUW_RS09260,ABUW_RS09285
IPR045758	IPR	Solute-binding protein AdeT 1/2	1; 3/ 4;0.00348;ABUW_RS00045,ABUW_RS00050,ABUW_RS01935
IPR000849	IPR	Sugar phosphate transporter	9; 2/ 2;0.00000;ABUW_RS13550,ABUW_RS14305
IPR005829	IPR	Sugar transporter, conserved site	1;11/23;0.00067;ABUW_RS07295,ABUW_RS08935,ABUW_RS10150,ABUW_RS10230,ABUW_RS12000,ABUW_RS12360,ABUW_RS13175,ABUW_RS13460,ABUW_RS13485,ABUW_RS15595,ABUW_RS18390
IPR029061	IPR	Thiamin diphosphate-binding fold	0; 5/11;0.01226;ABUW_RS10350,ABUW_RS10355,ABUW_RS14210,ABUW_RS14215,ABUW_RS14275
IPR002155	IPR	Thiolase	1; 5/ 9;0.00470;ABUW_RS08155,ABUW_RS08920,ABUW_RS10195,ABUW_RS12025,ABUW_RS17390
IPR016039	IPR	Thiolase-like	0; 5/13;0.03121;ABUW_RS08155,ABUW_RS08920,ABUW_RS10195,ABUW_RS12025,ABUW_RS17390
IPR020610	IPR	Thiolase, active site	1; 5/ 9;0.00470;ABUW_RS08155,ABUW_RS08920,ABUW_RS10195,ABUW_RS12025,ABUW_RS17390
IPR020615	IPR	Thiolase, acyl-enzyme intermediate active site	0; 4/ 8;0.01225;ABUW_RS08920,ABUW_RS10195,ABUW_RS12025,ABUW_RS17390
IPR020617	IPR	Thiolase, C-terminal	1; 5/ 9;0.00470;ABUW_RS08155,ABUW_RS08920,ABUW_RS10195,ABUW_RS12025,ABUW_RS17390
IPR020613	IPR	Thiolase, conserved site	1; 5/ 9;0.00470;ABUW_RS08155,ABUW_RS08920,ABUW_RS10195,ABUW_RS12025,ABUW_RS17390
IPR020616	IPR	Thiolase, N-terminal	1; 5/ 9;0.00470;ABUW_RS08155,ABUW_RS08920,ABUW_RS10195,ABUW_RS12025,ABUW_RS17390
IPR039420	IPR	Transcriptional regulatory protein WalR-like	0; 5/13;0.03121;ABUW_RS04055,ABUW_RS07345,ABUW_RS07395,ABUW_RS08285,ABUW_RS17600
IPR033248	IPR	Transketolase, C-terminal domain	0; 2/ 4;0.03289;ABUW_RS10350,ABUW_RS14210
IPR038404	IPR	TRAP transporter solute receptor DctP superfamily	1; 3/ 4;0.00348;ABUW_RS00045,ABUW_RS00050,ABUW_RS01935
IPR018769	IPR	Type VI secretion system spike protein VgrG2, domain of unknown function DUF2345	1; 2/ 3;0.01223;ABUW_RS12710,ABUW_RS13685
IPR017847	IPR	Type VI secretion system, RhsGE-associated Vgr family subset	1; 2/ 3;0.01223;ABUW_RS12710,ABUW_RS13685
IPR006533	IPR	Type VI secretion system, RhsGE-associated Vgr protein	1; 2/ 3;0.01223;ABUW_RS12710,ABUW_RS13685
IPR006015	IPR	Universal stress protein A family	9; 2/ 2;0.00000;ABUW_RS04365,ABUW_RS08095
IPR006016	IPR	UspA	9; 2/ 2;0.00000;ABUW_RS04365,ABUW_RS08095
IPR037026	IPR	Vgr protein, OB-fold domain superfamily	1; 2/ 3;0.01223;ABUW_RS12710,ABUW_RS13685

ClassID	Class	Description	Single_list
00040 Pentose and glucuronate interconversions [PATH:ko00040]	KEGG	ko00040	0; 2/ 4;0.0262;ABUW_RS09375,ABUW_RS14515
00071 Fatty acid degradation [PATH:ko00071]	KEGG	ko00071	1; 6/11;0.0022;ABUW_RS05995,ABUW_RS07905,ABUW_RS08155,ABUW_RS10670,ABUW_RS14310,ABUW_RS17390
00350 Tyrosine metabolism [PATH:ko00350]	KEGG	ko00350	1; 2/ 3;0.0126;ABUW_RS09080,ABUW_RS10130
00362 Benzoate degradation [PATH:ko00362]	KEGG	ko00362	0; 8/21;0.0079;ABUW_RS08920,ABUW_RS08925,ABUW_RS08930,ABUW_RS08940,ABUW_RS08945,ABUW_RS08950,ABUW_RS09135,ABUW_RS09185
00500 Starch and sucrose metabolism [PATH:ko00500]	KEGG	ko00500	0; 2/ 4;0.0262;ABUW_RS15160,ABUW_RS15165
00620 Pyruvate metabolism [PATH:ko00620]	KEGG	ko00620	0; 7/22;0.0262;ABUW_RS03605,ABUW_RS11945,ABUW_RS13490,ABUW_RS16065,ABUW_RS16500,ABUW_RS16505,ABUW_RS16550
00630 Glyoxylate and dicarboxylate metabolism [PATH:ko00630]	KEGG	ko00630	0; 5/14;0.0262;ABUW_RS09445,ABUW_RS11345,ABUW_RS11855,ABUW_RS12185,ABUW_RS14935
00640 Propanoate metabolism [PATH:ko00640]	KEGG	ko00640	0; 6/13;0.0068;ABUW_RS03135,ABUW_RS10665,ABUW_RS17385,ABUW_RS18420,ABUW_RS18525,ABUW_RS18530
00650 Butanoate metabolism [PATH:ko00650]	KEGG	ko00650	1;10/23;0.0017;ABUW_RS00865,ABUW_RS07690,ABUW_RS10330,ABUW_RS10335,ABUW_RS10455,ABUW_RS12020,ABUW_RS14275,ABUW_RS14915,ABUW_RS15610,ABUW_RS18410
00660 C5-Branched dibasic acid metabolism [PATH:ko00660]	KEGG	ko00660	1; 2/ 3;0.0126;ABUW_RS16835,ABUW_RS16840
00910 Nitrogen metabolism [PATH:ko00910]	KEGG	ko00910	0; 3/ 7;0.0262;ABUW_RS08280,ABUW_RS08300,ABUW_RS08305
05133 Pertussis [PATH:ko05133]	KEGG	ko05133	9; 2/ 2;0.0000;ABUW_RS09975,ABUW_RS11245
4Fe-4S	KEYWORDS	keyword	0;13/ 46;4.1e-02;ABUW_RS03365,ABUW_RS04630,ABUW_RS08300,ABUW_RS08305,ABUW_RS08315,ABUW_RS08320,ABUW_RS09190,ABUW_RS12335,ABUW_RS12420,ABUW_RS16255,ABUW_RS16840,ABUW_RS17645,ABUW_RS18525
Acetoin catabolism	KEYWORDS	keyword	1; 2/ 3;1.3e-02;ABUW_RS10350,ABUW_RS10355
Acetylation	KEYWORDS	keyword	1; 3/ 4;5.6e-03;ABUW_RS00865,ABUW_RS07690,ABUW_RS18410
Acyltransferase	KEYWORDS	keyword	0;13/ 44;2.9e-02;ABUW_RS01245,ABUW_RS07195,ABUW_RS08155,ABUW_RS08920,ABUW_RS10345,ABUW_RS10455,ABUW_RS11655,ABUW_RS11750,ABUW_RS12025,ABUW_RS14750,ABUW_RS14830,ABUW_RS16505,ABUW_RS17390
Antioxidant	KEYWORDS	keyword	9; 2/ 2;0.0e+00;ABUW_RS01670,ABUW_RS03090
Aromatic hydrocarbons catabolism	KEYWORDS	keyword	2;15/ 27;9.9e-06;ABUW_RS08910,ABUW_RS08915,ABUW_RS08930,ABUW_RS08940,ABUW_RS09110,ABUW_RS09120,ABUW_RS09135,ABUW_RS09570,ABUW_RS11990,ABUW_RS11995,ABUW_RS12190,ABUW_RS13510,ABUW_RS14220,ABUW_RS14310,ABUW_RS16465
Cell membrane	KEYWORDS	keyword	0;32/115;5.6e-03;ABUW_RS00110,ABUW_RS00260,ABUW_RS00550,ABUW_RS01270,ABUW_RS01480,ABUW_RS01485,ABUW_RS02130,ABUW_RS03380,ABUW_RS04920,ABUW_RS05290,ABUW_RS07425,ABUW_RS07790,ABUW_RS07905,ABUW_RS08170,ABUW_RS08895,ABUW_RS08970,ABUW_RS09260,ABUW_RS09355,ABUW_RS09440,ABUW_RS10275,ABUW_RS10305,ABUW_RS11265,ABUW_RS11515,ABUW_RS11620,ABUW_RS11625,ABUW_RS12640,ABUW_RS14130,ABUW_RS14215,ABUW_RS14305,ABUW_RS16070,ABUW_RS16440,ABUW_RS17125
FAD	KEYWORDS	keyword	0;12/ 33;8.1e-03;ABUW_RS00630,ABUW_RS01835,ABUW_RS02975,ABUW_RS02980,ABUW_R

ClassID	Class	Description	Single_list
			S05995,ABUW_RS08405,ABUW_RS09620,ABUW_RS10660,ABUW_RS10665,ABUW_RS10875,ABUW_RS11970,ABUW_RS12005
Lipid biosynthesis	KEYWORDS	keyword	1; 2/ 3;1.3e-02;ABUW_RS07385,ABUW_RS10015
Lipid metabolism	KEYWORDS	keyword	1; 2/ 3;1.3e-02;ABUW_RS14290,ABUW_RS16035
NAD	KEYWORDS	keyword	0; 9/ 21;5.6e-03;ABUW_RS04615,ABUW_RS05435,ABUW_RS09445,ABUW_RS09630,ABUW_RS12145,ABUW_RS13495,ABUW_RS14285,ABUW_RS16100,ABUW_RS16670
Oxidoreductase	KEYWORDS	keyword	0; 8/ 20;1.2e-02;ABUW_RS03570,ABUW_RS09195,ABUW_RS10160,ABUW_RS11455,ABUW_RS11850,ABUW_RS13440,ABUW_RS14225,ABUW_RS18150
Plasmid	KEYWORDS	keyword	1; 3/ 4;5.6e-03;ABUW_RS02535,ABUW_RS10000,ABUW_RS14210
Reference proteome	KEYWORDS	keyword	0;24/ 86;1.2e-02;ABUW_RS03290,ABUW_RS03295,ABUW_RS03310,ABUW_RS04350,ABUW_RS04365,ABUW_RS05145,ABUW_RS05595,ABUW_RS07515,ABUW_RS07525,ABUW_RS08095,ABUW_RS08195,ABUW_RS09455,ABUW_RS10460,ABUW_RS10770,ABUW_RS12200,ABUW_RS12515,ABUW_RS12705,ABUW_RS12710,ABUW_RS12950,ABUW_RS13515,ABUW_RS13685,ABUW_RS14675,ABUW_RS15330,ABUW_RS15715
Transferase	KEYWORDS	keyword	9; 2/ 2;0.0e+00;ABUW_RS16890,ABUW_RS18530
operon_0013	operons	NZ_CP008706.1;ID=gene-ABUW_RS00110;Name=ABUW_RS00110;gbkey=Gene;gene_biotype=protein_coding;locus_tag=ABUW_RS00110;old_locus_tag=ABUW_0022	9; 2/ 2;0.0e+00;ABUW_RS00110,ABUW_RS00115
operon_0059	operons	NZ_CP008706.1;ID=gene-ABUW_RS00540;Name=ABUW_RS00540;gbkey=Gene;gene_biotype=protein_coding;locus_tag=ABUW_RS00540;old_locus_tag=ABUW_0109	1; 3/ 5;9.9e-03;ABUW_RS00540,ABUW_RS00550,ABUW_RS00555
operon_0112	operons	NZ_CP008706.1;ID=gene-ABUW_RS01015;Name=ABUW_RS01015;gbkey=Gene;gene_biotype=protein_coding;locus_tag=ABUW_RS01015;old_locus_tag=ABUW_0205	9; 2/ 2;0.0e+00;ABUW_RS01015,ABUW_RS01020
operon_0158	operons	NZ_CP008706.1;ID=gene-ABUW_RS01475;Name=ABUW_RS01475;gbkey=Gene;gene_biotype=protein_coding;locus_tag=ABUW_RS01475;old_locus_tag=ABUW_0300	1; 3/ 4;2.4e-03;ABUW_RS01480,ABUW_RS01485,ABUW_RS01490
operon_0168	operons	NZ_CP008706.1;ID=gene-ABUW_RS01595;Name=ABUW_RS01595;gbkey=Gene;gene_biotype=protein_coding;locus_tag=ABUW_RS01595;old_locus_tag=ABUW_0324	9; 2/ 2;0.0e+00;ABUW_RS01595,ABUW_RS01600
operon_0185	operons	NZ_CP008706.1;ID=gene-ABUW_RS01760;Name=ABUW_RS01760;gbkey=Gene;gene_biotype=protein_coding;locus_tag=ABUW_RS01760;old_locus_tag=ABUW_0359	1; 2/ 3;1.1e-02;ABUW_RS01760,ABUW_RS01765
operon_0211	operons	NZ_CP008706.1;ID=gene-ABUW_RS02150;Name=ABUW_RS02150;gbkey=Gene;gene_biotype=protein_coding;locus_tag=ABUW_RS02150;old_locus_tag=ABUW_0438	9; 2/ 2;0.0e+00;ABUW_RS02150,ABUW_RS02155
operon_0235	operons	NZ_CP008706.1;ID=gene-ABUW_RS02355;Name=ABUW_RS02355;gbkey=Gene;gene_biotype=protein_coding;locus_tag=ABUW_RS02355;old_locus_tag=ABUW_0479	1; 2/ 3;1.1e-02;ABUW_RS02355,ABUW_RS02360
operon_0279	operons	NZ_CP008706.1;ID=gene-ABUW_RS02970;Name=ABUW_RS02970;gbkey=Gene;gene_biotype=protein_coding;locus_tag=ABUW_RS02970;old_locus_tag=ABUW_0604	9; 2/ 2;0.0e+00;ABUW_RS02970,ABUW_RS02975
operon_0312	operons	NZ_CP008706.1;ID=gene-ABUW_RS03285;Name=ABUW_RS03285;gbkey=Gene;gene_biotype=protein_coding;locus_tag=ABUW_RS03285;old_locus_tag=ABUW_0667	9; 3/ 3;0.0e+00;ABUW_RS03285,ABUW_RS03290,ABUW_RS03295
operon_0317	operons	NZ_CP008706.1;ID=gene-ABUW_RS03365;Name=ABUW_RS03365;gbkey=Gene;gene_biotype=protein_coding;locus_tag=ABUW_RS03365;old_locus_tag=ABUW_0684	9; 2/ 2;0.0e+00;ABUW_RS03365,ABUW_RS03370
operon_0332	operons	NZ_CP008706.1;ID=gene-ABUW_RS03490;Name=ABUW_RS03490;gbkey=Gene;gene_biotype=protein_coding;locus_tag=ABUW_RS03490;old_locus_tag=ABUW_0709	9; 2/ 2;0.0e+00;ABUW_RS03490,ABUW_RS03495
operon_0347	operons	NZ_CP008706.1;ID=gene-ABUW_RS03650;Name=ABUW_RS03650;gbkey=Gene;gene_biotype=protein_coding;locus_tag=ABUW_RS03650;old_locus_tag=ABUW_0741	0; 2/ 4;3.3e-02;ABUW_RS03650,ABUW_RS03655
operon_0358	operons	NZ_CP008706.1;ID=gene-ABUW_RS03970;Name=ABUW_RS03970;gbkey=Gene;gene_biotype=protein_coding;locus_tag=ABUW_RS03970;old_locus_tag=ABUW_0811	1; 2/ 3;1.1e-02;ABUW_RS03975,ABUW_RS03980
operon_0393	operons	NZ_CP008706.1;ID=gene-ABUW_RS04345;Name=ABUW_RS04345;gbkey=Gene;gene_biotype=protein_coding;locus_tag=ABUW_RS04345;old_locus_tag=ABUW_0886	9; 3/ 3;0.0e+00;ABUW_RS04345,ABUW_RS04350,ABUW_RS19720
operon_0409	operons	NZ_CP008706.1;ID=gene-ABUW_RS04485;Name=ABUW_RS04485;gbkey=Gene;gene_biotype=protein_coding;locus_tag=ABUW_RS04485;old_locus_tag=ABUW_0914	9; 2/ 2;0.0e+00;ABUW_RS04485,ABUW_RS04490
operon_0426	operons	NZ_CP008706.1;ID=gene-ABUW_RS04610;Name=ABUW_RS04610;gbkey=Gene;gene_biotype=protein_coding;locus_tag=ABUW_RS04610;old_locus_tag=ABUW_0940	9; 2/ 2;0.0e+00;ABUW_RS04610,ABUW_RS04615
operon_0437	operons	NZ_CP008706.1;ID=gene-ABUW_RS04735;Name=ABUW_RS04735;gbkey=Gene;gene_biot	1; 3/ 4;2.4e-03;ABUW_RS04740,ABUW_RS04745,ABUW_RS04750

ClassID	Class	Description	Single_list
		ype=protein_coding;locus_tag=ABUW_RS04735;old_locus_tag=ABUW_0965	
operon_0446	operons	NZ_CP008706.1;ID=gene-ABUW_RS04825;Name=rbtA;gbkey=Gene;gene=rbtA;gene_biotype=protein_coding;locus_tag=ABUW_RS04825;old_locus_tag=ABUW_0984	9; 2/ 2;0.0e+00;ABUW_RS04825,ABUW_RS04830
operon_0447	operons	NZ_CP008706.1;ID=gene-ABUW_RS04835;Name=ABUW_RS04835;gbkey=Gene;gene_biotype=protein_coding;locus_tag=ABUW_RS04835;old_locus_tag=ABUW_0986	9; 3/ 3;0.0e+00;ABUW_RS04835,ABUW_RS04840,ABUW_RS04845
operon_0454	operons	NZ_CP008706.1;ID=gene-ABUW_RS04930;Name=ABUW_RS04930;gbkey=Gene;gene_biotype=protein_coding;locus_tag=ABUW_RS04930;old_locus_tag=ABUW_1005	9; 2/ 2;0.0e+00;ABUW_RS04930,ABUW_RS20695
operon_0474	operons	NZ_CP008706.1;ID=gene-ABUW_RS05155;Name=ABUW_RS05155;gbkey=Gene;gene_biotype=protein_coding;locus_tag=ABUW_RS05155;old_locus_tag=ABUW_1050	1; 2/ 3;1.1e-02;ABUW_RS05160,ABUW_RS05165
operon_0479	operons	NZ_CP008706.1;ID=gene-ABUW_RS05205;Name=ABUW_RS05205;gbkey=Gene;gene_biotype=protein_coding;locus_tag=ABUW_RS05205;old_locus_tag=ABUW_1060	9; 2/ 2;0.0e+00;ABUW_RS05205,ABUW_RS05210
operon_0480	operons	NZ_CP008706.1;ID=gene-ABUW_RS05215;Name=ABUW_RS05215;gbkey=Gene;gene_biotype=protein_coding;locus_tag=ABUW_RS05215;old_locus_tag=ABUW_1062	2; 4/ 5;5.5e-04;ABUW_RS05220,ABUW_RS05225,ABUW_RS05230,ABUW_RS05235
operon_0514	operons	NZ_CP008706.1;ID=gene-ABUW_RS05590;Name=ABUW_RS05590;gbkey=Gene;gene_biotype=protein_coding;locus_tag=ABUW_RS05590;old_locus_tag=ABUW_1142	9; 2/ 2;0.0e+00;ABUW_RS05590,ABUW_RS05595
operon_0542	operons	NZ_CP008706.1;ID=gene-ABUW_RS05840;Name=xdhA;gbkey=Gene;gene=xdhA;gene_biotype=protein_coding;locus_tag=ABUW_RS05840;old_locus_tag=ABUW_1196	9; 3/ 3;0.0e+00;ABUW_RS05840,ABUW_RS05845,ABUW_RS05850
operon_0554	operons	NZ_CP008706.1;ID=gene-ABUW_RS05990;Name=ABUW_RS05990;gbkey=Gene;gene_biotype=protein_coding;locus_tag=ABUW_RS05990;old_locus_tag=ABUW_1226	9; 2/ 2;0.0e+00;ABUW_RS05990,ABUW_RS05995
operon_0588	operons	NZ_CP008706.1;ID=gene-ABUW_RS06530;Name=ABUW_RS06530;gbkey=Gene;gene_biotype=protein_coding;locus_tag=ABUW_RS06530;old_locus_tag=ABUW_1339	1; 2/ 3;1.1e-02;ABUW_RS06530,ABUW_RS06535
operon_0629	operons	NZ_CP008706.1;ID=gene-ABUW_RS07150;Name=ABUW_RS07150;gbkey=Gene;gene_biotype=protein_coding;locus_tag=ABUW_RS07150;old_locus_tag=ABUW_1467	9; 4/ 4;0.0e+00;ABUW_RS07150,ABUW_RS07155,ABUW_RS07160,ABUW_RS07165
operon_0642	operons	NZ_CP008706.1;ID=gene-ABUW_RS07250;Name=csuAB;gbkey=Gene;gene=csuAB;gene_biotype=protein_coding;locus_tag=ABUW_RS07250;old_locus_tag=ABUW_1487	1; 4/ 6;2.4e-03;ABUW_RS07250,ABUW_RS07260,ABUW_RS07265,ABUW_RS07275
operon_0650	operons	NZ_CP008706.1;ID=gene-ABUW_RS07345;Name=ABUW_RS07345;gbkey=Gene;gene_biotype=protein_coding;locus_tag=ABUW_RS07345;old_locus_tag=ABUW_1506	0; 4/10;3.9e-02;ABUW_RS07345,ABUW_RS07380,ABUW_RS07385,ABUW_RS07390
operon_0655	operons	NZ_CP008706.1;ID=gene-ABUW_RS07425;Name=ABUW_RS07425;gbkey=Gene;gene_biotype=protein_coding;locus_tag=ABUW_RS07425;old_locus_tag=ABUW_1521	9; 2/ 2;0.0e+00;ABUW_RS07425,ABUW_RS07430
operon_0667	operons	NZ_CP008706.1;ID=gene-ABUW_RS07515;Name=ABUW_RS07515;gbkey=Gene;gene_biotype=protein_coding;locus_tag=ABUW_RS07515;old_locus_tag=ABUW_1540	9; 4/ 4;0.0e+00;ABUW_RS07515,ABUW_RS07520,ABUW_RS07525,ABUW_RS07530
operon_0691	operons	NZ_CP008706.1;ID=gene-ABUW_RS07785;Name=ABUW_RS07785;gbkey=Gene;gene_biotype=protein_coding;locus_tag=ABUW_RS07785;old_locus_tag=ABUW_1594	9; 2/ 2;0.0e+00;ABUW_RS07785,ABUW_RS07790
operon_0697	operons	NZ_CP008706.1;ID=gene-ABUW_RS07820;Name=ABUW_RS07820;gbkey=Gene;gene_biotype=protein_coding;locus_tag=ABUW_RS07820;old_locus_tag=ABUW_1601	9; 2/ 2;0.0e+00;ABUW_RS07820,ABUW_RS07825
operon_0705	operons	NZ_CP008706.1;ID=gene-ABUW_RS07895;Name=eutC;gbkey=Gene;gene=eutC;gene_biotype=protein_coding;locus_tag=ABUW_RS07895;old_locus_tag=ABUW_1618	9; 3/ 3;0.0e+00;ABUW_RS07895,ABUW_RS07900,ABUW_RS07905
operon_0714	operons	NZ_CP008706.1;ID=gene-ABUW_RS07960;Name=ABUW_RS07960;gbkey=Gene;gene_biotype=protein_coding;locus_tag=ABUW_RS07960;old_locus_tag=ABUW_1631	9; 4/ 4;0.0e+00;ABUW_RS07960,ABUW_RS07965,ABUW_RS07970,ABUW_RS07975
operon_0715	operons	NZ_CP008706.1;ID=gene-ABUW_RS07980;Name=ABUW_RS07980;gbkey=Gene;gene_biotype=protein_coding;locus_tag=ABUW_RS07980;old_locus_tag=ABUW_1635	1; 3/ 4;2.4e-03;ABUW_RS07980,ABUW_RS07985,ABUW_RS07990
operon_0742	operons	NZ_CP008706.1;ID=gene-ABUW_RS08160;Name=ABUW_RS08160;gbkey=Gene;gene_biotype=protein_coding;locus_tag=ABUW_RS08160;old_locus_tag=ABUW_1675	9; 3/ 3;0.0e+00;ABUW_RS08160,ABUW_RS08165,ABUW_RS08170
operon_0757	operons	NZ_CP008706.1;ID=gene-ABUW_RS08280;Name=ABUW_RS08280;gbkey=Gene;gene_biotype=protein_coding;locus_tag=ABUW_RS08280;old_locus_tag=ABUW_1701	9; 2/ 2;0.0e+00;ABUW_RS08280,ABUW_RS08285
operon_0758	operons	NZ_CP008706.1;ID=gene-ABUW_RS08290;Name=ABUW_RS08290;gbkey=Gene;gene_biotype=protein_coding;locus_tag=ABUW_RS08290;old_locus_tag=ABUW_1703	1; 4/ 6;2.4e-03;ABUW_RS08300,ABUW_RS08305,ABUW_RS08310,ABUW_RS08315

ClassID	Class	Description	Single_list
operon_0778	operons	NZ_CP008706.1;ID=gene-ABUW_RS08530;Name=ABUW_RS08530;gbkey=Gene;gene_biotype=protein_coding;locus_tag=ABUW_RS08530;old_locus_tag=ABUW_1751	9; 3/ 3;0.0e+00;ABUW_RS08530,ABUW_RS08535,ABUW_RS08540
operon_0803	operons	NZ_CP008706.1;ID=gene-ABUW_RS08700;Name=ABUW_RS08700;gbkey=Gene;gene_biotype=protein_coding;locus_tag=ABUW_RS08700;old_locus_tag=ABUW_1787	1; 2/ 3;1.1e-02;ABUW_RS08700,ABUW_RS08705
operon_0822	operons	NZ_CP008706.1;ID=gene-ABUW_RS08910;Name=ABUW_RS08910;gbkey=Gene;gene_biotype=protein_coding;locus_tag=ABUW_RS08910;old_locus_tag=ABUW_1831	8;12/13;1.4e-09;ABUW_RS08910,ABUW_RS08915,ABUW_RS08920,ABUW_RS08925,ABUW_RS08930,ABUW_RS08935,ABUW_RS08940,ABUW_RS08945,ABUW_RS08950,ABUW_RS08960,ABUW_RS08965,ABUW_RS08970
operon_0823	operons	NZ_CP008706.1;ID=gene-ABUW_RS08975;Name=ABUW_RS08975;gbkey=Gene;gene_biotype=protein_coding;locus_tag=ABUW_RS08975;old_locus_tag=ABUW_1844	0; 2/ 4;3.3e-02;ABUW_RS08985,ABUW_RS08990
operon_0828	operons	NZ_CP008706.1;ID=gene-ABUW_RS09040;Name=ABUW_RS09040;gbkey=Gene;gene_biotype=protein_coding;locus_tag=ABUW_RS09040;old_locus_tag=ABUW_1857	3; 7/ 9;3.4e-05;ABUW_RS09045,ABUW_RS09050,ABUW_RS09055,ABUW_RS09065,ABUW_RS09070,ABUW_RS09075,ABUW_RS09080
operon_0840	operons	NZ_CP008706.1;ID=gene-ABUW_RS09190;Name=ABUW_RS09190;gbkey=Gene;gene_biotype=protein_coding;locus_tag=ABUW_RS09190;old_locus_tag=ABUW_1887	9; 2/ 2;0.0e+00;ABUW_RS09190,ABUW_RS09195
operon_0846	operons	NZ_CP008706.1;ID=gene-ABUW_RS09240;Name=ABUW_RS09240;gbkey=Gene;gene_biotype=protein_coding;locus_tag=ABUW_RS09240;old_locus_tag=ABUW_1897	0; 2/ 4;3.3e-02;ABUW_RS09250,ABUW_RS09255
operon_0847	operons	NZ_CP008706.1;ID=gene-ABUW_RS09260;Name=ABUW_RS09260;gbkey=Gene;gene_biotype=protein_coding;locus_tag=ABUW_RS09260;old_locus_tag=ABUW_1902	9; 2/ 2;0.0e+00;ABUW_RS09260,ABUW_RS09265
operon_0848	operons	NZ_CP008706.1;ID=gene-ABUW_RS09270;Name=ABUW_RS09270;gbkey=Gene;gene_biotype=protein_coding;locus_tag=ABUW_RS09270;old_locus_tag=ABUW_1904	9; 2/ 2;0.0e+00;ABUW_RS09270,ABUW_RS09275
operon_0867	operons	NZ_CP008706.1;ID=gene-ABUW_RS09435;Name=denD;gbkey=Gene;gene=denD;gene_biotype=protein_coding;locus_tag=ABUW_RS09435;old_locus_tag=ABUW_1937	1; 2/ 3;1.1e-02;ABUW_RS09440,ABUW_RS09445
operon_0868	operons	NZ_CP008706.1;ID=gene-ABUW_RS09450;Name=ABUW_RS09450;gbkey=Gene;gene_biotype=protein_coding;locus_tag=ABUW_RS09450;old_locus_tag=ABUW_1942	0; 2/ 4;3.3e-02;ABUW_RS09450,ABUW_RS09455
operon_0870	operons	NZ_CP008706.1;ID=gene-ABUW_RS09470;Name=ABUW_RS09470;gbkey=Gene;gene_biotype=protein_coding;locus_tag=ABUW_RS09470;old_locus_tag=ABUW_1947	9; 2/ 2;0.0e+00;ABUW_RS09470,ABUW_RS09475
operon_0871	operons	NZ_CP008706.1;ID=gene-ABUW_RS09480;Name=ABUW_RS09480;gbkey=Gene;gene_biotype=protein_coding;locus_tag=ABUW_RS09480;old_locus_tag=ABUW_1949	9; 2/ 2;0.0e+00;ABUW_RS09480,ABUW_RS09485
operon_0872	operons	NZ_CP008706.1;ID=gene-ABUW_RS09490;Name=ABUW_RS09490;gbkey=Gene;gene_biotype=protein_coding;locus_tag=ABUW_RS09490;old_locus_tag=ABUW_1951	9; 3/ 3;0.0e+00;ABUW_RS09490,ABUW_RS09495,ABUW_RS09500
operon_0881	operons	NZ_CP008706.1;ID=gene-ABUW_RS09565;Name=ABUW_RS09565;gbkey=Gene;gene_biotype=protein_coding;locus_tag=ABUW_RS09565;old_locus_tag=ABUW_1967	1; 2/ 3;1.1e-02;ABUW_RS09570,ABUW_RS09575
operon_0885	operons	NZ_CP008706.1;ID=gene-ABUW_RS09615;Name=ABUW_RS09615;gbkey=Gene;gene_biotype=protein_coding;locus_tag=ABUW_RS09615;old_locus_tag=ABUW_1977	9; 2/ 2;0.0e+00;ABUW_RS09615,ABUW_RS09620
operon_0887	operons	NZ_CP008706.1;ID=gene-ABUW_RS09630;Name=ABUW_RS09630;gbkey=Gene;gene_biotype=protein_coding;locus_tag=ABUW_RS09630;old_locus_tag=ABUW_1980	9; 3/ 3;0.0e+00;ABUW_RS09630,ABUW_RS09635,ABUW_RS09640
operon_0917	operons	NZ_CP008706.1;ID=gene-ABUW_RS09965;Name=ABUW_RS09965;gbkey=Gene;gene_biotype=protein_coding;locus_tag=ABUW_RS09965;old_locus_tag=ABUW_2052	2; 4/ 5;5.5e-04;ABUW_RS09965,ABUW_RS09970,ABUW_RS09975,ABUW_RS09985
operon_0941	operons	NZ_CP008706.1;ID=gene-ABUW_RS10180;Name=ABUW_RS10180;gbkey=Gene;gene_biotype=protein_coding;locus_tag=ABUW_RS10180;old_locus_tag=ABUW_2096	0; 2/ 4;3.3e-02;ABUW_RS10190,ABUW_RS10195
operon_0955	operons	NZ_CP008706.1;ID=gene-ABUW_RS10310;Name=ABUW_RS10310;gbkey=Gene;gene_biotype=protein_coding;locus_tag=ABUW_RS10310;old_locus_tag=ABUW_2122	9; 2/ 2;0.0e+00;ABUW_RS10310,ABUW_RS10315
operon_0957	operons	NZ_CP008706.1;ID=gene-ABUW_RS10330;Name=ABUW_RS10330;gbkey=Gene;gene_biotype=protein_coding;locus_tag=ABUW_RS10330;old_locus_tag=ABUW_2126	9; 6/ 6;0.0e+00;ABUW_RS10330,ABUW_RS10335,ABUW_RS10340,ABUW_RS10345,ABUW_RS10350,ABUW_RS10355
operon_0974	operons	NZ_CP008706.1;ID=gene-ABUW_RS10475;Name=ABUW_RS10475;gbkey=Gene;gene_biotype=protein_coding;locus_tag=ABUW_RS10475;old_locus_tag=ABUW_2156	9; 2/ 2;0.0e+00;ABUW_RS10475,ABUW_RS10480
operon_0986	operons	NZ_CP008706.1;ID=gene-ABUW_RS10660;Name=ABUW_RS10660;gbkey=Gene;gene_biotype=protein_coding;locus_tag=ABUW_RS10660;old_locus_tag=ABUW_2193	9; 2/ 2;0.0e+00;ABUW_RS10660,ABUW_RS10665
operon_0994	operons	NZ_CP008706.1;ID=gene-ABUW_RS10760;Name=ABUW_RS10760;gbkey=Gene;gene_biot	9; 3/ 3;0.0e+00;ABUW_RS10760,ABUW_RS10765,ABUW_RS10770

ClassID	Class	Description	Single_list
		ype=protein_coding;locus_tag=ABUW_RS10760;old_locus_tag=ABUW_2213	
operon_1004	operons	NZ_CP008706.1;ID=gene-ABUW_RS10890;Name=ABUW_RS10890;gbkey=Gene;gene_biotype=protein_coding;locus_tag=ABUW_RS10890;old_locus_tag=ABUW_2240	9; 2/ 2;0.0e+00;ABUW_RS10890,ABUW_RS10895
operon_1036	operons	NZ_CP008706.1;ID=gene-ABUW_RS11265;Name=ABUW_RS11265;gbkey=Gene;gene_biotype=protein_coding;locus_tag=ABUW_RS11265;old_locus_tag=ABUW_2316	9; 2/ 2;0.0e+00;ABUW_RS11265,ABUW_RS11270
operon_1048	operons	NZ_CP008706.1;ID=gene-ABUW_RS11330;Name=ABUW_RS11330;gbkey=Gene;gene_biotype=protein_coding;locus_tag=ABUW_RS11330;old_locus_tag=ABUW_2330	9; 4/ 4;0.0e+00;ABUW_RS11330,ABUW_RS11335,ABUW_RS11340,ABUW_RS11345
operon_1056	operons	NZ_CP008706.1;ID=gene-ABUW_RS11445;Name=ABUW_RS11445;gbkey=Gene;gene_biotype=protein_coding;locus_tag=ABUW_RS11445;old_locus_tag=ABUW_2353	1; 3/ 4;2.4e-03;ABUW_RS11450,ABUW_RS11455,ABUW_RS11460
operon_1062	operons	NZ_CP008706.1;ID=gene-ABUW_RS11510;Name=ABUW_RS11510;gbkey=Gene;gene_biotype=protein_coding;locus_tag=ABUW_RS11510;old_locus_tag=ABUW_2366	9; 2/ 2;0.0e+00;ABUW_RS11510,ABUW_RS11515
operon_1066	operons	NZ_CP008706.1;ID=gene-ABUW_RS11540;Name=ABUW_RS11540;gbkey=Gene;gene_biotype=protein_coding;locus_tag=ABUW_RS11540;old_locus_tag=ABUW_2372	9; 2/ 2;0.0e+00;ABUW_RS11540,ABUW_RS11545
operon_1076	operons	NZ_CP008706.1;ID=gene-ABUW_RS11620;Name=ABUW_RS11620;gbkey=Gene;gene_biotype=protein_coding;locus_tag=ABUW_RS11620;old_locus_tag=ABUW_2389	1; 3/ 5;9.9e-03;ABUW_RS11620,ABUW_RS11625,ABUW_RS20205
operon_1077	operons	NZ_CP008706.1;ID=gene-ABUW_RS11645;Name=madM;gbkey=Gene;gene=madM;gene_biotype=protein_coding;locus_tag=ABUW_RS11645;old_locus_tag=ABUW_2394	2; 6/ 9;5.5e-04;ABUW_RS11645,ABUW_RS11650,ABUW_RS11655,ABUW_RS11665,ABUW_RS11680,ABUW_RS11685
operon_1082	operons	NZ_CP008706.1;ID=gene-ABUW_RS11720;Name=ABUW_RS11720;gbkey=Gene;gene_biotype=protein_coding;locus_tag=ABUW_RS11720;old_locus_tag=ABUW_2409	1; 2/ 3;1.1e-02;ABUW_RS11725,ABUW_RS11730
operon_1085	operons	NZ_CP008706.1;ID=gene-ABUW_RS11745;Name=ABUW_RS11745;gbkey=Gene;gene_biotype=protein_coding;locus_tag=ABUW_RS11745;old_locus_tag=ABUW_2414	9; 2/ 2;0.0e+00;ABUW_RS11745,ABUW_RS11750
operon_1091	operons	NZ_CP008706.1;ID=gene-ABUW_RS11800;Name=ABUW_RS11800;gbkey=Gene;gene_biotype=protein_coding;locus_tag=ABUW_RS11800;old_locus_tag=ABUW_2425	9; 3/ 3;0.0e+00;ABUW_RS11800,ABUW_RS11805,ABUW_RS11810
operon_1099	operons	NZ_CP008706.1;ID=gene-ABUW_RS11855;Name=katE;gbkey=Gene;gene=katE;gene_biotype=protein_coding;locus_tag=ABUW_RS11855;old_locus_tag=ABUW_2436	9; 2/ 2;0.0e+00;ABUW_RS11855,ABUW_RS11860
operon_1101	operons	NZ_CP008706.1;ID=gene-ABUW_RS11870;Name=ABUW_RS11870;gbkey=Gene;gene_biotype=protein_coding;locus_tag=ABUW_RS11870;old_locus_tag=ABUW_2439	9; 2/ 2;0.0e+00;ABUW_RS11870,ABUW_RS11875
operon_1102	operons	NZ_CP008706.1;ID=gene-ABUW_RS11880;Name=ABUW_RS11880;gbkey=Gene;gene_biotype=protein_coding;locus_tag=ABUW_RS11880;old_locus_tag=ABUW_2441	9; 2/ 2;0.0e+00;ABUW_RS11880,ABUW_RS11885
operon_1108	operons	NZ_CP008706.1;ID=gene-ABUW_RS11915;Name=ABUW_RS11915;gbkey=Gene;gene_biotype=protein_coding;locus_tag=ABUW_RS11915;old_locus_tag=ABUW_2449	1; 2/ 3;1.1e-02;ABUW_RS11915,ABUW_RS11920
operon_1115	operons	NZ_CP008706.1;ID=gene-ABUW_RS11980;Name=ABUW_RS11980;gbkey=Gene;gene_biotype=protein_coding;locus_tag=ABUW_RS11980;old_locus_tag=ABUW_2462	3; 5/ 6;1.1e-04;ABUW_RS11985,ABUW_RS11990,ABUW_RS11995,ABUW_RS12000,ABUW_RS12005
operon_1129	operons	NZ_CP008706.1;ID=gene-ABUW_RS12180;Name=ABUW_RS12180;gbkey=Gene;gene_biotype=protein_coding;locus_tag=ABUW_RS12180;old_locus_tag=ABUW_2503	9; 2/ 2;0.0e+00;ABUW_RS12180,ABUW_RS12185
operon_1130	operons	NZ_CP008706.1;ID=gene-ABUW_RS12190;Name=ABUW_RS12190;gbkey=Gene;gene_biotype=protein_coding;locus_tag=ABUW_RS12190;old_locus_tag=ABUW_2505	9; 4/ 4;0.0e+00;ABUW_RS12190,ABUW_RS12195,ABUW_RS12200,ABUW_RS12205
operon_1159	operons	NZ_CP008706.1;ID=gene-ABUW_RS12485;Name=ABUW_RS12485;gbkey=Gene;gene_biotype=protein_coding;locus_tag=ABUW_RS12485;old_locus_tag=ABUW_2570	0; 5/11;1.5e-02;ABUW_RS12515,ABUW_RS12520,ABUW_RS12525,ABUW_RS12530,ABUW_RS12535
operon_1169	operons	NZ_CP008706.1;ID=gene-ABUW_RS12630;Name=ABUW_RS12630;gbkey=Gene;gene_biotype=protein_coding;locus_tag=ABUW_RS12630;old_locus_tag=ABUW_2600	1; 3/ 4;2.4e-03;ABUW_RS12630,ABUW_RS12635,ABUW_RS12640
operon_1174	operons	NZ_CP008706.1;ID=gene-ABUW_RS12700;Name=ABUW_RS12700;gbkey=Gene;gene_biotype=protein_coding;locus_tag=ABUW_RS12700;old_locus_tag=ABUW_2616	9; 3/ 3;0.0e+00;ABUW_RS12700,ABUW_RS12705,ABUW_RS12710
operon_1175	operons	NZ_CP008706.1;ID=gene-ABUW_RS12715;Name=ABUW_RS12715;gbkey=Gene;gene_biotype=protein_coding;locus_tag=ABUW_RS12715;old_locus_tag=ABUW_2619	9; 2/ 2;0.0e+00;ABUW_RS12715,ABUW_RS12720
operon_1207	operons	NZ_CP008706.1;ID=gene-ABUW_RS13030;Name=ABUW_RS13030;gbkey=Gene;gene_biotype=protein_coding;locus_tag=ABUW_RS13030;old_locus_tag=ABUW_2684	9; 2/ 2;0.0e+00;ABUW_RS13030,ABUW_RS13035

ClassID	Class	Description	Single_list
operon_1218	operons	NZ_CP008706.1;ID=gene-ABUW_RS13095;Name=xseA;gbkey=Gene;gene=xseA;gene_biotype=protein_coding;locus_tag=ABUW_RS13095;old_locus_tag=ABUW_2698	9; 2/ 2;0.0e+00;ABUW_RS13095,ABUW_RS13100
operon_1219	operons	NZ_CP008706.1;ID=gene-ABUW_RS13105;Name=ABUW_RS13105;gbkey=Gene;gene_biotype=protein_coding;locus_tag=ABUW_RS13105;old_locus_tag=ABUW_2700	9; 2/ 2;0.0e+00;ABUW_RS13105,ABUW_RS13110
operon_1227	operons	NZ_CP008706.1;ID=gene-ABUW_RS13175;Name=ABUW_RS13175;gbkey=Gene;gene_biotype=protein_coding;locus_tag=ABUW_RS13175;old_locus_tag=ABUW_2715	9; 2/ 2;0.0e+00;ABUW_RS13175,ABUW_RS13180
operon_1261	operons	NZ_CP008706.1;ID=gene-ABUW_RS13435;Name=ABUW_RS13435;gbkey=Gene;gene_biotype=protein_coding;locus_tag=ABUW_RS13435;old_locus_tag=ABUW_2767	0; 2/ 4;3.3e-02;ABUW_RS13440,ABUW_RS13450
operon_1265	operons	NZ_CP008706.1;ID=gene-ABUW_RS13490;Name=ABUW_RS13490;gbkey=Gene;gene_biotype=protein_coding;locus_tag=ABUW_RS13490;old_locus_tag=ABUW_2778	9; 8/ 8;0.0e+00;ABUW_RS13490,ABUW_RS13495,ABUW_RS13500,ABUW_RS13505,ABUW_RS13510,ABUW_RS13515,ABUW_RS13520,ABUW_RS13525
operon_1273	operons	NZ_CP008706.1;ID=gene-ABUW_RS13580;Name=ABUW_RS13580;gbkey=Gene;gene_biotype=protein_coding;locus_tag=ABUW_RS13580;old_locus_tag=ABUW_2796	9; 2/ 2;0.0e+00;ABUW_RS13580,ABUW_RS13585
operon_1292	operons	NZ_CP008706.1;ID=gene-ABUW_RS13750;Name=ABUW_RS13750;gbkey=Gene;gene_biotype=protein_coding;locus_tag=ABUW_RS13750;old_locus_tag=ABUW_2829	1; 2/ 3;1.1e-02;ABUW_RS13755,ABUW_RS13760
operon_1308	operons	NZ_CP008706.1;ID=gene-ABUW_RS13905;Name=ABUW_RS13905;gbkey=Gene;gene_biotype=protein_coding;locus_tag=ABUW_RS13905;old_locus_tag=ABUW_2860	1; 2/ 3;1.1e-02;ABUW_RS13910,ABUW_RS20270
operon_1317	operons	NZ_CP008706.1;ID=gene-ABUW_RS13980;Name=ABUW_RS13980;gbkey=Gene;gene_biotype=protein_coding;locus_tag=ABUW_RS13980;old_locus_tag=ABUW_2878	1; 5/ 8;2.1e-03;ABUW_RS13980,ABUW_RS13990,ABUW_RS13995,ABUW_RS14015,ABUW_RS20660
operon_1335	operons	NZ_CP008706.1;ID=gene-ABUW_RS14130;Name=ABUW_RS14130;gbkey=Gene;gene_biotype=protein_coding;locus_tag=ABUW_RS14130;old_locus_tag=ABUW_2910	9; 2/ 2;0.0e+00;ABUW_RS14130,ABUW_RS14135
operon_1347	operons	NZ_CP008706.1;ID=gene-ABUW_RS14210;Name=ABUW_RS14210;gbkey=Gene;gene_biotype=protein_coding;locus_tag=ABUW_RS14210;old_locus_tag=ABUW_2927	9; 4/ 4;0.0e+00;ABUW_RS14210,ABUW_RS14215,ABUW_RS14220,ABUW_RS14225
operon_1357	operons	NZ_CP008706.1;ID=gene-ABUW_RS14275;Name=ABUW_RS14275;gbkey=Gene;gene_biotype=protein_coding;locus_tag=ABUW_RS14275;old_locus_tag=ABUW_2941	1; 7/13;2.1e-03;ABUW_RS14275,ABUW_RS14285,ABUW_RS14290,ABUW_RS14295,ABUW_RS14300,ABUW_RS14305,ABUW_RS14310
operon_1401	operons	NZ_CP008706.1;ID=gene-ABUW_RS14745;Name=ABUW_RS14745;gbkey=Gene;gene_biotype=protein_coding;locus_tag=ABUW_RS14745;old_locus_tag=ABUW_3038	0; 2/ 4;3.3e-02;ABUW_RS14750,ABUW_RS14760
operon_1417	operons	NZ_CP008706.1;ID=gene-ABUW_RS14910;Name=cntB;gbkey=Gene;gene=cntB;gene_biotype=protein_coding;locus_tag=ABUW_RS14910;old_locus_tag=ABUW_3072	3; 5/ 6;1.1e-04;ABUW_RS14910,ABUW_RS14915,ABUW_RS14920,ABUW_RS14925,ABUW_RS14935
operon_1437	operons	NZ_CP008706.1;ID=gene-ABUW_RS15160;Name=otsB;gbkey=Gene;gene=otsB;gene_biotype=protein_coding;locus_tag=ABUW_RS15160;old_locus_tag=ABUW_3122	9; 2/ 2;0.0e+00;ABUW_RS15160,ABUW_RS15165
operon_1446	operons	NZ_CP008706.1;ID=gene-ABUW_RS15235;Name=ABUW_RS15235;gbkey=Gene;gene_biotype=protein_coding;locus_tag=ABUW_RS15235;old_locus_tag=ABUW_3138	9; 3/ 3;0.0e+00;ABUW_RS15235,ABUW_RS15240,ABUW_RS15245
operon_1455	operons	NZ_CP008706.1;ID=gene-ABUW_RS15330;Name=ABUW_RS15330;gbkey=Gene;gene_biotype=protein_coding;locus_tag=ABUW_RS15330;old_locus_tag=ABUW_3157	9; 2/ 2;0.0e+00;ABUW_RS15330,ABUW_RS20305
operon_1477	operons	NZ_CP008706.1;ID=gene-ABUW_RS15550;Name=ABUW_RS15550;gbkey=Gene;gene_biotype=protein_coding;locus_tag=ABUW_RS15550;old_locus_tag=ABUW_3204	9; 2/ 2;0.0e+00;ABUW_RS15550,ABUW_RS15555
operon_1490	operons	NZ_CP008706.1;ID=gene-ABUW_RS15730;Name=ABUW_RS15730;gbkey=Gene;gene_biotype=protein_coding;locus_tag=ABUW_RS15730;old_locus_tag=ABUW_3240	0; 2/ 4;3.3e-02;ABUW_RS15730,ABUW_RS15745
operon_1519	operons	NZ_CP008706.1;ID=gene-ABUW_RS16060;Name=ABUW_RS16060;gbkey=Gene;gene_biotype=protein_coding;locus_tag=ABUW_RS16060;old_locus_tag=ABUW_3306	1; 3/ 5;9.9e-03;ABUW_RS16065,ABUW_RS16070,ABUW_RS16075
operon_1521	operons	NZ_CP008706.1;ID=gene-ABUW_RS16090;Name=ABUW_RS16090;gbkey=Gene;gene_biotype=protein_coding;locus_tag=ABUW_RS16090;old_locus_tag=ABUW_3312	9; 3/ 3;0.0e+00;ABUW_RS16090,ABUW_RS16095,ABUW_RS16100
operon_1524	operons	NZ_CP008706.1;ID=gene-ABUW_RS16130;Name=ABUW_RS16130;gbkey=Gene;gene_biotype=protein_coding;locus_tag=ABUW_RS16130;old_locus_tag=ABUW_3320	9; 3/ 3;0.0e+00;ABUW_RS16130,ABUW_RS16135,ABUW_RS16140
operon_1559	operons	NZ_CP008706.1;ID=gene-ABUW_RS16500;Name=ABUW_RS16500;gbkey=Gene;gene_biotype=protein_coding;locus_tag=ABUW_RS16500;old_locus_tag=ABUW_3395	9; 2/ 2;0.0e+00;ABUW_RS16500,ABUW_RS16505
operon_1588	operons	NZ_CP008706.1;ID=gene-ABUW_RS16825;Name=leuB;gbkey=Gene;gene=leuB;gene_bioty	0; 2/ 4;3.3e-02;ABUW_RS16835,ABUW_RS16840

ClassID	Class	Description	Single_list
		pe=protein_coding;locus_tag=ABUW_RS16825;old_locus_tag=ABUW_3460	
operon_1618	operons	NZ_CP008706.1;ID=gene-ABUW_RS17100;Name=ABUW_RS17100;gbkey=Gene;gene_biotype=protein_coding;locus_tag=ABUW_RS17100;old_locus_tag=ABUW_3515	9; 2/ 2;0.0e+00;ABUW_RS17100,ABUW_RS17105
operon_1638	operons	NZ_CP008706.1;ID=gene-ABUW_RS17385;Name=fadB;gbkey=Gene;gene=fadB;gene_biotype=protein_coding;locus_tag=ABUW_RS17385;old_locus_tag=ABUW_3572	9; 2/ 2;0.0e+00;ABUW_RS17385,ABUW_RS17390
operon_1681	operons	NZ_CP008706.1;ID=gene-ABUW_RS17925;Name=ABUW_RS17925;gbkey=Gene;gene_biotype=protein_coding;locus_tag=ABUW_RS17925;old_locus_tag=ABUW_3681	9; 2/ 2;0.0e+00;ABUW_RS17925,ABUW_RS17930
operon_1727	operons	NZ_CP008706.1;ID=gene-ABUW_RS18390;Name=ABUW_RS18390;gbkey=Gene;gene_biotype=protein_coding;locus_tag=ABUW_RS18390;old_locus_tag=ABUW_3777	0; 3/ 7;3.9e-02;ABUW_RS18390,ABUW_RS18410,ABUW_RS18420
operon_1735	operons	NZ_CP008706.1;ID=gene-ABUW_RS18470;Name=ABUW_RS18470;gbkey=Gene;gene_biotype=protein_coding;locus_tag=ABUW_RS18470;old_locus_tag=ABUW_3793	1; 3/ 4;2.4e-03;ABUW_RS18470,ABUW_RS18475,ABUW_RS18485
operon_1739	operons	NZ_CP008706.1;ID=gene-ABUW_RS18515;Name=ABUW_RS18515;gbkey=Gene;gene_biotype=protein_coding;locus_tag=ABUW_RS18515;old_locus_tag=ABUW_3805	1; 4/ 6;2.4e-03;ABUW_RS18515,ABUW_RS18520,ABUW_RS18525,ABUW_RS18530
PF00111	Pfam	2Fe-2S iron-sulfur cluster binding domain	0; 4/ 9;1.9e-02;ABUW_RS05840,ABUW_RS09075,ABUW_RS10115,ABUW_RS14910
PF00725	Pfam	3-hydroxyacyl-CoA dehydrogenase, C-terminal domain	2; 4/ 5;6.5e-04;ABUW_RS03135,ABUW_RS12020,ABUW_RS12730,ABUW_RS17385
PF02737	Pfam	3-hydroxyacyl-CoA dehydrogenase, NAD binding domain	2; 4/ 5;6.5e-04;ABUW_RS03135,ABUW_RS12020,ABUW_RS12730,ABUW_RS17385
PF07724	Pfam	AAA domain (Cdc48 subfamily)	0; 2/ 4;2.9e-02;ABUW_RS08825,ABUW_RS13285
PF17871	Pfam	AAA lid domain	1; 2/ 3;1.1e-02;ABUW_RS08825,ABUW_RS13285
PF12806	Pfam	Acetyl-CoA dehydrogenase C-terminal like	9; 4/ 4;0.0e+00;ABUW_RS01835,ABUW_RS02975,ABUW_RS02980,ABUW_RS11970
PF00694	Pfam	Aconitase C-terminal domain	9; 3/ 3;0.0e+00;ABUW_RS16255,ABUW_RS16835,ABUW_RS18525
PF00330	Pfam	Aconitase family (aconitate hydratase)	1; 3/ 4;3.0e-03;ABUW_RS16255,ABUW_RS16840,ABUW_RS18525
PF00441	Pfam	Acyl-CoA dehydrogenase, C-terminal domain	2;11/20;8.7e-05;ABUW_RS01835,ABUW_RS02975,ABUW_RS02980,ABUW_RS05995,ABUW_RS06650,ABUW_RS10660,ABUW_RS10665,ABUW_RS11970,ABUW_RS12005,ABUW_RS13505,ABUW_RS15600
PF02770	Pfam	Acyl-CoA dehydrogenase, middle domain	1;10/21;8.7e-04;ABUW_RS01835,ABUW_RS02975,ABUW_RS02980,ABUW_RS06650,ABUW_RS10660,ABUW_RS10665,ABUW_RS11970,ABUW_RS12005,ABUW_RS13505,ABUW_RS15600
PF02771	Pfam	Acyl-CoA dehydrogenase, N-terminal domain	1;12/24;1.6e-04;ABUW_RS01835,ABUW_RS02975,ABUW_RS02980,ABUW_RS05995,ABUW_RS06650,ABUW_RS09045,ABUW_RS10660,ABUW_RS10665,ABUW_RS11970,ABUW_RS12005,ABUW_RS13505,ABUW_RS15600
PF08240	Pfam	Alcohol dehydrogenase GroES-like domain	0; 3/ 8;5.0e-02;ABUW_RS10330,ABUW_RS12605,ABUW_RS15610
PF00171	Pfam	Aldehyde dehydrogenase family	0; 8/25;2.9e-02;ABUW_RS05435,ABUW_RS12145,ABUW_RS12355,ABUW_RS13495,ABUW_RS14915,ABUW_RS16475,ABUW_RS16670,ABUW_RS18420
PF00561	Pfam	alpha/beta hydrolase fold	1; 7/13;1.6e-03;ABUW_RS01595,ABUW_RS02535,ABUW_RS07195,ABUW_RS08930,ABUW_RS09185,ABUW_RS10455,ABUW_RS16465
PF01425	Pfam	Amidase	0; 2/ 4;2.9e-02;ABUW_RS09475,ABUW_RS12565
PF13193	Pfam	AMP-binding enzyme C-terminal domain	0; 5/14;3.2e-02;ABUW_RS00865,ABUW_RS07690,ABUW_RS11920,ABUW_RS15985,ABUW_RS18410
PF00004	Pfam	ATPase family associated with various cellular activities (AAA)	0; 3/ 7;3.0e-02;ABUW_RS08825,ABUW_RS13285,ABUW_RS13920
PF00144	Pfam	Beta-lactamase	1; 2/ 3;1.1e-02;ABUW_RS08170,ABUW_RS17125
PF04273	Pfam	Beta-lactamase hydrolase-like protein, phosphatase-like domain	1; 2/ 3;1.1e-02;ABUW_RS10310,ABUW_RS10315
PF13533	Pfam	Biotin-lipoyl like	0; 3/ 6;1.9e-02;ABUW_RS04745,ABUW_RS09480,ABUW_RS15310
PF10431	Pfam	C-terminal, D2-small domain, of ClpB protein	0; 2/ 4;2.9e-02;ABUW_RS08825,ABUW_RS13285
PF00199	Pfam	Catalase	9; 2/ 2;0.0e+00;ABUW_RS11855,ABUW_RS12185
PF02417	Pfam	Chromate transporter	9; 2/ 2;0.0e+00;ABUW_RS10275,ABUW_RS11515
PF02861	Pfam	Clp amino terminal domain, pathogenicity island component	9; 2/ 2;0.0e+00;ABUW_RS08825,ABUW_RS13285
PF02515	Pfam	CoA-transferase family III	0; 2/ 4;2.9e-02;ABUW_RS03150,ABUW_RS12200
PF01144	Pfam	Coenzyme A transferase	1; 5/ 8;1.9e-03;ABUW_RS08910,ABUW_RS08915,ABUW_RS09120,ABUW_RS11990,ABUW_RS11995
PF00775	Pfam	Dioxygenase	1; 2/ 3;1.1e-02;ABUW_RS08945,ABUW_RS08950
PF00378	Pfam	Enoyl-CoA hydratase/isomerase	0; 5/13;2.7e-02;ABUW_RS03135,ABUW_RS04935,ABUW_RS13490,ABUW_RS16065,ABUW_RS17385
PF00743	Pfam	Flavin-binding monooxygenase-like	0; 3/ 6;1.9e-02;ABUW_RS02130,ABUW_RS09620,ABUW_RS10875
PF07995	Pfam	Glucose / Sorbosone dehydrogenase	9; 5/ 5;0.0e+00;ABUW_RS00270,ABUW_RS07425,ABUW_RS08585,ABUW_RS09260,ABUW_RS09285
PF00255	Pfam	Glutathione peroxidase	9; 2/ 2;0.0e+00;ABUW_RS11455,ABUW_RS18150
PF02798	Pfam	Glutathione S-transferase, N-terminal domain	0; 3/ 7;3.0e-02;ABUW_RS11725,ABUW_RS11730,ABUW_RS16890
PF13488	Pfam	Glycine zipper	9; 2/ 2;0.0e+00;ABUW_RS13250,ABUW_RS14775
PF00682	Pfam	HMGL-like	9; 3/ 3;0.0e+00;ABUW_RS11950,ABUW_RS12195,ABUW_RS16550
PF00180	Pfam	Isocitrate/isopropylmalate dehydrogenase	1; 2/ 3;1.1e-02;ABUW_RS05275,ABUW_RS14935
PF01476	Pfam	LysM domain	0; 2/ 4;2.9e-02;ABUW_RS15080,ABUW_RS19650
PF07690	Pfam	Major Facilitator Superfamily	0;16/47;3.5e-03;ABUW_RS04920,ABUW_RS08935,ABUW_RS09355,ABUW_RS09440,ABUW_RS09485,ABUW_RS10150,ABUW_RS12000,ABUW_RS12190,ABUW_RS13175,ABUW_RS13460,ABUW_RS13485,ABUW_RS13550,ABUW_RS14220,ABUW_RS14305,ABUW_RS15595,ABUW_RS18390
PF08241	Pfam	Methyltransferase domain	1; 2/ 3;1.1e-02;ABUW_RS01700,ABUW_RS10460
PF00384	Pfam	Molybdopterin oxidoreductase	1; 3/ 4;3.0e-03;ABUW_RS04630,ABUW_RS08305,ABUW_RS08315

ClassID	Class	Description	Single_list
PF04879	Pfam	Molybdopterin oxidoreductase Fe4S4 domain	1; 2/ 3;1.1e-02;ABUW_RS08305,ABUW_RS08315
PF01568	Pfam	Molydopterin dinucleotide binding domain	9; 3/ 3;0.0e+00;ABUW_RS04630,ABUW_RS08305,ABUW_RS08315
PF03446	Pfam	NAD binding domain of 6-phosphogluconate dehydrogenase	1; 2/ 3;1.1e-02;ABUW_RS09445,ABUW_RS16070
PF14833	Pfam	NAD-binding of NADP-dependent 3-hydroxyisobutyrate dehydrogenase	1; 2/ 3;1.1e-02;ABUW_RS09445,ABUW_RS16070
PF00724	Pfam	NADH:flavin oxidoreductase / NADH oxidase family	0; 3/ 8;5.0e-02;ABUW_RS09190,ABUW_RS09255,ABUW_RS13715
PF00881	Pfam	Nitroreductase family	0; 2/ 4;2.9e-02;ABUW_RS04610,ABUW_RS07870
PF00577	Pfam	Outer membrane usher protein	9; 3/ 3;0.0e+00;ABUW_RS07970,ABUW_RS09975,ABUW_RS11245
PF13953	Pfam	PapC C-terminal domain	9; 3/ 3;0.0e+00;ABUW_RS07970,ABUW_RS09975,ABUW_RS11245
PF13954	Pfam	PapC N-terminal domain	9; 3/ 3;0.0e+00;ABUW_RS07970,ABUW_RS09975,ABUW_RS11245
PF13296	Pfam	Putative type VI secretion system Rhs element Vgr	1; 2/ 3;1.1e-02;ABUW_RS12710,ABUW_RS13685
PF12146	Pfam	Serine aminopeptidase, S33	9; 3/ 3;0.0e+00;ABUW_RS09110,ABUW_RS09575,ABUW_RS09615
PF19582	Pfam	Solute-binding protein AdeT 1/2	1; 3/ 4;3.0e-03;ABUW_RS00045,ABUW_RS00050,ABUW_RS01935
PF00083	Pfam	Sugar (and other) transporter	0; 4/ 8;1.1e-02;ABUW_RS07295,ABUW_RS10230,ABUW_RS12360,ABUW_RS18390
PF02803	Pfam	Thiolase, C-terminal domain	1; 5/ 9;3.9e-03;ABUW_RS08155,ABUW_RS08920,ABUW_RS10195,ABUW_RS12025,ABUW_RS17390
PF00108	Pfam	Thiolase, N-terminal domain	1; 5/ 9;3.9e-03;ABUW_RS08155,ABUW_RS08920,ABUW_RS10195,ABUW_RS12025,ABUW_RS17390
PF02780	Pfam	Transketolase, C-terminal domain	0; 2/ 4;2.9e-02;ABUW_RS10350,ABUW_RS14210
PF04717	Pfam	Type VI secretion system/phage-baseplate injector OB domain	1; 2/ 3;1.1e-02;ABUW_RS12710,ABUW_RS13685
PF10106	Pfam	Uncharacterized protein conserved in bacteria (DUF2345)	1; 2/ 3;1.1e-02;ABUW_RS12710,ABUW_RS13685
PF00582	Pfam	Universal stress protein family	9; 2/ 2;0.0e+00;ABUW_RS04365,ABUW_RS08095
PF00107	Pfam	Zinc-binding dehydrogenase	0; 3/ 7;3.0e-02;ABUW_RS10330,ABUW_RS12605,ABUW_RS15610

Chapter 5 Appendices

A5.1 Differentially Expressed Genes for DMSO Control vs Pomalidomide

Locustag	Gene	logFC	PValue	Pomalidomide 5mM_1	Pomalidomide_5mM_2	Pomalidomide_5mM_3	DMSO CON_1	DMSO CON_2	DMSO CON_3
ABUW_RS00040		1.386	0.00313823	3.231	2.714	1.834	10.294	4.327	5.767
ABUW_RS00710		1.837	0.00295127	3.732	5.468	5.550	7.043	15.463	30.235
ABUW_RS01115		1.458	0.040869	0.683	0.851	0.386	2.763	1.154	1.455
ABUW_RS01125		-1.406	0.0127699	1.183	0.851	1.400	0.596	0.288	0.377
ABUW_RS02215		1.134	0.0043218	2.094	2.147	2.365	4.659	4.270	5.551
ABUW_RS02230		-1.179	0.0137472	3.004	2.592	1.255	0.379	1.269	1.401
ABUW_RS02300		-1.084	0.0331709	2.458	2.430	1.882	1.138	0.519	1.509
ABUW_RS02810		1.955	0.045317	0.228	0.081	0.000	0.704	0.231	0.323
ABUW_RS03050		-1.115	0.00241579	9.649	11.016	10.280	3.738	5.943	4.635
ABUW_RS03435		1.048	0.00773652	29.902	29.646	40.395	36.895	64.161	105.471
ABUW_RS04720		1.689	0.0361819	0.319	0.648	0.338	0.704	0.346	3.234
ABUW_RS05230		-1.389	0.000479076	2.776	4.253	3.668	1.571	1.327	1.186
ABUW_RS05235		-1.247	0.00752512	11.287	4.334	3.909	2.817	1.904	3.449
ABUW_RS05440		-1.928	0.000841621	6.144	3.321	2.799	1.571	1.269	0.377
ABUW_RS05730	bauC	2.357	0.0137627	0.000	0.567	0.193	0.650	0.288	3.180
ABUW_RS05765	basF	1.290	0.00262952	1.593	1.377	1.544	2.438	3.866	4.743
ABUW_RS06285		1.037	0.0214521	0.592	0.932	0.386	1.896	1.039	1.078
ABUW_RS06345		-1.809	0.036616	0.637	0.567	0.386	0.108	0.231	0.108
ABUW_RS06780		-1.641	0.0444412	0.501	0.243	0.531	0.000	0.231	0.162
ABUW_RS06860		2.490	0.0200144	0.091	0.081	0.097	0.704	0.115	0.755
ABUW_RS06935		-1.054	0.0145036	1.638	1.620	1.689	0.758	0.519	1.078
ABUW_RS07195		1.154	0.00225314	8.739	6.278	10.376	25.030	13.444	17.785

Locustag	Gene	logFC	PValue	Pomalidomide 5mM_1	Pomalidomide_5mM_2	Pomalidomide_5mM_3	DMSO CON_1	DMSO CON_2	DMSO CON_3
ABUW_RS07260	csuB	-2.077	0.0349136	0.455	0.405	0.869	0.108	0.115	0.162
ABUW_RS07265	csuC	-1.070	0.00407623	2.822	6.035	5.116	2.817	1.731	2.102
ABUW_RS07405		-3.540	0.0095693	0.182	0.851	0.434	0.000	0.000	0.108
ABUW_RS07645		-1.014	0.00575007	4.733	6.278	3.571	2.384	3.462	1.455
ABUW_RS07950		-1.621	0.022138	1.138	0.932	2.124	0.433	0.692	0.216
ABUW_RS08035		1.099	0.0102178	40.097	25.718	51.302	44.155	85.394	120.938
ABUW_RS08070		1.680	0.00706855	2.685	4.131	4.681	3.576	12.694	20.588
ABUW_RS08085		3.263	0.0290483	0.000	0.000	0.048	0.163	0.346	0.108
ABUW_RS08280		-1.135	0.0271651	1.320	2.876	3.861	0.650	1.385	1.617
ABUW_RS08870		-1.088	0.0113008	2.503	3.362	2.220	0.867	1.904	1.078
ABUW_RS09085	feaR	-2.650	0.0149497	2.276	0.203	0.820	0.217	0.288	0.000
ABUW_RS09110	pcaD	1.150	0.0246972	0.819	1.620	1.593	3.576	3.116	2.317
ABUW_RS09475	iaaH	-1.256	0.0211666	1.821	2.066	0.965	0.975	0.923	0.162
ABUW_RS09620		-1.025	0.00258243	11.606	10.773	9.508	3.792	5.135	6.737
ABUW_RS09660		-1.175	0.00243313	5.097	2.511	4.585	1.625	1.385	2.317
ABUW_RS09670		-1.188	0.0192225	2.048	1.904	1.207	0.704	1.096	0.485
ABUW_RS10120		-1.278	0.00228078	14.200	4.982	7.818	3.413	3.058	4.581
ABUW_RS10155		-1.702	0.00645728	2.913	1.944	2.413	0.542	0.923	0.755
ABUW_RS10365		-1.459	0.000503824	30.858	16.808	16.650	9.535	7.905	5.928
ABUW_RS10520		1.761	0.0109521	4.415	5.670	12.355	6.935	24.176	44.463
ABUW_RS10525		2.329	0.0140294	0.819	0.567	0.241	0.433	1.269	6.575
ABUW_RS10600		1.779	0.00153221	0.910	0.608	1.255	2.763	2.250	4.365
ABUW_RS10615		1.154	4.78416e-05	2.640	3.524	3.668	5.309	7.385	9.216
ABUW_RS10630		1.149	0.0101713	8.648	12.879	18.967	13.870	24.984	50.714
ABUW_RS10635		1.447	0.00816503	6.827	5.630	9.652	7.368	22.676	30.019
ABUW_RS10640		1.293	0.0206044	10.423	9.761	12.838	11.865	22.733	46.133
ABUW_RS10790		-1.195	0.000206092	8.283	7.979	5.888	3.792	3.924	1.994
ABUW_RS11300		-1.424	0.000922388	7.328	4.617	3.475	3.034	1.616	1.078
ABUW_RS11470		-1.033	0.00687401	218.463	126.927	223.741	77.366	115.109	85.584
ABUW_RS11670		-1.096	0.0490415	1.229	2.349	1.351	0.542	1.558	0.269
ABUW_RS11850		-1.235	0.0329533	2.412	2.754	1.158	0.379	1.327	1.024
ABUW_RS11885		-2.661	0.00457736	0.546	1.175	1.544	0.054	0.173	0.269
ABUW_RS11920		-1.441	0.000474622	129.303	89.546	80.645	45.076	44.544	20.695
ABUW_RS11925		-1.142	0.000474718	68.907	59.090	51.543	30.285	33.061	18.055
ABUW_RS12265		-2.380	0.0440497	0.546	1.013	0.193	0.108	0.231	0.000
ABUW_RS12310	paaD	-1.374	0.000645887	33.225	16.119	14.575	11.540	7.212	5.874
ABUW_RS12315	paaC	-1.640	0.00943682	60.077	18.225	26.447	16.091	10.617	6.845
ABUW_RS12320	paaB	-1.870	0.00118312	19.525	6.075	9.652	3.738	2.943	2.910
ABUW_RS12325	paaA	-2.684	0.00312692	182.872	28.107	56.756	14.574	14.944	12.126
ABUW_RS12330	paaZ	-1.681	0.0125158	201.350	49.653	64.719	38.846	30.350	29.211
ABUW_RS12750		-1.273	0.0173547	42.737	16.200	10.955	16.470	8.597	3.826
ABUW_RS12995		-1.763	0.0492905	0.956	0.486	0.290	0.325	0.115	0.054
ABUW_RS13030		1.545	0.0115844	0.728	0.405	0.531	2.492	1.385	0.970
ABUW_RS13120		-1.657	0.0282691	1.274	1.296	2.220	0.704	0.346	0.431
ABUW_RS13285	clpB	-1.037	0.0240381	1465.660	2109.969	1747.025	870.205	872.119	852.442

Locustag	Gene	logFC	PValue	Pomalidomide 5mM_1	Pomalidomide_5mM_2	Pomalidomide_5mM_3	DMSO CON_1	DMSO CON_2	DMSO CON_3
ABUW_RS13395		-1.615	0.0390689	0.273	0.810	1.351	0.163	0.115	0.485
ABUW_RS13435		-1.692	9.4796e-07	35.955	29.484	33.494	7.856	10.559	12.180
ABUW_RS13440		-1.278	3.34807e-06	21.437	15.431	16.747	8.235	7.270	6.575
ABUW_RS13445		-1.261	0.00400511	7.464	7.331	9.073	5.039	3.000	1.886
ABUW_RS13530		-1.016	0.0111093	21.573	26.487	82.817	20.100	18.117	26.300
ABUW_RS13600		-1.225	0.0029789	1071.562	699.881	812.968	469.505	387.448	248.290
ABUW_RS13625		-1.043	0.00215507	10.149	9.275	11.824	6.230	6.405	2.533
ABUW_RS14080		-1.474	0.0037944	13.973	8.181	6.515	6.556	2.654	1.078
ABUW_RS14160		1.514	0.0142421	18.433	24.584	29.729	22.971	58.161	126.489
ABUW_RS15365	upp	1.211	0.00749826	167.079	180.387	195.701	208.693	230.449	818.165
ABUW_RS15500		-2.447	0.0169539	0.637	0.648	0.290	0.108	0.173	0.000
ABUW_RS15705		-1.743	0.0298727	293.423	24.746	36.824	34.457	42.236	29.372
ABUW_RS15985		-1.517	4.20104e-05	67.405	36.450	34.893	19.667	17.656	11.156
ABUW_RS16185		3.421	0.00995189	1.866	1.458	3.040	63.767	1.385	2.156
ABUW_RS16295		1.117	0.0367819	29.811	30.051	31.370	24.434	27.926	145.352
ABUW_RS16475		1.129	0.00531119	643.738	578.786	585.945	981.595	2417.469	557.210
ABUW_RS16500		-1.723	0.00345284	465.281	220.401	195.122	143.300	73.739	49.744
ABUW_RS16540		1.105	0.0333643	208.769	186.584	435.707	231.827	596.203	958.721
ABUW_RS16965		-1.418	0.0155624	9.512	52.893	9.797	8.614	9.693	8.893
ABUW_RS17065		-1.172	0.0355612	17.887	28.472	16.312	11.161	10.040	6.683
ABUW_RS17680		1.208	0.00673356	6.417	4.982	7.384	7.097	14.309	21.827
ABUW_RS18015		-1.307	0.0063972	15.110	7.169	7.336	4.118	4.443	3.395
ABUW_RS18095		1.169	0.0107106	1.274	1.863	0.869	3.196	3.404	2.587
ABUW_RS20185		1.486	0.0471009	0.091	0.162	0.145	0.108	0.462	0.593
ABUW_RS20235		2.698	0.00766436	0.046	0.081	0.048	0.379	0.519	0.377
ABUW_RS20295		-2.793	0.044122	0.455	0.324	0.097	0.000	0.000	0.108
ABUW_RS20505		-1.497	0.0299092	0.546	0.486	1.400	0.379	0.115	0.323